COMPLETED
505
Y 3. N 88:27/0082/v.3
FEB 25 1987

NUREG/CP-0082
Vol. 3

Proceedings of the U.S. Nuclear Regulatory Commission

# Fourteenth Water Reactor Safety Information Meeting

Volume 3
- Equipment Qualification
- Mechanical and Structural Research
- Seismic Research
- Nuclear Plant Aging

ORIGINAL

Held at
National Bureau of Standards
Gaithersburg, Maryland
October 27-31, 1986

**U.S. Nuclear Regulatory Commission**

**Office of Nuclear Regulatory Research**

Proceedings prepared by
Brookhaven National Laboratory

NOTICE

These proceedings have been authored by a contractor of the United States Government. Neither the United States Government nor any agency thereof, or any of their employees, makes any warranty, expressed or implied, or assumes any legal liability or responsibility for any third party's use, or the results of such use, of any information, apparatus, product or process disclosed in these proceedings, or represents that its use by such third party would not infringe privately owned rights. The views expressed in these proceedings are not necessarily those of the U.S Nuclear Regulatory Commission.

Available from

Superintendent of Documents
U.S. Government Printing Office
P.O. Box 37082
Washington D.C. 20013-7082

and

National Technical Information Service
Springfield , VA 22161

NUREG/CP-0082
Vol. 3
RD, RM, RV

Proceedings of the U.S. Nuclear Regulatory Commission

# Fourteenth Water Reactor Safety Information Meeting

Volume 3
- Equipment Qualification
- Mechanical and Structural Research
- Seismic Research
- Nuclear Plant Aging

Held at
National Bureau of Standards
Gaithersburg, Maryland
October 27-31, 1986

Date Published: February 1987

Compiled by: Allen J. Weiss

**Office of Nuclear Regulatory Research**
**U.S. Nuclear Regulatory Commission**
**Washington, DC 20555**

Proceedings prepared by
Brookhaven National Laboratory

I

BLANK PAGE

II

# ABSTRACT

This six-volume report contains 156 papers out of the 175 that were presented at the Fourteenth Water Reactor Safety Information Meeting held at the National Bureau of Standards, Gaithersburg, Maryland, during the week of October 27-31, 1986. The papers are printed in the order of their presentation in each session and describe progress and results of programs in nuclear safety research conducted in this country and abroad. Foreign participation in the meeting included thirty-four different papers presented by researchers from Canada, Czechoslovakia, Finland, Germany, Italy, Japan, Mexico, Spain, Sweden, Switzerland and the United Kingdom. The titles of the papers and the names of the authors have been updated and may differ from those that appeared in the final program of the meeting.

BLANK PAGE

PROCEEDINGS OF THE
14th WATER REACTOR SAFETY INFORMATION MEETING

October 27-31, 1986

Published in Six Volumes

## GENERAL INDEX

VOLUME 1

- Plenary Session
- Severe Accident Sequence Analysis
- Risk Analysis/PRA Applications
- Reference Plant Risk Analysis - NUREG-1150
- Innovative Concepts for Increased Safety of Advanced Power Reactors

VOLUME 2

- Research in Nondestructive Evaluation
- Environmental Effects in Primary System Components
- Pressure Vessel Research
- Irradiation Effects on RPV Steels
- Degraded Piping Research

VOLUME 3

- Equipment Qualification
- Mechanical and Structural Research
- Seismic Research
- Nuclear Plant Aging

VOLUME 4

- ECCS Rule Revision
- Integral Systems Testing
- Separate Effects/Experiments and Analyses
- 2D/3D Research

VOLUME 5

- Nuclear Plant Analyzer and Code Development
- International Code Assessment Program
- Industry Safety Research

VOLUME 6

- TMI-2 Analyses
- Fission Product Release and Transport in Containment
- Severe Accident Source Term
- Containment Systems Research/Containment Loads Analysis

BLANK PAGE

# REGISTERED ATTENDEES

## 14th WATER REACTOR SAFETY INFORMATION MEETING

Abel, P.S.
Mitre Corporation
1820 Dolley Madison Blvd.
McLean, VA 22102

Acker, D.
Commissariat A L'Energie Atomique
DEMT-Centre d'Etudes Nucleaires de SACLAY
91191 GIF S/YVETTE
FRANCE

Adams, R.E.
Oak Ridge National Laboratory
P.O. Box Y, Bldg. 9108 MS-2
Oak Ridge, Tennessee 37831

Addabbo, C.
CEC-JRC
Ispra
21020, Italy

Akers, D.W.
EG&G Idaho
P.O. Box 1625
Idaho Falls, Idaho 83415

Aksan, N.S.
EIR
5303 Wuerenlingen
Switzerland

Allen, R.A.
E.I. du Pont de Nemours Co.
Bldg. 707-C, Room 331
Savannah River Plant
Aiken, SC 29808

Allison, C.M.
EG&G Idaho
P.O. Box 1625
Idaho Falls, Idaho 83415

Almenus, K.K.
University of Maryland
College Park, Maryland 20742

Alonso, A.
Madrid Polytechnical University
Jose Gutierrez Abascal, 2
28006 Madrid, Spain

Andersen, J.G.
General Electric Company
175 Curtner Avenue, M/C 186
San Jose, California 95125

Andersen, P.S.
Dynatrek, Inc.
2115 E. Jefferson Street
Rockville, Maryland 20852

Anderson, G.E.
Babcock & Wilcox
109 Woodberry Lane
Lynchburg, VA 24502

Anderson, J.M.
Bechtel Power Corporation
15740 Shady Grove Road
Gaithersburg, MD 20877

Anderson, R.P.
Argonne National Laboratory
9700 S. Cass Avenue
Argonne, IL 60539

Arcieri, W.C.
ENSA, Inc.
15825 Shady Grove Road
Rockville, Maryland 20850

Ardron, K.H.
CEGB Generation Development & Construction Div.
Barnett Way, Barnwood
Gloucester, United Kingdom GL47RS

Arendts, J.G.
INEL
1325 Presto #4
Idaho Falls, Idaho 83402

Armstrong, D.A.
Washington Public Power Supply System
3000 George Washington
Richland, WA 99352

Arrington, E.A.
Chubu Electric Power
900 17th St., N.W.
Suite 714
Washington, D. C. 20006

Asaka, H.
Japan Atomic Energy Research Institute
3000 Trinity Drive #23
Los Alamos, New Mexico

Azarm, M.A.
Brookhaven National Laboratory
Building 130
Upton, New York 11973

Bandyopadhyay, K.K.
Brookhaven National Laboratory
Building 129
Upton, New York 11973

Bari, R.A.
Brookhaven National Laboratory
Building 130
Upton, New York 11973

Bass, B.R.
Oak Ridge National Laboratory
P.O. Box P
Oak Ridge, Tennessee 37831

Basselier, J.E.
Belgonucleaire
25 rue de Camp De Mars
Brussel, Belgium 1050

Bayless, P.D.
EG&G Idaho, Inc.
P.O. Box 1625
Idaho Falls, ID 93415

Beliaev, G.K.
OKG Aktiebolag
Box 1746(Birger Jarlsgatan 41A)
11187 Stockholm
Sweden

Benjamin, A.S.
Sandia National Laboratory
Division 6411
Albuquerque, New Mexico 87185

Bennett, J.C.
Los Alamos National Laboratory
Mail Stop 5576
Box 1663
Los Alamos, New Mexico 87544

Beranek, F.
Savannah River Laboratory
Aiken, South Carolina 29808

Bergeron, K.D.
Sandia National Laboratory
P.O. Box 5800
Albuquerque, New Mexico 87185

Berman, M.
Sandia National Laboratory
Division 6427
Albuquerque, New Mexico 87185

Bernard, M.G.
Commissariat A L'energie Atomique, France
Ceng, Seth, 85X 38041 Grenoble-Cedex
Grenoble 38041
France

Berry, D.L.
Sandia National Laboratory
Organization 6447
Albuquerque, New Mexico 87185

Beswick, E.
Central Electricity Generating Board
Booths Hall, Chelford Road
Knutsford, Cheshire WA16 8Q9
England

Beyer, R.F.
Westinghouse
206 Navajo Road
Pittsburgh, PA 15241

Bian, S.H.
Battelle Northwest Laboratory
P.O. Box 999
Richland, WA 99352

Binner, W.
Austrian Research Center Seibersdorf
Seidersdorf A-2444
Austria

Blanco, J.
Madrid Polytechnical University
Jose Gutierrez Abascal, 2
28006 Madrid
Spain

Board, S.J.
Berkeley Nuclear Laboratories
Berkeley, Gloucestershire
United Kingdom

Boeanert, P.A.
U. S. Nuclear Regulatory Commission
Washington, D. C. 20555

Borsum, R.B.
Babcock & Wilcox
7910 Woodmont Avenue
Bethesda, Maryland 20814

Boyack, B.E.
Los Alamos National Laboratory
P.O. Box 1663
Los Alamos, New Mexico 87544

Bradley, D.R.
Sandia National Laboraotry
Albuquerque, New Mexico 87109

Bray, M.A.
INEL
P.O. Box 1625
Idaho Falls, Idaho 83415

Brittain, I.
United Kingdom Atomic Energy Authority
Atomic Energy Establishment Winfrith
Dorchester, Dorset DT28DH
England

Broughton, J.M.
EG&G Idaho
P.O. Box 1625
Idaho Falls, Idaho 83402

Brust, B.W.
Battelle Northwest Laboratory
505 King Avenue
Columbus, Ohio 43201

Bryan, R.H.
Oak Ridge National Laboratory
P.O. Box Y
Oak Ridge, Tennessee 37831

Buescher, B.J.
INEL
Idaho Falls, Idaho 84301

Bussac, J.M.
Commissariat A L'Energie Atomique
Centre D'Etudes Nucleaires
De Fontenay-Aux-Roses- Cedex 92265
France

Buxton, L.D.
Sandia National Laboratory
Division 6444
Albuquerque, New Mexico 87185-5800

Camp, A.L.
Sandia National Laboratory
P.O. Box 5800, Org. 6412
Albuquerque, New Mexico 87185

Campbell, D.J.
JBF Associates
1000 Technology Park Center
Knoxville, TN 37932

Campbell, J.F.
H.M. Nuclear Installations Inspectorate
Room 735, Thames House South
Millbank, London, SWIP 4QJ
London, England

Carey, C.
Tennessee Valley Authority
400 W Summit Hill Drive
Knoxville, TN 37923

Carroll, D.E.
Sandia National Laboratory
Org. 6449
P.O. Box 5800
Albuquerque, New Mexico 87185

Carter, H.R.
Babcock & Wilcox
1562 Beeson Street
Alliance, Ohio 44601

Casper, H.F.
Gesellschaft fur Reactorsicherheit
Schweitnergasse
Koln, Federal Republic of Germany

Catalawi, L.
Framatome
Tour Fiat Cedex 16
Paris-La-Defense 92084
France

Catton, I.
University of California
Los Angeles, CA 90024

Cavlina, N.
University of Zagreb
Faculty of Electrical Engineering
Zagreb, Yugoslavia

Chae, S.
Korea Advanced Energy Research Institute
P.O. Box 7
Daeduk-Danji
Choong-Nam, Korea

Chambers, R.
EG&G Idaho, Inc.
P.O. Box 1625
Idaho Falls, ID 83415

Charlton, T.R.
EG&G Idaho, Inc.
P.O. Box 1625
Idaho Falls, Idaho 83415

Chen, J.C.
Lehigh University
Whitaker Lab #5
Bethlehem, Pennsylvania 18015

Chen, J.T.
U. S. Nuclear Regulatory Commission
Washington, D. C. 20555

Chen, P.
Taiwan Power Company
242, Roosevelt Road, Sec. 3
Taipei, Taiwan
Federal Republic of China

Chen, W.
Taiwan Power Company
242, Roosevelt Road, Sec. 3
Taipei, Taiwan
Federal Republic of China

Chiang, F.K.
Long Island Lighting Company
P.O. Box 618
North Country Road
Wading River, New York 11792

Chona, R.
University of Maryland
College Park, MD 20742

Chopra, O.K.
Argonne National Laboratory
9700 S. Cass Avenue
Argonne, IL 60565

Chu, R.Y.
Ontario Hydro
700 University Avenue
Toronto, Ontario M5G 1X6
Canada

Chung, H.M.
Argonne National Laboratory
9700 S. Cass Avenue
Argonne, IL 60565

Church, J.P.
Savannah River Laboratory
Aiken, South Carolina 29808

Cole, R.K.
Sandia National Laboratory
P.O. Box 5800
Albuquerque, New Mexico 87185

Condie, K.G.
EG&G Idaho
P.O. Box 1625
Idaho Falls, Idaho 83415

Conine, J.C.
Knolls Atomic Power Laboratory
P.O. Box 1072
Schenectady, New York 12301

Cook, K.V.
Oak Ridge National Laboratory
P.O. Box X
Bldg. 4500S
Oak Ridge, Tennessee 37831

Corwin, W.R.
Oak Ridge National Laboratory
P.O. Box X
Oak Ridge, Tennessee 37831

Cox, R.F.
United Kingdom Atomic Energy Authority
Wigshaw Lane
Culcheth, Warrington, Cheshire
United Kingdom

Crawford, T.J.
American Electric Power Service Corporation
1 Riverside Plaza
Columbus, Ohio 43215

Croucher, D.W.
EG&G Idaho, Inc.
P.O. Box 1625
Idaho Falls, Idaho 83415

Crutzen, S.J.
CEC Joint Research Center, Ispra
Ispra I-21020
Italy

Cummings, G.E.
Lawrence Livermore National Laboratory
P.O. Box 808, L-198
Livermore, California 94550

Cushman, R.A
Niagara Mohawk
300 Erie Blvd. West
Syracuse, New York 13202

Cybulskis, P.
Battelle Northwest Laboratory
1160 Cindy Ellen Court
Columbus, Ohio 43229

Czech, J.J.
KWU
Hammerbacherstr
Erlangen
Federal Republic of Germany

Dahlgren, D.A.
Sandia National Laboratory
Dept. 6440
P.O. Box 5800
Albuquerque, New Mexico 87185

Dallman, R.J.
EG&G Idaho, Inc.
P.O. Box 1625
Idaho Falls, Idaho 83415

Damerell, P.J.
MPR Associates, Inc.
1050 Connecticut Avenue, N.W.
Washington, D. C. 20036

Darlaston, J.
Central Electricity Generating Board
Berkeley Nuclear Lab.
Berkeley, Gloucestershire GL13 9PB
United Kingdom

Davidson, E.M.
Florida Power Corporation
P.O. Box 14042
St. Petersburg, Florida 34311

Debenham, A.A.
United Kingdom Atomic Energy Authority
Wigshaw Lane
Culcheth, Warrington, Cheshire WA34NE
United Kingdom

Deem, R.E.
New York Power Authority
120 Main Street
White Plains, New York 10601

Deletre, G.
CEA-IPSN
Centre d'etades nucleaires
Fontenay aux Roses
France 92 265

Dietershagen, H.P.
General Electric
River Road
Schenectady, New York 12302

Dimarto, M.
University of Maryland
Mechanical Engineering Department
College Park, Maryland 20742

Doctor, S.R.
Battelle Northwest Laboratory
Battelle Blvd.
Richland, WA 99352

Dodd, C.V.
Oak Ridge National Laboratory
P.O. Box X
Oak Ridge, TN 37831

Duce, S.W.
EG&G Idaho, Inc.
P.O. Box 1625
Idaho Falls, Idaho 83415

DuCharme, A.
Sandia National Laboratory
P.O. Box 5800
Albuquerque, New Mexico 87185

Duco, J.J.
CEA Institut De Protection Et De Surete Nuclear
CEN/FAR B.P. N° 6
92265 Fontenay Aux Roses Cedex
France

Durkin, M.S.
DOD
8603 Brand Court
Clinton PG
Maryland 20735

East, G.R.
Stone & Webster Engineering Corporation
P.O. Box 2325
Boston, MA 02107

Ebeling-Koning, D.B.
Westinghouse
P.O. Box 355
Pittsburgh, PA 15230

Echavarri, L.E.
Consejo De Seguridad Nuclear
C/Sor Angela De La Cruz, 3
Madrid 28020
Spain

Ehlers, K.D.
Brown Boveri Reaktor GmbH
Postfach 5143
Dudenstr. 44, D-6800 Mannheim 1
Mannheim, Germany D-6800

Eidam, G.R.
Bechtel National Laboratory
P.O. Box 72
Middletown, PA 17057

Eissenberg, D.M.
Oak Ridge National Laboratory
Bldg. 9201-3
P.O. Box Y
Oak Ridge, Tennessee 37830

Evans, M.G.
NUS Corporation
910 Clopper Road
Gaithersburg, Maryland 20878

Fabic, S.
Dynatrek, Inc.
2115 E. Jefferson Street
Rockville, Maryland 20852

Fabry, A.M.
SCK-CEN
Boeretang
2400 Mol, Belgium

Falls, O.B.
NucleDyne Energy Corporation
728 W. Michigan Avenue
Jackson, Michigan 49201

Farrar, C.R.
Los Alamos National Laboratory
Mail Stop J576
Los Alamos, New Mexico 37545

Fell, J.
United Kingdom Atomic Energy Authority
AEE Winfrith
Dorchester, Dorset DT2 8DH
England

Feltus, M.
New York Power Authority
123 Main Street
White Plains, New York 10601

Ferch, R.
Atomic Energy Control Board
P.O. Box 1046
Station "B"
Ottawa, Ontario K1P5S9
Canada

Finley, M.T.
Baltimore Gas & Electric Company
P.O. Box 1535
Lusby, Maryland 20657

Fischer, S.R.
Middle South Utilities
639 Loyola
New Orleans, LA 70114

Ford, C.E.
G.E.C.- Energy Systems
Cambridge Road, Whetstone
Leicestershire, England

Fulford, J.
NUS Corporation
910 Clopper Road
Gaithersburg, Maryland 20878

Gallagher, W.J.
NUS Corporation
910 Clopper Road
Gaithersburg, Maryland 20878

George, P.T.
Central Electricity Generating Board
Booths Hall
Knutsford, Cheshire
England

Ghosh, S.
Central Electricity Generating Board
Booths Hall
Knutsford, Cheshire
England

Gibbon, S.H.
Philadelphia Electric Co.
510-1 2301 Market Street
Philadephia, PA 19101

Gibson, I.H.
United Kingdom Atomic Energy Authority
AEE winfrith
Dorchester, Dorset DT2 8DH
England

Gieseke, J.A.
Battelle Northwest Laboratory
505 King Avenue
Columbus, Ohio 43201

Ginsberg, T.
Brookhaven National Laboratory
Bldg. 820
Upton, New York 11973

Gitnick, B.
ENSA, Inc.
15825 Shady Grove Road
Rockville, Maryland 20850

Goldberg, F.
U.S. Nuclear Regulatory Commission
Mail Stop P-808
Washington, D. C. 20555

Golden, D.W.
EG&G Idaho
P.O. Box 1625
Idaho Falls, Idaho 83401

Goodwin, K.E.
U.S. Department of Energy
19901 Germantown Road, DP-133.1
Germantown, Maryland 20545

Gottula, R.C.
Exxon Nuclear Company
2101 Horn Rapids Road
Richland, WA 99352

Greene, G.A.
Brookhaven National Laboratory
Bldg. 820
Upton, New York 11973

Greene, S.R.
Oak Ridge National Laboratory
Martin Marietta Energy Systems, Inc.
P.O. Box Y
Oak Ridge, TN 37831

Griffith, P.
MIT
Room 7-044, MIT
Cambridge, MA 02139

Guppy, J.G.
Brookhaven National Laboratory
Building 475B
Upton, New York 11973

Guthrie, G.L.
Westinghouse
7170 Davenport, Apt. 203
Santa Barbara, California 93117

Haga, T.
Japan Nuclear Power Engineering Test Center
Mita Kokusai Bldg.
Mita 1-4-28, Minato-ku
Tokyo 108, Japan

Hammar, L.H.
Swedish Nuclear Power Inspectorate
Box 27106
10252 Stockholm, Sweden

Hammond, R.P.
Telephos
P.O. Box 1735
Santa Monica, California 90406

Hansen, C.M.
Roy F. Weston, Inc.
955 L'Enfant Plaza, 8th Floor
Washington, D.C. 20024

Hanson, D.J.
EG&G Idaho
P.O. Box 1625
Idaho Falls, Idaho 83415

Hanson, R.G.
EG&G Idaho
P.O. Box 1625
Idaho Falls, Idaho 83501

Hara, H.
Japan Nuclear Power Engineering Test Center
Mita Kokusai Bldg.
Mita 1-4-28, Minato-ku
Tokyo 108, Japan

Harbison, S.A.
HM Nuclear Installations Inspectorate
Room 701, Thames House South, Millbank
London, England SW1P4QL

Harper, F.T.
Sandia National Laboratory
P.O. Box 5800, Organization 6412
Albuquerque, New Mexico 87185

Harrington, R.M.
Oak Ridge National Laboratory
P.O. Box Y
Oak Ridge, Tennessee 37831

Hashimoto, K.
Japan Atomic Research Institute
Tokai-mura
Naka-gun, Ibaraki-ken 319-11
Japan

Haskin, E.
Sandia National Laboratory
P.O. Box 5800, Division 6415
Albuquerque, New Mexico 87185

Hatmaker, W.A.
Oak Ridge National Laboratory
P.O. Box X
Oak Ridge, Tennessee 37831

Hawthorne, R.
Materials Engineering Associates
9700B Martin Luther King Jr., Highway
Lanham, Maryland 20706

Hazzan, M.J.
Stone & Webster
3 Executive Campus
Cherry Hill, New Jersey 08034

Heck, C.L.
Westinghouse
P.O. Box 355
Pittsburgh, PA 15125

Hedrick, R.A.
Technology for Energy Corporation
One Energy Center, Lexington Drive
Knoxville, Tennessee 37922

Henlez, V.
National Bureau of Standards
Gaithersburg, Maryland 20899

Henninger, R.J.
Los Alamos National Laboratory
Group Q-9, Mail Stop K553
Los Alamos, New Mexico 87544

Hertlein, R.J.
Kraftwerk Union AG, R 152
Hammerbacherstr. 12+14
Erlangen, 8520
Federal Republic of Germany

Hewitt, G.F.
Harwell Laboratory
Thermal Hydraulics Div., B-392
Oxfordshire OX11 ORA
United Kingdom

Higgins, J.
MPR Associates, Inc.
1050 Connecticut Avenue, N.W.
Washington, D. C. 20555

Hill, P.R.
Pennsylvania Power & Light Co.
Two North Ninth Street
Allentown, Pennsylvania 18101

Hill, R.C.
Idaho National Engineering Laboratory
P.O. Box 1625
Idaho Falls, Idaho 83415

Hirons, T.J.
Los Alamos National Laboratory
212 Canada Way
Los Alamos, New Mexico 87544

Hodge, S.A.
Oak Ridge National Laboratory
P.O. Box Y
Building 9104-1
Oak Ridge, Tennessee 37831

Hofmayer, C.H.
Brookhaven National Laboratory
Building 129
Upton, New York 11973

Hojo, T.
MAPI
1267-5, Muramatsu, Tokai-mura
Ibaragi, Japan

Holman, G.S.
Lawrence Livermore National Laboratory
P.O. Box 808, L-197
Livermore, California 94509

Holmstrom, H.L.
Technical Research Centre of Finland (VTT)
P.O. Box 169
SF-00181 Helsinki
Finland

Hoopingarner, K.R.
Battelle - Pacific Northwest Laboratory
P.O. Box 999
Richland, WA 99352

Hosoda, S.
Century Research Center Co.
2, Nihonbashi-Honcho 3-Chome
Chuo-ku, Tokyo 103
Japan

Hsiue, J.
Taiwan Power Company
242, Roosevelt Road, Sec. 3
Taipei, Taiwan
Federal Republic of China

Hsu, Y.Y.
University of Maryland
College Park, Maryland 20742

Hutton, P.H.
Battelle, Pacific Northwest Laboratories
P.O. Box 999
Richland, Washington 99352

Hyman, C.R.
Oak Ridge National Laboratory
P.O. Box Y
Building 9104-1, Room 18
Oak Ridge, Tennessee 37831

Iguchi, T.
Japan Atomic Energy Research Institute
Tokai-mura, Naka-gun
Ibaraki-ken 319-11
Japan

Imai, T.
JEPIC
1726 MST, N.W.
Washington, D. C. 20036

Irani, A.
GPU Nuclear
100 Interpace Parkway
Parsippany, New Jersey 07054

Irwin, G.R.
University of Maryland
Department of Mech. Engr.
College Park, Maryland 20742

Ishii, M.
Argonne National Laboratory
9700 South Cass Avenue
Argonne, IL 60559

Iskander, S.K.
Oak Ridge National Laboratory
P.O. Box X
Oak Ridge, Tennessee 37831

Iwamura, T.
Japan Atomic Energy Research Institute
Tokai-mura, Naka-gun
Ibaraki-ken
319-11, Japan

Jacobs, P.T.
EG&G Idaho, Inc.
P.O. Box 1625
Idaho Falls, Idaho 23415

Jageler, E.F.
Combustion Engineering
1000 Prospect Hill Road
Windsor, CT 06095

Jamet, P.
CEA
DEMT/SMTS/CAMS
Gif Sun Yuette
91191, France

Jansky, J.F.
BTB - Leonberg
725 Leouberg
Rilkestr. 5
Germany

Jeanmougin, N.M.
ETEC
P.O. Box 1449
Canoga Park, California 91304

Jensen, R.T.
ITI
P.O. Box 1604
Idaho Falls, Idaho 83401

Jenson, S.E.
Exxon Nuclear Company
2101 Horn Rapids Road
Richland, WA 99352

Johnson, G.L.
Lawrence Livermore National Laboratory
L-195, P.O. Box 808
Livermore, CA 94550

Jones, D.D.
SA AEC
Delindaba
Pretoria, TVL
Private BAG X25C
Republic of South Africa

Jonsson, N.O.
AB Asea-Atom
P.O. Box 53
Vasteras 72104
Sweden

Kam, F.B.
Oak Ridge National Laboratory
P.O. Box X
Building 3001, MS-004
Oak Ridge, Tennessee 37831

Kannberg, L.D.
Battelle, Pacific Northwest Laboratories
P.O. Box 999
Richland, Washington 99352

Kanninen, M.F.
Southwest Research Institute
P.O. Drawer 28510
San Antonio, Texas 78284

Karwat, H.
Techn. Universitat Munchen
8046 Garching Forschungsgelande
Garching, D8046
Federal Republic of Germany

Kashima, K.
Central Res. Institute of Elec. Power Industry
11-1, Iwato Kita 2-Chome
Komae-shi
Tokyo 201
Japan

Kato, W.Y.
Brookhaven National Laboratory
Building 197C
Upton, New York 11973

Kato, Y.
Hitachi Ltd.
3-1-1, Hitachi, Japan
Hitachi, Japan

Keaney, W.R.
General Associates Corp.
P.O. Box 762
Worthington, Ohio 43085

Keating, R.
MPR Associates, Inc.
1050 Connecticut Avenue, N.W.
Washington, D. C. 20555

Khan, R.
Baltimore Gas & Electric Co.
Calvert Cliffs Nuclear Power Plant
Lusby, MD 20657

Khatib-Rahbar, M.
Brookhaven National Laboratory
Building 130
Upton, New York 11973

Kim, D.
Korea Advanced Energy Research Institute
P.O. Box 7
Kaeduck-Danji
Choong-Nam, Korea

Kim, M.
University of Wisconsin-Madison
336 ERB, 1500 Johnson St.
Madison, WI 53706

King, D.J.
Bechtel
15740 Shady Grove Road
Gaithersburg, Maryland 20877

Kinnersly, S.R.
United Kingdom Atomic Energy Authority
AEE Winfrith
Dorchester, Dorset DT2 8DH
England

Kirchner, R.
JBS Associates, Inc.
1000 Technology Park Center
Knoxville, TN 37922

Klausnitzer, E.N.
KWU
Hammerbacherstrasse 72+74
D-8520 Erlangen
Federal Republic of Germany

Kleimola, F.W.
Nucledyne Engineering Corporation
728 W. Michigan Avenue
Jackson, Michigan 49201

Kloeg, P.J.
KEMA
Utrechtseweg 310
Arnhem 6812 AR
The Netherlands

Klorig, W.N.
Aptech Engineering Services
101 1/2 S. Union Street
Alexandria, VA 22314

Knight, T.D.
Los Alamos National Laboratory
Los Alamos, New Mexico 87545

Koizumi, Y.
Japan Atomic Research Institute
Tokai-mura
Naka-gun, Ibaraki-ken 319-11
Japan

Kot, C.A.
Argonne National Laboratory
9700 S. Cass Avenue
Building 335
Argonne, Illinois 60439

Krantz, E.A.
EG&G Idaho, Inc.
Box 1625
Idaho Falls, Idaho 83415

Kress, T.S.
Oak Ridge National Laboratory
P.O. Box Y
Oak Ridge, TN 37831

Krueger, G.A.
Philadelphia Electric
2301 Market Street
Philadelphia, PA 19101

Kukita, Y.
Japan Atomic Research Institute
Tokai-mura
Naka-gun, Ibaraki-ken 319-11
Japan

Kupperman, D.S.
Argonne National Laboratory
Materials & Components, Bldg. 212
9700 S. Cass Avenue
Argonne, IL 60439

Kurtz, R.J.
Battelle, Pacific Northwest Laboratory
P.O. Box 999
Richland, Washington 99352

Kusama, Y.
Japan Atomic Energy Research Institute
1233 Watanuki-machi
Takasaki, gunma-ken 370-12
Japan

Kussmaul, K.
Staatliche Materialprufungsanstalt (MPA)
Univ. of Stuttgart
Pfaffenwaldring 32
D-7000 Stuttgart 80
Federal Republic of Germany

Laats, T.
EG&G Idaho
P.O. Box 1625
Idaho Falls, Idaho 83415

Lampe, D.A.
Utility Resource Associates
1700 Rockville Pike
Suite 400
Rockville, Maryland 20852

Lang, P.M.
Department of Energy
Washington, D. C. 20545

Larragoite, L.S.
Baltimore Gas & Electric Company
P.O. Box 1535
Lusby, Maryland 20657

Lee, H.C.
University of Maryland
College Park, Maryland 20742

Lee, N.E.
Combustion Engineering
1000 Prospect Hill Road
Windsor, CT 06095

Leung, R.K.
Ontario Hydro, HII
700 University Avenue
Toronto, Ontario M5G 1X6
Canada

Lidbury, D.P.
United Kingdom Atomic Energy Authority
Warrington, Cheshire WA3 6AT
United Kingdom

Liesch, K.J.
Gesellschaft fur Reaktorsicherheit
Forschungsgelande
8046 Garching
West Germany

Lin, E.
Taiwan Power Company
242, Roosevelt Road, Sec. 3
Taipei, Taiwan
Federal Republic of China

Lincoln, F.W.
Westinghouse-Bettis
P.O. Box 79
West Mifflin, PA 15642

Loewenstein, W.B.
Electric Power Research Institute
3412 Hillview Avenue
Palo Alto, California 94303

Loss, F.J.
Materials Engineering Associates
9700-B Martin Luther King, Jr., Highway
Lanham, Maryland 20706

Lowe, A.L.
Babcock & Wilcox
P.O. Box 10935
Lynchburg, Virginia 24506-0935

Lubnow, T.
MPR Associates, Inc.
1050 Connecticut Avenue, N.W.
Washington, D. C. 20555

MacDonald, P.E.
EG&G Idaho, Inc.
P.O. Box 1625
Idaho Falls, Idaho 83415

Maeda, T.
Japan Nuclear Power Engineering Test Center
Mita Kokusai Bldg.
Mita 1-4-28, Minato-ku
Tokyo 108, Japan

Majorana, G.
Ansaldo S.P.A.
Via Dei Pescatori 35
Genova  16129
Italy

Makoto, N.
Japan NUS
7-1 Nishi-Shinzuku 2 chome
Shinozuku, Tokyo, Japan

Malcher, L.
Kernforschingszentrum
Postfach 3640 D 7500 Karlsruhe
West Germany

Malherbe, J.
Commissariat A L'Energie Atomique
DEMT-Centre d'Etudes Nucleaires de SACLAY
91191 GIF SUR YVETTE CEDEX
France

Malinauskas, A.M.
Oak Ridge National Laboratory
P.O. Box X
Building 4500S, A174
Oak Ridge, Tennessee  37831

Mandl, R
KWU
Hammerbacherstr. 12
Erlangen, 852
Federal Republic of Germany

Marschall, C.W.
Battelle Northwest Laboratory
505 King Avenue
Columbus, Ohio  43201

Marsili, P.
ENEA
Via Vitaliano Brancati 48
Roma
00144  Italy

Mavko, B.
Jozef Stefan Institute/Yugoslavia
Ljubljana, Yugoslavia

McCabe, D.E.
Materials Engineering Associates
9700B Martin Luther King, Jr., Highway
Lanham, Maryland  20706-1837

McCardell, R.K.
EG&G Idaho
Rt. #4 Box 4221
Rigby, Idaho  83442

McGoff, D.J.
U.S. Department of Energy
NE-40
Washington, D. C.  20545

McIntyre, B.A.
Westinghouse Electric Corporation
Box 355, Monroeville Energy Center
Mail Stop 4-11
Pittsburgh, PA  15230

McIntyre, M.
Rolls Royce & Associates Limited
P.O. Box No. 31
Derby DE28BJ
United Kingdom

McMahon, P.M.
Bechtel
Shady Grove road
Gaithersburg, Maryland  20877

McPherson, G.D.
U.S. Department of Energy
Office of Reactor Deployment
Washington, D. C.  20545

Medich, C.
SIET
Via Nino Bixio 27
Piacenza, Italy  29100

Medina, M.
CNSNS
Insurgentes Sur 1806
01030 Mexico

Megahed, M.M.
INEL
488 D Street, #24
Idaho Falls, Idaho  83402

Meincke, J.A.
Consumers Power Company
1945 W. Parnall Road
Room P24-416
Jackson, Michigan  49201

Mercier, O.M.
EIR
Wurenlingen, 5305
Switzerland

Merkle, J.G.
Oak Ridge National Laboratory
P.O. Box Y
Oak Ridge, TN  37830

Mew, I.D.
New York Power Authority
123 Main Street
White Plains, New York  10601

Meyer, L.C.
EG&G Idaho, Inc.
P.O. Box 1625
Idaho Falls, Idaho  83415

Meyzaud, Y.
Framatome
Tour Fiat Cedex 16
Paris-La Defense  92084
France

Milella, P.P.
ENEA
Via V. Brancati 48
Roma, 00144
Italy

Miller, C.D.
CBI Industries
1501 N. Division St.
Plainfield, IL  60544

Miller, C.S.
EG&G Idaho, Inc.
P.O. Box 1625
Idaho Falls, Idaho  83415

Modro, S.M.
Austrian Research Center Seibersdorf
c/o EG&G Idaho, Inc.
P.O. Box 1625
Idaho Falls, Idaho  83415

Mohr, C.L.
Mohr and Associates
1440 Agnes
Richland, WA  99352

Moore, J.G.
United Kingdom Atomic Energy Authority
Wigshaw Lane
Culchetch, Warrington, Cheshire
WA3 4NE United Kingdom

Motley, F.E.
Los Alamos National Laboratory
P.O. Box 1663
Los Alamos, New Mexico  87544

Mueller, U.
KfK W. Germany
75 Karlsruhe, Bad Wurt
Federal Republic of Germany

Muhlestein, L.D.
Westinghouse Hanford Co.
P.O. Box 1970
Richland, Washington  99352

Muramoto, T.
Chubu Electric Power
900 17th Street, N.W.
Suite 714
Washington, D. C.  20006

Murao, Y.
Japan Atomic Energy Research Institute
Tokai-mura, Ibaraki-ken
Japan 319-11

Murase, M.
Hitachi Limited
1168 Moriyama-cho
Hitachi-shi, Iibaraki
316, Japan

Murata, K.K.
Sandia National Laboratory
P.O. Box 5800
Albuquerque, New Mexico  87185

Murphy, G.A.
Oak Ridge National Laboratory
P.O. Box Y
9201-3 MS-5
Oak Ridge, TN  37830

Murphy, K.G.
U. S. Nuclear Regulatory Commission
877 LLlewelyn Road
Berwyn, PA  19312

Murray, R.C.
Lawrence Livermore National Laboratory
P.O. Box 808, L-197
Livermore, California  94550

Naff, S.A.
EG&G Idaho, Inc.
Kraftwerk Union-R15
Hammerbacherstr. 12-14, Postfach 3220
8520 Erlangen
Federal Republic of Germany

Nair, P.K.
Southwest Research Institute
6220 Culebra Street
San Antonio, Texas  78250

Kakagawa, S.
Kansai Electric Power Co., Inc.
1100 17th Street, N.W
Suite 500
Washington, D. C.  20036

Nakajima, H.
Japan Atomic Energy Research Institute
Tokai-mura, Ibaraki-ken
319-11, Japan

Nakamura, T.
Japan Atomic Research Institute (ORNL)
c/o Chemical Tech. Div., ORNL
P.O. Box X
Oak Ridge, TN  37831

Nanstad, R.K.
Oak Ridge National Laboratory
P.O. Box X
Oak Ridge, Tennessee  37830

Naus, D.J.
Oak Ridge National Laboratory
P.O. Box Y
Oak Ridge, Tennessee 37831

Neti, S.
Lehigh University
Mechanical Engineering
Bethlehem, PA 18015

Niemczyk, S.J.
Cull Engineering
1545 18th Street, N.W. #112
Washington, D. C. 20036

Nithianandan, C.K.
Babcock & Wilcox
3315 Old Forest Road
Lynchburg, VA 24506

Niyogi, K.K.
United Engineers & Construction, Inc.
30 South 17th Street
Philadelphia, PA 19101

Nomura, T.
Hitachi Works of Hitachi, Ltd.
1-1 Saiwai-Cho, 3-Chome
Hitachi-Shi, Ibaraki-Ken
Japan

North, P.
EG&G Idaho, Inc.
P.O. Box 1625
1580 Sawtelle Street
Idaho Falls, Idaho 93415

Nourbakhsh, H.P.
Brookhaven National Laboratory
Upton, New York 11973

Nuhm, A.P.
Technicatome (Groupe CEA)
Centre d' Etudes Nucleaires Cadarache
St. Paul-Lez-Durance 13115
France

O'Kula, K.R.
Savannah River Laboratory
773-41A
Aiken, South Carolina 29808

Ohki, A.
Hitachi Ltd.
3-1-1 Saiwai-Cho
Hitachi, Ibaragi
317, Japan

Ohno, T.
Japan Nuclear Power Engineering Test Center
Mita-Kokusai Bldg.
Mita 1-4-28, Minato-ku
Tokyo 108, Japan

Olson, R.C.
Baltimore Gas & Electric Co.
CCNPP-NEF-DES
Lusby, Maryland 20657

Omoto, A.
The Tokyo Electric Power
1901 L Street, N.W.
Suite 720
Washington, D. C. 20036

Onesto, A.T.
ETEC
P.O. Box 1449
Canoga Park, CA 91304

Osakabe, M.
Japan Atomic Research Institute
Tokai-mura
Naka-gun, Ibaraki-ken 319-11
Japan

Pajot, J.J.
General Electric Company/KAPL
P.O. Box 1072
Schenectady, New York 12301-1072

Palazzi, G.
ENEA
ENEA C.R.E Casaccia-S.P. Anguillarese Km. 1300
Roma, Italy 00060

Pan, J.
University of Michigan
Mechanical Engineering & Applied Mechanics
Ann Arbor, MI 48109

Pardoen, G.C.
University of California
516 Engineering, UCI
Irvine, CA 92717

Park, C.K.
Brookhaven National Laboratory
Upton, New York 11973

Pasculli, A.
ENEA Disp.
Via V. Brancati No. 48
Rome
00144, Italy

Paul, D.J.
Aptech Engineering Services
795 San Antonio Road
Palo Alto, California 94303

Paul, K.D.
Rheinisch Westfalischer TUV
Steubenstr. 53
4300 Essen 1
Federal Republic of Germany

Pavinich, W.A.
Babcock & Wilcox
P.O. Box 11165
Lynchburg, VA 24506-1165

Pekoske, J.
Northeast Utilities
Berlin, Connecticut 06037

Pellissier-Tanon, A.
FRAMATOME
Tour Fiat Cedex 16
Paris, La Defense
92084, France

Peng, N.
Taiwan Power Company
242, Roosevelt Road, Sec. 3
Taipei, Taiwan
Federal Republic of China

Pereira, K.
Atomic Energy Control Board
P.O. Box 1046, Station "B"
Ottawa, Ontario KIP559
Canada

Pertmer, G.A.
University of Maryland
College Park, Maryland 20742

Philippacopoulos, A.J.
Brookhaven National Laboratory
Bldg. 129
Upton, New York 11973

Piirto, A.S.
Teollisuuden Voimaoy
Industrins Kraft AB
27160 [illegible], Ste 220
Bethesda, Maryland 20814

Pilch, M.
Sandia National Laboratory
12417 Morrow Avenue, N.E.
Albuquerque, New Mexico 87112

Podowski, M.Z.
Rensselaer Polytechnic Institute
Tibbits Avenue
Troy, New York 12180-3590

Pointer, W.
GRS
80 Forschungsgelande
Garching 8046
Federal Republic of Germany

Posakony, G.J.
Battelle, Pacific Northwest Laboratory
P.O. Box 999
Richland, Washington 99352

Prassinos, P.G.
Lawrence Livermore National Laboratory
P.O. Box 808, L-196
Livermore, California 94550

Prelewicz, D.A.
ENSA, Inc.
15825 Shady Grove Road
Suite 170
Rockville, Maryland 20850

Prine, D.W.
GARD Div. Chamberlain
7449 N. Natchez
Niles, ID 60648

Pugh, C.E.
Oak Ridge National Laboratory
P.O. Box Y
Oak Ridge, Tennessee 37831

Rahn, F.
Electric Power Research Institute
3412 Hillview Avenue
Palo Alto, CA 94303

Redden, E.F.
U.S. Department of Energy
19901 Germantown Road, DP-133.1
Germantown, Maryland 20545

Renner, H.
NUS Corporation
910 Clopper Road
Gaithersburg, Maryland 20878

Reponen, H.
U. S. Nuclear Regulatory Commission
Mail Stop 212
Bethesda, Maryland 20815

Reynen, J.
CEC
2100 M St., N.W.
Washington, D. C. 20037

Rib, L.N.
LNR Associates
8605 Grimsby Court
Potomac, MD 20854

Richter, K.
MPA Stuttgart
Plaftenweldring 32
Stuttgart
Federal Republic of Germany

Rinckel, M.A.
Babcock & Wilcox
E 3315 Old Forest Road
Lynchburg, VA 24503

Romano, A.J.
Brookhaven National Laboratory
Building 197C
Upton, New York 11973

Ross, C.P.
DuPont
10024-203 Stedwick Road
Gaithersburg, Maryland 20879

Rosse, F.
United Engineers International
30 South 17 St.
Philadelphia, PA 19101

Rupprecht, S.D.
Westinghouse
P.O. Box 355
Pitttsburgh, PA 15146

Saffell, B.
Battelle Northwest Laboratory
505 King Avenue
Columbus, Ohio 43201

Saluja, J.K.
Viking Systems International
121 N. Highland Avenue
Pittsburgh, Pennnsylvania 15206

Salyards, L.E.
Baltimore Gas & Electric Company
P.O. Box 1535
Lusby, Maryland 20657

Samanta, P.K.
Brookhaven National Laboratory
Building 130
Upton, New York 11973

Sandervag, O.S.
Studsvik Energiteknik AB
S-61182 Nykoping
Sweden

Saponaro, G.
ENEA
Via Vitaliano Brancati, 48
00144 Roma
Italy

Savy, J.
Lawrence Livermore National Laboratory
Livermore, CA 94550

Scarborough, J.C.
JCS Limited
6936 Race Horse Lane
Rockville, Maryland 20852

Schack, W.J.
Argonne National Laboratory
9700 S. Cass Avenue
Argonne IL 60519

Schally, P.J.
GRS
Schwertnergasse 1
Koln 5000
Federal Republic of Germany

Schmitt, A.P.
Commissariat Energie Atomique
CEN-FAR-IPSN-BPu6
Fonteway-aux-Roses, France 92265

Schneider, K.
Kraftwerk Union
Hammerbacher Str. 14+16
Erlangen, 852
Federal Republic of Germany

Schultz, M.A.
Penn State University
615 Summersea Road
Mashpee, MA 02649

Schwartz, C.W.
University of Maryland
College Park, Maryland 20742

Scott de Martinville, E.F.
Cea/IPSN/DERS/SEAREL
CEN/CADARACHE - BPI
St. Pal lez Durance 13108
France

Seals, J.C.
Babcock & Wilcox
1701 Danbury Drive
Lynchburg, VA 24502

Severud, L.K.
Westinghouse Hanford Company
P.O. Box 1970
Richland, Washington, D. C. 99352

Shah, N.H.
Babcock & Wilcox
P.O. Box 1260
Lynchburg, VA 24502

Shaner, B.J.
Westinghouse-Bettis
P.O. Box 79
West Mifflin, PA 15122

Shannon, R.H.
Consultant
P.O. Box 2264
Rockville, Maryland 20852

Sharma, R.S.
American Electric Power
One Riverside Plaza
Columbus, Ohio 43215

Sharp, D.A.
Savannah River Laboratory
Aiken, South Carolina 29808

Shimeck, D.D.
Westinghouse Electric Corporation
Box 355, Monroeville Energy Center
Mail Stop 4-11
Pittsburgh, PA 15230

Shiralkar, B.S.
General Electric Company
175 Curtner Avenue, M/C 186
San Jose, California 95125

Silver, E.G.
Oak Ridge National Laboratory
Building 9201-3, MS-5, P.O. Box Y
Oak Ridge, Tennessee 37831

Simms, N.T.
Duke Power Company
P.O. Box 33189
Charlotte, North Carolina 28242

Slaughter, G.M.
Oak Ridge National Laboratory
P.O. Box X
Building 4500S
Oak Ridge, Tennessee 37831-6152

Smith, D.L.
Wyle Laboratories
1841 Hillside Avenue
Norco, California 91760

Snoek, C.W.
Chalk River Nuclear Laboratory
Chalk River, Ontario KOJ1JO
Canada

Snyder, A.W.
Sandia National Laboratory
Org. 6400
P.O. Box 5800
Albuquerque, New Mexico 87111

So, C.
Atomic Energy of Canada Ltd.
Whiteshell Nuclear Res. Establishment
Pinawa, Manitoba, ROE1LO
Canada

Soda, K.
Japan Atomic Research Institute
Tokai-mura
Naka-gun, Ibaraki-ken 319-11
Japan

Solberg, D.E.
U. S. Nuclear Regulatory Commission
Washington, D. C. 20555

Sorenson, R.J.
Battelle, Pacific Northwest Laboratory
P.O. Box 999
Richland, Washington 99352

Speelman, J.E.
ECN
Westerduinweg
Petter, NH 1755 LE
Netherlands

Spindler, B.
CEA
Ceng-Seth-85X-38041 Grenoble Cedex
Grenoble, France

Squarer, D.
Westinghouse Electric Corporation
P.O. Box 355
Expo Mart 200W
Pittsburgh, Pennsylvania 15230-0355

Srinivasan, M.G.
Argonne National Laboratory
9700 S. Cass, Bldg. 335
Argonne, IL 60439

St. John, K.
Yankee Atomic Electric Company
1671 Worcester Road
Framingham, Massachusetts 01701

Stadtke, H.
Euratom, JRC-ISPRA
ISPRA
I-21027, Italy

Stanford, R.E.
Consultant
10 Plantation Court
Rockville, MD 20852

Steele, R.
EG&G Idaho, Inc.
P.O. Box 1625
Mail Stop TSB
Idaho Falls, Idaho 83415

Steinhilber, H.
LBF
Bartningstr. 27
Darmstadt
6100 West Germany

Stepp, J.C.
Electric Power Research Institute
3412 Hillview Avenue
Palo Alto, CA 94303

Stratton, W.R.
Stratton & Associates
2 Acoma Lane
Los Alamos, New Mexico 87544

Stubbe, E.J.
Tractebel
31 Rue De La Science
1040 Brussels, Belgium

Subudhi, M.
Brookhaven National Laboratory
Building 130
Upton, New York 11973

Sundaram, R.K.
Yankee Atomic Electric Company
1671 Worcester Road
Framingham, MA 01701

Suwa, H.
Japan NUS Company, Ltd.
7-1, Nishi-Shinjuki 2 Chome, Shinjuki-ku
Tokyo 163
Japan

Swan, D.I.
Rolls Royce & Associates Ltd.
P.O. Box 31
Derby, United Kingdom DE28BJ

Tabuchi, M.
Mitsubishi Atomic Power Industries
4-1, shibakouen 2-Chome, Minato-Ku
Tokyo 105
Japan

Tang, H.T.
Electric Power Research Institute
3412 Hillview Avenue
Palo Alto, California 94303

Tang, Y.K.
Electric Power Research Institute
3412 Hillview Avenue
Palo Alto, California 94303

Tasaka, K.
Japan Atomic Research Institute
Tokai-mura
Naka-gun, Ibaraki-ken 319-11
Japan

Taylor, J.H.
Brookhaven National Laboratory
Building 130
Upton, New York 11973

Tazawa, K.
Japan NUS Company, Ltd.
7-1, Nishi-Shinjuki 2 Chome, Shinjuki-ku
Tokyo 163
Japan

Thomas, E.W.
Bechtel Power
15740 Shady Grove Road
Gaithersburg, Maryland 20877

Thomas, G.R.
Electric Power Research Institute
3412 Hillview Avenue
Palo Alto, California 94303

Tice, D.R.
United Kingdom Atomic Energy Authority
Salwick
Preston, Lancashire PR40RR
United Kingdom

Tokuine, T.
Japan Nuclear Power Engineering Test Center
Mita-Kokusai Bldg.
Mita 1-4-28, Minato-ku
Tokyo 108, Japan

Tolley, B.J.
European Commission
Rue De La Loi 200
Brussel, Belgium 1049

Tolman, B.
EG&G Idaho, Inc.
P.O. Box 1625
Idaho Falls, Idaho 83401

Tong, L.
TAI
9733 Lookout Place
Gaithersburg, Maryland 20879

Trammell, H.E.
Oak Ridge National Laboratory
Martin Marietta Energy Systems, Inc.
P.O. Box Y
Oak Ridge, TN 37831

Trolle, M.
Swedish Nuclear Power Inspectorate
Box 27106
10252 Stockholm, Sweden

Tsuchiya, A.
Toyo Engineering Corporation
2-17-7 Higashinakahara
Hiratsuka, Kanagawa
254 Japan

Tsuge, A.
Mitsubishi Heavy Industries, Ltd.
2-1-1 Shinhama, Arai-cho
Takasago, Hyogo Pref. 676
Japan

Tsunoyama, S.
Nippon Atomic Industry Company
4-1, Ukishima-cho, Kawasaki-ku
Kawasaki, Kanagawa
210 Japan

Tuomisto, H.J.
Imatran Voima Oy
P.O. Box 138
00101 Helsinki
Finland

Turland, B.D.
UKAEA Culham Laboratory
Culham Lab. Abingdon
Oxon 3DB, England

Tuzla, K.
Lehigh University
Chemical Eng. Dept.
Whitaker Lab. #5
Bethlehem, PA 18015

Valentin, R.A.
Argonne National Laboratory
9700 S. Cass Avenue
Argonne, Illinois 60439

Valtonen, K
Finnish Centre for Radiation and Nucl. Safety
P.O. Box 268
SF-00101 Helsinki
Finland

van Deusen, D.E.
American Electric Power Service Corporation
1 Riverside Plaza
Columbus, Ohio 43215

Vasudevan, N.
Babcock & Wilcox
Old Forest Road
Lynchburg, VA 24502

Vayssier, G.L.
Ministry of Social Affairs and Employment
P.O. Box 69
2270 Ma Voorburg
The Netherlands

Vesely, W.E.
Science Applications International Corporation
Suite 245
2929 Kenny Road
Columbus, Ohio 43221

Villadoniga, J.I.
Consejo De Seguridad Nuclear
C/Sor Angela De La Cruz, 3
Madrid 28020
Spain

von Riesemann, W.A.
Sandia National Laboratory
P.O. Box 5800
Albuquerque, New Mexico 87185

Wagner, K.C.
EG&G Idaho, Inc.
P.O. Box 1625
Idaho Falls, Idaho 83415

Wahba, A.B.
GRS-MBH
8046 Garching
Federal Republic of Germany

Wahba, M.
Ontario Hydro
700 University Avenue
Toronto, Ontario M5G 1X6
Canada

Washington, K.E.
Sandia National Laboratory
P.O. Box 5800
Albuquerque, New Mexico 87185

Watanabe, T.
Japan Atomic Energy Research Institute
Tokai-mura, Ibaraki-ken 319-11
Japan

Weaver, W.L.
EG&G Idaho, Inc.
P.O. Box 1625
Idaho Falls, Idaho 83415

Webb, S.W.
Sandia National Laboratory
P.O. Box 5800
Albuquerque, New Mexico 87185

Weber, C.F.
Oak Ridge National Laboratory
P.O. Box X
Building 6002-B
Oak Ridge, Tennessee 37831-6357

Weerakkody, S.D.
Penn State University
Nuclear Engineering
231 Sackett
University Park, PA 16802

Weiss, A.J.
Brookhaven National Laboratory
Building 197C
Upton, New York 11973

Weiss, P.A.
Kraftwerk Union AG, R 515
Hammerbacherstr. 12+14
Erlangen, 8520
Federal Republic of Germany

Wells, J.E.
Lawrence Livermore National Laboratory
P.O. Box 808, L-196
Livermore, CA 94550

Wessel, E.T.
Consultant
3570 Meadowgate Drive
Murrysville, Pennsylvania 15668

Westphal, H.
Gesellschaft fur Reaktorsicherheit
Schwertnergasse
Cologne, NRW 5000
Federal Republic of Germany

Wheatley, C.J.
UKAEA Attache, Sandia National Laboratory
Division 6425
P.O. Box 5800
Albuquerque, New Mexico 87185

White, J.E.
Oak Ridge National Laboratory
P.O. Box X
Oak Ridge, Tennessee 37831

White, J.R.
J.R. White Consulting
2100 Belmont Avenue
Idaho Falls, Idaho 83401

Whitesel, R.N.
GPU Nuclear Corporation
1 Upper Pond Road
Parsippany, New Jersey 07054

Whitkop, P.G.
E.I. duPont de Nemours and Co.
Savannah River Laboratory
Building 773-41A
Aiken, SC 29808

Wilkowski, G.M.
Battelle Northwest Laboratory
505 King Avenue
Columbus, Ohio 43201

Williams, J.F.
Baltimore Gas & Electric
4131 Birch Drive
Huntingtown, Maryland 20639

Williams, K.A.
Science Applications International Corporation
2109 Air Park Road, SE
Albuquerque, New Mexico 87106

Wilson, G.E.
EG&G Idaho, Inc.
P.O. Box 1625
Idaho Falls, Idaho 83415

Winegardner, K.
Battelle, Pacific Northwest Laboratory
P.O. Box 999
Richlard, Washington, D. C. 99352

Winkler, F.
KWU/FBG
Ringstrasse 1g
Spardorf, Bayerly
D-8521 West Germany

Winslow, S.G.
Oak Ridge National Laboratory
Martin Marietta Energy Systems, Inc.
P.O. Box X
Oak Ridge, TN 37831

Witt, F.J.
Westinghouse
P.O. Box 355
Pittsburgh, PA 15146

Wolf, J.R.
EG&G Idaho
P.O. Box 1625
Idaho Falls, Idaho 83415

Wolf, L.
PHDR/KfK
Karlsruhe, 7500
Federal Republic of Germany

Wolfert, K.F.
Gesellschaft fur Reaktorsicherheit
Forschungsgelande
8046 Garching
West Germany

Worledge, D.H.
Electric Power Research Institute
784 Finchwood Way
San Jose, CA 95720

Wright, A.L.
Oak Ridge National Laboratory
P.O. Box X, Bldg. 4500N
Oak Ridge, Tennessee 37831

Wu, P.
U. S. Nuclear Regulatory Commission
Washington, D. C. 20555

Wulff, W.
Brookhaven National Laboratory
Buildng 475B
Upton, New York 11973

Yang, C-Y.
INER
P.O. Box 3
Lungtan 32500, Taiwan
Republic of China

Yang, Y.
Atomic Energy Council
67, Lane 144
Keelung road, Section 4
Taipei, Taiwan, 107
Rep. of China

Yokoyama, T.
Babcock & Wilcox
2400-I Weeping Willow Drive
Lynchburg, VA 24501

Yonomoto, T.
Japan Atomic Research Institute
Tokai-mura
Naka-gun, Ibaraki-ken 319-11
Japan

Yoon, K.K.
Babcock & Wilcox
P.O. Box 10935
Lynchburg, VA 24506

Young, R.
UKAEA/SRD
Wigshaw Lane
Culcheth, Cheshire
WA3 4NE, United Kingdom

Zdarek, J.
Czechoslovak Embassy
3900 Linnean Avenue, N.W.
Washington, D. C. 20008

Zhou, R.
Institute of Atomic Energy of PRC
P.O. Box 275 (59)
Beijing
People's Republic of China

# PROCEEDINGS OF THE
# FOURTEENTH WATER REACTOR SAFETY INFORMATION MEETING

October 27-31, 1986

## TABLE OF CONTENTS - VOLUME 3

Page

ABSTRACT . . . . . . . . . . . . . . . . . . . . . . . . . . . . . . . . iii
GENERAL INDEX . . . . . . . . . . . . . . . . . . . . . . . . . . . . . . v
REGISTERED ATTENDEES . . . . . . . . . . . . . . . . . . . . . . . . . . vii

### EQUIPMENT QUALIFICATION
Chairperson: G. H. Weidenhamer (NRC)

Functionality and Leak Integrity of Containment Penetration Systems Subjected to Design Basis Dynamic Loads . . . . . . . . . . . . . . . . . . 1
R. Steele, Jr., R. C. Hill and J. A. Close (INEL)

Parameters Important to Reactor Coolant Pump Seal Stability During Station Blackout . . . . . . . . . . . . . . . . . . . . . . . . . . . 19
R. C. Hill (INEL) and D. B. Rhodes (AECL)

Dynamic Load Effects on Gate Valve Operability . . . . . . . . . . . . . . 31
R. Steele, Jr., P. E. MacDonald and J. G. Arendts (INEL)

Progress on Qualification Testing Methodology Study of Electric Cables . . . . . . . . . . . . . . . . . . . . . . . . . . . . . . . . 43
Y. Kusama et al. (JAERI)

General Technical Requirements for Special Valves Used in Nuclear Power Plants . . . . . . . . . . . . . . . . . . . . . . . . . . 65
J. Zdarek and F. Jukl (SRI, Czechoslovakia)

Effectiveness and Safety Aspects of Selected Decontamination Methods for LWRs . . . . . . . . . . . . . . . . . . . . . . . . . . . . 77
S. W. Duce and F. B. Simpson (INEL)

### MECHANICAL AND STRUCTURAL RESEARCH
Chairperson: J. J. Burns (NRC)

Probability of Failure in BWR Reactor Coolant Piping . . . . . . . . . . . 87
G. Holman and C. K. Chou (LLNL)

SSI and Structural Benchmarks . . . . . . . . . . . . . . . . . . . . . . 107
A. J. Philippacopoulos, C. A. Miller and C. J. Costantino (BNL), and H. Graves (NRC)

## MECHANICAL AND STRUCTURAL RESEARCH
(Cont'd)

Page

NRC Valve Performance Test Program -- Check Valve Testing . . . . . . . . . 121
N. M. Jeanmougin (ETEC)

Piping nd Fitting Dynamic Reliability Program . . . . . . . . . . . . . . . 147
D. Guzy (NRC)

6-Inch Diameter Pipe Seismic Fragility Test . . . . . . . . . . . . . . . . 153
W. P. Chen, V. DeVita and A. T. Onesto (ETEC)

Pipe Damping Studies . . . . . . . . . . . . . . . . . . . . . . . . . . . 179
A. G. Ware (INEL)

Nonlinear Piping Damping and Response Predictions . . . . . . . . . . . . . 199
L. K. Severud et al. (HEDL)

Examples of NRC Research Products Used in Regulation. . . . . . . . . . . . 219
N. R. Anderson (NRC)

## SEISMIC RESEARCH
Chairperson: A. Murphy (NRC)

Component Fragility Research Program: Prioritization and Demonstration Testing . . . . . . . . . . . . . . . . . . . . . . . . 229
G. S. Holman and C. K. Chou (LLNL)

Synthesizing Seismic Fragility of Components by Use of Existing Data. . . 255
K. K. Bandyopadhyay and C. H. Hofmayer (BNL)

Seismic Margins Review of Nuclear Power Plants: Program Overview and Status. . . . . . . . . . . . . . . . . . . . . . . . . . . . . 261
R. C. Murray, P. G. Prassinos and G. E. Cummings (LLNL)

Validation of Seismic Soil-Structure Interaction Analysis Methods . . . . 277
C. A. Kot, M. G. Srinivasan and B. J. Hsieh (ANL),
and Y. K. Tang and R. P. Kassawara (EPRI)

HDR Phase II Vibrational Experiments. . . . . . . . . . . . . . . . . . . 295
L. Malcher (KfK) and C. A. Kot (ANL)

The Seismic Category I Structures Program . . . . . . . . . . . . . . . . 313
J. G. Bennett, C. R. Farrar and W. E. Dunwoody (LANL)

## NUCLEAR PLANT AGING
Chairperson: J. Vora (NRC)

Page

Risk Evaluations of Aging Phenomena: The Linear Aging Reliability Model and Its Extensions. . . . . . . . . . . . . . . . . . . . . . . . . 335
W. E. Vesely (SAIC)

An Interim Assessment of Reactor Protection System Aging. . . . . . . . . . 351
P. T. Jacobs (INEL)

Overview of Recent Operating Experience Regarding Plant Aging . . . . . . 369
M. A. Caruso and G. M. Holahan (NRC)

Application of Diagnostics to Determine Motor Operated Valve Operational Readiness . . . . . . . . . . . . . . . . . . . . . . . . . 389
D. M. Eissenberg (ORNL)

The Interactive Effects of Relay and Circuit Breaker Aging in a Safety-Related System . . . . . . . . . . . . . . . . . . . . . . . . . 403
G. J. Toman et al. (FRC) and W. Gunther (BNL)

Nuclear Service Emergency Diesel Generator Aging Research . . . . . . . . . 419
K. R. Hoopingarner, J. W. Vause III and D. A. Dingee (PNL)

# FUNCTIONALITY AND LEAK INTEGRITY OF CONTAINMENT PENETRATION SYSTEMS SUBJECTED TO DESIGN BASIS DYNAMIC LOADS[a]

Robert Steele, Jr., Robert C. Hill, James A. Close
Idaho National Engineering Laboratory
Idaho Falls, Idaho 83415

## ABSTRACT

The results of testing typical U.S. nuclear power plant containment piping penetrations during seismic excitation are presented. Full-sized hardware, including the containment wall penetration, piping, pipe supports, and the isolation valve, were subjected to seismic excitation typical of levels specified in U.S. nuclear power plant designs. The effect of the seismic excitation on valve leakage and operability and the effect on overall system integrity were studied. All hardware performed well and showed no degradation as a result of the seismic loads.

## INTRODUCTION

The containment structure at a nuclear power plant provides the final protective boundary to prevent uncontrolled radioactive releases during normal operation and off-normal or accident situations. Because it performs this important safety function, containment integrity has been the subject of considerable investigation and research. One potential failure that has been identified is leakage through the many piping penetrations. The typical containment penetration system (CPS) includes the actual penetration assembly through the containment wall, the process piping, two isolation valve assemblies, and the associated piping supports.

The Idaho National Engineering Laboratory (INEL) is investigating the behavior of typical CPSs under typical seismic excitation and accident loads. The objectives of the research are to develop a technical basis for assessing the adequacy of nuclear industry seismic qualification standards and, in subsequent research, to determine margins in design bases and severe accident containment loadings. The dynamic qualification of line-mounted mechanical equipment is an area of equipment qualification where the industry standards are still in draft form. As a part of this research program, three full-scale CPS configurations were recently subjected to triaxial simulated seismic loadings, and the response of the systems with respect to leak integrity, valve operability, and overall structural capacity was observed. This paper presents a description of the experiments and the results that were obtained.

---

[a] Work supported by the U.S. Nuclear Regulatory Commission, Office of Nuclear Regulatory Research, under DOE Contract No. DE-AC07-76ID01570.

# EXPERIMENT DESIGN

The basic approach used in this project was to mount typical CPSs in a fixture and dynamically excite the entire assembly at typical operating basis earthquake (OBE) and safe shutdown earthquake (SSE) accelerations. To permit use of a smaller assembly, only the portion of the CPS installed inside the containment was tested; this is readily justified on the basis that the piping inside the containment will see representative accelerations due to amplification by the building and its internal structures. The piping located outside of the containment would have a negligible effect on the building response, and the penetration assembly effectively prevents all loads and moments from being transmitted from one side of the containment wall to the other. Throughout this program, strong emphasis has been placed on maximizing the typicality of hardware and loads and on concentrating on those CPSs that would present the highest risks if they failed.

Three systems, chosen for accident testing based on their importance during severe accident conditions, were subjected to seismic testing. The first system tested was an 8-in. purge and vent CPS containing a butterfly valve assembly. The purge and vent system provides a direct path from the containment to the atmosphere and could allow fission products to escape if it failed during a severe accident.

The second system selected for testing was a 2-in. CPS, typical of the many support systems that penetrate containment. A survey of representative Final Safety Analysis Reports (FSARs) showed that small bore piping penetrations of the 1- to 4-in. size outnumbered larger sizes by a factor of 3 or 4 and accounted for nearly half of the more than 100 containment penetrations. Additionally, the valve-to-pipe weight ratio was considerably higher than for the larger valves and presented a unique feature that is appropriate for investigation. Globe valves are commonly used in these systems; therefore, a globe valve assembly was included in this configuration.

The third CPS chosen was an 8-in. system representing containment spray configurations. The spray system is important to accident mitigation in its heat removal function. Typical of containment spray systems, this configuration included a gate valve assembly.

All valves, purchased supports, and valve operators were typical of those used in the nuclear industry and were manufactured by vendors who have supplied the majority of these components to domestic nuclear power plants.

The 8-in. containment spray system, mounted in the test fixture, is shown in Figure 1. In its overall dimensions, the assembly is about 14 ft wide, 25 ft long, and 8 ft high. The fixture, fabricated from 14-in. square tubing, weighs approximately 23,000 lb. The various components are labeled in Figure 1. The penetration assembly is a Code-certified[a] component obtained from surplus; the piping is Schedule 40 carbon steel; the valve is an ANSI

---

[a] American Society of Mechanical Engineers, Boiler and Pressure Vessel Code.

BEST COPY AVAILABLE

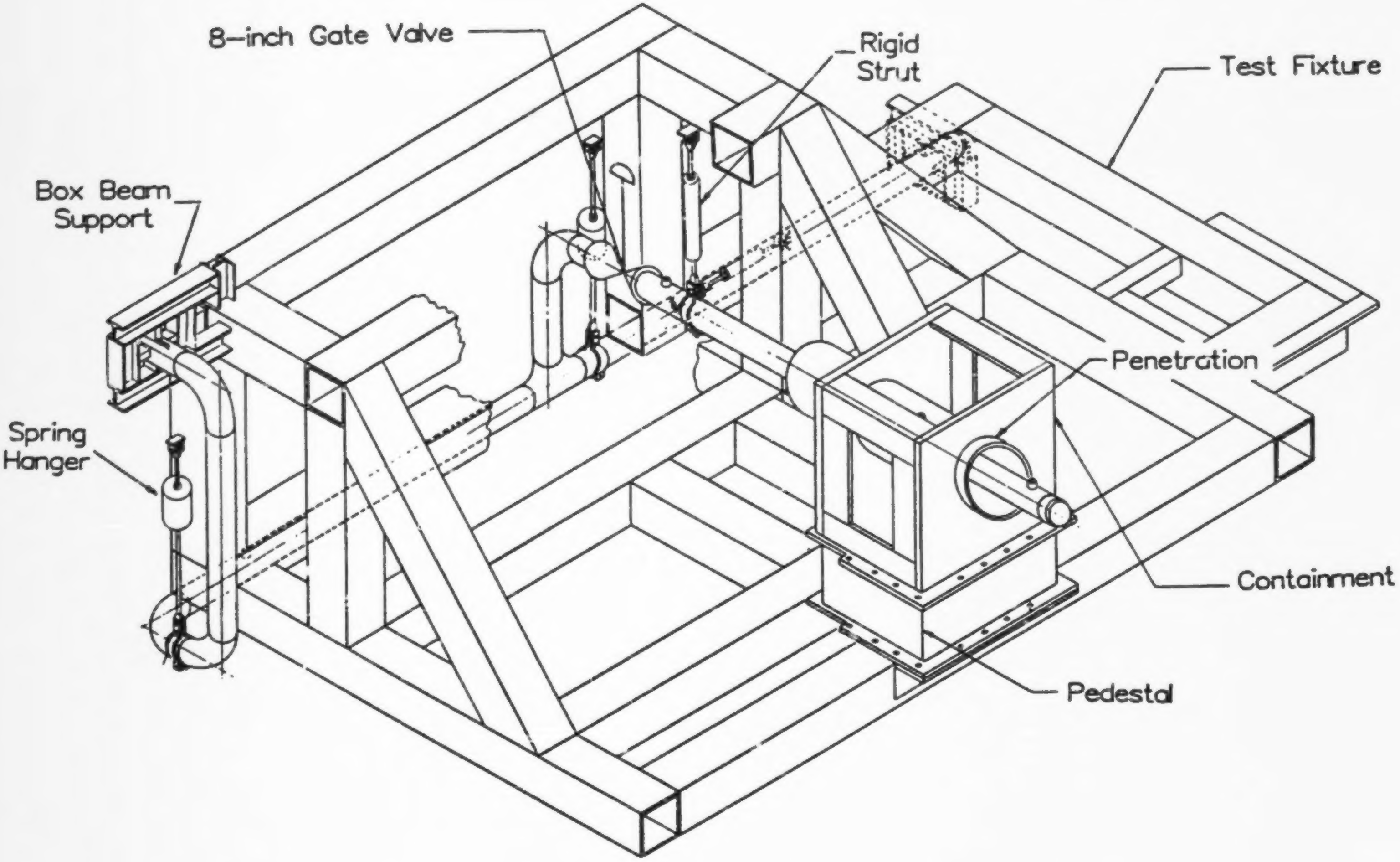
8-inch Gate Valve
Rigid Strut
Test Fixture
Box Beam Support
Penetration
Spring Hanger
Containment
Pedestal

Figure 1. Sketch showing 8-in. piping system with gate valve installed in test fixture.

150-psi-rated gate valve, also obtained from surplus, and was procured to Section III, Class 2, ASME Code; the spring hanger and rigid struts were procured to the Code; and the box beam supports were fabricated with typical gaps and alignment tolerances. Load ratings for the piping supports were typical of similar units installed in domestic nuclear power plants.

The entire assembly was mounted on pneumatic supports and was dynamically excited with hydraulic actuators. Excitation was applied simultaneously and independently on the three principal axes. As in the case when selecting components, emphasis was placed on defining test loads (acceleration response spectra) that were typical of those specified for nuclear power plants. A detailed review of 17 FSARs was performed to determine representative required response spectra at the one-third and two-thirds containment heights. These elevations were chosen since the majority of the purge and vent systems penetrate the containment at about two-thirds of the containment height and most containment spray and typical support systems penetrate at about the one-third containment height. The FSARs that were reviewed covered large dry, ice condenser, Mark I and II, and subatmosphere containment designs. The test response spectra developed for the horizontal and vertical accelerations are shown in Figures 2 and 3. These spectra are considered to be typical, and no attempt was made to envelope all of the spectra studied.

Two basic types of measurements were taken during the dynamic experiment: acceleration, displacement, and strain to determine actual dynamic inputs and responses; and measurements associated with valve behavior, such as leakage, stroke time, and operator current. The piping system was pressurized to permit measurement of leakage or actuator current required to open the valve at various times during the test sequence. In Figure 4, a schematic of the instrumentation installed on the 8-in. systems shows the sensor locations. The sensors used to measure piping system response were located in areas of piping/support interfaces, and the valve accelerations were measured at points that define the deflected mode shapes.

## TEST CONDUCT AND RESULTS

Each of the three systems was separately subjected to the testing sequence using the single test fixture. The testing sequence is summarized in Table 1. Test conditions for each system are given in Table 2. Baseline data included leakage measurements through the valve when pressurized from either side, valve stroke time from open-to-close and close-to-open, and valve actuator current and voltage measurements when both closing and opening. Opening current and voltage were measured both with the system at atmospheric pressure and with the system at pressure (on one side of the valve at a time) for the initial unseating of the valve. No testing was performed with fluid flowing through the systems.

Testing at 0.1 OBE was performed to check out instrumentation, to confirm reasonably repeatable measurements, and to detect any early indications of unexpected system response.

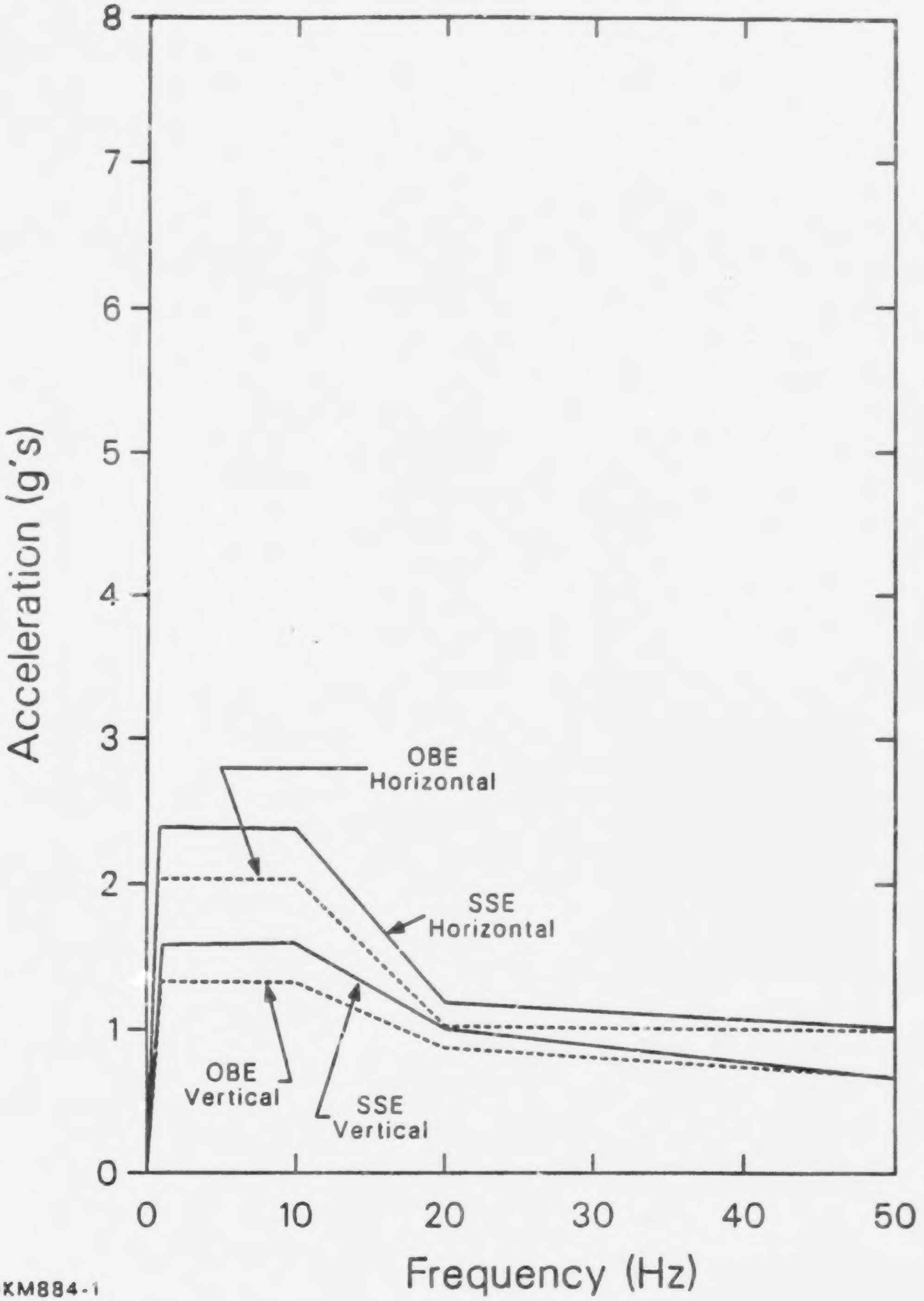

DKM884-1

Figure 2. Specified input acceleration response spectra for 1/3 containment height.

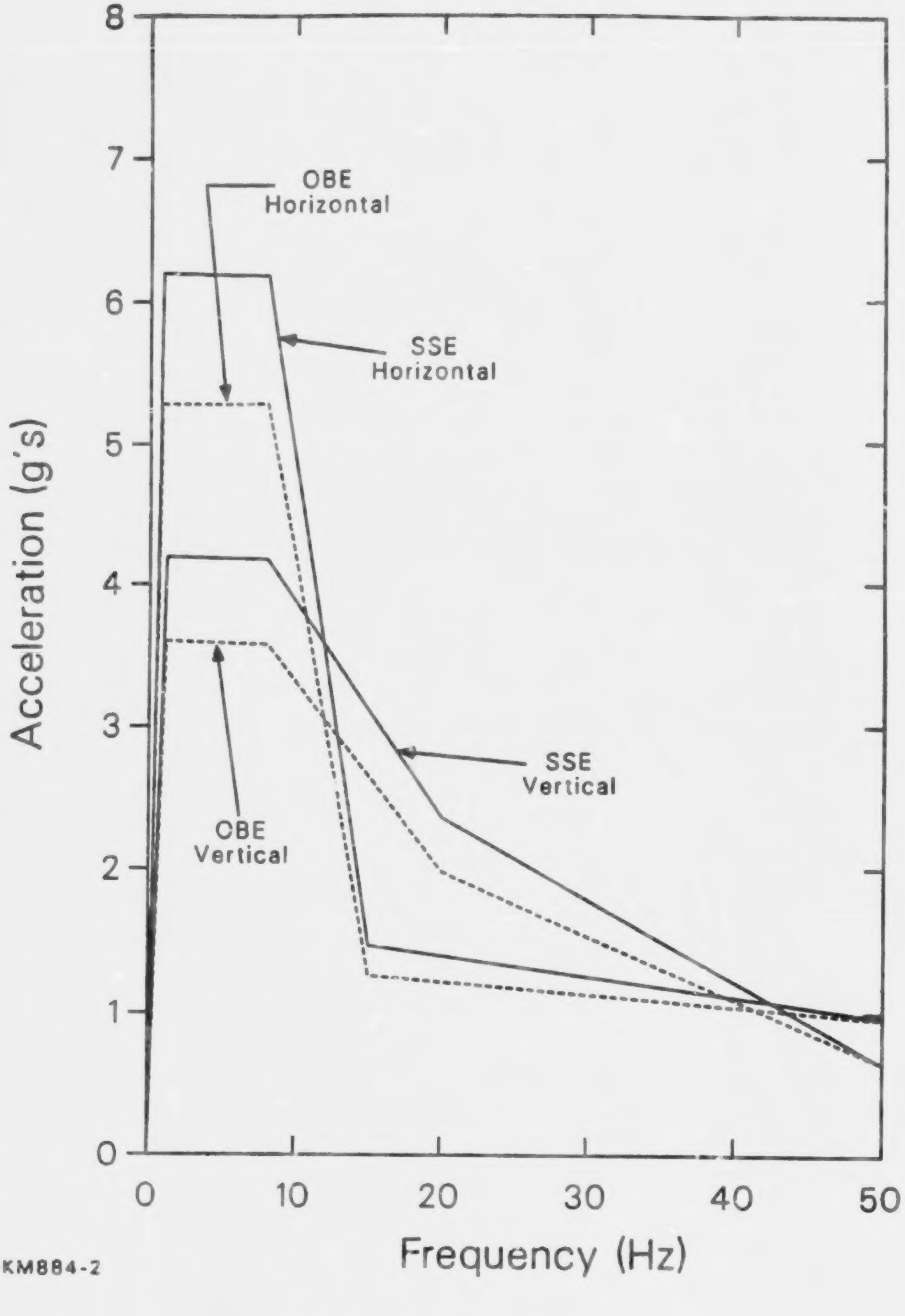

DKM884-2

Figure 3. Specified input acceleration response spectra for 2/3 containment height.

BEST COPY AVAILABLE

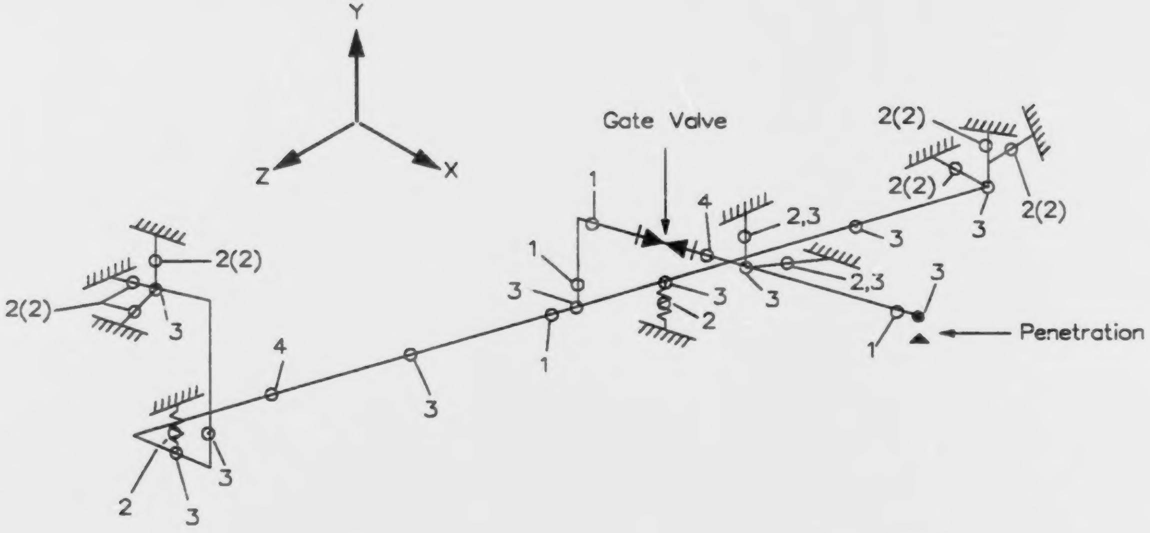
Y
Z
X
Gate Valve
Penetration
1
2(2)
2,3
3
4
2

Key

1- Strain Gages on Pipe (6 channels)
2- Strain Gages on Support (1 channel)
3- Accelerometers (3 channels)
4- Static Pressure (1 channel)

For Each Valve

| | |
|---|---|
| 3 | Accelerometers |
| 1 | Stem Position |
| 6 | Uniaxial Strain |
| 2 | Strain Rosette |

Figure 4. Schematic of piping and instrumentation used for 8-in. system with gate valve.

MGH01546

TABLE 1. SUMMARY OF SEISMIC TESTING SEQUENCE FOR THREE CPSs

| Baseline Measurements and Conditioning | | | | | Seismic Testing | | | |
|---|---|---|---|---|---|---|---|---|
| Pre-Seismic Baseline Measurements | During 0.1 OBE (5 min) | After 0.1 OBE | During 0.1 OBE (5 min) | After 0.1 OBE | During OBE (30 sec) | After OBE | During SSE (30 sec) | After SSE |
| Stroke[a] and seat leakage test | Stroke valve during test period | Visual inspection, stroke[a] and seat leakage test | Seat leakage test | Visual inspection, stroke[a] and seat leakage test | Seat leakage test | Visual inspection, stroke[a] and seat leakage test | Stroke valve during test period | Visual inspection, stroke[a] and seat leakage test |

Note test sequence proceeds from left to right.

Note test sequence proceeds from left to right.

---

a. The stroke test consists of measuring valve operator motor current and the stroke time as the valve moves full stroke (from closed to open and/or vice versa).

TABLE 2. TEST CONDITIONS FOR THREE CPSs

| Valve | Test Pressure (psig) | Test Medium |
|---|---|---|
| 2-in. globe | 150 | Gas |
| 8-in. butterfly | 60 | Gas |
| 8-in. gate | 100 | Water |

Leakage through the valves was the primary performance parameter of interest during the OBE excitation. The system pressure was stabilized at the conditions noted in Table 2. Fluid leaking past the valve seat was contained in the CPS piping and collected directly (in the case of the water used in gate valve testing) or indirectly through water displacement from a graduated cylinder. The valves were not cycled during the OBE excitation.

During the SSE excitation, the valves were cycled to determine the effects of seismic motion on valve actuator current demands.

In all cases, the baseline tests (operating current, stroke time, and leakage) were repeated after each dynamic excitation to detect any changes in leakage or actuator demands.

The specified horizontal input acceleration response spectrum for SSE and a typical measured spectrum, applicable to the purge and vent CPS, are shown in Figure 5. Also shown are response spectra from Diablo Canyon, SONGS 2 and 3, and Zimmer, which were the three highest spectra in the 17 FSARs studied. Consistent with Nuclear Regulatory Commission Regulatory Guide 1.61, 2% critical damping has been applied to these spectra for SSE. The spectra apply to the input to the test rig and simulate containment motion driving the piping system. At low frequencies, the test input acceleration was lower than the specified level. This is considered to be of little significance since the first natural frequency of the piping was measured at about 4 Hz, and no significant amplification of the input acceleration is expected below 2 Hz.

The three plant specific spectra are considered to be representative of the highest levels expected for CPSs. On this basis, the actual excitation applied during the test is expected to envelope more than 90% of U.S. nuclear power plants in the important frequency range of 2 to 33 Hz.

Figure 6 illustrates comparable specified, measured, and plant specific input response spectra for the containment spray and small bore systems. The three plant specific spectra (Summer, Diablo Canyon, and SONGS 2 and 3) were chosen because they were the highest of the spectra identified at this elevation on the containment. As can be seen in this figure, the actual test input again exceeded the specified and highest plant specific accelerations in the frequencies above 2 Hz.

## RESULTS

The results of the valve leakage and operability testing are shown in Figures 7 through 11 and are discussed below.

Leakage through the 2-in. globe valve is shown in Figure 7. The initial leak rate is much higher than would be expected in a typical valve when initially installed or after routine maintenance but is considered representative of a poorly functioning valve that would be identified during plant inspections. The important observation is that seismic excitation did not further increase the leakage. The leakage decreased significantly during testing, but the cause cannot be specifically attributed to the positive effects of vibration, repeated cycling, or both.

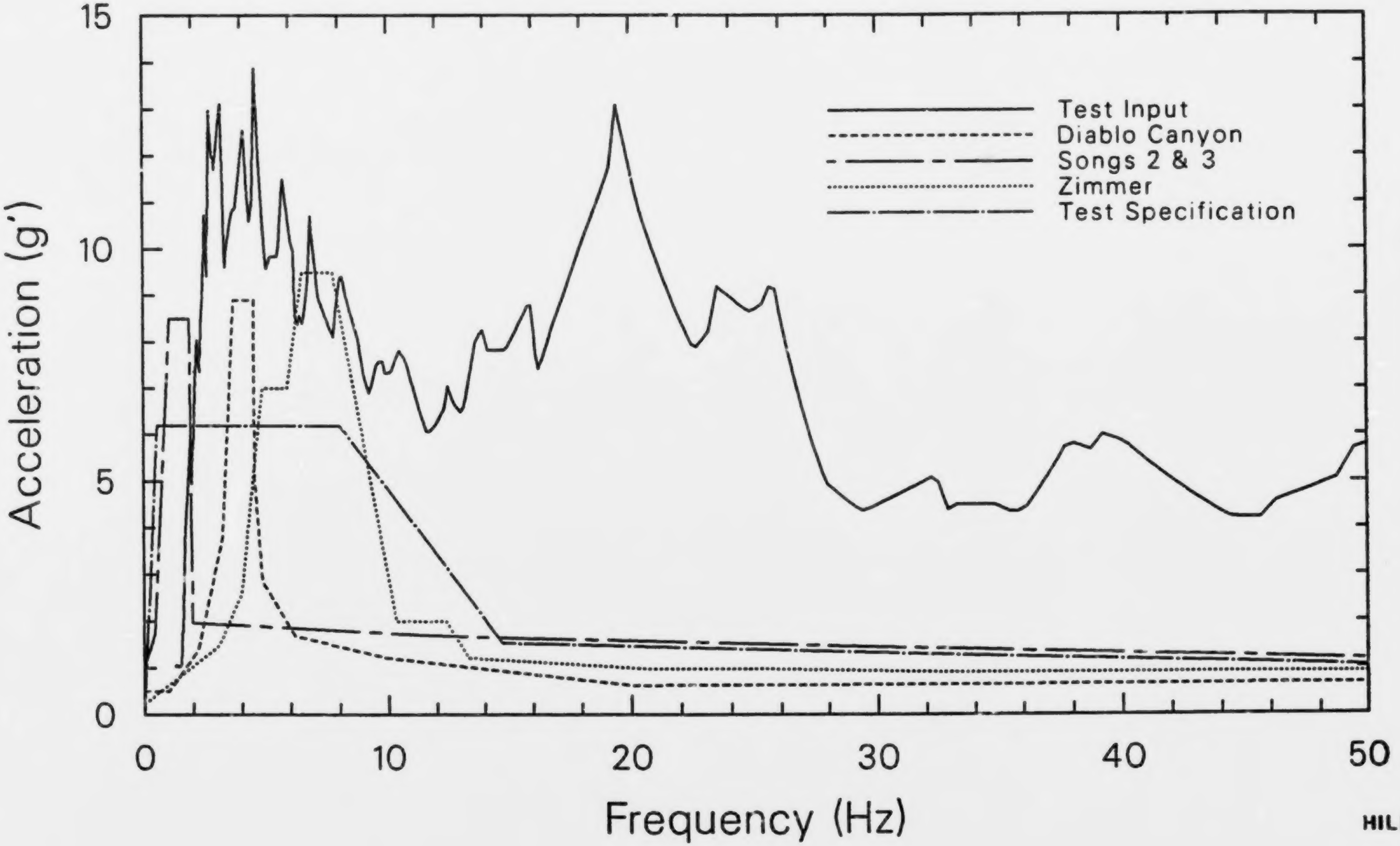

Figure 5. Test response spectrum for 2/3 height exceeded specified input and highest plant specific spectra at frequencies above 2 Hz.

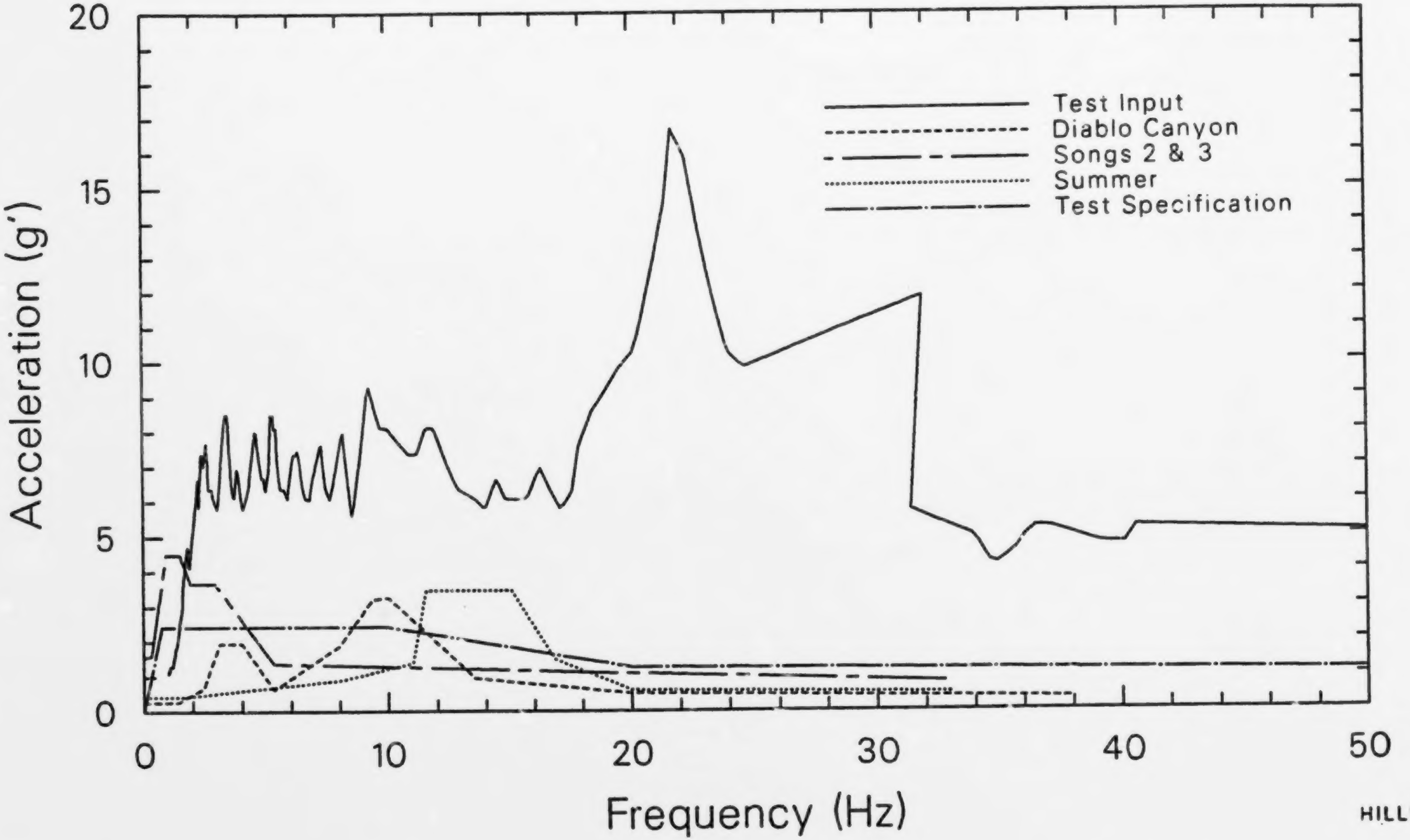

HILL986-2

Figure 6. Test response spectrum for 1/3 height exceeded specified input and highest plant specific spectra at frequencies above 2 Hz.

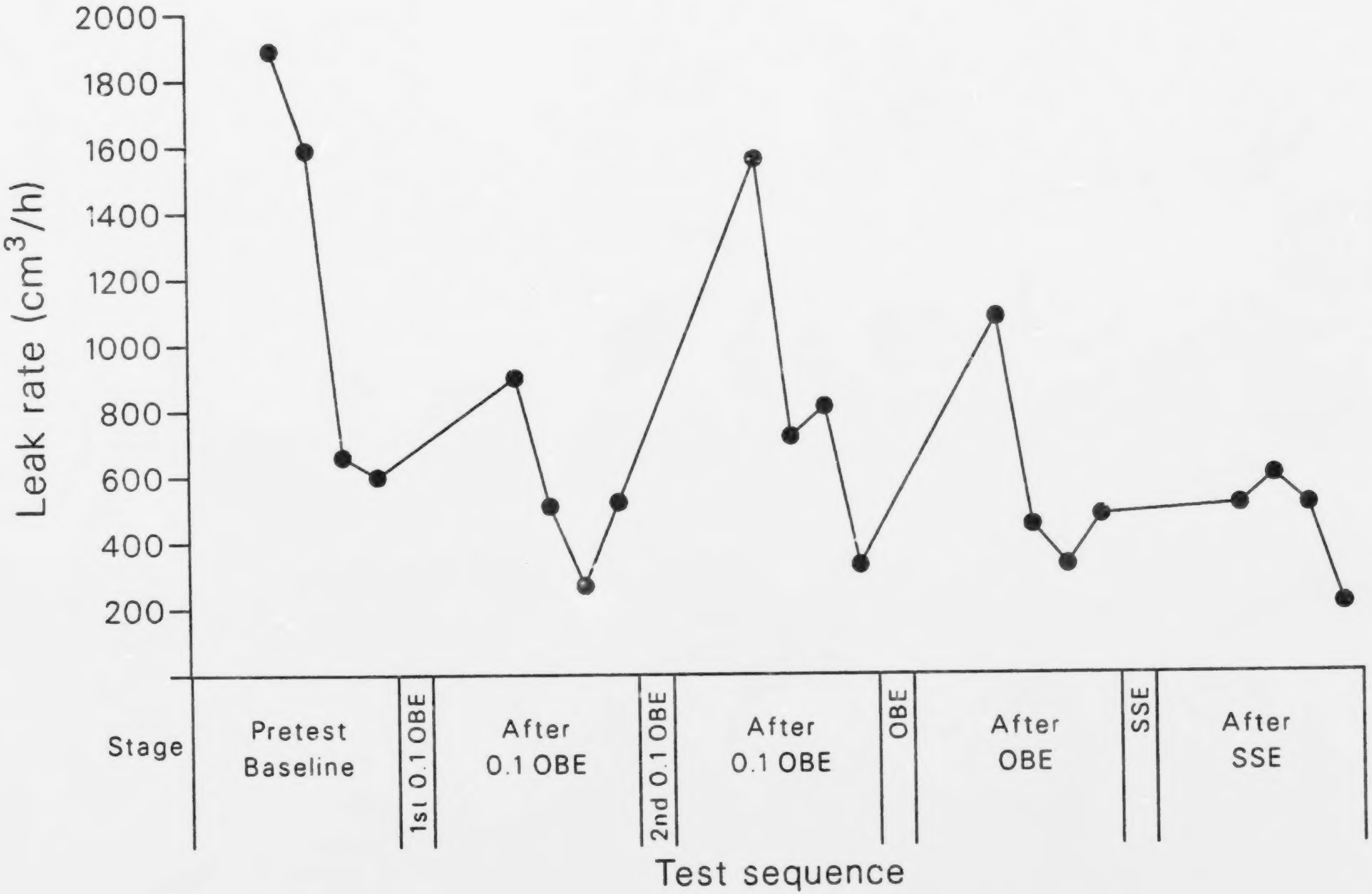

Figure 7. Leak rates through 2-in. globe valve.

Actuator current measurements for the 2-in. globe valve are shown in Figure 8. The actuator current showed some initial increase with cycling; however, this occurred prior to the stronger seismic excitations and is attributed to packing drag on the valve stem. Graphite will frequently transfer from new packing to the valve stem during early operation and increase stem drag until equilibrium is reached. Recorded stroke times in all cases were constant within the repeatability of the limit switches and measuring system components at 35 seconds.

Figure 9 shows the actuator current measured during testing of the butterfly valve included in the purge and vent CPS. The current varied more than in the case of the 2-in. globe valve, but no trends are apparent, and again, the important observation is that no degradation was caused by the dynamic excitation. Stroke times were constant at 8 seconds. No measurable leakage occurred through the 8-in. butterfly valve during the test.

The 8-in. gate valve performance is shown in Figures 10 and 11. Leakage remained unmeasurable during most of the test, but increased to 300 $cm^3$/hr during the OBE excitation. The leakage decreased to zero following the OBE, and the valve did not leak measurably during the remaining test steps. The actuator current decreased from its initial baseline value following the 0.1 OBE excitation, but rose to an intermediate level during and after the SSE. A possible explanation for the variation in actuator current is the gradual migration of water between the valve stem and packing during the early cycling, which would tend to provide lubrication, or slight wearing-in, of the metal-to-metal sliding surfaces. Stroke times were constant at 41 seconds throughout the test. As in the case of the butterfly and globe valves, the seismic excitation did not degrade operability.

The gate and globe valves did not complete their full strokes prior to shutdown of the SSE dynamic excitation. In both cases, the actuator current increased 10 to 15% at the time of shutdown. This is attributed to the beneficial effect of the vibration in reducing friction.

A detailed evaluation of the piping response has not been completed yet. However, posttest visual examinations did not reveal any damage to the piping, supports, or penetration.

## CONCLUSIONS

On the basis of the hardware chosen for testing, the seismic excitation applied, and the measurements and observations discussed above, the conclusion is that typical CPSs, located in typical containments, will not be adversely affected by typical SSE excitation. This conclusion applies to the operability and leak integrity of the valves and to the structural integrity of the piping, penetrations, and supports.

A companion project at the INEL seismically tested an 8-in. motor operated gate valve in an in situ environment. The preliminary results from that program also support the conclusion that the structural integrity of valves in a nuclear piping system will not be damaged from the loads resulting from a credible seismic event.

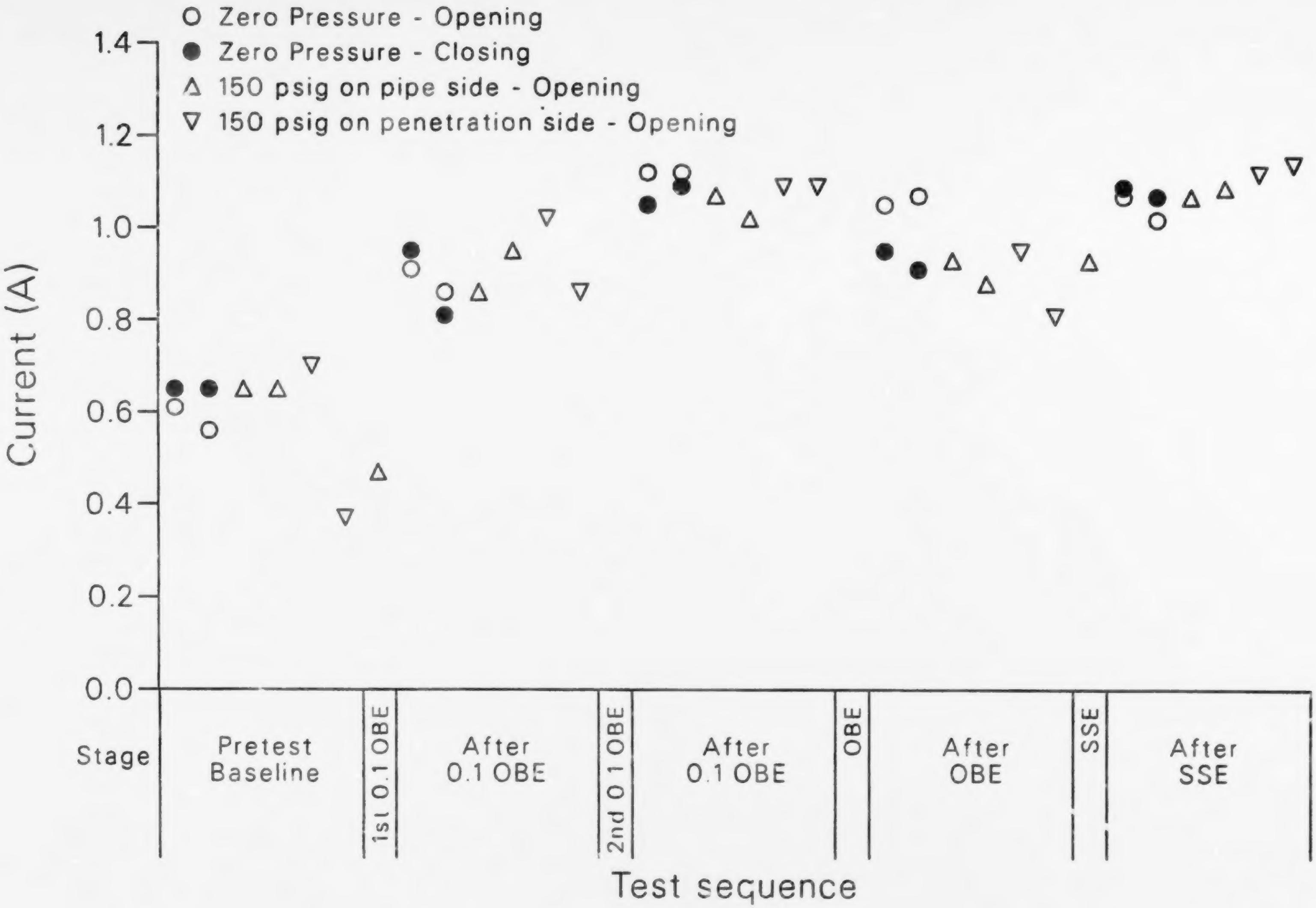

Figure 8. Actuator motor currents for 2-in. globe valve.

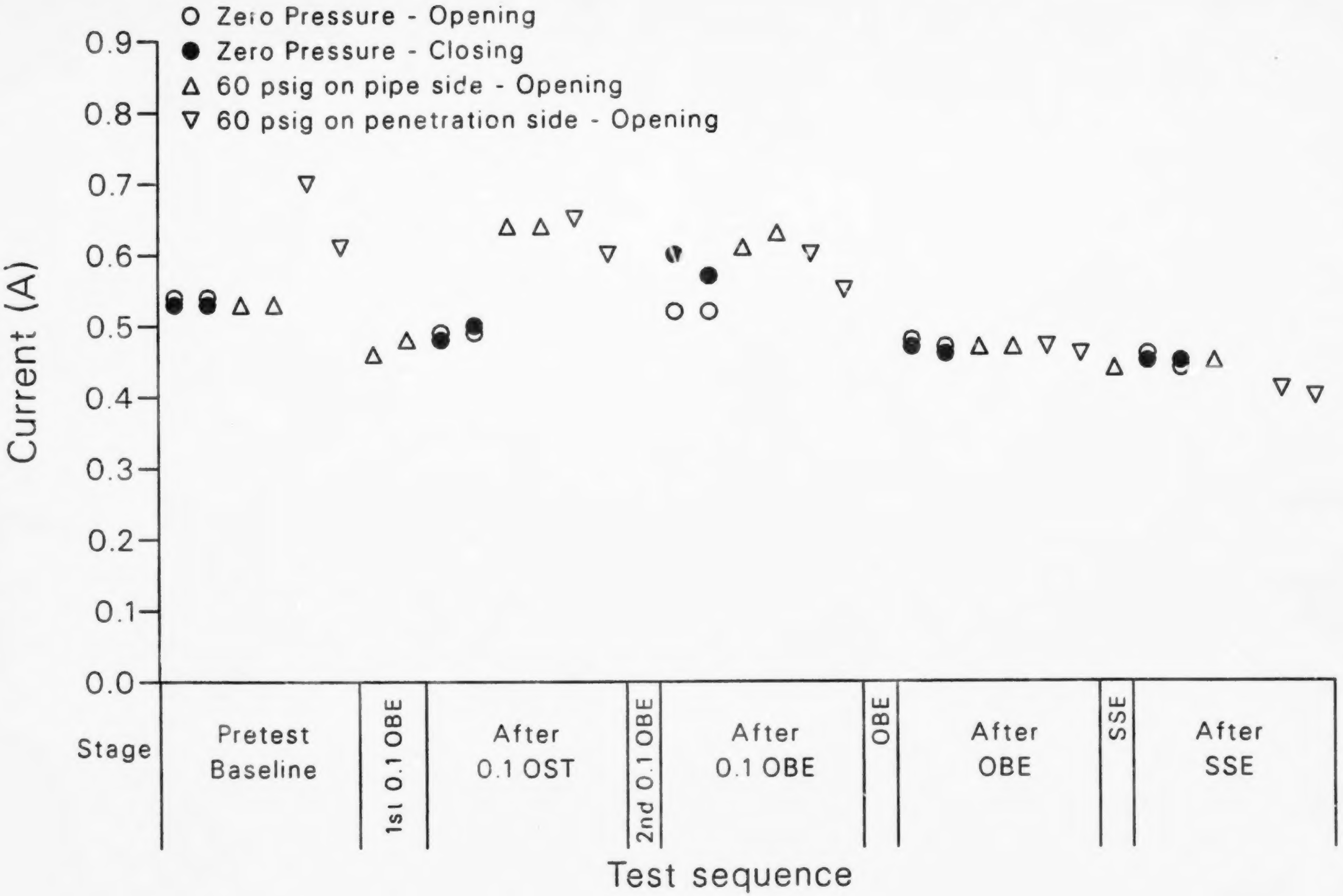

Figure 9. Actuator motor currents for 8-in. butterfly valve.

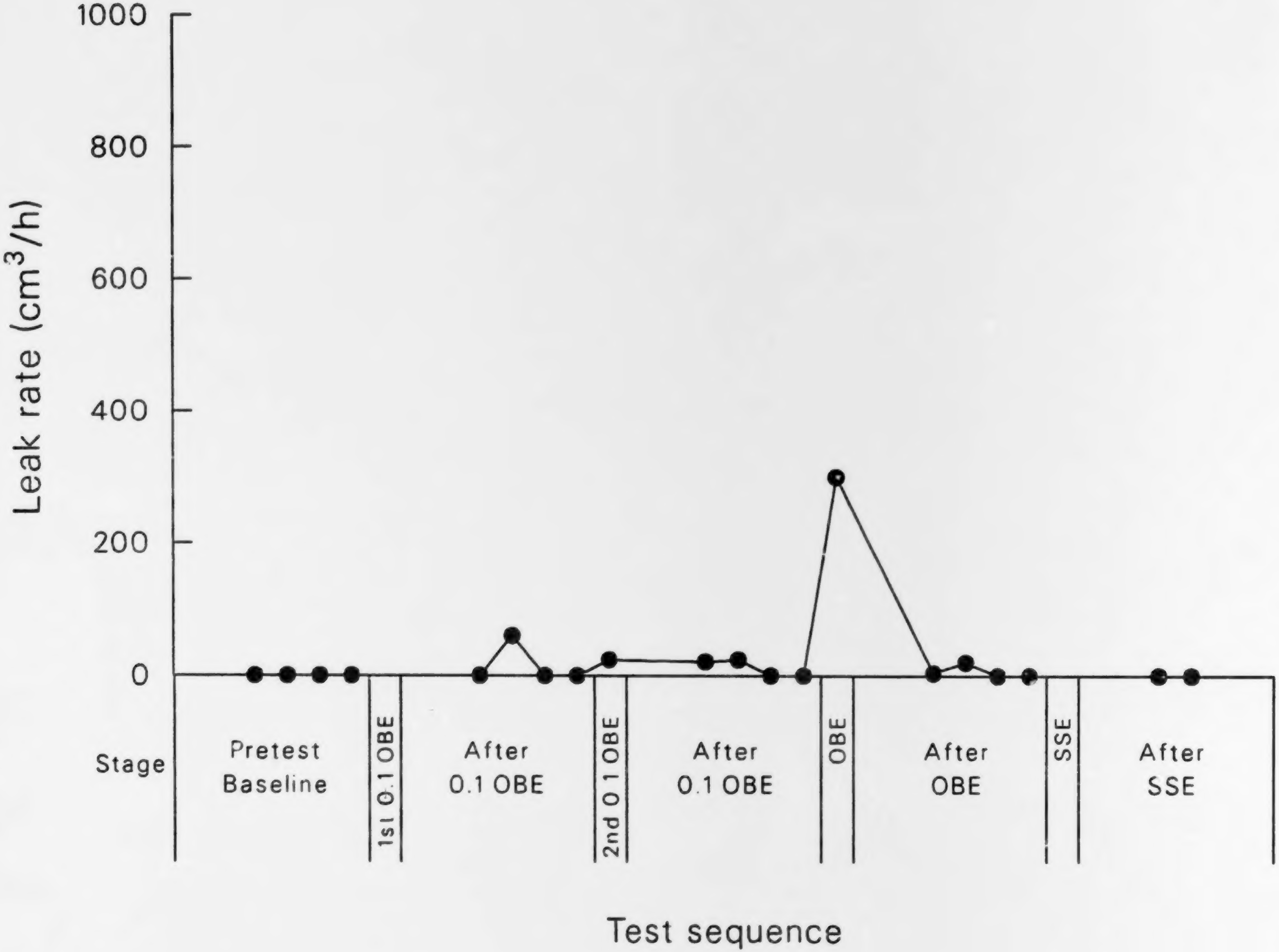

Figure 10. Leak rates through 8-in. gate valve.

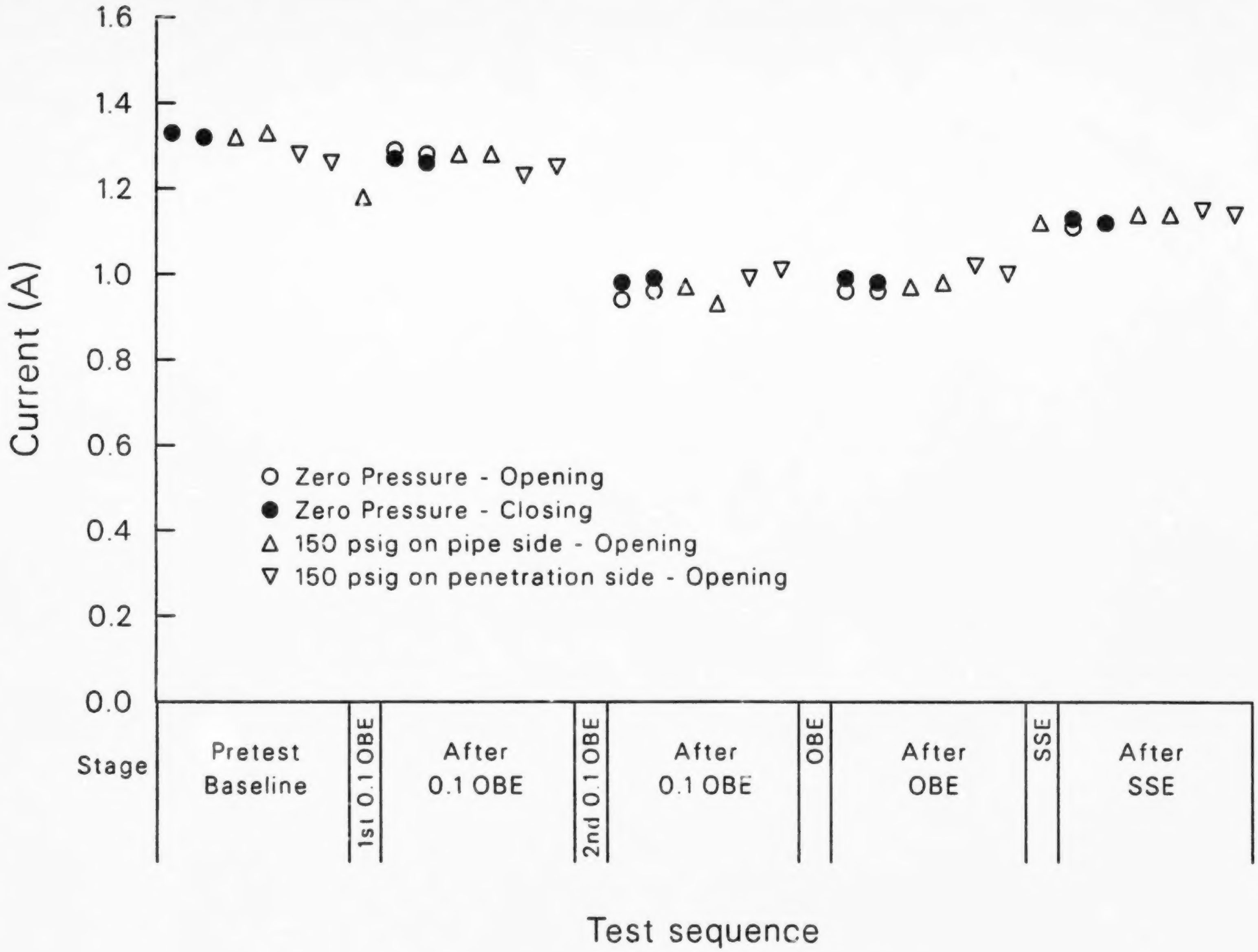

Figure 11. Actuator motor currents for 8-in. gate valve.

# NOTICE

This report was prepared as an account of work sponsored by an agency of the United States Government. Neither the United States Government nor any agency thereof, or any of their employees, makes any warranty, expressed or implied, or assumes any legal liability or responsibility for any third party's use, or the results of such use, or any information, apparatus, product or process disclosed in this report, or represents that its use by such third party would not infringe privately owned rights. The views expressed in this report are not necessarily those of the U.S. Nuclear Regulatory Commission.

# PARAMETERS IMPORTANT TO REACTOR COOLANT PUMP SEAL STABILITY DURING STATION BLACKOUT[a]

R. C. Hill
Idaho National Engineering Laboratory
EG&G Idaho
Idaho Falls, ID 83401
(208) 526-8306

D. B. Rhodes
Atomic Energy of Canada Limited
Chalk River, Ontario
Canada KOJ 1JO
(613) 584-3311

## ABSTRACT

An assessment is made of the ability of typical Reactor Coolant Pump (RCP) Shaft Seals to withstand the conditions predicted for a station blackout (loss of all alternating current power) at a nuclear power station. Several factors are identified that are key to seal stability including inlet fluid conditions, pressure downstream of the seal, and geometrical details of the seal rings. Limits for stable seal operation are determined for various combinations of these factors, and the conclusion is drawn that some RPC seals would be near or over the threshold of instability during a station blackout. If the threshold were exceeded, significant leakage of coolant from the primary coolant system could be expected.

## INTRODUCTION

The Reactor Coolant Pumps (RCPs) that circulate coolant through light water reactor (LWR) primary coolant systems contain rotary end-face seals to prevent leakage of primary coolant along the pump shaft into the containment. Failure of these precision components results in breaching the primary coolant system pressure boundary, and may, depending on severity, result in a breach large enough to cause a small loss of coolant accident (LOCA).

As a result of several seal failures, the U.S. Nuclear Regulatory Commission (NRC) performed a study to determine the significance of seal failures with respect to risk. The conclusion was that such failures could dominate the overall probability of core melt due to small-break LOCAs.

Following this determination, the NRC initiated a research program to provide the necessary technical understanding to support a licensing position that assures RCP seal failures do not pose an unacceptable risk. That program included evaluating seal failures based on reported events, evaluating seal cooling system reliability, evaluating mechanical and maintenance induced failures, and determining the effect of a loss of cooling on seal performance. The research presented in this paper was performed by Atomic Energy of Canada Limited in Chalk River, Ontario,

---

[a] Work supported by the U.S. Nuclear Regulatory Commission, Office of Nuclear Regulatory Research, under DOE Contract No. DE-AC07-76ID01570.

Canada. This work addresses seal performance during a loss of seal cooling with emphasis on the temperatures and pressures that could be expected during a station blackout (loss of both off-site and on-site ac power). The objective of the project is to identify and quantify the parameters that have the most influence on seal behavior when seal cooling is lost.

## REACTOR COOLANT PUMP SEAL DESIGN

The basic operation of reactor coolant pump seals is described below. Although the different pump manufacturers have variations among their designs, the general behavior of their seals is similar. The overall assembly is made up of three or four stages of face seals, one stage is represented in a simplified manner in Figure 1. High pressure flow that communicates with the primary coolant system water is either injected from an external system or is taken directly from the primary coolant system, through a thermal barrier heat exchanger, into the seal assembly. The leakage flow, or actual flow through the seal, passes between the rotating seal ring (shaft mounted) and the nonrotating seal ring (mounted on the pump housing). One seal is mounted so limited axial motion is permitted to maintain a virtually constant gap between the seal rings during relative axial shaft motion caused by thermal and pressure induced expansions. In Figure 1, this capability is shown on the nonrotating seal ring. A polymer secondary seal prevents leakage between the seal ring and the housing but permits relative motion between the two. The gap between the seal rings is determined by a balance of forces on the movable seal ring. Friction between the secondary seal and the seal ring tends to impede motion in either direction. The hydrostatic pressure on the back side of the seal ring and the spring load tend to close the gap. (Some designs do not include the axial loading spring.) The distributed pressure load across the face of the seal ring tends to open the gap. A graphical representation of the pressure distribution is shown in Figure 2. The pressure gradient increases near the inside diameter (ID) of the seal ring due to the reduced flow area.

During normal operation (single-phase flow), the seal is stable, that is, if the gap opens up for some reason, the pressure distribution over the seal face changes by becoming more linear (flatter) across the radial width of the seal. This decreases the overall pressure force acting to separate the seal rings and the gap will decrease. If the gap closes due to some perturbation, the pressure drop will occur more predominately near the ID of the seal; thus, increasing the force (integrated pressure times area) acting on the face of the seal ring, and the seal ring will be driven back with a resulting increase in the gap.

In a station blackout, cooling water to the thermal barrier and power to the seal injection pumps are lost resulting in hot water, approaching primary coolant system conditions, entering the seal assembly. As this flow passes between the seal faces, it flashes to the relatively low pressure region at the ID of the seal assembly. The reducing fluid density causes a higher pressure gradient near the ID of the gap and results in an increase in the distributed pressure load which tends to open the seals (refer to the two-phase flow curves in Figure 2) and in a worst case could

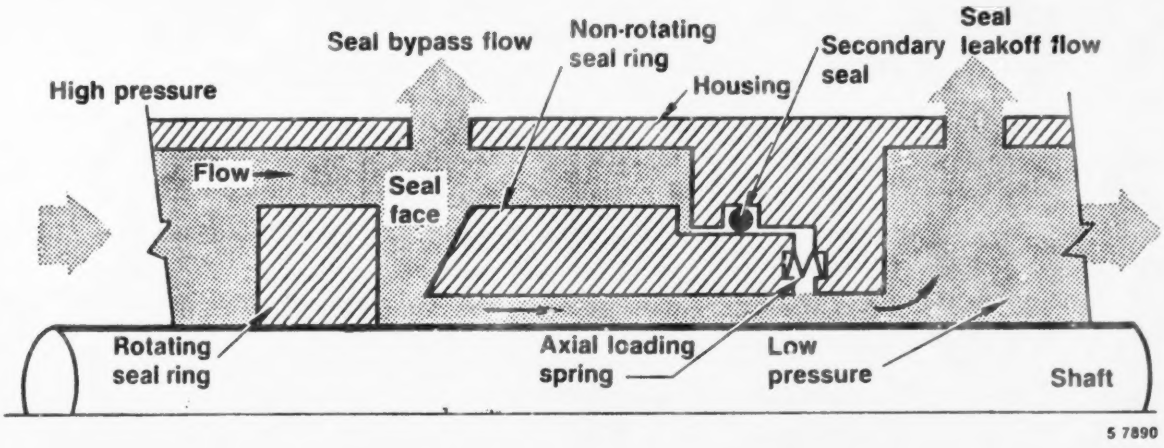
Seal bypass flow
Non-rotating seal ring
Seal leakoff flow
Secondary seal
Housing
High pressure
Flow
Seal face
Rotating seal ring
Axial loading spring
Low pressure
Shaft
5 7890

Figure 1. RCP Shaft Seals Limit Leakage from Primary Coolant System.

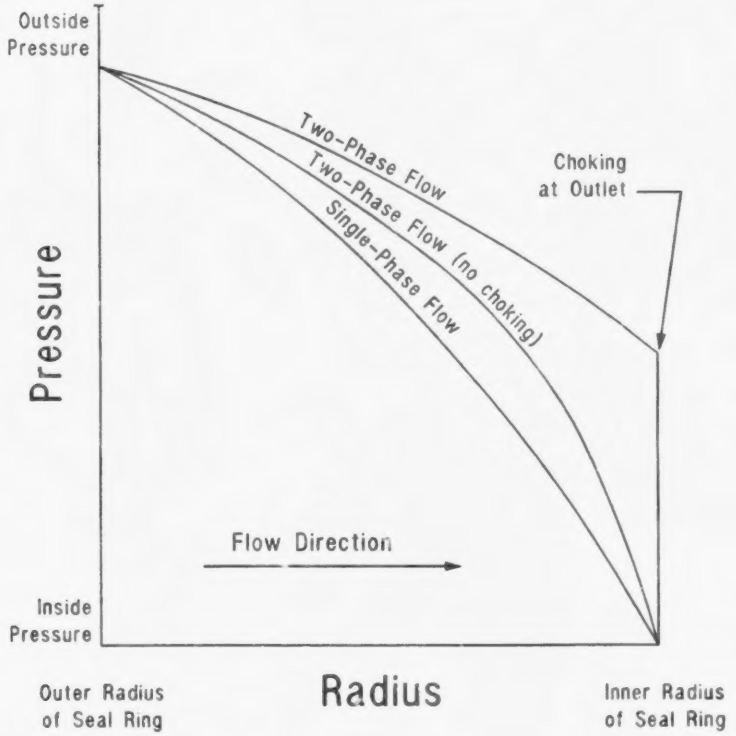

Figure 2. Pressure Profile in Gap Varies with Fluid Conditions.

cause the seal to become unstable and pop open. In this unstable, open position a relatively large opening is presented for coolant to leak from the primary coolant system.

The manner in which the various seal stages are connected is different for each vendor. Some designs direct the seal leak-off flow to the next stage rather than collecting it separately; also, some control the seal bypass flow in order to maintain intermediate pressures at the outside diameter (OD) of succeeding stages, thus limiting the ΔP across any given seal stage. While these differences certainly have importance in the overall stability consideration, the basic concern in this research is the performance of a general, single seal stage under various inlet fluid conditions, as influenced by seal geometry.

## PROGRAM DESCRIPTION AND RESULTS

A computer code developed specifically for seal analysis was used to determine the seal behavior as a function of changes in various parameters. The code assumes homogeneous, equilibrium, two-phase flow through a seal modeled as shown in Figure 3. For all analyses and experiments, the shaft has been assumed stationary since the pump will coast down before the water in the seal assembly increases significantly in temperature during a station blackout.

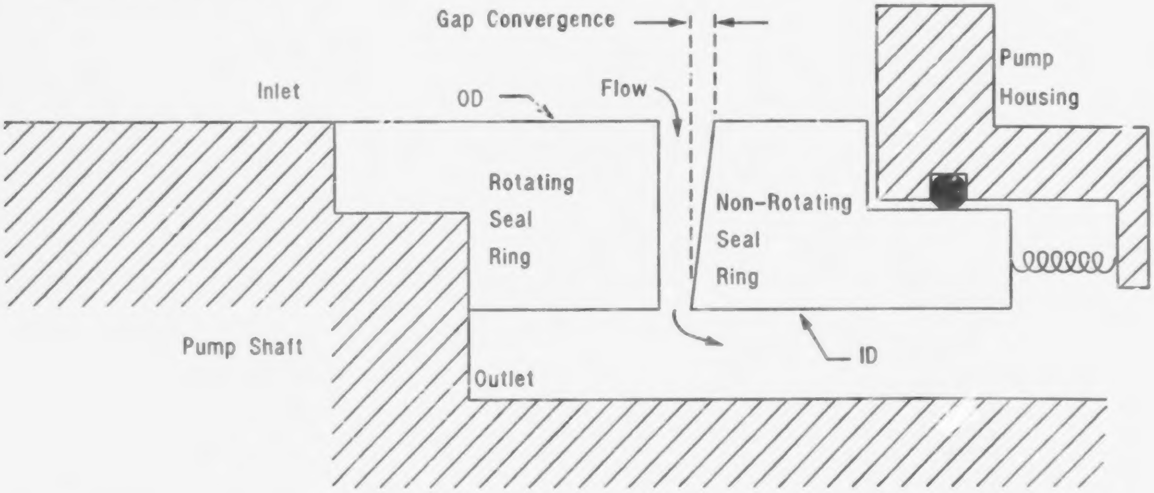

Figure 3. Analytical model considers various fluid conditions and seal ring geometries.

Inputs to the analysis included geometrical parameters (seal ring ID and OD and gap convergence or taper between seal faces); fluid conditions including temperature, pressure, and quality at the seal OD (inlet); and the back pressure (pressure at the seal ID). An iterative routine converges on a gap between the seal faces that results in balanced forces on the axially movable ring.

The specific objective was to determine the ranges and combinations of the various parameters that would define a threshold for instability.

Instability is defined to be the condition in which the minimum opening force (pressure between the seal faces integrated over the area of the movable seal ring) is larger than the closing forces. The latter include the pressure acting on the back side of the seal (also a function of back pressure) spring load, and friction of the secondary seal which may act in either direction.

The analysis employed several simplifying assumptions as listed below:

1. Flow is quasistatic and purely radial
2. Flow is turbulent with a constant friction factor or laminar
3. Gap is axisymmetric, that is, the rings are not tilted relative to each other
4. Two phases are homogeneously mixed and are in thermal equilibrium
5. No heat conduction occurs to the surrounding environment
6. Inlet flow is isentropic.

The effects of changing the various input parameters are discussed in the following paragraphs. The ranges for the parameters were determined by estimating the actual values that could be expected in a postulated station blackout. Since virtually all of the specific dimensions are vendor proprietary, judgment based on experience with typical face seal assemblies was used in the parameter selections.

To facilitate presentation of the analytical results in a format independent of specific geometries, a "critical balance ratio" is used as defined below.

The critical balance ratio, $B_{crit}$, is the minimum nondimensionalized closing force, B, required to prevent the seals from separating due to the pressure distribution in the gap. The nondimensionalized closing force can be expressed as

$$B = \frac{\text{Hydraulic closing force + spring force} \pm \text{friction force}}{(P_{OD} - P_{ID})\ (\text{area of seal face})}$$

where

$P_{OD}$ is the inlet pressure in Figure 3.

$P_{ID}$ is the outlet pressure in Figure 3.

With this definition, stability will exist if $B > B_{crit}$; and the smaller $B_{crit}$ is relative to B, the more margin to instability. The balance ratio, B, for most RCP pumps is in the range of 0.60 to 0.75.

## INLET FLUID CONDITIONS

Inlet fluid conditions affect seal stability in two opposing ways. As saturation conditions are approached, the amount of flashing in the gap increases, causing the pressure profile to become more bowed which increases the opening force on the ring. Opposing this tendency to open is an increased entrance loss at the OD of the seal rings. The net result of these two phenomena is a relatively constant critical balance ratio when fluid conditions are near saturation. As subcooling increases, a transition to fully stable operation occurs. This effect is shown in Figure 4. The dashed portion of the curve represents a condition wherein the seal will not pop open (become unstable) but may have higher leak rates than in fully stable operation.

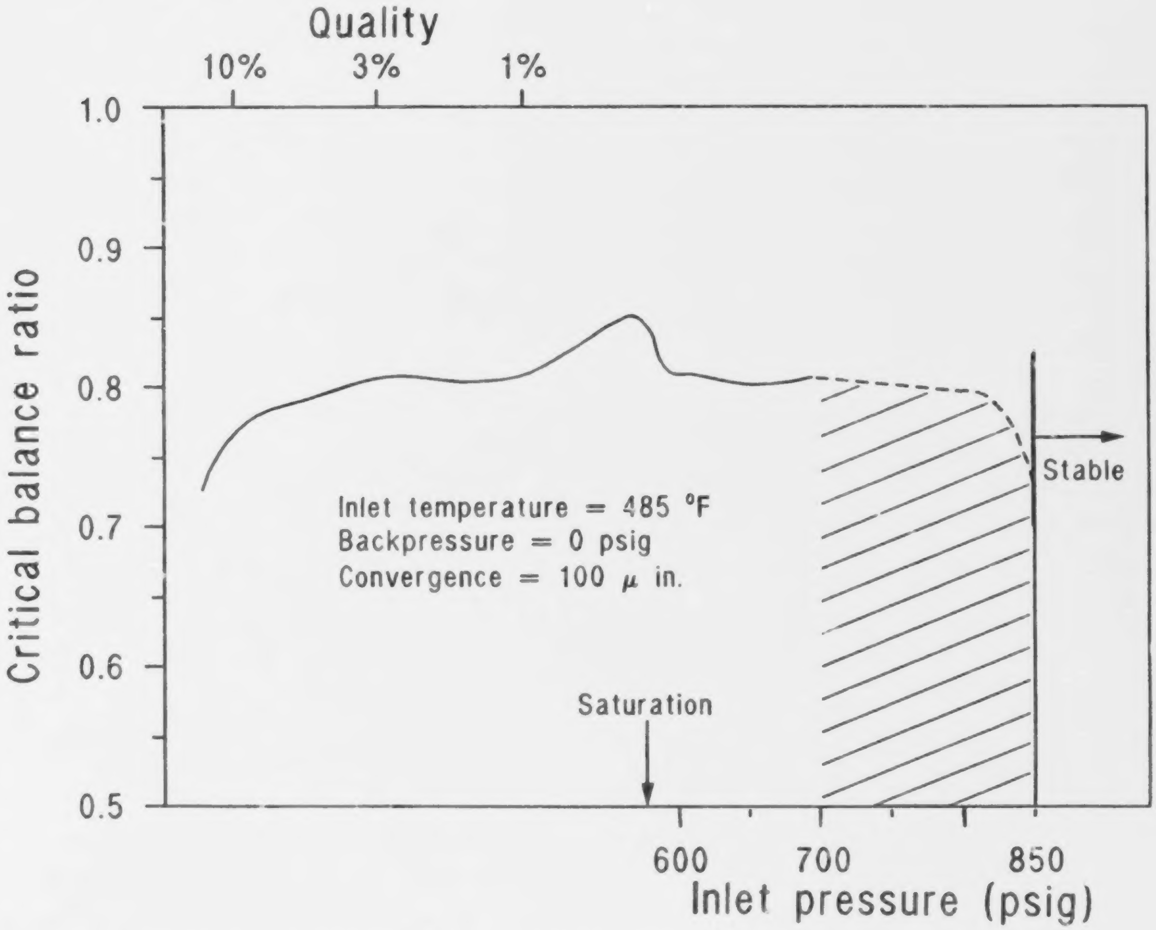

Figure 4. Sufficient inlet fluid subcooling assures stability.

## BACK PRESSURE

The back pressure or the pressure at the ID (see Figure 3) of the seal is determined both by the seal design and restrictions in the leak-off path. Increasing the back pressure has three effects--it increases the average pressure between the seal faces, increases the pressure on the back side of the seal ring, and flattens the pressure profile across the seal face as a result of reduced flashing in the gap. The overall effect of increasing back pressure is to reduce the net opening force (increase stability) as shown in Figure 5.

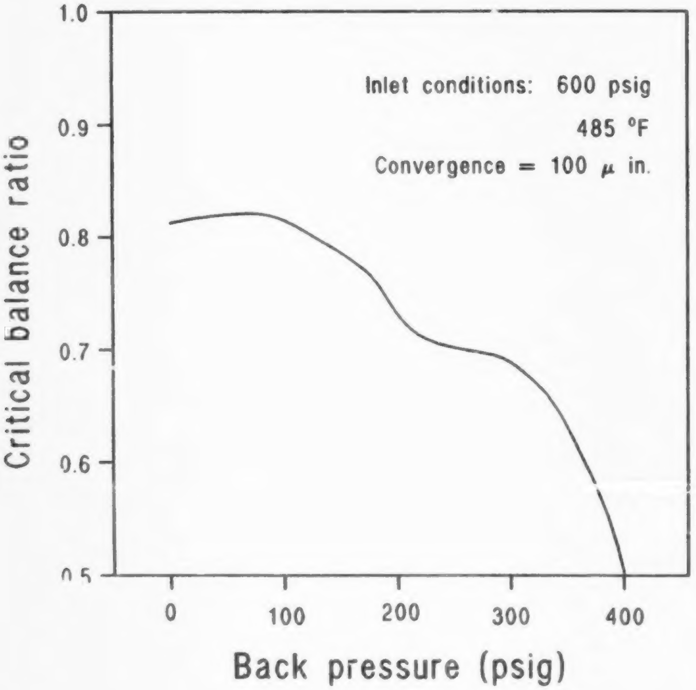

Figure 5. Increasing back pressure improves stability.

## SEAL FACE CONVERGENCE

The seal convergence (see Figure 3) has a strong effect on the pressure profile, and therefore, is important to stability. Figure 6 shows the calculated critical balance ratio as a function of convergence for selected fluid conditions. From a qualitative standpoint, the effect of convergence is consistent with earlier descriptions of the pressure profile behavior. As the convergence increases, more of the pressure drop occurs near the seal ID. This, in turn, provides a more bowed profile with an increase in the integrated pressure load, and therefore, an increased opening force. If the seal became divergent (minimum gap at the OD), the pressure distribution would be such that only the back pressure would act across the seal face. With the inlet pressure forcing the rings together, no instability should occur. However, in this case of divergent seal faces, another seal geometry parameter is important--the seal surface condition.

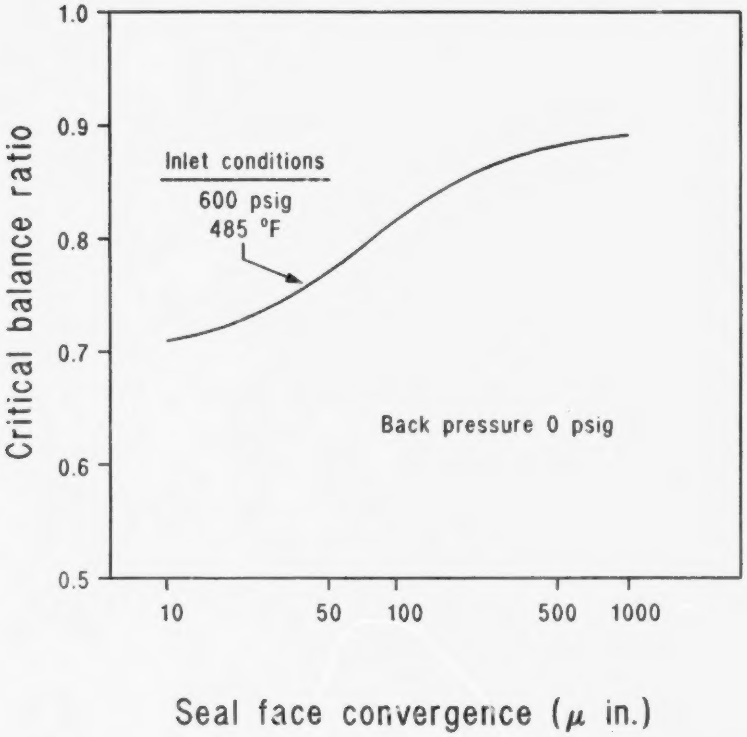

Figure 6. Reducing seal face convergence improves stability.

A roughened or worn surface would permit flow to pass between the seal faces and establish a pressure profile comparable to the two-phase curves in Figure 2. The minimum leakage that will cause instability in parallel and divergent seal faces is shown in Figure 7 as a function of balance ratio.

The behavior of divergent seals is important in the overall stability of the seal assembly. In some designs, hot water flowing through the first and second stages will induce thermal distortions large enough to cause the second stage to achieve a divergent gap. If the second stage remains stable, sufficient back pressure will be generated for the first stage to also remain stable. Figure 5 shows the effect of back pressure on stability. On the other hand, instability in the second stage would result in a low back pressure on the first stage, and consequently, in a much higher critical balance ratio (less stable condition) on the first stage.

## FRICTION TESTING

A specific area of concern in the analysis was the magnitude of the friction drag on the movable seal ring. As a result of hydrostatic loads and the relative thermal expansions within the pump and seal assembly, the seals would separate during a station blackout if the movable ring were restricted from sliding over the secondary seal. Earlier research in this program, documented in NUREG/CR-4077, entitled "Reactor Coolant Pump Shaft Seal Behavior During Station Blackout," determined that some of the

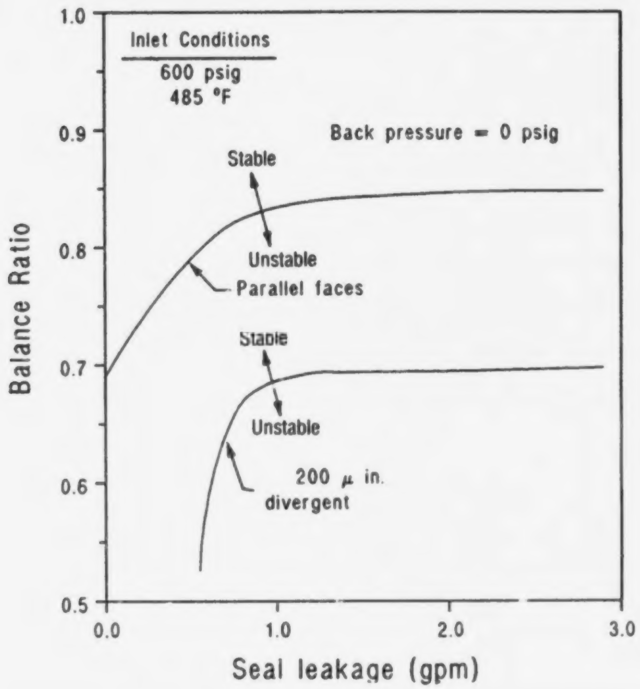

Figure 7. Divergent seal faces may also become unstable with leakage.

secondary seals will extrude into the gap, due to seal material degradation in the station blackout environment. The resulting increase in the friction drag force on the ring would cause a decrease in the effective closing force and result in less margin to instability. Another effect of high temperature is embrittlement of some secondary seals. Small-scale tests were performed to measure the change in friction drag on several secondary seal configurations. The tests showed that friction between degraded secondary seals and the movable ring would be on the order of two to four times the normal values. This force is relatively small compared to typical hydraulic loads and the effects of secondary seal degradation are concluded to be of second order importance with respect to seal stability. One pump vendor has identified a substitute o-ring material that will function adequately in station blackout environments; plans are currently being made for the material change in that vendor's pumps.

A potentially significant factor concerning seal embrittlement that was not investigated is the effect of typical wear on the metal surface in contact with the secondary seal. If the secondary seal was subjected to high temperature while pressed into surface irregularities caused by wear, the friction drag could be considerably higher than in the case of a smooth surface.

## STABILITY TESTING

A limited amount of experimental testing at representative temperatures and pressures was performed to benchmark or confirm the analysis. The tests were made with simulated seal rings having a diameter of about six inches. Although typical RCP seal rings are about eight inches in diameter, analysis showed that size differences would account for variations on only 2% in the predicted critical balance ratio-larger seals being more stable. The test rig is shown in a simplified sketch in Figure 8. The injection flow entered the pressure vessel at the OD of the seal rings. The annular chamber between the OD of the seal rings and the pressure vessel was sealed so flow could only pass between the seal faces. A measured, controlled load was applied to the axially movable ring (rotor) through an externally mounted load controller.

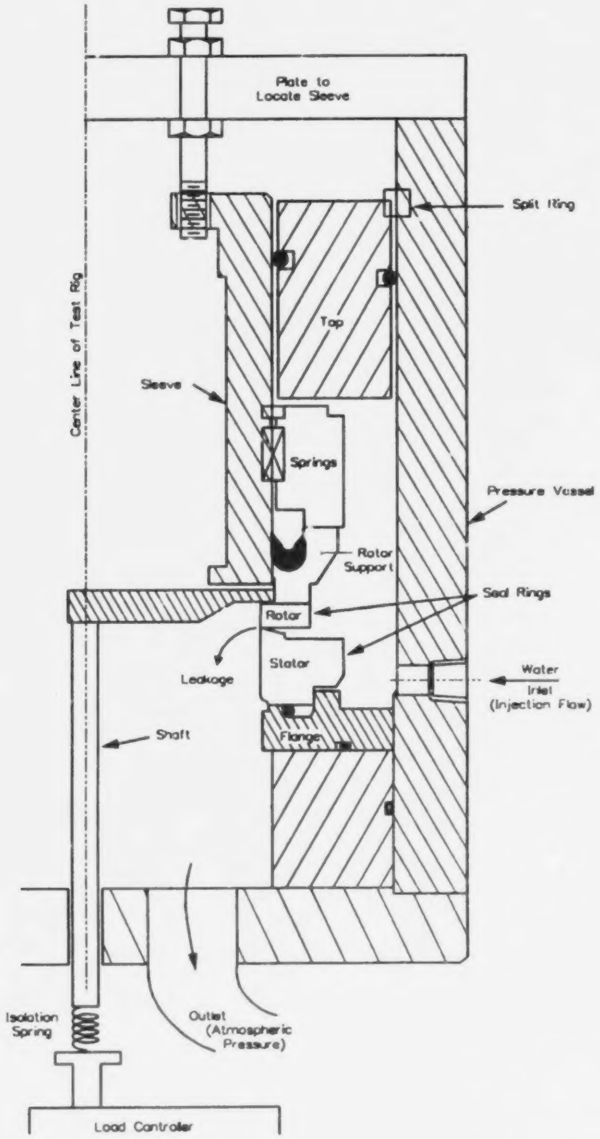
Plate to Locate Sleeve
Split Ring
Top
Sleeve
Center Line of Test Rig
Springs
Pressure Vessel
Rotor Support
Seal Rings
Rotor
Stator
Leakage
Water Inlet (Injection Flow)
Shaft
Flange
Isolation Spring
Outlet (Atmospheric Pressure)
Load Controller

Figure 8. Testing performed to confirm analysis.

Hot water was supplied to the fixture at temperatures ranging from 435°F to 490°F and pressures up to 1200 psig. Testing was performed by (1) loading the seals at a high load, using the load controller, to prevent flow; (2) opening the supply line from the hot water supply to the fixture; (3) reducing the seal closing load to initiate flow and allow temperature and pressure distributions to stabilize; and (4) further decreasing the seal load until the seal opening force caused the seals to pop open. By calculating the hydraulic closing force and measuring the applied load, the net closing force at the threshold to instability could be determined. With the ring geometry and inlet pressure known (and zero back pressure) $B_{crit}$ was identified. The experimental results are plotted in Figure 9 and are compared to analytical results for similar conditions. The conclusion is that the analysis and experimental results are, generally, in reasonable agreement through the range of temperatures and pressures tested. The back pressure was atmospheric pressure in all cases, and a single gap convergence value of about 100 μ in. was used.

## CONCLUSIONS

Firm conclusions are difficult to reach on seal survivability in a station blackout without a detailed knowledge of the plant specific time dependent conditions and the specific seal and associated piping system configuration. However, the following general conclusions can be reached that can be used in assessing the capability of specific seals to withstand station blackout conditions:

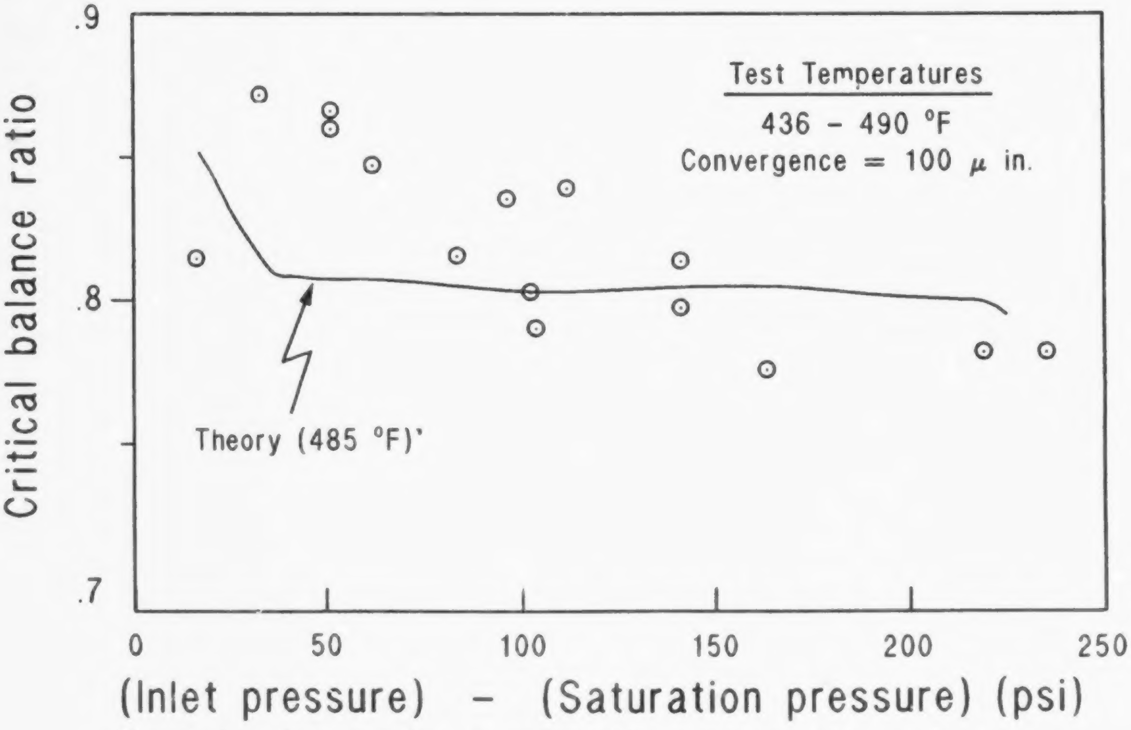

Figure 9. Test results in reasonable agreement with analysis.

BEST COPY AVAILABLE

1. Balance ratio has been identified as a parameter for quantifying seal stability margins under station blackout conditions. General knowledge indicates some of the RCP shaft seals currently in use are designed close to or less than the critical balance ratios calculated for station blackout conditions. If the actual balance ratio is less than the critical balance ratio for the specific station blackout conditions, seal instability and high leakage can be expected.

2. All current RCP seal designs are subject to some degree of inherent instability under two-phase flow conditions. This effect can be minimized provided that:

   a. Inlet pressure is kept sufficiently above saturation

   b. Back pressure is kept sufficiently high

   c. Seal convergence is sufficiently low.

3. Seals that are divergent are not immune to instability and will "pop open" if a maximum stable leakage is exceeded because of scratches and wear on the seal face.

4. Based on the results of high temperature extrusion tests and subsequent action by one manufacturer to specify a superior elastomer material, extrusion failure of secondary seals is not expected. Experimentally-determined values for friction forces of degraded secondary seals are of a second-order importance relative to seal instability; however, for some designs, the friction force would likely be considerably higher when typical surface wear is present.

The research discussed above does not provide assurance that current RCP shaft seals would reliably survive station blackout conditions without high leakage from the primary coolant system.

NOTICE

This report was prepared as an account of work sponsored by an agency of the United States Government. Neither the United States Government nor any agency thereof, or any of their employees, makes any warranty, expressed or implied, or assumes any legal liability or responsibility for any third party's use, or the results of such use, or any information, apparatus, product or process disclosed in this report, or represents that its use by such third party would not infringe privately owned rights. The views expressed in this report are not necessarily those of the U.S. Nuclear Regulatory Commission.

# DYNAMIC LOAD EFFECTS ON GATE VALVE OPERABILITY[a]

Robert Steele, Jr., Philip E. MacDonald, James G. Arendts
Idaho National Engineering Laboratory
Idaho Falls, Idaho 83415

## ABSTRACT

The Idaho National Engineering Laboratory (INEL) participated in an internationally sponsored seismic research program conducted at the decommissioned Heissdampfreaktor (HDR) located in the Federal Republic of Germany. An existing piping system was modified by installation of an 8-in., naturally aged, motor-operated gate valve from a U. S. nuclear power plant and a piping support system of U. S. design. Six other piping support systems of varying flexibility from stiff to flexible were also installed at various times during the tests. Additional valve loadings included internal hydraulic loads and, during one block of tests, elevated temperature. The operability and integrity of the aged gate valve and the dynamic response of the various piping support systems were measured during 25 representative seismic events.

## INTRODUCTION

The qualification of equipment increases the confidence that equipment will operate as designed when subjected to design basis loadings. Nuclear equipment qualification is typically performed to industry standards, some of which have only an analytical or an extrapolated basis for the qualification technology they contain. This is especially true with line-mounted equipment where the dynamic input is always analytically determined.

The Environmental and Dynamic Qualification of Mechanical and Electrical Equipment Program being conducted at the Idaho National Engineering Laboratory (INEL) and sponsored by the United States Nuclear Regulatory Commission, Office of Nuclear Regulatory Research, is performing research to establish a technical basis to assess the adequacy and to improve these qualification standards. The dynamic qualification of line-mounted mechanical equipment is one area of this research where the industry standard is still in draft form.

The seismic research program conducted by Kernforschungszentrum Karlsruhe (KfK) at HDR provided a unique opportunity to study the behavior of a motor-operated gate valve in an in situ environment subjected to representative seismic loadings.

---

[a] Work supported by the U.S. Nuclear Regulatory Commission, Office of Nuclear Regulatory Research, under DOE Contract No. DE-AC07-76ID01570.

The objectives of the INEL activities associated with this multinational experimental program were to:

1. Measure the effects of various dynamic and hydraulic loads on gate valve operability during a series of representative seismic events. The dynamic loads were varied by placing the valve in a very flexible, a flexible, a typical U.S. stiff, and four energy-absorbing-type piping support systems and by varying the magnitude and frequency of the excitation.

2. Provide data for comparison of valve response due to multiaxis in situ seismic loads and valve response due to single-effects loadings typical of valve qualification testing.

3. Provide piping system response (strain, acceleration, and displacement) data for a very flexible, a flexible, a typical U.S. stiff, and four energy-absorbing piping support systems during a series of reasonably representative seismic events. The information will be used to evaluate support systems and verify the Seismic Methodology Analysis Chain with Statistics (SMACS) computer code.

4. Provide data on the behavior of a typical U.S. stiff and a very flexible piping system which can be used to assist in the evaluation of the applicability of nonnuclear seismic experience data to nuclear piping systems.

This paper presents the preliminary test results from the first three tests performed. Valve operability and the performance of the seismically active supports are addressed.

## EXPERIMENTAL PROGRAM

The experiments at the HDR facility consisted of mechanical excitation of the HDR building and the subsequent excitation of the systems and components inside the structure. Excitation of the building was accomplished by a large, twin-arm, rotary mass shaker (designed by ANCO Engineers, Inc.) which was spun up in the balanced condition to the desired starting frequency and then, through the use of an explosive bolt, allowed to go into the unbalanced state, imparting a mechanical loading to the highest structural floor [31 m (100 ft)] in the building. The components and systems in the building responded with both vertical and horizontal motion due to the complex dynamic response of the building.

An aged, motor-operated gate valve and various types of piping supports were installed in and on an existing HDR piping system. This piping system is called the Versuchskreislauf (VKL) piping system, and it is located between the 18- and 24-m elevations in the HDR facility, as shown in Figure 1. The VKL system basically consists of two parallel flow loops connected to a large vessel called the HDU and a manifold or header, as shown in Figure 2. The VKL piping system is constructed of stainless steel

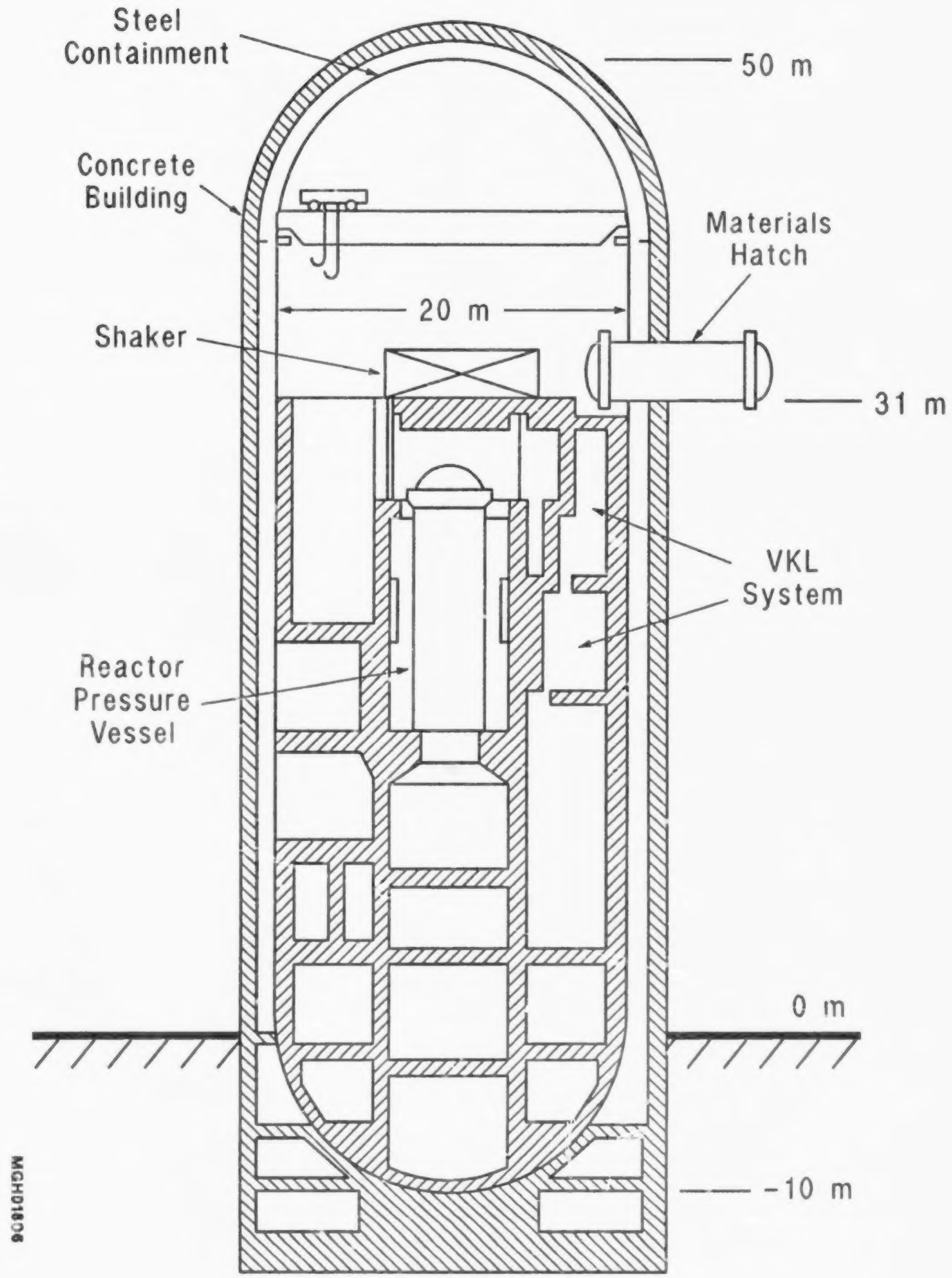
Steel
Containment
50 m
Concrete
Building
Materials
Hatch
20 m
Shaker
31 m
VKL
System
Reactor
Pressure
Vessel
0 m
-10 m
MGHD1806

Figure 1. A simplified cross section of the HDR facility, showing the shaker, VKL piping system, and the reactor pressure vessel.

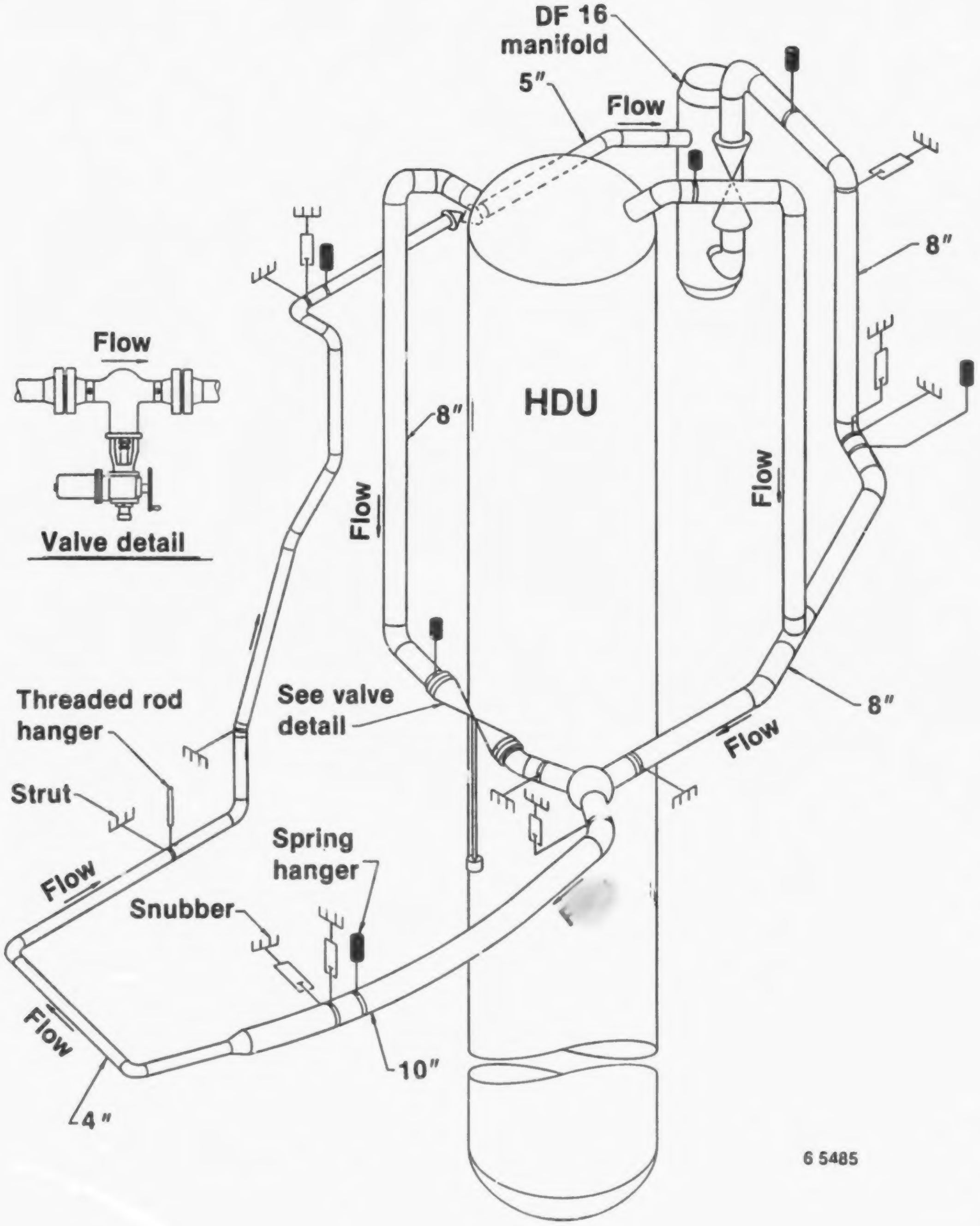
DF 16 manifold
5"
Flow
8"
Flow
Valve detail
8"
HDU
Flow
Flow
Threaded rod hanger
See valve detail
8"
Flow
Strut
Spring hanger
Flow
Snubber
Flow
10"
4"
6 5485

Figure 2. The VKL system with the U.S. stiff support system installed.

BEST COPY AVAILABLE

(equivalent to U.S. Type 347) in four pipe sizes (also shown in Figure 2). The system is electrically heated and is capable of operation at pressurized water reactor (PWR) secondary or boiling water reactor (BWR) primary pressure/temperature conditions. A maximum differential pressure of 26.5 BAR (385 psid) was applied across the valve by placing an orifice in the parallel flow line.

The aged, 8-in., motor-operated gate valve was thoroughly refurbished before installation in the VKL system at the location shown in Figure 2. The aged valve had seen approximately 25 years of service in a nuclear power plant as a boiler feedwater header safety injection isolation valve. The refurbishment included replacement of the seals, gaskets, and motor operator grease and work on the gate sealing surfaces. One side of the wedge and seat-sealing surface was weld-repaired using a hard facing filler material and lapped. The valve was then subjected to the applicable single-effects qualification tests outlined in ANSI B16.41 (QV-4), "Functional Qualification Requirements for Power Operated Active Valve Assemblies for Nuclear Power Plants."

Seven different piping support systems were installed on the VKL piping. These support systems included a typical U.S. stiff, a KfK-designed very flexible, a Kraftwerk Union (KWU) flexible, and four energy-absorbing support systems. The four energy-absorbing systems included an impact system, a ductile flexure system, and two different types of viscous mass energy-absorbing designs. The VKL deadweight supports consisted of the six spring hanger type supports and the one threaded rod support shown on Figure 2. These deadweight supports were installed during all the tests. The additional supports installed for the seven dynamic support configurations are listed in Table 1.

TABLE 1. TYPE OF SUPPORTS USED IN THE HDR/VKL TESTS

| Support System Name | Rigid Supports | Snubbers | Viscous Mass Supports | Impact Supports | Spring Supports |
|---|---|---|---|---|---|
| U.S. stiff | 6 | 6[a] | 0 | 0 | 0 |
| KfK very flexible | 2 | 0 | 0 | 0 | 0 |
| KfK flexible | 5 | 0 | 0 | 0 | 0 |
| EPRI/Cloud impacting | 6 | 0 | 0 | 6 | 0 |
| EPRI/Bechtel energy-absorbing | 6 | 0 | 0 | 0 | 4 |
| Gerb energy-absorbing | 5 | 0 | 2 | 0 | 0 |
| ANCO energy-absorbing | 6 | 0 | 6 | 0 | 0 |

---

a. Five mechanical snubbers and one hydraulic snubber.

BEST COPY AVAILABLE

The U.S. stiff system consisted of six additional rigid supports, five mechanical snubbers, and one hydraulic snubber at the locations shown in Figure 2. This system was designed using the expected HDR structural response, the NUPIPE-II computer code, and the response spectra analysis techniques and equations of NC-3600, Summer 1979 Addenda of the ASME Code, to calculate representative stresses. The KfK very flexible and KWU flexible systems consisted of only two and five additional rigid supports, respectively (no snubbers). The EPRI/Cloud support system retained the six additional rigid supports shown in Figure 2 but replaced the snubbers with impact supports built on box beam principles with specified gaps. Seismic energy is dissipated when the piping impacts the supports. The EPRI/Bechtel system consisted of replacing the six snubbers with four devices made of ductile flexures in a box. Seismic energy was absorbed through the deformation of the ductile flexures. The Gerb and ANCO energy-absorbing devices consisted of a highly viscous bituminous liquid inside of a small vessel with a damping rod. Either two or six of these devices replaced the U.S. snubbers; and, in the case of the Gerb system, only five of the rigid supports were installed.

## EXPERIMENTAL RESULTS

The valve and VKL piping system were subjected to 25 seismic-type excitations with initial shaker starting frequencies of 1.6 to 8 Hz. Internal piping fluid temperature included both ambient (25 to 40°C) and elevated at 210°C. Table 2 lists the test number, internal piping temperature, piping support configuration, shaker eccentricity in kilogram meters, starting frequency in hertz, piping system flow, and valve functional requirements. The instruments used to monitor the VKL system and the valve response to the dynamic and hydraulic loadings are listed in Table 3.

Figure 3 shows the measured acceleration response spectrum developed from the response of the HDU vessel support and a typical U.S. west coast nuclear power plant design seismic response spectrum for an internal structure at an elevation of about one-half the containment height. The HDU vessel movement was greater than the HDR wall movement and was the forcing function influencing the VKL piping system behavior. The typical west coast containment structure movement would also be expected to strongly influence nearby piping system behavior during seismic events. The similarity of the two spectra suggests that the VKL piping system and valve results are typical of predicted commercial plant behavior during seismic events.

Figure 4 shows the valve body and valve actuator response spectra (acceleration in the x direction in g's as a function of frequency) for Test 40.36, which began with a 5.6-Hz shaker starting frequency. Comparison of the two plots indicates that the valve generally responded as a rigid body at low and high frequencies. However, the spectra indicate that there was significant amplification of the actuator response as compared with valve body response for frequencies between 8 and 25 Hz. This amplification would have been caused by either (a) some flexibility in the yoke of the actuator to the valve body mounting or (b) rotation of the piping at the valve body location (amplification due to the actuator being offset from the

TABLE 2. TEST MATRIX

| Test Number | Temperature (C) | Supports[a] Configuration | Eccentricity (kg/m) | Frequency (Hz) | VKL Flow (tons/h) | Valve Operation |
|---|---|---|---|---|---|---|
| T 40.34 | 20 | 1 | 4700 | 6.0 | 90 | Cycle |
| T 40.35 | 20 | 1 | 4700 | 8.0 | 90 | Cycle |
| T 40.36 | 20 | 1 | 8200 | 5.6 | 90 | Cycle |
| T 40.37 | 20 | 1 | 27800 | 2.1 | 90 | Cycle |
| T 40.40 | 20 | 5 | 4700 | 8.0 | 90 | Cycle |
| T 40.20 | 20 | 3 | 4700 | 8.0 | 90 | Cycle |
| T 40.60 | 20 | 6 | 4700 | 8.0 | 90 | Cycle |
| T 40.50 | 20 | 4 | 4700 | 8.0 | 90 | Cycle |
| T 40.70 | 20 | 7 | 4700 | 8.0 | 90 | Cycle |
| T 40.10 | 20 | 2 | 4700 | 8.0 | 90 | Cycle |
| T 40.30 | 20 | 1 | 4700 | 8.0 | 90 | Cycle |
| T 40.31 | 20 | 1 | 6450 | 6.0 | 90 | Cycle |
| T 40.41 | 20 | 5 | 6450 | 6.0 | 90 | Cycle |
| T 40.21 | 20 | 3 | 6450 | 6.0 | 90 | Cycle |
| T 40.11 | 20 | 2 | 6450 | 6.0 | 90 | Cycle |
| T 40.51 | 20 | 4 | 6450 | 6.0 | 90 | Cycle |
| T 40.52 | 210 | 4 | 8200 | 4.5 | 90 | Cycle |
| T 40.32 | 210 | 1 | 8200 | 4.5 | 90 | Cycle |
| T 40.42 | 210 | 5 | 8200 | 4.5 | 90 | Cycle |
| T 40.12 | 210 | 2 | 8200 | 4.5 | 90 | Cycle |
| T 40.22 | 50 | 3 | 8200 | 4.5 | 90 | Cycle |
| T 40.12A | 210 | 2 | 8200 | 4.5 | 90 | Cycle |
| T 40.14 | 40 | 2 | 33000 | 1.6 | 90 | Cycle |
| T 40.16 | 30 | 2 | 54000 | 1.6 | 0 | Open |
| T 40.13 | 30 | 2 | 67000 | 1.6 | 0 | Open |

---

a. Support configuration.

1. U.S. stiff
2. KfK very flexible
3. KfK flexible
4. EPRI/Cloud impacting
5. EPRI/Bechtel energy-absorbing
6. Gerb energy-absorbing
7. ANCO energy-absorbing

TABLE 3. VKL INSTRUMENTATION SUMMARY

| Type Instrument | On Piping | On Valve | At Support Base |
|---|---|---|---|
| Accelerometers | 36 | 10 | 12 |
| Strain gages | 45 | 14 | -- |
| Displacement | 11 | -- | |
| Pressure | -- | 1 (internal) | -- |
| Differential pressure | -- | 2 (internal) | -- |
| Valve position | -- | 2 | -- |
| Valve current | -- | 1 | -- |
| Valve voltage | -- | 1 | -- |
| Temperature | 3 | 1 (internal) | -- |
| Flow rate | 1 (internal) | -- | -- |
| Video camera | 1 | 1 | -- |

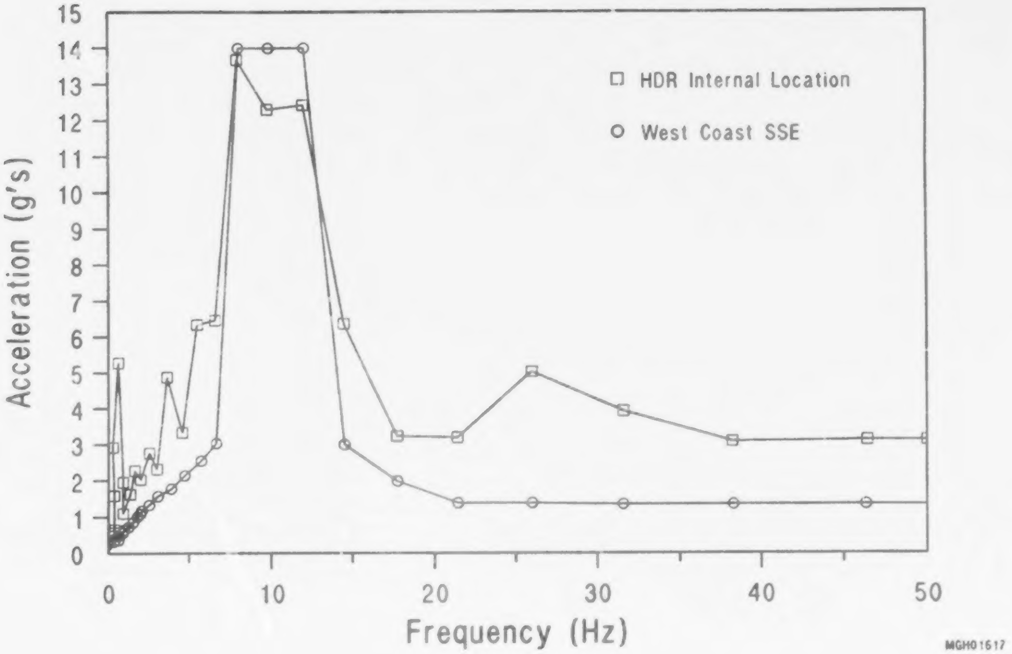

Figure 3. Acceleration response spectra of west coast SSE vs. HDR internal location.

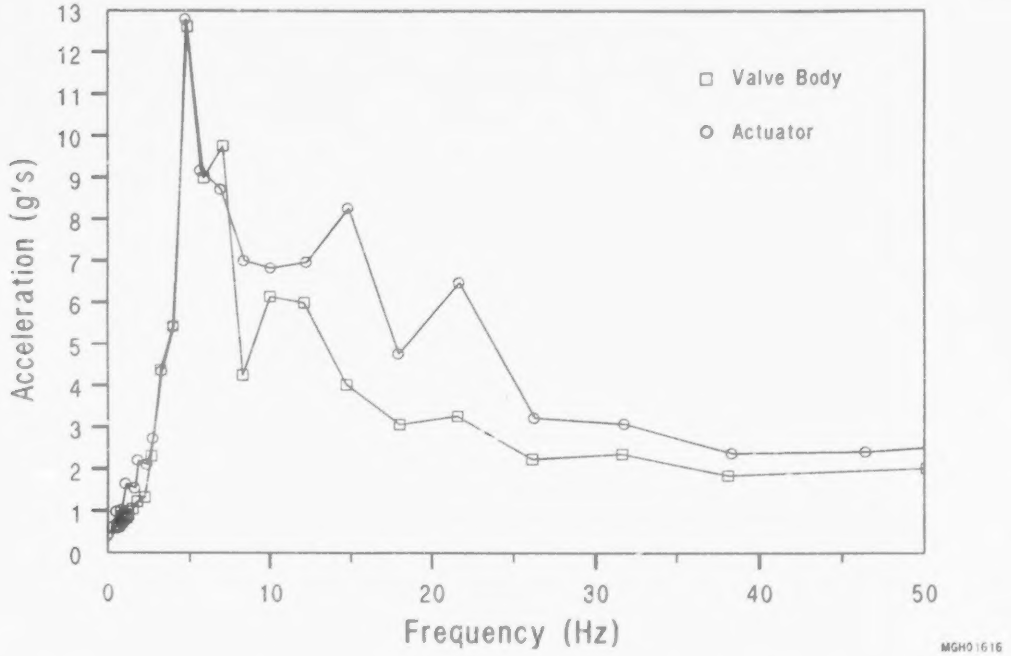

Figure 4. Acceleration response spectra of valve body and actuator.

pipe centerline). There was no indication of an actuator yoke bending mode in this frequency range during the single-effects qualification tests performed to the ANSI B16.41 standard. (The first fundamental frequency was determined to be approximately 28 Hz.) Therefore, it is likely that the relatively high actuator amplification indicated on Figure 4, which is as much as a factor of two at some frequencies, is caused by pipe dynamic response. This suggests that *in situ* seismic responses may cause some components to respond differently than they do during bench testing, and this should be considered in the qualification process.

Figure 5 shows the valve position and valve current during operation both prior to dynamic loading and during Tests 40.34 and 40.36, with initial shaker starting frequencies of 6.0 and 5.6 Hz, respectively. The differential pressure across the valve was approximately 384 psid in all cases. Figure 5 clearly indicates that valve stroke time and current were not influenced by the dynamic loadings during Tests 40.34 and 40.36.

Figure 6 shows the pin force versus time of a snubber which failed to resist input motion shortly after Test 40.34 began and a snubber which did resist input motion. In total, four mechanical snubbers of one manufacturer were replaced, three for failure to resist dynamic movement and one for locking up with a 0.01 m (1/2-in.) piping displacement. The cause of the apparent snubber malfunction is under investigation. One mechanical snubber of another manufacturer (Pacific Scientific) and one hydraulic snubber (Bergen-Paterson) were exposed to all the stiff system tests and performed within design requirements. The four replacement Pacific Scientific mechanical snubbers also performed within design requirements.

## CONCLUSIONS

The aged, 8-in., motor-operated gate valve installed in the VKL piping system was unaffected by the seismic loadings it was subjected to during the first three tests of the HDR test program. A companion project at the INEL seismically tested three other valves of nuclear quality and found no change in performance due to seismic loads. These results support the conclusion that in a nuclear piping system, the pressure boundary and load carrying structure of a qualified valve will not be damaged by the loads resulting from a seismic event.

The unexpected *in situ* amplification of the actuator response and the high frequency content of the response require additional analyses to determine the possible impact on the present qualification requirements of ANSI B16.41. Of specific interest are the qualification requirements of the actuator control components (switches, positioners, etc.) that are mounted in the valve assembly.

Four mechanical snubbers of the same manufacturer malfunctioned during the first four tests, three for failure to lock up properly during the first test and one for locking up with the pipe deflected after the fourth test. This may be a generic problem with this brand of snubbers, and investigations are continuing to determine the cause.

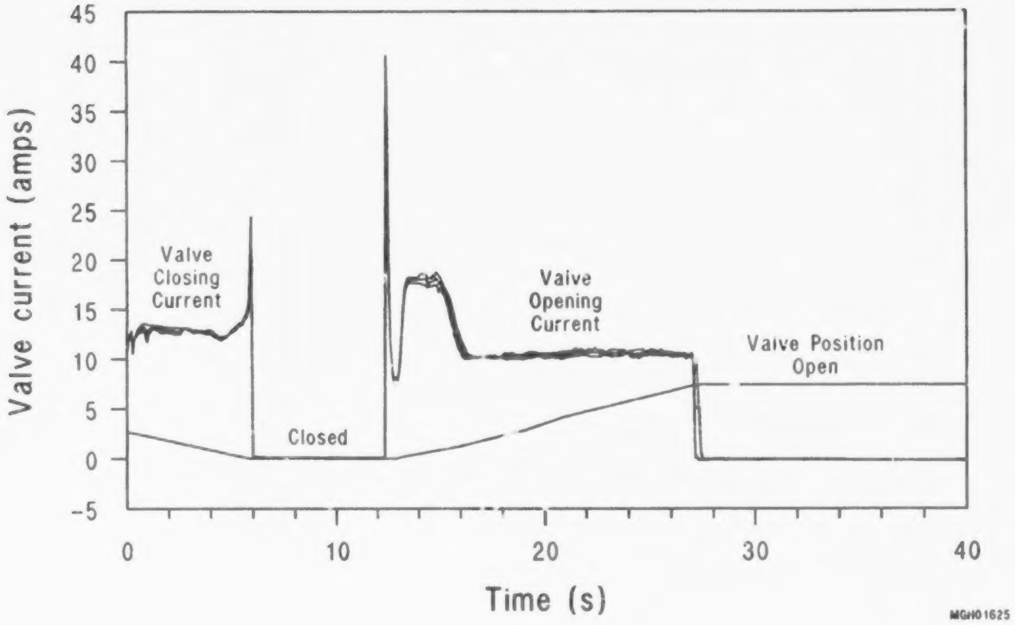

Figure 5. Valve position and valve current before dynamic loading and during Tests 40.34 and 40.36.

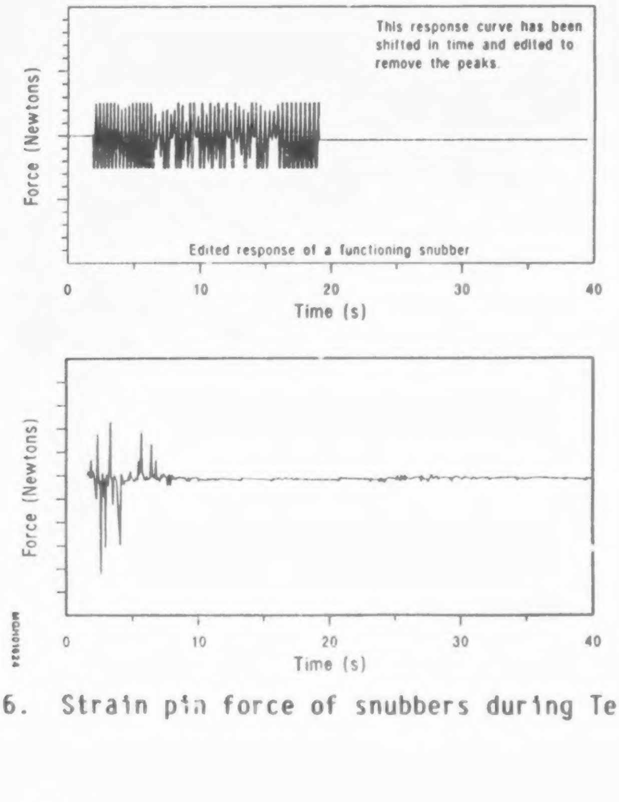

Figure 6. Strain pin force of snubbers during Test 40.34.

AVAILABLE

# NOTICE

This report was prepared as an account of work sponsored by an agency of the United States Government. Neither the United States Government nor any agency thereof, or any of their employees, makes any warranty, expressed or implied, or assumes any legal liability or responsibility for any third party's use, or the results of such use, of any information, apparatus, product, or process disclosed in this report, or represents that its use by such third party would not infringe privately owned rights. The views expressed in this paper are not necessarily those of the U.S. Nuclear Regulatory Commission.

BLANK PAGE

# Progress on Qualification Testing Methodology Study of Electric Cables

Y.Kusama, T.Yagi, S.Okada, M.Ito, M.Yoshikawa, K.Yoshida,
N.Tamura, W.Kawakami
Japan Atomic Energy Research Institute (JAERI), Takasaki
Radiation Chemistry Research Establishment

## ABSTRACT

Five kinds of insulating and jacketing materials such as ethylenepropylene rubber, crosslinked polyethylene, silicone rubber, chlorosulfonated polyethylene and chloroprene used for nuclear power plants were exposed to various sequential LOCA testing environments composed of pre-irradiation and the following steam/spray exposure. Experimental conditions of exposures in the sequential tests were systematically altered in order to estimate the effect of these conditions on mechanical and electrical degradations. Water sorption during the steam/spray exposure was investigated as well.

The experimental data show that factors effective to cause mechanical degradation were irradiation dose. dose rate. irradiation atmosphere and steam temperature. Irradiation under oxidative conditions such as at low dose rate, at elevated temperature and in pressurized oxygen caused remarkable electrical degradation and large water sorption during subsequent steam/spray exposure.

It can be concluded that degradation under various simultaneous LOCA exposures, in which irradiation and steam/spray are applied simultaneously. even an extreme case of a long term test will be well simulated by applying suitable sequential test conditions such as pre-irradiation under oxidative environments followed by high temperature air-containing steam exposures.

## 1. INTRODUCTION

Safety-related electrical cables (class 1E) in nuclear power plants are supposed to be exposed to radiation. high temperature steam. spray. and in certain cases. air, simultaneously when a LOCA (loss of coolant accident) occurs. These cables are required to be functional even if they are subjected to a LOCA at the end of their intended service life. To confirm the integrity of the cables under LOCA, qualification tests have been carried out under simulated environments which were specified by individual countries according to types of their reactors.

In Japan. cable makers qualify their cables by the sequential method based on the recommendation issued by IEEJ in 1982(1). In the 13th meeting. we compared mechanical and electrical degradations of Hypalons and EPR's under four kinds of simultaneous LOCA environments (one week duration and three months duration for both air-free and air-containing) with those under various combinations of the pre-irradiations and the steam/spray exposures, and discussed a possibility of simulation of the simultaneous environments by selecting suitable conditions in the sequential methods. In the present work, we develop the comparison to the water sorption as well as the mechanical and electrical properties of five kinds of insulating materials, on the basis of more detailed data in the sequential LOCA exposures.

## 2. EXPERIMENTAL

### 2.1 Materials

Five kinds of insulating and jacketing materials such as ethylenepropylene rubber(EPR), crosslinked polyethylene(XLPE), silicone rubber(SiR), chlorosulfonated polyethylene(Hypalon) and chloroprene(CR) were exposed to various conditions of sequential LOCA-environments. The thickness of the samples was about 1 mm. Dumbbell-shaped samples and sheets of 8x8 $cm^2$ were used for a tensile test and electrical property measurements, respectively. These samples included materials formulated for cables of general use (marked with asterisk) for fire-retardant safety-related cables used in nuclear power plants as listed in Table 1.

### 2.2 LOCA Simulation

The sequential test is composed of two procedures, that is irradiation, which will be called pre-irradiation hereafter, and steam/spray exposure. Both pre-irradiation and steam/spray conditions were systematically altered in order to find adequate conditions which can bring about the degradation to the same degree as four kinds of simultaneous environments reported previously as shown in Table 2(2).

The experimental conditions were summarized and listed in Table 2.

Pre-irradiations:

Sheet and dumbbell-shaped samples were irradiated with Co-60 gamma rays up to 2 MGy with a dose rates ranging from 0.45 to 10 kGy/h in air at room temperature. The above dose rate range can cover Japanese PWR plant qualification test conditions.

In some cases, samples were pre-irradiated under oxidative conditions as elevated temperature (50,70,90 °C) and in pressurized oxygen (0.5MPa, at room temperature) in which oxygen supply was expected to be sufficient to approach complete oxidation of the samples.

Steam/spray Exposure:

The steam/spray exposures following the pre-irradiations were performed under various conditions as shown in Table 2 by using a LOCA-simulating apparatus SEAMATE-II(4,5,6).

Quantity and composition of the chemical spray were according to IEEE Std. 323-1974(6). In most cases, the irradiated samples were exposed to saturated steam and air-containing steam (0.05MPa) of constant temperature at 120 °C.

Effect of temperature in steam/spray exposure on the degradations was investigated in the range from 120 to 160°C for both cases of air-free and air-containing steam. The effect of air partial pressure in steam environments on the degradations was also investigated in the range from 0.05 to 0.5 MPa.

### 2.2 Measurement

Tensile properties were measured by using an Instron tension tester (type 1130) and Shimazu Autograph (type DCS-500) with a cross head speed of 500 mm/min.

Volume resistivity at 1 minute after impression of the 500 V D.C. was measured by a high resistance meter and a resistivity cell (Yokogawa-Hewlett-Packard 4329A and 16008A). All the measurements were performed at room temperature two weeks after the LOCA exposures.

## 3. RESULTS AND DISCUSSION

### 3.1 Effect of pre-irradiation conditions on the degradation of tensile and electrical properties

Figures 1 to 5 show the tensile properties and the volume resistivity of the insulating and jacketing materials irradiated under various conditions. In these figures, Tb,Eb, and Tbo, Ebo, are the tensile strength and elongation at break and volume resistivity and their original values, respectively. Values in these figures except for XLPE are averages of the numbers of samples of the same kind listed in Table 1.

Mechanical properties , especially elongation at break markedly decreases with increasing dose. Mechanical degradation except for XLPE is slightly dependent upon the irradiation conditions. For the XLPE, rapid decrease in the elongation at break is observed when the sample is irradiated under oxidative conditions such as irradiation at low dose rate, at elevated temperature or in pressurized oxygen.

Volume resistivity of the insulating materials, on the other hand, is influenced in some extent by irradiation conditions. Larger decrease in volume resistivity of EPR, XLPE and SiR are observed under oxidative irradiation and the decreases are within two orders of magnitude by 1.5 MGy irradiation which is supposed to be subjected in PWR-LOCA.

### 3.2 Effect of irradiation conditions on the degradation caused by subsequent steam/spray exposure

Materials irradiated to 1.5 MGy under the various conditions shown in Table 2 were exposed to air free and air-containing 0.05MPa) steam/spray environments at 120°C.

In many cases, influences of irradiation conditions on the degradation are more obvious when they exposed to air-containing steam than air-free steam environment. Figures 6 to 10 show mechanical degradation of above materials exposed to the air-containing (0.05MPa) steam.

Figure 6 shows effect of pre-irradiation conditions on the mechanical properties of the EPR in the following steam/spray exposure. Remarkable dose rate effect on the mechanical degradation, especially on the tensile strength, is observed during steam exposure. irradiation at low dose rate causes greater degradation than irradiation at high dose rate. In order to estimate dose rate dependence on the mechanical degradation in the following steam/spray exposure, the time when the toughness reduced to half of the original value was plotted against dose rate. Dose rate dependence on the rate of degradation of toughness for the EPR in the following steam/spray exposure is estimated to be about -1st power.

Figure 7 shows effect of pre-irradiation conditions on the mechanical properties of the XLPE. In this case, dose rate dependence is not remarkable. Usually, elongation at break is recovered by steam exposure when the sample was irradiated in air at room temperature. Elongation recovery, on the other hand, was not observed when the sample was irradiated at elevated temperature. Irradiation in pressurized oxygen causes great mechanical degradation in the subsequent steam exposure, and the measurement was impossible.

Figure 8 to 10 show results of SiR, Hypalon and CR. Mechanical degradation of the SiR is not influenced by not only dose rate but also irradiation temperature and atmosphere. Hypalon shows a dose rate dependence on the mechanical degradation. Large decrease in the mechanical property, especially elongation at break is observed when the sample is irradiated at oxidative conditions such as at elevated temperature and in pressurized oxygen as compared with irradiation at non oxidative conditions. CR shows a significant decrease in the elongation at break irradiated under oxidative conditions, especially in pressurized oxygen.

Figure 11 shows volume resistivity of EPR and XLPE irradiated under various conditions followed by air-containing steam exposure at 120°C. Decrease in volume resistivity is remarkable when the samples are irradiated at lower dose rate than at high dose rate irradiation. The largest resistivity decrease is caused for EPR when the sample is irradiated in pressurized oxygen.

It is considered that unstable oxidized species formed during pre-irradiation does not affect the mechanical degradation prior to steam exposure, but these species decompose and promote mechanical degradation when they are exposed to the steam environment. Formation of these species mainly depends on irradiation conditions, because oxygen can diffuse sufficiently through the samples in the case irradiated at low dose rate, at elevated temperature or in pressurized oxygen.

Figure 12a,12b show effect of irradiation conditions on the water sorption of EPR and Hypalon in the following air-containing steam exposure. Higher water sorption is observed when the samples are irradiated under oxidative conditions than when irradiated at high dose rate.

### 3.3 Effect of Steam Temperature on the degradation of insulating materials

Samples irradiated to 1.5MGy with a dose rate of 10 kGY/h were exposed to air-free and air-containing steam at 120, 140, and 160°C for 264 hours, respectively.

Figure 13 shows the effect of steam temperature on the degradation of Hypalon and EPR. Both mechanical and electrical properties degrade significantly with increasing temperature, especially in air-containing steam environment. Higher decrease in volume resistivity and water sorption are brought about by exposure to high temperature air-containing steam.

This may indicate that resistivity decreases are caused by absorbed and retained water molecules inside the materials due to the oxidized substances formed during pre-irradiation. Exposure to high temperature air-containing steam promotes futher oxidation which may cause futher resistivity decrease(7,8,9,10).

The silicone rubber is not influenced by the amount of air added to steam environments, but great decrease in mechanical property is caused by high temperature steam exposure. This may be caused by hydrolysis of the material with chemical spray solution at high temperature.

### 3.4 Effect of air over pressure in steam exposure on the degradation of insulating materials

Samples irradiated up to 1.5MGy with a dose rate of 10 kGy/h in air at room temperature were exposed to steam/spray environments at 120°C for 264 hours where air added to saturated steam by 0.05, 0.13, 0.25 and 0.5 MPa.

Figure 14 shows mechanical and electrical properties of Hypalon, EPR and XLPE. Slight changes in the mechanical properties of the materials except for XLPE are caused by air added to the steam at levels up to 0.25MPa, but significant damages are seen at 0.5MPa. On the other hand, increasing air content does not always promote resistivity decrease. For some EPR, resistivity decrease is the most remarkable when the additional air partial pressure is 0.05MPa. As reported before, the suppression of the resistance decrease for EPR with increasing oxygen content in the steam may result from the removal of electrically sensitive species from the materials. This is assumed to be brought about by mechanical degradation which may proceed oxygen diffusion into the samples.

### 3.5 Effect of spray on the degradation of the insulating materials

Samples irradiated at room temperature in air with 10 kGy/h and at 70°C in air with 5 kGy/h were exposed to air-containing steam with and without spray for 264 hours.

Figure 15 shows degradation behaviors of toughness, resistivity and water sorption of the materials. Spray promotes mechanical degradation of Hypalon and XLPE. On the contrary, SiR is scarcely influenced by spray. Mechanical degradation of the EPR exposed to steam/spray or spray-free environments depends on pre-irradiation conditions, that is, larger damage is observed under the exposure to spray-free environment when the sample is pre-irradiated at high dose rate. However, presence of spray in steam environment does not affect the mechanical degradation when the irradiation is carried out at elevated temperature.

Presence of spray in the steam exposure does not affect the electrical degradation of the XLPE and the SiR, but enhances that of the EPR. Contrary to the mechanical degradation, larger resistivity decrease of the Hypalon is observed when the sample is irradiated at elevated temperature.

These complicated phenomena are assumed to be due to accumulation of the oxidized species in the materials and their extraction from the materials by chemical spray or some times chemical reaction with spray solution.

We have mentioned the effect of pre-irradiation conditions and steam/spray exposure conditions on the mechanical and electrical degradation of the insulating materials. Extensive data obtained under various sequential LOCA exposures are shown by using radar chart, in order to compare degradation and to find suitable conditions which can bring about same extent of degradation produced under the various simultaneous environments as shown in Table 2.

Figures 16, 17 and 18 show ultimate elongation, resistivity and water sorption of the EPR exposed to various sequential LOCA exposures, respectively. Elongation and resistivity are normalized to the original values, and water sorption is weight increase normalized to the initial weight. Smaller radii in Figures 16 and 17 correspond to lager degradation, but in Figure 18 lager radii correspond to large water sorption. In these figures, solid lines and dotted lines show data obtained under air-containing steam and air-free steam environments, respectively. It is obvious that factors effective to cause mechanical degradation for the EPR are radiation dose, dose rate and irradiation atmosphere. For electrical degradation and the water sorption, dose rate and irradiation atmosphere as well as steam temperature enhance degradation. As shown in Figure 16, irradiation under oxidative condition followed by air-containing steam exposure can produce same degree of degradation obtained under a long term simultaneous exposure (three months with air shown by the circle sim-D).

Figures 19, 20 and 21 show degradation behaviors of the Hypalon under various sequential LOCA exposures. Dose, dose rate as well as steam temperature are effective to cause mechanical degradation. Steam temperature is the most effective for the electrical degradation. In addition to steam temperature, irradiation atmosphere is effective to enhance water sorption.

For XLPE, additional air in the steam exposure as well as irradiation atmosphere causes mechanical degradation, and in

AVAILABLE

addition, steam temperature remarkably degrades electrical properties.

For SiR, on the other hand, high temperature steam exposure other than irradiation dose affects the mechanical degradation. Only steam temperature causes resistivity decrease.

For CR, effects of irradiation condition are not obvious because mechanical degradation is too great when the sample is irradiated up to 1.5MGy.

## 4. CONCLUSION

Effects of simulated LOCA-conditions in sequential method on the mechanical and electrical properties and on water sorption of the insulating materials were systematically investigated. It can be concluded that factors effective to cause mechanical degradation are irradiation dose, dose rate, irradiation atmosphere and steam temperature. Electrical degradation and water sorption are influenced by oxidative irradiation such as irradiation at low dose rate, at elevated temperature or in pressurized oxygen. Especially, significant damages were caused by irradiation under oxidative environments and with subsequent exposure to high temperature air-containing steam.

Degradation under various simultaneous LOCA exposures including even an extreme case of long term air-containing exposure will be well simulated by a short period sequential test condition. for example, pre-irradiation carried out under oxidative conditions and following exposure to high temperature air-containing steam/spray environments.

## REFERENCE

(1) "Proposed environmental and flame test method of electric wires and cables for nuclear power station", Inst. Electrical Engineers of Japan Technical Report(Part 2) No. 139 Nov. 1982 IEEJ (Tokyo)

(2)S.Okada, Y.Kusama, M.Ito, T.Yagi, M.Yoshikawa, K.Yoshida, N.Tamura, W.Kawakami, "Progress on Qualification Testing Methodology Study of Electric Cables", Proceedings of the U.S. Nuclear Regulatory Commission NUREG/CP-0071 Oct. (1985)

(3) S. Tanaka, Y. Nakase, Y.Kusama, M.Ito, S.Okada, K.Yoshida, "Engineering data of SEAMATE-II, 1.Rapid heating test", JAERI-M 9361 (1981)

(4) S.Tanaka, Y.Nakase, S.Okda, M.Ito, Y. Kusama, K.Yoshida, "Engineering data of SEAMATE-II, 2. Test on the characteristics of temperature regulation in the pressure vessel", JAERI-M 9699 (1981)

(5) S.Okada, Y.Nakase, Y.Kasahara, S.Tanaka, M.Ito, Y.Kusama, K.Yoshida, "Constitution and performance of the electrical loading system in SEAMATE-II", JAERI-M 9706 (1981)

(6) IEEE Std. 323-1974. "IEEE Standard for Qualifying Class 1E Equipment for Nuclear Power Generating Stations". IEEE Inc., New York (1974)

(7) T.Yagi, Y.Kusama, M.Ito, S.Okada, M.Yoshikawa, K.Yoshida, "Swelling Behavior of gamma ray Irradiated Elastomers in Boiling Spray Solution". JAERI-M 83-072 (1983)

(8) S.Okada, M.Yoshikawa, M.Ito, Y.Kusama, T.Yagi, K.Yoshida, "Effects of LOCA-Simulating environments on electric property change of insulating materials". IEEJ Meeting on Electrical Insulation Materials, EIM-82-109 (1982)

(9) M.Yoshikawa, T.Seguchi, K.Yoshida, "Effect of radiation-induced oxidation and steam exposure on electrical insulation of high polymer", ibid., EIM-83-121 (1983)

(10) Y.Kusama, T.Yagi, M.Ito, M.Yoshikawa, S.Okada, K.Yoshida, "Effect of temperature in sequential LOCA exposure on the degradation of insulating materials", ibid., EIM-84-136 (1984)

Table 1 Insulating and jacketing materials for the cables tested under various sequential LOCA environments

| Sample Name | | Specification |
|---|---|---|
| Hypalon | A* , B* | Standard |
| | C , D | Unspecified |
| EPR | A* | Standard |
| | B , C | Unspecified |
| XLPE | A* | Standard |
| Chloroprene | B* | " |
| | A , C | Unspecified |
| Silicone | A , B | " |

Table 2 Test conditions of simultaneous LOCA exposures (2)

| CASE | TEST PERIOD | DOSE RATE (kGy/h) | DOSE (MGy) | AIR PARTIAL PRESSURE IN STEAM (MPa) |
|---|---|---|---|---|
| Sim-A | ~1 Week | 10 | up to 1.5 | 0 |
| Sim-B | ~3 Months | 0.6 | up to 1.4 | 0 |
| Sim-C | ~1 Week | 10 | up tp 1.5 | 0.05 |
| Sim-D | ~3 Months | 0.6 | up to 1.4 | 0.05 |

Temperature profile: PWR LOCA Profile and 120°C

Table 3 Test conditions of sequential LOCA exposures

| Pre-irradiation | Steam/spray Exposure |
|---|---|
| Dose : | Temperature: |
| 0.25 ~ 2.0MGy | 120, 140, 160°C |
| Dose Rate: | Air Over Pressure: |
| 0.45, 1, 5, 10 kGy/h | 0, 0.05, 0.13, 0.25, 0.5 MPa |
| Irradiation Temperature: | Chemical Spray: |
| R.T, 50, 70, 90°C | Yes, No |
| Irradiation atmosphere | |
| in Air at R.T. | |
| in Pressurized Oxygen (0.5MPa) | |

AVAILABLE

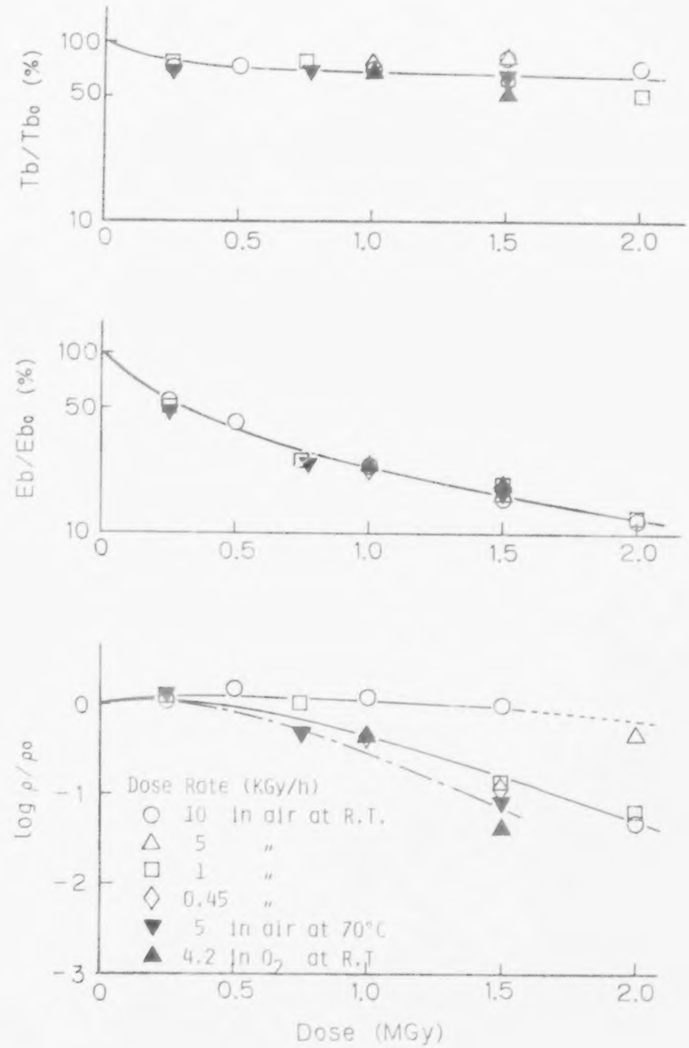

Fig. 1 Mechanical and electrical properties of the ethylenepropylene rubber irradiated under various conditions.

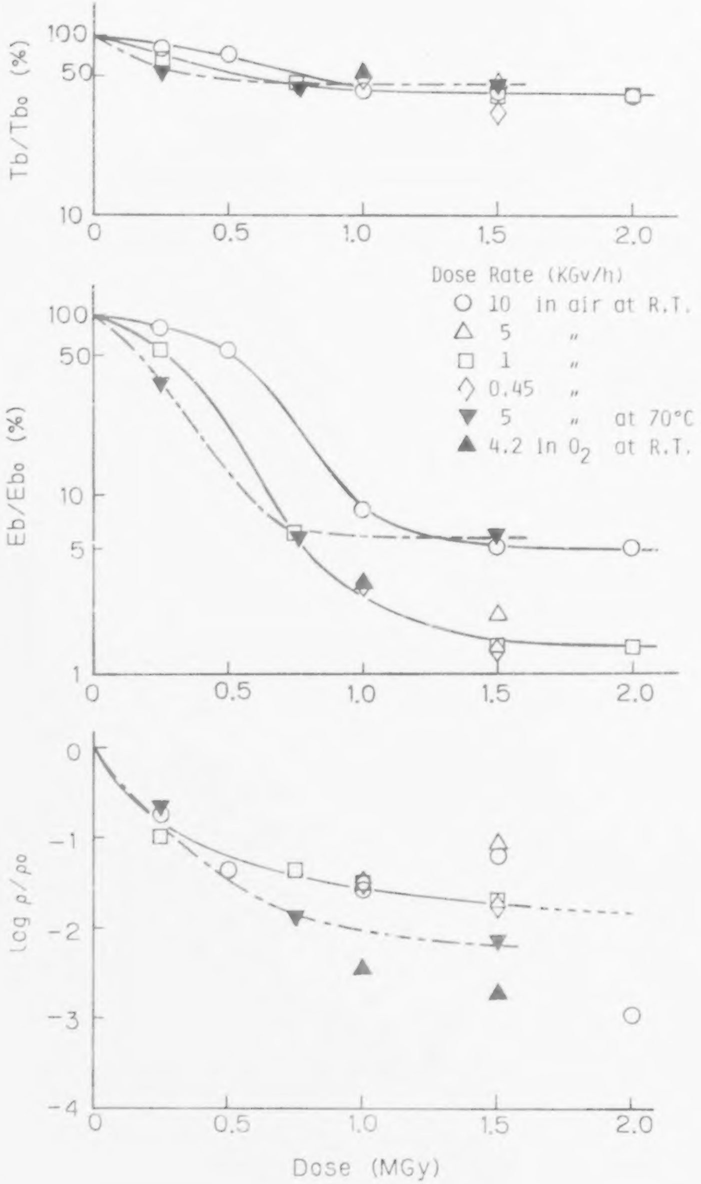

Fig. 2 Mechanical and electrical properties of the crosslinked polyethylene irradiated under various conditions.

AVAILABLE

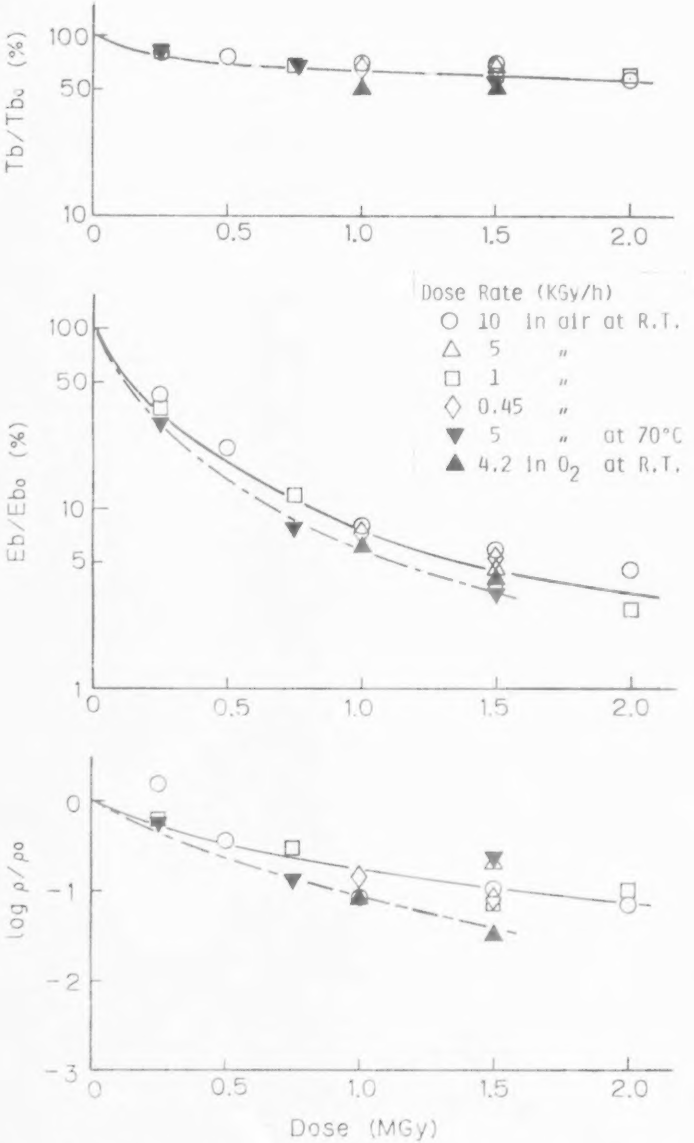

Fig. 3 Mechanical and electrical properties of the silicone rubber irradiated under various conditions.

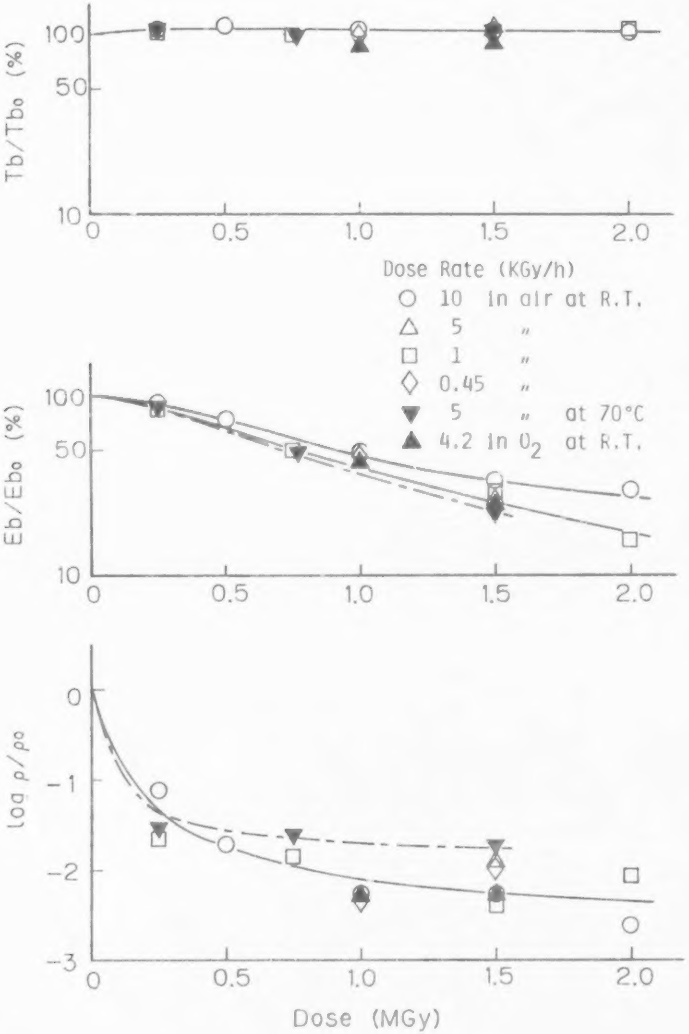

Fig. 4 Mechanical and electrical properties of the Hypalon irradiated under various conditions.

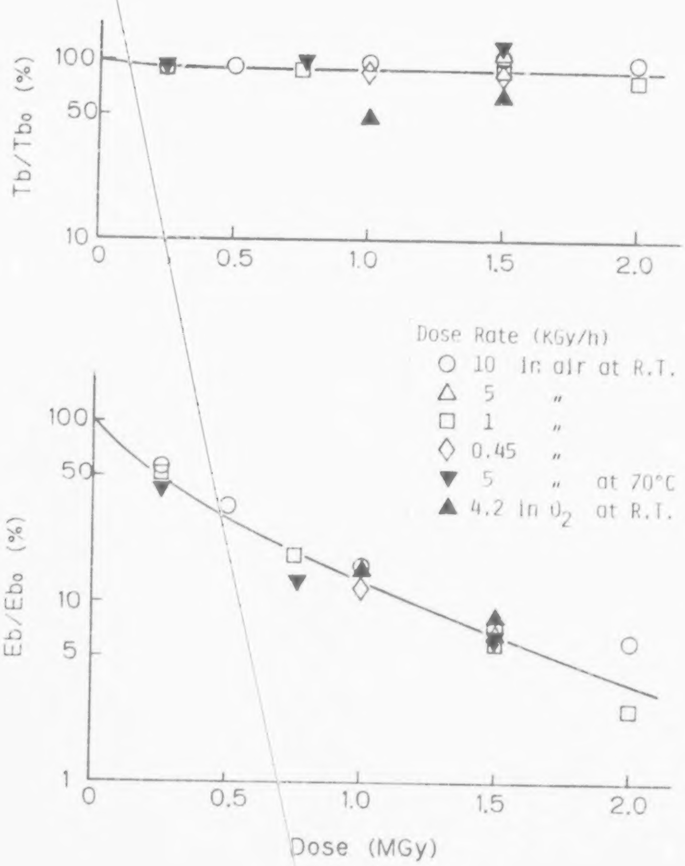

Fig. 5 Mechanical and electrical properties of the chloroprene irradiated under various conditions.

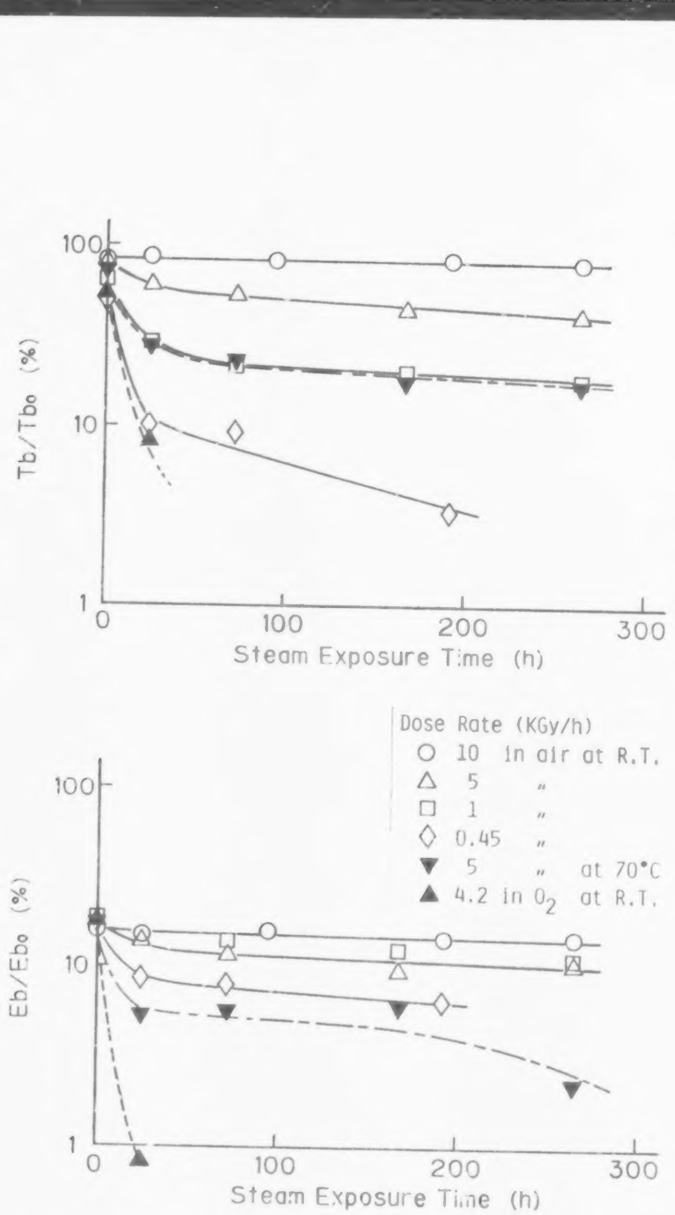

Fig. 6 Effect of pre-irradiation conditions on the mechanical properties of the ethylene-propylene rubber in the following steam/spray exposure.

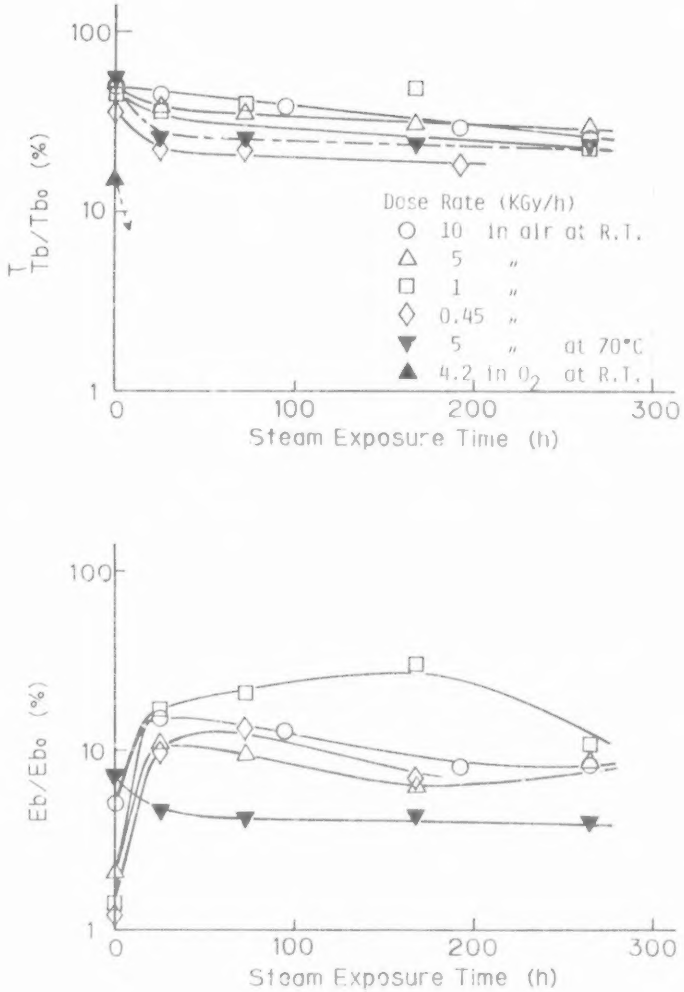

Fig. 7 Effect of pre-irradiation conditions on the mechanical properties of crosslinked polyethylene in the following steam/spray exposure.

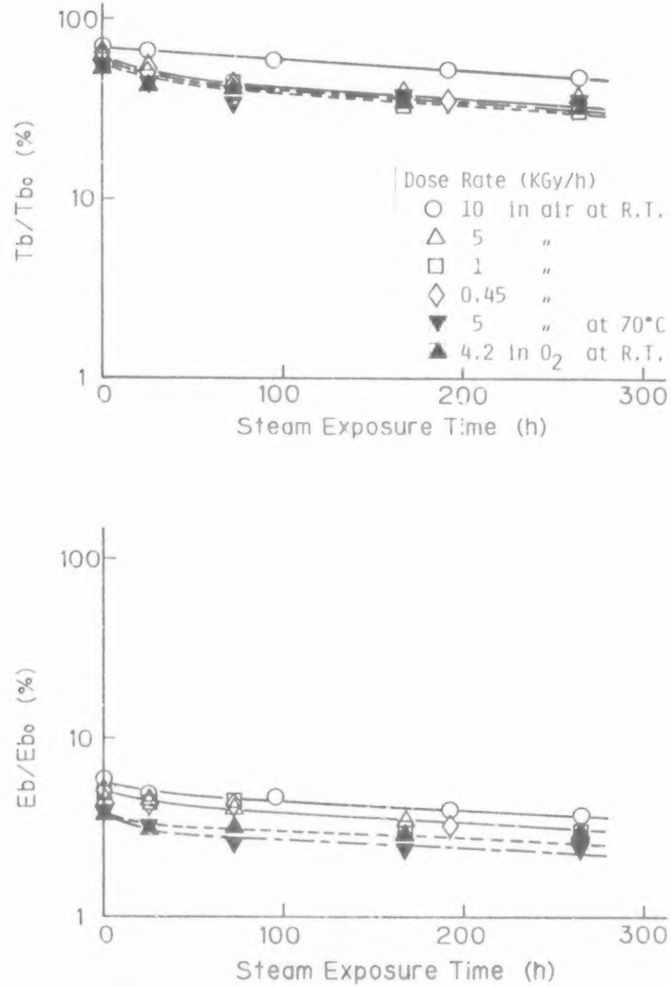

Fig. 8 Effect of pre-irradiation conditions on the mechanical properties of the siicone rubber in the following steam/spray exposure.

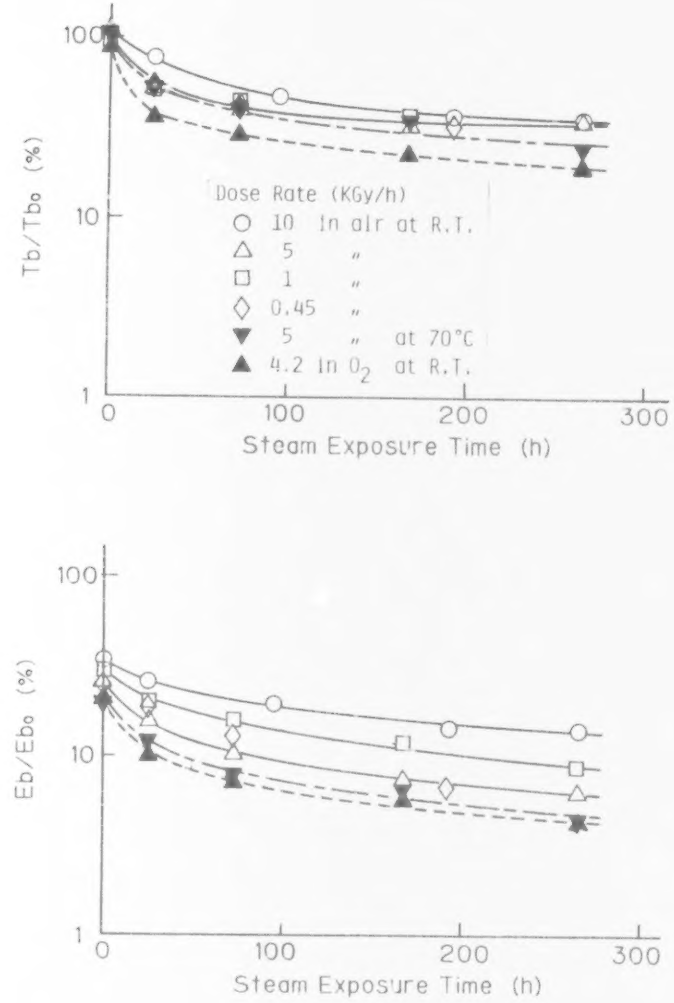

Fig. 9 Effect of pre-irradiation conditions on the mechanical properties of the Hypalon in the following steam/spray exposure.

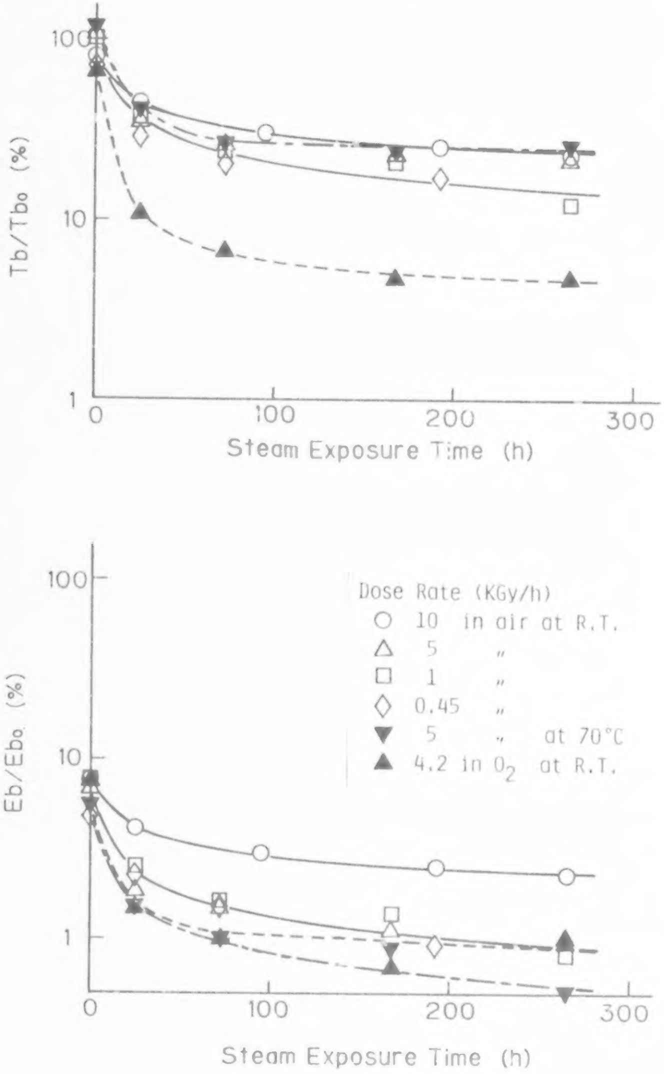

Fig. 10 Effect of pre-irradiation conditions on the mechanical properties of the chloroprene in the following steam/spray exposure.

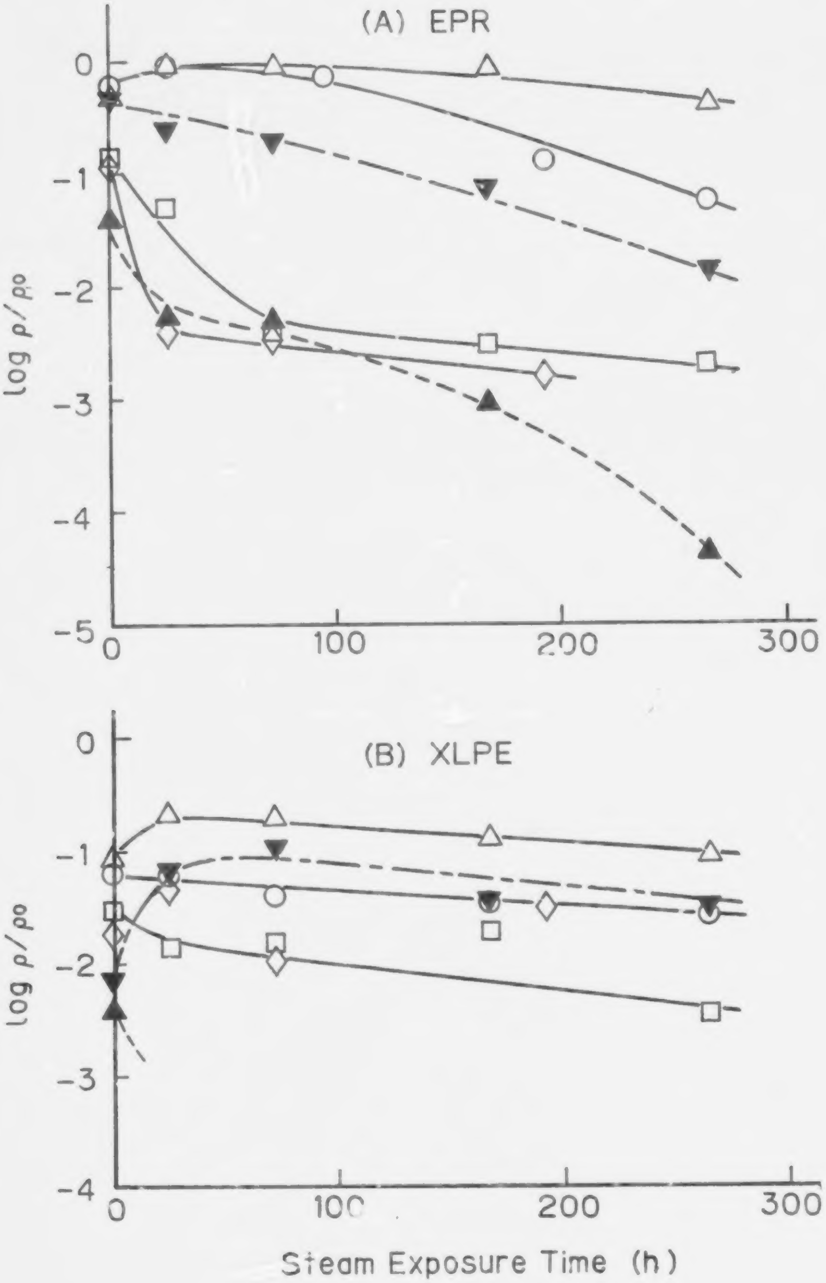

Fig. 11 Effect of pre-irradiation conditions on volume resistivity of the EPR and XLPE in the following steam/spray exposure.

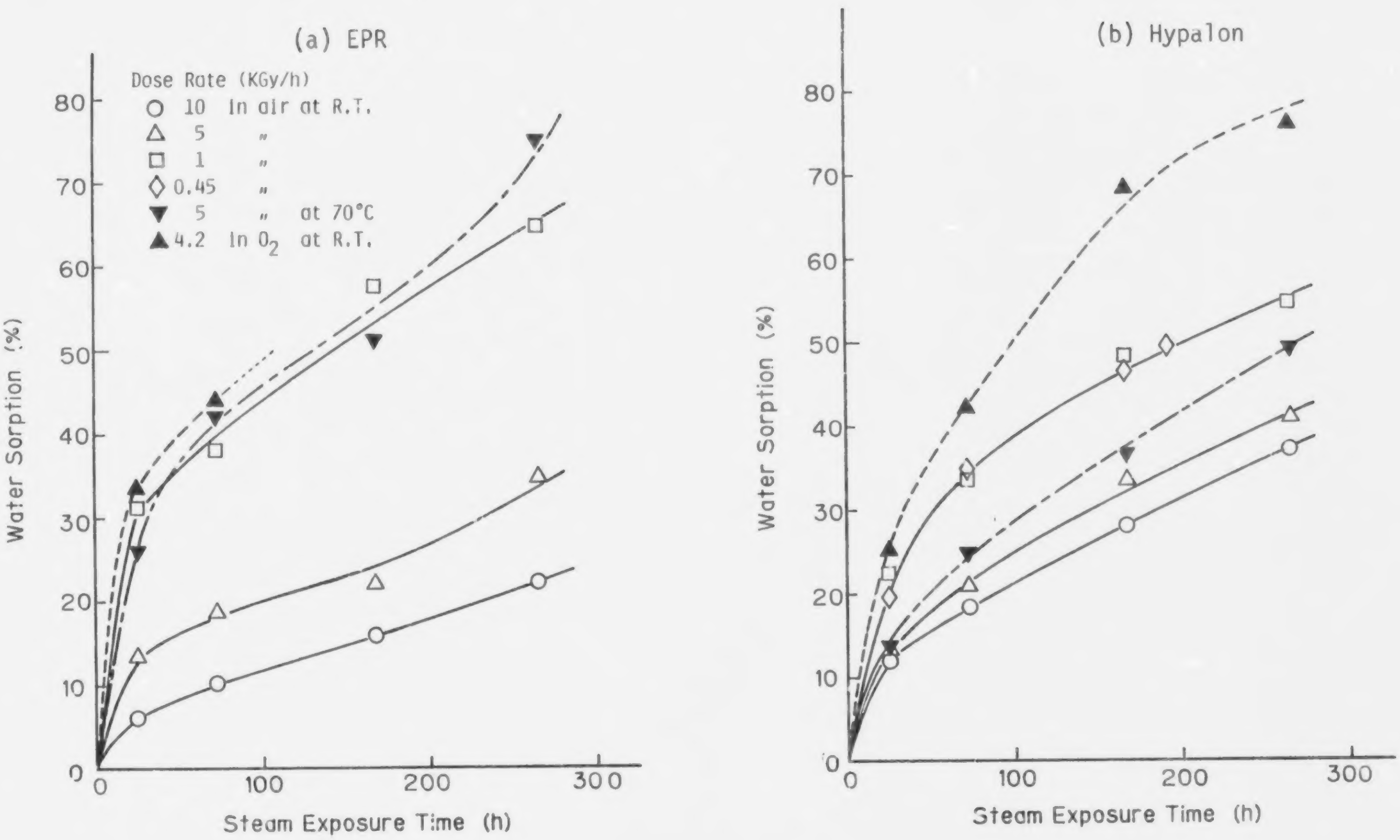

Fig. 12a,b Effect of pre-irradiation conditions on the water sorption of EPR and Hypalon in the following air-containing steam exposure.

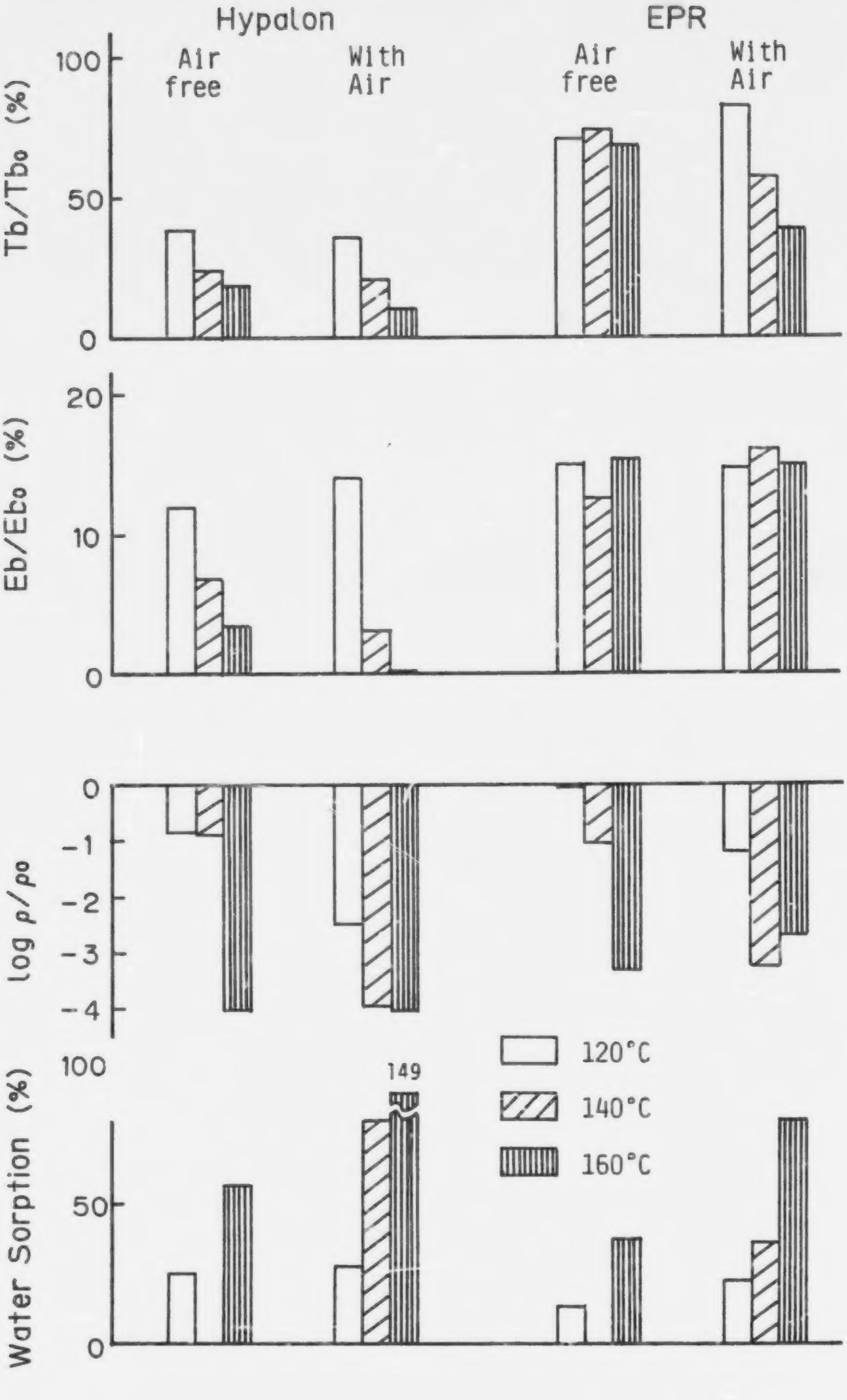

Fig. 13 Effect of steam temperature on mechanical and electrical properties and water sorption of the EPR and Hypalon in the following air free and air-containing steam exposure.

BEST COPY AVAILABLE

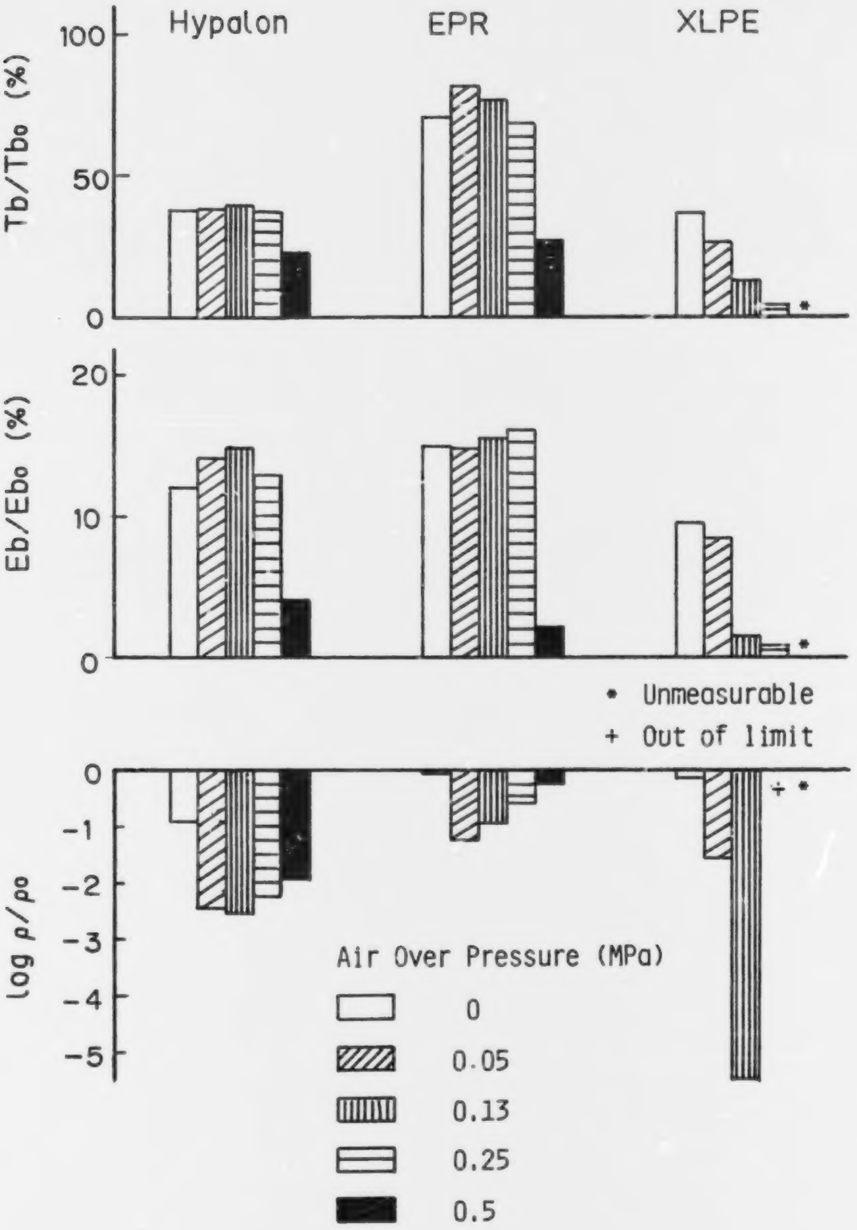

Fig. 14 Effect of air over pressure in steam/spray exposure on the mechanical and electrical degradation of the insulating materials.

BEST COPY AVAILABLE

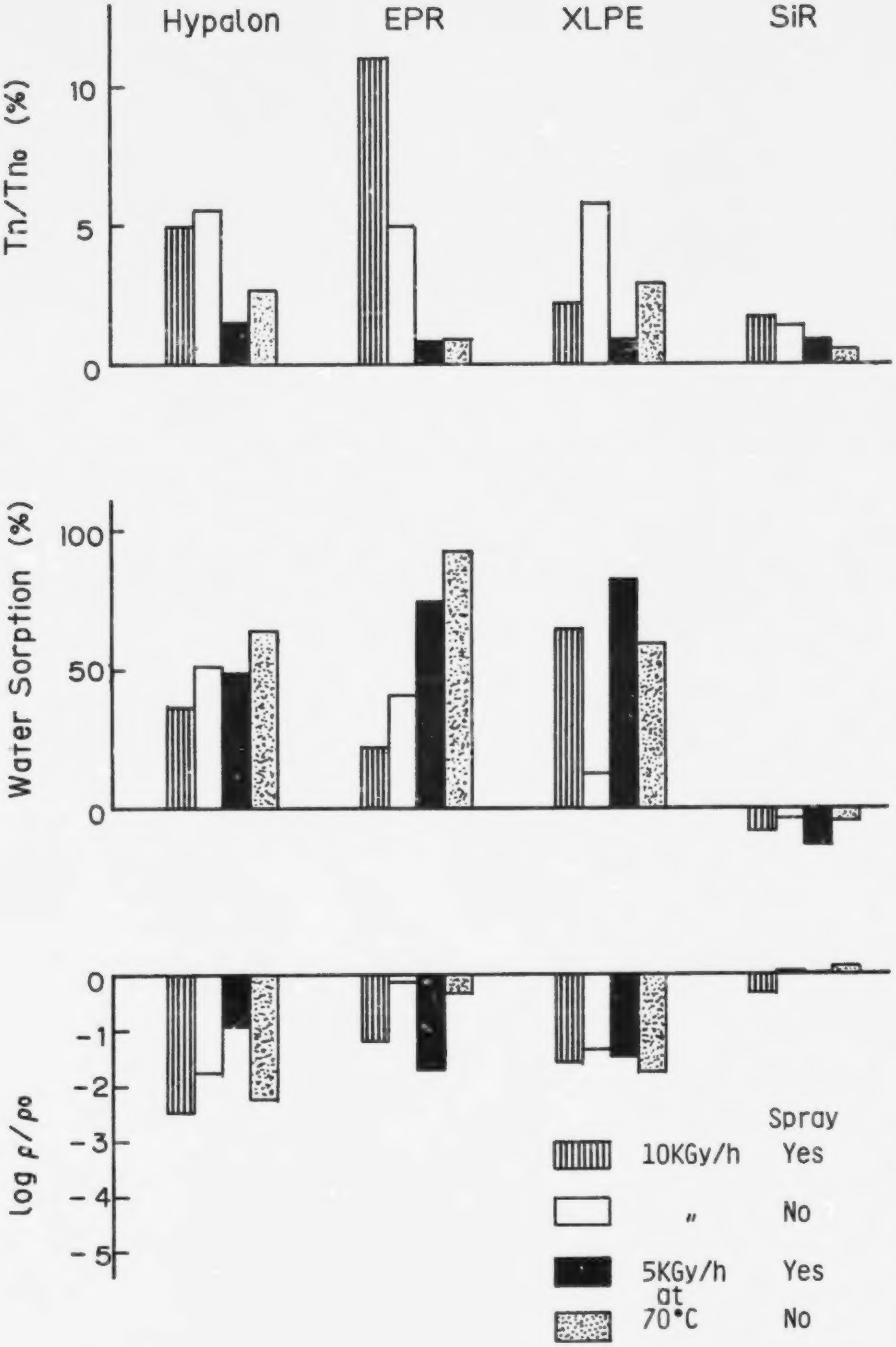

Fig. 15 Effect of spray on degradation of toughness, volume resistivity and water soption of the insulating materials.

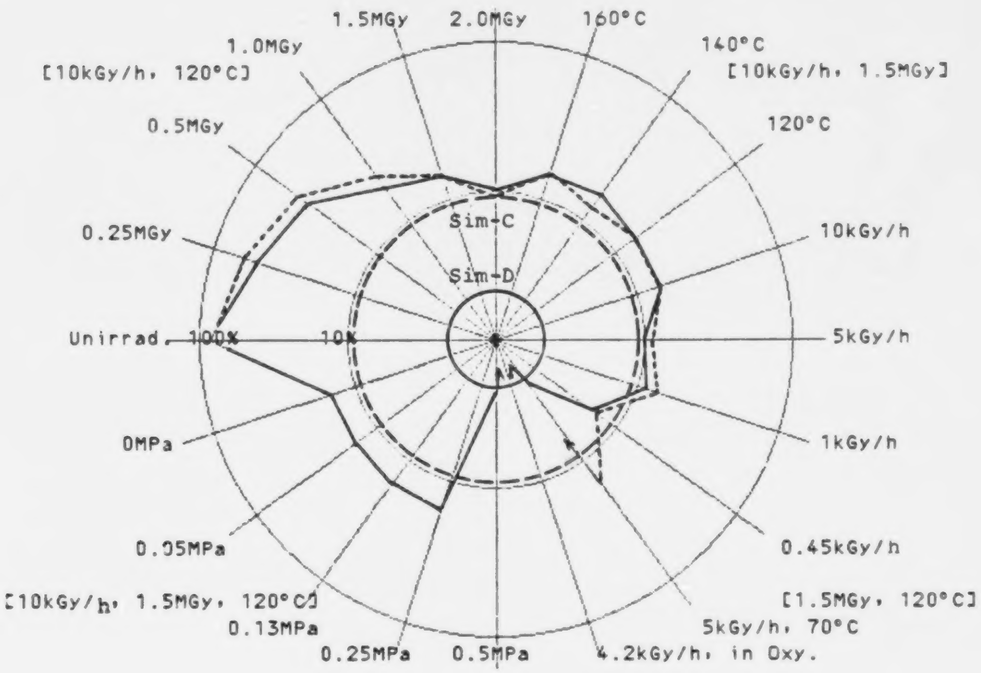

Fig. 16 Ultimate elongation of the EPR exposed to various sequential LOCA environments.

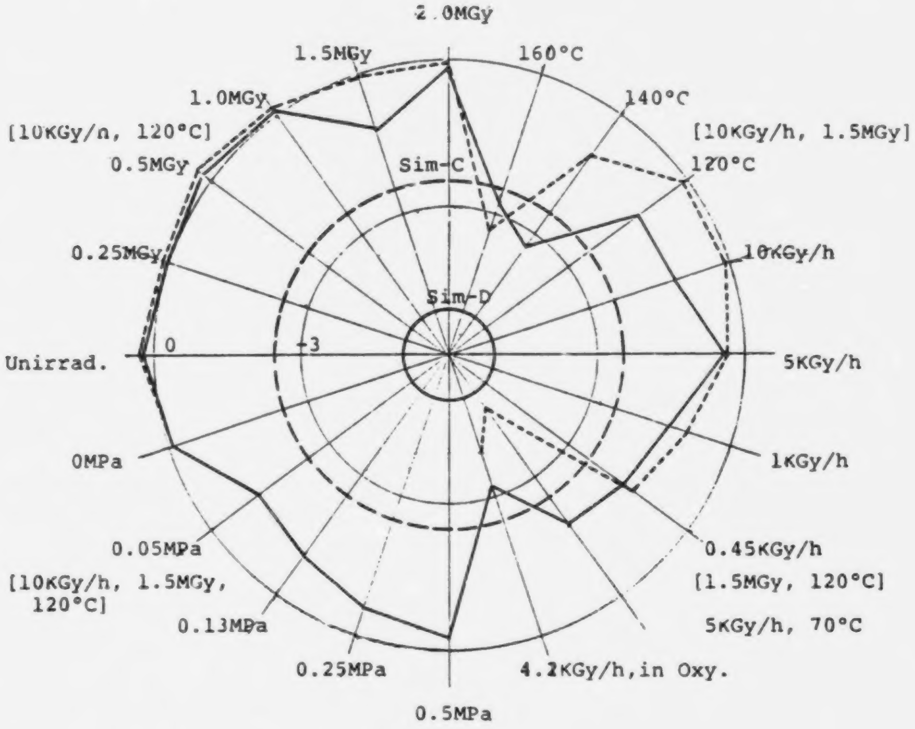

Fig. 17 Ultimate volume resistivity of the EPR exposed to various sequential LOCA environments.

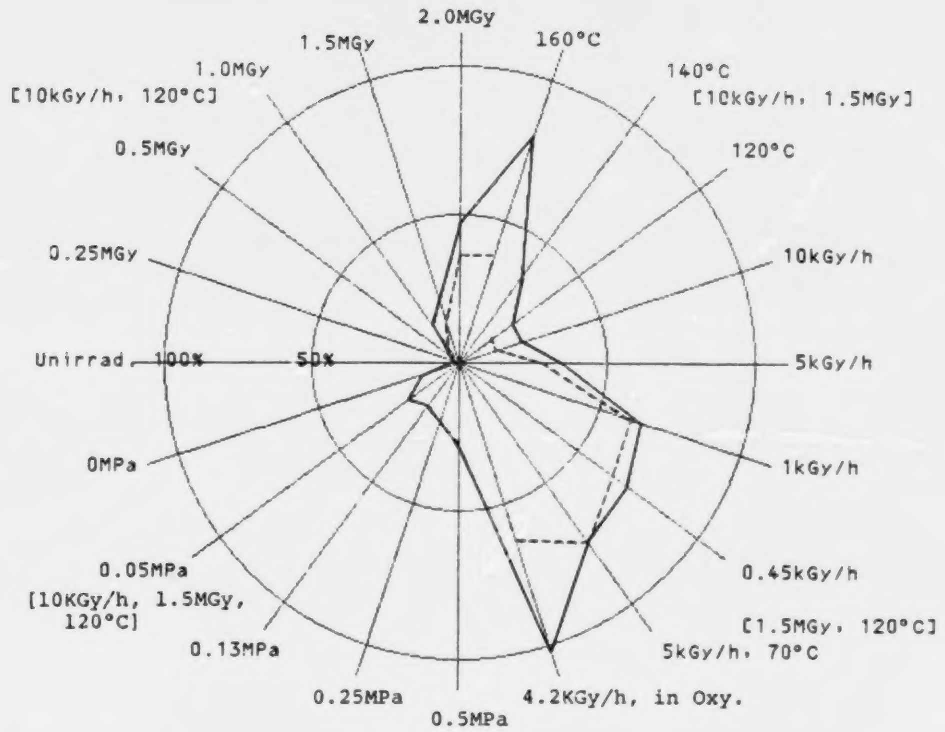

Fig. 18 Water sorption of the EPR exposed to various sequential LOCA environments.

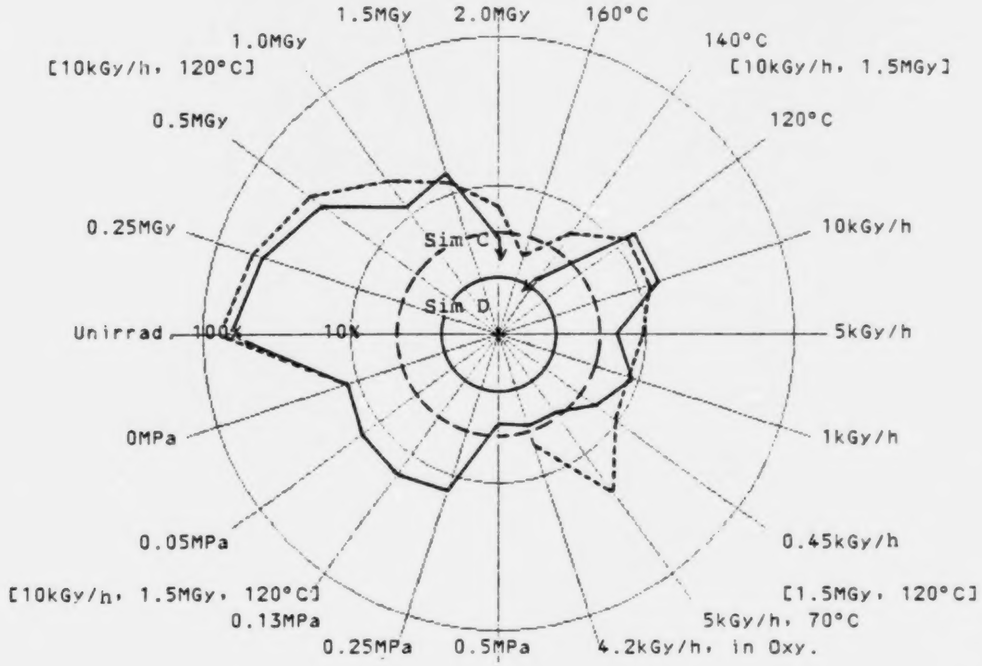

Fig. 19 Ultimate elongation of the Hypalon exposed to various sequential LOCA environments.

BEST COPY AVAILABLE

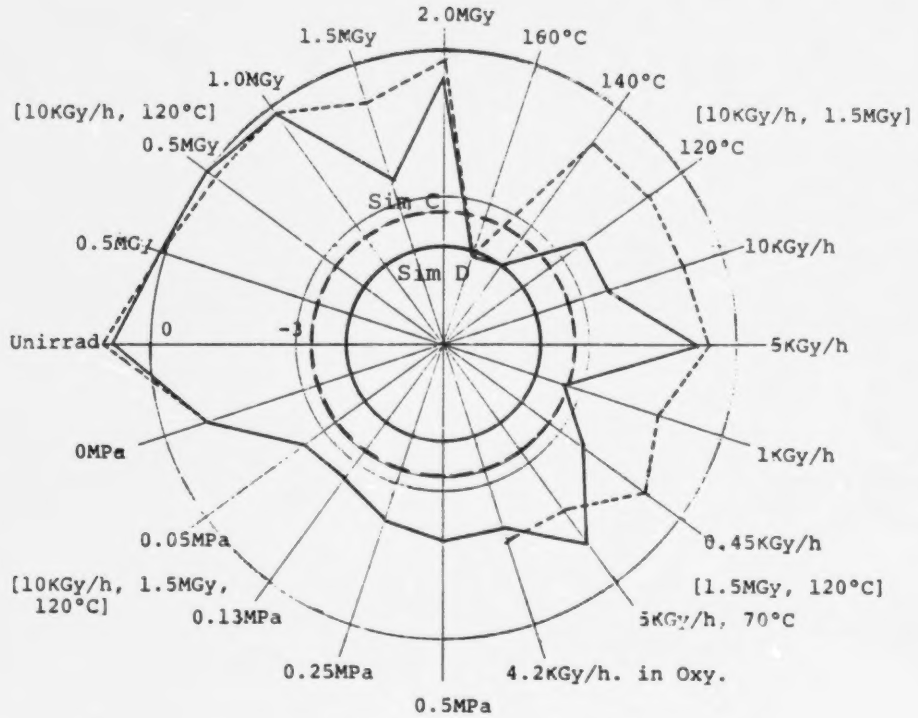

Fig. 20 Ultimate volume resistivity of the Hypalon exposed to various sequential LOCA environments.

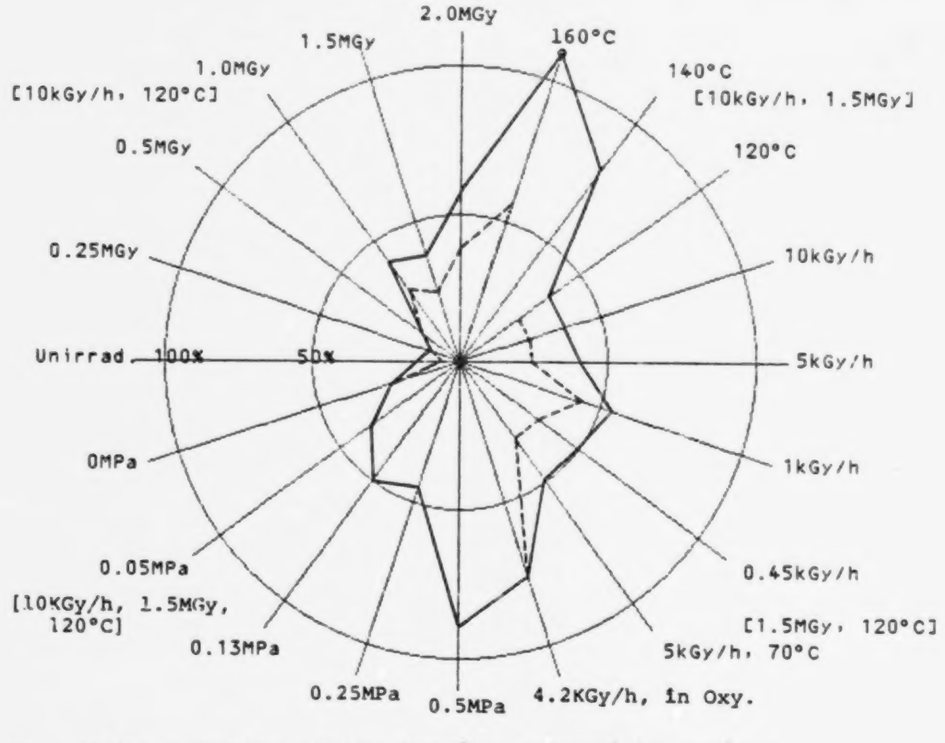

Fig. 21 Water sorption of the Hypalon exposed to various sequential LOCA environments.

# General Technical Requirements for Special Valves Used in Nuclear Power Plants

J. Zdarek, F. Jukl

Sigma Research Institute, Prague
Czechoslovakia

## Abstract

The "General Requirements for Special Valves Used in Nuclear Power Plants" /OTT-82/ have been developed for purposes of quality improvement and standardization. Within the scope of OTT-82 fall all types and sizes of special valves used in pipelines and systems of nuclear power plants /NPP/ with PWR and RBMK /boiling water cooled, graphite moderated, chanel type/ reactors.

OTT-82 involves comprehensive design data and requirements for production, inspections, testing, packaging, transportation storage of the valves and manufacturer guarantees.

## Introduction

To satisfy the requirements of designers and users of nuclear power plants and to ensure reliable operation of this highly demanding apparatus, the manufacturers of valves must systematically prove that the technical parameters of their products has been met.

This proof is accomplished by several successive steps as follows:

a/ Checking the technical parameters stated in the technical specifications of the relevant type series of valves on the basis of test results and calculation of prototypes prior to beginning their series production.

b/ Periodical checking of selected technical parameters in the course of series production.

c/ Checking the technical parameters at substantial changes in the design or technology of the individual model.

d/ Following up and analyzing the failure rate /trouble incidence/, repairability, and/or of other statistical quantities characteristic of nuclear power plants under operating conditions.

Due to the complexity of the above steps, this paper shall deal only with step a/.

## Qualitative Determination

Evalution of the qualitative parameters is generally carried out on selected prototypes, representative of the type series. In selecting these prototypes, their number is chosen according to the sizes in the type series, their design and similarities with respect to the following generalization of possible conclusions reached on the basis of calculations and tests for the entire type series.

The main parameters subjected to checking by calculation and experiment are as follows:

a/ Functional ability under nominal operating conditions.

b/ Strength and services life under nominal operating conditions.

c/ Resistance to breakdowns and seismic effects.

d/ Hydraulic parameters.

e/ Properties of materials used, purchased components, extent of keeping to the instructions of production and installation.

The methodology of calculations and tests, together with their evaluation detailed below, were selected by following the specifications of standards /2/, methods introduced by the SIGMA Research Institute /3/, experimental capabilities of the SIGMA Concern and of other cooperating Czechoslovak organizations.

## Functional Capability of Valves at Nominal Operating Conditions

The valve meets functional requirements at nominal operating conditions if it is proved that for a certain time, expressed in time units or number of operating cycles /open - closed - open/ it performs within required limits of probability in the following areas:

1. Closing valve /gate valve, quick-acting gate valve, bellows-sealed globe valve, quick-acting bellows-sealed globe valve/

a/ No occurrence of medium leakage through the external surface.

b/ In the position marked closed, the closure of the valve seals completely.

c/ During closing or opening of the valve the control moment or force does not exceed the stated value.

d/ The time of shifting the closure from one extreme position to the other does not exceed the stated value.

2. Control valve /control bellows-sealed globe valve/

a/ No leakage of the medium through the external surface.

b/ At the given pressure gradient on the valve, an amount of medium specified for the relevant opening of the valve flows through it.

c/ When closing or opening the valve, the control moment or force does not exceed the stated value.

d/ The stated value for the time of shifting the closure from one extreme position to the other is not exceeded.

3. Check valve /butterfly check valve, return valve/

a/ There is no leakage of the medium through the external surface.

b/ In the position marked closed, the closure of the value seals at the pressure gradient stated on the valve. At the magnitude of reversed pressure gradient stated on the valve, the closure opens.

c/ At the stated speed of the medium flowrate or magnitude of the pressure gradient stated on the valve, the closure is in a fully opened position.

The functional ability is demonstrated for a certain period of time or for a certain number of working cycles on the one hand by calculation the probability of trouble-free operation for selected representatives of the type series according to the methodology stated in /4/ and, on the other hand, experimentally.

The experimental demonstration of functional capability is carried out as follows:

1. Closing and control valves; on a hot-water stand at pressure, temperature and pressure gradients on the valve which are nearest to the nominal operating parameters and with the flow

rate of the medium within limits of the experimental equipment.

2. Check valves; on a water stand at a nominal flow rate, temperature, pressure, and pressure gradient on the valve within limits of the experimental equipment.
3. Quick-acting valves, approximately at one third of the working cycles on a water stand with a nominal flow rate and pressure gradient. On the remaining number of cycles the same method is used as on the closing and control valves, i.e., the hot-water stand.

For tests of functional capability at nominal operating parameters, usually a minimum of three representatives of a type series are chosen. The fittings are subjected to 1.5 times the nominal number of working cycles if no fault occurs. If in the stated period a fault /repairable/ occurs, then the test continues up to three times the nominal number of operating cycles or up to four repairable faults following immediately one after the other. Specification of faults is carried out for every type series separately before beginning the tests.

## Strength and Service Life at Nominal Operating Conditions

The valve has the requried service life and strength at nominal operating conditions when the values of stress induced by internal pressure, temperature, nominal temperature changes, effects of external forces nad moments transferred from the piping, /its own weight, dilatation/ do not exceed the values of allowable stresses as stated according to /2/ and the cumulative damage of the material caused by low-cycle fatigue of the individual components of stress does not exceed the value 1.

The strength and service life of prototype are verified on the main components of the valve subjected to stress by the full operating load, i.e., on the body, including pipe connections, on the cover, wedges, the cone, the screwed cover to body flanges, spindle, and or other parts.

The verification proceeds by means of calculations so that in selected cases the calculated values are supplemented and made more precise by strain-gage or photoelasticimetric measurements on prototypes or models. The calculated values of stress and service life of the body and cover are determined for every size of the evaluated series: stress is determined by an analytic method according to the principles specified in point /3/. This calculation is then checked on selected prototypes and the stress concentration at selected points by the final element method /FEM/.

Experimental checking of stresses is carried out for stationary loads caused by internal pressure, and/or by external moments and forces under normal temperature; stress arising from external moments is checked usually only in the plane with a lower rigidity. The loading parameters for strength tests are generally selected up to the values of the nominal loads according to the relevant technical conditions.

Resistance of Valves to Effects of Breakdown and Earthquake

1. Valves are resistant to the effects of breakdown when:

a/ The calculated values of stress and damage of the basic components of the valve subjected to effects of temperature and pressure changes caused by a breakdown of the relevant piping systems do not exceed, when added to the values specified for nominal operating conditions, the permissible value.

b/ The closing, control and check valve maintains its functional ability after 10 temperature impacts, when the body, which is warmed up to the nominal operating temperature, is suddenly cooled by inside flow of cold water at a rate of approximately 5 m/sec.

c/ The check valve maintains its functional ability after 10 closing movements by a return impact carrier out from a completely open state at the initial speed of the reversed water flow of 1 m/sec.

d/ The valve with an electric actuator maintains its functional ability at a voltage reduction to the minimum value specified in the relevant operating conditions.

e/ The quick-acting valve with a pneumatic actuator maintains its functional ability within the entire range of the control air pressure specified by the relevant operating conditions; at a shut-down of the pressure air source for a determined period of time, it is capable of carrying out the determined number of working cycles following immediately one after the other.

f/ Valves designed to work in the containment maintain their functional ability after all types of accidents including LOCA, accident as specified in the general technical requirements for special valves for nuclear power plants.

2. Valves are resistant to seismic effects when:

a/ The stress and damage caused to the body /especially to the pipe connections/ by forces and moments transferred from the vibrating piping to the valve during an earthquake do not exceed the permissible value.

b/ The stress and damage to the basic components of the valve caused by vibrations of the valve itself as a result of an earthquake do not exceed the permissible value.

c/ During an earthquake and the time immediately afterwards, the valve maintains its functional ability as specified below.

Only valves with an electric or pneumatic actuator are subjected to tests and checking of seismic resistance since by calculations generally only such valves, due to the distribution of mass, are less resistant to seismic effects.

The checking of resistance to temperature changes in cases of breakdown proceeds by the calculation method of final elements on two-dimensional models.

The experimental verification of seismic resistance of valves is as follows: within the range of 5-25 Hz and/or 50 Hz/, the natural frequency, modes of vibration and/or damping of the valve fixed by the bottom of the body /welded into a rigid holder by the neck of the valve, in individual cases another method is used/ are determined. The influence of the connecting piping is ignored. It is the rule that for valves, which can be used without dampers, the minimum frequency /first natural frequency/ must by higher than 20 Hz. For such valves, the checking by calculation of the stress of the basic components is carried out quasi statically for effects according to /1/. The calculations and/or experimental verification of stresses in the yoke, cover flange, bolts of cover connection and spindle of closing and control valves is made gradually under excitation in two directions in the plane perpendicular to the spindel for the entire amplitude of acceleration of the excitation force of approximately 30 m/sec$^2$ in the center of the through-flow part of the body.

The functional capability of the valve under seismic effects is judged on the basis of tests on a direct-acting co-axial vibration table where the seismic effects are simulated by a sinusoid excitation force of an acceleration amplitude of approximately 30 m/sec$^2$ at a frequency of 5 up to 25 Hz and/or up to 50 Hz/,increasing in steps of 1 Hz.

The valve closed by the nominal moment must have the specified tightness of the closure and the external tightness, after a simulated earthquake with time delay in one level of frequency, for a duration of at least 10 vibrations. The cold tightness test takes place after termination of the earthquake simulation with the nominal working pressure. The valve must remain controllable, i.e., the actuator of the valve must shift the closure from one extreme position to the other. The test proceeds so that the valve, in which there is no pressure of the medium under cold conditions closes and opens with delays on the basis of constant excitation frequency with the length of the control time. Both the above-mentioned tests are carried out on closing and control valves gradually for excitation in two directions, perpendicular to the axis of the spindle, on the swing check valves in the flow direction, on the check globe valves in the direction of the cone movement.

## Hydraulic Parameters of Valves

As hydraulic parameters of valves we consider:

a/ on closing and check valves, the coefficients of hydraulic resistance for full opening of the valve.

b/ on check valves the minimum speed or pressure gradient on the valve necessary for complete opening of the closure.

c/ on control valves the flow rate coefficient for full opening of the valve and the control characteristic, i.e., the dependence of the flow rate coefficient on the opening of the valve.

The hydraulic parameters are usually checked experimentally on cold water stands.

## Specified Properties of Materials Used, Purchased Sub-Components, Range of Observation of Production and Installation Instructions

On all metallic materials detailed checking of completeness and correctness of the certifications relating to the relevant mechanical and chemical properties takes place over the entire range according to the relevant technical conditions as well as random testing of selected properties.

As regards seals, their detailed checking includes completeness and correctness of certifications where as the random testing concerns specific weight resistance of sealing materials to temperature and content of chlorides. With lubricants used, the completeness of the certificates is checked and random tests of resistance to temperature and radioactive radiation are carried out experimentally.

On semi-products and manufactured metallic components, detailed testing for faults in the basic and welding materials are usually carried out radiographically.

Detailed checking of purchased components /for instance bellows, electric actuators, etc./ includes completeness and correctness of certifications; random experimental testing with reference to the technical parameters such as for instance to the bellows where a test is made of the number of working cycles before a failure occurs. The actuators are checked for resistance to the effects of a complete breakdown.

On assembled valves, the setting /adjustment/ of the control and regulating elements is checked as well as tightening of screws and bolts. Especially careful testing is carried out on the strength and impermeability of the body and of its connections as well as the tightness of the closure and determination is made of the magnitude of the necessary control moment for a tight closure of the closing valves and control capacity of the control valves.

Checked in detail on all prototypes of valves designated for tests are the values of surface roughness and hardness, observation of alignment and perpendicularity of the component parts which have a decisive influence on the functional properties, i.e., strength and service life of the valves.

## Literature

/1/ General technical requirements on special valves for nuclear power plants, Moscow 1982 /OTT-82/

/2/ Rascot standards

Normy rascota na procnost elementov reaktorov, parogeneratorov, sosudov, truboprovodov atomnych elektrostancij, opytnych i isledovatelskich jadernych reaktorov, Moskva 1973

Dopolneniji k Normam rascota ... Moskva 1980

GOST 95 44-75

/3/ Sima J.: Calculation of strength and service life for bodies of valves - Methodics I and II

Reports on research work by SIGMA Research Institute Olomouc 1981 and 1982

/4/ OST 26-07-821-75

/5/ Methodologies of tests and calculations of special valves for nuclear power plants - SIGMA Research Institute 1984

/6/ Colebroock: Turbulent Flow in Pipes With Particular Reference to the Translation Region Between the Smooth and Rough Pipe Laws. J. Inst. Civ. Engrs., Vol 11 /1938 - 39/, p. 133.

# Effectiveness and Safety Aspects of Selected Decontamination Methods for LWRs[†]

S. W. Duce, F. B. Simpson
EG&G Idaho Inc., Idaho National Engineering Laboratory

## ABSTRACT

During the years 1984 and 1985 in-situ chemical decontamination processes were applied extensively in boiling water reactor (BWR) primary coolant recirculation systems (PCRSs) to help facilitate system replacement or inservice inspections, and more limited in pressurized water reactor (PWR) steam generators to facilitate tube plugging or sleeving operations. During these two years four chemical decontamination processes were observed: CAN-DECON, LOMI, DOW NS-1 and PNS CITROX A at a total of nine different facilities, seven BWRs and two PWRs. These chemical decontaminations were performed to reduce the man-rem that would be received by the work force to perform the specified task(s). This paper presents information and results on (a) base metal attack during the process application, (b) methods used to protect critical components, (c) activity removed, (d) man-rem savings, and (e) waste forms and volumes.

---

[†] Work supported by the U. S. Department of Energy under Doe Contract No. DE-AC07-76ID01570

# INTRODUCTION

In October of 1983 the Nuclear Regulatory Commission (NRC) Office of Nuclear Regulatory Research funded this program with the objective to obtain information on chemical decontamination processes that the NRC might be expected to review. Information was to focus on methods, effectiveness, and safety aspects of the chemical decontamination processes as they were applied in PCRSs at commercial nuclear power reactors. This information was to be obtained through observation of the process application in light water reactors (LWRs).

During the years 1984 and 1985 in-situ chemical decontamination processes were applied extensively in BWR PCRSs to help facilitate system replacement or inservice inspections, and more limited in PWR steam generators to facilitate tube plugging or sleeving operations. During these two years four chemical decontamination processes were observed: CAN-DECON, LOMI, DOW NS-1 and PNS CITROX A at a total of nine different facilities, seven BWRs and two PWRs. The facilities visited were Pilgrim Nuclear Power Station, Monticello Nuclear Generating Plant, Millstone Nuclear Power Station Unit No. 1, Palisades Nuclear Plant, Quad Cities Nuclear Power Station Unit No. 1, Peach Bottom Atomic Power Staion Unit No. 2., Dresden Nuclear Power Station Unit No. 1, Cooper Nuclear Station, and Millstone Nuclear Power Station Unit No. 2. In addition to the nine facilities visited, information on four other decontaminations was obtained: Brunswick Steam Electric Station, Milstone Nuclear Power Station Unit No. 2 (1983), Quad Cities Nuclear Power Station Unit No. 2, and Robert E. Ginna Nuclear Station. At each of the nine facilities a questionnaire was filled out that addressed several different aspects of the decontamination process. Later, as equipment was obtained, confirmatory and supplemental measurements were made with an Eberline E-530N radiation survey meter, thermoluminescent dosimeters (TLDs), and a tungsten-shielded Ortec CPD-1 Intrinsic Germanium Gamma-ray Detector with a Davidson Multichannel Analyzer.

The confirmatory and supplemental measurements using the Eberline E-530N and the TLDs were made to enable the program personnel to evaluate the techniques being used to determine the DFs, as well as to evaluate other techniques that could be used to determine the DFs. Measurements with the intrinsic germanium detector were made to determine if the various radionuclides that were included in the oxide films were being removed selectively or if the chemical decontamination processes were acting independently of the nature of the radionuclide. These gamma spectral measurements were also made to provide background measurements for future measurements of the recontamination rate of primary coolant systems following a chemical decontamination.

## PROGRAM RESULTS

In general there are two major areas of safety concern: system hardware and personnel, whether they be facility or member of the public. Concerning the first area of system hardware there were three main areas of focus: reduction in system integrity due to pipe wall thinning, chemical attack on other critical system components, and plant radwaste systems. Prior to application at the nuclear facilities all of the chemical decontamination processes had been tested in laboratory experiments to determine if the process enhanced intergranular attack (IGA) or intergranular stress corrosion cracking (IGSCC). None of the processes used showed any enhancement of IGA or IGSCC in their initial testing programs. However, later testing of the CAN-DECON LND-101A process showed "...that under aggressive laboratory conditions this reagent can cause IGA and an increased susceptibility to IGSCC on highly sensitized 304 SS and Inconel 600."[1] A new CAN-DECON process reagent LND-107, which should result in lower corrosion rates, has been developed by London Nuclear and can replace the LND-101A process.

In addition to the laboratory tests, artifacts from the system to be decontaminated were sent to the vendor for testing to determine proper application process parameters and to quantify the attack on the base metals by the chemical process. During the application of the chemical process, artifact coupons were installed in the vendor process system to measure the attack on the base metal for the actual application parameters. In all cases, regardless of the chemical process, the attack on the piping system base metal was within acceptable limits.

Concern for chemical attack on other critical system components was taken seriously at all facilities. Several different methods were used to ensure that the decontamination chemicals did not move into systems where their affect was unknown or not desirable. In PWR steam generators the common practice was to install plugs into the hot and cold leg coolant lines to prevent chemicals from leaking into the reactor system. These plugs were pressure tested, prior to injecting any chemicals into the system, at pressures that would exceed the expected operational pressures.

In BWRs the methods used to prevent decontamination solutions from moving into systems where they were not wanted were greatly varied. In one case the PCRS was physically cut loose from the reactor vessel ensuring the decontamination chemicals would not enter the reactor vessel. As the PCRS was to be removed following the decontamination this was considered by the utility and General Electric as an acceptable option. However, most facilities used plugs in the suction lines and solution level administrative controls in the risers to prevent the decontamination solutions from entering the reactor vessel. Administrative controls also varied with utility, with some utilities allowing decontamination solution to be injected one to two feet up in the risers inside the annulus, while others did not allow the solution to get higher than the elbow outside the vessel. There were some cases where the decontamination solutions were deliberately sent through the annulus area via the suction lines, in an effort to remove the oxide film that had built up in the annulus. In general these methods were effective in protecting the critical components. In the few rare cases where small amounts of chemicals did get into the reactor vessel or piping the vendors were able to remove the chemicals in a minimum time using their ion-exchange systems.

There were few instances where system leaks occurred. In those few situations that did occur the chemical solutions were normally contained and cleaned up before they could enter the facility radwaste treatment system. In the one instance where the decontamination solution did enter the radwaste treatment system the system was able to handle the decontamination chemicals without special treatment.

Personnel safety, be it facility personnel or member of the public, was probably the most significant driving factor for performing a chemical decontamination, albeit the greatest concern was for facility personnel. Chemical decontamination processes were selected because of the large dose (i.e., man-rem) savings that could be realized by removing the highly radioactive oxide films that had built up on the internal pipe surfaces. Table 1 lists the number of curies by radionuclide removed from each BWR facility for which information was available and Table 2 lists the curies by radionuclide removed from each PWR for which information was available. Average total curies of gamma emitting activity removed from all facilities were 51.4 Ci.

Man-rem savings are listed in Table 3 for all facilities for which information was available. Average man-rem savings for all facilities was 1482 man-rem. The range of man-rem savings for BWRs was >450 to 2193 and for PWRs 1400 to 3660 man-rem. Several utilities, showing a strong ALARA commitment, chose chemical decontamination methods solely for the dose reduction to personnel and not because they felt that there would be dollar savings.

Radioactive low level wastes generated from the chemical decontamination process were generally solidified ion-exchange resins. There was one instance where liquids were solidified and one instance where the resins were dewatered. Table 4 lists the chemical decontamination generated radwaste volumes and waste forms. Average waste volumes from the chemical decontamination was ~150 $ft^3$, with the range being 80 to 1020 $ft^3$. Note that the calculated average does not include the Monticello nor the Pilgrim waste volumes as the two facilities' waste volumes were not representative of the norm due to other extenuating circumstances

In many instances the facilities were able to significantly reduce the volume of radioactive wastes going to the burial grounds by taking advantage of the Quadrex Recycle Center in Oak Ridge, TN. The recycle center received the stainless steel pipe, that had been removed from the PCRSs, and; using other chemical and electro-chemical techniques, decontaminated the pipe so that it could be sold for scrap metal to the public. Current experience shows a 75% reduction in volume of material that would have been sent to a burial ground. An example of typical volume from a PCRS replacement is 3500 $ft^3$ pipe received and 774 $ft^3$ of waste buried. The 3500 $ft^3$ is a close approximation of actual pipe volume, actual burial volume would probably have been greater by a factor of two, at a minimum, due to waste in packaging the pipe in appropriate containers for burial. Processing the waste material through a recycle center showed a concern for the public on the part of the utilities, by minimizing the volume and lowering the exposure rate of the wastes going to the low level waste burial grounds, which should result in lower doses to future generations.

## CONCLUSIONS

The conclusions from this study, pertinent to this paper, are as follows:

a) Current chemical decontamination processes have been extensively tested.

b) Coupon results have shown acceptable levels of metal removal.

c) Current practices for preventing decontamination solutions into PCRS piping and reactor vessels are varied.

d) Average curies removed from BWRs was 51.3.

e) Average curies removed from PWRs was 46.3.

f) Average man-rem savings for all facilities was 1482.

g) Average normal decontamination waste volume was 150 $ft^3$.

h) Average volume of pipe processed through a recycle center results in a 75% reduction in volume going to a commercial burial ground.

The results of this NRC program have been published as NUREG/CR-4445, "Effectiveness and Safety Aspects of Selected Decontamination Processes", Aug. 1986. This document is available through the NRC Public Document Room or the National Technical Information Service.

## REFERENCES

1: V. C. Turner, "Corrosion Data From London Nuclear," The Second Seminar on Chemical Decontamination of BWRs, Charlotte, NC, June 3-5, 1986

BEST COPY AVAILABLE

TABLE 1 RADIOACTIVITY REMOVED FROM PCRSs AND RWCSs

| | | Radionuclides (Ci) | | | | | | | |
|---|---|---|---|---|---|---|---|---|---|
| Facility | System | Co-60 | Co-58 | Mn-54 | Cr-51 | Fe-59 | Zn-65 | Other | Total |
| Pilgrim | PCRS | 45.7 | 3.2 | 3.9 | ND | ND | 0.9 | 39.4[a] | 93.1 |
| Monticello | PCRS | 26.0 | 1.5 | 3.9 | 1.5 | 0.3 | 6.4 | 0.4 | 40.0 |
| Monticello | RWCS | 3.15 | 0.08 | 0.26 | 7.6 | ND | 3.64 | 0.01 | 14.74 |
| Millstone U-1 | PCRS | 36.8 | 3.9 | 12.6 | ND | 1.3 | ND | ND | 54.6 |
| Millstone U-1 | RWCS | 3.0 | ND | ND | ND | ND | ND | ND | 4.4 |
| Quad Cities U-1 | PCRS | 107.8 | 4.3 | ND | 1.8 | 1.2 | ND | 2.7 | 117.8 |
| Quad Cities U-1 | RWCS | 10.4 | 0.4 | ND | 1.2 | 0.08 | ND | 0.1 | 12.2 |
| Quad Cities U-2 | PCRS | 135.6 | 3.4 | 6.1 | 0.4 | 1.1 | 2.4 | 3.3 | 152.3 |
| Cooper | PCRS | 14.9 | 1.2 | 2.4 | 0.3 | 0.03 | 0.2 | 0.37 | 19.4 |
| Brunswick | RWCS | 3.6 | 0.6 | 1.7 | 3.0 | 0.2 | 0.1 | ND | 9.1 |
| | | | | | | | | Total (Ci) = | 517.6 |

---

a. 36 2 Ci of $^{55}$Fe.

ND. No Data

TABLE 2 ACTIVITY REMOVED (Ci)

| | A Steam Generator[a,b] | | B Steam Generator | | |
|---|---|---|---|---|---|
| Isotope | Ginna | Millstone[c] | Ginna | Palisades | Millstone[c] |
| Co-58 | 13.0 | ND | 14.3 | 33.5 | 17.2 |
| Co-60 | 17.1 | ND | 17.7 | 10.3 | 48.4 |
| Others | 3.6 | ND | 5.6 | 1.3 | 3.4 |
| Total | 33.6 | ND | 37.6 | 45.1 | 69 |

---

a. No data available for the Millstone 83 decontamination.

b. Palisades "A" steam generator not decontaminated.

c. May 85 decontamination.

TABLE 3 MAN-REM SAVINGS USING CHEMICAL DECONTAMINATION

| | Man-Rem Expenditure | | |
|---|---|---|---|
| Facility | Projected w/o Decontamination | Actual With Decontamination | Projected Savings |
| Pilgrim[c] | 3840 | 1785 | 2055 |
| Monticello[c] | ND | ND | 800 |
| Millstone U-1[d] | 2000 | 668 | 1332 |
| Quad Cities U-1[d] | 1624 | 511 | 1113 |
| Quad Cities U-2[d] | 2654 | 461 | 2193 |
| Palisades[b] | ND | ND | 1400[e] |
| Peach Bottom U-2[c] | 5438 | 3838 | 1600[f] |
| Cooper[c] | >1900 | 1422 | >450 |
| Millstone U-2[a,b] | 4300 | 640 | 3660 |
| Millstone U-2[b] | ND | ND | 1400 |
| Ginna | ND | ND | 300 |

---

a. Decontamination performed in August 1983.
b. PWR SG work.
c. PCRS pipe replacement.
d. PCRS ISI and weld overlays.
e. Initial projected savings, however the actual job performed was greatly reduced.
f. Includes a 350 man-rem penalty for work performed to isolate the Rx vessel.
ND No Data

TABLE 4 CHEMICAL DECONTAMINATION GENERATED RADWASTE

| Plant | Date | Type | Process | Waste Form | Waste |
|---|---|---|---|---|---|
| Millstone Unit No. 2 | 8/83 | Steam Generator Channel Head | Ce/Ku OZOX | Ion exchange pressure vessels dewatering and then solidification with DOW binder (In-situ). | Ten 18ft$^3$ pressure vessels total of (180 ft$^3$) |
| Quad Cities Unit No. 2 | 9/83 | PCRS | LN-CAN-DECON | Ion exchange resins slurried to liner then solidified using cement/lime. | 46 ft$^3$ resins<br>80 ft$^3$ solidified volume |
| Monticello | 3/84 | PCRS and RWCU | Quadrex LOMI | Ion exchange resins slurried to liner then solidified using cement/lime. | 700 ft$^3$ resins<br>1020 ft$^3$ solidified volume |
| Quad Cities Unit No. 1 | 4/84 | PCRS and RWCU | LN-CAN-DECON | Ion exchange resins slurried to liners then solidified using cement/lime. | 60 ft$^3$ resins<br>120 ft$^3$ solidified volume |
| Millstone Unit No. 1 | 5/84 | PCRS and RWCU | LN-CAN-DECON | Ion exchange resins slurried to liner then solidified using cement/lime. | 60 ft$^3$ resins<br>160 ft$^3$ solidified volume* |
| Peach Bottom Unit No. 2 | 7/84 | PCRS | LN-CAN-DECON | Ion exchange resins slurried to liners then solidified using cement/lime. | 52 ft$^3$ resins<br>80 ft$^3$ solidified volume |
| Pilgrim | 8/84 | PCRS and RWCU | IT/PN DOW NS-1 | Liquid from reverse osmosis unit and ion exchange resins. Both solidified using cement/lime. | 1300 gallons liquid<br>90 ft$^3$ resins<br>607 ft$^3$ solidified volume |

TABLE 4 CHEMICAL DECONTAMINATION GENERATED RADWASTE (cont'd)

| Plant | Date | Type | Process | Waste Form | Waste |
|---|---|---|---|---|---|
| Palisades | 8/84 | Steam Generator Channel Head | LN-CAN-DECON | Ion exchange resins slurried to liner then solidified using cement/lime. | 120 ft$^3$<br>Solidified volume |
| Cooper | 12/84 | PCRS | PN Citrox | Ion exchange resins slurried to liner then solidified using cement/lime. | 175 ft$^3$ resins<br>290 ft$^3$ solidified volume |
| Millstone Unit No. 2 | 5/85 | Steam Generator Channel Head | PN Citrox | Ion exchange resins slurried to liner then dewatered. | |

| | |
|---|---|
| CE | Combustion Engineering |
| KU | Kraftwesk Union |
| LN | London Nuclear |
| IT | IT Nuclear |
| PN | Pacific Nuclear |

---

* Includes plant generated waste not associated with the decontamination.

# PROBABILITY OF FAILURE IN BWR REACTOR COOLANT PIPING*

G. Holman and C.K. Chou

Lawrence Livermore National Laboratory
University of California
P.O. Box 808 / Livermore, California 94550

## ABSTRACT

The Lawrence Livermore National Laboratory (LLNL) has estimated the probability of double-ended guillotine break (DEGB) in the reactor coolant piping of Mark I boiling water reactor (BWR) plants. Two causes of pipe break are considered: crack growth at welded joints and the seismically-induced failure of component supports. For the former a probabilistic fracture mechanics model is used, for the latter a probabilistic support reliability model. To account for effects of intergranular stress corrosion cracking (IGSCC), a probabilistic model was developed based on experimental and field data compiled from several sources. Times to crack initiation and crack growth rates for Types 304 and 316NG stainless steel are correlated to material-specific "damage parameters" which consolidate the separate effects of coolant environment (temperature, dissolved oxygen content, level of impurities), stress (including residual stress), and degree of sensitization. Results to date show IGSCC clearly dominates the probability of failure in 304SS recirculation piping, mainly due to cracks that initiate within a few years after plant operation has begun. Replacing Type 304 piping with 316NG reduces failure probabilities by several orders of magnitude.

## 1. Introduction

The Lawrence Livermore National Laboratory (LLNL), through its Nuclear Systems Safety Program, has performed probabilistic reliability analyses of PWR and BWR reactor coolant piping for the NRC Office of Nuclear Regulatory Research. Specifically, LLNL has estimated the probability of a double-ended guillotine break (DEGB) in the reactor coolant loop piping of PWR plants, and in the main steam, feedwater, and recirculation piping of BWR plants. For these piping systems, the results of these investigations provide NRC with one technical basis on which to:

(1) reevaluate the current general design requirement that DEGB be postulated in the design of nuclear power plant structures, systems, and components against the effects of postulated pipe breaks. Recent NRC rulemaking actions, based in large part on the results of our PWR evaluations, now provide a means for

---

* "This work was supported by the United States Nuclear Regulatory Commission under a Memorandum of Understanding with the United States Department of Energy."

eliminating dynamic effects of reactor coolant loop breaks (e.g., pipe whip, jet impingement) as a basis for PWR plant design.

(2) determine if an earthquake could induce a DEGB and thus reevaluate the design requirements that pipe break loads be combined with those resulting from a safe shutdown earthquake (SSE). Recent revisions in the NRC Standard Review Plan, for example, now allow decoupling of SSE and DEGB loads for PWR reactor coolant loop piping.

(3) make licensing decisions concerning the replacement, upgrading, or redesign of piping systems, or addressing such issues as the need for pipe whip restraints on reactor coolant piping.

In estimating the probability of DEGB, LLNL considers two causes of pipe break; pipe fracture due to the growth of cracks at welded joints ("direct" DEGB) and pipe rupture indirectly caused by the seismically-induced failure of critical supports or equipment ("indirect" DEGB).

Although the investigations discussed here have been limited to the specific piping systems mentioned earlier, the techniques used to assess piping reliability are sufficiently general that they could be conveniently applied to other piping systems.

## 2. General Approach

Generic evaluations of reactor coolant loop piping were completed for PWR nuclear steam supply systems manufactured by Westinghouse, Combustion Engineering, and Babcock & Wilcox. In these evaluations, LLNL performed the following:

(1) estimated the probability of direct DEGB taking into account such contributing factors as the initial size (depth and length) of pre-existing fabrication flaws, pipe stresses due to normal operation and sudden extreme loads (such as earthquakes), the crack growth characteristics of pipe materials, and the capability to detect cracks or to detect a leak if a crack were to penetrate the pipe wall. For this purpose, LLNL developed a probabilistic fracture mechanics model using Monte Carlo simulation techniques, implemented in the PRAISE (Piping Reliability Analysis Including Seismic Events) computer code.

(2) estimated the probability of indirect DEGB by identifying critical supports or equipment whose failure could result in pipe break, determining the seismic "fragility" (relationship between seismic response and probability of failure) of each, and then combining this result with the probability that an earthquake occurs producing a certain level of excitation ("seismic hazard").

(3) for both causes of DEGB, performed sensitivity studies to identify key parameters affecting the probability of pipe break.

(4) for both causes of DEGB, performed uncertainty studies to quantify how uncertainties in input data affect the uncertainty in the final estimated probability of pipe break.

The results of these evaluations consistently indicated that the probability of a DEGB in PWR reactor coolant loop piping is extremely small, about le-7 events per reactor-year from indirect causes, and less than le-10 events per reactor-year from direct causes. It was also found that thermal stresses dominated the probability of direct DEGB, and that earthquakes contributed only negligibly. These results suggested that the DEGB design requirement -- and with it related design issues such as coupling of DEGB and SSE loads, asymmetric blowdown, and the need to install pipe whip restraints -- warranted reevaluation for PWR reactor coolant loop piping. Details of these investigations have been extensively documented elsewhere [1,2,3,4] and will not be discussed here except as they relate to the BWR study.

The objectives and approach of the BWR study have been essentially the same except that different dominant failure mechanisms were added. LLNL has so far limited its investigation to Mark I plants, which have recirculation piping particularly susceptible to the effects of intergranular stress corrosion cracking (IGSCC). An initial pilot study based on the Brunswick plant operated by Carolina Power & Light has been completed, the results of which were presented at the 13th NRC Water Reactor Safety Research Information Meeting [5] along with the results of preliminary evaluations of certain other Mark I plants.

## 3. Double-Ended Guillotine Break Caused by Crack Growth

The probability of "direct" DEGB in reactor coolant piping is estimated using a probabilistic fracture mechanics model implemented in the PRAISE computer code and associated pre- and post-processing routines. Details of the model are documented elsewhere [6,7] and will not be repeated here, but can be summarized as follows.

For a given weld joint in a piping system, the probability of failure (i.e., leak or break) is estimated using a Monte Carlo simulation technique. As diagramed in Fig. 1, each replication of the simulation -- of which a typical simulation may include many thousand -- begins with a pre-existing flaw having initial length and depth randomly selected from appropriate distributions. These distributions in turn relate the probability of crack existence. Fatigue crack growth is then calculated using a Paris growth model, to which are applied stresses associated with normal operating conditions and postulated seismic events. The influence of such factors as non-destructive examination (NDE) and leak detection is also considered through the inclusion of appropriate statistical distributions (e.g., probability of crack non-detection as a function of crack size). Leak occurs when a crack grows through the pipe wall, break when failure criteria based on net section stress (for austenitic materials) or tearing modulus (for carbon steels) are exceeded.

Completing all replications for a given weld joint and tabulating those cracks that cause failure yields the cumulative probability of failure as a function of time at that weld. If only pre-existing cracks are considered, then "stratified sampling" can be applied to assure that initial crack samples are selected only from those sizes that can potentially cause pipe break. Through this technique, very low failure probabilities (less than one in a million) can be reliably estimated from only a few thousand replications of the Monte Carlo simulation.

After the failure probabilities at all weld joints in a piping system have been estimated, a "systems analysis" combines these results with the non-conditional crack existence probability (a function of total volume of weld material) and seismic hazard (which relates the occurrence rates of earthquakes as a function of peak ground acceleration) to obtain the non-conditional probabilities of leak and DEGB.

This was the basic approach followed in our evaluations of PWR reactor coolant loop piping. One significant factor complicating the evaluation of BWR piping, however, was the need to include effects of intergranular stress corrosion cracking (IGSCC). When present, IGSCC not only accelerates the growth rate of existing flaws, but also causes new cracks to initiate after plant operation has begun. The effect of these "initiated" cracks on the probability of DEGB must be therefore be considered in addition to that of pre-existing flaws.

Recirculation piping in older BWR plants, particularly those characterized by the General Electric Mark I containment design, has been found in recent years to be susceptible to intergranular stress corrosion cracking. Stress corrosion cracking occurs in stainless steel piping (in the Mark I plants, Type 304) when the "appropriate" (in an adverse sense) conditions of "sensitization" -- material properties conducive to IGSCC that result from prolonged exposure to high temperatures during welding -- environment, and stress are met. Earlier versions of PRAISE treated the effect of IGSCC on pre-existing cracks through a simple relationship between growth rate and the stress intensity factor at the crack front; crack initiation was not modeled at all. It is important to note that this model was *not* applied in our PWR evaluations because operating experience has indicated that IGSCC is not a problem in PWR reactor coolant loop piping.

As part of our BWR study we developed an advanced IGSCC model for the PRAISE code [8]. This model is semi-empirical in nature, and is based on experimental and field data compiled from several sources. Using probabilistic techniques, the model addresses the following IGSCC phenomena:

- **crack initiation**, including the effects of environment, applied loads, and material type (i.e., sensitization). Crack location, time of initiation, and velocity upon initiation are all defined by appropriate distributions based on experimental data.

  "Initiated" cracks are considered separately from pre-existing cracks until one of the following two criteria are satisfied: (1) the crack attains a depth of 0.1 inch, or (2) the velocity of the crack estimated according to the Paris growth law exceed the initiation velocity. Beyond this point, "initiated" and "fracture mechanics" cracks are treated identically.

- **crack growth rate**, including effects of environment, applied loads, and material type.

- **multiple cracks**. Because our earlier evaluations were based on pre-existing flaws only, each Monte Carlo replication included one crack only. Inclusion of crack initiation requires that multiple cracks be considered during each replication.

- **crack linking**. Treating multiple cracks requires that their potential linkage into larger cracks be considered. This is done using linkage criteria specified in Section XI of the ASME Boiler and Pressure Vessel Code.

The model covers not only the Type 304 stainless steel found in most Mark I recirculation piping, but Type 316NG ("nuclear grade") steel as well, a low-carbon alloy widely regarded as an IGSCC-resistant replacement for Type 304. Crack growth rates and times-to-initiation for each material are correlated against "damage parameters" which consolidate the separate influences of several individual parameters. The damage parameters are multiplicative relationships among exponential terms which individually describe the effects of the various phenomena on IGSCC behavior, including:

- **environment**, specifically coolant temperature, dissolved oxygen content, and level of impurities.
- **applied loads**, including both constant and variable loads to account for steady-state operation and plant loading or unloading, respectively.
- **residual stresses**. Steady-state pipe loads due to welding residual stresses are considered in addition to fatigue loads.
- **material sensitization.**

Figures 2 and 3 show, respectively, times-to-initiation and crack growth rates for Type 304 stainless steel, the material on which the initial development of the model was based. The solid curved lines in Fig. 2 show crack growth rates predicted by the earlier IGSCC model in PRAISE for oxygen concentrations of 0.2 ppm (typical during plant operation) and 8 ppm (typical during startup); the relatively close agreement implies that the earlier model gave reasonable crack growth rates despite its much simpler approach.

The damage parameters in the 304SS model were based on the results of both constant-load (CL) and constant extension rate (CERT) IGSCC laboratory tests. Many other factors were considered during initial model development, but were later excluded from consideration either because they were judged to be of secondary influence for 304SS, or because suitable operating data was not available to exercise them in a plant-specific evaluation. Although the present model was developed for 304SS, adapting the correlation scheme for Type 316NG was a relatively straightforward matter of defining new damage parameters based on appropriate laboratory data; the basic functional form of the model was otherwise left unchanged. Two features unique to the 316NG model are, however, noteworthy:

- where both CERT and CL data were available for 304SS, only CERT data was available for 316NG. These data were used to define constant-load growth rates and times-to-initiation in 316NG under the assumption that the creep behavior of both alloys is similar.
- as noted earlier, three conditions are necessary for IGSCC in austenitic steels: stress, environment, and sensitization. In 304SS, whenever stress corrosion cracking occurs in laboratory

tests intended to simulate operating BWR conditions, it is most often intergranular. In 316NG, however, CERT specimens fail by transgranular stress corrosion cracking (TGSCC), whereas IGSCC *is* observed in fracture mechanics specimens. Since the relative influence of environment and loading on TGSCC in 316NG appears similar to that of IGSCC in 304SS, the available TGSCC data were used to predict cracking in 316NG.

Residual stresses are treated as a random variable in the Monte Carlo simulation. Distributions of residual stress as a function of distance from the inner pipe wall were developed from experimental data for three categories of nominal pipe diameter. For large lines (20 to 26 inches), residual stresses took the form of a damped cosine through the wall as based on data collected by General Electric and Argonne National Laboratory (see Fig. 4). The nominal tensile stress at the inner pipe wall is about 40 ksi. For intermediate-diameter (10 to 20 inches) and small-diameter (less than 10 inches) lines, a linear distribution was assumed through the pipe wall with respective inside wall stresses of 9.3 ksi and 24.4 ksi.

The 304SS model was benchmarked by comparing predicted leak rates under nominal BWR applied load conditions against actual leak and crack indication data made available to us by the NRC Office of Nuclear Reactor Regulation (NRR). During benchmarking we quickly ascertained that residual stress was the parameter most influencing the predicted leak rates, and we therefore opted to "tune" the model on this basis. A variety of schemes were considered before we settled on adjusting the stress magnitude (using a multiplication factor) to bring the model into agreement with the field data. Figures 5 and 6, respectively, compare predicted leak rates and number of NDE indications greater than 10 and 50 percent of wall thickness with the corresponding field data for various adjustment factors. As these figures show, surprisingly large reduction factors had to be applied to bring the model into line with the field data, suggesting that factors other than residual stress may be more influential than we first concluded.

## Probability of Direct DEGB

Applying this model in our Brunswick pilot study, we estimated the leak and DEGB probabilities in the original recirculation piping (both loops combined) to be about 0.68/py and 9.0e-4/py, respectively, when IGSCC is present. During development of the IGSCC model, we found that its complexity greatly increased computer time requirements for its execution (up to three CPU hours *per weld*). We therefore grouped the welds in the Brunswick recirculation piping, taking those welds with the highest applied loads in each group. We then estimated the leak and DEGB probabilities at each of these representative welds and performed a systems analysis assuming that these leak and DEGB probabilities applied to all welds in the respective group. These weld-by-weld probabilities and the resultant system probabilities are presented in Table 1 for both leak and DEGB. These results apply to the existing recirculation piping at Brunswick. A replacement configuration, fabricated from Type 316NG and including fewer welds (eliminating, for example, the recirculation pump bypass piping), has been proposed for the Brunswick plant. For purposes of comparison, Table 1 includes the number of replacement welds in each pipe group.

These analyses further indicated that if IGSCC is not a factor, thermal fatigue is the primary cause of direct DEGB, and the probability of break is similar to that in PWR reactor coolant loop piping (see Ref. 5). As for PWR reactor coolant loop piping, earthquakes contribute only negligibly to the probability of direct DEGB.

Note that these results imply about one leak for each plant-year of operation. Field observations, however, indicate that the actual leak frequency is closer to one in every ten plant-years of operation, which led us to conclude that our predicted leak probabilities -- and by implication, DEGB probabilities as well -- were between one and two orders of magnitude high. Inclusion of an impurities term in the 304SS model (which had not been done originally) resulted in a slight reduction in the estimated failure probabilities.

Table 2 summarizes cumulative leak probabilities for Types 304 and 316NG weldments at five-year intervals up to 20 years of operation. At the time of publication, equivalent DEGB probabilities had not yet been generated. Results for 316NG are presented both for initiated cracks and for pre-existing cracks, the latter case reflecting only the effect of stress corrosion cracking on crack growth and not only the addition of new "initiated" cracks to the overall population. Two observations are significant here:

- at any given time, the estimated failure probability in 304SS is some two to three orders of magnitude higher than in 316NG.
- the time required to reach a given leak probability is about six times as long in 316NG as it is in 304SS.

These results also show that where failure is 304SS is *always* dominated by initiated cracks (i.e., resulting from stress corrosion), while in 316NG the initiated cracks dominate the probability of leak only after about 12 years (see Fig. 7). Once cracks are present, growth rates are nominally the same in either material. Consequently, the predicted difference in behavior between the two materials is due to differences in the times-to-initiation.

## 4. Double-Ended Guillotine Break Indirectly Induced by Earthquakes

If earthquakes and pipe breaks are considered as purely random events, the probability of their simultaneous occurrence is negligibly low. However, if an earthquake could cause DEGB, then the probability of simultaneous occurrence would be significantly higher. Our study of direct DEGB concluded that earthquakes were not a significant contributor to this failure mode. However, another way in which DEGB could occur would be for an earthquake to cause the failure of component supports or other equipment whose failure in turn would cause a reactor coolant pipe to break.

Two additional causes of pipe break were therefore considered in our evaluation of BWR reactor coolant piping: failure of "intermediate" pipe supports and supports for light loop components (e.g., recirculation pumps), and failure of heavy component supports.

### 4.1 Failure of Heavy Component Supports

Evaluating the probability of indirect DEGB involves the following four steps:

(1) identify "critical" components whose failure could induce a DEGB. For each component, estimate the conservatism and the uncertainty in the calculated structural responses for various loading conditions, such as dead weight, thermal expansion, pressure, and seismic loads. In our PWR evaluations, we identified as critical components the reactor pressure vessel supports, the steam generator supports, and the reactor coolant pump supports. A BWR, of course, has no steam generators and the failure of coolant pump supports was considered as part of the direct DEGB evaluation. Therefore, the only critical components that we considered in our Brunswick indirect DEGB evaluation were those making up the reactor support structure.

(2) for each critical component, develop a fragility description for each failure mode. The fragility of a component may be based on several factors (see Table 3). Each fragility description relates the probability of structural failure conditioned on the occurrence of an earthquake of given peak ground acceleration.

(3) calculate the overall "plant level" fragility to account for all significant failure modes and the associated fragility descriptions.

(4) calculate the non-conditional probability of indirect DEGB by convolving the plant level fragility with an appropriate description of seismic hazard. "Seismic hazard" relates the probability of occurrence of an earthquake exceeding a given level of peak ground acceleration.

Typical descriptions of seismic hazard are shown in Fig. 8, in this case generic seismic hazard curves that we developed for plant sites east of the Rocky Mountains (see Ref. 2 for details). For Brunswick, we found that the probability of indirect DEGB was about 2e-8 events per reactor-year, with a 90th-percentile value (confidence limit) of 5e-7 per reactor-year. We found that the "star" stabilizer at the top of the reactor pressure vessel, which restrains the RPV against lateral motion in the event of an earthquake, was the primary contributor to failure.

### 4.2 Failure of "Intermediate" Supports

Reactor coolant loops in PWR plants typically have small length-to-diameter ratios and, because of their stiffness, are supported solely by the major loop components (reactor pressure vessel, reactor coolant pumps, and steam generators); therefore, no additional supports are needed. However, recirculation loop piping in BWR plants is longer and smaller-diameter (typically 12 to 26 inches), and requires additional support from spring- or constant-load hangers. This piping may also have numerous snubbers to reduce stresses in the event that an earthquake occurs. Each recirculation loop at Brunswick, for example, has a snubber pair each on the inlet and outlet lines, as well as a snubber triplet at the top and at the bottom of the recirculation pump.

The potential effect of intermediate support failure on estimating the probability of direct DEGB is two-fold:

(1) support failure would redistribute applied stresses at weld joints, in turn affecting crack growth rates as well as the failure criteria used to define when pipe break occurs.

(2) accounting for stress redistribution would require an individual PRAISE evaluation for each support failure scenario, dramatically increasing the computational effort involved. For example, even if only four supports were addressed, sixteen separate PRAISE runs would be required to cover all possible combinations and permutations of support failure.

Our evaluations of indirect DEGB (i.e., support reliability) in PWR reactor coolant loop piping were based on the assumption that failure of a heavy component (e.g., steam generator) support unconditionally led to pipe break. This assumption was regarded as conservative (in reality a pipe would likely experience severe inelastic deformation before actually breaking) but nevertheless resulted in very low DEGB probabilities. To have assumed that failure of a snubber or a constant-load support would similarly cause a DEGB in BWR recirculation piping would have been unreasonably conservative. We therefore developed a more detailed approach to incorporate the effect of support fragility into the probabilistic fracture mechanics evaluation, which we used to investigate the effect of support failure on the probability of direct DEGB for our reference "pilot" plant. After identifying support failure scenarios, we calculated the pipe stresses for each. We then performed sensitivity analyses -- again using the generic seismic hazard curves that we had developed for plant sites east of the Rocky Mountains -- which indicated that the probability of DEGB due to hanger and snubber failure was about the same (about 1e-8 events per reactor year) as that of indirect DEGB due to the failure of the RPV support structure. We concluded that we could neglect support failure in our subsequent direct DEGB evaluations.

## 5. Summary and Discussion

The results of our evaluations to date clearly show that IGSCC dominates the probability of direct DEGB in recirculation piping fabricated from Type 304 stainless steel. In general, we have observed that:

- residual stresses appear to be the dominate factor influencing the number of cracks initiated and, to a lesser degree, their growth rates. In the absence of IGSCC, thermal stresses dominate the probability of direct DEGB; earthquakes contribute only negligibly.

- initiated cracks always dominate the probability of leak (and by inference, break probabilities as well) in Type 304 stainless steel piping. By contrast, the influence of initiated cracks in Type 316NG piping first becomes apparent after about 12 years of operation.

- the per-weld probability of leak in Type 316NG piping is between two and three orders of magnitude lower than that in piping fabricated from Type 304 stainless steel. Based on our past experience, this trend should hold true for break probabilities as well.

Type 316NG piping owes its improved SCC performance to crack initiation times being much longer than in 304SS piping. Crack velocities upon initiation are also significantly lower than in 304SS. Although the growth rate of "fracture mechanics" cracks in 316NG is *somewhat* lower than in 304SS, in general once cracks do initiate, their growth rates are nominally the same in either material. This result points to the *number* of cracks, rather than their growth behavior, as being the dominant influence on relative leak probabilities in Types 304 and 316NG stainless steel piping.

Although we are now in the process of explicitly estimating DEGB probabilities in Type 316NG piping (using the Brunswick pilot plant as our case study), we expect break probabilities to behave accordingly. Our past experience has shown that break probabilities are typically three to four orders of magnitude lower than leak probabilities. On the basis of the DEGB probabilities estimated for Type 304 recirculation loop piping (Table 1), and taking into account the fact that proposed 316NG recirculation loop configurations have significantly fewer welds than current 304SS configurations, we anticipate that system DEGB probabilities should be on the order of 1e-6 per reactor-year.

# REFERENCES

1. G. Holman, "Double-Ended Breaks in Reactor Primary Piping", Lawrence Livermore National Laboratory, Report UCRL-91731 (October 1984). Presented at the 12th NRC Water Reactor Safety Research Information Meeting, Gaithersburg, Maryland, October 22-26, 1984.

2. Probability of Pipe Failure in the Reactor Coolant Loops of Westinghouse PWR Plants, Lawrence Livermore National Laboratory, Report UCID-19988, NUREG/CR-3660, Vols. 1-4 (1984).

3. Probability of Pipe Failure in the Reactor Coolant Loops of Combustion Engineering PWR Plants, Lawrence Livermore National Laboratory, Report UCRL-53500, NUREG/CR-3663, Vols. 1-3 (1984).

4. Probability of Pipe Failure in the Reactor Coolant Loops of Babcock & Wilcox PWR Plants, Lawrence Livermore National Laboratory, Report UCRL-53644, NUREG/CR-4290, Vols. 1-2 (1985).

5. G. Holman, et al., "Pipe Ruptures in BWR Plants", Lawrence Livermore National Laboratory, Report UCRL-93181 (October 1985). Presented at the 13th NRC Water Reactor Safety Research Information Meeting, Gaithersburg, Maryland, October 22-25, 1985.

6. D. Harris, et al., Probabilistic Fracture Mechanics Models Developed for Piping Reliability Assessment in Light Water Reactors, Lawrence Livermore National Laboratory, Report UCRL-15490, NUREG/CR-2301 (April 1982).

7. T. Lo, et al., "Failure Probability of PWR Reactor Coolant Loop Piping," Lawrence Livermore National Laboratory, Report UCRL-86249 (February 1984).

8. Probability of Failure in BWR Reactor Coolant Piping, Volume 3: Probabilistic Treatment of Stress Corrosion Cracking in 304 and 316NG BWR Piping Weldments, Lawrence Livermore National Laboratory, Report UCID-20914, NUREG/CR-4792 (November 1986).

Table 1. Probability of direct DEGB, Brunswick recirculation piping (current loop configuration).

| Weld Group | Diameter (in) | Welds/Loop[1] | $P_{Leak}$[2] | $P_{DEGB}$[2] |
|---|---|---|---|---|
| Suction | 26 | 10 (11) | 5.3e-6<br>(5.3e-3) | 1.3e-6<br>(1.3e-5) |
| Discharge | 26 | 6 (5) | 9.0e-4<br>(5.4e-3) | 5.0e-5<br>(3.0e-4) |
| Header | 20 | 5 (2) | 3.2e-3<br>(1.6e-2) | 5.0e-6<br>(2.5e-5) |
| Riser | 12 | 20 (12) | 1.2e-2<br>(2.3e-1) | 4.0e-6<br>(8.0e-5) |
| Bypass | 3 | 10 (0) | 8.8e-3<br>(8.8e-2) | 3.0e-6<br>(3.0e-5) |
| Total, both loops (with IGSCC) | | 102 | 6.8e-1/py | 9.0e-4/py |
| Total, both loops (w/o IGSCC) | | 102 | 3.6e-7/py | 7.7e-12/py |

Notes:

(1) Value in parantheses is number of welds in proposed replacement configuration.

(2) Events per weld-year. Value in parantheses is events per plant-year for weld group considered.

BEST COPY AVAILABLE

Table 2. Cumulative leak probabilities as a function of time for 304SS and 316NG weldments.

| | Time (yr) | | | | |
|---|---|---|---|---|---|
| Pipe Size | 2 | 5 | 10 | 15 | 20 |
| **Type 304 (initiating)** | | | | | |
| Small | <2.0e-3 | 2.0e-3 | 3.0e-3 | 9.4e-2 | 1.5e-1 |
| Medium | <1.0e-3 | <1.0e-3 | 7.0e-3 | 3.8e-2 | 8.5e-2 |
| Large | <1.0e-3 | 1.0e-3 | 6.0e-3 | 1.0e-2 | 1.9e-2 |
| **Type 316NG (initiating)** | | | | | |
| Small | --- | --- | <5.0e-5 | 1.0e-4 | 6.5e-4 |
| Medium | --- | --- | --- | --- | --- |
| Large | --- | --- | --- | --- | --- |
| **Type 316NG (pre-existing)** | | | | | |
| Small | 8.0e-6 | 1.5e-5 | 2.5e-5 | 3.5e-5 | 4.4e-5 |
| Medium | 1.1e-6 | 1.5e-5 | 4.0e-5 | 8.5e-5 | 1.3e-4 |
| Large | 6.0e-7 | 2.3e-6 | 9.0e-6 | 1.4e-5 | 1.7e-5 |

Table 3. Parameters considered in developing component fragilities

Structural Response

- Ground spectrum used for design
- Structural damping
- Site characteristics (rock or soil, shear wave velocity, thicknesses of different strata)
- Fundamental frequency of internal structure if uncoupled analysis was performed
- Interface spectra for NSSS points of connection to structure if uncoupled analysis was performed
- Input ground spectra resulting from synthetic time history applied to structural model

NSSS Response

- Method of analysis (time history or response spectrum, etc.)
- Modeling of NSSS and structure (coupled or uncoupled)
- NSSS system damping
- NSSS fundamental frequency or frequency range
- If uncoupled analysis was performed, whether envelope or multi-support spectra were used

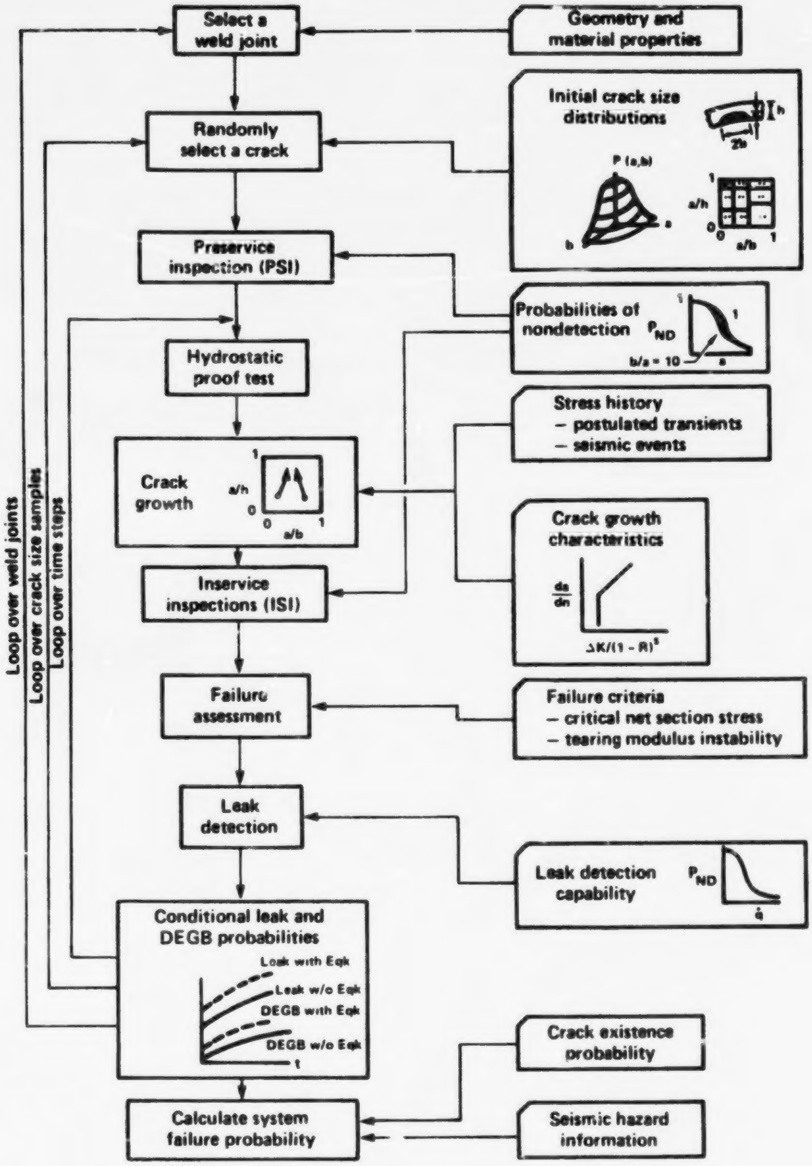
Select a weld joint
Geometry and material properties
Randomly select a crack
Initial crack size distributions
h
2b
P (a,b)
a/h
1
0
a/b
b
a
Preservice inspection (PSI)
Probabilities of nondetection
P_ND
b/a = 10
Hydrostatic proof test
Stress history
– postulated transients
– seismic events
Crack growth
Crack growth characteristics
da/dn
ΔK/(1 – R)^s
Inservice inspections (ISI)
Failure assessment
Failure criteria
– critical net section stress
– tearing modulus instability
Leak detection
Leak detection capability
P_ND
q̇
Conditional leak and DEGB probabilities
Leak with Eqk
Leak w/o Eqk
DEGB with Eqk
DEGB w/o Eqk
t
Crack existence probability
Calculate system failure probability
Seismic hazard information
Loop over weld joints
Loop over crack size samples
Loop over time steps

Fig. 1. Flowchart of the probabilistic fracture mechanics model implemented in the PRAISE computer code.

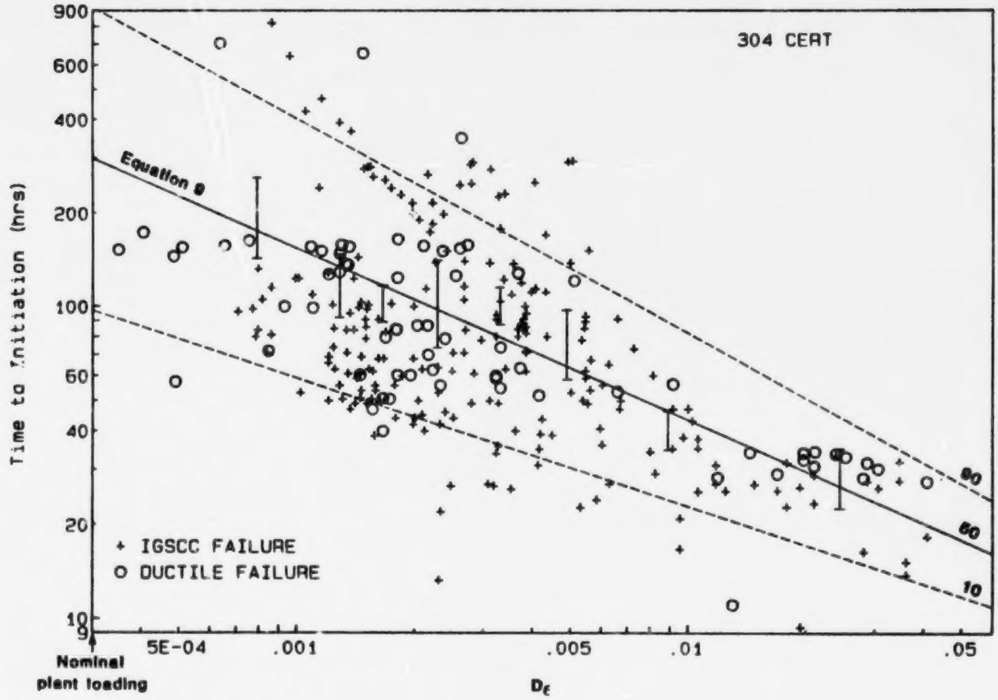

Fig. 2. Time-to-initiation for IGSCC cracks in 304SS as a function of damage parameter, plant loading/unloading.

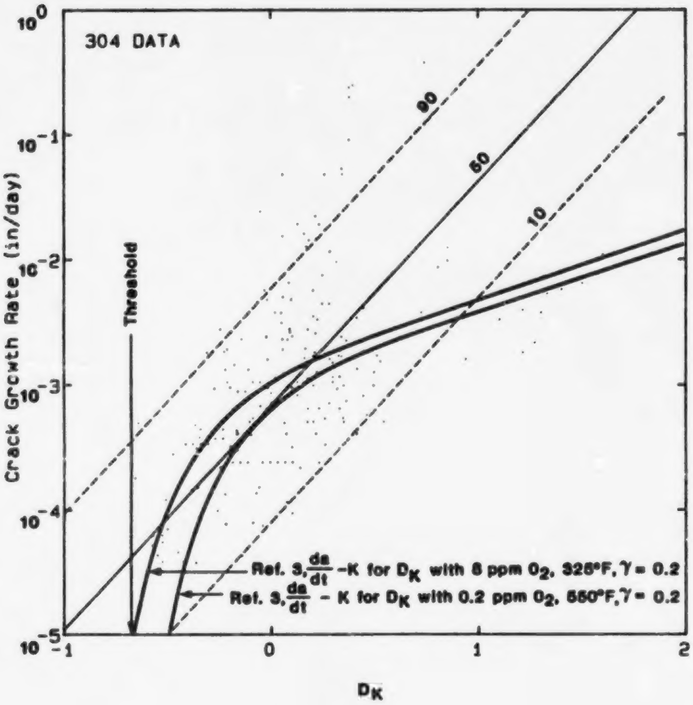

Fig. 3. IGSCC crack growth rate in 304SS as a function of damage parameter, steady-state operation. The solid lines represent crack growth rates predicted by the earlier IGSCC model in PRAISE.

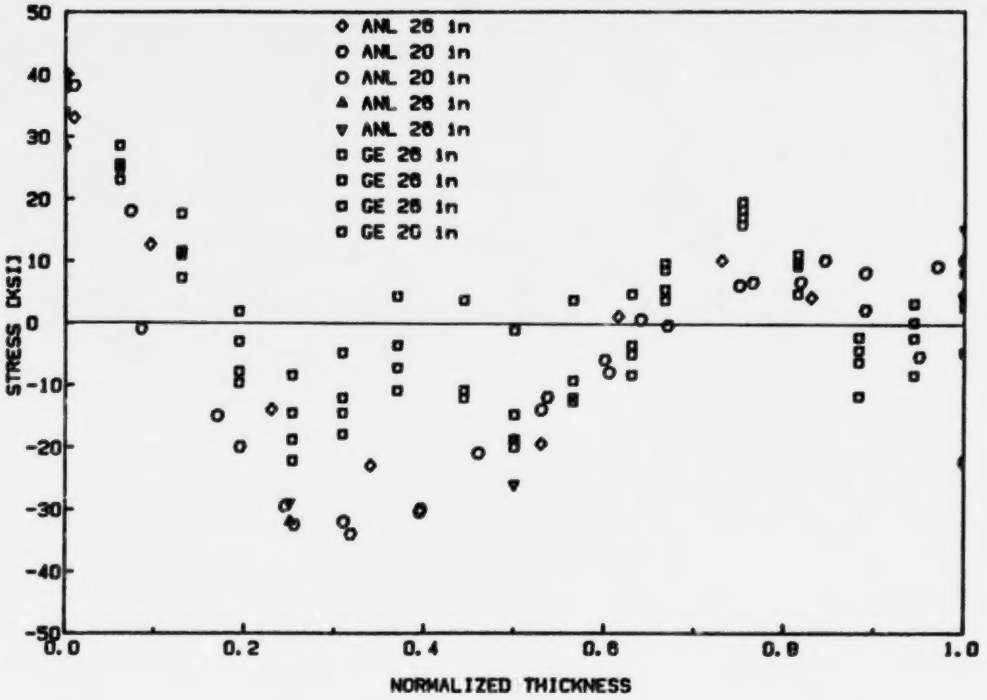

Fig. 4. Residual stress data for large-diameter (20 to 26 inches) piping as a function of distance from the inner wall.

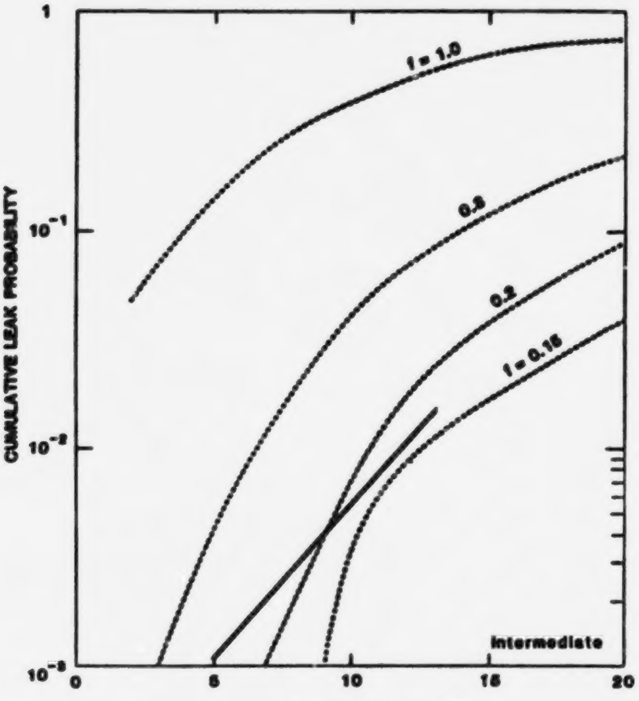

Fig. 5. Comparison of leak probabilities derived from field data with leak probabilities estimated by PRAISE for various values of residual stress adjustment factor (304SS).

BEST COPY AVAILABLE

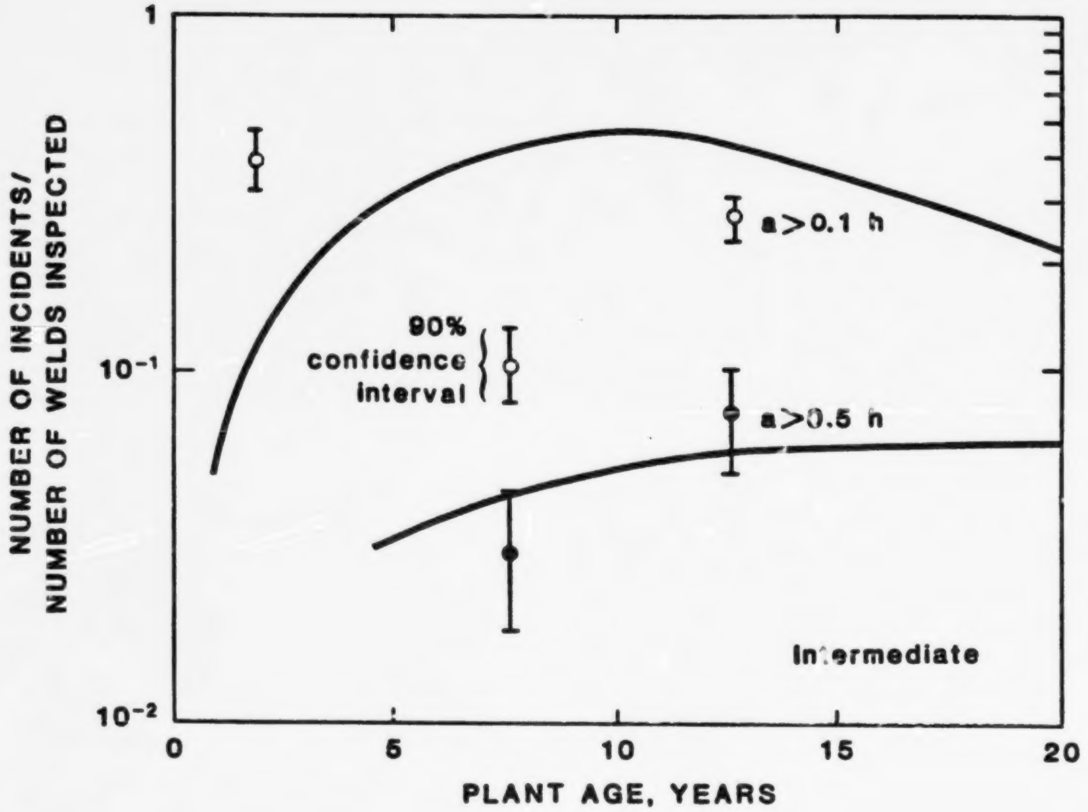

Fig. 6. Comparison of crack indications derived from field data with PRAISE results for various values of residual stress adjustment factor (304SS).

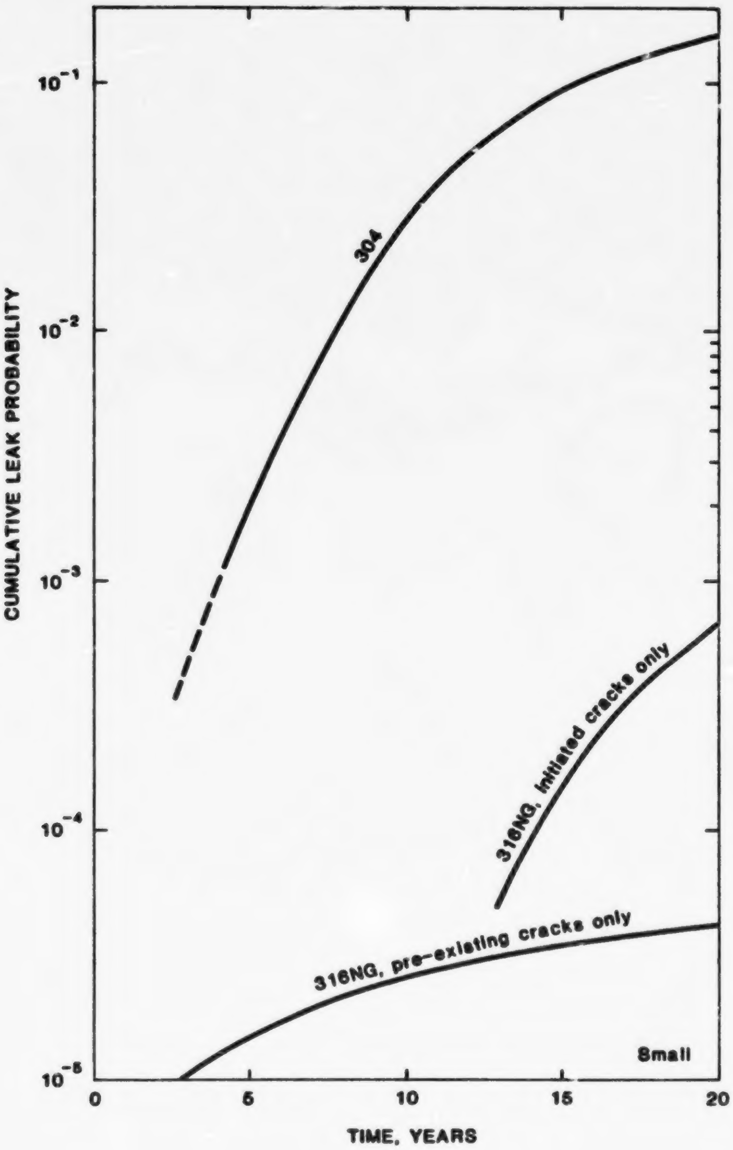

Fig. 7. Cumulative leak probability as a function of time for small-diameter weldments fabricated from Types 304 and 316NG stainless steel.

# DISCLAIMER

This document was prepared as an account of work sponsored by an agency of the United States Government. Neither the United States Government nor the University of California nor any of their employees, makes any warranty, express or implied, or assumes any legal liability or responsibility for the accuracy, completeness, or usefulness of any information, apparatus, product, or process disclosed, or represents that its use would not infringe privately owned rights. Reference herein to any specific commercial products, process, or service by trade name, trademark, manufacturer, or otherwise, does not necessarily constitute or imply its endorsement, recommendation, or favoring by the United States Government or the University of California. The views and opinions of authors expressed herein do not necessarily state or reflect those of the United States Government or the University of California, and shall not be used for advertising or product endorsement purposes.

# SSI AND STRUCTURAL BENCHMARKS

A.J. Philippacopoulos, C.A. Miller, C.J. Costantino
Brookhaven National Laboratory
Upton, NY 11973

H. Graves
Office of Nuclear Regulatory Research
U.S. Nuclear Regulatory Commission
Washington, DC 20555

## INTRODUCTION

This paper presents the latest results of the ongoing program entitled, "Standard Problems for Structural Computer Codes", currently being worked on at BNL for the USNRC, Office of Nuclear Regulatory Research. During FY 1986, efforts were focussed on three tasks, namely, (1) an investigation of ground water effects on the response of Category I structures, (2) the Soil-Structure Interaction Workshop and (3) studies on structural benchmarks associated with Category I structures.

The objective of the studies on ground water effects is to verify the applicability and the limitations of the SSI methods currently used by the industry in performing seismic evaluations of nuclear plants which are located at sites with high water tables. In a previous study by BNL (NUREG/CR-4588), it has been concluded that the pore water can influence significantly the soil-structure interaction process. This result, however, is based on the assumption of fully saturated soil profiles. Consequently, the work was further extended to include cases associated with variable water table depths. In this paper, results related to "cut-off" depths beyond which the pore water effects can be ignored in seismic calculations, are addressed. Comprehensive numerical data are given for soil configurations typical to those encountered in nuclear plant sites. These data were generated by using a modified version of the SLAM code which is capable of handling problems related to the dynamic response of saturated soils.

Further, the paper presents some key aspects of the Soil-Structure Interaction Workshop (NUREG/CP-0054) which was held in Bethesda, MD on June 16-18, 1986. This workshop was set up with the following objectives: (1) to examine the SSI related licensing concerns and various procedures and alternatives jointly by the regulators, practitioners, researchers, utilities and other interested groups in the light of the recent analytical and

---

*This work was performed under the auspices of the U.S. Nuclear Regulatory Commission.

experimental development; (2) to examine the areas of greater uncertainties and means to address them; (3) to review the licensing criteria in the SSI area with an overall view and discuss suggestions to improve the licensing process; and (4) to present results of recent USNRC research. During the workshop the emphasis was placed on particular aspects related to the Unresolved Safety Issue (USI) A-40, "Seismic Design Criteria".

Finally, recent efforts related to the task on the structural benchmarks are described. The objective of this task is to develop benchmark problems which can be used to validate methods and computer codes used by the industry in making predictions of the behavior of Category I structures. Each benchmark consists of an experimental observation which is compared with code predictions. The structural loads, the response characteristics as well as the uncertainties in strength are discussed for one benchmark problem, namely a shear wall benchmark.

## INFLUENCE OF GROUND WATER ON SSI

Soil-structure interaction evaluations of nuclear category I structures are typically performed using continuous or finite element methods which assume that the foundation medium is of the dry type. Under this program, BNL developed a methodology which extends currently available SSI methods to include pore water effects in seismic response evaluations of nuclear structures located at saturated sites. The method was implemented into a computer code which was subsequently used to develop response solutions for the case involving rigid footings resting on saturated uniform deposits (NUREG/CR-4588). The results obtained show that the pore water causes the horizontal mode of the response to increase by more than 50%. Furthermore, the radiation damping associated with rocking mode increases by a factor of more than two as compared with the case of the dry foundation. The frequency variation of the rocking stiffness is further modified due to the influence of the pore water. Finally, with respect to the vertical response it was found that the damping increases by factors of more than four.

The studies performed for the footing case were then extended by considering a model of a typical containment building. Numerical results obtained by BNL indicate that due to the pore water pressure, the rocking response of the reactor containment was significantly reduced.

More recent work on this subject dealt with saturated sites in which the ground water table was located at some depth below the ground surface. The objective was to generate criteria to allow the analyst engineer the ability to judge when ground water effects are significant for a particular problem. For this purpose frequency-dependent interaction coefficients were obtained for typical foundation configurations in which the water table depth was treated as a free parameter. These coefficients were plotted together with the corresponding results from the dry case.

In order to develop solutions for interaction coefficients, a variety of calculations were made using the finite element computer program developed previously (NUREG/CR-4588). For the two-phased soil-fluid system, the governing equations of motion were discretized into a set of nodal equations for the skeleton displacements and the relative water displacements. For any given frequency of steady state motion, the numerical solution is obtained, from which the corresponding soil and pore water stresses can be calculated.

The specific problem investigated is shown in Figure 1. A rigid surface footing of width 2a is located at the surface of the elastic halfspace and moved in the three coordinate directions (horizontal, rocking and vertical modes) in a steady state manner, from which the total forces developed on the footing are calculated. The corresponding influence coefficients are then determined as a function of frequency of the steady state motion. All the data generated is then plotted as a function of dimensionless frequency

$$\lambda = a\Omega/V_s$$

where a is the half footing width, $\Omega$ is the input frequency of the steady state motion and $V_s$ is the shear wave velocity of the dry soil. The specific properties of the soil and water used in the calculations are defined in Figure 1. These are typical for a relatively stiff silty sand.

As mentioned previously, the primary goal of this numerical study has been to determine the influence of the depth to the ground water table (GWT) on the standard interaction coefficients. In the previous study (NUREG/CR-4588), calculations were made for the two cases of either fully saturated soil (GWT at the ground surface) or dry soil (GWT at infinite depth). In this study, the computer program was modified to allow for placing the ground water table at various depths, considering the soil above the GWT as dry. In all the calculations performed, a simplified one-dimensional transmitting boundary was used. As will be seen in some of the following data, this simplified transmitting formulation is reasonably adequate for these calculations. However, in studying more realistic problems, an improved two-dimensional formulation is required. A continuum type of formulation which can be used to generate consistent transmitting boundary was also developed (NUREG/CR-4784).

Calculations were performed with different mesh sizes, i.e., shallower mesh and the deeper mesh. In all cases, the bottom and side boundaries are subjected to the one-dimensional transmitting boundary condition mentioned above. Obviously, the required symmetry conditions are applied on the left boundary.

Next, results are discussed for the finite element mesh which is shown in Figure 2. This is made up of uniform rectangular elements, fourteen laterally (B/A = 7) and eight vertically (D/A = 4). Based upon previous calculations, this mesh is adequate to treat wave propagation up to a dimensionless frequency of 2.5 to 3. All calculations presented herein are thus limited to a maximum dimensionless frequency of 2. Calculations were then performed for a variety of configurations, moving the GWT from the ground surface to a depth specified by H/A = 3.5 (seven elements below the footing). Figure 3 presents horizontal interaction coefficients (stiffness and damping) for a variety of the depth to the GWT. As may be noted from the lower figure, the damping coefficient rapidly decays from the fully saturated case to the dry case, until at a depth ratio of 1.0, at which the damping coefficients are essentially identical to the dry problem. From the upper plot of Figure 3, however, it may be noted that the horizontal stiffness coefficient does not quickly converge to the dry case. Similar data is shown in Figure 4, which shows additional results for the lower depths to the GWT. As can be seen, the damping coefficients still show the independence with the GWT at these depths, with the stiffness coefficients essentially showing relatively uniform results below a dimensionless depth of 2.0.

Similar data using this model for the rocking stiffness and damping are shown in Figures 5 and 6. As may be noted, the damping essentially approaches the dry data at depths below 0.5 while the rocking stiffness converges to the dry case at depths of 1.5. The small differences at the higher frequencies probably are unreal if actual material damping effects were considered in the calculations. All the data at the deeper depths shown in Figure 6 show essentially complete agreement with the dry data at depths below 1.5.

## SOIL STRUCTURE INTERACTION WORKSHOP

The objective of this workshop was to discuss licensing review criteria and related issues in Soil-Structure Interaction (SSI) area and obtain some guidance to assist the NRC staff in the upcoming revision of the SSI related Standard Review Plan (SRP) sections. Further, the specific objective of the last of the workshop session, was to present summaries prepared by each of the panels of the previous four sessions. It is remarkable that this workshop was extremely successful in achieving both of the objectives. Discussions throughout the workshop remain focused on the broader review criteria related issues. The summaries presented by moderators of technical sessions were prepared after lengthy discussions among panel members. These summaries not only provided definite guidance useful for the development of licensing review criteria but also addressed the specific issues and questions identified in the workshop program.

Time and again, thoughout the workshop beginning with Harold Denton's opening address, it was observed that it is necessary to avoid the compounding of conservatism in each step (seismic input, site analysis, SSI analysis, etc.,) of the seismic analysis/design process such that final results do not contain unquantifiable, excessive conservatism. In order to do so, the effective interaction between different desciplines, such as seismology, geotechnical and structural, involved in the seismic design process is very crucial. The effective interaction should lead to clear understanding of needs of different desciplines and assumptions used in various steps, thus providing consistancy between various steps. The interaction between the regulatory agency and the design organization was also discussed. Some of the foreign participants indicated that the licensing review process in their countries was more interactive and started early enough to establish acceptable technical approaches prior to the detailed designs. The concern with excessive conservatism also led to a discussion of performance versus prescriptive requirements. Desirability of specifying a performance criterion over prescriptive requirements were expressed by a number of participants. A truly performance criterion may allow one to perform an analysis using best available techniques and then adding known margin to the final design. However, it was noted that a true performance criterion, in terms or probability of exceedance of some critical parameter, may not be feasible.

The degree of prescriptiveness could also vary depending on how explicitly and systematically one accounts for uncertainties in each step of the analysis. In any event, the staff's proposed revision in the SSI area is very likely to be less prescriptive than the current version.

The objective of Session 2 was to apprise the audience of the state-of-the-art approaches for ground motion estimation. In this light, four currently used approaches were discussed. The ensuring discussion, again, greatly emphasized the interactions between engineers and seismologists to best define the ground motion parameters to achieve the desired desing/analysis objectives. A need for revising Appendix A to 10 CFR Part 100 was also discussed. It was noted that in the U.S. the regulatory process is primarily geared to satisfy the legal requirements and technical considerations, in many cases, are secondary.

In Session 3, with respect to the seismic input to be used in the SSI analysis, the importance of the site effects and the use of the site-specific spectra (defined at finished grade or rock surface) were emphasized. The past experience of using a broad-banded site-independent spectra in a SSI analysis has led to some inconsistent results. The discussion in Session 3 centered on the most controversial element of the current licensing criteria, that is the location if input motion for SSI analysis. The current requirement of defining the control motion at the foundation level in the free-field was examined and discussed at great length.

With respect to the current requirement for SSI methodologies, it was noted that licensing review criteria should not try to regulate "misuse" or "abuse" certain SSI methods or procedures; however, the proper implementation of these procedures should be assured through some other means. In this light, a number of participants pointed out a need for developing simple models to identify critical parameters and to judge the adequacy of the results obtained from a complex analysis. Sensitivity studies and systematic parametric variation should be a part of an SSI analysis.

In Session 5, four invited papers were presented. These papers described some of the more pertinent sources of data (both currently available and planned) that can be used to verify soil-structure interaction methods. These papers also described some correlation studies that were performed using the data to validate various aspects of the SSI problem. A fifth paper was presented by staff of ENEA-Fast Reactor Department (Italy) describing an experimental program being conducted as an integral part of the construction of a breeder reactor. The data sources discussed were: (1) Fukushima, (2) Humboldt Bay, (3) Lotung experiments in Taiwan, (4) SIMQUAKE experiments, (5) HDR shaker tests in Germany, and (6) Japanese shaker and high explosive tests. Much of the discussion regarding correlation studies centered on the liftoff problem. It was generally agreed that this was only important for the higher level earthquakes.

The NRC staff, with consideration of the above have discussed general observations and specific conclusions and recommendations of each of the technical panel sessions. The staff is currently preparing the draft revision of the affected SRP sections. These sections will be issued for public comment prior to finalizing the staff acceptance criteria.

## STRUCTURAL BENCHMARKS

BNL efforts associated with the task of developing structural benchmarks for Category I structures was begun during the last quarter of FY 1986. The objectives of this phase of the overall program are to:

1. Locate experimental data that is useful for benchmarking problems.

2. Relate the parameters of the experimental conditions to nuclear power plant structures and loadings of interest. The program is focused on the seismic response of Category I, shear wall structures.

3. Generate computer solutions for the selected benchmark problems.

4. Correlate the computer solutions with the experimental data. These correlations may then be used to establish the acceptance criteria by which other methods and computer programs may be evaluated when compared with the experimental benchmark data.

BNL examined the data collected on the shear wall tests performed and planned to be performed at Los Alamos National Laboratory. An extensive series of tests are being performed on 1/30 to 1/4 scale model shear wall structures. Both stiffness and strength characteristics of the walls and assemblies of walls are being measured. Stiffness characteristics at both low and high stress levels are considered. These tests have been under way since FY 1980.

The reports describing the work performed to date and the planned work were reviewed. A visit was made to Los Alamos on August 26, 1986 during which the program was discussed with Los Alamos personnel. The measured stiffness of walls have been significantly less than that predicted by standard strength of material models (typical of those used in modeling nuclear power plant structures). It is possible that this reduced stiffness results because of the boundary conditions existing in the tests which are likely different from those found in power plant structures. The loads were applied to the test structures at a point rather than distributed across the top surface of the wall, representing one of the differences with prototype walls. The second difference occurs at the base of the wall. The test walls were clamped to the load frame and lift off likely occurred for some of the walls.

A SAP finite element model of one of the test walls was developed at BNL to investigate the effects of these boundary conditions. Five runs were made as follows:

BEST COPY AVAILABLE

| Run # | Input Load | Base Boundary Condition | Computed Stiffness/ Theoretical Stiffness |
|---|---|---|---|
| 1 | Dist. Across Top | Fully Fixed | 0.911 |
| 2 | Concentrated | Fully Fixed | 0.540 |
| 3 | Concentrated | Release 30% Base | 0.371 |
| 4 | Concentrated | Release 10% Base | 0.511 |
| 5 | Concentrated | Release 40% Base | 0.202 |

As may be seen in problems 1 and 2, the application of a concentrated rather than distributed load reduces the stiffness of the wall to 54%. The base support results in further reduction.

The work under the Structural Benchmarks Program will be continued during FY 1987. Particularly

1. The literature review begun during the past year will be completed. There is an extensive body of literature dealing with shear wall problems. It is essential that this review be performed in a selective manner so that the scope is manageable. The significant problems (uncertainties) as defined in the following task will be used to identify the types of shear wall problems that are of interest. Preliminary screening of data sources will be used to limit the scope of the review and to focus the review in problems of principal interest.

2. The list of uncertainties identified under this task will be expanded. As the literature review proceeds, the data sources will be evaluated against the uncertainties. The goal in selecting benchmark problems will be to obtain a cross section of problems that relate to as many of the uncertainties as possible.

3. Computer solution will be developed for each of the benchmark problems. Acceptance criteria will also be developed which may be used to test the acceptability of alternative methods of solution.

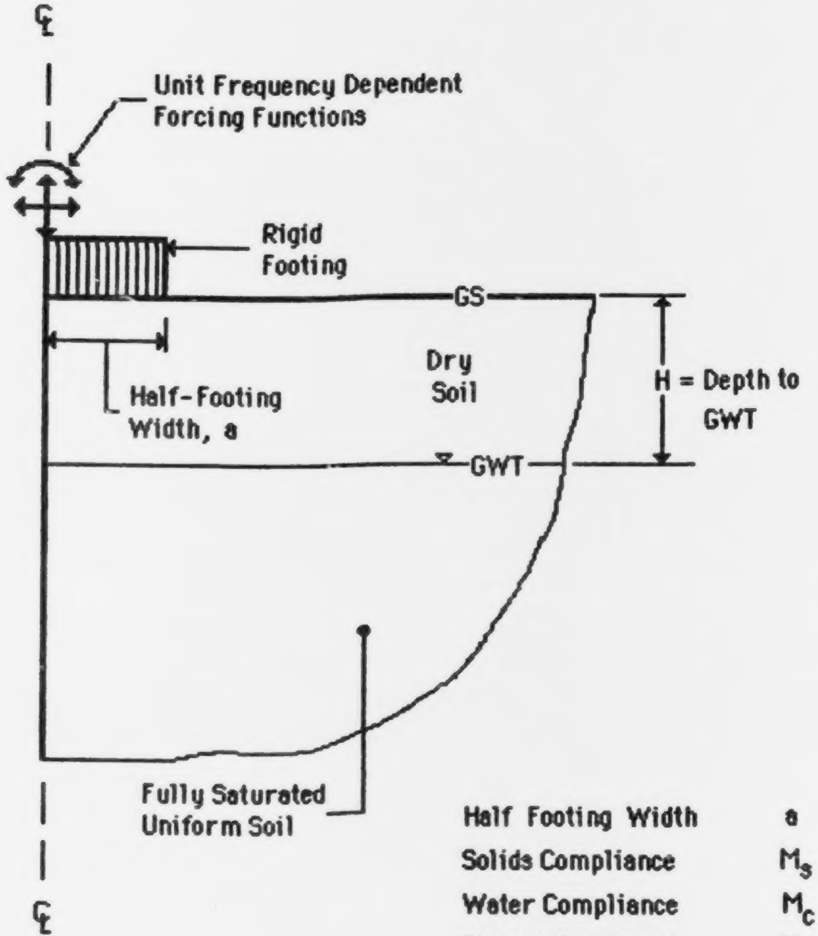
℄
Unit Frequency Dependent Forcing Functions
Rigid Footing
GS
Dry Soil
Half-Footing Width, a
H = Depth to GWT
GWT
Fully Saturated Uniform Soil
℄

| | | |
|---|---|---|
| Half Footing Width | a | 300 inches |
| Solids Compliance | $M_s$ | 14,000 psi |
| Water Compliance | $M_c$ | 293,900 psi |
| Shear Wave Speed | $V_s$ | 448.72 fps |
| Dry P Wave Speed | $V_c$ | 777.19 fps |
| Poisson's Ratio | $\nu$ | 0.25 |
| Dry Soil Density | $\gamma_d$ | 107.47 pcf |
| Sat. Soil Density | $\gamma_s$ | 129.31 pcf |
| Soil Permeability | k | $10^{-1}$ to $10^{-6}$ cm/sec |

Figure 1 - Rigid Footing Atop an Elastic Soil in a Two-Dimensional Plane Strain Configuration

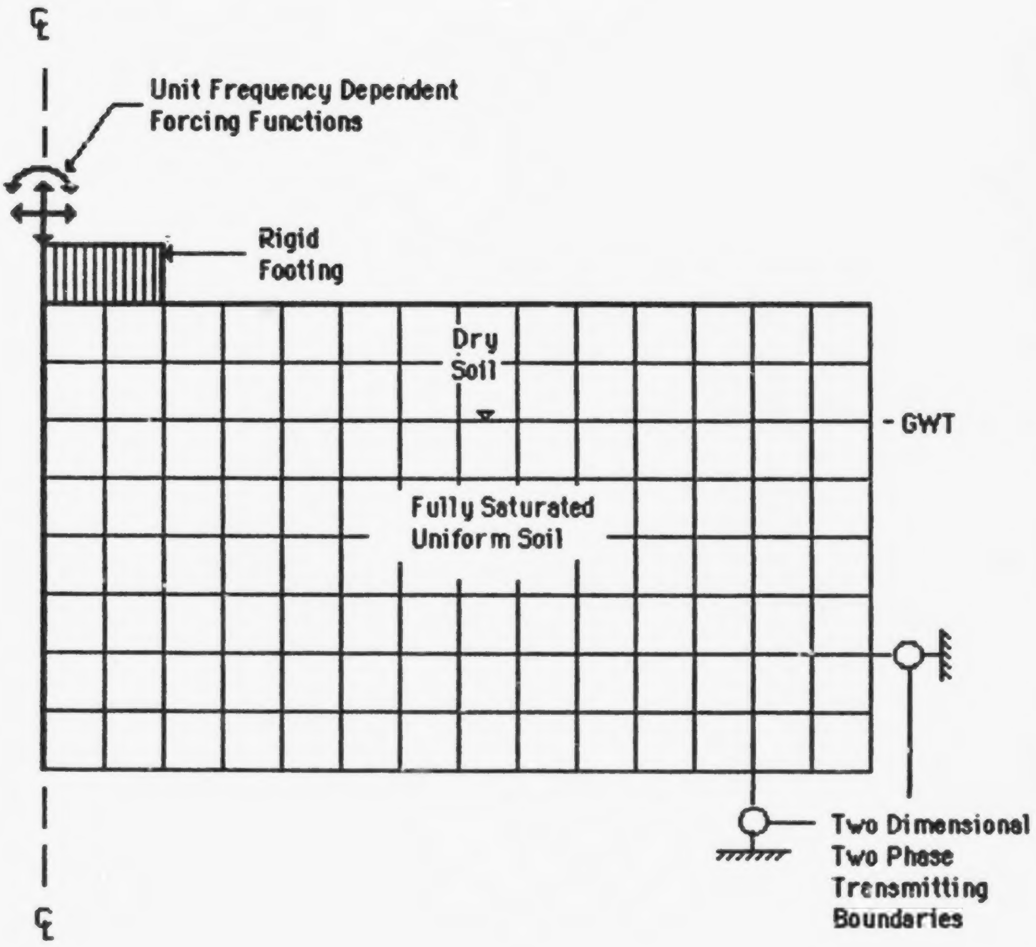

℄
Unit Frequency Dependent Forcing Functions
Rigid Footing
Dry Soil
- GWT
Fully Saturated Uniform Soil
Two Dimensional Two Phase Transmitting Boundaries
℄

Figure 2 - Model 1 Finite Element Mesh

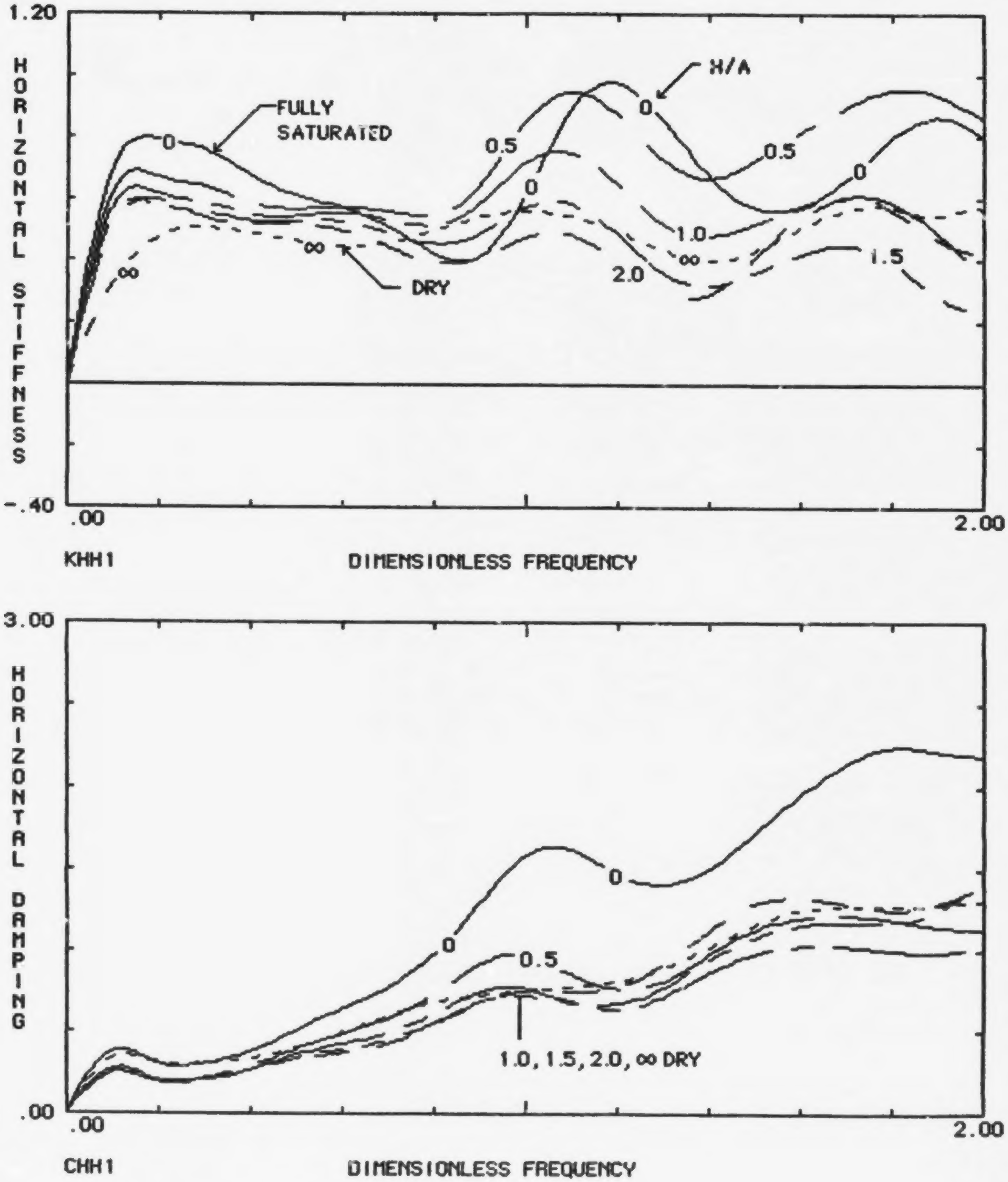

Figure 3 - Horizontal Interaction Coefficients Using Model 1 For A Uniform Soil

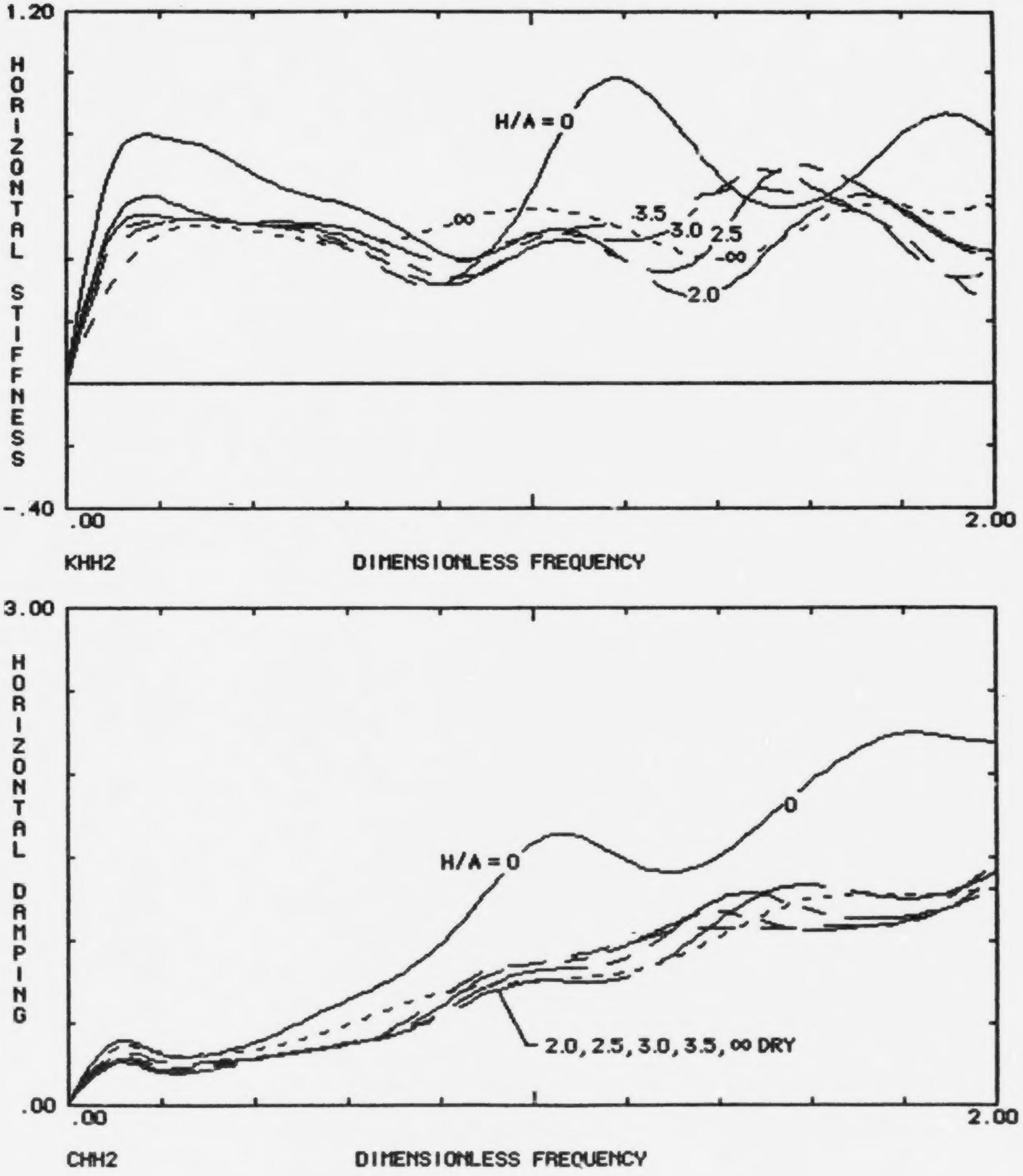

Figure 4 - Horizontal Interaction Coefficients Using Model 1 For A Uniform Soil

BEST COPY AVAILABLE

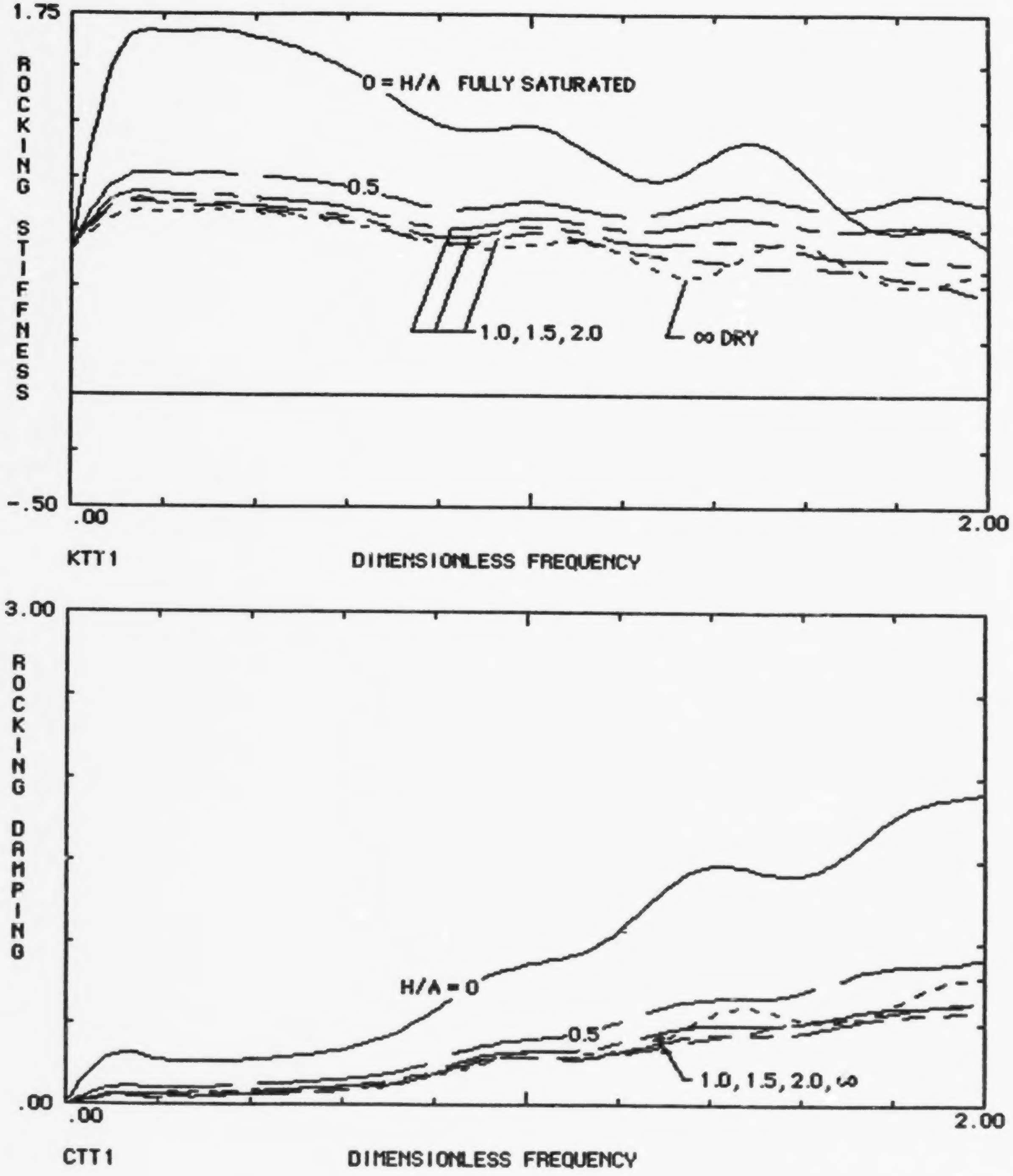

Figure 5 - Rocking Interaction Coefficients Using Model 1 For A Uniform Soil

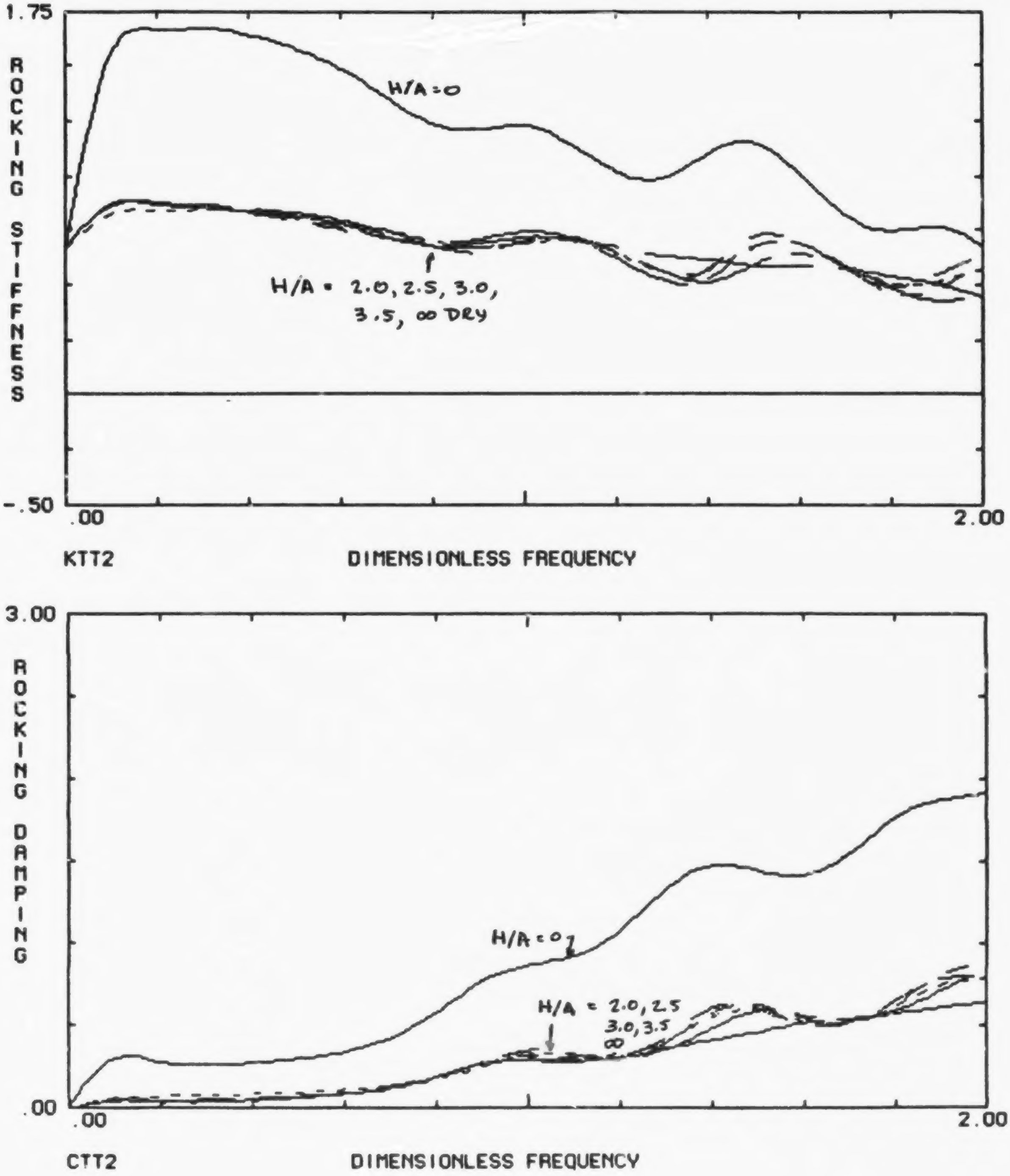

Figure 6 - Rocking Interaction Coefficients Using Model 1 For A Uniform Soil

BLANK PAGE

# NRC VALVE PERFORMANCE TEST PROGRAM--CHECK VALVE TESTING

N. M. Jeanmougin
Energy Technology Engineering Center

## ABSTRACT

The Valve Performance Test Program addresses the current requirements for testing of pressure isolation valves (PIVs) in light water reactors. Leak rate monitoring is the current method used by operating commercial power plants to survey the condition of their PIVs. ETEC testing of three check valves (4-inch, 6-inch, and 12-inch nominal diameters) indicates that leak rate testing is not a reliable method for detecting impending valve failure. Acoustic emission monitoring of check valves shows promise as a method of detecting loosened internals damage.

Future efforts will focus on evaluation of acoustic emission monitoring as a technique for determining check valve condition. Three gate valves also will be tested to evaluate whether the check valve results are applicable to gate type PIVs.

## CURRENT REGULATORY REQUIREMENTS:

Pressure isolation valves (PIVs) isolate the high pressure primary reactor coolant system from connected lower pressure piping systems. Commercial nuclear power plants are required to periodically leak test PIVs in accordance with Section XI of the ASME Boiler & Pressure Vessel Code. The acceptable leak rate across the PIVs is defined in the technical specifications for each plant. The Nuclear Regulatory Commission allows a leakage rate of one-half gpm per inch of nominal valve diameter, but no more than five gpm on any valve. Leakage through the PIVs is monitored and limited for two safety reasons. First, leak rates are monitored to detect imminent failure of the valves' ability to serve as a pressure barrier. Second, the overall leak rate from the high pressure system to the low pressure system must not exceed the low pressure system's pressure relief and radiological processing capabilities.

EG&G prepared a study for the NRC on leak test requirements for PIV's. As part of this study, a survey was conducted of nine plants to obtain information about actual in-plant experience with leak rate testing of PIVs. The study indicated that current utility practice is to conduct PIV leak tests at reduced pressures and to extrapolate to leak rates at normal plant operating pressure, 2235 psig. This practice is allowable using the correlation given in Section XI of the ASME Code. The correlation is based on a ratio of the differential pressure across the valve during normal operation to the differential pressure across the valve during the leak test raised to the one-half power. The correlation is theoretically correct for turbulent flow across the valve ignoring temperature effects.

## VALVE PERFORMANCE TEST PROGRAM--OBJECTIVES

The objectives of the Valve Performace Test Program, currently being conducted at the Energy Technology Engineering Center (ETEC) are to:

1. Evaluate the use of valve leakage as an indicator of valve condition.
2. Evaluate the ASME Code Section XI method for extrapolating leak rates to higher differential pressure conditions.
3. Evaluate the use of acoustic emission monitoring for quantifying valve leakage and as an indicator of valve condition.
4. Evaluate the use of motor signature monitoring as a measure of gate valve operability.

The test program is being performed under contract to the U.S. Nuclear Regulatory Commission (NRC).

## TEST RESULTS

Check valve testing was completed in fiscal year 1986 and is the subject of this paper. The check valves tested have nominal diameters of four, six and twelve inches. Cycling of the check valves, interspersed with leak rate measurements, was performed to assess the correlation between valve wear and leak rate. The valves were subjected to long-term flashing to evaluate the effects of erosion on valve seating surfaces. In addition, testing of the check valves with loosened internals examined the capability of check valves to perform their pressure isolation function with damaged internals. Acoustic emission traces were recorded throughout the check valve leak rate measurements and loosened internals testing.

## FOUR-INCH CHECK VALVE TESTING

### Test Article Description

During fiscal year 1985, the three check valves were installed in the test facility (see Figure 1). The four-inch check valve is a 1,500 lb swing check valve with buttweld ends. The body is fabricated from 316 stainless steel to ASME Section III, Class 1 standards. The seating surfaces have a Stellite hard facing. The valve was manufactured by the Nuclear Valve Division of the Borg-Warner Corporation.

### Life-Cycle Testing

The four-inch check valve was subjected to baseline leak rate testing followed by ten dry cycles (cycles in a nitrogen atmoshpere), fifty wet cycles, and one hundred and fifty additional wet cycles. The wet cycles were made in borated water at 250 F and 2,250 psid. Leak rate tests, at a range of temperatures

BEST COPY AVAILABLE

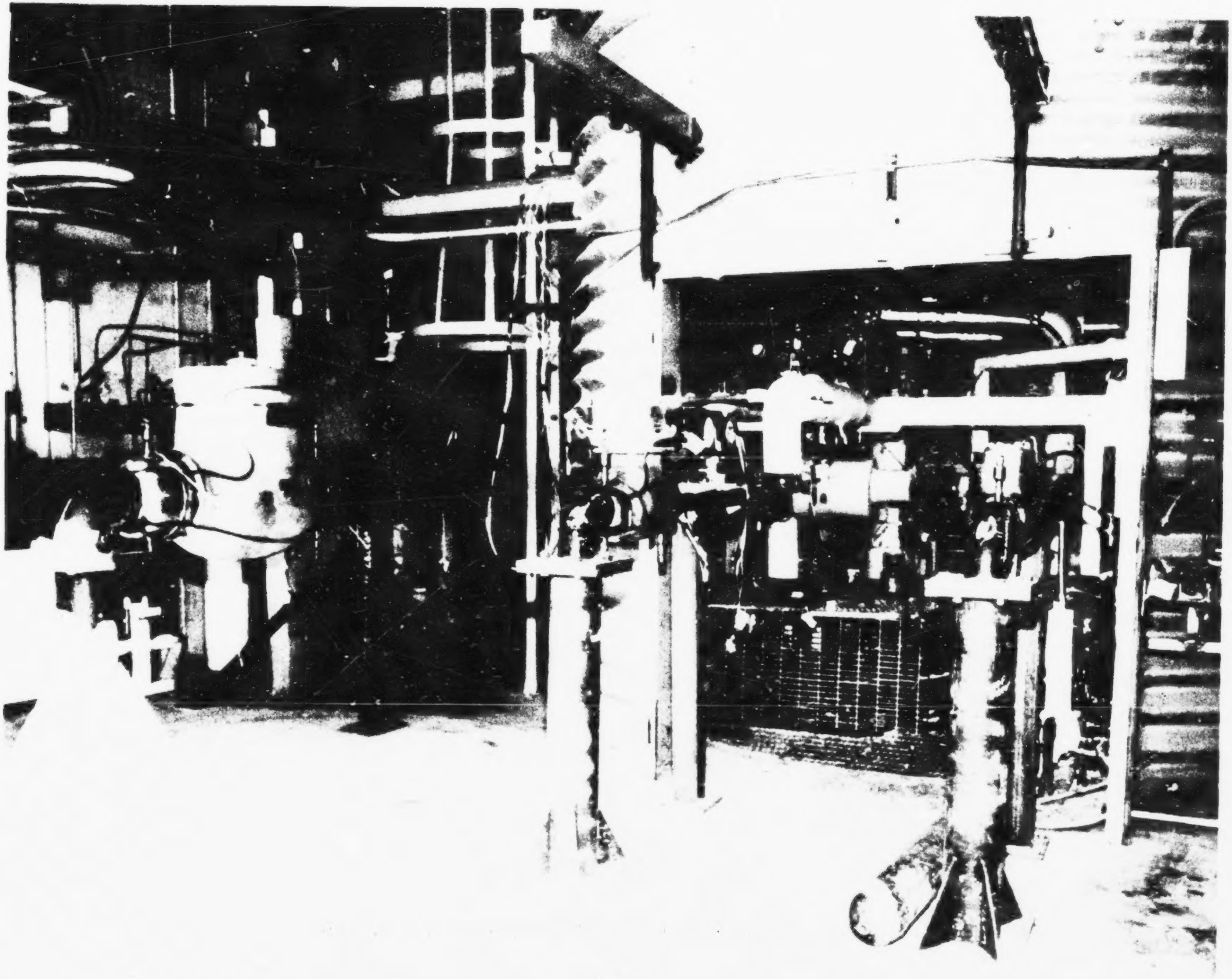

and differential pressures were conducted after each set of dry and wet cycles.

The leak rate across the four-inch check valve did not increase significantly during the program of life cycling. The baseline leak rate was approximately 4 x 10-5 lb/sec. Following the dry cycles, the leak rate across the four-inch valve was too small to be measured, less than 9 x 10-7 lb/sec, perhaps indicating that the valve seating surfaces had "worn in." After the first fifty wet cycles, the valve leak rate was in the measureable region, in the range of 1 x 10-5 lb/sec, similar to the baseline leak rates. The next one hundred and fifty wet cycles had minimal impact on the measured leak rate, marginally increasing the average leak rate to 2 x 10-5 lb/sec.

The leak rate did not vary significantly with either pressure or temperature, except at the lowest differential pressures. The relatively high leak rate at low differential pressures, less than approximately 350 psid, indicates that the valve was not seated tightly. The sealing force for a swing check valve is provided by the pressure difference across the valve; therefore, a minimum differential pressure is required for proper sealing.

### Long-Term Flashing

The life cycle testing of the four-inch check valve indicated that wear due to dry and wet cycling does not cause significant damage to check valve seating surfaces. Therefore, a long-term flashing test was initiated to evaluate the effect of erosion on check valve leak rates. The long-term flashing test was not part of the original program plan, but was added with the concurrence of NRC.

The test began in August of 1985 and continued until late January, 1986. When the long-term flashing test was begun, life cycling of the four-inch check valve had been completed. During long-term flashing, the water on the upstream side of the valves was maintained at 550 F and 1500 psig. Ambient pressure was maintained on the downstream side of the valves. After contacting several operating commercial nuclear power plants, these conditions were determined to be within the range of typical operating conditions for a LWR PIV. During the test, the leak rate across the four-inch check valve increased only slightly to approximately 1 x 10-4 lb/sec.

### Loosened Internals Testing

Following the completion of the long term flashing test in late January, 1986, loosened internals testing of the four-inch check valve was initiated.

The four-inch check valve was wet cycled ten times prior to loosened internals testing to obtain baseline acoustic emissions traces. When leak rate tests were attempted a differential pressure could not be established across the valve, indicating that the valve was not seating. A boroscope was used for in-situ inspection of the valve internals, but the cause of the failure could not be identified. It should be noted that the standard leak rate inspection of PIVs would identify malfunctions of this type once a failure occurred. However, the leak rate monitoring did not indicate impending valve failure.

Since, the next scheduled activity was the removal of the bonnet to loosen the clapper assembly stud, the valve was disassembled for further examination. Problems were encountered during disassembly. The bonnet nuts had galled to the studs; some of the studs broke while they were being removed. New bolts had to be fabricated. In addition, the valve bonnet had galled to the valve body despite the anti-seizure lubricant that was applied during valve manufacture. Special tools, including a spanner wrench, had to be fabricated to remove the bonnet. Similar tools were fabricated to remove the twelve-inch check valve bonnet. The valve disassembly was videotaped.

The valve body, bonnet and clapper assembly were examined with the clapper assembly removed. The clapper stud was deformed by impact with the valve bonnet during cycling, see Figure 2. The four-inch check valve had been subjected to over two hundred cycles during the life cycle phase of testing. The valve bonnet was damaged at the point of contact with the stud, see Figure 3. Although the stud was damaged, it did not appear to be the cause of the valve failure. The exact reason why the valve failed to close could not be identified.

There is concern that check valve failure can be caused by the internal components working loose and becoming incapable of performing their design function. These types of failure occured at San Onofre, Unit 1, contributing to the loss of power and water hammer event which occured on November 21, 1985. At San Onofre, see Reference 1, deformation of the stud was observed in two check valves. The clapper had separated from the hinge arm in both these check valves. Separation of the clapper and the hinge arm did not occur during life cycling of the four-inch check valve in the Valve Performance Program.

At San Onofre, three check valves were found in which the nut which locks the clapper into place had worked loose. The clappers of these valves were found to be caught inside the seat ring. During the Valve Performance Program, the nut on the four-inch check valve did not work loose. In fact, due to the stud deformation, the nut could not be removed without cutting the stud. The design of the four-inch check valve specified a seal weld between the nut and the stud which probably prevented the nut from working loose.

For the first phase of the loosened internals tests, the seal weld was cut, the deformed stud replaced, and the nut backed off two full turns, approximately 0.16 inches, as shown in Figure 4. The maintenance manual for the four-inch check valve was not available (the valve was purchased from a utility), so the manufacturer was contacted to obtain the proper procedure for reassembly of the valve. A manufacturer`s representative verbally described the procedure. However, after reassembly, a pressure differential could not be established across the valve; the valve was not seating. A boroscope and an X-ray examination were made. The X-ray showed that the clapper was too low and was getting hung up on the seat. The manufacturer was contacted and visited the facility. It was discovered that the reassembly procedure had

[illegible] Valve Hinge Assembly
[illegible]

BEST COPY AVAILABLE

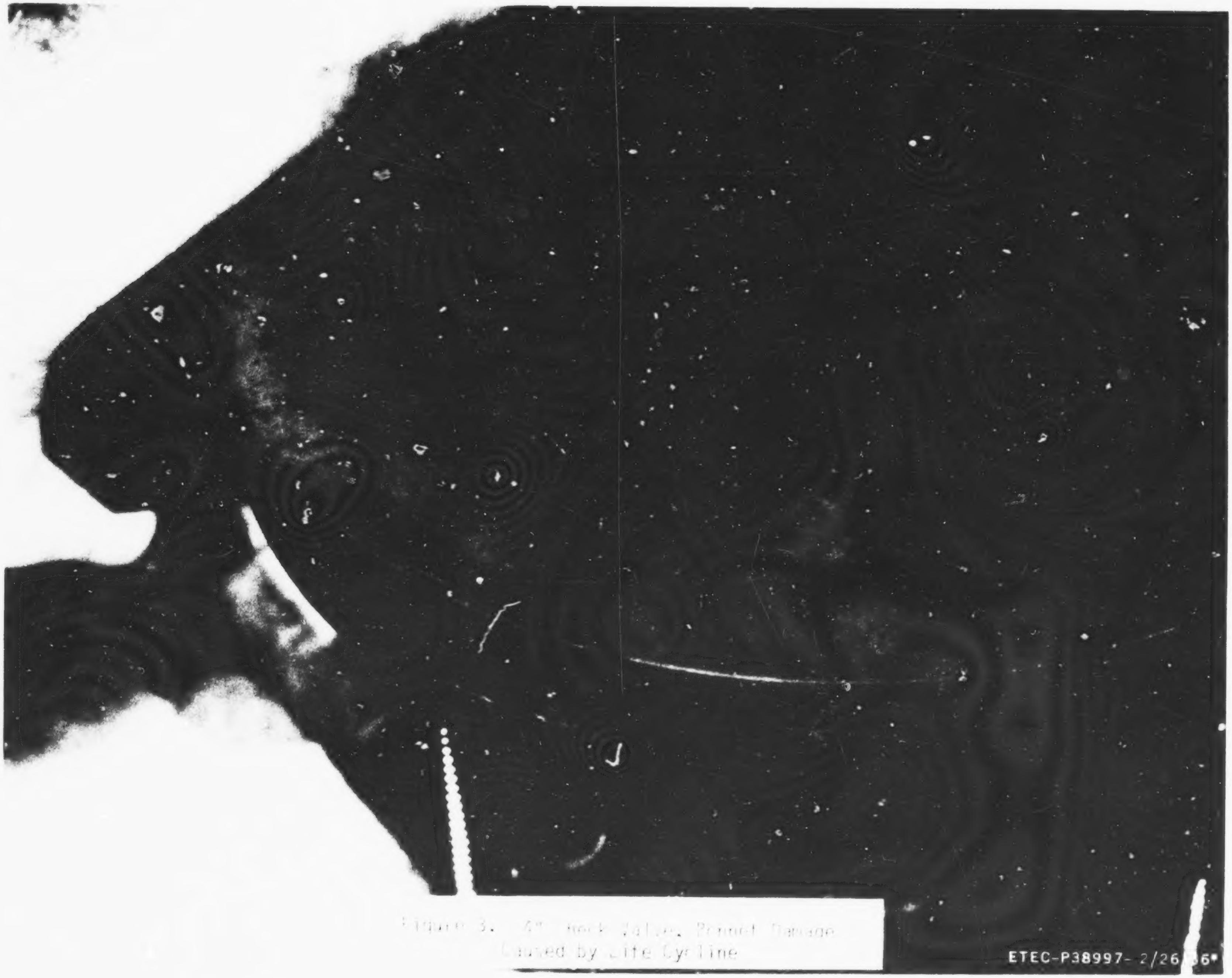
ETEC-P38997- 2/26/[illegible]6

Figure 3. 4" Check Valve, Poppet Damage Caused by Life Cycling

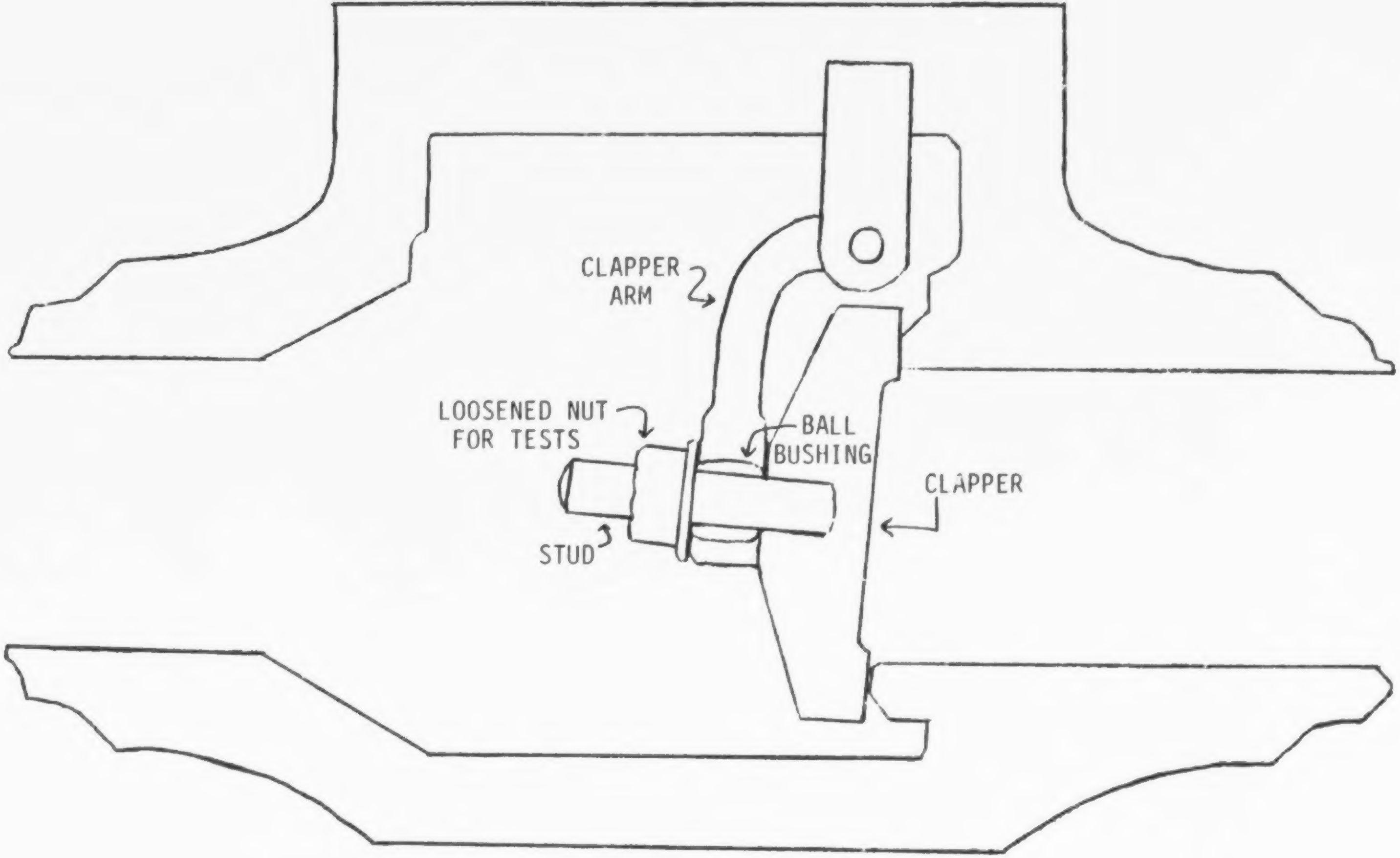
BONNET
CLAPPER ARM
LOOSENED NUT FOR TESTS
BALL BUSHING
CLAPPER
STUD

Figure 4. 4" Check Valve Simplified Schematic

been revised. The bonnet was removed and the clapper assembly readjusted allowing the valve to seat properly.

This experience emphasizes the importance of having up-to-date procedures.

Following valve reassembly, leak rate measurements were made. The leak rate was measured at 250 F and at a range of differential pressures from 150 psi to 2,200 psi. The leak rate varied from 1.4 x 10-4 lb/sec at low differential pressures to 7 x 10-5 lb/sec at higher differential pressures. The average was approximately 1.2 x 10-4 lb/sec. This rate is roughly the same as the leak rate measured after completion of the long-term flashing test, and is well within the range of acceptable PIV leak rates. The valve then was cycled five times and the leak rate measurements were repeated. The average leak rate from the second set of leak rates was equal to that of the first, 1.2 x 10-4 lb/sec.

The purpose of the sequence of leak tests and cycling was twofold: first, to determine if the valve reseats in a reproducible manner, as determined by leak rate, with its internals loosened; secondly, to obtain acoustic emission (AE) traces of the valve cycle to evaluate whether the degraded condition of the valves could be identified using AE data. The results of the leak rate tests indicate that the valve did seat in a reproducible manner. The acoustic emissions data will be discussed later.

For the second phase of loosened internals testing, the clapper assembly nut was backed off an additional four rotations. This resulted in a free length of 0.5 inches between the front of the nut and the back of the clapper. The sequence of leak tests, five wet cycles, leak tests, five wet cycles, and leak tests was repeated. The leak rate was consistently very low during all the leak tests, approximately 2 x 10-4 lb/sec, indicating that leak rate is not a good diagnostic technique for this check valve condition.

## SIX-INCH CHECK VALVE TESTING

### Test Article Description

The six-inch swing check valve is a 1,500 lb valve with buttweld ends. Its body is fabricated from 304 stainless steel with a Stellite hard facing on the seating surfaces. The valve was manufactured by the Atwood & Morrill Company to the requirements of ASME Code, Section III for Class 2 valves. A Class 2 valve is built to the same design as a Class 1 valve, but the quality assurance documentation requirements are not as stringent.

### Life Cycle Testing

During fiscal year 1985, the six-inch check valve was dry cycled but not wet cycled. The results of this initial testing were similar to the results obtained with the four-inch check valve: very low leak rates in the as-received condition (8 x 10-5 lb/sec) and no measureable leak rate following the dry cycles.

When wet cycling of the six-inch valve was initiated during fiscal year 1986, a water hammer problem was encountered and the cycling was interrupted after ten cycles had been completed. The facility was modified by adding a standpipe to the inlet line. The six-inch check then was subjected to seventy five additional wet cycles (eighty five total wet cycles). Leak tests conducted after the cycling indicated that the seating surfaces had suffered only minor damage during the life cycling, the average leak rate was 2 x 10-3 lb/sec.

## Long-Term Flashing Tests

The six-inch and twelve-inch check valves were subjected to long-term flashing concurrently with the four-inch check valve in August of 1985. At that time the six-inch check had been dry cycled but had not been wet cycled. Its leak rate before the flashing test was not measureable. At the end of the long-term flashing test, the leak rate had increased slightly to an average of 4.4 x 10-4 lb/sec. The minor increase in leak rate indicates that the ability of the six-inch check valve to function as a pressure barrier was not impaired by erosion damage to its seating surfaces.

The leak rate also was measured at intervals during the long-term flashing test. It varied but was always small. Changes in the leak rate often occurred after the valves were cycled; probably due to particulate matter either being swept off or deposited on the seating surfaces during the cycling.

## Loosened Internals Testing

The valve was dissambled for loosened internals testing and the clapper assembly and valve body were examined after completion of the wet cycling program. Although the six-inch check valve leak rates after life cycling and the long term flashing were well within the allowable leak rate for PIVs, they were higher than the leak rates across either the four-inch or twelve-inch check valves. Examination of the valve seating surfaces did not show any damage account for the higher leak rates. Differences in valve design may account for the higher leak rate. Unlike the four-inch valve, the six-inch check valve did not substain damage to the clapper assembly, bonnet or valve body during the cycling, see Figure 5. The four-inch check valve was cycled more than the six-inch check valve, approximately two hundred and one hundred cycles, respectively.

The internals of the six-inch valve were loosened as shown in Figure 6. The bolt to clevis assembly weld was ground off and the bolt was loosened 0.27 inches. After the internals were compromised the valve was cycled five times, leak tests were conducted, the valve was cycled five additional times and the leak tests were repeated. The average leak rate after the first set of cycles was almost the same as the leak rates measured before the loosened internals test, 1.5 x 10-3 lb/sec versus 1.9 x 10-3 lb/sec. After the second set of cycles, the leak rate decreased by an order of magnitude to 1.9 x 10-4 lb/sec. The decrease may indicate some inconsistency in seating of the six-inch check

Figure 5. 6" Check Valve Clapper Assembly after Life Cycling

BEST COPY AVAILABLE

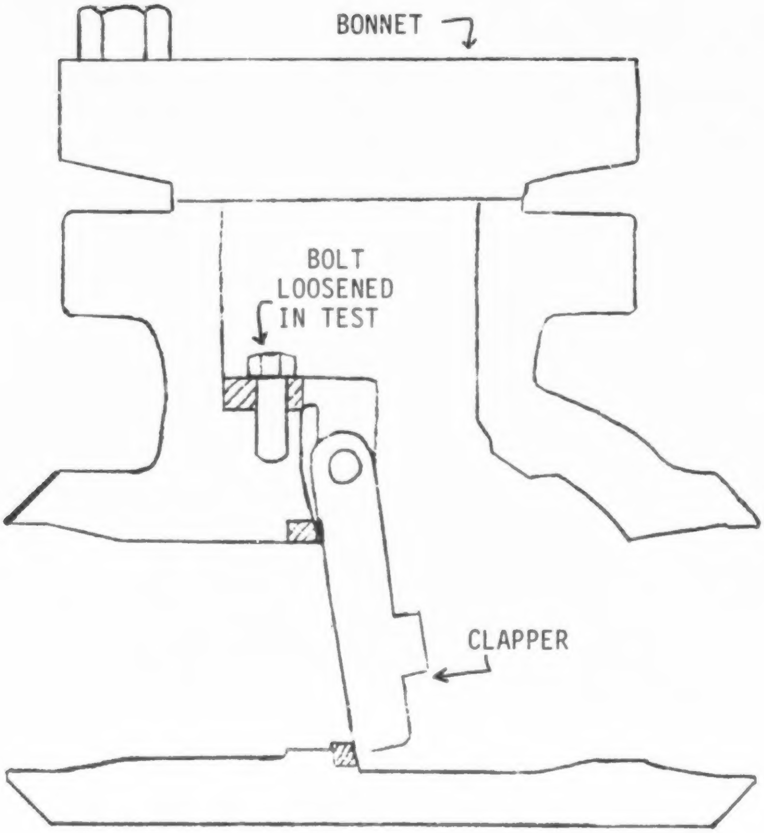
BONNET
BOLT LOOSENED IN TEST
CLAPPER

Figure 6. 6" Check Valve simplified schematic

valve with loosened internals or may be due to particulate matter dislodging from the seat thereby producing a better seal.

The six-inch valve internals were loosened a second time with the bolt being loosened a total of 0.5 inches. After five wet cycles, the leak rate was 1.0 x 10-4 lb/sec. the same as before the additional loosening. Following five additional cycles, the average leak rate was measured as 1.1 x 10-3 lb/sec. Thus the inconsistency in measured leak rate was repeated. The valve was reseating differently after being cycled. However, the leak rates were so small that it would be impractical to expect utilities to detect similar variations.

## TWELVE-INCH CHECK VALVE TESTS

### Test Article Description

The twelve-inch check valve is a swing check valve manufactured by the Nuclear Valve Division of Borg-Warner. Its general design is similar to that of the four-inch check valve used in this test program. It is a 1,500 lb valve with buttwelded ends, a 316 stainless steel body and Stellite hard facing on the seating surfaces. The valve was manufacted per requirements of Section III of the ASME Code. It is a Class 1 valve.

### Life Cycle Testing

The twelve-inch check valve was not cycled during fiscal year 1985. During fiscal year 1986, the twelve-inch valve was wet cycled twenty times at 250 F and 2,250 psid, the number of cycles which could be made with one full load of supply water. The life cycling of the twelve-inch valve was abbreviated because life cycling did not significantly damage the seating surfaces of the four-inch and six-inch check valves. As for the smaller diameter check valves, the twelve-inch valve leak rate was very small following the wet cycling. The average baseline leak rate was 4.0 x 10-6 lb/sec, after long term flashing the average leak rate was 7.7 x 10-4 lb/sec, and following the wet cycles the average leak rate was 3.6 x 10-4 lb/sec.

### Long-Term Flashing Tests

The long-term flashing of the twelve-inch check valve was done prior to cycling of the valve. The erosion produced by flashing across the valve resulted in a small increase in flow rate. But as later examination would show, neither the cycling nor flashing caused significant damage to the twelve-inch check valve seating surfaces.

### Loosened Internals Testing

The valve was disassembled for loosened internals testing and the clapper assembly, valve body, and seating surfaces were examined. No significant damage was found. The seating surfaces were cleaned before reassembly.

The twelve-inch valve is similar in design to the four-inch check valve. However, there are two bolts in the twelve-inch valve clapper assembly as seen in Figure 7. The first phase of the loosened internals test consisted of loosening the stud nut on the back of the clapper assembly. The weld between the nut and the stud was cut and the nut was loosened 1.12 inches. If the nut were loosened more than 1.12 inches, the clapper arm could completely slide off the ball bushing (see Figure 7). This would probably cause the clapper arm to hang up on the outer edge of the bushing preventing the clapper from seating. By loosening the nut 1.12 inches, the test program evaluated whether the valve could seat with the integrity of its internal assembly compromised, rather than illustrating that it was possible to loosen the internals to a degree that would ensure that the clapper did not seat. The ability of leak rate testing to identify impending valve failure also was examined.

The valve was cycled six times and the leak rate was measured. The leak rate was lower than it was prior to the loosening, 7 x 10-6 lb/sec versus 3.6 x 10-4 lb/sec. Cleaning of the seating surfaces probably accounts for the decreased leak rate. After five additional cycles, the measured leak rate was somewhat larger, 1.2 x 10-5 lb/sec.

For the second phase of the loosened internals testing, the nut on the back of the clapper was retightened. The clevis assembly bolt (see Figure 7) was loosened 2 rotations (0.15 inches), this allowed the clapper assembly to rotate freely. In order to loosen the clevis assembly, it was necessary to cut two welds: one between the bolt and the clevis; and the second between the clevis and the bonnet. After the valve was cycled five times, the average measured leak rate was 4.5 x 10-4 lb/sec. The leak rate measured following an additional five cycles was 3.8 x 10-5 lb/sec. Although these results show some inconsistency in leak rate following cycling, the leak rates are consistently low, well within allowable PIV limits. It would be difficult to accurately measure leak rates of this magnitude in operating plants.

## ANALYSIS RESULTS

### ASME Correlation

The correlation given in Section XI of the ASME Boiler and Pressure Vessel Code is used by commercial nuclear power plants to extrapolate valve leak rates measured at low differential pressures to leak rates at larger differential pressures. The correlation was developed to allow utilities to conduct the required valve leak rate tests at low differential pressures during plant shutdowns rather than requiring them to match the differential pressure conditions which exist during normal plant operation. The correlation is based on the square root ratio of the differential pressure during operation to the differential pressure during leak rate testing as shown below. The correlation does not include temperature affected parameters such as visosity or density.

$$Lo = Lt \sqrt{(\Delta Po/\Delta Pt)}$$

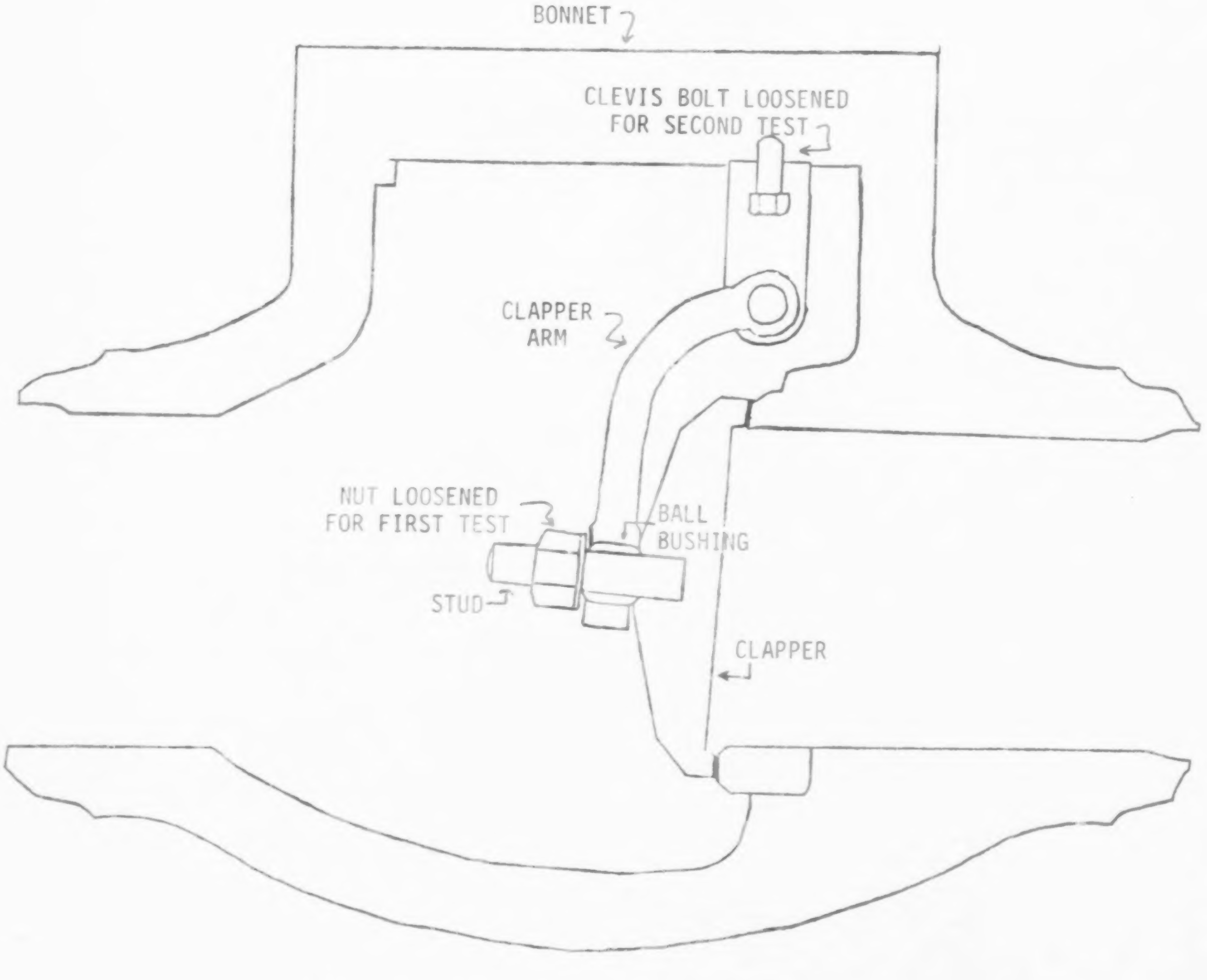
BONNET
CLEVIS BOLT LOOSENED FOR SECOND TEST
CLAPPER ARM
NUT LOOSENED FOR FIRST TEST
BALL BUSHING
STUD
CLAPPER

Figure 7. 12" Check Valve Simplified Schematic

To evaluate the accuracy of this correlation, the check valve leak rates were measured over a range of differential pressures. Leak rate measurements also were made at various temperatures to determine whether fluid temperature affects the correlation. The graphs shown in Figures 8 to 10 compare the measured leak rates to those extrapolated from the leak rate measured at the lowest differential pressure using the ASME Code correlation. In most cases, the code correlation results in conservative predictions, that is, the measured leak rate is less than predicted using the correlation. This holds true for leak rates measured during the loosened internals testing as illustrated in Figures 11 and 12. Although the correlation did not give conservative results in all cases, the measured leak rates never greatly exceeded the predicted leak rate.

Because the check valve leak rates measured during this test program are very low, less than 3 x 10-3 lb/sec, it may be difficult to extrapolate the results of these tests to leak rates in the range of .1 to 5 gpm. However, the results obtained illustrate the importance of applying an adequate differential pressure across the face of the valve during the leak rate testing. The sealing force for swing check valves is supplied by the differential pressure across the valve face. If the applied differential pressure is too low, the valve will not seal properly and overly conservative results will be obtained. In some cases, the leak rate measured at low differential pressures exceeded the leak rate measured at higher differential pressures. No relationship between temperature and measured leak rate was discerned (see Figure 13).

## Acoustic Emission Monitoring

There were four acoustic emission measurement systems installed on the test valves. The systems were supplied by ETEC, Argonne National Lab (ANL), Oak Ridge National Lab (ORNL), and the Naval Ship Research & Development Center. Each of the four acoustic emission systems had a transducer installed on the valve (see Figure 14) and another transducer installed on the valve inlet pipe (see Figure 15).

The original purpose of the acoustic emission systems was to evaluate the effectiveness of acoustic emission techniques for detecting, quantifying, and trending valve leakage. However, during the course of the program, one of the acoustic emission systems was adjusted to obtain acoustic traces of valve cycling during the loosened internals testing. The objective was to evaluate whether loosened internals could be detected with acoustic emission monitoring during valve cycling. Since the ETEC and ORNL systems were very similar, the ETEC transducers were chosen to be readjusted to monitor the acoustic frequencies produced during valve cycling.

The leak rates measured during the check valve testing were very small, less than 3 x 10-3 lb/sec. These small leak rates are below the range of reliable measurement for acoustic emission systems. Therefore, the data could not be used to evaluate acoustic emission monitoring as a method for quantitative leak rate measurement. The acoustic emission monitoring during leak rate

FIGURE 8: 4" CHECK VALVE

Post 50 Wet Cycles, Ambient Temperature

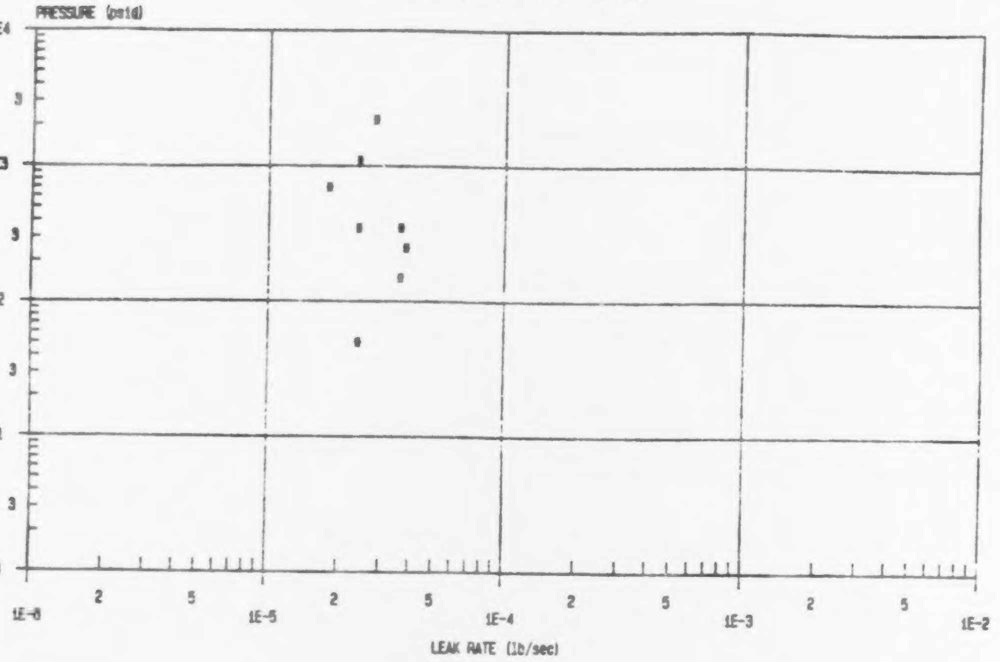

FIGURE 9: 6" CHECK VALVE

Baseline Data, Ambient Temperature

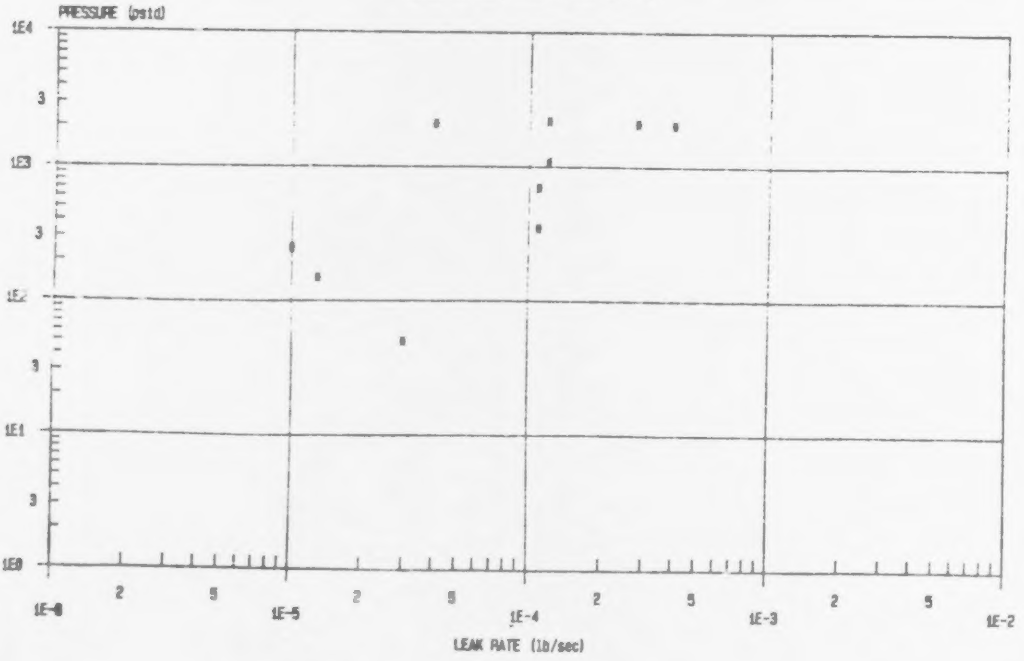

## FIGURE 10: 12" CHECK VALVE

Post Long-Term Flashing, 250F

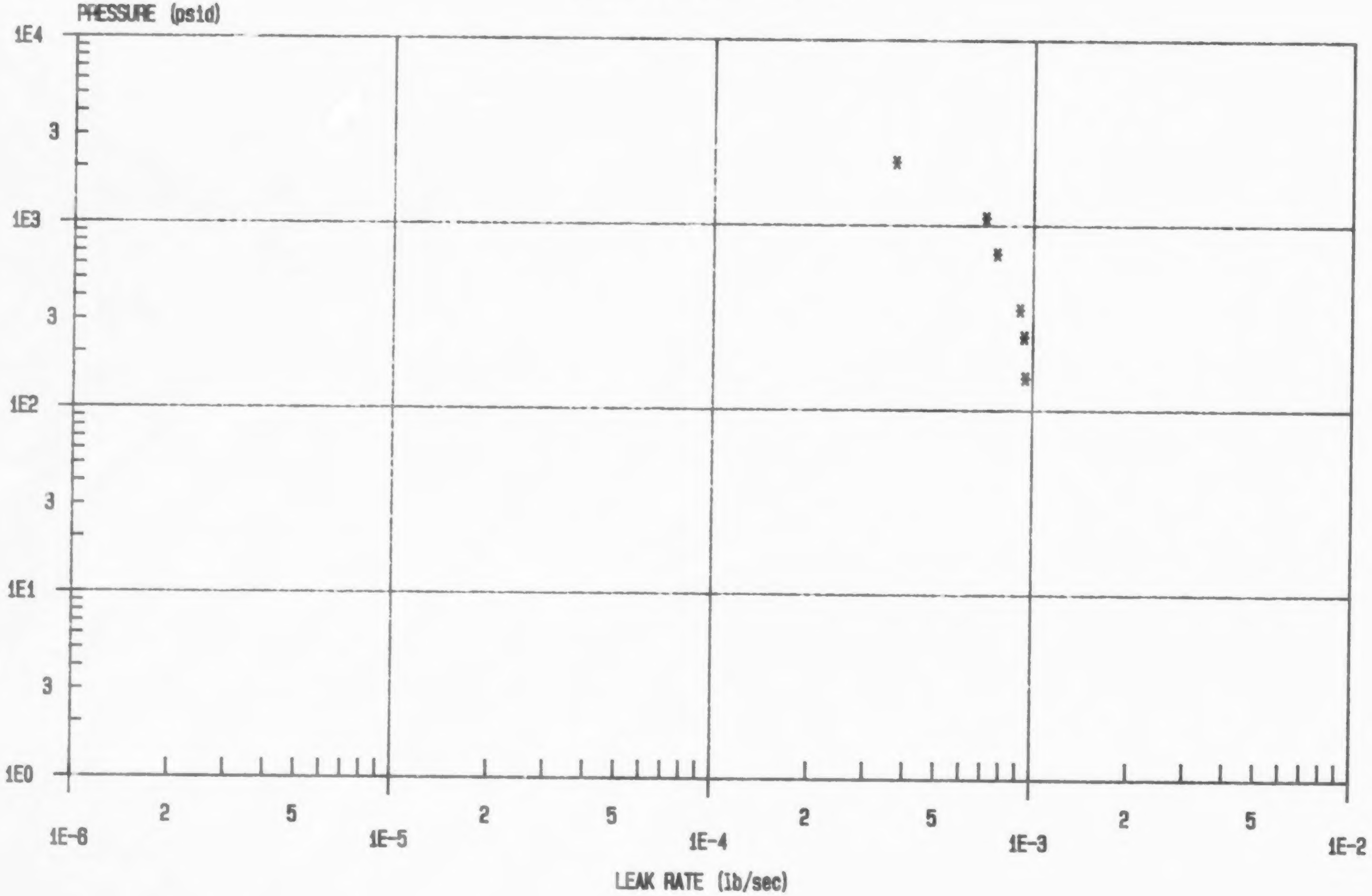

138

FIGURE 11: 4" CHECK VALVE

Internals Loosened 0.5"

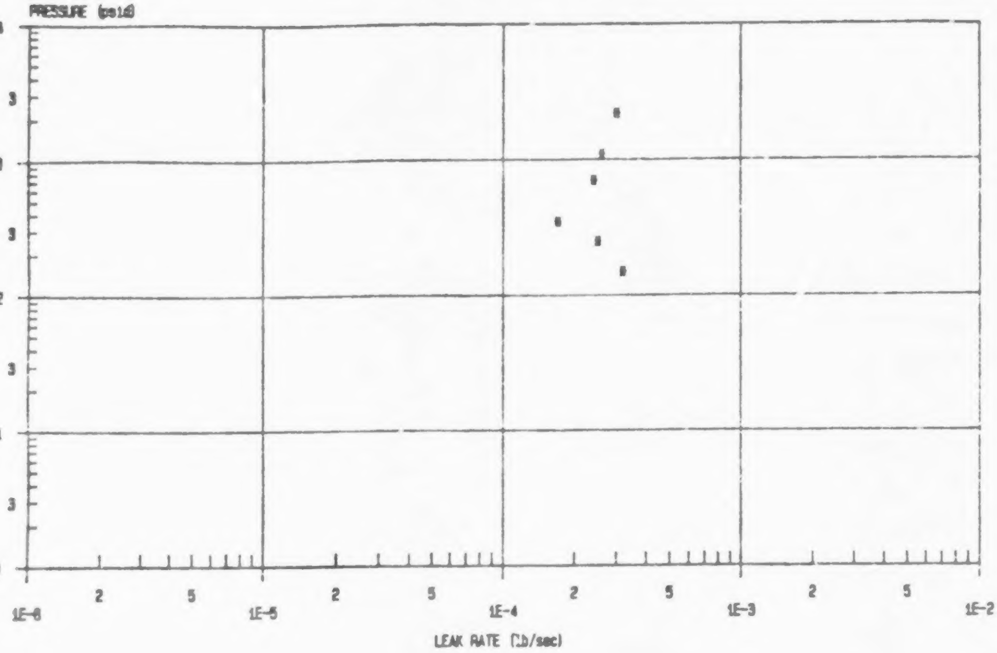

FIGURE 12: 6" CHECK VALVE

Internals Loosened 0.5"

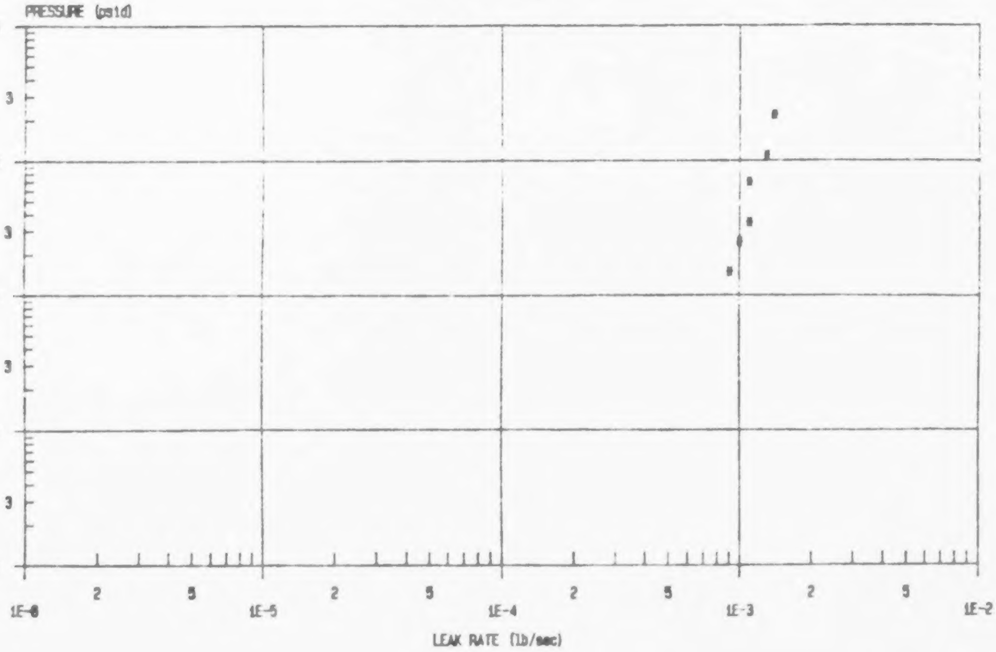

# FIGURE 13: EFFECTS OF TEMPERATURE

4" Check Valve—250F, 350F, 450F, 550F

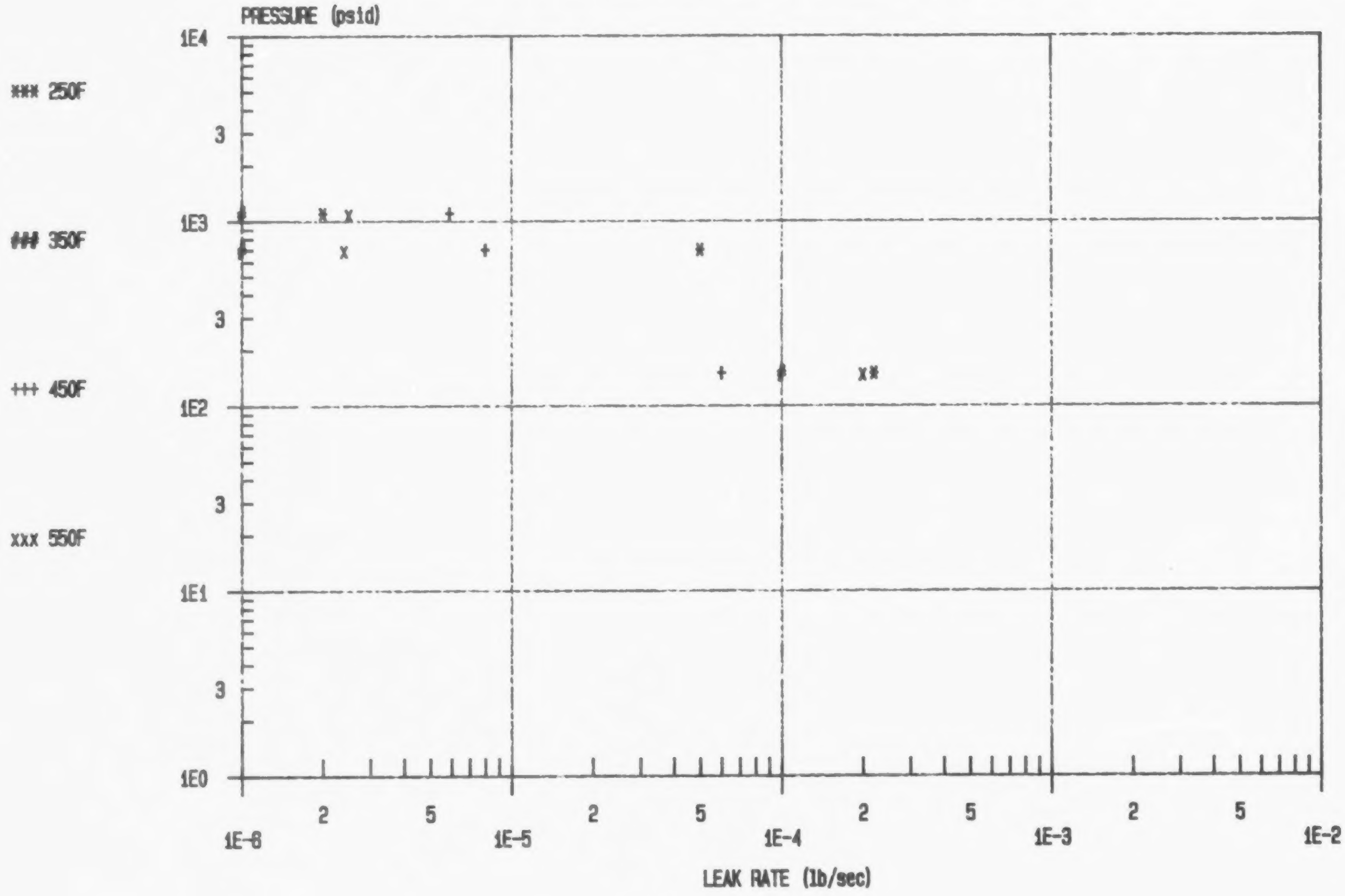

140

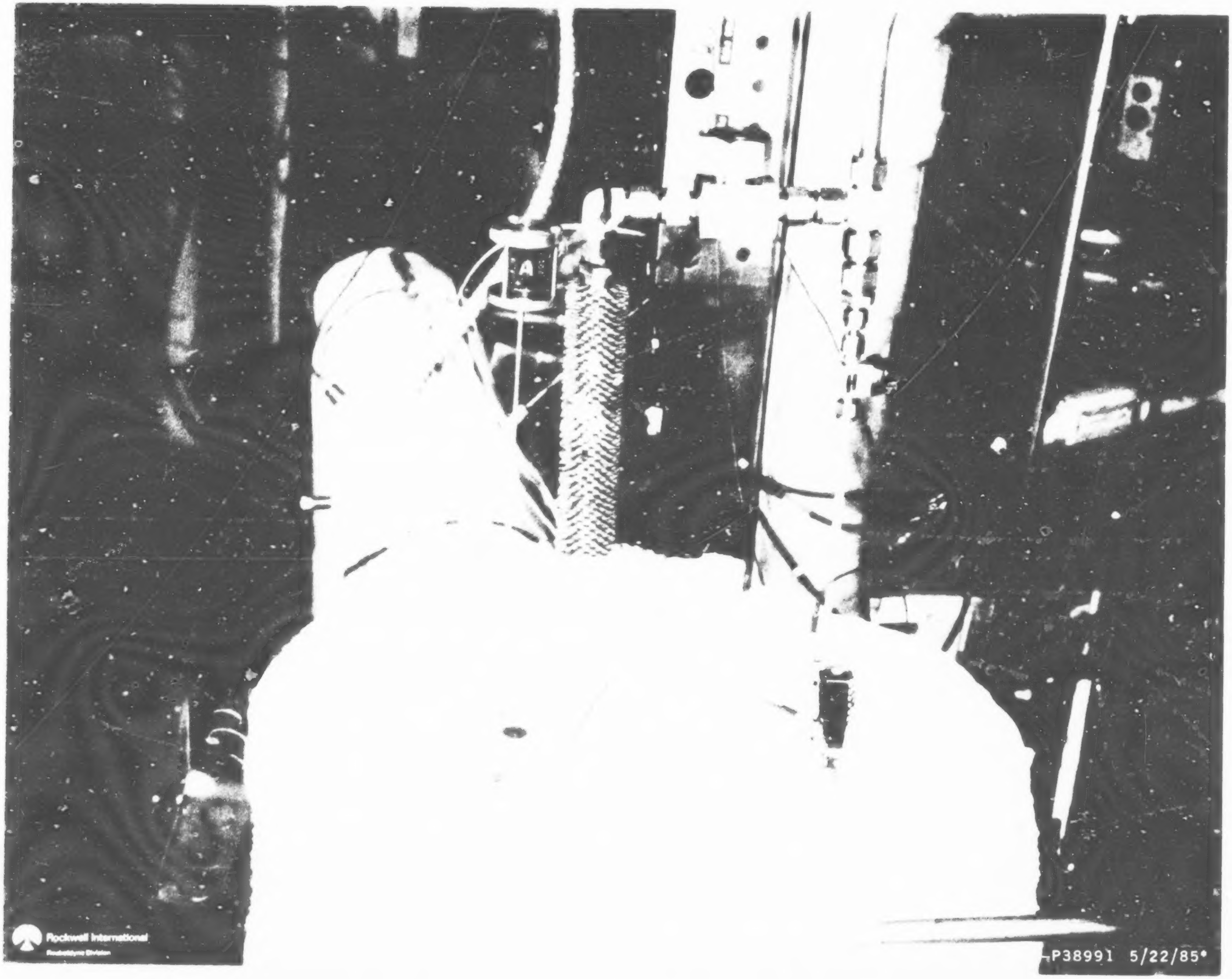
A
Rockwell International
Rocketdyne Division
P38991 5/22/85

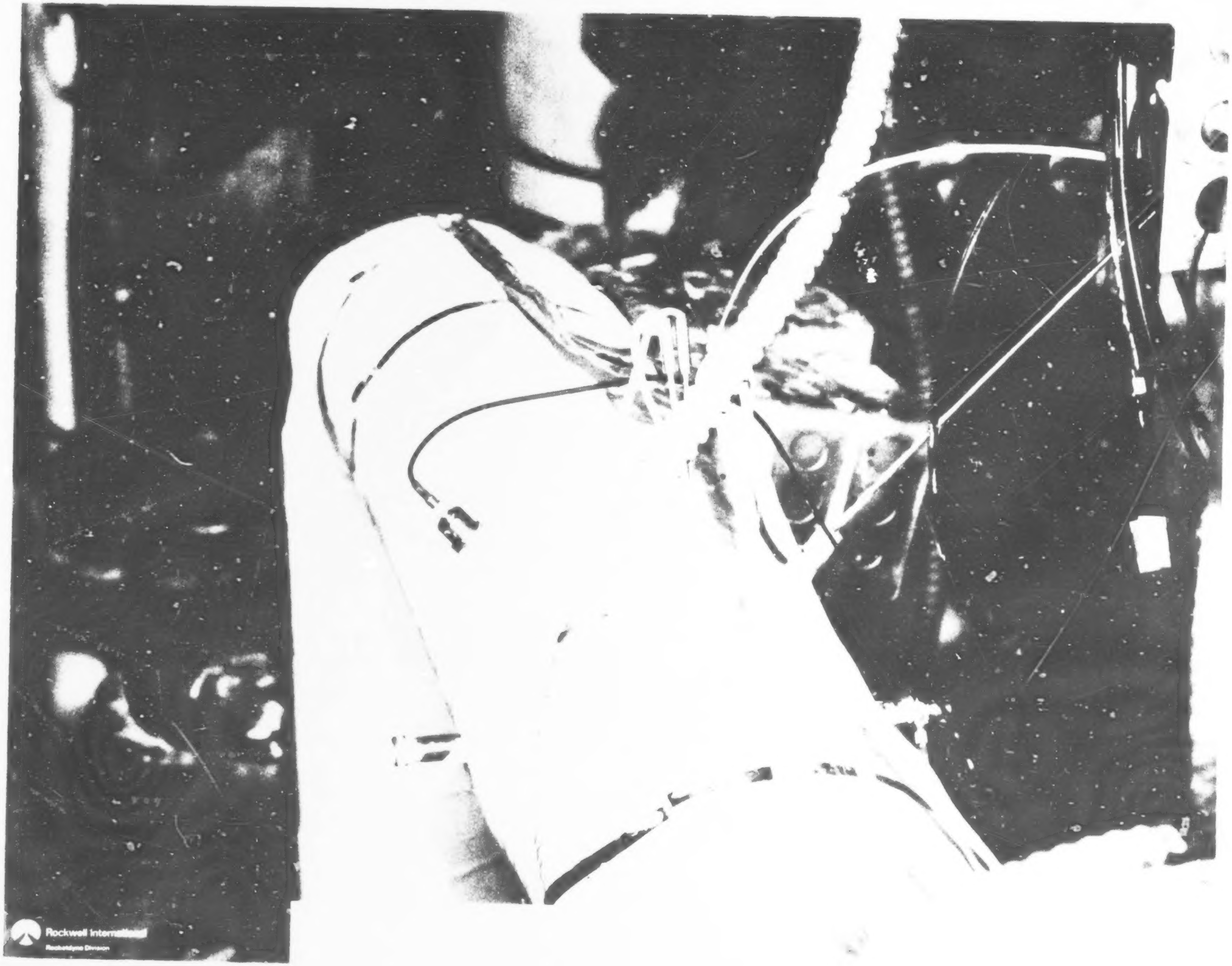
Rockwell International
Rocketdyne Division

testing will continue through the gate valve portion of the testing. Hopefully, the gate valve data will be useful in evaluating acoustic emissions monitoring for qualitative and quantitative trending of valve leak rate.

The acoustic emission data was shared with ANL, ORNL, and the Naval Ship Research & Development Center. In addition, a representative from Leak Dynamics Company visited ETEC during the long term flashing program and monitored the acoustic emission traces of the four-inch check valve. Leak Dynamics is under contract to the Nuclear Regulatory Commission (NRC). These organizations will make independent evaluations of the data for the NRC programs in which they participate.

Although the low leak rates measured during the check valve testing prevented an accurate evaluation of the ability of acoustic emission monitoring to quantify valve leak rate, the acoustic emission equipment was extremely valuable for another purpose. The acoustic emission traces made of the valve cycling during the loosened internals tests indicate that acoustic emission monitoring may be effective in detecting this check valve condition. Figure 16 shows two acoustic emission traces recorded during testing of the six-inch check valve. The first is a trace of cycle made with the valve internals in the as-received condition. The second is a cycle trace recorded after the first loosening of the valve clapper assembly. The second trace shows two high amplitude peaks whereas the first shows only one. The difference is attributed to a different seating pattern with loosened internals.

A new phase of check valve testing during fiscal year 1987 will focus on identifying an acoustic emission monitoring technique which can be used by utilities to detect loosened check valve internals.

## CONCLUSIONS

Leak rate testing did not identify whether the integrity of a check valve clapper or clevis assembly had been compromised, even when the clapper restraining nut was almost detached from the stud.

Leak rate monitoring was not effective in predicting impending failure of the four-inch check valve. However, leak rate testing did indicate that the failure had occured.

Life cycling of check valves can damage the clapper assembly. Although this type damage did not result in any valve failures during the Valve Performance Program, the damage to the clapper stud on the four inch check valve indicates that valve failure could occur during plant operation. A possible scenario could include failure of the clapper stud.

Life cycling of check valves does not significantly degrade the seating surfaces of the valves.

Acoustic emmission shows promise as a technique to identify loosened valve internals.

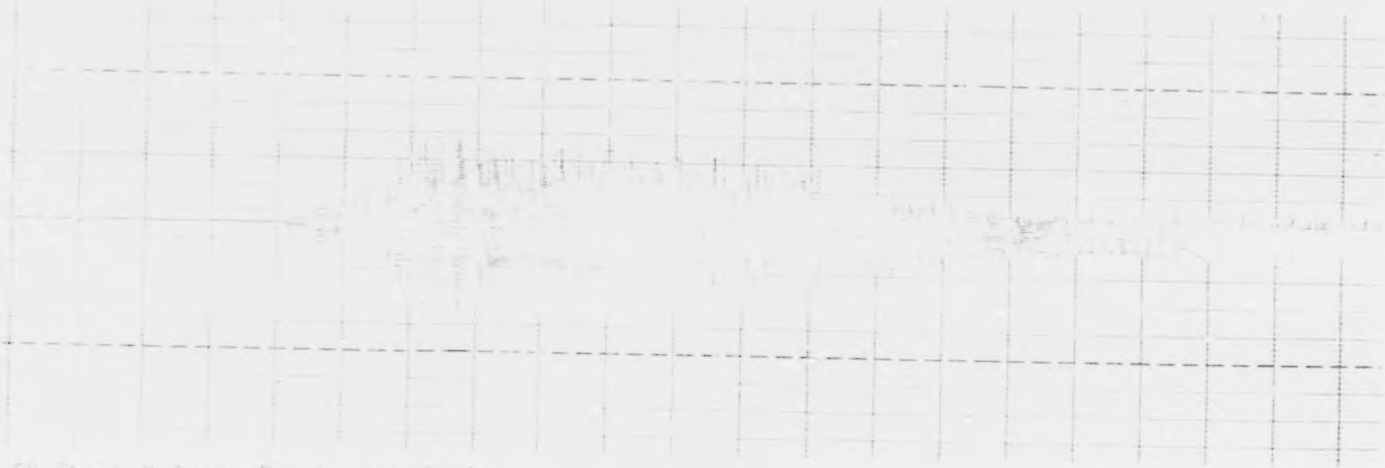

6" Check Valve: Pre-Loosen Cycle

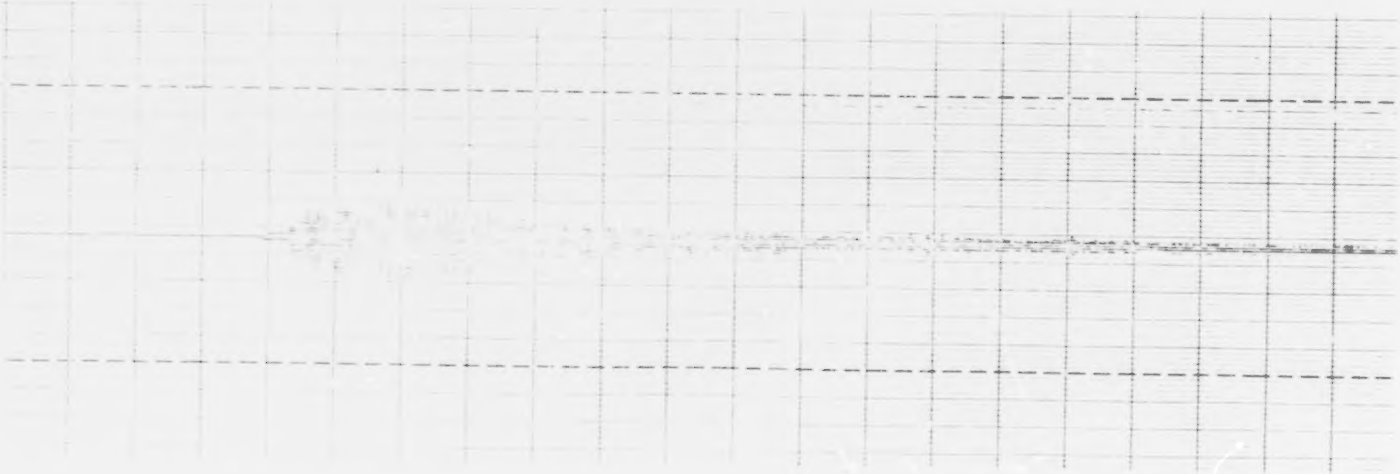

6" Check Valve: Cycle After First Loosening of Clapper Assembly

Figure 16. 6" Check Valve Cycles, Acoustic Emission Traces

## References

1. NUREG-1190, "Loss of Power and Water Hammer Event at San Onofre, Unit 1, on November 21, 1985," U.S. Nuclear Regulatory Commission, January 1986.

BLANK PAGE

# Piping and Fitting Dynamic Reliability Program

Dan Guzy

USNRC

The NRC Piping Review Committee (PRC) recognized the potential benefit that could come from improving ASME Code piping design criteria for dynamic loads, but unfortunately the data and information available at the time of writing NUREG 1061 was too limited to allow them to make specific standards recommendations in this area. The data was "limited" in the sense that while it gave indications that the margins-to-failure were much greater than assumed when the current ASME Code rules were written (see References 1 through 3 for background on these rules), the true margins to failure were not well quantified. In order to develop improved and realistic design criteria, the actual level of failure and the mechanisms that contribute to this failure should be understood. Experience data and dynamic test data available to the PRC showed mostly "non-failures", particularly for dynamic inertial loadings. The PRC thus did not recommend immediate changes to the ASME Code rules, but instead recommended as a high priority research activity that tests be undertaken to identify seismic design margins and failure modes for typical piping systems. The research that will be discussed below is a direct result of this recommendation.

Inertial loadings from dynamic events such as earthquakes are time-varying and have limited durations and energy content. ASME Code requirements now, however, evaluate these like gravity and other sustained piping loads by Equation (9) of Sections NB/NC/ND 3600. Cross-sectional plastic collapse is assumed to be the dominate failure mode for these loads. But an increasing amount of analytic and test data has shown that piping inertial loads behave differently than static loads. The margins-to-failure are greater than are predicted by current theoretical limit-load estimations, and ratcheting and fatigue appear to be the principal failure modes. If these new insights into dynamic piping failure can be demonstrated systematically and conclusively then significant changes can be made with regards to how the ASME Code sets limits on inertial stresses. This would dramatically change the nature of piping system design and could in turn reduce the number of snubbers used in nuclear power plants.

To address this issue, the NRC and EPRI are cooperating jointly in the Piping and Fitting Reliability Research Program. The objectives of this program are:

- To identify failure mechanism and failure levels of piping components and systems under dynamic loadings.
- To provide a data base that will improve our prediction of piping system response and failure due to high level dynamic loads.
- To develop an improved, realistic and defensible set of piping design rules for inclusion into the ASME Code.

The joint EPRI/NRC program began in the Spring of 1985, and will take approximately 3 years to complete. General Electric of San Jose is the main contractor and performs the overall management, coordination and integration of the program. General Electric has worked with consultants to develop test matrices, configurations, data acquisition procedures, and plans for analytical studies. Analysis is performed mainly by General Electric of San Jose and testing is performed by subcontractors. EPRI and the NRC approve program planning and review results as they develop. The NRC's contribution to this program is primarily through funding of piping system and component tests. Reference 4 is the first report to be published in this program.

Piping component tests are being conducted at ANCO Engineers. The objective is to systematically obtain dynamic data failure for components under severe (but characteristic) seismic, and high frequency loadings. Elbows, tees, reducers, support connections, nozzles and lugs are being tested. The test specimens consist of both carbon and stainless steel 6" piping components with various thicknesses and internal pressures. Both in-plane and out-of-plane loadings are applied to the components; driven at one end by hydraulic actuators and having weights at the other end. High level time history inputs are repeated until the component ruptures. Table 1 presents the results to date.
The 40 component tests will be completed probably in late

BEST COPY AVAILABLE

1987, with the NRC and EPRI each funding 20 tests. Also, an elbow will be failed under static loading as a reference test. Systematic evaluation of these tests will take place after this task is completed, but some preliminary conclusions can be made now from the tests performed so far:

1. Failure levels are much higher than previously believed - 15 to 20 times higher than Level D allowable limits and measured moments are higher than theoretical collapse moments.

2. Ratcheting and fatigue, not collapse, are the observed failure mechanisms for all cases.

3. Functionality failure did not occur. Piping components bulged and cracked, they did not collapse and crimp.

4. Equivalent linear damping values were computed to be much higher than design values (on the order of 30% of critical damping).

As a separate task in this EPRI/NRC program, three different 6" piping systems will also be tested to failure under simulated earthquake, hydrodynamic, and water hammer loadings. The NRC will fund the seismic and hydrodynamic load tests in 1987. These pressurized systems will use components compatible with those above to provide a correlation of system behavior to the component test results.

A separate but related NRC-sponsored pipe system test was conducted at ETEC in 1986 (Ref. 5). The objectives of this test were to demonstrate the feasibility of failing a representative piping system under a high earthquake-like load, and to provide information and insights needed in the test planning of the main EPRI/NRC program. The 6" piping system withstood a 30g seismic input without rupturing the piping, although ratchetting was observed. This input was 15 to 20 times the Level D design limit. The system was eventually failed by applying sine-burst inputs at the system's resonance frequency. Strain concentration and ratchetting were the cause of rupture.

The basic phenomena of fatigue ratcheting will be studied at General Electric of Schenectady using laboratory specimens. (EPRI is the sole funder of this task). Since at the present time there is no standard laboratory test specimen which addresses this failure behavior, specimen designs had to be developed. Both uniaxial and bending loads will be applied. The influence of different material and temperatures will be studied. The outcome of this task will be the basis for evaluating ratchet effects under dynamic fatigue for ASME Code pipe materials.

The results of the three types of tests discussed above will be analyzed and synthesized to form the basis of failure criteria for the combined static and dynamic loading of nuclear piping components. These criteria will be design-oriented and applicable for ASME Class 1, 2, and 3 piping. Analytical studies will be made to develop and justify the alternative piping design rules. A strong liason is maintained with the NRC licensing staff, the PVRC, and the ASME Section III Code body which ultimately makes the rule changes.

The EPRI/NRC program outlined above is directed primarily at evaluating and improving the piping design rules in Section III of the ASME Code. ASME and PVRC activities related to support and nozzle design will play a role in the acceptance of the future piping design rules. Integration of this program with the International Piping Integrity Research Group's program will also serve to justify or improve rules now in Section XI of the ASME Code. (Current plans are now to retest the piping systems discussed above with cracked piping sections in strategic locations.) Additional work will be sponsored later by the NRC and EPRI to use the failure information obtained to validate or improve seismic risk piping fragility models.

Table 1

EPRI/NRC PIPING AND FITTING DYNAMIC RELIABILITY PROGRAM COMPONENT TEST SUMMARY
6 in. Components Seismic Input

| Test No. | Type | Mat. | Sch. | Press. (psi) | Load | Dyn. Mom./Lim. Mom. | PP Cyclic Strain | Input/Level D | No. TH | Fail. Mode | Residual Strain |
|---|---|---|---|---|---|---|---|---|---|---|---|
| 1 | E | CS | 80 | 1500 | I-P | 1.21 | 1.5% | 15 | 5.0 | NF | No data |
| + | (Retest) | | 80 | 2600 | I-P | 1.21 | 1.5% | 15 | 0.5 | FR | No data |
| 2 | E | CS | 80 | 1500 | 0-P | 1.04 | 1.4% | 15 | 5.0 | NF | No data |
| + | (Retest) | | 80 | 2600 | 0-P | 1.04 | 1.4% | 15 | 4.5 | FR | No data |
| 3 | E | SS | 10 | 400 | I-P | 2.36 | 2.4% | 21 | 3.5 | FR | 3.5% |
| 4 | E | CS | 40 | 1000 | I-P | 1.83 | 2.0% | 18 | 2.5 | FR | No data |
| 5 | E | CS | 40 | 1700 | I-P | 2.06 | 2.0% | 21 | 3.5 | FR | 13.8% |
| 6 | E | SS | 40 | 1700 | I-P | 2.00 | 2.0% | 19 | 3.5 | FR | 16% |
| 7 | E | SS | 40 | 1000 | I-P | 1.8 | 2.0% | 23 | 4.5 | FR | 9% |
| 8 | E | SS | 40 | 0 | I-P | 1.8 | 2.0% | 24 | 5.0 | NF | 1.5% |
| 9 | T | SS | 40 | 1700 | 0-P | 2.5 | 2.2% | 21 | 1.5 | FR | 8% |
| 10 | T | SS | 40 | 1000 | 0-P | 2.4 | 2.2% | 21 | 2.5 | FR | 6.5% |
| 11 | T | SS | 10 | 400 | 0-P | 1.0 | Later | Later | 0.5 | FR | 3% |
| 12 | T | SS | 40 | 1700 | I-P | 2.3 | 2.2% | 27 | 2.5 | FR | 11% |

SYMBOLS & NOTES:

I-P = In-plane
0-P = Out-of-plane
E = Elbow
T = Tee
No. TH = Number of high level time history inputs to cause failure
FR = Fatigue ratcheting failure
NF = No failure
Residual strain = measured by 2 inch scratch marks
Input/ Level D = Calculated stress using linear response spectrum analysis, 2% damping, +15% broadening and actual sled input, $(B_2M/Z)$, divided by Level D allowable (3Sm)
Dyn Mom/Lim Mom = Measured maxium dynamic moment divided by theoretical limit load (Ref. Moore and Rodabaugh, J. of Pressure Vessel Technology, Nov. 1982)

## References

1. "Background for Changes in the 1981 Edition of the ASME Nuclear Power Plant Components Code for Controlling Primary Loads in Piping Systems", S. E. Moore and E. C. Rodabaugh, Journal of Pressure Vessel Technology, Volume 104, November 1982.

2. NUREG/CR-0261, "Evaluation of the Plastic Characteristics of Piping Products in Relation to ASME Code Criteria", E. C. Rodabaugh and S. E. Moore, July 1978.

3. NUREG/CR-2137, "Realistic Seismic Design Margins of Pumps, Valves, and Piping", E. C. Rodabaugh and K. D. Desai, June 1981.

4. W. F. English, "Piping and Fitting Dynamic Reliability Program First Semi-Annual Progress Report May-October 1985, NEDC-31272," November 1985 .

5. Draft ETEC Report, 6-inch Diameter Pipe Seismic Fragility Test.

# 6-INCH-DIAMETER PIPE SEISMIC FRAGILITY TEST

W. P. Chen
V. DeVita
A. T. Onesto

ENERGY TECHNOLOGY ENGINEERING CENTER

P.O. Box 1449
Canoga Park, California 91304

## ABSTRACT

This paper contains the test results and assessments of seismic fragility tests performed on a 6-in.-diameter piping system. The objective of the test was to investigate the ability of a piping system to withstand high level dynamic seismic and other loadings. The test was performed in the ETEC Seismic Fragility Test Facility. Levels of loadings achieved during seismic testing were 20 to 30 times larger than usually specified for Safe Shutdown Earthquakes (SSE's) of contemporary nuclear power plants. Based on failure data obtained during seismic and other dynamic testing, it was concluded that nuclear piping systems are inherently stronger to resist dynamic seismic loadings than currently permitted by design criteria in existing codes and standards or would be predicted by the probabilistic risk assessment (PRA) and several proposed nonlinear methods of failure analysis.

# 1.0 INTRODUCTION

The Seismic Design Task Group of the U. S. Nuclear Regulatory Commission (NRC) Piping Review Committee has recommended that, in view of the limited data base of piping failures, test research programs for verifying seismic design margins and identifying failure modes in nuclear power plant piping should be supported by the NRC. The need for these programs was identified by the Seismic Design Task Group of the Piping Review Committee during a comprehensive review of NRC piping requirements as part of an ongoing effort to improve the reliability of piping in nuclear power plants. The Seismic Design Task Group found during its consideration of overall design margins that the achievement of an optimum balance among all factors affecting piping design was made difficult because of a lack of real failure information for piping, particularly for seismic loads.

Nuclear power plant piping systems are currently designed to resist high level dynamic loadings such as earthquakes by conservative analysis methods and criteria. In particular, internal forces and moments due to seismic loads are determined by linear elastic analysis and the resulting stresses at each cross section of the piping system are evaluated as primary stresses in accordance with Section III of the ASME B&PV Code (ASME Code). This design practice is sufficient to prevent the overall collapse of piping systems but is conservative. It ignores the increased load capacity of typically highly redundant piping systems where the material ductility permits load redistributions and frequency shifts due to inelastic behavior. Also, in the current design approach, the implications of the inherent displacement limited response of piping systems to the applied seismic input are disregarded.

BEST COPY AVAILABLE

The objective of the ETEC tests was to investigate the ability of the piping system to withstand high level dynamic seismic and other loadings by: (1) testing the piping system to failure under dynamic loads; (2) characterizing the high level dynamic response; (3) identifying the failure mode; and (4) providing a benchmark test for quantifying the analytical conservatism for (a) current design criteria, (b) failure predictions based on several emerging nonlinear piping response analysis methods, and (c) probabilistic risk assessment (PRA) methods for piping systems. This paper contains the test results and assessments of the test performed on the 6-in. diameter piping system.

# 2.0 TEST DESCRIPTION

## 2.1 Test Article Description

The configuration of the piping system utilized in the test (test article) was as shown in Figure 2-1. The test article consisted of some 48 ft of 6-in. diameter and 17 ft of 3-in. diameter carbon steel piping and components, and included a simulated valve assembly. E1 through E9 identify elbow locations.

The test article was fabricated from materials procured in accordance with the requirements of American Society of Testing Materials (ASTM) materials specifications which were identical to the corresponding ASME Code, Section II material specifications. Fabrication, including welding and inspection, were in accordance with ASME Code, Section III, Class 1 requirements.

Prior to testing, the test article was hydraulically proof tested in accordance with ASME Code Section III, Class 1 requirements. The liquid utilized for the proof pressure test was oil. Subsequent to proof pressure testing but prior to dynamic testing, the test article was internally pressurized to 1000 psi. Provisions were made to entrap approximately 800 in.$^3$ (approximately 4% of the total volume) of air and gas during pressurization. This pressurized condition was maintained during dynamic testing and was selected as a means of reducing potential variations in the 1000 psi internal pressure in the test article due to variations in ambient temperature during testing.

## 2.2 Test Article Installation

The test article was installed in the ETEC Seismic Fragility Test Facility by: (1) attachment of the three welding neck flanges at test article supports S1, S3, and S5 to three of the facility shaker tables; and (2) by installation of a pipe support at test article support S2 (see Figure 2-1). S1, S2, S3, and S5 identify support locations. Restraint of the test article at support S2 was provided by an assembly constructed from commercially available components, i.e., a pipe clamp and two rigid struts. The vertical strut was attached to the floor of the test facility and the horizontal strut was attached to a rigid vertical stanchion.

Additionally, allowance was made to apply horizontal input motions to the test article at support S2 which were identical to the horizontal base input motions applied at supports S1, S3, and S5. These motions were provided by a fourth shaker table to which the vertical stanchion was attached.

## 2.3 Test Article Instrumentation

The test article was instrumented with 6 accelerometers, 30 strain gages, and 1 pressure transducer. In addition, each of the four shaker tables utilized in the test were instrumented with one accelerometer to measure table acceleration in the direction of motion, and one linear variable differential transformer (LVDT) for table displacement measurement in the direction of motion. The locations of the test article instruments are shown in Figures 2-2 and 2-3. One pressure transducer was mounted immediately above the 3-in. pipe flange at support S5.

## 2.4 Test Input Motions

The input base motions planned during testing are described in Table 2-1. The seismic input motions are based on the acceleration-time history and associated response spectrum shown in Figures 2-4 and 2-5, respectively. The time history amplitude was scaled to achieve the three levels of seismic testing described in Table 2-1. Alternately, the input motions were to be based on a similarly scalable artificial time history.

The peak spectral response frequency (7 Hz) was not "tuned" to coincide with the test article natural frequency (5 Hz) since this condition is expected to be investigated in an upcoming NRC/EPRI cooperative research study. Pretest analysis did not suggest a need to tune the input to produce a piping failure.

Initially, only the three seismic tests were planned. The load levels were selected on the basis of the 17.1 g ZPA level predicted by ETEC (and later corroborated by Hanford Engineering Development Laboratory [HEDL] to cause failure of the test article and previous ETEC experience gained during similar testing of a 3-in. diameter piping system. However, provisions were made to conduct repeated sine burst testing to failure of the test article if failure did not occur during the seismic tests. The three frequencies of the displacements in the sine burst tests (4, 5 and 6 Hz) were selected to bracket and coincide with the fundamental frequency of the test article observed during testing. This frequency was observed to be 5 Hz. In fact, only the 4 Hz sine burst test was completed: test article failure occurred during the 5-Hz test (Figure 2-6).

During seismic testing, differences in amplitude of displacements of up to 3/4 in. (approximately 5% of the maximum approximately 15 in. peak-to-peak motions) were observed between the displacement at supports S3 and S5 during the nominal 25 g high level seismic test. This difference was attributed to a scaling anomaly which will be corrected during future testing. Fortunately, the effects of this difference were limited to the 3-in. branch piping of the test article which was far removed from the critical section of 6-in. pipe for the tests.

## 2.5 Test Observations

No visual indications of damage were observed prior to high level seismic testing. However, two such indications were observed at the end of the high level test: a 2-in. wide circumferential bulge was found in the vertical leg of the test article 8 in. above support S1, and the permanent set of the test article was found to be of the order of 2 in. The residual circumferential strain in the bulge was approximately 2.3%.

As previously mentioned, failure of the test article occurred during the 5-Hz sine burst test. The failure was located in the previously observed circumferentially bulged area in the test article and occurred during the 6th of the 11 planned full amplitude cycles. The test was promptly terminated to prevent possible damage to the seismic tables.

During the termination of the test, the horizontal rigid strut at support S2 was damaged. The rod end attached to the clamp at support S2 was bent as a result of the increased torsional deflections of the pipe between elbows E4 and E5 (Figure 2-1). The increased deflections were due to the decrease in restraint of the test article piping resulting from the failure. Frictional forces at the clamp were exceeded causing the clamp to rotate around the pipe and subsequent misalignment and bending of the horizontal strut.

## 3.0 TEST RESULTS

The results of the three seismic and two sine burst tests are arranged for convenience to address the following test objectives:

1) Characterize high level dynamic response
2) Quantify conservatisms in current design criteria and failure analysis methods
3) Identify failure modes.

### 3.1 Characterization of Dynamic Response

The dynamic response of the test article was characterized by parameters which describe the overall and localized response of the test article. The overall or general parameters include acceleration values at specific locations or averaged values for several locations. Localized parameters include strains and strain ranges. Additional characterization parameters include test article permanent set and support loads.

Variations of the response parameters with increasing levels in test seismic inputs are described in the following.

### 3.1.1 Acceleration Response

The overall response of the test article was characterized by peak acceleration attained at locations throughtout the test article. Accordingly, peak accelerations measured during test at all accelerometer locations (Figure 2-3) are shown as functions of seismic ZPA in Figure 3-1. The figure indicates the expected behavior: the increasing resistance of the test article to respond to increasing levels of seismic input.

### 3.1.2 Amplification Ratio

Alternately, the overall response was characterized by the amplification ratio, $G_{out}/G_{in}$, where $G_{in}$ is the input ZPA and $G_{out}$ is the selected peak acceleration(s) of interest. This ratio is shown plotted in Figure 3-2 as a function of seismic ZPA for the three directions of response. For convenience, $G_{out}$ in each direction was selected to be the average of all peak accelerations in the given direction measured during testing. The plots indicate that the amplification ratios decrease with increasing levels of seismic loadings.

The relative amplification factor $(G_{out} - G_{in})/G_{in}$ is also shown plotted in Figure 3-2 in the X-direction, the direction of the seismic input. This plot was based on the average peak X-direction accelerations measured during testing. Extrapolation of the plot gives a value of approximately 6.0 for zero input which is in good agreement with the anticipated value based on the input response spectra: the peak accelerations of the response spectra are six times the ZPA accelerations.

### 3.1.3 Strains and Strain Ranges

Strain gage data indicated that internal load redistribution, if any, was minor: inelastic behavior was limited to localized regions in the test article. Stresses associated with strains measured in the elbows and near the supports were in excess of the yield strength of the material, and residual strains were accumulated at these locations. However, stresses corresponding to strains measured in straight portions of pipe remote from elbows and supports were in the material elastic range, and negligible residual strains were observed at these locations.

For each of the seismic tests, the data indicate that the most highly strained elbow was elbow E5 (gage location G8), and the critical support-related piping was the 6 in. vertical leg at support S1 (gage location G1). Prior to failure of the critical gage at location G8 on the elbow, the maximum strain measured in the elbow (12,500 in./in.) appeared to be 50% higher than that in the pipe (8,100 in./in.) but is believed to reflect conditions in highly localized areas in the elbow. Other strains in the elbow were low (approximately 3000 in./in. to 6000 in./in.) in comparison to the maximum strain.

The longitudinal strain ranges observed at gage location G1 are shown in Figure 3-3 where the strain range is defined to be the difference between the maximum and minimum strains during any test. The figure indicates the decreasing rate of increase of strain range with increasing levels of seismic input.

### 3.1.4 Strain Ratchetting

Strain ratchetting was limited during testing to localized areas in the test article, i.e., the failure zone and the E4 (gage location G4) and E5 (gage location G8) elbows.

The maximum accumulated residual strains in the failure zone were 0.7% and 9.2% in the longitudinal and circumferential directions, respectively (Figure 3-4). The large strain in the circumferential direction occurred in the 2-in. wide circumferential bulge first observed after the high-level seismic test. This bulge continued to grow during the 4-Hz sine burst test and subsequently ruptured during the 5-Hz sine burst test.

Wall thinning, i.e., radial strain, in the failure zone was found to be between 10% and 15%. The magnitude of these radial strains, together with the magnitudes of the 0.7% longitudinal and 9.2% circumferential strains, confirms the results of a simplified ratchetting strain analysis which indicated that subsequent to repeated cycling, the total radial and circumferential ratchetting strains will be approximately equal in magnitude and the axial ratchetting strains negligible.

Although the maximum accumulated strain in elbow E4 was 40% of that in the failure zone, and there was visible evidence (circumferential bulging) of the accumulation in the failure zone, no corresponding visible evidence of bulging was found in the elbow. This was attributed to differences between the extent of the areas of ratchetting in the elbow and the failure zone.

In general, the results indicate that the cross-sectional stress in the piping system is more important than localized peak stresses from an overall piping system response point of view.

### 3.1.5 Support Loads

The horizontal rigid strut at support S2 was instrumented with strain gages to determine strut loadings. The average strains and resulting loads shown in Figure 3-5 are plotted as a function of seismic ZPA level and harmonic sine burst peak g level: the characteristic decreasing rate of increase of strut load is exhibited in Figure 3-5.

### 3.1.6 Internal Pressure

Pressure fluctuations observed during testing are summarized in Table 3-1.

One-per-cycle pressure fluctuations observed during testing are believed caused by fluid inertial loads; a pipe volume reduction of approximately 200 to 250 $in.^3$ would be required to produce these recorded fluctuations. Figure 3-6 shows the relationship between the range in pressure fluctuations and input seismic level: the characteristic decreasing rate of increase in range of pressure fluctuations is exhibited.

### 3.1.7 Pipe Permanent Set

Permanent set in the test article during seismic testing was determined by monitoring the position of the pipe near accelerometer location A3 after each test. The vertical displacements after the low and intermediate level seismic tests were negligible. At the completion of the high-level 25-g seismic test, the permanent displacements were 1 7/8 in. north, 3/4 in. east, and 11/16 in. downward. Additionally, a 6° set in the north direction was observed in the vertical pipe above support S2.

The horizontal permanent displacements observed during seismic testing are shown in Figure 3-7.

### 3.1.8 System Damping

Estimates of system damping were made based on amplification ratios obtained from spectral data and the results of the 4 Hz sine burst test. Estimates obtained for the three levels of seismic testing are contained in Table 3-2 and Figure 3-8.

To the extent that the test results were examined, no evidence of softening of the piping system with increasing levels of seismic input was observed during testing. Final conclusions regarding softening are deferred pending further inspection of the system response test data.

## 3.2 Post-Test Examinations

Subsequent to failure of the test article, examinations of the test article were conducted. These examinations included visual inspections and dimensional data checks as well as metallographic and scanning electron microscope (SEM) inspections of the failure zone. The results of general overall examinations and detailed examinations of the failure zone are reported separately for convenience in the following.

### 3.2.1 General Examination - Excluding Failure Zone

Visual examinations of the test article and dimensional data checks were performed following failure of the test article. Visible signs of damage were found only in the vertical leg of the test article above support S1. Furthermore, no anomalies were found in the dimensional data for the straight pipe sections and the elbows examined.

### 3.2.2 Examination of Failure Zone

A detailed examination of the failure zone was conducted to determine the mode of failure. Results of examination based on the visual, metallograpic, and SEM techniques are provided in the following.

Visual Examination - Visual examinations of the failure zone found that in addition to the primary through-wall fracture, cracking of the internal surface as well as wall thinning and diametral growth had occurred in the highly strained, plastically deformed, circumferential bulge. The examination of the primary through-wall fracture indicated that failure was due principally to overloading under tension and plane stress conditions during the failure cycle. Examinations of the failure zone found multiple circumferentially oriented surface cracks.

Post-test diametric and wall thickness data in the vertical leg of pipe indicated that diametric growth (up to 9%) had occurred in the first foot of pipe above the fracture but was attenuated at two feet away from the fracture. The wall thickness data indicated maximum thinning of the order of 25%. However, in general, thinning in the circumferentially bulged area of the pipe was between 10% and 15%.

Metallographic Examination - Metallographic examination of specimens from the upper half on the south side of the fracture revealed an equiaxed structure of ferrite and pearlite (normal for carbon steel) except for localized elongation of the surface. The grain flow indicated the fracture propagated from the inside to the outside surface. An increase in microhardness, presumably due to strain hardening, was also found near the fracture. A series of parallel transgranular cracks could be seen on the inside surface as rounded, blunt penetrations rather than knifelike cracks.

Scanning Electron Microscope (SEM) Examination - SEM examinations were performed on sample specimens from the upper half on the south side of the fracture.

A specimen from a single slant fracture site from the south side exhibited a structure consisting primarily of equiaxed dimples. The dimples are formed by microvoid coalescence and are indicative of ductile fracture. Equiaxed dimples are characteristic of tension failure.

All surfaces were scanned for fatigue striations but none were found. However, even if fatigue striations had been present on the fresh fracture surface, they were probably obliterated by the deformation during crack closure impact. The absence of striations did not preclude the possibility of fatigue fracture since striations are not always found on fatigue fractures.

Failure Mode - Based on visual, SEM, and metallographic examination, the fracture was primarily a ductile tension failure. Some brittle fracture could have occurred and been masked by deformation after fracture, but no evidence of fatigue was found. Fracture initiated on the inside surface and propagated to the outside.

# 4.0 CONCLUSIONS AND RECOMMENDATIONS

Testing to failure of the 6-in. piping system was achieved in the ETEC Seismic Fragility Test Facility. Failure of the test article did not occur during the 30 g ZPA seismic loading but occurred during the 5 Hz sine burst test. Based on the test data and observations, the following conclusions and recommendations were developed.

## Test to Failure

Testing to failure of moderate-sized piping systems is currently achievable in the ETEC Seismic Fragility Test Facility. Such testing is essential for proper assessment of conservatisms in current-design criteria and proposed analytic methodologies and provides experimental justification for more realistic seismic design criteria currently under consideration for existing codes and standards.

Although the 6-in. piping system did not fail during seismic testing at loading levels in excess of that predicted to cause failure, the test demonstrated the feasibility of testing to failure using sine burst tests. However, in retrospect, it was felt that failure under seismic loadings could have been achieved by subjecting the piping system to either (1) an increased level of seismic loading with ZPA of approximately 50 g or (2) repeated application of the 25 g ZPA seismic loading.

## Characterization of Dynamic Response

The test results indicated an increasing resistance of the piping system to respond to increasing levels of seismic loadings. This characteristic was exhibited by the overall response of the piping system as measured by the peak accelerations or amplifications. This characteristic was also demonstrated by the local response as measured by strain ranges in the vicinity of the failure zone.

Strain gage data indicated that minor redistribution of internal loadings occurred in the highly stressed elbows due to local yielding. Otherwise, the strains and associated stresses in straight sections of pipe remote from elbows and supports were in the material elastic range. The circumferential, longitudinal and average radial residual strains at the failure location were 9.2%, 0.7% and -12%, respectively.

Based on the test results, damping was estimated to be between 1-6%, 3-12% and 13-22% for the low, intermediate and high level seismic tests, respectively, and 19% for the 4 Hz sine burst test.

## Failure Mode

Failure, i.e., rupture, of the test article was attributed to incremental ratchetting due to internal pressure that resulted in wall thinning and subsequent fracture due to tensile overloading during the failure cycle. No evidence of fatigue failure was found. Failure was initiated locally on the inside surface of the pipe with rapid circumferential propagation subsequent to growth through the wall.

Failure occurred in a circumferential bulge observed after high level seismic testing in the vertical leg of pipe above the critical support. Increase in growth and subsequent rupture occurred during the 5 Hz sine burst test. Local wall thinning of up to 25% (10 to 12% average) was found in the bulge during post-test examinations.

Figure 2-1 Test Article Configuration

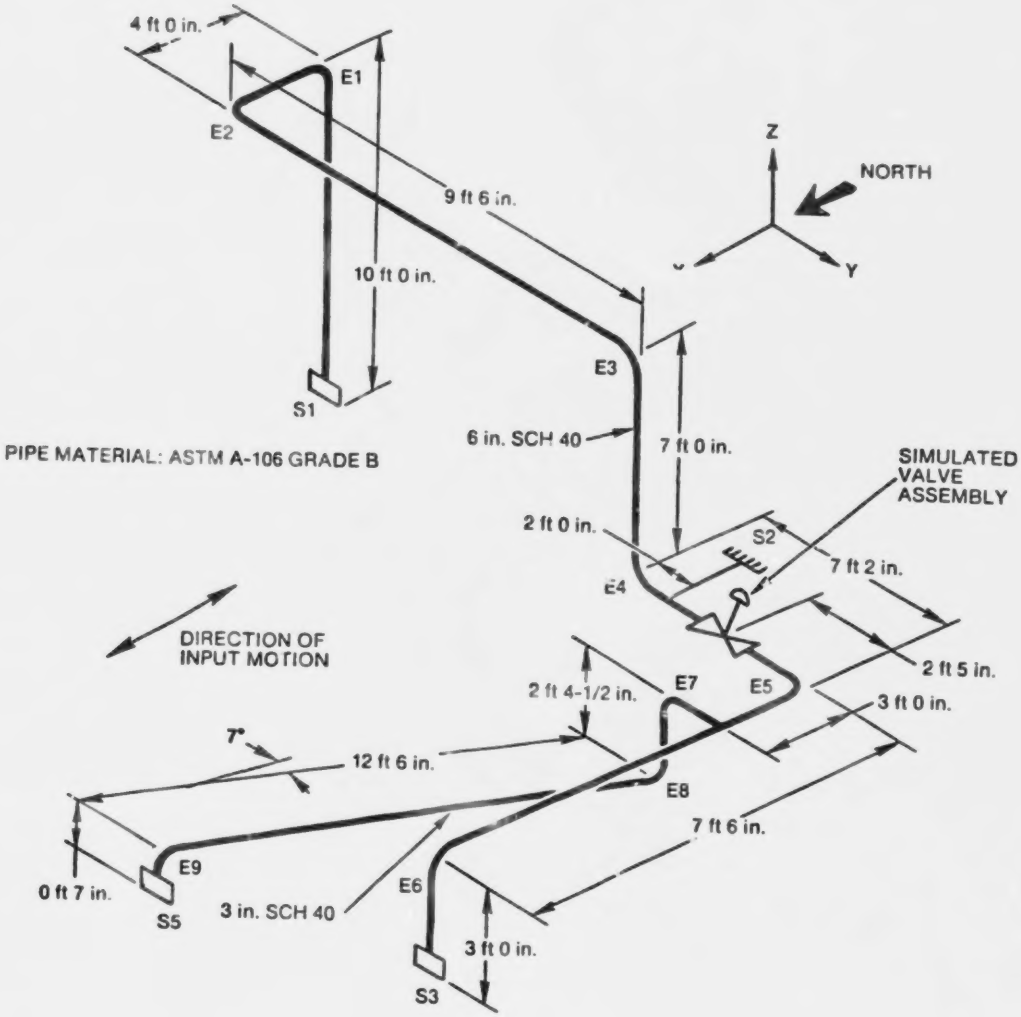
4 ft 0 in.
E1
E2
Z
NORTH
Y
9 ft 6 in.
10 ft 0 in.
E3
S1
6 in. SCH 40
7 ft 0 in.
PIPE MATERIAL: ASTM A-106 GRADE B
SIMULATED
VALVE
ASSEMBLY
2 ft 0 in.
S2
7 ft 2 in.
E4
DIRECTION OF
INPUT MOTION
2 ft 5 in.
2 ft 4-1/2 in.
E7
E5
3 ft 0 in.
7°
12 ft 6 in.
E8
7 ft 6 in.
E9
0 ft 7 in.
S5
3 in. SCH 40
E6
3 ft 0 in.
S3

Figure 2-2 Test Article Instrumentation - Accelerometer Locations

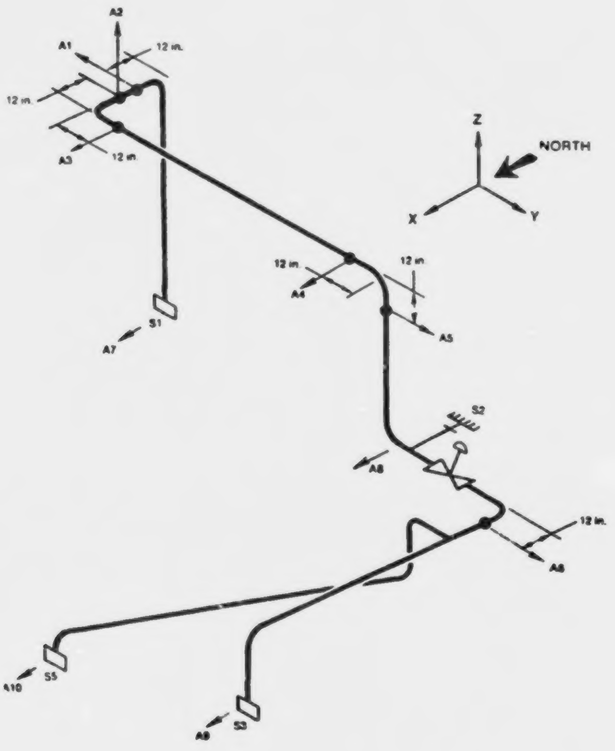
A2
A1
12 in.
12 in.
A3
12 in.
Z
NORTH
X
Y
12 in.
A4
12 in
A5
S1
A7
S2
A8
12 in.
A6
S5
A10
S3
A9

Figure 2-3 Test Article Instrumentation - Strain Gage Locations

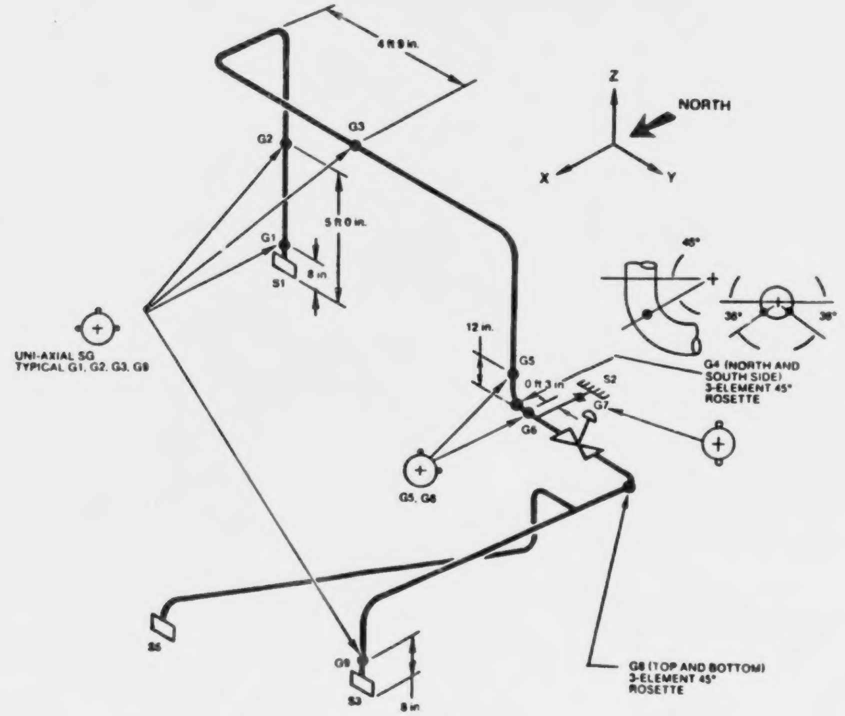
4 ft 9 in.
Z
NORTH
X
Y
G2
G3
5 ft 0 in.
G1
S1
8 in
45°
36°
36°
UNI-AXIAL SG
TYPICAL G1, G2, G3, G9
12 in.
G5
0 ft 3 in
S2
G4 (NORTH AND SOUTH SIDE) 3-ELEMENT 45° ROSETTE
G7
G6
G5, G6
S5
G9
S3
8 in
G8 (TOP AND BOTTOM) 3-ELEMENT 45° ROSETTE

Figure 2-4

SEISMIC ACCELERATION DATA
FOR
ETEC PIPING SYSTEM DEMONSTRATION TEST

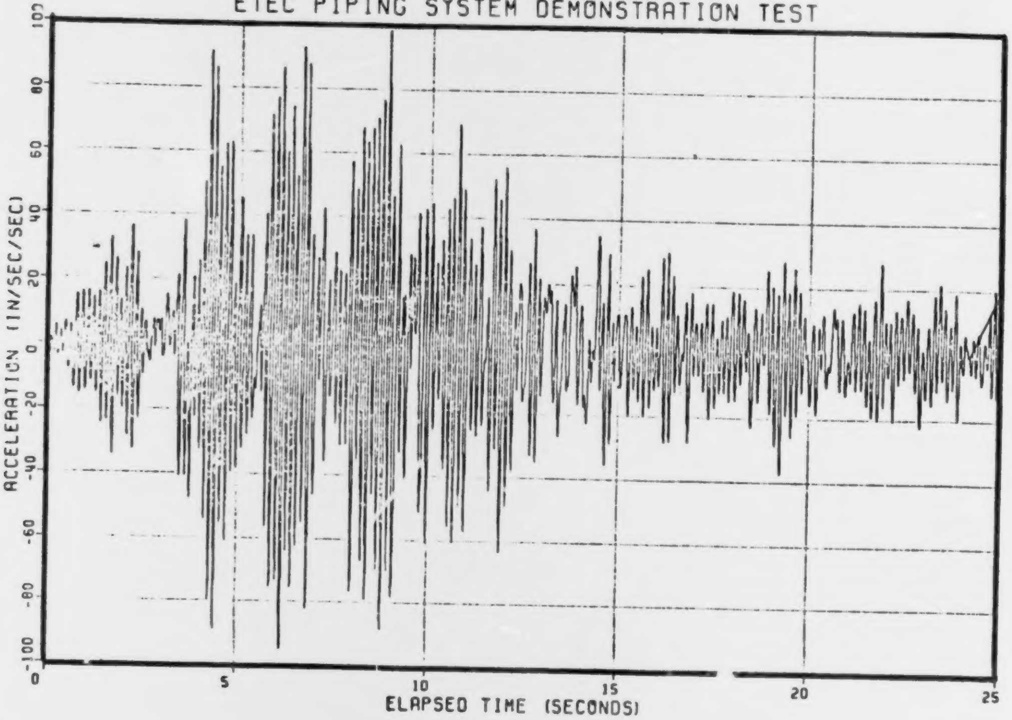

Figure 2-5

REQUIRED RESPONSE SPECTRA FOR 6 INCH PIPE TEST
5% DAMPING

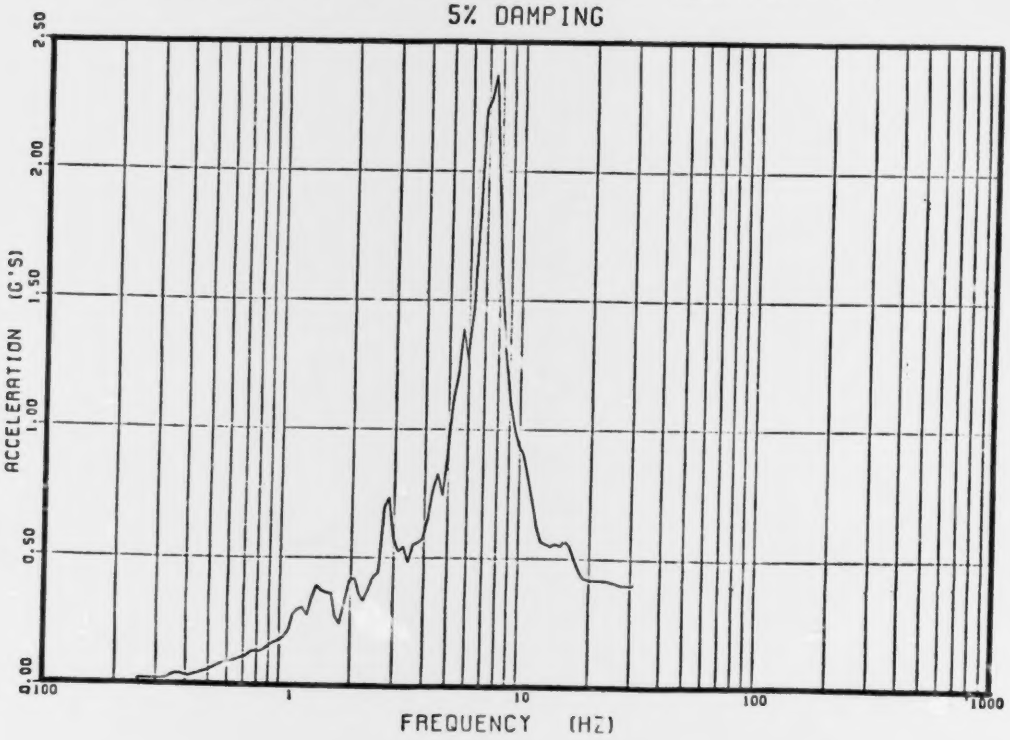

Table 2-1 Planned Test Article Base Input Motions

| Input Motion | Description |
|---|---|
| Low Level Seismic | Synchronous time history of 15 seconds duration. Response spectrum with 5-g nominal (7.5 g actual) ZPA |
| Intermediate Level Seismic | Synchronous time history of 15 seconds duration. Response spectrum with 14-g (13 g actual) nominal ZPA |
| High Level Seismic | Synchronous time history of 15 seconds duration. Response spectrum with 24-g nominal (30 g actual) ZPA |
| Sine burst -4 Hz | Synchronous harmonic displacements: 8 cycles at ± 7 in. maximum displacement and 11.5 g nominal (18 g actual) maximum acceleration |
| Sine burst - 5 Hz | Synchronous harmonic displacements: 11 cycles at ± 7 in. maximum displacement and 11.7 g nominal (48 g actual) maximum acceleration |
| Sine burst - 6 Hz | Synchronous harmonic displacements: 7 cycles at ± 5 in. maximum displacement and 18.4 g nominal maximum acceleration |

Figure 2-6 Actual Sine Burst Input

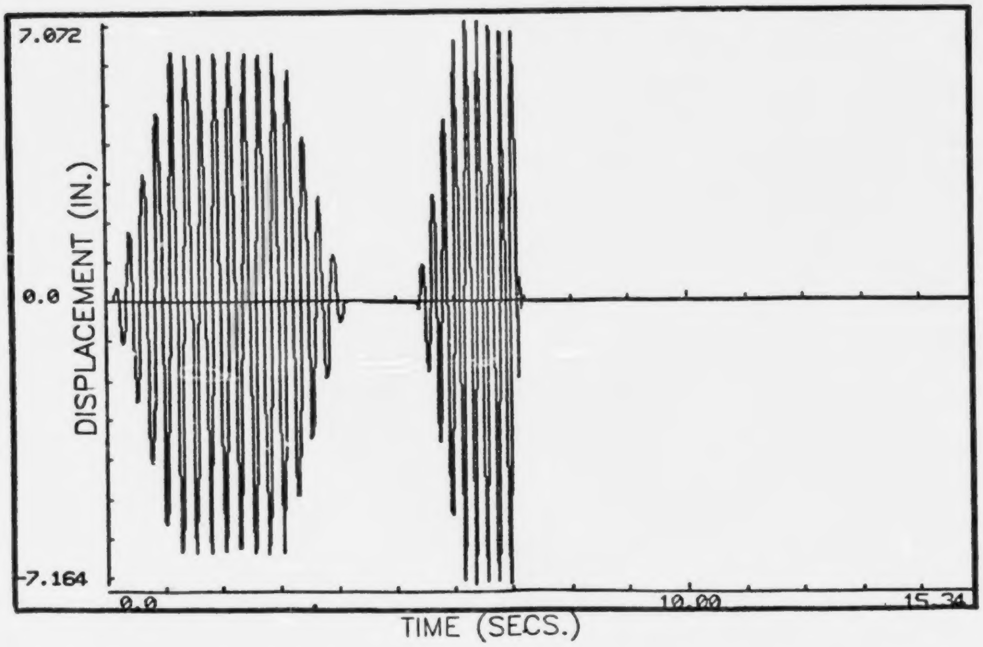

Figure 3-1 Test Article Acceleration Due to Seismic Input

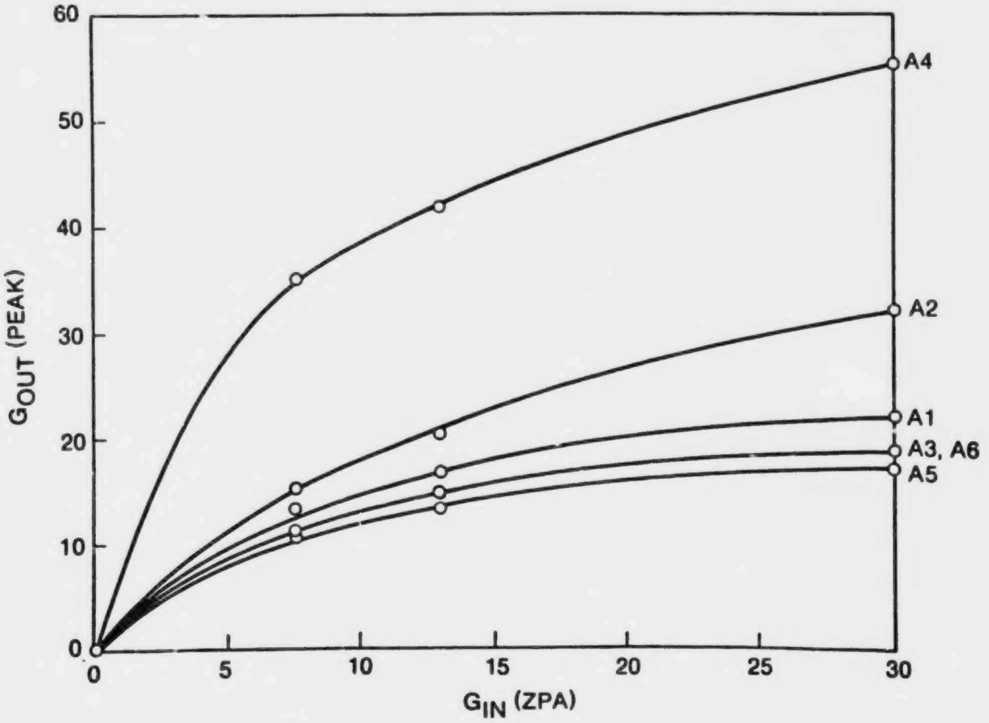

Figure 3-2 Amplification Ratio

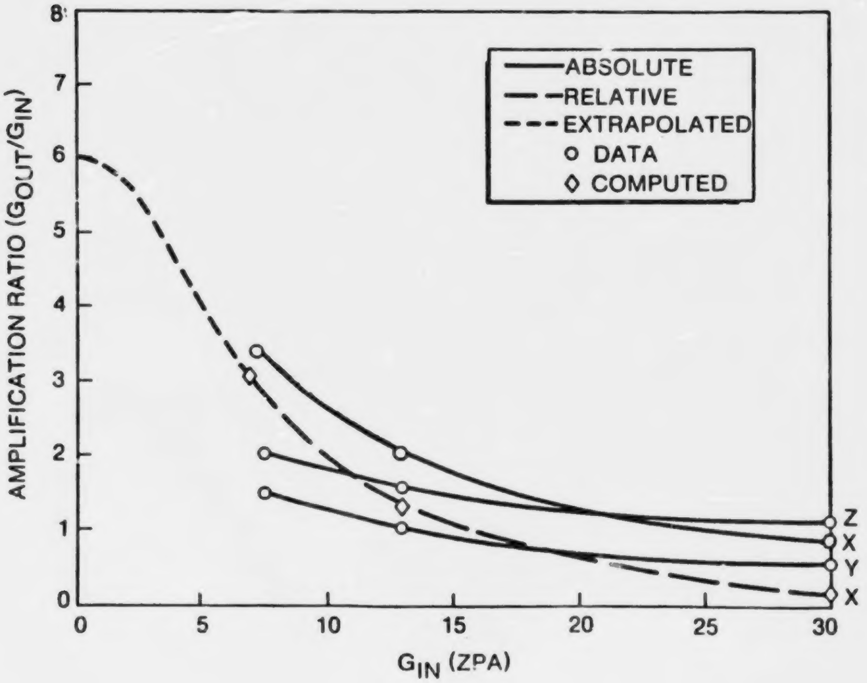

Figure 3-3 Strain Range at Gage Location G1

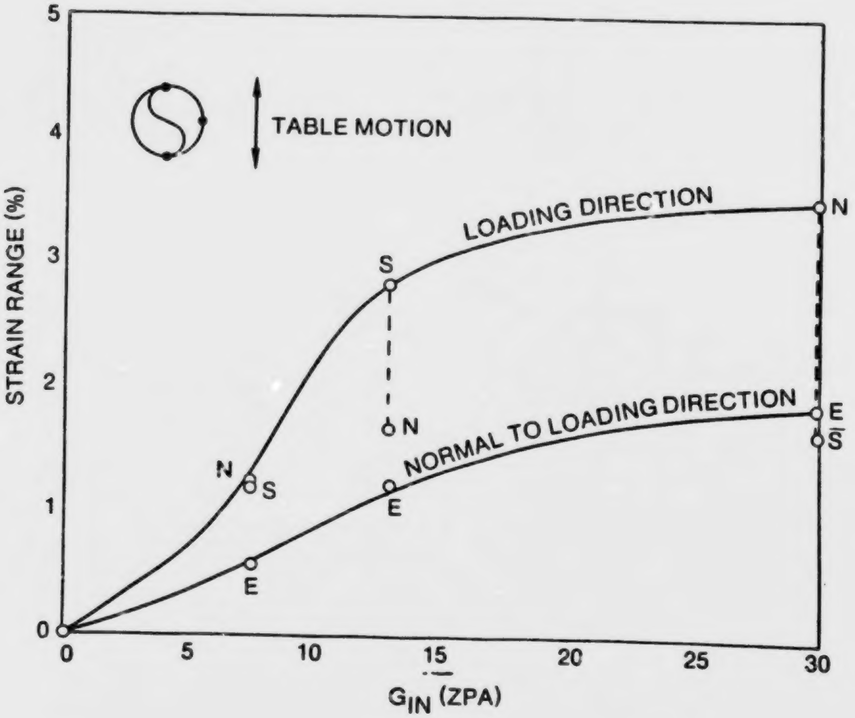

Figure 3-4 Circumferential/Longitudinal Strain Ratchet at Failure Location

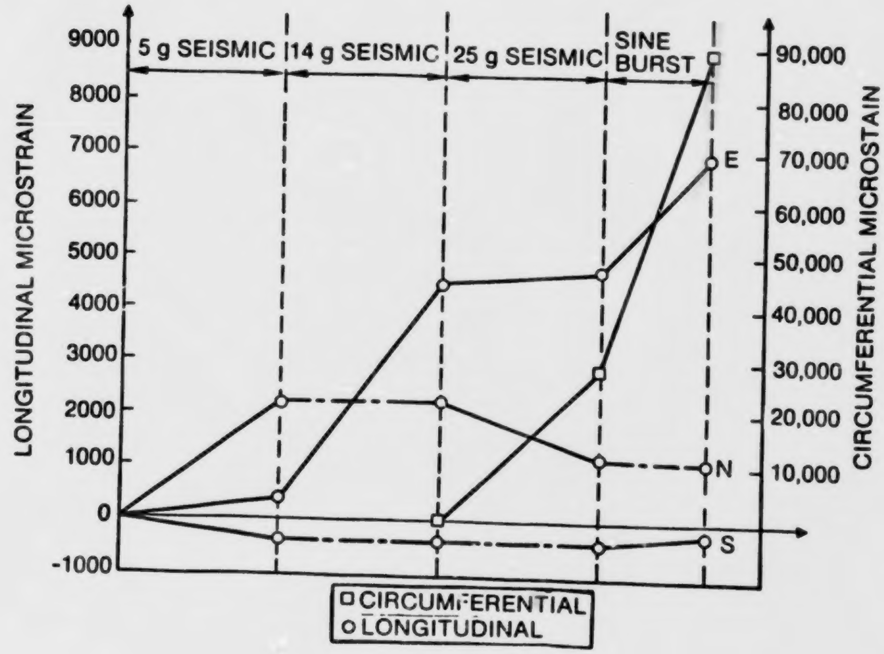

Figure 3-5 Horizontal Strut Loads

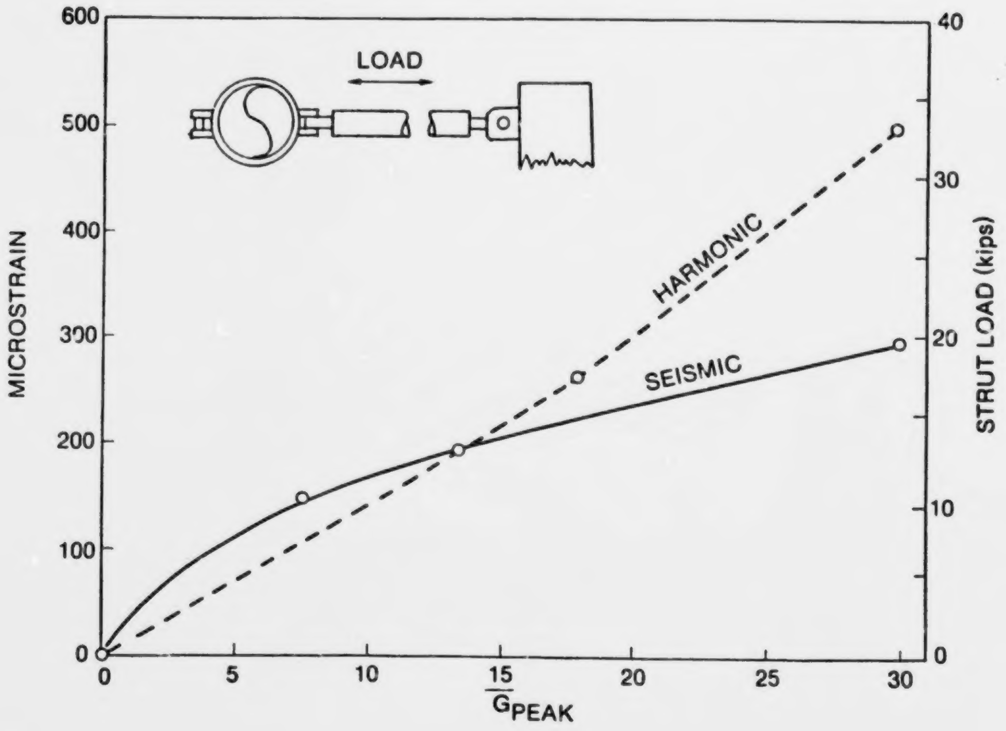

Figure 3-7 Test Article Set During Seismic Testing

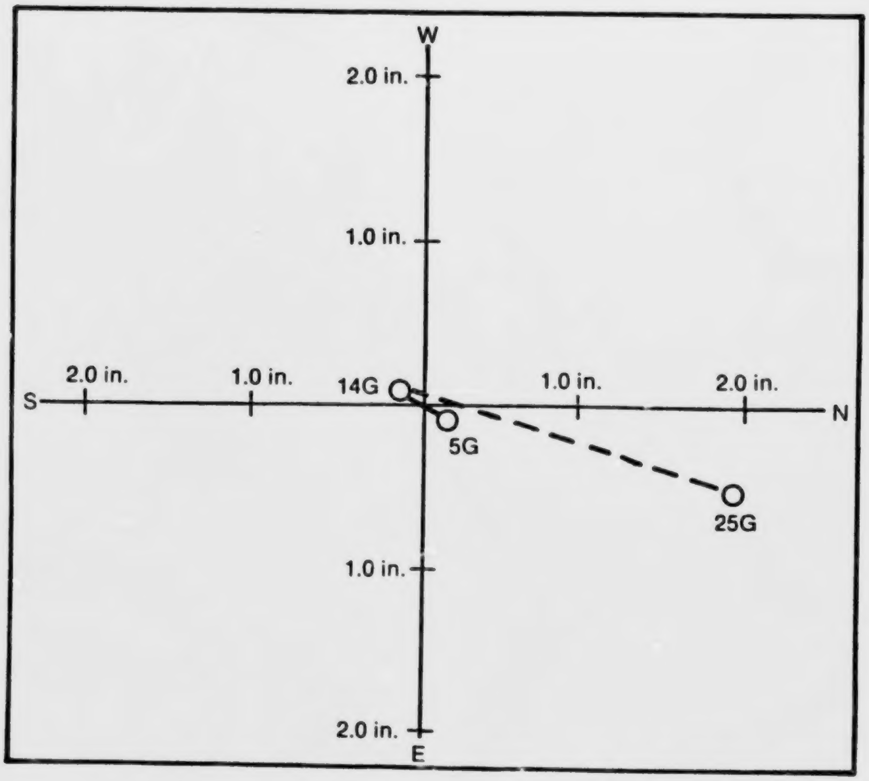

Table 3-1 Internal Pressure Variations

| | Internal Pressures (psi) | | |
|---|---|---|---|
| Test | $P_{start}$ | $P_{end}$ | $P_{max}/P_{min}$ |
| 5 g Seismic | 1025 | 960 | 1130 / 865 |
| 14 g Seismic | 1040 | 960 | 1210 / 850 |
| 25 g Seismic | 1050 | 950 | 1250 / 790 |
| Sine Burst - 4 Hz | 1100 | 1000 | 1230 / 800 |
| Sine Burst - 5 Hz | 1000 | 0* | 1330 / 720 |

---

*Test article failed.

Figure 3-6 Internal Pressure Fluctuations

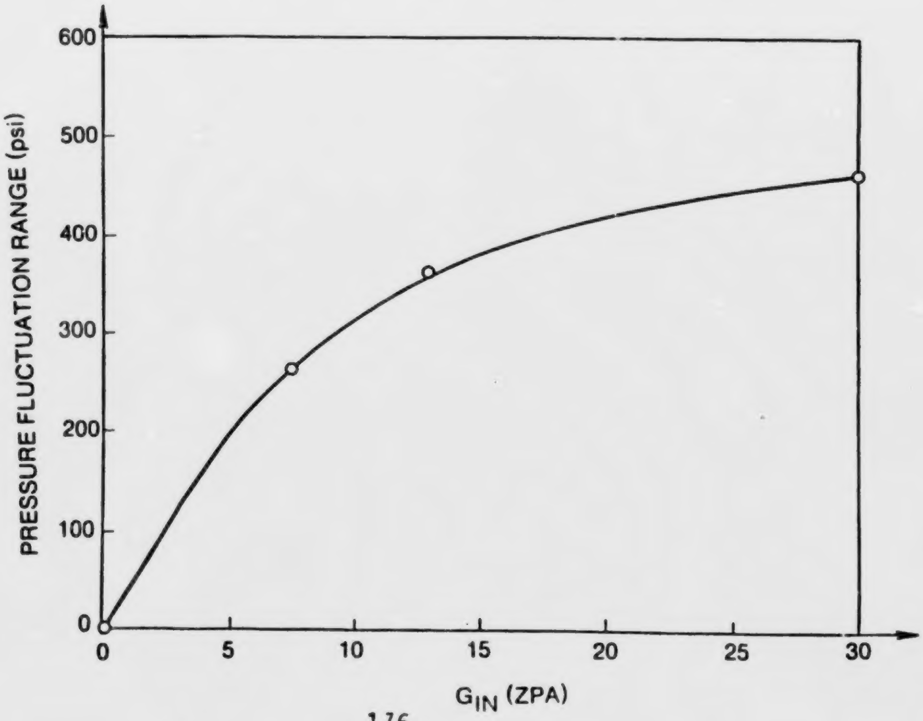

Table 3-2 Estimated System Damping

| Test | Estimated Damping |
|---|---|
| Low-level seismic test<br>5 g nominal (7.5 g actual) ZPA | 1-6% |
| Intermediate-level seismic test<br>14 g nominal (13 g actual) ZPA | 3-12% |
| High-level seismic test<br>25 g nominal (30 g actual) ZPA | 13-22% |
| 4 Hz sine burst test<br>11.5 g nominal (18 g actual)<br>maximum acceleration | 19% |

Figure 3-8 Estimated System Damping

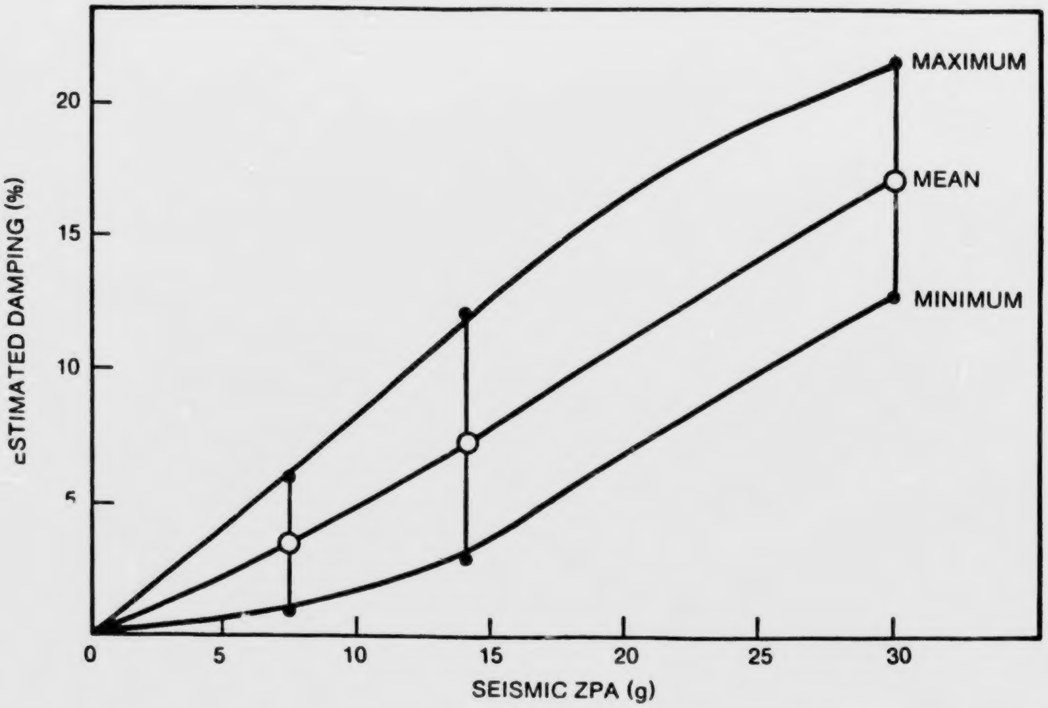

BEST COPY AVAILABLE

BLANK PAGE

# PIPE DAMPING STUDIES[a]

A.G. Ware
Idaho National Engineering Laboratory
EG&G Idaho, Inc.
Idaho Falls, Idaho

## ABSTRACT

The Idaho National Engineering Laboratory (INEL) is conducting a research program to assist the United States Nuclear Regulatory Commission (USNRC) in determining best-estimate damping values for use in the dynamic analysis of nuclear power plant piping systems. This paper describes four tasks in the program that were undertaken in FY-86. In the first task, tests were conducted on a 5-in. INEL laboratory piping system and data were analyzed from a 6-in. laboratory system at the ANCO Engineers facility to investigate the parameters influencing damping in the seismic frequency range. Further tests were conducted on 3- and 5-in. INEL laboratory piping systems as the second task to determine damping values representative of vibrations in the 33 to 100 Hz range, typical of hydrodynamic transients. In the third task a statistical evaluation of the available damping data was conducted to determine probability distributions suitable for use in probabilistic risk assessments (PRAs), and the final task evaluated damping data at high strain levels.

## INTRODUCTION

The Idaho National Engineering Laboratory (INEL) has been conducting a research program to assist the United States Nuclear Regulatory Commission (USNRC) in determining best-estimate damping values for use in the design and analysis of nuclear power plant (NPP) piping systems.[1] The results of this program have been used by the Pressure Vessel Research Committee (PVRC) to propose higher allowable pipe damping values[2] than in Regulatory Guide (RG) 1.61.[3] Higher damping values allow more flexible systems with fewer supports, making the piping better able to expand and contract during thermal loadings, less susceptible to fatigue, less costly, and will reduce inspection, maintenance, and worker radiation exposure. The PVRC proposal has been approved as Code Case N-411 to the American Society of Mechanical Engineers Boiler and Pressure Vessel Code (ASME Code),[4] and in Revision 24 to USNRC RG 1.84.[5] Comparisons of RG 1.61 and PVRC curves for piping system damping are shown in Figure 1. The benefits of this change in allowable damping values are already being demonstrated as a cost-savings measure on commercial nuclear power plants. For example, Gilbert/Commonwealth, Inc., has determined that 10 of the 23 snubbers in one

---

[a] Work supported by the U.S. Nuclear Regulatory Commission, Office of Nuclear Regulatory Research, under DOE Contract No. DE-AC07-761D01570.

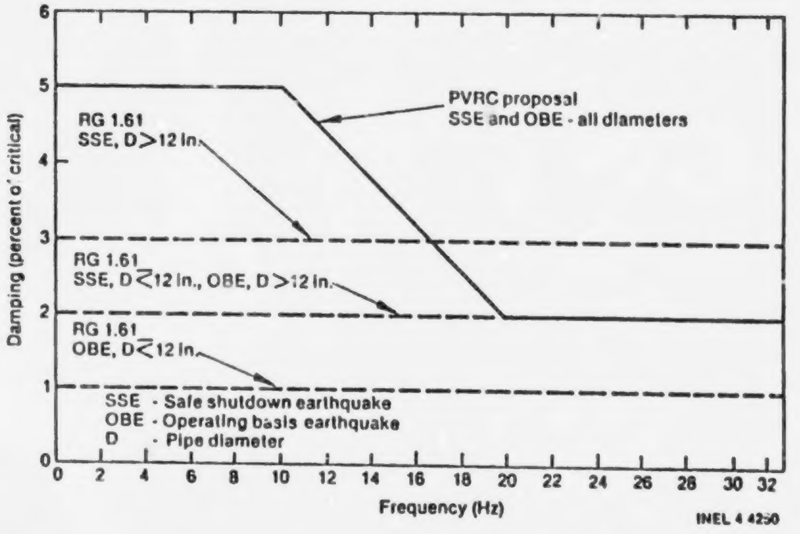

Figure 1. Comparison of RG 1.61 and PVRC pipe damping curves.

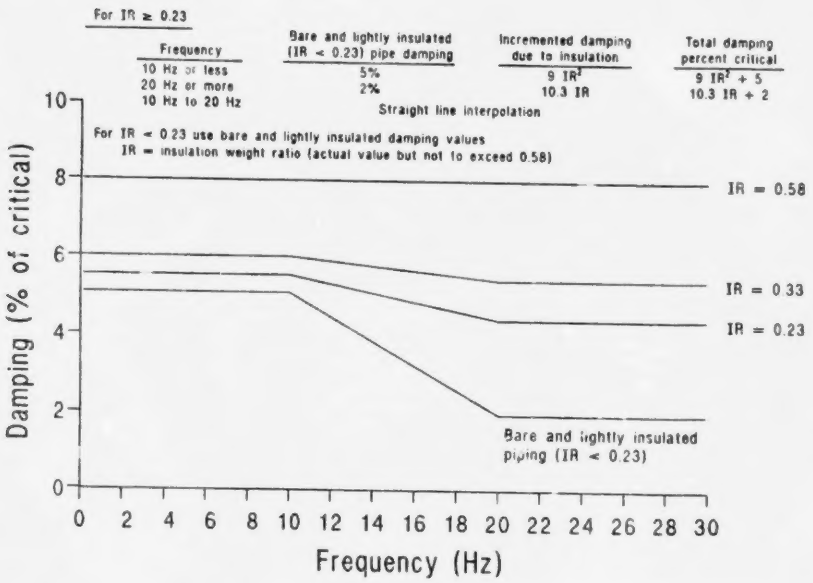

Figure 2. HEDL proposal for heavily insulated piping.

BEST COPY AVAILABLE

nuclear piping system could be eliminated using the revised damping values.[6] Using PVRC damping and other new techniques (zero deflection criteria and peak shifting), 18 of the 23 snubbers could be eliminated or replaced by rigid hardware. Similarly, using PVRC damping and independent support motion (ISM) techniques, 76% of the snubbers in three Commonwealth Edison piping systems (main steam, standby liquid control, and residual heat removal) could be eliminated.[7] Since nuclear power plant piping systems include several hundred (over 1000 per unit on recently completed plants) snubbers, the savings in design, procurement, installation, and maintenance of snubbers are considerable. The PVRC proposal has subsequently been modified as shown in Figure 2 to include the effects of heavily insulated piping based on data from the Hanford Engineering Development Laboratory (HEDL).[8] The first task described in this paper included conducting additional tests on a 5-in. INEL laboratory piping system and evaluating ANCO Engineers 6-in. laboratory piping system vibration data to further examine the parameters influencing damping in the seismic frequency range, and to add data to the already existing data base in support of the PVRC recommendations.

The allowable damping values in RG 1.61 and the PVRC proposals cover only the seismic frequency range, 0 to 33 Hz. However, there are several transients in which the forcing frequencies on piping are > 33 Hz. These are mainly fluid induced, such as water hammer, pressure relief valve discharge, and loss-of-coolant-accident (LOCA) related hydrodynamic loads. Neither RG 1.61 nor the ASME Code provides guidelines for damping values to be used for these high-frequency loads. With no official guidelines, the usual approach has been to use the RG 1.61 values for high-frequency analyses, although these values of damping have not been specifically approved for use in this frequency range nor for fluid-induced transients. Recognizing the need for allowable damping values at higher modal frequencies, the USNRC and the INEL expanded the pipe damping research program to cover modal frequencies in the 33 to 100 Hz range. This was the second task in the FY-86 research program.

A considerable amount of work has recently been performed by the Lawrence Livermore National Laboratory on probabilistic risk assessment (PRA) analyses of seismic safety margins. A risk assessment is conducted using a Seismic Safety Margins Research Program (SSMRP) methodology that has been developed as part of this program. To actually assess the effect of an earthquake on a given NPP using SSMRP methodology, specific information concerning the site and plant geometries, the seismic input, the structure and piping response, and the component fragilities must be known or assumed as input to the SMACS computer code.[9] Damping is one of the piping response parameters. Previously, parameter values have been sampled from assumed probability distributions according to a Latin hypercube sampling procedure. The mean values and uncertainties for piping system damping have not yet been determined from actual vibration test data. The third research task was to conduct statistical analyses of damping data for those piping systems in the nuclear piping data bank that are representative of light water reactor (LWR) NPPs, and from tests in which the excitation was of the order that might be expected during a significant seismic or hydrodynamic event. Thus future

SSMRP analyses can be conducted using piping system damping values obtained from actual test data, rather than assumed probability distributions.

It was recognized by the authors of RG 1.61 that damping was amplitude dependent, and thus they allowed an extra 1% of critical damping for the higher level safe shutdown earthquake (SSE) than for the operating basis earthquake (OBE). Since the issue of RG 1.61 in 1973, considerably more damping tests have been conducted worldwide at higher strain levels, and our knowledge of piping system damping at plastic strain levels has been increased. It has been noted that once the strain level in the piping system reaches a certain strain threshold, approximately the material yield stress (Sy), the damping tends to increase significantly.[10] This phenomenon has been attributed to material damping in the piping and supports. Because of the increased damping at high strain levels, the use of linear elastic stress analysis methods with RG 1.61 or PVRC damping will result in drastic overpredictions of the bending moments and stresses in piping systems excited sufficiently to vibrate in the plastic range. This will cause a significant design margin to be present in the stress analysis predictions. Consequently, the USNRC has authorized the INEL to evaluate high strain level damping data from recent and ongoing pipe vibration testing, and to outline ways to combine and present these data. A further objective of this fourth FY-86 research task is to provide quantitative measures of response margins in terms of piping damping values.

## LABORATORY PIPING TESTS AT SEISMIC FREQUENCIES

The first INEL damping tests were conducted on straight sections of 3-in and 8-in carbon steel piping.[11] From these tests, the effects of various typical piping supports and amplitude ranges were investigated. Using the results of these essentially one-dimensional tests, a more complicated three-dimensional 5-in laboratory piping system was designed and a series of experiments were conducted to determine the correlation of excitation type (shaker and snapback), supports, amplitude, insulation (insulated and uninsulated), response frequency, and pressure on pipe damping.[12] A diagram of the test configuration is shown in Figure 3.

Another series of piping vibration tests has been conducted for the USNRC and the Electric Power Research Institute (EPRI) by ANCO Engineers on two 6-in laboratory piping systems, shown in Figure 4. An extensive series of experiments using a variety of test excitation methods, supports, and response amplitudes was completed by ANCO Engineers as part of this program. The USNRC furnished the INEL with the raw data from these tests to reduce and to evaluate the damping results. In addition to the main series of tests on the ANCO laboratory system, the INEL participated in another, smaller, series of tests in which ANCO supplied the excitation to the system and the INEL collected and analyzed the data.

The effects of varying a number of parameters on damping has been investigated in these two series[12] and will be discussed individually below.

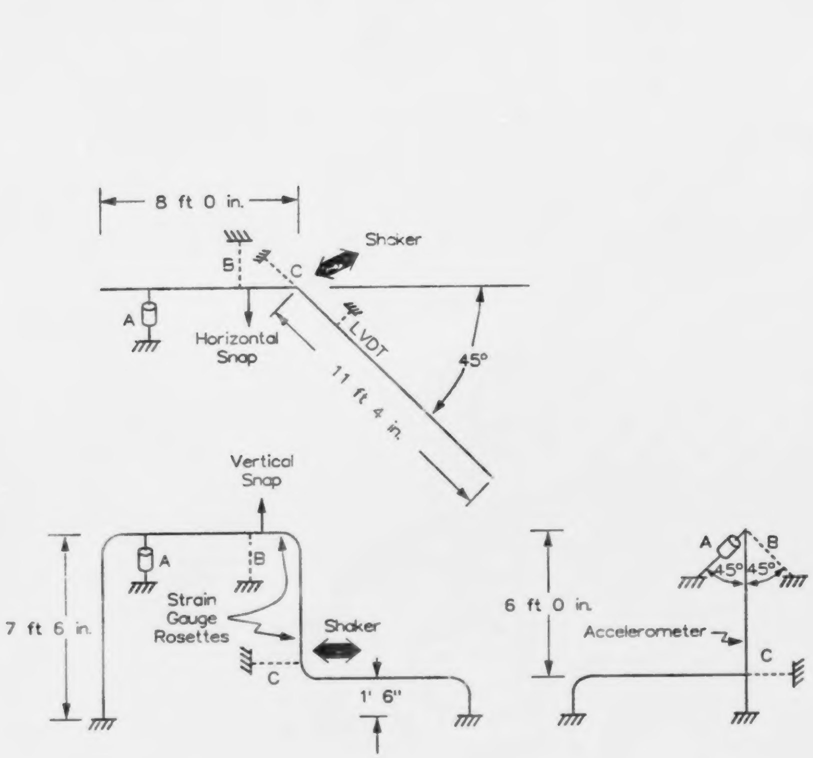
8 ft 0 in.
Shaker
B
C
A
Horizontal Snap
LVDT
11 ft 4 in.
45°
Vertical Snap
A
B
7 ft 6 in.
Strain Gauge Rosettes
Shaker
C
1' 6"
6 ft 0 in.
A
B
45°
45°
Accelerometer
C

Figure 3. INEL 5-in. piping system configuration.

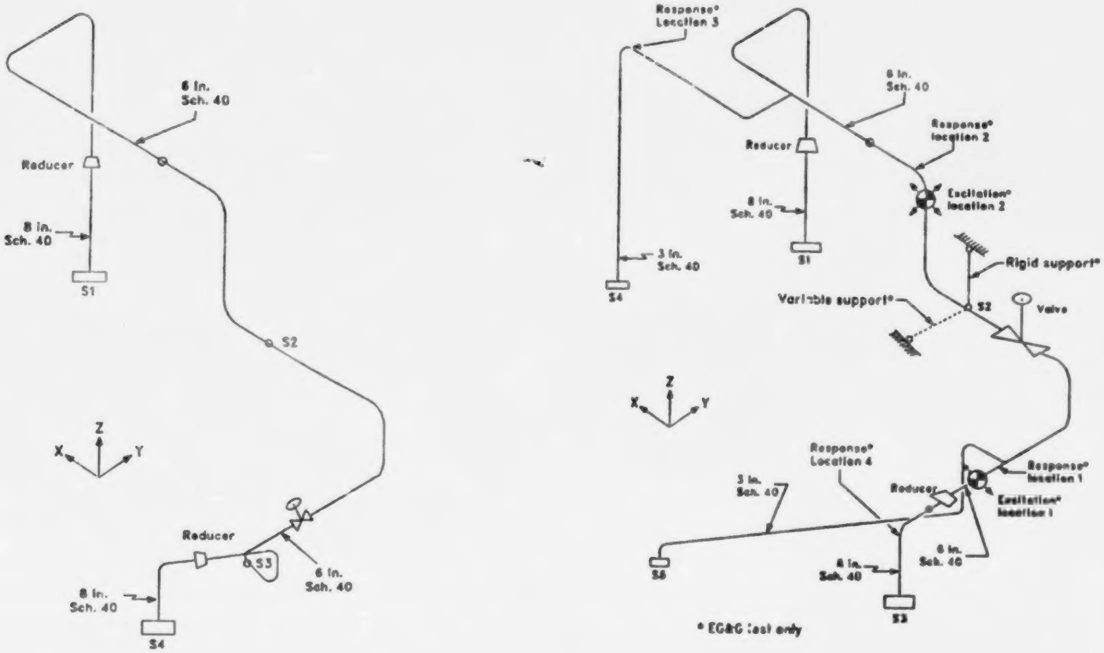
6 in. Sch. 40
Reducer
8 in. Sch. 40
S1
S2
X
Z
Y
Reducer
S3
6 in. Sch. 40
8 in. Sch. 40
S4
Response* Location 3
6 in. Sch. 40
Response* location 2
Reducer
Excitation* location 2
8 in. Sch. 40
S1
3 in. Sch. 40
S4
Rigid support*
Variable support*
S2
Valve
X
Z
Y
Response* Location 4
3 in. Sch. 40
Reducer
Response* location 1
Excitation* location 1
8 in. Sch. 40
6 in. Sch. 40
S6
S3
* EG&G test only

Figure 4. ANCO laboratory piping systems.

BEST COPY AVAILABLE

## Pressure

Damping tended to decrease with increasing pressure for the INEL 5-in. system with end supports only, while the damping did not change with pressure when a support was added at location A in Figure 3. Overall, the effect of pressure on damping at seismic levels is considered minimal when compared to the other influecing parameters.

## Supports

Starting with no supports and adding a rigid strut at location C in Figure 3 in the INEL tests had little effect on system damping, while adding a support at A or B increased the damping. A mechanical snubber dissipated the most energy producing, the highest damping levels in any of the lower excitation level tests. During swept sine, random, and simulated earthquake excitation tests, there was no noticable support effect in the ANCO series, while in the impulse tests the cases with mechanical snubbers at both intermediate supports produced higher damping than did other support conditions.

## Frequency

In contrast to much of the data in the technical literature which shows an inverse frequency to damping relationship, the INEL series uninsulated pipe, shaker excitation data showed damping was fairly constant with mode number. For the insulated pipe, shaker excitation data, damping was lowest at the first mode (8 Hz), was maximum around 15 Hz, then decreased with frequency. In the uninsulated pipe, snapback excitation tests, the only frequency dependence was for the mechanical snubber configurations, where an inverse frequency to damping relationship was apparent. It is concluded that the frequency effect often noted is really a result of the interaction of the modes with the supports. Those modes causing high loads in energy dissipating supports have higher damping. The lower modes have significant interactions with the supports for larger piping systems common to most nuclear power plants, while most of the vibrational motion of the higher modes takes place between supports, often at lower amplitudes of vibration. In the ANCO test series there was a definite trend of an inverse frequency to damping relationship for the swept sine, random, and simulated earthquake tests (Figure 5), but no such trend was observed for the impulse tests.

## Insulation

The INEL test series shaker excitation tests showed a pronounced increase in damping in all modes when the insulation was added (Figure 6), while the snapback excitation tests showed virtually no effect on the few modes that responded. This was probably more of an excitation method effect rather than an amplitude effect. The piping was continually vibrated against the insulation during the shaker tests, resulting in considerable energy loss due to friction. However, the insulation moved freely with the pipe during the snapback tests, with no additional energy being input to the system during cycling, and when resistance was encountered, both pipe and insulation

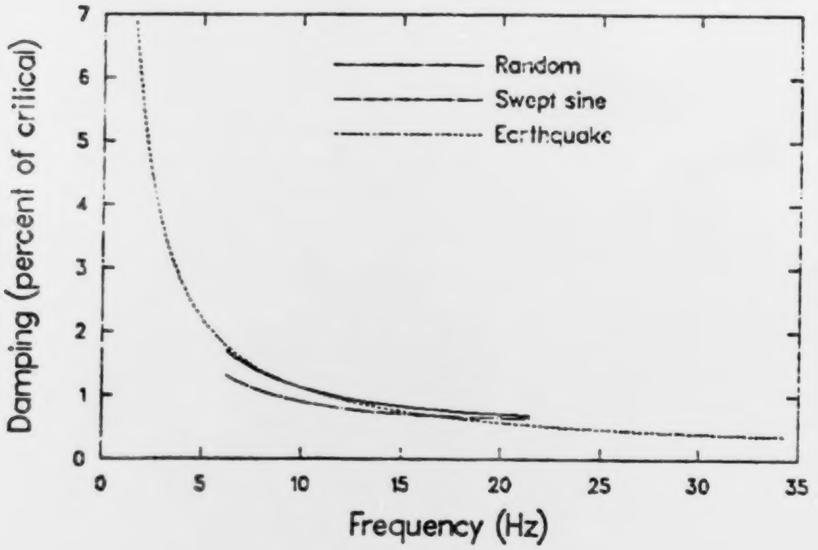

Figure 5. ANCO 6-in. system excitation method results.

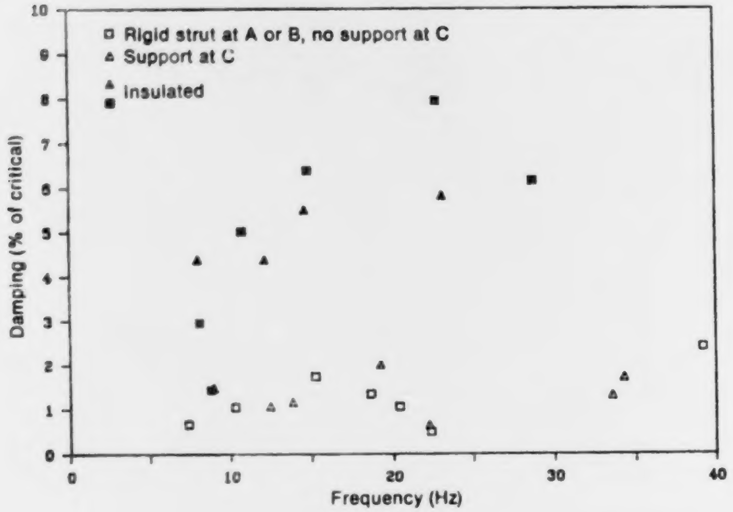

Figure 6. Effect of insulation on INEL 5-in. system.

changed directions in a consistent manner. Since only a few modes could be identified for the snapback excitation, insulated pipe series, the other modes may have been so heavily damped that the free vibration decay did not excite them. The shaker tests would be more representative of an earthquake, which produces random motions.

### Amplitude

The INEL high-level test series, at dominant frequencies of around 7, 9, and 18 Hz, all showed a trend of increasing damping with strain level. Although the low-level damping was about 1% of critical for all three test sets in the series, the slope of the increase was different for each higher level case. This is probably because of the difference in mode shapes. Damping is proportional to the ratio of the dissipated energy to the total energy. Since each mode shape places an individual stress pattern in the piping and since the vibrational energy associated with each mode shape is unique from those of other mode shapes, it stands to reason that the ratio of the two will have its own value for each case. Furthermore, each mode shape will cause the pipe to impact with the supports at a different force level. An important point to note is that the same effect was noted for the higher frequency (18 Hz) case as for the lower frequency cases. Some of the data in the ANCO series exhibited a similar trend.

### Excitation method

Base band random excitation (excitation over a wide range of frequencies) produced generally higher damping in the INEL tests than did the swept sine tests. This is attributed to lower resolution of the data and nonuniform energy distribution among the modes for base band excitation. Since the number of lines of resolution are constant as set by the data analyzer (400 spectral lines of resolution in these tests), more data points are concentrated in the region of the damping versus frequency curve used to calculate the damping for narrow band data acquisition than for the broader base band excitation. Thus there are more data points to better define the shape of the curve for half-power damping calculations. Excitation levels high enough to produce a good measure of damping were achieved by concentrating the excitation energy in only one or two modes. The zoom random (excitation of only one or two modes at a time) and swept sine methods were judged to produce comparable damping levels. The swept sine method is more time consuming and fatigues the metal in the pipe more rapidly; consequently, the zoom random was the preferred method of excitation in the tests. In the ANCO series the swept sine, random, and simulated earthquake excitation methods all produced almost the same results. The impulse tests gave similar low damping levels, but did not match quite as closely as the other excitation tests for any frequencies. In particular, the damping was slightly higher in the higher frequency range for the impulse tests.

### Calculational method

For the low response level tests where the damping was fairly constant with response amplitude, the half-power, curve-fit, and logarithmic decrement methods gave approximately the same results. However, at higher response levels where damping was not constant with response amplitude, the half-power method gave a damping value between the extremes of the logarithmic-decrement computed points. Each method offers its own unique advantage. The logaritmic decrement method is good for tracking damping when it is amplitude dependent through a decaying amplitude range. It is difficult to use when multiple modes are excited, and extensive digital filtering of the data may be required. The curve-fit and half-power methods are much easier to perform; yet they provide only a single average damping value for each test, even if the amplitude is varying nonlinearly. The curve-fit method is judged to be more accurate than the half-power method because it considers both the amplitude and phase of the response. In order to achieve the best understanding of the damping associated with a piping system, excitation should be undertaken by a variety of methods and damping calculated using several methods. Then, based upon a comparison of results, a better overall perspective can be gained. This approach would highlight some of the inconsistencies which are often observed in the damping test results.

## HIGH FREQUENCY DAMPING EVALUATION

The plan followed in conducting this research task was to review published literature and the USNRC/INEL nuclear piping data bank for high-frequency damping results, conduct tests at high frequencies on laboratory 3-in. and 5-in. piping systems at the INEL, evaluate the data and recommend damping values for use in analyses of piping vibrations at high frequencies.[12]

Relevant high-frequency piping system damping data was found in only two references. Kraftwerk Union (KWU) in the Federal Republic of Germany conducted a vibration test series on 250-mm (10-in.) NPP piping, with and without insulation. There were two high-frequency modes each with two data points, one insulated and the other uninsulated, for each mode. The General Electric Company also conducted vibration tests on BWR piping systems. The excitation was by safety relief valve (SRV) discharge transients, and these tests provided the only data in this review in which excitation was produced by bona fide fluid-induced transients. High damping values of 5.9%, 7.1%, and 16% of critical were reported at 28 Hz, near the upper frequency limit of the seismic range.

High-frequency damping values in an INEL test series using a section of 3-in. straight pipe ranged from one to three percent of critical for the configuration with no intermediate supports. For configurations with intermediate supports, high-frequency damping values ranged from 3% to 7% percent of critical; averaging 4.1% of critical. The high-frequency damping values were generally $\geq$ damping values for the seismic range. Intermediate supports supplied an additional 2% to 3% of critical damping at high frequencies.

The 5-in. INEL laboratory system in Figure 3 that included elbows, bends, and reducers was also tested at higher frequencies, both in the insulated and uninsulated conditions and at high and low stress levels. Results for the uninsulated cases with no intermediate supports showed that the modes above 60 Hz had significantly higher damping than did the lower modes. For the uninsulated pipe with a rigid strut as the intermediate support, damping increased at frequencies above 50 Hz and the higher level excitations that produced stresses near Sy resulted in higher damping than did the lower level (Sy/4) case. At frequencies > 50 Hz, results for the mechanical and hydraulic snubbers were comparable to the rigid strut results. Damping values at frequencies > 50 Hz ranged from 2% to 8% of critical (uninsulated condition). For the higher excitation levels in which pipe stress was near Sy, damping ranged from 4% to 12% of critical which is 2% to 4% of critical higher than for the lower excitation case in which pipe stress was about Sy/4. However, no definite difference was noted between the supported and unsupported condition damping values in the insulated test results. Damping in the high-frequency range was scattered from 3% to 7% of critical (insulated condition). For modes with low damping, i.e. below 1% of critical, insulation increased the damping. For modes > 50 Hz for which the damping was already high, insulation had minimal effect on damping.

The data chosen as the basis for estimating high-frequency damping values was heavily weighted by the results of the INEL high-frequency 3-in. and 5-in. tests (Figure 7). One characteristic of the data worth noting is that damping appears to be higher when insulation is present (Figure 8). Another feature of interest is that damping levels were greater at the higher excitation levels, i.e., when stress levels were near Sy, and for systems

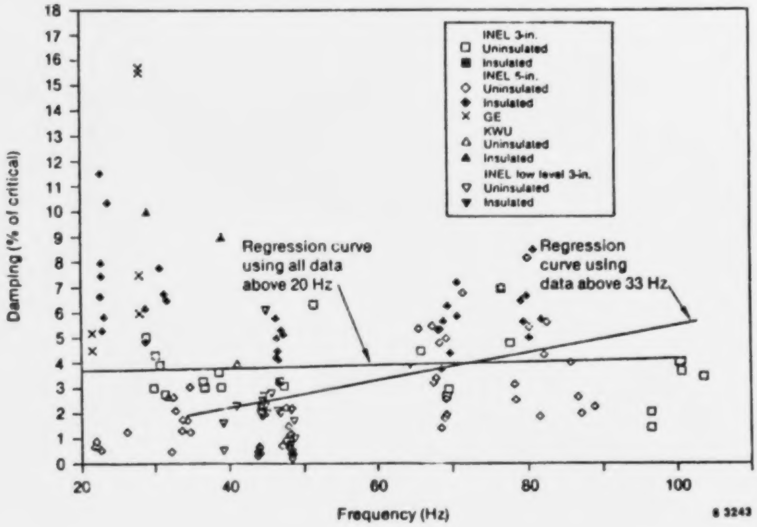

Figure 7. High frequency test data.

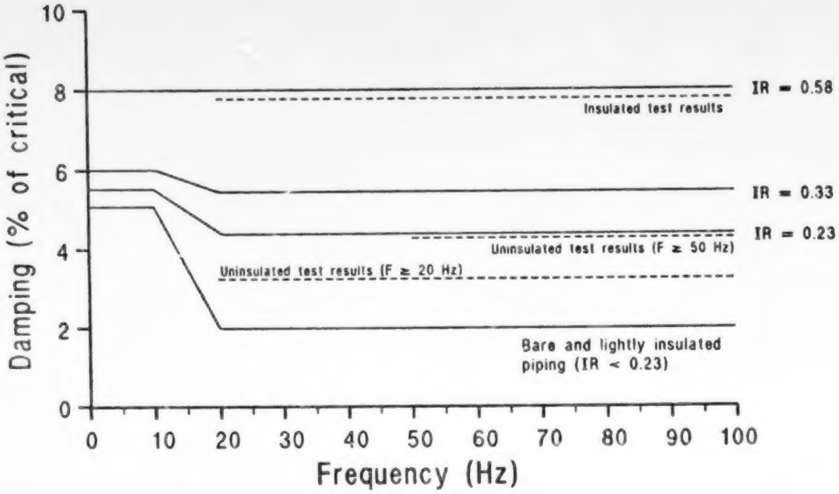

Figure 8. Comparison of high-frequency results to PVRC curve.

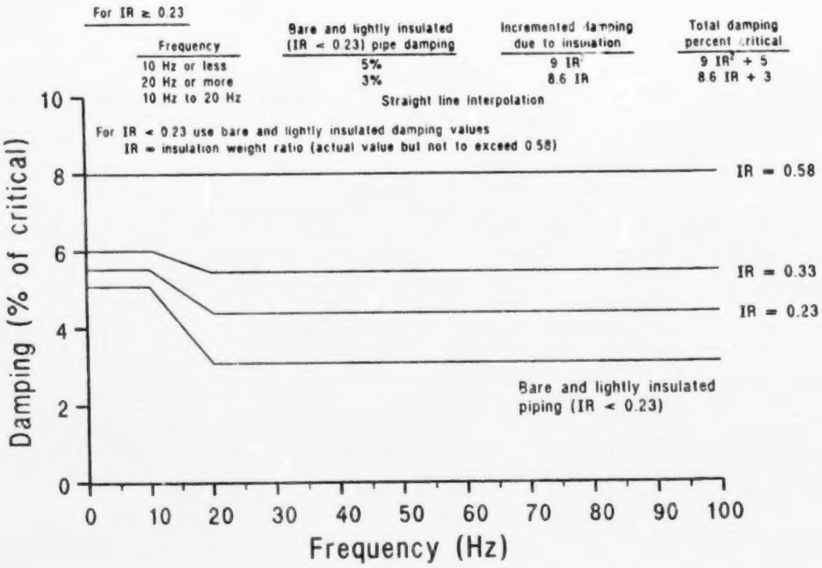

For IR ≥ 0.23

| Frequency | Bare and lightly insulated (IR < 0.23) pipe damping | Incremented damping due to insulation | Total damping percent critical |
|---|---|---|---|
| 10 Hz or less | 5% | $9 IR^2$ | $9 IR^2 + 5$ |
| 20 Hz or more | 3% | $8.6 IR$ | $8.6 IR + 3$ |
| 10 Hz to 20 Hz | Straight line interpolation | | |

For IR < 0.23 use bare and lightly insulated damping values
IR = insulation weight ratio (actual value but not to exceed 0.58)

Figure 9. High-frequency representation of test data.

BEST COPY AVAILABLE

with intermediate supports, which are more representative of conditions which would be found in actual nuclear piping systems. It was concluded that suitable representations of the test data could be achieved by increasing the PVRC uninsulated piping curve (Figure 1) from 2 to 3% of critical damping for frequencies >20 Hz, and by extending the proposed insulated curves (Figure 2) to 100 Hz at the recommended levels as shown in Figure 9.

## STATISTICAL DISTRIBUTION OF DATA

Test data from 27 LWR type piping systems where the piping had been vibrated at levels representative of at least moderate severity seismic or hydrodynamic transients were chosen for a statistical damping study.[14] Most of these piping systems are in actual NPPs, and the lowest mode was < 8 Hz for over 80% of them. Thus a great deal of the damping data was from low frequency piping systems. The data were broken into eight groups (see Table 1) representing all data and data used in the original USNRC regression analysis, NPP and test (laboratory) systems, insulated systems, and pipe sizes of > or < 12 in. A further categorization was conducted (see Table 2), separating the data into three runs that represented all data, one data point

TABLE 1. DATA GROUPS

| GROUP | DESCRIPTION |
|---|---|
| 1 | All data |
| 2 | Data used in original PVRC regression analysis |
| 3 | Data from NPP piping systems |
| 4 | Data from test or laboratory piping systems |
| 5 | Data from insulated piping systems |
| 6 | Data from all piping systems > 12 in. |
| 7 | Data from all piping systems < 12 in. |
| 8 | Data from NPP piping systems < 12 in. |

TABLE 2. NUMBER OF DAMPING VALUES IN EACH SUBDIVISION

| RUN | Description |
|---|---|
| 1 | all damping values |
| 2 | one damping value per mode representing the average of the damping values for that mode from multiple tests on the same system |
| 3 | a single damping value for each system representing the highest excitation of the lowest mode. |

per mode for each data set, and the damping of the lowest mode at the highest excitation for each data set, respectively.

In the first part of this study damping was treated as independent of frequency (or mode number). The statistical analysis showed that a lognormal fit provided a suitable approximation of the raw data (see Figure 10 for histogram and cumulative distribution plot of group 1, run 2). A statistical summary is presented in Table 3. Average damping values ranged from 3.38% of critical for test systems to 4.41% of critical for NPP systems < 12 in. in the

TABLE 3. NORMAL AND LOGNORMAL DISTRIBUTION PARAMETERS; % OF CRITICAL DAMPING (SEE TABLES 1 AND 2 FOR DESCRIPTIONS OF GROUPS AND RUNS)

| | | ASSUMED NORMAL DIST. | | ASSUMED LOGNORMAL DIST. | | | |
|---|---|---|---|---|---|---|---|
| GROUP | RUN | ARITHMETIC MEAN | ARITHMETIC STAN. DEV | GEOMETRIC MEAN | GEOMETRIC STAN. DEV. | MEDIAN | BETA |
| 1 | 1 | 3.84 | 3.33 | 2.82 | 2.28 | 3.0 | 0.82 |
| | 2 | 4.45 | 3.82 | 3.36 | 2.16 | 3.5 | 0.77 |
| | 3 | 6.96 | 5.67 | 5.06 | 2.36 | 4.8 | 0.86 |
| 2 | 1 | 4.22 | 3.53 | 3.29 | 2.06 | 3.3 | 0.72 |
| | 2 | 4.38 | 3.12 | 3.56 | 1.91 | 3.3 | 0.65 |
| | 3 | 7.42 | 4.07 | 6.50 | 1.75 | 6.3 | 0.56 |
| 3 | 1 | 4.04 | 3.52 | 3.08 | 2.12 | 3.1 | 0.75 |
| | 2 | 4.37 | 3.61 | 3.35 | 2.11 | 3.4 | 0.75 |
| | 3 | 7.62 | 5.93 | 5.67 | 2.30 | 5.3 | 0.84 |
| 4 | 1 | 3.38 | 2.80 | 2.32 | 2.57 | 2.6 | 0.94 |
| | 2 | 4.72 | 4.55 | 3.39 | 2.32 | 3.6 | 0.84 |
| | 3 | 4.45 | 3.96 | 3.28 | 2.39 | 3.1 | 0.87 |
| 5 | 1 | 3.70 | 3.39 | 2.68 | 2.32 | 3.0 | 0.84 |
| | 2 | 4.40 | 3.62 | 3.36 | 2.14 | 3.4 | 0.76 |
| | 3 | 7.73 | 5.92 | 5.74 | 2.32 | 5.8 | 0.84 |
| 6 | 1 | 4.16 | 4.04 | 3.05 | 2.27 | 3.2 | 0.82 |
| | 2 | 4.48 | 3.03 | 3.72 | 1.83 | 3.5 | 0.60 |
| | 3 | 7.47 | 4.67 | 6.10 | 1.98 | 6.1 | 0.68 |
| 7 | 1 | 3.72 | 3.03 | 2.75 | 2.28 | 3.0 | 0.82 |
| | 2 | 4.43 | 4.33 | 3.12 | 2.38 | 3.3 | 0.87 |
| | 3 | 6.61 | 6.39 | 4.44 | 2.61 | 4.4 | 0.96 |
| 8 | 1 | 4.41 | 3.26 | 3.55 | 1.94 | 3.3 | 0.66 |
| | 2 | 4.84 | 4.48 | 3.39 | 2.49 | 3.6 | 0.91 |
| | 3 | 8.68 | 7.13 | 6.13 | 2.67 | 6.3 | 0.98 |

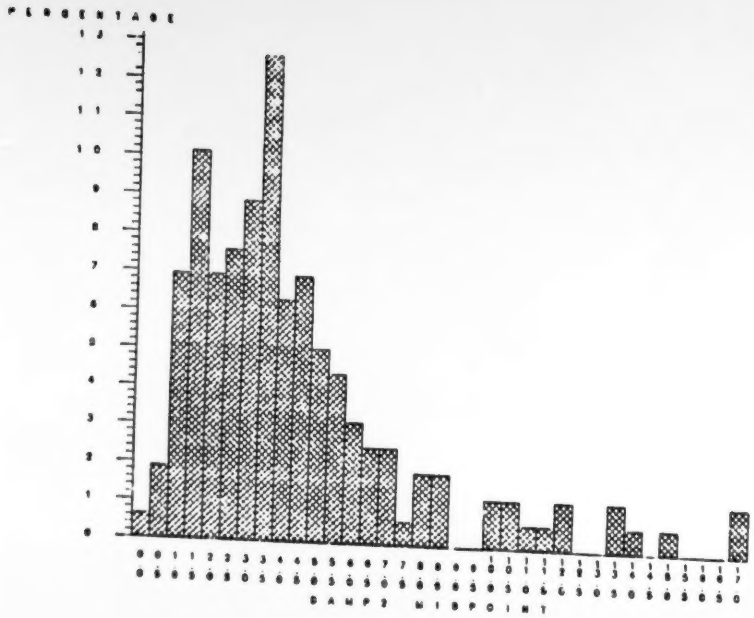

(a) Histogram

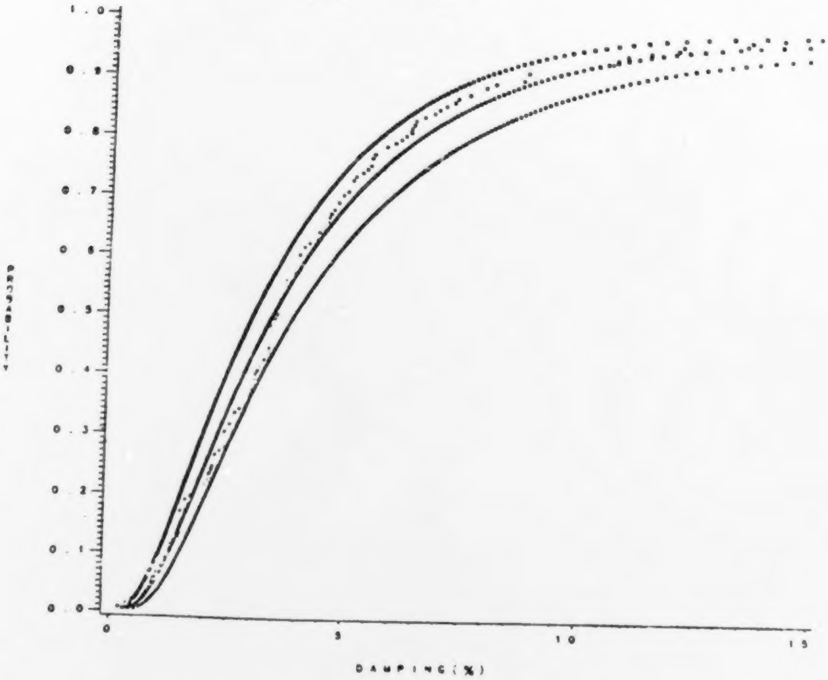

(b) Cumulative distribution plot.

Figure 10. Group 1, Run 2 data.

Run 1 cases (duplicate tests for each system included). When duplicate tests were eliminated (Run 2), the averages for all groups were nearly the same, ranging from 4.38% of critical to 4.84% of critical. Damping values ranged from 4.45% of critical for test systems to 8.68% of critical for NPP systems < 12 in. in Run 3, consisting of the lowest mode at its highest excitation level for each data set.

The fact that Run 3 values are higher is not surprising since in many tests the lowest mode was the most heavily excited, with little of the input energy being concentrated in the higher modes. Tests have shown that damping values are relatively lower in the lightly excited modes. Thus the Run 3 values are probably the most representative of the damping that might be expected in the most heavily seismically excited modes. The Run 2 values would give the best sets of values to use over the entire frequency range, because some of the unequal weighting by the data sets with more damping values than others has been eliminated, while multiple modes have been retained. The standard deviation is fairly large in all 24 subdivisions (8 groups, 3 runs/group), reflecting the generally wide scatter in the data.

The geometric mean damping values calculated for the lognormal distribution fits are all lower than the average values. This is a result of the averaging of the natural logarithms of the damping values which gives a higher weighting to the lower raw data values.

Most of these data were from tests in which the maximum stresses in the piping systems were ≤ OBE levels. Very few of the damping values were recorded at stress levels represenatative of an SSE. Therefore, the conclusions reached in this report are most applicable to OBE events. Since damping values are generally higher at SSE levels than at OBE levels, the results can be considered to be lower than comparable SSE damping values.

## EVALUATION OF DAMPING AT HIGH STRAIN LEVELS

Although the concept of damping as related to a linear elastic system is not strictly defined for elastoplastic piping system vibrations, a concept of equivalent damping was used in Reference 15 to estimate the response margins in predicted piping system behavior. The equivalent damping concept used was based on the computed linear damping that would cause amplifications of an elastic system to match the available experimental data at high strain levels. The theoretical variation of damping and frequency with ductility (the ratio of the total elastoplastic displacement to the elastic displacement) is shown in Figures 11 and 12. Damping is shown to increase at higher ductilities using both an energy concept and the logarithmic decrement method. The increase also depends on the change in system stiffness due to the formation of progressive plastic hinges leading to collapse.

High strain damping data from eight different sources are plotted on a common basis as a function of ductility in Figure 13. For stiff systems the data tend to follow the theoretical elastic-perfectly-plastic (EPP) curve, while for more flexible systems the damping is somewhat lower. At the highest observed strain levels, the damping values are estimated to be 30 to

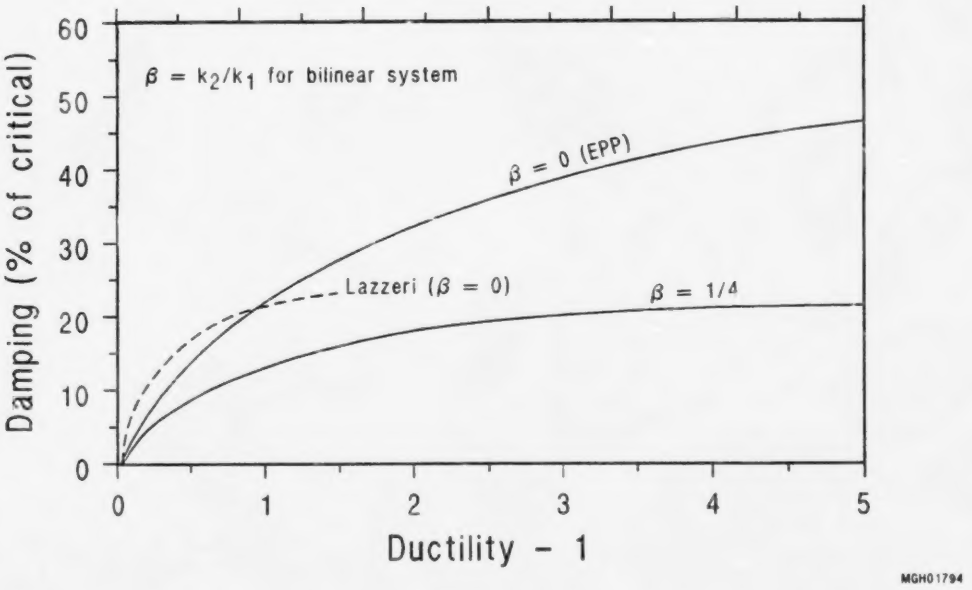

Figure 11. Theoretical variation of damping with ductility.

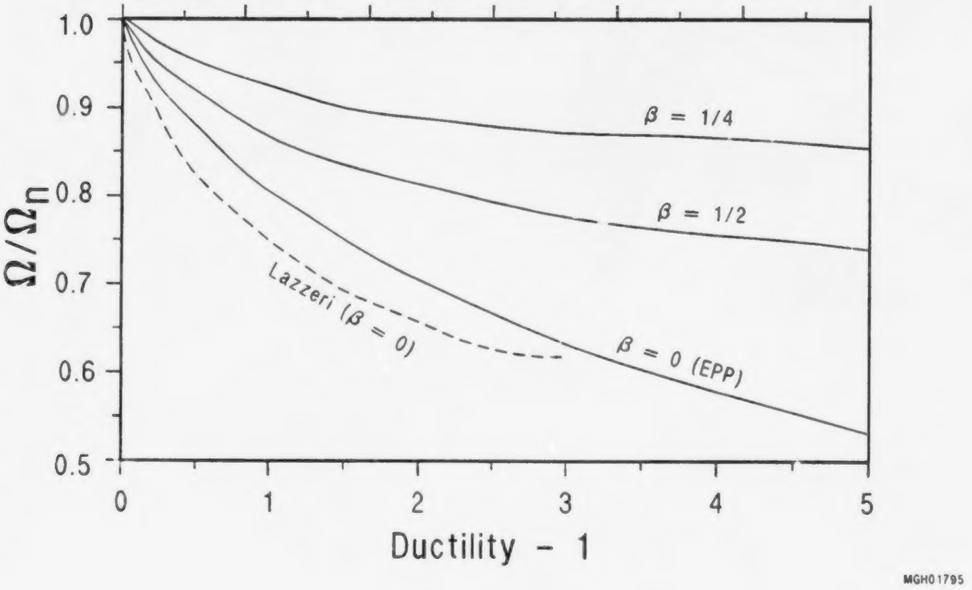

Figure 12. Frequency shift due to ductility.

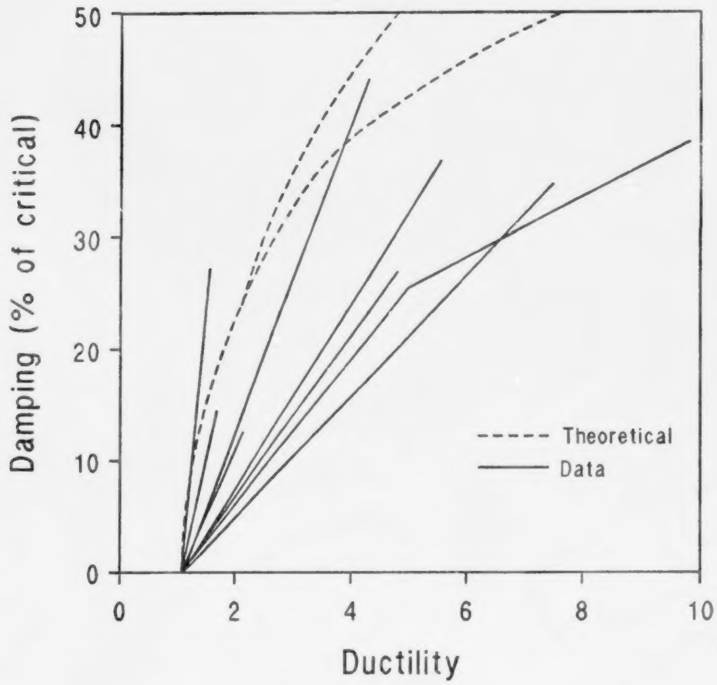

Figure 13. Test data compared with theoretical EPP curves.

50% of critical. This results in a response margin of actual input acceleration to linear elastic computed acceleration (using 5% of critical damping) of from 2.5 to 3 for seismic excitations and from 6 to 10 for sinusoidal excitations.

Although an estimate has been made as to the expected damping and response margins of piping systems at the time of failure, such information is not well suited to predict piping system failure by itself. The proper method is to conduct an inelastic analysis that accounts for the nonlinear change in system properties at high load levels. This must include a model of system geometry and the determination of successive plastic hinges that will occur before system failure. The 30 to 50% damping values stated in this report would not be used in such analyses because the material hysteresis or revised plastic spectra in the mathematical model will already take into account this energy dissipation. Rather, a representative elastic damping value such as 5% for actual nuclear power plant piping systems and 1 to 2% for laboratory systems should be used.

What does the 30 to 50% of critical damping for piping systems at failure mean? If a linear elastic analysis were to be performed on a system with hinges at the locations at which the cross-section had yielded, this damping would be required to predict the response motion. However, at 50% of critical damping there is no dynamic amplification of the motion. Thus at the time of failure the piping system appears to be forced into a plastic dynamic deflection shape with all of the input energy being absorbed by the system by means of changing its plastic shape. Therefore, the use of high strain level damping would not be recommended for analyses at ductility levels > 2 to 3 (20% to 30% of critical damping).

## SUMMARY

Four tasks aimed at describing the parameters that influence damping in nuclear power plant piping systems were performed at the INEL in FY-86. In the first two of these tasks the parameters were investigated in the seismic (< 33 Hz) and high frequency (33 to 100 Hz) ranges. Results of the third task showed that a lognormal probability distribution of damping was found to give a good statistical representation of the data, and the means and standard deviations of damping for several combinations of parameters were determined for use in PRA analyses. The final task evaluated damping at high strain levels, and concluded that once plastic action begins, the apparent damping begins to steadily increase with strain level.

## REFERENCES

1. A.G. Ware and J.G. Arendts, "The NRC/EG&G Nuclear Piping System Damping Study Program", Paper K17/3, Transactions of the 8th International Conference on Structural Mechanics in Reactor Technology (SMiRT), Brussels, Belguim, pp. 285-290, 1985.

2. Welding Research Council Bulletin 300, "Technical Position on Criteria Establishment", ISSN 0043-2326, 1984.

3. U.S. Atomic Energy Commission, "Damping Values for Seismic Design of Nuclear Power Plants", Regulatory Guide 1.61, 1973.

4. American Society of Mechanical Engineers, ASME Boiler and Pressure Vessel Code, Section III, Nuclear Power Plant Components, Division 1, 1983 Edition.

5. U.S. Nuclear Regulatory Commission, "Design and Fabrication Code Case Acceptability: ASME Section III Division 1", Regulatory Guide 1.84, Rev. 24. 1986.

6. L.P. Buchanan, "Snubber Optimization Results on In-plant Piping System", Seismic Engineering for Piping Systems, Tanks, and Power Plant Equipment, American Society of Mechanical Engineers, PVP-Vol. 108, pp. 31-42, 1986.

7. R. Srinivasan, J.J. Marianyi, and J.T. Fox, "A Snubber Reduction Pilot Program", Seismic Engineering for Piping Systems, Tanks, and Power Plant Equipment, American Society of Mechanical Engineers, PVP-Vol. 108, pp. 177-183, 1986.

8. M.J. Anderson, M.R. Lindquist, and L.K. Severud, Further Considerations for Damping in Heavily Insulated Pipe Systems, HEDL-SA-3258-SP, Hanford Engineering Development Laboratory, Richland, Washington, 1985.

9. J.J. Johnson et al., SMACS--Seismic Methodology Analysis Chain with Statistics, Lawrence Livermore National Laboratory, Livermore, California, NUREG/CR-1780, UCRL-53021, Vol. 9, 1981.

10. A.G. Ware, "Pipe Damping", Proceeding of the U.S. Nuclear Regulatory Commission 13th Water Reactor Safety Research Information Meeting, Gaithersburg, Maryland, October 1985, NUREG/CP-0072, Vol. 3, pp. 73-82, 1986.

11. A.G. Ware and G.L. Thinnes, Damping Results for Straight Sections of 3 in. and 8 in. Unpressurized Pipes, NUREG/CR-3722, EGG-2305, EG&G Idaho, Inc., Idaho Falls, Idaho, 1984.

12. A.G. Ware and J.G. Arendts, Pipe Damping--Laboratory Tests in the Seismic Range, NUREG/CR-4529, EGG-2447, EG&G Idaho, Inc., Idaho Falls, Idaho, 1986.

13. A.G. Ware, Pipe Damping--Results of Vibration Tests in the 33 to 100 Hertz Frequency Range, NUREG/CR-4562, EGG-2450, EG&G Idaho, Inc., Idaho Falls, Idaho, 1986.

14. A.G. Ware and T.M. Kimes, "Statistical Evaluation of Light Water Reactor Piping Damping Data Representative of Seismic and Hydrodynamic Events", EGG-EA-7260 (Draft), EG&G Idaho, Inc., Idaho Falls, Idaho, 1986.

15. A.G. Ware, "An Evaluation of Damping in Piping Systems at High Strain Levels", EGG-EA-7380 (Draft), EG&G Idaho, Inc., Idaho Falls, Idaho, 1986.

## NOTICE

This paper was prepared as an account of work sponsored by an agency of the United States Government. Neither the United States Government nor any agency thereof, or any of their employees, makes any warranty, expressed or implied, or assumes any legal liability or responsibility for any third party's use, or the results of such use, of any information, apparatus, product or process disclosed in this report, or represents that its use by such third party would not infringe privately owned rights. The views expressed in this paper are not necessarily those of the U.S. Nuclear Regulatory Commission.

BLANK PAGE

# NONLINEAR PIPING DAMPING AND RESPONSE PREDICTIONS*

L. K. Severud, E. O. Weiner, M. R. Lindquist, M. J. Anderson, S. E. Wagner

Hanford Engineering Development Laboratory
Westinghouse Hanford Company, Richland, WA

## ABSTRACT

The high level dynamic testing of four prototypic piping systems, used to provide benchmarks for analytical prediction comparisons, is overviewed. The size of pipe tested ranged from one-inch to six-inches in diameter and consisted of carbon steel or stainless steel material.

Failure of the tested systems included progressive gross deformation or some combination of ratchetting-fatigue. Pretest failure predictions and post test comparisons using simplified elastic and elasto-plastic methods are presented. Detailed non-linear inelastic analyses are also shown, along with a typical ratchet-fatigue failure calculation.

A simplified method for calculating modal equivalent viscous damping for snubbers and plastic hinges is also described.

Conclusions are made regarding the applicability of the various analytical failure predictive methods and recommendations are made for future analytic and test efforts.

## INTRODUCTION

The purpose of the research described herein is to provide the bases for recommending pseudo-linear-elastic methods and procedures to be used in predicting the high-level seismic response and failure of piping systems. These methods can then be used to assess the margins provided by the present ASME Code rules for piping seismic design, to reduce the number of needed piping restraints, to increase the piping reliability and contribute to Code improvements.

---

* Work sponsored by the U. S. Nuclear Regulatory Commission Office of Nuclear Research under FIN D1611 with the U. S. Department of Energy.

BEST COPY AVAILABLE

During 1986, the NRC/NRR sponsored fragility testing of a 6-inch diameter piping system at the Energy Technology Engineering Center (ETEC), Reference 1. Previously, a 1-inch pipe system was tested at Hanford Engineering Development Laboratory (HEDL), Reference 2, a 3-inch system at ETEC, and a branch 2 and 4-inch system at KWU, Reference 3. These test results provided correlation data for comparison to pre and post-test predictions using various simplified methods.

## DESCRIPTION OF TESTS

High level dynamic testing of piping systems has occurred on a world-wide basis and has included a variety of pipe sizes and configurations. Analytic predictive failure methods and correlations have been applied to four tested piping systems as described below.

### HEDL One-Inch Pipe Loop

A series of high level dynamic tests were performed on a heavily insulated one-inch diameter piping loop at Hanford Engineering Development Laboratory (HEDL), Reference 2. The HEDL piping loop consisted of a one-inch diameter, 304 stainless steel, schedule 40 pipe approximately 35 feet long. It contained nine elbows and/or bends along with risers and one liquid metal valve. The loop was insulated with stand-off insulation with an inner heater annulus and outer metal cover similar to that planned for LMFBR pipe systems. The test article, shown in Figure 1, was unpressurized during the tests.

The dynamic loading of the HEDL one-inch diameter pipe loop consisted of a time history loading that correlated to a specified seismic response spectrum followed by sinusoidal loading at the first natural frequency of the system. No failure of piping components was noted during time history seismic loading at several input load levels.

During the progressively increasing sinusoidal load steps, gross deformation of the test piping system progressively developed. This ratchet-type deformation was correlated to the formation of plastic hinges at specific locations. Permanent local deformation of the pipe wall (see Figure 1) was first noted near the vertical support at node 99 and a plastic hinge subsequently developed at this location. Pipe plastic bending started at a base input load level between 0.2 g's and 0.5 g's. As the load steps increased, permanent deformation also increased, with the vertical portion of the pipe system (nodes 22-24) gradually rotating (with the top moving in a positive Z direction). A second increase in the deformation rate of this vertical portion initiated at about 1.5 g's base load input, implying that a second plastic hinge was operative. Testing continued up to 2.8 g's where it was terminated. Progressive gross deformation (ratcheting) led to very near collapse of the piping system. After completion of testing, the insulation was removed and a second region of plastic deformation was found on the pipe section between nodes 35 and 36. Despite the gross deformations that occurred as a result of the testing, the pressure boundary of the piping system remained intact.

## ETEC Six-Inch System

High level dynamic testing was accomplished at the Energy Technology Engineering Center (ETEC) on a configuration consisting of mainly six-inch diameter pipe, Reference 1. The test article, Figure 2, was constructed of approximately forty-eight feet of six-inch diameter and seventeen feet of three-inch diameter carbon steel schedule 40 bare piping and components, including a simulated valve assembly. The test article was pressurized at 1000 psi during the test.

The dynamic loading of the ETEC six-inch diameter test article consisted of a time history loading that represented a specific seismic response spectrum followed by sinusoidal "burst" loading at three frequencies. The time history loadings, which did not cause failure, were performed at three levels of zero period acceleration (ZPA): 7.5 g, 13 g, and 30 g. The sinusoidal burst tests were at 4 HZ (8 cycles), and 5 HZ (11 cycles).

A local rupture failure of the piping test article occurred during the 5 HZ sinusoidal burst test. The location of the rupture was near the anchor at location S1. Prior to actual failure, a two inch wide circumferential bulge indicative of ratchetting was observed at location S1 following the high level (30 g actual ZPA) seismic test. Subsequently, failure occurred during the second sine burst test. Rupture occurred in the previously observed circumferential bulge during the 6th of the planned 11 cycles of maximum displacement of the 5 HZ harmonic input. Failure resulted from a 300 degree circumferential break in the bulge; a classic double-ended guillotine break was avoided with prompt termination of testing. Failure of the test article was attributed to incremental ratchetting due to internal pressure in the piping system resulting in wall thinning and bulging and subsequent fracture due to tensile overloading.

## ETEC Three-Inch System

High level dynamic testing was performed at ETEC on a three-inch diameter test article. The configuration, Figure 3, consisted of approximately fifty-one feet of three-inch diameter schedule 40 carbon steel piping. The test environment consisted of 15 second time history loadings at three levels of acceleration ZPA: 5 g, 14 g, and 30 g and sinusoidal burst tests at 3.4 HZ, 4.7 HZ, and 6 HZ.

Failure of the test article occurred during the sinusoidal burst loading at 6 HZ, at approximately 25 g load level. Failure took place in the crotch region of the tee with a crack developed that is typical of fatigue failure associated with local peak strains and stress concentrations.

## KWU Four-Inch/Two-Inch System

A stainless steel test article consisting of a four-inch diameter main pipe line with a two-inch diameter branch line was tested by the German Kraftwerk Union (KWU), Reference 3. The piping configuration, Figure 4, consisted of approximately forty-one feet of four-inch and seventeen feet of two-inch diameter pipe. Wall thickness of the piping was 0.165 inch and 0.114 inch respectively.

The test loading consisted of two time history load inputs and a harmonic excitation. The time histories represented (1) a standard-type broadened and enveloped floor earthquake response spectrum and (2) a "natural" free field time history.

Although local distortion occurred, failure of the piping test article did not occur as a result of the test load inputs. The greatest measured distortion was approximately 1% local strain near the anchor on the two-inch diameter branch line for the sinusoidal testing and slightly less for seismic testing.

## ANALYSES FOR NONLINEAR RESPONSE PREDICTIONS

The following simplified elastic, elastic-plastic, and nonlinear inelastic methods were employed:

a. A standard ASME Class 1 and 2 design analysis
b. The Newmark modified spectra method (Reference 4)
c. The Campbell/Kennedy/Thrasher dynamic/static margin ratio method (Reference 5)
d. A progressive hinge simplified limit analysis method by Jaquay (Reference 6)
e. Seismic PRA-type piping fragility estimations using two procedures. (Reference 7 and 8)
f. A nonlinear transient dynamic inelastic analysis using the NONPIPE computer code (Reference 9)

### Simplified Methods

A number of simplified elastic and elasto-plastic methods and a nonlinear method for predicting piping system collapse failure under dynamic loading have been referenced. Each of the methods require estimation or calculation of structural parameters unique to the particular method. Features of each of the methods are briefly summarized in Table 1. Shown in the Table for each method are the significant parameters considered in the analysis, the analysis approach, and the limiting criteria.

The methods of Table 1 are listed in ascending order of detail, complexity, cost, and degree of accuracy and information provided. All methods are practical and not unduly costly. Except for the ASME Code-type linear elastic method, the key input parameters include choice of: (1) damping or dynamic amplification factors, (2) effective yield strength of material, (3) component limit load factors, (4) system ductility ratio (maximum strain) and effective yield point, and (5) a criteria of failure, such as collapse, fatigue, accumulated strain, ratchet-fatigue, etc.

## System Ductility Ratio and Equivalent Yield Point

The Newmark and D/S simplified methods utilize the concept of reduced system response as a result of inelastic action. This is based upon the premise that even a slight amount of inelastic action reduces the response of the structure significantly due to non-linear behavior. The inelastic action is accounted for in these methods by the introduction of parameters called the system ductility ratio and the equivalent yield point strength. The system ductility ratio is a measure of the elastic plus inelastic capability of the structure, see Figure 5. It is important to recognize that the system ductility ratio is based upon the ductility that is determined from the resistance-displacement relationship of the structural system as a whole, rather than from, for example, the moment-rotation capacity of a particular joint, or the ductility of a particular element or component of the structure. Since the system ductility ratio represents the energy absorption capacity of the structure as a whole, it is generally substantially lower than the material ductility by itself, due to strain concentrations.

For the seismic collapse failure levels predicted herein, appropriate maximum ductility ratios have been calculated for each piping multi-degree-of-freedom system. It is recognized that ductility ratio calculations for structural systems are approximate in nature. Studies were made to assess the sensitivity of calculated ductility ratios to variations of other parameters in a given structural system.

## PRA-Type Methods

Probabilistic risk assessments of the piping systems were made using the methods described in References 7 and 8. Reference 7, referred to by the author as the "Zion Method," determines the fragility of a piping system by estimating the median safety factor and logarithmic standard deviation. The latter are determined from analysis of a number of typical piping systems. Reference 8, the "SSMRP Method," is similar except that analysis of the specific piping system under consideration is utilized.

## Nonlinear Inelastic Transient Dynamic Analyses

Nonlinear inelastic transient analysis provides more accurate predictions of the structural response of a system under time varying dynamic loads. These analyses typically require specialized computer programs to implement the analyses. The NONPIPE program, Reference 9, was used for inelastic analyses of the piping systems involved in high level dynamic testing.

NONPIPE provides relatively inexpensive means of inelastic dynamic analysis of piping systems by the uncoupling of bending, torsion and axial responses. Nonlinearities include those due to material inelastic response. By uncoupling the moment and axial responses, bending definition in the plastic range may be specified by trilinear load-deflection curves of bending and torsion components. NONPIPE utilizes the direct stiffness method, with a trapezoidal rule for time marching. Plastic effects are included by a tangential stiffness matrix.

## ANALYTICAL PREDICTIONS AND TEST FINDINGS

A series of analyses were performed, on each of the above described piping systems, to assess collapse failure under the high level test dynamic loads. Analytical prediction methods and limiting criteria are those previously discussed and shown in Table 1. The piping system material and relavent properties are shown in Table 2. A summary of the analytical results and test finding is presented in Table 3. A detailed discussion is given below.

In Table 3 is a summary for the HEDL one-inch diameter pipe loop. Since total collapse of the piping system was not achieved at the maximum test level (2.8 g's base input), all of the methods underpredicted when failure would occur. The ASME level D allowable limit was less than one-quarter of the level when gross deformation occurred. The Newmark and the dynamic/static ratio methods predicted a collapse load approximately equal to test loading where initiation of the second plastic hinge occurred. Test failure level, however, was somewhat difficult to define and the occurrence of the second hinge probably occurred over a range of test load values.

The inelastic analysis of the HEDL one-inch pipe loop correctly predicted the location of initial hinge formation. No collapse was predicted at 2.5 g base input acceleration, with maximum strain calculated as 2.5 percent. Analytical pipe magnification factors decreased with increasing load level and agreed well with test data as shown in Figure 6.

Table 3 also presents a summary of the analytical predictions and some of the test findings for the ETEC six-inch diameter pipe system. As can be seen, the linear analysis ASME Code method underpredicted the test demonstrated load capacity by more than an order of magnitude. The simplified elastic-plastic response spectra methods underpredicted by about a factor of 3 and the static progressive hinge underpredicted the collapse capacity by about a factor of 2.

The nonlinear transient dynamic inelastic analyses of the ETEC six-inch system did not predict a dynamic instability or system collapse mode even at 30 g's base input. Both static and dynamic inelastic solutions were obtained. Figure 7 shows the maximum strains under dynamic loading are dynamically magnified relative to static response. However, the formation of plastic hinges in the piping system at high level loading does not induce a dynamic instability like it does under static loading. Thus, the static analysis underpredicts response at low level loading but it overpredicts response at high level loading.

The controlling failure mode of the ETEC six-inch test system, as has been noted, was not system collapse. Rather, it was a local cracking/rupture. We believe it was induced by hoop ratcheting from the combined sustained pressure stresses and cyclic dynamic stresses. This is a ratchet-fatigue failure mode. It will be discussed later.

Table 3 summarizes the failure predictions for the ETEC three-inch diameter pipe system. As with the other test systems, the various methods underpredicted the collapse level of the piping system. The nonlinear inelastic analyses did not achieve instability even with a condition of 14% local strain range.

Table 3 contains a summary of the failure predictions for the KWU four-inch/two-inch system. Testing did not achieve collapse or failure of the system under the maximum loads (about 5.5 g's ZPA seismic time history input or 4 g's harmonic input), but did provide high measured strains at a few locations. The standard ASME Class 1 analysis indicated a Level D (Faulted) loading allowable of about 1.4 g's, or about one-third of the testing level experienced. The inelastic analyses gave reasonably good agreement between the 0.90% measured and calculated 0.80% strain amplitude at the critical location (Point (2), Figure 4).

## RATCHET-FATIGUE FAILURE

The failure of the ETEC six inch diameter pipe system occurred when the straight pipe section just above sliding table S1, Figure 2, ruptured. A circumferential through-wall crack, extending over 300 degrees around the pipe, was developed.

A post-test standard ASME Class 1 fatigue analysis was performed for the ruptured pipe location. Estimates were made of the strain range for each test event. Best fit average fatigue curves, instead of the code allowable fatigue curve was used.

The fatigue analysis calculated a cumulative usage factor of 0.13 to 0.27 for the entire test series. As a usage factor of unity indicates fatigue failure, the standard fatigue analysis overpredicted the pipe cyclic life.

The pipe "elephant foot" bulge failure mode, depicted in Figure 8, suggests that the hoop ratchet strain could have exhausted the material ductility and reduced the pipe cycle life capacity. To assess the ratchet mode of failure by ductility exhaustion, an analysis (using the ratchet strain per cycle formula from Reference 10) was accomplished and summarized in Reference 11. Since tensile tests indicated the material elongation was about 35 percent, about 30 to 40 cycles of 3 to 4 percent strain range superposed on the sustained hoop stress appear sufficient to exhaust the ductility.

The ductility reduction due to the ratchet strain accumulation has an interaction with the cyclic fatigue life. Figure 9 depicts an approximate analysis of the ratchet-fatigue interaction. Using this approximate interaction method, the ratchet-fatigue usage factors were computed to be 1.1 to 1.2. As the computed usage factor reaches unity, the analysis indicates failure as it happened during the last test.

The ratchet-fatigue conditions need the sustained internal pressurization. It appears that the noncycling pressure loading, normally not included in ASME Code fatigue assessments, may be an important parameter --- especially for low cycle fatigue from strain ranges above a few percent.

AVAILABLE

## SIMPLIFIED PREDICTION METHOD FOR DAMPING DUE TO PLASTIC HINGES AND SNUBBERS

Nuclear power plant piping designs of the last decade have incorporated many seismic restraints and snubbers to assure adequacy to withstand earthquakes. The design methods have conservatively utilized very low damping values. In the past few years much experimental damping data of piping responding elastically has been gathered. This led to new proposals by industrial groups, such as the Pressure Vessel Research Council (PVRC), for higher design damping allowables and the ASME adopted an interim Code Case N-411.
Interest in high-level inelastic response and tests-to-failure have resulted in research programs sponsored by the U.S. Department of Energy (DOE), the U.S. Electric Power Research Institute (EPRI), and the U.S. Nuclear Regulatory Commission (NRC). The effective equivalent damping associated with the inelastic response is also of interest for use in simplified analyses.

Simplified methods for calculating modal equivalent viscous damping for plastic hinges and snubbers were also developed. These methods were used to assess damping energy distribution in four pipe systems in high-level response.

The methods described provide simple techniques for calculating the total modal equivalent viscous damping coefficient. It is determined as the sum of damping due to (a) plastic hinges, (b) snubbers, and the pipe system exclusive of (a) and (b).

The equivalent viscous damping coefficient, $\xi$, for the piping system is approximated by Equation (1):

$$\xi = \Delta W / [4\pi (KE)] \qquad (1)$$

where, $\Delta W$ = energy loss per cycle and

KE = maximum kinetic energy or strain energy of the system.

The energy loss, $\Delta W$, is made up of those losses due to plastic hinges, snubbers, and the other damping sources.

The plastic hinge energy loss, $\Delta W_p$, is approximated by

$$\Delta W_p = 4 \sum_{i=1}^{K} \left[ M_{pi} \left( \theta_{mi} - \theta_{yi} \right) \right] \qquad (2)$$

where, K = number of plastic hinges in system,

where, $M_{pi}$ = effective limit moment of plastic hinge i,
$\theta_{mi}$ = maximum angle amplitude hinge i rotates through, and
$\theta_{yi}$ = angle amplitude to initiate plastic hinge i yielding.

The snubber energy loss, $\Delta W_s$, is approximated by:

$$\Delta W_s = \pi \sum_{j=i}^{L} \left[ C_j \; W_N \; X^2_{Mj} \right] \qquad (3)$$

where, $C_j$ = damping coefficient of snubber j,
$W_N$ = circular frequency of mode N, and
$X_{Mj}$ = maximum displacement of snubber j.

The energy loss due to viscous damping, exclusive of $\Delta W_p$ and $\Delta W_s$ losses, is expressed by a damping coefficient $\xi_v$ in conjunction with equation (1).

An example of the simple method results and correlation to experimental data follows. For a high-level test (2.5 g's ZPA) a small bore heavily insulated pipe system with one mechanical snubber experimentally revealed dynamic magnifications equivalent to 40 to 50 percent damping. At low levels, the piping system was elastic and the equivalent damping was about 10 percent. The calculated equivalent increment of damping for one plastic hinge was 16 percent and with two hinges it was 29 percent. The single mechanical snubber provided only 1 percent damping. Thus, adding 30% to the 10% low-level damping gives a good correlation to the experimental 40% measured equivalent damping value.

A number of correlations of the calculated damping values per the above methods have been made to piping experimental findings. These comparisons of calculated and experimental data, of numerous piping systems at multiple levels of response, are presented in Reference 11. Good correlations were found. The simple methods provide a useful tool in assessing the extent plasticity and snubbers add to piping system damping during high-level inelastic response.

## CONCLUSIONS AND RECOMMENDATIONS

1. Pre-test failure predictions of several high level dynamic tests using a number of simplified pseudo-linear-elastic methods, all underestimated the ability of the pipe systems to withstand very high seismic loads without collapse. As an example, for the ETEC six-inch diameter system, the Newmark and dynamic/static ratio methods indicated collapse at about 10 g's. The progressive hinge method gave collapse at 8 to 16 g's depending on use of a dynamic magnification factor of 2 or 1 respectively. The seismic PRA-type fragility average estimate was 4.4 and 8.8 g's for the Zion and SSMRP methods. The test actually withstood 30 g's without collapse.

2. Pre-test inelastic transient dynamic analyses using the NONPIPE program correctly predicted no collapse load up to the limit of the analyses:

2.8 g's, 30 g's, 30 g's, and 5.5 g's ZPA for the WHC one-inch test loop, ETEC six-inch system, ETEC three-inch system, and KWU four-inch/two-inch systems respectively. The analyses predicted a maximum strain range that correlated very well with strain gage data from these tests.

3. The reduction of dynamic magnification with increasing plastic response of the piping under high level shaking is a major factor in limiting response well below current elastic response spectra predictions. Current ASME Class 1 and 2 methods, intended to protect against collapse, gave allowable shake levels that are one order of magnitude below that withstood by the demonstration test.

4. The reduction of dynamic amplification with plastic response is due conceptually to two factors: (1) internal energy dissipation resulting in higher damping and ductility ratios, and (2) resonant de-tuning due to system increased flexibility. Simplified plastic reduced spectra techniques, such as herein used with the Newmark and the D/S ratio methods, do not account for the second factor. This omission could partially explain the strength underpredictions by the simplified methods.

5. All of the simplified elastic failure prediction methods require that a characteristic parameter be established, whether it be system ductility ratio, D/S factor, or magnification factor. More work is needed to develop methods and procedures to quantify these parameters to account for inelastic response.

6. Ductility ratios for the piping system (the ratio of the maximum displacement to that at effective yield) are much less than material ductility ratios at tensile failure. The appropriate ratios for the WHC stainless steel pipe and the ETEC carbon steel pipe systems were in the 5 to 10 range. Higher system ductility ratios will not raise the collapse capacities predicted by the pseudo-linear elastic methods up to the 50 to 100% higher levels withstood experimentally.

7. The progressive hinge method predicts the sequence of plastic hinge formation and permits a visualization of the system collapse mechanism. The method gives results consistent with other methods provided proper magnification factors are selected.

8. Failure of the ETEC six-inch demonstration pipe system did occur after extensive multiple high level seismic and sinusoidal burst tests. The failure mode involved local cracking and section rupture near one pipe leg support, where ratcheting produced a bulge in the pipe diameter. Post-test analyses herein reported indicate to the authors that the failure was by ratchet-fatigue and/or ductility exhaustion.

9. Correlations of test and calculated high-level piping dynamic response show good promise for simplified inelastic prediction methods. More tests and correlations are needed to establish a reasonable data base and to develop reliable methods for establishing safe design. This includes establishing procedures for conservatively accounting for the inelastic energy absorption and dynamic response of the piping system and

establishing code acceptance criteria such as allowable ductility ratios, allowable strain criteria, or static allowable stress or load criteria. This work is consistent with the NRC Piping Review Committee recommendations (Reference 12).

10. It is recommended that additional pipe systems, that have or will be tested to high levels, be analyzed with simplified inelastic methods for response and failure mode assessments. In particular, the piping components tested under the EPRI/NRC piping and fitting program at GE (Reference 13) and the NRC pipe tests (Reference 14) at HDR and Todatsu (NUPEC) should be used to develop the needed design methods and code limits.

## REFERENCES

1. A. T. Onesto, W. O. Chen, and V. DeVita, 6-Inch Diameter Pipe Seismic Fragility Test, Draft NUREG Report to NRC, ETEC, July, 1986. Also, A. Onesto, "Piping System Fragility Tests" paper presented at 14th WRSM, 1986, Washington D.C.

2. M. R. Lindquist, M. J. Anderson, L. K. Severud, E. O. Weiner, "High Level Dynamic Testing and Analytical Correlations for a Small Bore Piping System," ASME PVP Conference Special Publication PVP-Volume 108, July, 1986.

3. E. Haas, et al, "Experimental and Analytical Investigation of the Dynamic Response of a Branched Piping System Due to Elasto-Plastic Behavior", Trans. of the 8th SMIRT, paper K 15/3, Brussels, Belgium, August 1985.

4. N. M. Newmark, "A Response Spectrum Approach for Inelastic Seismic Design of Nuclear Reactor Facilities," Transactions Third International Conference on Structural Mechanics in Reactor Technology (London), Paper K5/1, Volume 4, Part K, 1975.

5. R. D. Campbell, R. P. Kennedy, R. D. Thrasher, Inelastic Response of Piping Systems Subjected to In-Structure Seismic Excitation, ASME Paper 83-PVP-50.

6. K. Jaquay, "A Simplified Limit Analysis Approach for Seismic Design of Ductile Piping System," Presentation at the ASME Winter Annual Meeting, New Orleans, December 9-14, 1984.

7. R. P. Kennedy and M. K. Ravindra, "Seismic Fragilities for Nuclear Power Plant Risk Studies", Nuclear Engineering and Design, Volume 79 (1984) No. 1, May 1984.

8. Seismic Safety Margins Research Program Phase I Final Report, U.S. Nuclear Regulatory Commission NUREG CR-2015.

9. NONPIPE, A computer Program for Nonlinear Analysis of Piping Systems-User Information Manual, Engineering Decision Analysis Company, Inc., Palo Alto, CA, September 30, 1983.

10. H. G. Edmunds and F. J. Beer, Notes on Incremental Collapse in Pressure Vessels", Journal of Mech. Engr. SCI, Volume 3, No. 3, 1961.

11. M. J. Anderson, M. R. Lindquist, L. K. Severud S. E. Wagner, E. O. Weiner, Dynamic Inelastic Piping Response, Damping, and Failure Predictions for Four Piping Systems, Draft NUREG Report to be published, 1986.

12. Report of the U.S. Nuclear Regulatory Commission Piping Review Committee, U.S. NRC NUREG-1061, Volume 5, 1985.

13. W. F. English, Piping and Fitting Dynamic Reliability Program First Semi-Annual Progress Report, May - October 1985, General Electric NEDC-31272, EPRI Contract RP-1543-15, November, 1985.

14. Seismic Safety Research Program Plan, US NRC NUREG-1147, 1985, pp. F-8 and F-12.

15. S. S. Manson, Thermal Stress and Low-Cycle Fatigue, McGraw-Hill, 1966, pp. 174-175.

16. J. F. Harvey, Pressure Vessel Design, Van Nostrand Nuclear Science Series, New York, NY, 1963, pp 194-195.

TABLE 1

COMPARISON OF PIPING RESPONSE COLLAPSE FAILURE PREDICTIONS

| METHOD | SIGNIFICANT PARAMETERS | ANALYSIS APPROACH | LIMITING CRITERIA |
|---|---|---|---|
| Linear Elastic | • Response Spectra<br>• Damping Ratio | Dynamic Analysis with Elastic Spectra | $3S_M$, $3S_H$ of ASME Code, Cl 1 or 2 For Level D |
| Newmark (Reference 4) | • Response Spectra<br>• Damping Ratio<br>• Effective Yield Point<br>• System Ductility | 1) Reduce Spectra<br>2) Dynamic Analysis with Plastic Spectra | 1) Effective Yield Point<br>2) System Ductility Ratio (Max Strain) |
| Dynamic/Static Margin Ratio (Reference 5) | • Response Spectra<br>• Damping Ratio<br>• D/S Factor (Sys Ductility)<br>• Effective Yield Point | 1) Dynamic Analysis with Elastic Spectra<br>2) Reduce Results by D/S Factor | 1) Effective Yield Point<br>2) System Ductility Ratio (Max Strain) |
| Static Progressive Hinge (Reference 6) | • Component Hinge Strengths<br>• System Collapse (Limit Load) | 1) Static Analyses for g-loads and Plastic Hinges<br>2) Reduce Results by Eff Dynamic Ampl Factor | 1) Enough Plastic Hinges to Cause System Instability and Collapse<br>2) Dynamic Amplification Factor |
| Nonlinear, Inelastic (Reference 9) | • Time History Input<br>• Damping<br>• Elbow Inelastic Stiffness | Time-History Dynamic Analysis | 1) System Instability<br>2) Max Strain and Strain Range |

AVAILABLE

## TABLE 2

### MODEL PROPERTIES USED IN ANALYSIS

| | HEDL 1-IN DIA PIPING | KWU 2-IN/4-IN PIPING | ETEC 3-IN PIPING | ETEC 6-IN PIPING |
|---|---|---|---|---|
| MATERIAL | 304 S.S | 304 S.S | SA-106, GR.B. | SA-106, GR.B. |
| EFFECTIVE YIELD, KSI | 54 | 54 | 53 | 53 |
| SYSTEM DUCTILITY RATIO | 5 | 3 | 10 | 10 |

## TABLE 3

### SUMMARY OF ANALYTICAL PREDICTIONS AND TEST FINDINGS

| | ANALYTIC METHOD | HEDL 1 IN DIA. PIPING | KWU 2-IN/4-IN DIA. PIPING | ETEC 3-IN DIA. PIPING | ETEC 6-IN DIA PIPING |
|---|---|---|---|---|---|
| A. | ASME CLASS 1, $3S_M$ LEVEL D, G'S | 0.36 SINE | 1.9 ZPA | 1.4 ZPA | 2.0 ZPA |
| B. | ASME CLASS 2, $3S_H$, G'S | 0.34 | 1.7 | 1.0 | 1.4 |
| C. | NEWMARK METHOD, G'S | 1.55 | 4.8 | 10.2 | 10.0 |
| D. | DYNAMIC/STATIC MARGIN RATIO, G'S | 1.58 | 4.5 | 10.0 | 9.7 |
| E. | PROGRESSIVE HINGE, STATIC LOAD, G'S | | | | |
| | () = DYN. MAGNIF. FACTOR | 1.50 (1.8) | 3.0 (5.0) | 10.6 (2.0) | 8.1 (2.0) |
| | | 2.70 (1.0) | 15.2 (1.0) | 21.2 (1.0) | 16.2 (1.0) |
| F. | PRA-TYPE FRAGILITY | | | | |
| | ZION METHOD, G'S | -- | 7.8 | 4.4 | 4.4 |
| | SSMRP METHOD, G'S | -- | 11.5 | 5.2 | 8.8 |
| G. | NONLINEAR INELASTIC DYNAMIC | | | | |
| | LOAD LEVEL, G'S | 2.5 | 4.0 SINE | 30.0 | 30.0 |
| | STRAIN RANGE, PERCENT | 2.5 | 1.6 | 14.0 | 4.1 |
| | TEST FINDINGS | | | | |
| A. | MAX. BASE INPUT, G'S | 2.8 SINE, 2 $H_Z$<br>0.5 ZPA | 4.0 SINE, 8.9 $H_Z$<br>5.5 ZPA | 30.0 ZPA<br>25.0 SINE, 6 $H_Z$ | 30.0 ZPA<br>18.7 SINE, $5H_Z$ |
| B. | NO FAILURES FOR ALL ZPA'S | | | | |
| C. | FAILURE MODE | RATCHETING-GROSS DEFORMATION | NONE | FATIGUE | PATCHET/FATIGUE OR DUCTILITY EXHAUSTION |

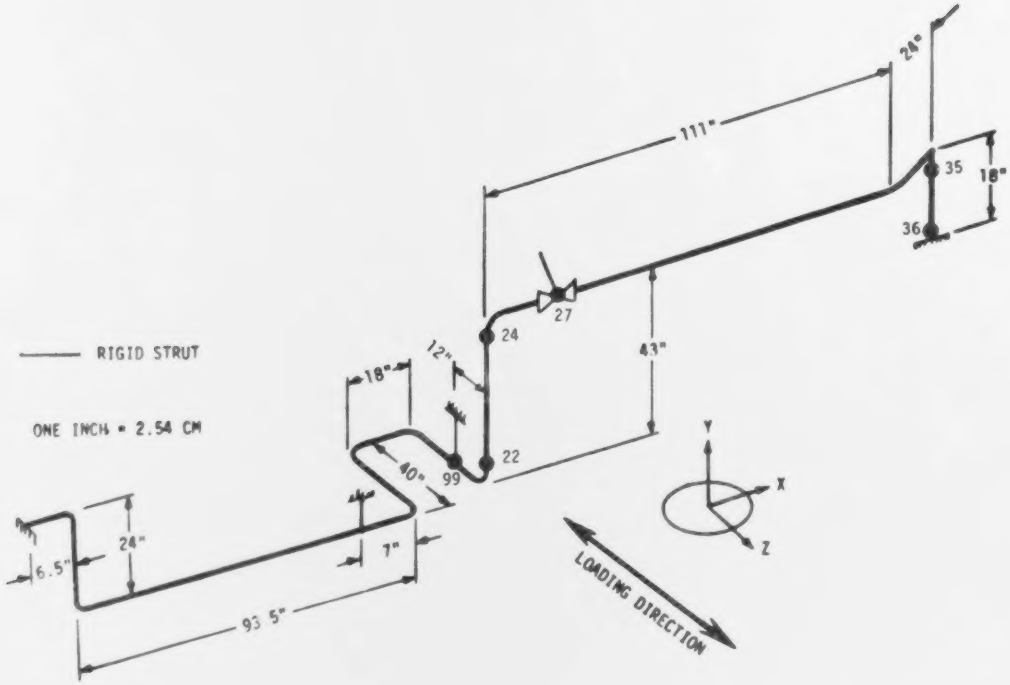
RIGID STRUT
ONE INCH = 2.54 CM
111"
24"
35
18"
36
27
24
43"
12"
18"
22
99
40"
24"
6.5"
7"
93.5"
Y
X
Z
LOADING DIRECTION

FIGURE 1, HEAVILY INSULATED SMALL BORE (1" DIAMETER) STAINLESS STEEL PIPE SYSTEM

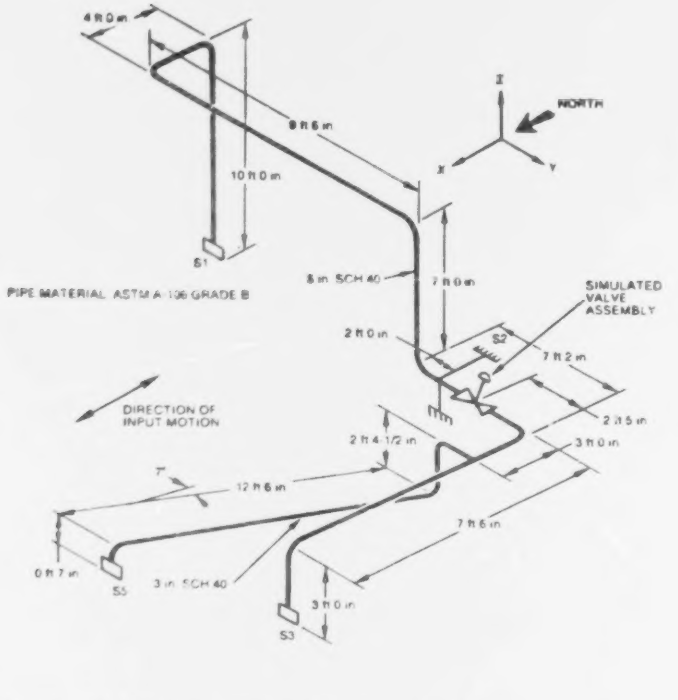
4 ft 0 in
9 ft 6 in
10 ft 0 in
S1
NORTH
Z
X
Y
PIPE MATERIAL ASTM A-106 GRADE B
8 in SCH 40
7 ft 0 in
SIMULATED VALVE ASSEMBLY
2 ft 0 in
S2
7 ft 2 in
DIRECTION OF INPUT MOTION
2 ft 5 in
2 ft 4-1/2 in
3 ft 0 in
7"
12 ft 6 in
7 ft 6 in
0 ft 7 in
S5
3 in SCH 40
3 ft 0 in
S3

FIGURE 2, UNINSULATED MILD STEEL (6" DIAMETER) PIPE SYSTEM

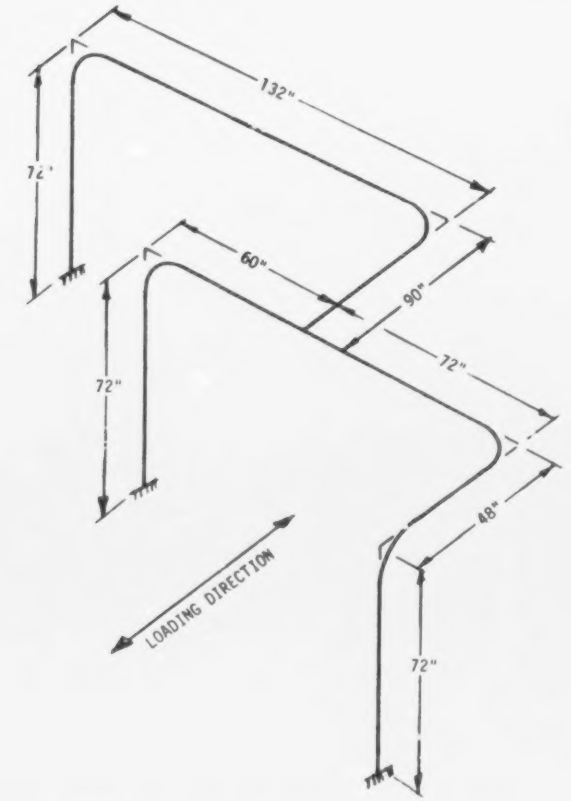
132"
72"
60"
90"
72"
72"
48"
LOADING DIRECTION
72"

FIGURE 3, UNINSULATED MILD STEEL (3" DIAMETER) PIPE SYSTEM

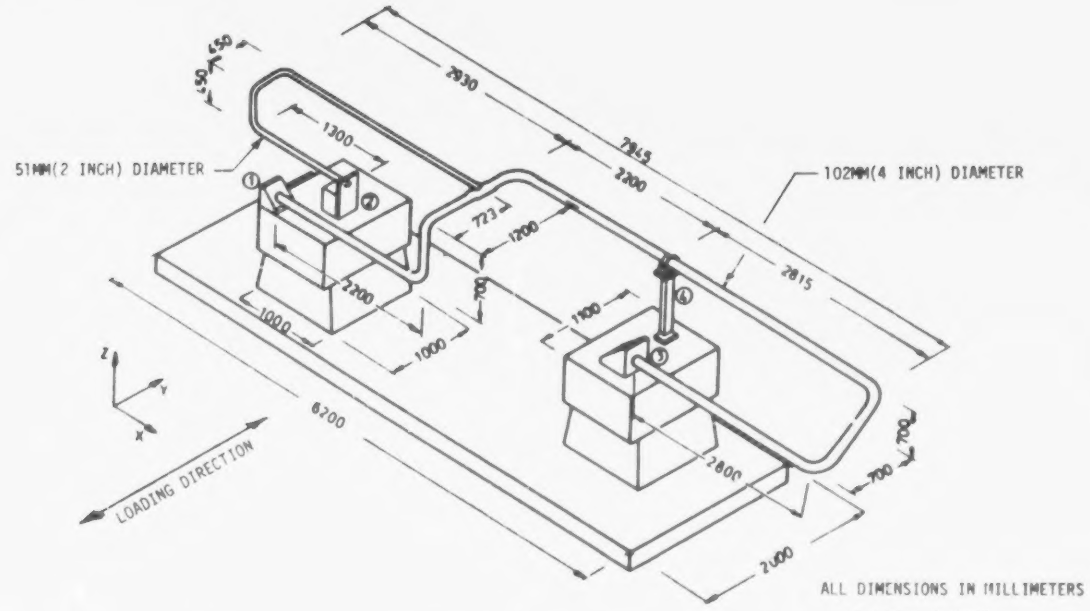
650
650
2930
1300
51MM(2 INCH) DIAMETER
7945
2200
102MM(4 INCH) DIAMETER
①
②
723
1200
2815
700
2200
④
1000
1100
1000
③
Z
Y
X
6200
700
LOADING DIRECTION
2800
700
2000
ALL DIMENSIONS IN MILLIMETERS
25.4 MM = 1 INCH

FIGURE 4, UNINSULATED STAINLESS STEEL (4" AND 2" DIAMETER) PIPE SYSTEM

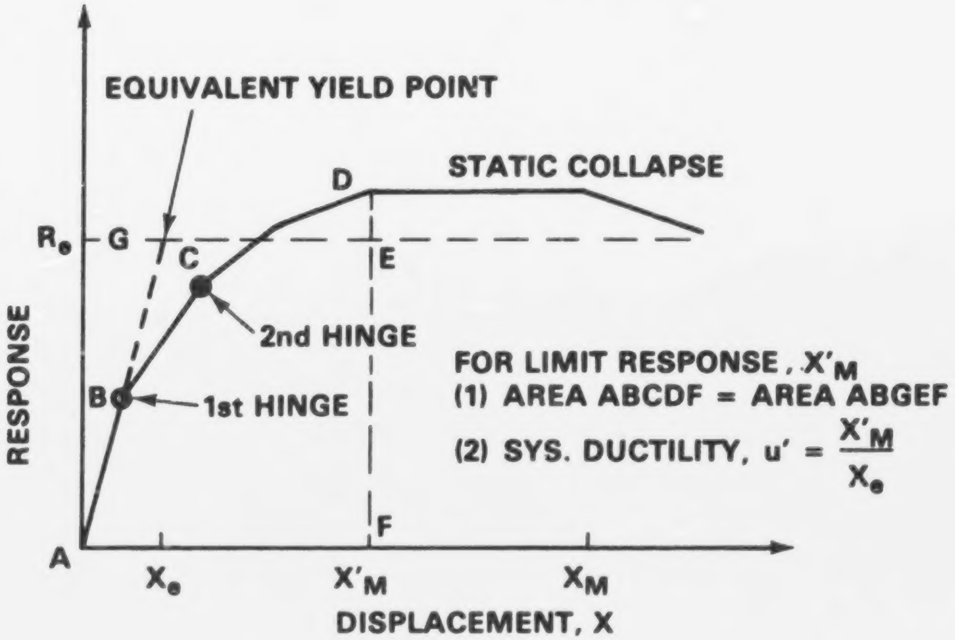
EQUIVALENT YIELD POINT
STATIC COLLAPSE
D
$R_e$
G
C
E
2nd HINGE
B
1st HINGE
RESPONSE
FOR LIMIT RESPONSE, $X'_M$
(1) AREA ABCDF = AREA ABGEF
(2) SYS. DUCTILITY, $u' = \frac{X'_M}{X_e}$
F
A
$X_e$
$X'_M$
$X_M$
DISPLACEMENT, X

FIGURE 5, TYPICAL SYSTEM RESPONSE SHOWING DEFINITION OF SYSTEM DUCTILITY AND EQUIVALENT YIELD POINT

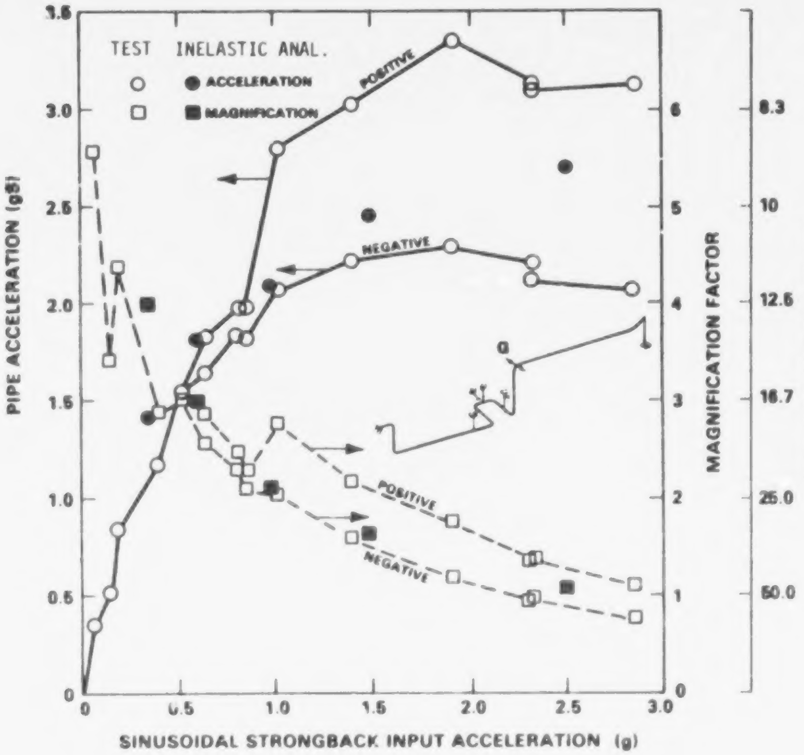

FIGURE 6, INELASTIC ANAYSIS RESULTS VS. TEST RESULTS, HEDL SMALL BORE SYSTEM

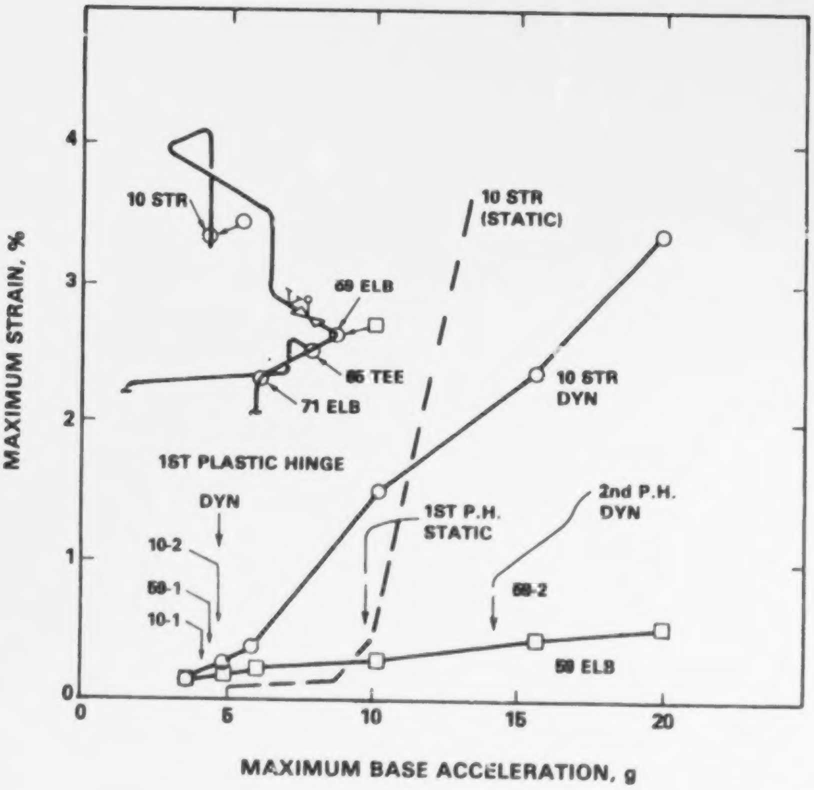

FIGURE 7, ETEC 6 INCH DIAMETER TEST, ANALYTICAL RESULTS

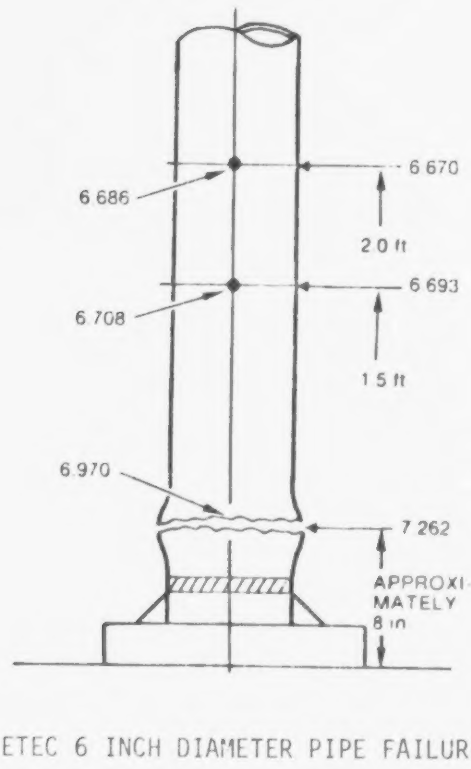
6.686
6.670
2.0 ft
6.708
6.693
1.5 ft
6.970
7.262
APPROXIMATELY 8 in

FIGURE 8, ETEC 6 INCH DIAMETER PIPE FAILURE AREA

# RATCHET-FATIGUE INTERACTION

- COFFIN FATIGUE EQ., $N_F = \left(\frac{C}{\Delta\varepsilon_P}\right)^2$ , REFERENCES 15 and 16

- RATCHETING $\varepsilon_R \cdot N$ REDUCES C

- RATCHET-FATIGUE EQ., $N_{RF} = \left(\frac{C - \varepsilon_R \cdot N}{\Delta\varepsilon_P}\right)^2$

$$= \left[\frac{0.46 - \varepsilon_R \cdot N}{\Delta\varepsilon_t - 0.0037}\right]^2$$

- INTERACTION FACTOR

$$N_{RF}/N_F = \left[1 - \frac{\varepsilon_R \cdot N}{C}\right]^2$$

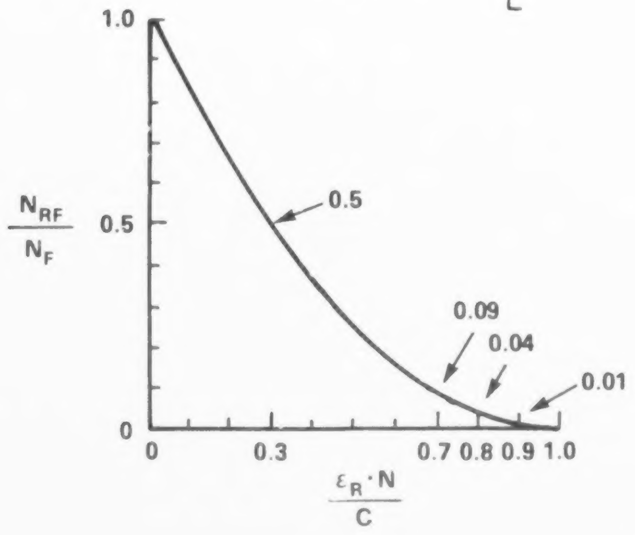

HEDL 8610-061.2

FIGURE 9, APPROXIMATE RATCHET-FATIGUE INTERATION

BLANK PAGE

# Examples of NRC Research Products Used in Regulation

Newton R. Anderson, Section Leader
Engineering Issues Branch
Division of Safety Review and Oversight
Office of Nuclear Reactor Regulation
Nuclear Regulatory Commission

Abstract:

The key to effective research is a close relationship between information needs and research results. This can only be achieved by close cooperation between the "researchers" and the "regulators." At the NRC, this relationship has matured over the years until now the researchers participate in definition of the information needs and the regulators help define the research programs.

The more formal means of ensuring a close match between needs and results include joint research groups, oversight working groups, and a system of Research Information Letters (RILs). On an informal basis there are many day to day discussions and meetings on the various programs which ensure effective program guidance and early identification of significant findings.

This paper describes both the formal and informal researcher/regulation interface and discusses some examples of how specific research programs are utilized in the regulatory process.

Specific programs described are the pressurized thermal shock program, the seismic margins program and the Category 1 structures program. Other examples cited are the aging and life extension programs.

# Examples of NRC Research Products Used in Regulation

Newton Anderson

Research is an essential part of the regulatory process. Research information is provided for the vital regulatory tasks including 1) developing an adequate technical basis for rulemaking and regulatory decisions to support licensing and inspection activities, 2) assessing the effectiveness and feasibility of safety improvements and 3) improving the basic understanding of those phenomena for which analytical methods are necessary for supporting licensing decisions. The research product normally takes the form of NRC standards, regulations and guides. Ongoing research efforts form the basis for licensing decisions and as such are referenced in Safety Evaluation Report.

The office of Nuclear Reactor Regulation (NRR) is responsible for regulating operating nuclear reactors, for reviewing applications for construction permits and operating licenses and for issuing permits and licenses after all regulatory requirements are met. The emphasis for the past several years has been on ensuring the safety of operating reactors since no new applications for licenses have been received during this period.

The key to effective research is a close relationship between information needs and research results. Close cooperation between researchers and regulators was essential as the NRC role changed from the emphasis on reactor licensing during the early 1970's to ensuring the safety of operating reactors in the 1980's. The regulatory role is again changing as both researchers and regulators prepare for the challenge of assessing the safety impact of plant aging and developing both the technical basis and the legal and policy framework for license extension.

In this changing regulatory environment, it is essential that close cooperation and a spirit of teamwork exist between the researchers (RES) and the regulators (NRR). This cooperation exists on both a formal and an informal basis. The more formal means include development and review of long range research plans by RES, endorsement of research programs by NRR, submittal and approval of RES program briefs, and a system of research information letters (RILs). In addition, contractor reports are extensively reviewed both by RES and NRR before publication. On an informal basis there are frequent personal contacts and informal meetings to discuss regulatory needs and research programs. This close and continuing contact ensures the efficient use of research dollars and maximizes the effectiveness of regulatory programs.

To illustrate the role research plays in regulation several examples follow. Although the cited examples are in the area of structural, mechanical and seismic research, comparable relationships exist in other technical areas.

## Pressurized Thermal Shock

Pressurized Thermal Shock events involve unintended rapid cooling of the steel reactor pressure vessel to a low temperature concurrent with or followed by repressurization of the vessel. If a flaw or crack exists at a location where the toughness of the vessel's inner surface has been decreased excessively by neutron irradiation, severe PTS events could cause failure of the vessel.

From 1970 through 1982, there were eight significant PTS events in operating reactors. None of these events resulted in reactor vessel failures but all resulted in substantial cooldown of the reactor coolant while at high pressure or with rapid return to high pressure. The most severe of these events occurred at Rancho Seco on March 20, 1978 when the reactor coolant system was cooled from 582°F to 285° in less than one hour, while pressure remained at about 2,000 psig. In addition, there were 24 other events identified from operating experience searches which had one or more characteristics of a severe PTS event.

PTS was designated as an Unresolved Safety Issue (USI A-49) in January 1982 after it became apparent that PTS was a significant safety concern for operating reactors. A complete review of the studies which resulted in resolution of the PTS issue are outside the scope of this paper. The discussion is presented to illustrate the coordination of research programs with the regulatory activities.

Following the Rancho Seco event, a series of meetings between RES and NRR was held and a program outlined which included expanding the RES Heavy Section Steel Technology (HSST) Program at ORNL to include a PTS test program, development of an RES program at PNL to develop models to make probability estimates of reactor vessel crack propagation and failure, and initiation of a program at ORNL to perform a complete PRA for PTS risk at 3 prototype plants, to determine types of transients that are significant contributors, their frequency and severity, etc. In addition, NRR initiated a technical assistance contract with PNL to assist in developing a regulatory position and performing cost benefit analyses for the proposed resolution of the issue. A steering group was formed to help guide the activities. Both RES and NRR participated plus a number of well known expert consultants in the various technical areas. An industry group was formed and contributed to the technical resolution by performing independent analyses and providing plant information on reactor vessel chemistry and plant specific information on vessel fluence.

The resolution of the PTS issue resulted in a rule (10 CFR 50.61) which requires licensees of Pressurized Water Reactors (PWRs) with pressure vessels for which the reference temperature ($RT_{NDT}$) is projected to exceed the screening criteria before the expiration date of their license, to submit their plans for a flux reduction program to avoid exceeding the screening criterion. If the screening criterion is predicted to be exceeded in spite of practical flux reduction measures, the licensee must submit a plant specific safety analysis at least three years before the expected date the screening criterion will be exceeded. Following issuance of the PTS rule, a Regulatory Guide, jointly written by RES and NRR is being prepared. This Regulatory

Guide references prototype analyses for use by utilities in performing plant specific analyses if required by the PTS rule, and provide detailed guidance for performing such analyses.

The PTS example deviates from the more formal approach to initiating and utilizing research products. It does, however, demonstrate the flexibility and the spirit of cooperation that exists and can be focused on a difficult technical and licensing issue.

## Seismic Margins Program

In November, 1982, the U.S. Geological Survey (USGS) issued a letter that stated their position that the 1886 Charleston South Carolina earthquake could not be associated with a geologic structure unique to that area. This implies that there is some possibility however small, that the level of ground motion associated with a Charleston sized earthquake could occur at other locations along the eastern seaboard. Also, more recently high seismic accelerations were recorded at sites in New Brunswick, Canada, New Hampshire and Arkansas. These developments indicated that a re-evaluation of the seismicity at certain Eastern U.S. sites should be undertaken.

Together with NRR, RES initiated two major programs designed to re-affirm the seismic design basis at nuclear plant sites, the eastern seismicity program and the seismic margins program.

The Eastern Seismicity program is designed to develop the technology and procedures for estimating the seismic hazard at a site, and conducting investigations aimed at reducing the uncertainty in this estimate. The seismic margins program is designed to assess the seismic adequacy of plant structures, piping and components in the event that the seismic hazard re-evaluation results in a somewhat higher design basis earthquakes at some plant sites.

Industry groups with support from the Electric Power Research Institute have also developed both an eastern seismicity program and a seismic margins program and are working closely with the NRC/RES which should ensure a resolution acceptable to both the NRC and the nuclear industry.

The licensing need is clear in this case. The seismic design basis for certain eastern sites may need to be reassessed; and a procedure is needed to evaluate, if necessary, some plants at a level higher than the original design basis.

In addition, the severe accident policy implementation statement (SECY-86-76) requires that all operating reactors must be reviewed for severe accidents. This review includes the consideration of seismic events. The seismic margins program is designed to provide a tool to fill this need.

Both of these programs are funded and directed by RES but are guided by working groups with representation from both NRR and RES. This arrangement has proven to be very successful in ensuring that research programs are formulated and conducted in a way that give the maximum chance of producing reasonable answers to licensing questions. In addition, the seismic margins program PWR trial plant review which is underway currently has been tailored to answer a current licensing need at the trial plant as well as to provide information to answer the generic licensing questions for longer term application.

Other seismic programs which contribute to current and projected licensing concerns include the following.

1. Investigation of soil response to earthquakes which will improve the capability of predicting plant response to seismic events.

2. Validation of seismic calculational models which is designed to obtain experimental information to be used to develop criteria for judging predictions of the behavior of nuclear plants subjected to large earthquakes.

3. BWR risk assessment program to improve the models and procedures for assessing seismic risk.

4. Seismic component fragilities program which is primarily a collection of test and experience data as well as a review of fragilities used in past PRA studies. Some testing is also planned.

## Seismic Category I Structures Program

Because of the increasing emphasis on operating plant safety, understanding the response of existing structures is a higher priority than the design of new structures. Nuclear power plant structures are much different than commercial structures in that they are more like an irregular box consisting of shear walls with low aspect ratios. These buildings are more stiff than slender high rise or frame-type construction. With the continuous improvement in our understanding of Eastern U.S. Seismicity and changing perspective on seismic design requirements, the NRR staff felt that the following needs should be addressed by a research program:

1. understanding the behavior of Category I structures (other than the containment) subjected to earthquake loads beyond design. The behavior of structures loaded such that both elastic and inelastic response occurs is of interest;

2. identify the changes in floor response spectra at various magnitudes and duration of input loading; and

3. identify the changes in damping associated with the various magnitudes and duration of input loading.

In order to address the above NRR needs, the RES initiated a program, Seismic Category I Structures Program, in FY-1980 with the following specific objectives:

1. Develop experimental data for determining the sensitivity of structural behavior in the elastic and inelastic response range (including changes in floor response spectra) to variations in configuration, design practices and earthquake loading;

2. Develop experimental data to enable validation of computer programs used to predict the behavior of Category I structures during earthquake loading that causes elastic and inelastic response; and

3. Develop a method for representing damping in the inelastic range, and demonstrate how this damping changes when structural response goes from the elastic to the inelastic ranges.

The Seismic Category I Structures Program is a combination experimental and analytical program with the initial work heavily emphasizing the experimental aspects to develop a good data base. In the latter phases of this program the emphasis is on more analytical development with verification experiments used to validate the sensitivity of certain significant geometry configuration changes. A Test Review Group (TRG) consisting of nationally known experts was formed to provide assistance and advice in conducting the program and evaluating the results.

The experimental program started with static and dynamic testing of isolated shear walls using small scale models. This investigation indicated that the initial stiffness of these walls was significantly less than the stiffness computed assuming an uncracked concrete section (a common assumption made in design). Subsequent investigation of scale models representing typical auxiliary and diesel-generator type buildings also resulted in similar findings. The difference between calculated and experimentally determined stiffness could potentially affect the shape of calculated floor response spectra.

To assure that the stiffness effect was not largely due to atypical aggregate and reinforcement in the concrete or to modeling effects, an additional experiment called "TRG" was undertaken. This TRG structure was specifically constructed with the typical size aggregate and reinforcing. Both large-scale and small-scale tests were conducted. The results from these tests also appear to confirm the reduction in the initial stiffness.

Review of these results by the NRR and RES technical staff plus review by the Technical Review Group (TRG) and the technical staff of the Los Alamos Laboratory resulted in recommendations for quasi-static testing of models with various aspect ratios and percentage of reinforcing to establish the magnitude of reduction in the total stiffness and separating the contribution of bending and shear stiffness.

This program not only represents close cooperation between NRR and RES in developing a program to achieve specific regulatory objectives but also continuous and on-going involvement of both groups in addressing significant findings.

Aging and Life Extension

The issue of plant aging and life extension is becoming increasingly important with the first application for a license renewal expected within the next 5 to 7 years.

ABLE

NRR comments on the long range research plan identified the need for a research program to investigate the safety aspects of aging processes in nuclear plants and develop guidance for license renewal applications. Initiation of aging research was also recommended by the ACRS in their 1983 report to Congress.

As operating reactors advance in age there is a need to understand the time related degradation of structures, components and systems. The potential impact of this degradation on safety must be understood and measures must be developed to successfully mitigate significant aging degradation.

A related challenge is the development of appropriate policy and regulations to allow efficient processing of applications for license renewals or extensions.

In a memo dated November 25, 1985, the NRC Executive Director requested the Office Directors of NRR, RES, IE and NMSS to provide a coordinated plan for the technical integration of four major technical programs including "aging." The first of the major areas to be addressed is plant aging. An interoffice group, TIRGALEX (Technical Integration Review Group for Aging and Life Extension) was formed and chaired by RES. The objective of the group is to ensure the coordination and integration of technical activities among NRC offices and staff and with contractors to identify, prioritize and coordinate these tasks necessary to address and resolve major regulatory issues from an agency perspective.

TIRGALEX identified a broad spectrum of safety and regulatory issues ranging from fundamental policy questions to detailed technical issues. The most pressing issues are fundamental policy issues, such as:

o Should license renewals be based on current licensing criteria, the criteria in effect when the plant was built, or on some other set of criteria? Use of current licensing criteria for license renewal could severely limit the benefits of life extension since it would have a major "ratcheting" effect on many plants.

Early resolutions to these kinds of issues are critical for establishing a stable, predictable regulatory climate for life extension.

In addition to policy issues, there are a large number of issues of a technical nature. For example,

o Is annealing a feasible and effective method of mitigating embrittlement of reactor vessels and thereby extending vessel life?

o Regulatory requirements themselves sometimes cause aging or accelerate other aging mechanisms (e.g., the requirement for frequent fast starts of diesel generators). How can these aging effects be alleviated, while continuing to assure adequate protection of public health and safety?

There are certainly additional issues that have not yet been explicitly identified. To ensure a reasonably comprehensive identification of all the relevant issues, particularly the detailed technical issues, TIRGALEX developed a structured approach for systematically identifying and analyzing the safety and regulatory issues associated with aging and life extension.

AEOD, IE, NRR, and RES all have programs that are related to aging and life extension. AEOD, through its programs involving LER data and the NPRDS database, provides valuable data and methods for assessments of aging effects on operating reactors. IE, through its inspection-related programs, addresses the detection and control of aging degradation along with other causes of safety system degradation. NRR, through programs such as the Plant Life Extension Policy project and the Maintenance and Surveillance Program, is addressing regulatory policy and positions needed for aging and life extension. RES through the Nuclear Plant Aging Research Program and programs covering key reactor structures and components, is concentrating on the technical base for regulatory policy and positions.

Industry has been increasingly active over the last few years. A joint industry, EPRI, and DOE program was initiated in 1984 to identify issues associated with life extension. In 1985, detailed technical studies were started on two pilot plants (Surry 1 and Monticello) and a study on the regulatory aspects of life extension was commissioned by AIF's National Environmental Studies Project. Results to date were presented at a joint industry EPRI/DOE life extension seminar in August 1986. Industry has established a framework for planning and integrating life extension activities (Enclosure 3). A steering committee called NUPLEX (Nuclear Plant Life Extension) is coordinating the efforts of several working groups focusing on technical activities, codes and standards, licensing matters, and policy considerations.

Codes and standards committees are also becoming very active in this area. ASME is planning to establish a special coordinating committee under the Board of Nuclear codes and Standards to direct the overall thrust of life extension code activities. ASME Section XI has a special working group on plant life extension considerations. IEEE is also active. NRC staff are participating in these codes and standards activities.

Several foreign countries (e.g., West Germany, Canada, France and Italy) have aging-related programs. Japan and France have initiated programs specifically directed toward life extension. The IAEA recently convened a technical committee meeting on "Safety Aspects of Nuclear Power Plant Aging" (September 1-5. 1986). Further exchanges of information concerning foreign programs are planned.

Considering the large amount of relevant work, a concerted effort is needed to coordinate and exchange information to minimize duplication of efforts and to maximize the effectiveness of the NRC programs.

Plant aging and license extension is a much broader area of cooperation than an NRR/RES cooperative effort. Other NRC offices, the nuclear industry and codes and standards committees are all involved. This approach demonstrates the ability of the NRC to focus substantial resources on an important safety issue and to integrate their activities with industry and utility groups.

The preceding examples of NRR utilization of Research efforts and products and of the cooperative efforts and programs is not meant to be a definitive technical treatise but is presented to demonstrate how the regulatory process works in the area of developing information to support nuclear plant regulation.

BLANK PAGE

# COMPONENT FRAGILITY RESEARCH PROGRAM: PRIORITIZATION AND DEMONSTRATION TESTING[*]

G.S. Holman and C.K. Chou

Lawrence Livermore National Laboratory
University of California
P.O. Box 808 / Livermore, California

## ABSTRACT

Current probabilistic risk assessment (PRA) methods for nuclear power plants utilize seismic "fragilities" -- probabilities of failure conditioned on the severity of seismic input motion -- which are based largely on limited test data and on engineering judgement. As part of the NRC Component Fragility Research Program (CFRP), the Lawrence Livermore National Laboratory (LLNL) developed procedures for fragilities testing. These procedures were applied to evaluate actual seismic capacities of motor control center (MCC) electrical devices, to develop seismic "fragility curves" suitable for PRA application, and to suggest various methods of improving MCC seismic performance. In other CFRP activities, LLNL used "high-level" qualification data to develop fragility descriptions for selected equipment, and identified candidate components for future comprehensive fragilities testing using similar procedures.

## 1. Introduction

Current probabilistic risk assessment (PRA) methods for nuclear power plants utilize component fragilities which are for the most part based on a limited data base and engineering judgement. The seismic design of components is based on code limits and NRC requirements that do not reflect the actual capacity of a component to resist failure. In order to improve the present component fragility data base and establish component seismic design margins, the NRC commissioned a Component Fragility Research Program (CFRP). The CFRP is being conducted in two phases. Phase I has consisted of parallel efforts to (1) develop and demonstrate procedures for performing component tests to obtain new fragilities data, (2) identify through systematic grouping components influencing plant safety and therefore candidate for independent NRC testing, and (3) compile and evaluate existing fragilities data obtained from various sources. The results of these three

---

[*] "This work was supported by the United States Nuclear Regulatory Commission under a Memorandum of Understanding with the United States Department of Energy."

activities form the basis for a comprehensive evaluation of component behavior, based both on available data and on new testing, to be performed in Phase II of the program.

During Phase I, the Lawrence Livermore National Laboratory (LLNL) has performed component testing and prioritization, while the existing fragilities data base has been compiled by the Brookhaven National Laboratory (BNL). The specific objectives of the Phase I LLNL effort have been as follows:

### Component Prioritization

- systematically identify and categorize electrical and mechanical components influencing plant safety, taking into account system and subsystem functional descriptions, operating and maintenance experience, expert opinion, past PRA results, regulatory concerns and existing test data.
- collect and utilize existing test data and operating experience to judge the relative seismic capacity of each component identified.
- identify "very important, low seismic capacity" components which then become priority candidates for future comprehensive testing.

### Demonstration Testing

- develop procedures for component fragilities and seismic margins testing and demonstrate the effectiveness of these procedures through actual component tests.
- obtain useful fragilities and seismic margins data for the components tested.
- enhance understanding of failure mechanisms of the components tested.

Our Phase I demonstration testing program and component prioritization activities are documented in separate NUREG reports [1,2].

## 2. Component Fragility

"Fragility" is a term commonly used to describe the conditions under which a component (or, in general, a structure, a piping system, or piece of equipment) would be expected to fail. In this paper we are concerned with *seismic* fragility, in other words, what levels of seismically induced input motion would be required to cause component failure; it is important to keep in mind, however, that fragility can in principle be defined for *any* input condition affecting component performance. Failure can be characterized as either functional (e.g., erratic behavior, failure to perform intended function) or physical, or as the exceedance of some predetermined performance criteria (such as a limit given in a design code).

One interpretation of component fragility -- which we will refer to as the "fragility level" -- evolves from qualification testing. In seismic qualification testing, a component is subjected to input motion characterized by a specified waveform describing input level (seismic acceleration) as a function of frequency. The component is "qualified" if it continues to perform its intended function when its response to this input motion -- the "test response spectrum," or TRS -- meets or exceeds pre-determined acceptance limits (the "required response spectrum," or RRS). In qualification testing, the TRS is usually measured at the component support points.

Although it may establish the adequacy of a component for a particular seismic environment, a successful qualification test does not directly provide data on what input motion levels actually result in component failure. This can be (and sometimes is) done by retaining the original input spectrum and then increasing the input *level* until "failure" (however it is defined) occurs. The TRS at failure represents the "fragility level" (or "ruggedness") of the component; the difference between the fragility level and the qualification level thus represents the seismic margin or "reserve capacity" of the component.

Fragility is described differently when used for PRA purposes or for other types of probabilistic analysis. In this case, the fragility of a component represents the probability of its failure -- or more rigorously speaking, the probability of attaining a defined "limit state" -- conditioned upon the occurrence of some level of forcing or response function. It may be expressed in terms of a local response parameter (for example, input motion at the component mounting location) or can be tied to a more global forcing function such as free field peak ground acceleration (PGA). Note however that when fragility is anchored to a forcing function, the further removed the component is from that forcing function, the more factors there are (such as structural response and soil-structure interaction) that must be considered in the fragility description.

The probability of failure is typically described by a family of "fragility curves" plotted at various levels of statistical confidence (see Fig. 1). The central, or "median" function represents the fragility analyst's best estimate of the "true" fragility of the component taking into account all significant factors which, in the analyst's judgement, might contribute to failure. The central point (50% probability of failure) on this curve represents the "median capacity" of the component; ideally, this probabilistic value would correspond with the deterministic "fragility level" of the component. The fragility function is a cumulative distribution usually characterized by a lognormal function with this median value and a logarithmic standard deviation $\beta_R$ which describes the "random" variation in the parameters affecting fragility. In a description of seismic fragility, for example, this parameter might represent the differences in real earthquake ground motion compared to the input motion that a component is subjected to in qualification or fragilities testing. Note that the random uncertainty controls the slope of the fragility function; the less random uncertainty, the steeper the fragility function becomes. As random uncertainty is reduced towards zero, the fragility "curve" approaches a step function with its break point at the fragility level of the component.

The 5% function and 95% function in Fig. 1 represent the "modeling uncertainty" in the median fragility function. These bounds, which may also be referred to as 5% and 95% confidence limits, are based on the assumption that there is uncertainty in the *median* capacity; this uncertainty is characterized by a logarithmic standard deviation $_U$. Simply stated, the 5% confidence limit implies the following:

- there is only a 5% subjective probability that the actual fragility *level* is less than the median capacity indicated for the 5% fragility function.
- there is a 95% subjective probability ("confidence") that the "true" fragility function for the component would be equal to or greater than the 5% function.

Modeling uncertainty, often described as "lack of knowledge" about the component in question, reflects the adequacy (or inadequacy) of information -- component damping values, for example -- used by the fragility analyst to form his judgements about component capacity. Thus, modeling uncertainty in fragility descriptions has a subjective rather than a "random" basis as is true in the statistical sense.

For any given component, empirically developing a statistically meaningful seismic fragility would require that a large population of identical components (e.g., several hundred or several thousand) be subjected to successively higher levels of acceleration and the distribution of failures (however "failure" is defined) be recorded as a function of acceleration level. Practical constraints on time and resources clearly make this infeasible for a single component under well-defined load conditions, let alone for the effectively infinite combinations and permutations of component type, manufacturer, mounting, and loading conditions that could be identified for actual nuclear power plants. Therefore, an alternative approach is necessary to experimentally gain an insight into fragility.

Our approach to assessing fragility takes advantage of the fact that for certain PRA applications, a limited or "lower bound" fragility description may be adequate. In a probabilistic analysis, failure occurs only when the probability distributions of response and fragility overlap; therefore, only the lower tail end of the fragility curve may be of interest from a PRA standpoint. For components having a high seismic capacity (high "ruggedness"), the overlap of the response and fragility distributions could conceivably be so small under all credible loading conditions as to imply that the probability of failure is negligibly low.

One method of developing a "lower bound" fragility is to estimate a so-called "HCLPF" (for High Confidence, Low Probability of Failure) capacity for the component that takes into account both the random and modeling uncertainty in the median capacity. The definition of HCLPF used in the CFRP is that adopted by the LLNL Seismic Design Margin Program, namely that value of the forcing or response function (in this case, seismic acceleration) for which we have "95% confidence" that the probability of "failure" is less than 5 percent [3]. If the median capacity of a component is defined by a peak acceleration with value A, the corresponding HCLPF capacity (i.e., HCLPF acceleration) is obtained from the following numerical relationship:

$$A_{HCLPF} = A \exp\left[-1.65\,(\beta_R + \beta_U)\right]$$

where $\beta_R$ and $\beta_U$ represent the random and modeling uncertainties, respectively. The median capacity A can be determined by component tests, either to actual failure or to some threshold or "cut-off" limit. The cut-off might be applied, for example, in testing certain components whose actual median capacities were significantly above any response levels of regulatory interest.

The HCLPF capacity provides a practical means of addressing variations that inevitably arise between actual plant conditions and test conditions, variations that might otherwise be difficult to parametrically quantify by testing alone. For example, the random uncertainty $\beta_R$ allows for variations in real earthquake motion compared to test input motion, variations in building floor response, or (e.g., for cabinet-mounted electrical devices) random variations in cabinet response. The modeling uncertainty $\beta_U$ can account for variations in real damping values, or in component mounting conditions, or in the response of functionally similar components of different size or supplied by different manufacturers. These uncertainties can be quantified by systematically structuring test conditions in the form of "sensitivity studies" to investigating the effect of various parameters on the measured median capacity of the device tested. This was the basic approach taken in our Phase I demonstration tests.

The HCLPF approach has the added advantage that, in the absence of complete fragility data, a "lower bound" fragility can still be defined for a seismically qualified component by assuming its qualification level also represents its HCLPF capacity. Engineering judgement can then be applied to estimate the uncertainty parameters and thus make inferences about the median capacity.

Note that because the HCLPF capacity by definition presumes a five percent probability of failure, while "qualification" implies no failure, this approach tends to be conservative. It may in fact be overly conservative if qualification levels are low, as would be the case for many plants in the eastern United States. However, HCLPF capacities based on "high level" qualification data -- from plants in the western United States, for example -- can provide useful lower bound fragilities for plants having relatively low design basis earthquakes. The CFRP Phase I prioritization report [1] describes in detail how we used this approach to infer the actual capacity of selected electrical equipment.

In itself, the HCLPF capacity is a useful parameter on which to base regulatory decisions concerning seismic performance. However, extreme care must be exercised in selecting "reasonable" values of $\beta_R$ and $\beta_U$ when using a HCLPF capacity derived from qualification data to infer the actual capacity or "fragility level" of a component. The reasons for this are two-fold:

- as shown in Fig. 2, the slope of the fragility curve becomes more shallow as random uncertainty ($\beta_R$) increases. Therefore, the resultant median capacity on the 5% curve (and, for constant $\beta_U$, the inferred fragility level) also increases with increasing random uncertainty.

  As shown in Fig. 3, however, if the fragility level of the component is known (e.g., from actual failure tests), then the HCLPF capacity derived from the median capacity decreases with increasing random uncertainty.

- similarly, as modeling uncertainty ($\beta_U$) increases, the offset between the 5% fragility function and the 50% function also increases, implying an increase in the inferred fragility level. If, on the other hand, the fragility level is known, an increase in modeling uncertainty drives the HCLPF capacity towards lower (i.e., more conservative) values.

The above exercise illustrates how a "bottom-up" approach towards estimating median capacity (i.e., inferred from HCLPF capacity) can imply that fragility level increases with uncertainty, which is clearly nonconservative. This observation suggests that the reverse approach -- basing HCLPF capacities on measured fragility levels -- is preferable for assessing seismic performance. For a given fragility level, such a "top-down" approach yields lower (i.e., more conservative) HCLPF capacities as uncertainty increases.

## 3. Component Prioritization

In order to reduce to a manageable level the number of components included in a comprehensive test program, it was first necessary to review and prioritize components related to plant safety. Past efforts to develop generic minimum equipment lists through the use of probabilistic risk assessment models have met with limited success. The results of these efforts suggested that the apparent importance of components was strongly influenced by the component fragilities assumed in the analyses.

The results of such probabilistic analyses can also vary widely from plant to plant, being strongly influenced by the specific event trees and fault trees used in the analysis. The reasons for these variations include the following:

- event trees, which describe the postulated accident scenarios ("initiating events") potentially leading to core melt, depend on plant system design and operating procedures.

- fault trees, which describe the sequences of equipment failure leading to core melt given that an initiating event has occurred, similarly depend on plant system design. Of particular importance are such factors as redundancy (e.g., duplicate systems, multiple trains within a given system, multiple systems of different design but with the same safety function), effects of partial failure, the potential for "common-mode" failure (e.g., independent vs shared power sources), and the "fragility" of the components in these systems.

  When assessing the influence of fault trees on the apparent importance of certain components, it is also important to consider that *component* failure may not necessarily constitute a "failure" in a safety sense. For example, the safety significance of seismically-induced contact "chatter" -- uncommanded state changes -- in a motor controller would depend on electrical circuit design and the characteristics of the mechanical device (e.g., a pump motor) that the starter was connected to. Consequently, although a particular starter may have a certain fragility (e.g., defined on occurrence of chatter), its "importance" in a safety sense could be very different from one plant (or, for that matter, from one system) to the next.

For any given component or component type, its fragility -- or probability of failure -- will itself depend on many factors that may vary widely from plant-to-plant. These include the following:

- manufacturer-specific differences in design, as well as random variations in performance from component-to-component.

- the particular failure mode identified and its relationship to plant safety.

- the "external interface" between the component and its environment, primarily component mounting conditions.

- degradation ("aging") caused by such factors as temperature, vibration, and radiation.

- input load characteristics, which are influenced by site-specific soil behavior and structural response (e.g., component location) as well as to random variations in seismic input motion.

Clearly, feasibility considerations limit not only our ability to empirically develop broadly applicable "generic" fragilities, but to identify individual components as being "most important" to plant safety.

In view of these limitations, we took an alternate approach to systematically identify, categorize, and prioritize electrical and mechanical components. We based this approach primarily on the design of "typical" plant systems under both normal and abnormal operating conditions, supplemented by expert opinion on plant operating experience, past PRA results, and the results of industry qualification testing. The general approach taken in this effort proceeded in the following steps:

1. Identify "safety functions" necessary to maintain a plant in a safe condition ("normal operation"), or to safely bring the plant to and maintain it in a state of cold shutdown in the event of an earthquake ("accident mitigation").

2. For each safety function, identify associated plant systems (or sub-systems, as appropriate). The systems considered included those having only a normal operating function, those having only a designated safety function (i.e., for accident mitigation), and those having both operating and safety functions.

3. For each system, list major components based on system descriptions. Here "components" included items generally regarded as mechanical or electrical equipment. Such items as piping, tanks, heat exchangers, equipment supports, and structures were not included.

4. Within each system, group components according to whether they are "very important", "important", or "less important" to the system being able to perform its designated safety function.

5. Within each system, identify "high-", "intermediate-", or "low-capacity" components based on the anticipated ability of each to function during a postulated earthquake.

6. Rank each component by combining its importance and seismic capacity.

The specific criteria for defining importance and seismic capacity are outlined in the following discussion. The general process resulted in nine natural groups, that is, three levels of seismic capacity for each importance group. Those components ranked as "very important, low-capacity" became first-priority candidates for Phase II testing, while "important, low-capacity" or "very important, intermediate-capacity" were assigned as second-priority candidates.

The actual systematic prioritization of components was performed by a Component Identification Working Group formed of expert consultants from a wide range of engineering disciplines. The working group members were drawn primarily from the nuclear industry, and represented a number of nuclear steam supply vendors, architect-engineering firms, and utility owner-operators. The following discussion briefly summarizes describes how our prioritization of components was developed.

## Plant Safety Functions

The following plant functions were assumed to contribute to plant safety, either during normal operation or accident mitigation, or both:

1. Control reactivity
2. Control reactor coolant inventory
3. Maintain integrity of the reactor coolant pressure boundary
4. Maintain adequate core cooling
5. Remove decay heat
6. Maintain plant environment
7. Maintain containment integrity
8. Maintain adequate supply of electrical power
9. Provide control and instrumentation
10. Maintain vital auxiliaries

## Plant Safety Systems

Table 1 lists the plant systems considered in this evaluation, organized by safety function; for each safety function a system-by-system breakdown of components was then developed for consideration. The component list was based primarily on a review of system descriptions for Zion, a four-loop Westinghouse PWR plant. As a result, the systems considered tend to be PWR-oriented, although certain systems unique to boiling water reactor (BWR) plants were considered as well. Despite the strong PWR emphasis, we regard the resultant prioritization of components as reasonably representative of all plants, due to the fact that the *relative* importance of *systems* -- which may vary widely from plant-to-plant -- is not taken into account.

## Component Importance

For each system listed in Table 1, components were ranked according to their effect on the ability of that system to perform its intended safety function. No consideration was given to the relative importance of any one system compared to another, as this is highly variable from plant-to-plant. As discussed earlier, past attempts to use PRA techniques for defining "generic" importance lists have in fact indicated that the relative importance of plant systems is strongly dependent on the component fragilities assumed in the assessment.

After components were identified for a particular system, each was assigned to one of three importance groups -- very important ("VI"), important ("I"), or less important ("LI") -- according to the following guidelines:

| | |
|---|---|
| Very Important: | failure of the component would prevent the system from performing its designated function. In other words, component failure implies system failure. |
| Important: | failure of the component results in a significant reduction in system performance. |
| Less Important: | failure of the component would not significantly affect the performance of the system. |

Note that component "importance" or "safety significance" as used in this development is not intended to necessarily correspond with or to redefine equipment "important to safety" as used in NRC terminology. The assignment of a component to a particular importance group was based on the subjective judgement of the working group members.

In principle, the relative importance of a given component (or type of component if more than one are present) to a particular system could be affected by redundancy and by component performance characteristics. For example, if a pump is able to deliver only 50 percent of its rated flow, the relative importance of that pump would depend on how the flow reduction affects the ability of the overall system to perform its function, taking into account such factors as number of flow trains and the discharge capacities of other pumps in the system. Our prioritization scheme, however, recognized neither partial failure nor redundancy of components. The latter factor implies that common-mode failure is an important consideration; therefore, even redundant components may be categorized as "very important."

## Seismic Capacity

Component seismic capacity was characterized by local zero period acceleration (ZPA) at the component support location. The local response spectrum was assumed to be characterized by a relatively broad-band frequency content, with a ZPA of 2g (or greater) being postulated as an important threshold to denote "high capacity" components. For realistic definitions of earthquake ground motion and structural response, this local threshold (if considered as a structural floor response) is expected to encompass earthquakes inducing up to 1g peak ground acceleration (PGA) in the free field. For our purposes, three "capacity levels" were identified:

| | |
|---|---|
| Level 1: | component is expected to remain functional for local response greater than 2g ZPA ("high capacity"). |
| Level 2: | component "failure" is anticipated for local response between 1g and 2g ZPA inclusive ("intermediate capacity"). |
| Level 3: | component "failure" is anticipated for local response less than 1g ZPA ("low capacity"). |

where "failure" might be defined as either functional or physical failure, or both. Note that no detailed verification was undertaken of earthquake ground motions corresponding to Levels 1, 2, and 3 of local response, as this would depend on plant-specific structural and geological characteristics. Note also that the precise definition of "local response" depends on the particular mounting characteristics of the component in question. For example, the appropriate "local response" for motor control center (MCC) internals (e.g., relays, contactors) would be the in-cabinet response at each device location, while that for the MCC as a whole would be the structural "floor response" at the cabinet base.

## Comparison Against Data

Tables 2 through 4, respectively, summarize all low-, intermediate-, and high-capacity components identified in this evaluation, arranged according to importance group. After the reviewed components had been subjectively ranked by importance group and anticipated seismic capacity, a comparison was made with available qualification data as a check on the subjective seismic capacity level. The main source of data used for this purpose was a summary of qualification test results for Millstone Unit 3 (a Westinghouse PWR) provided by Northeast Utilities. This data was supplemented by similar data taken from a seismic re-evaluation program performed by the Pacific Gas & Electric Company for Diablo Canyon Units 1 and 2 (also a Westinghouse PWR) following discovery of the previously undetected "Hosgri" earthquake fault near the plant site.

Note that the "qualification level" for a particular component relates its performance at a specific test input level which in turn reflects the design basis earthquake for the plant site. It is *not* the "fragility level" of the component, and may in fact be an overly conservative representation of the point at which component "failure" would actually occur. As a result, a review of qualification data alone may not be sufficient for assessing the ultimate seismic capacity of certain plant equipment. For example, the "high capacity" rating of the certain components was supported by the Millstone qualification data despite the relatively low (0.18g) SSE requirement. Consequently, the subjective ranking of these components as "high capacity" appears to be reasonable. Not surprisingly, however, much of the Millstone qualification testing did not reach the 2g threshold ZPA that we had designated for Level 1 components owing *to* the low SSE requirement. Furthermore, when "high level" qualification data was considered for some components -- in this case from the PG&E evaluation program for the 0.75g Hosgri SSE — markedly different seismic capacity levels were often inferred.

Such discrepancies in inferred capacity more likely reflect test input rather than "actual" component capacity. If this is indeed the case, HCLPF capacities based on the low-level qualification data would clearly yield conservative -- perhaps overly conservative -- descriptions of component fragility. Conversely, if the "high-level" data can be shown to apply to equipment at the "low-level" plant site, then substantial margin between design basis and actual ultimate capacity would be demonstrated. Of course, the applicability of "high level" qualification data to plant equipment qualified for significantly lower SSE levels depends on the extent to which the equipment in the high-level tests was modified specifically to meet the higher SSE requirement as well as to other factors such as differences in mounting conditions.

It therefore remains to identify a suitable technical basis for resolving these discrepancies in inferred seismic performance. Two avenues are available for this purpose:

- detailed evaluation of existing data, preferably actual fragility data or, alternatively, high-level qualification data.

- fragility testing specifically structured to investigate the effects of various factors (e.g., mounting) n seismic performance.

In either case, the evaluation must address not only the "commonality" of like equipment at high- and low-level plant sites, but also specific factors (e.g., mounting) that potentially affect seismic performance. Typically, these factors are not systematically investigated as a part of qualification testing; any "sensitivity studies" performed during such tests generally arise out of necessity as equipment is modified in order to meet qualification requirements.

To demonstrate how "high-level" qualification testing can be used to assess ultimate seismic capacity, we developed fragility descriptions for five components based on high-level qualification data from the Hosgri requalification program. Although not true "fragility" data, these test results provided valuable information on component behavior under conditions exceeding any anticipated change in peak ground acceleration for eastern plant sites. The specific equipment that we evaluated included the following:

- 4160-volt metal-clad switchgear
- potential transformer 4160/120VAC
- safeguard relay boards
- emergency light battery pack
- station battery and racks

To describe equipment fragility, we assumed that the qualification test results represented the "high-confidence, low probability of failure" (HCLPF) value for each. After a thorough review of test conditions and test results (particularly relating to cabinet transmissibility), we used our judgement to estimate the uncertainty and random variability in the fragility description. This, in turn, provided us with a basis for inferring the median capacity of the equipment being considered.

Besides providing a basis for developing probabilistic fragility descriptions, these tests yielded insight into the influence of such parameters as support arrangement, cabinet rigidity and mass distribution on seismic capacity. In some cases the results of these tests identified practical -- and often relatively minor -- hardware modifications which substantially improved the seismic performance of the equipment tested.

The results of our assessment, described in Ref. 1, indicated that high-level qualification data can be used to infer ultimate capacity ("fragility level") provided that sufficient information is available from which to estimate how factors such as component mounting affect seismic performance. Our evaluation further indicated that many components included in the Hosgri evaluation were qualified in their standard commercial configurations or with relatively minor modifications. This result is encouraging because it suggests commonality among certain "standard" equipment items and therefore that high-level test results can be used to "confirm" seismic capacity levels -- at least for "high capacity" components -- assigned to like equipment at plants having lower SSE requirements.

However, as discussed earlier, such a "bottom-up" approach (i.e., fragility level estimated from HCLPF capacity) suggests that fragility level increases with uncertainty, which is clearly non-conservative. Extreme care must therefore be exercised in selecting the uncertainty parameters used to infer the component fragility level. Unfortunately, definitive information may not be available on certain factors potentially affecting seismic performance, such as component mounting, as these factors are not usually investigated systematically as a part of qualification testing; any "sensitivity studies" performed during such tests generally arise out of necessity as equipment is modified in order to meet qualification requirements.

This result implies that a "top-down" approach -- estimating HCLPF capacities from actual failure data measured in fragility tests -- is preferable for assessing seismic performance, particularly when developing detailed fragility descriptions for low-capacity equipment.

## 4. Phase I Demonstration Tests

As part of the Phase I CFRP, we performed actual tests to demonstrate our approach to fragility testing. The specific objectives of our Phase I demonstration tests were as follows:

- demonstrate, for a typical item of nuclear power plant hardware, that we could characterize its fragility.
- investigate the dependence of fragility on a specific "technical issue" affecting equipment behavior.
- generate useful information regarding the actual seismic capacity of the equipment tested.
- develop practical fragility descriptions based on the experimental data, suitable for application in probabilistic risk assessments.
- provide guidance for interpretation of test data available from other sources.

Although independent of our prioritization efforts, the Phase I demonstration tests also provided guidance on the level of effort necessary to do meaningful yet cost-effective fragilities testing, as well as on the level of detail appropriate for specifying candidate components for Phase II evaluation.

We selected as our test specimen a three-column Westinghouse Five-Star motor control center (MCC) containing 8 Westinghouse motor controllers of various types and sizes as well as 14 relays of different types and manufacturers. The Five-Star is the current basic model marketed by Westinghouse for industrial and power system applications; it is essentially identical to the Type W motor control center manufactured by Westinghouse from 1965 to 1975, various configurations of which are found in many nuclear power plants of this vintage. The particular electrical devices selected represented a sample of standard MCC devices typical in function of those found in actual plants, but are not necessarily generic for all similar devices.

It is important to note that the selection of an MCC as our test specimen was made with no intent to "target" motor control centers out of any special concern. Instead, we viewed the MCC as having certain characteristics which would allow us to best demonstrate our general approach to fragilities testing. While our prioritization activities have generally identified MCCs (and their internal devices) as important components, our selection of an MCC for demonstration testing did not depend on its importance relative to other components.

As our "technical issue" of interest, we investigated the effect of base flexibility on electrical device behavior by systematically varying the mounting configuration of the MCC. Besides addressing the specific question of how base mounting might affect device behavior, testing with different mounting configurations offers the following useful insights:

- if device (e.g., relay) behavior as a function of local in-cabinet response varies insignificantly with changes in the mounting of the MCC, this result would imply that fragility data from tests on individual devices would also apply for the same devices mounted in cabinets.

- by correlating device fragility only to local in-cabinet response (in particular, ZPA) independent of MCC mounting configuration and device location, the scatter in the experimental results (and thus the uncertainty in fragility descriptions developed from the data) should encompass such issues as variations in cabinet transmissibility and in-cabinet device location.

In these tests we investigated both the functional behavior of the individual electrical devices -- relays and starters -- and the structural response of the MCC cabinet for various levels of table input motion and for four different cabinet mounting configurations, although the cabinet itself was viewed mainly as a "typical" load transmission device between the floor and the devices. We conducted multiple tests on each of the following four mounting configurations: four bolts per column with top bracing, four bolts per column with no top bracing, four bolts per column with internal diagonal bracing, and two bolts per column with no top or internal bracing. We performed a total of 56 test runs, including 43 biaxial random motion tests (vertical plus one horizontal axis). Table input motions in the random motion tests ranged up to 2.5 g zero period acceleration (ZPA), which yielded in-cabinet spectral accelerations up to 10 g and higher at the device locations.

### Functional Behavior

We used contact "chatter" -- contact motion causing a momentary uncommanded change of state -- to characterize the functional behavior of each electrical device tested. For qualification purposes, chatter is usually defined as any uncommanded state change longer than a specified duration; the occurrence of chatter therefore indicates "failure" of the device. In our investigation, we did not test to pre-determined acceptance criteria, but instead recorded for each device the following parameters related to its functional behavior:

- the number of chatter events. Single events, such as momentary "bouncing" of contacts, often occur as a normal part of commanded state changes and therefore may not represent true chatters.
- the duration of individual chatter events. In our demonstration tests, we categorized chatter events according to duration, ranging from 2 ms (the threshold typically applied in qualification tests) to over 80 ms.
- the effect of device state on occurrence of chatter. Past tests on similar devices have indicated that spurious contact motion is highly dependent on whether or not the contact coil is energized at the time strong motion occurs.

We later used these parameters as a basis for developing probabilistic fragility descriptions ("fragility curves") for each type of electrical device in the MCC, referencing fragility to local ZPA at the device location. In addition to "best estimate" descriptions of device fragility, we estimated the random variability and modeling uncertainty to arrive at a "high confidence, low probability of failure" (HCLPF) capacity for each type of device. Figure 4 shows a representative set of curves developed from the test data, in this case for the Westinghouse Type AR armature-type relays installed in the MCC.

Aside from providing a basis for developing probabilistic fragility descriptions, our MCC tests also lent insight into the functional behavior of contact-operated electrical devices subjected to extreme levels of seismic input motion. The more significant observations made from the results of these tests include the following:

- for all devices, chatter occurred only when the device contacts were in their deenergized state. Without exception, no chatter of energized contacts was recorded.
- for all devices, virtually all chatter occurred when the MCC was tested in its front-to-back orientation. Only isolated instances of contact chatter were recorded when the MCC was tested in its side-to-side orientation; these were attributed to possible variations in local in-cabinet waveforms.

  Given the mounting orientation of most devices in the cabinet (i.e., direction of contact motion oriented with the front-to-back axis of the cabinet), these results imply that chatter is most likely to occur when the input motion is oriented with the direction of contact action. Virtually no chatter was observed when the input motion was oriented perpendicular to the direction of contact action.
- for starters, virtually all chatter occurred in auxiliary conacts. Only isolated occurrences of spurious main contact action were recorded, most of which could be attributed to contact "bounce" during a commanded state change.

BEST COPY AVAILABLE

- for all devices, normally-closed contacts consistently chattered at lower input levels and more often than normally-open contacts. This suggests for these devices that contact chatter is caused by armature movement rather than local response of the contact element.

- neither reed-type relay was observed to chatter, regardless of input level or MCC mounting configuration. This observation was not surprising considering the extremely low contact mass of the reed-type relays compared to that of the armature-type relays tested.

- the occurrence of chatter appears to correlate only weakly with local in-cabinet ZPA. The significant overlap in "chatter" and "no chatter" in-cabinet response spectra implies that spectral acceleration may be a more appropriate parameter to define the "threshold" above which chatter occurs.

- all 14 relays and all 8 starters responded normally to commanded changes of state for all input levels and MCC support configurations. This held true for each device regardless of whether it was initially energized or deenergized. Only in one case did a device not respond to a commanded state change; this was attributed to technician error.

- the results of single-axis, single-frequency tests performed on one Size 2 starter and one relay removed from the MCC indicate that chatter is most likely to occur for input motions in the 2.5 to 8 Hz range. This result further supports the conclusion that spectral acceleration, rather than ZPA, is a more appropriate basis for characterizing device fragility.

Our fragility estimates indicated that the median capacity ("best estimate" curve, 50 percent failure probability) of the MCC relays ranged from 5.2 to 6.1 g local ZPA, with HCLPF values ranging from 3.2 to 4.3 g local ZPA. When considered as a single group, these relays have a median estimated capacity of 5.6g and a HCLPF of 3.6g. Keep in mind these are local in-cabinet levels, not the motion at the cabinet base, and that input motion is oriented in the direction of contact action. No fragility description was developed for the reed-type relays because no chatter was observed.

The test data for Size 2 reversing and non-reversing starters yielded identical median capacities of 3.9g, and HCLPF capacities of 2.5g and 2.3g, respectively. Note that these results reflect auxiliary contact chatter; for all practical purposes, no chatter of main contacts was observed. The similarity in behavior is not surprising when it is considered that reversing and non-reversing starters differ only in the number of contact sets used (two vs one); the contact sets themselves are identical. For the two Size 3 starters tested, the median capacity was 6.5g local ZPA. The markedly different capacity compared to that of the Size 2 starters most likely results from the substantial difference in starter size.

Note that these results assume that input motion is oriented with the direction of contact motion. The results of our tests indicated that virtually no chatter occurs when the direction of input motion is perpendicular to that of contact motion.

The results of our tests -- the random motion tests on the MCC as well as sinusoidal tests on two devices removed from the cabinet -- also imply that local spectral acceleration is a more appropriate parameter for describing device fragility than local ZPA. Nevertheless, the results of this study demonstrate how test data can be used to develop practical fragilities for PRA applications.

## Structural Behavior

Vendor tests have shown that electrical devices such as those included in our tests typically show high resistance to structural failure; in other words, seismic excitation would be expected to affect functional behavior before any physical damage to the device occurred. Consequently, the only likely structural failures in our demonstration tests were those to the MCC cabinet itself. Types of possible damage anticipated included the following:

- non-destructive effects of cabinet shaking, such as cracking of paint.
- permanent, but non-destructive damage such as deformation of cabinet structures.
- cracking or breaking of welds, destruction of cabinet structures, pull-out or breaking of mounting bolts. Although outside the scope of our demonstration testing, pull-out of concrete anchors might also be expected to occur in actual plant applications.

We inspected the cabinet for signs of damage after each test. In later tests, as the likelihood of permanent cabinet damage increased, we also measured strain levels at selected locations on the cabinet frame. The more significant observations regarding structural behavior of the MCC cabinet include the following:

- our demonstration tests focussed on low-frequency input motions, i.e., less than 9 Hz. We found that with the brace at the top of the MCC, the resonant frequency of the cabinet frame was about 12 Hz, well above this level. Removing the top brace caused the front-to-back resonant frequency to drop to about 5 Hz. Reducing from four to two the number of mounting bolts per column further reduced the frame frequency to about 3.5 Hz.

  The effect of mounting configuration on cabinet response takes on added significance when the results of the single-axis single-frequency device tests are considered. The one relay and one starter tested both indicated highest sensitivity to input motions in the 2.5 to 8 Hz range. Removing the top brace from the MCC lowered the front-to-back frame frequency (i.e., in the direction of contact action for most devices in the MCC) from well outside this range to a point where it could conceivably have a significant effect on device behavior.

- the predominant resonances of the MCC draw-out units ("buckets") ranged from about 14 to 26 Hz, well outside the "sensitive" range indicated by the sinusoidal tests.
- we observed no cabinet damage when the MCC was braced at the top. Testing of the free-standing MCC in the side-to-side direction similarly caused no indication of structural damage until late in

the testing program. Although substantial damage was observed in later tests (in the form of cracked welds between the base frame and the vertical frame members), the cabinet nevertheless withstood some 20 strong motion tests at ZPA levels up to 1.9g before any significant damage was observed.

In general, our test results suggest that top bracing can increase the seismic capacity of both the MCC structure (by limiting cabinet motion) and the internal electrical devices (by increasing the resonant frequency of the cabinet frame).

## 5. Summary and Conclusions

The results of our Phase I prioritization efforts provide guidance regarding not only the urgency of assessing the seismic performance of various mechanical and electrical components, but also the nature and rigor of assessment procedures appropriate for the component in question. Options available for detailed assessment include comprehensive testing -- such as the parametric motor control center tests that we performed in our Phase I demonstration test program -- or evaluation of existing data, or some combination of the two. Our Phase I efforts have demonstrated that if appropriate data is available, either from existing sources or from specially-designed fragility test programs, insights into component capacity *can* be obtained and serviceable fragility functions *can* be generated for PRA applications. The question that remains, however, is one of how definitive the resultant descriptions of seismic performance actually are.

As discussed earlier, a "bottom-up" assessment of seismic capacity (i.e., fragility level estimated from HCLPF capacity) suggests that fragility level increases with uncertainty, which is clearly non-conservative. The fragility analyst must therefore exercise extreme care when selecting the uncertainty parameters used to infer the ultimate capacity, or "fragility level", of a component. Unfortunately, the information necessary to select these parameters may not be available from existing data, or may be difficult to assess consistently if attempts are made to consolidate data from several diverse sources. The less definitive the data on HCLPF-derived fragility descriptions are based, the higher their degree of inherent uncertainty.

For certain high-capacity components, this uncertainty may be tolerable if only a "lower bound" fragility -- a HCLPF capacity, for example, or a 5% fragility function -- is adequate for regulatory decision-making or for PRA applications. This may apply, for example, to the five Diablo Canyon components considered in this assessment. This may also be true for high-capacity components at plant sites with relatively low SSE requirements (e.g., in the eastern U.S.), provided that (1) the "high capacity" rating of these components can be substantiated, and (2) commonality in configuration and mounting conditions can be established between the in-plant components in question and those for which "high level" data is available.

In general, however, high inherent uncertainty implies that a "top-down" assessment -- estimating HCLPF capacities from measured fragility levels -- is still preferable for assessing seismic performance. This is particularly true when a detailed fragility function, rather than a "threshold" fragility description, is necessary for low-capacity equipment. Parametric "sensitivity" tests, even on a limited scale, are best-suited for this purpose when structured to systematically investigate how individual factors affect seismic performance.

Clearly, even for functionally identical components, variations among manufacturers and models, in size and type, and in mounting and loading conditions imply that any fragility estimate -- or, for that matter, other methods of assessing component performance -- will be based to a certain extent on engineering judgement. It is important that this judgement be supported by as firm a technical basis as possible within practical constraints. Our Phase I tests demonstrated that "testing for understanding" is a feasible and cost-effective means of assessing component fragility. This positive experience therefore suggests that Phase II tests be similarly conducted according to the following general steps:

(1) identify a representative component or sample of components for testing. Such a sample might not necessarily be "generic" in the purest statistical sense, but should attempt to include significant variations within a given component type (armature- vs reed-type relays, for example).

(2) identify failure modes and the relevant forcing or response functions. Characterize "failure" (either functional or physical) in terms of a suitable parameter that can be measured experimentally.

(3) identify factors or "technical issues" affecting component failure; such factors might include, but not necessarily be limited to, variations in mounting, input motion, and component damping. Design experimental program to parametrically vary those factors judged to be important.

(4) perform tests to identify when failure occurs, i.e., component median capacity. Such tests might, for example, follow qualification procedures (e.g., use of same input spectra) but at elevated input motion levels. Alternatively (particularly for "high capacity" components), test to a pre-determined level to establish a "lower bound" failure threshold.

(5) use test results to empirically estimate median capacity; note that this result is equivalent to the deterministic "fragility level" generated as a part of some qualification tests. Based on component behavior over all conditions considered, develop estimates of random variability and modeling uncertainty in the empirically derived median capacity.

Although this approach does not remove subjectivity from the process of describing component fragility, it does improve the basis on which these judgements are made. Furthermore, it can provide information useful on many levels, including:

- guidance to the fragility analyst as to what should be considered in developing a specific fragility description for a specific component.

- an aid for interpreting and applying test data obtained from other sources. This is particularly valuable, for example, when using qualification data to assess actual component capacity or when consolidating equipment data from several sources.

- an improved basis for defining test conditions if more rigorous testing of a specific component or component type is required.

- guidance for developing screening techniques for reviewing actual plant equipment ("walkdown" procedures) and suggesting modifications for enhancing the seismic capacity of critical components.

It is also important that such testing be viewed not necessarily as a replacement for, but also as a supplement to, evaluation of data from other sources.

## REFERENCES

1. G.S. Holman and C.K. Chou, et al., Component Fragility Research Program: Phase I Component Prioritization, Lawrence Livermore National Laboratory, NUREG report in preparation (September 1986).

2. G.S. Holman and C.K. Chou, Component Fragility Research Program: Phase I Demonstration Tests, Lawrence Livermore National Laboratory, NUREG report in preparation (May 1986).

3. R.J. Budnitz, et al., An Approach to the Quantification of Seismic Margins in Nuclear Power Plants, Lawrence Livermore National Laboratory, Report UCID-20444, NUREG/CR-4334 (August 1985).

Table 1. Systems identified according to plant safety function.

---

1. Reactivity Control

    1.1 Control Rod Insertion
    1.2 Accident Boration

2. Reactor Coolant Inventory Control

    2.1 Chemical and Volume Control System

    - Letdown
    - Charging (seal injection)

    2.2 Safety Injection Systems

    - High-head injection
    - Low-head injection
    - Residual heat removal
    - Core spray

    2.3 Reactor Coolant System (RCS) Pressure Relief

3. Reactor Coolant Pressure Boundary Integrity

    3.1 Reactor Coolant System
    3.2 RCS Pressure Relief System

4. Core Cooling

    4.1 Safety Injection Systems
    4.2 Residual Heat Removal System
    4.3 Main Steam (MS) System

5. Decay Heat Removal

    5.1 Auxiliary Feedwater System
    5.2 Reactor Coolant System
    5.3 RCS/MS Pressure Relief Systems
    5.4 Residual Heat Removal System

---

Table 1 (cont.). Systems identified according to plant safety function.

---

6. Plant Environment
    - 6.1 Containment Spray System
    - 6.2 Reactor Containment Fan Coolers
    - 6.3 Heating, Ventilating and Air Conditioning (HVAC) Systems
    - 6.4 Containment Purge System
    - 6.5 Containment Refrigeration System (ice condenser plants)

7. Containment Integrity
    - 7.1 Containment Isolation System
    - 7.2 Containment Spray System
    - 7.3 Containment Ventilation Systems
    - 7.4 Isolation Valve Seal Water System
    - 7.5 Penetration Pressurization System

8. Onsite Electrical Power
    - 8.1 Onsite AC Power System
    - 8.2 Onsite DC Power System

9. Instrumentation and Controls
    - 9.1 Instrument Air System
    - 9.2 Nuclear Instrumentation System (ex-core)
    - 9.3 Control Panels and Boards
    - 9.4 Local Instrumentation Racks
    - 9.5 Local Instruments
    - 9.6 Radiation Monitoring System
    - 9.7 Reactor Protection System
    - 9.8 Emergency Safety Function Sequencing System

10. Maintain Vital Auxiliaries
    - 10.1 Closed/Component Coolant Water System
    - 10.2 Service Water System
    - 10.3 Chilled Water System
    - 10.4 Fire Protection System

---

Table 2. Summary of components ranked as "low-capacity" (Capacity Level 3).

---

"Very Important" Components (Group VI-3)

ESF sequencers
Switchgear internals
Motor control center internals
Connections/mounting
DC distribution switchboard internals
Nuclear instrumentation equipment (ex-core)
Electrical distribution equipment
Ion chamber electrical connectiors
P/P transducers
P/P switches
Temperature switches
Flow switches
Relays
Process control equipment
Mechanical/electrical interlocks
Bistables
Indicators/power supplies

"Important" Components (Group I-3)

None identified

"Less Important" Components (Group LI-3)

Rod bottom indicators
Air handling units

---

Table 3. Summary of components ranked as "intermediate-capacity" (Capacity Level 2).

---

"Very Important" Components (Group VI-2)

- Reactor trip breakers
- Pilot-operated relief valves
- Safety valves
- Atmospheric dump valves
- Motor control center internals
- Batteries/battery racks
- ESF/RPS actuation cabinet internals
- Local instrument racks
- Control panels/boards internals
- Limit switches
- Air compressors
- Bearing cooling system equipment
- Fire detection devices
- Fire deluge equipment

"Important" Components (Group I-2)

- Seal injection filters
- Pressure relief valves (BWR)
- Vacuum relief valves
- Reactor coolant pump seals
- Louvers
- Air filters
- Radiation monitoring equipment
- Chiller units
- Strainers

"Less Important" Components (Group LI-2)

- Rod bottom indicators
- Dampers

---

Table 4. Summary of components ranked as "high-capacity" (Capacity Level 1).

---

"Very Important" Components (Group VI-1)

- Control rod drive equipment (BWR)
- Charging pumps and drives
- Motor-operated valves
- Check valves
- Explosive valves (BWR)
- Air-operated flow control valves
- Isolation valves
- Safety injection pumps and drives
- Residual heat removal pumps and drives
- Core spray pumps and drives
- Air-operated solenoid valves
- Main steam isolation valves
- Motor-operated flow control valves
- Auxiliary feedwater pumps and drives
- Containment spray pumps and drives
- Exhaust fans and drives
- Component cooling water pumps and drives
- Butterfly valves
- Air-operated valves
- Air-operated pressure control valves
- Diesel generators
- Diesel oil pumps and valves
- Diesel air accumulator
- Diesel lube oil equipment
- Combustion air intake louvers
- Isolation amplifiers
- Transformers
- Inverters

"Important" Components (Group I-1)

- Supply fans and valves

"Less Important" Components (Group LI-1)

- None identified

---

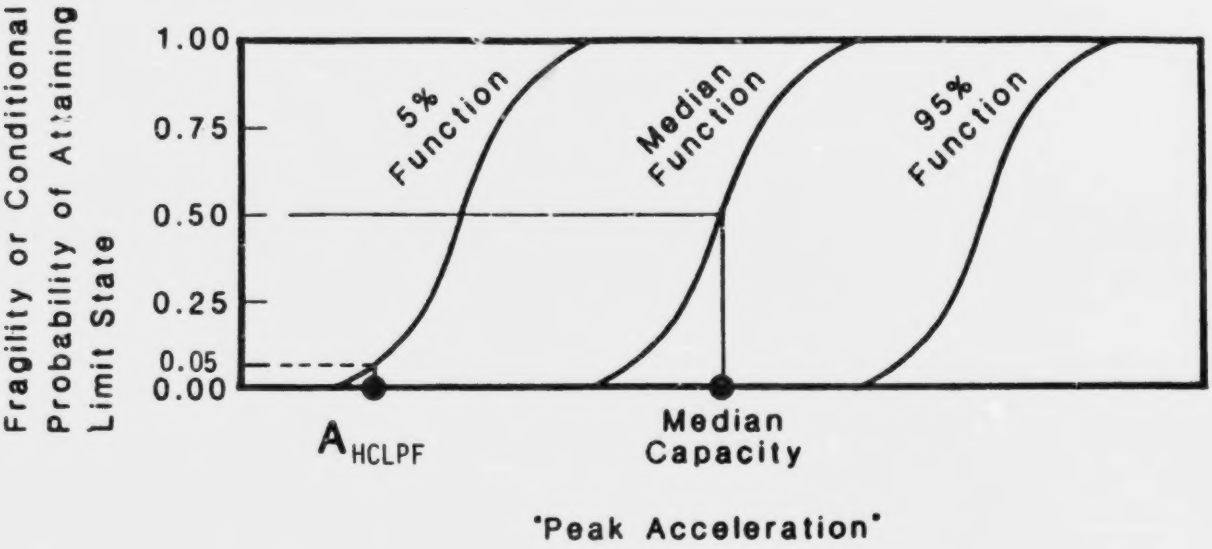

Fig. 1. Typical curve set representing component fragility.

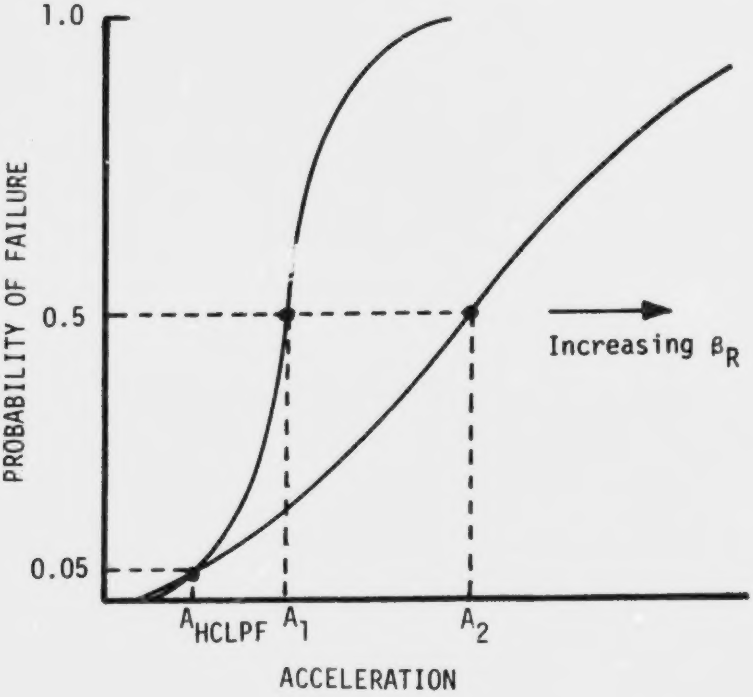

Fig. 2. Typical 5% fragility function showing how increasing random uncertainty affects median capacity derived from a HCLPF value. For constant $\beta_U$, the inferred fragility level of the component (i.e., median capacity of the 50% function) would be similarly affected.

BEST COPY AVAILABLE

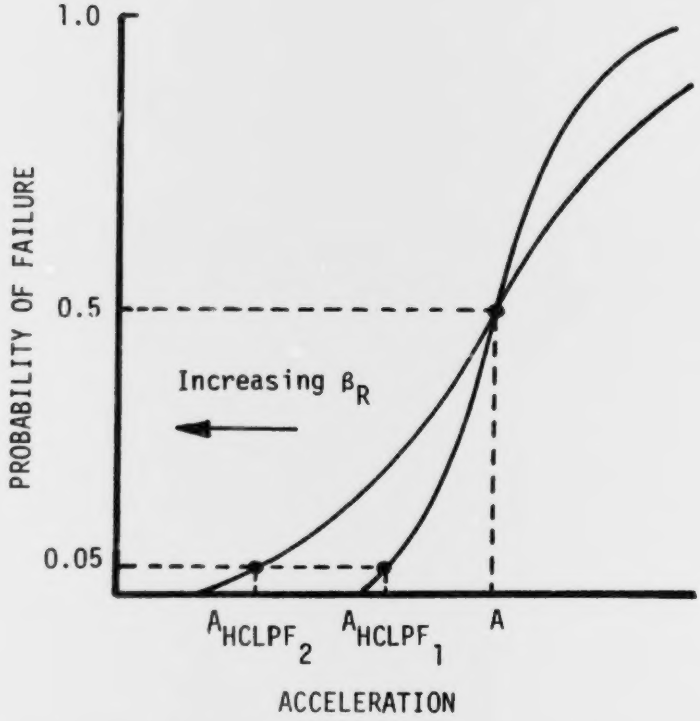

Fig. 3. Typical 5% fragility function showing how increasing random uncertainty affects the HCLPF value derived from a constant median capacity. For constant $_U$, the effect would be the same for HCLPF values derived from a constant component fragility level.

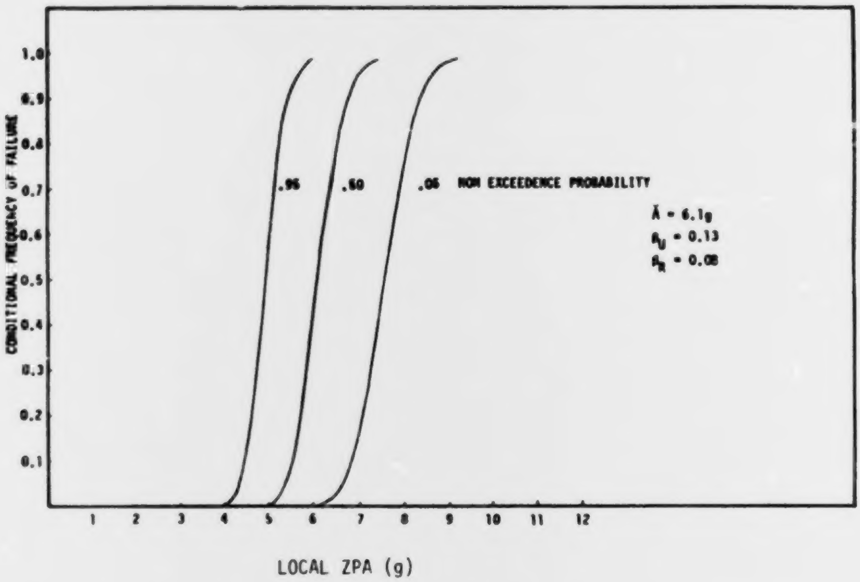

Fig. 4. Fragility curves for Westinghouse Type AR relays.

BEST COPY AVAILABLE

# Synthesizing Seismic Fragility of Components by Use of Existing Data*

K.K. Bandyopadhyay and C.H. Hofmayer
Brookhaven National Laboratory
Upton, NY 11973

## ABSTRACT

Brookhaven National Laboratory has completed Phase I of the Component Fragility Program and is now performing Phase II. The results of Phase I have been published in NUREG/CR-4659. In both Phases, existing test data for various models are utilized to determine the seismic fragilities of different equipment categories. This represents the first large scale attempt to assemble, compile and interpret the very large heretofore fragmented data base. In Phase I, a methodology has been established to compile the test data for variations of testing methods, vibration inputs, damping values, etc. Test response spectra have been used as a measure of the test vibration inputs. Fragility data have been collected and stored in a computerized data bank at BNL for many electrical and control equipment pieces. The data for Motor Control Centers (MCC) and Switchgears have been analyzed in Phase I for determination of the respective fragility levels. Additional test data are being collected in Phase II for these two equipment pieces, as well as other equipment categories. Statistical analyses are also being performed to estimate a single fragility descriptor for each equipment family.

## 1. INTRODUCTION

In FY 1985, under the sponsorship of the U.S. Nuclear Regulatory Commission, Brookhaven National Laboratory (BNL) initiated a research program to develop the seismic fragility levels of nuclear power plant equipment by use of existing test data. An introduction to this research program was presented in the Thirteenth Water Reactor Safety Meeting in October 1985 and published in NUREG/CP-0072 [1]. Phase I of the program was completed in March 1986 and the results were published in NUREG/CR-4659 [2]. BNL is now performing Phase II of the program and is continuing to collect and analyze existing test data. This paper summarizes the fragility analysis performed in Phase I and enumerates the observations made during the study. It also describes the scope and the status of Phase II of the program.

## 2. PHASE I ANALYSIS AND RESULTS

The data collected for the fragility analysis are the results of numerous test programs that utilized different testing techniques and vibration inputs, and presented the response spectra for different damping values. For compilation and assessment of these diverse test data, a standardization method has been developed to transform the entire data base for each equipment to an equivalent system. Test response spectra (TRS) have been used as a measure of the test vibration inputs. Independent biaxial multifrequency testing and TRS at 2% damping have been considered standard for convenience since the majority of the data in the BNL data base are in this form and consequently require no conversion. Single-axis or narrow band (e.g., sine beat) responses have been multiplied by a factor of 0.7 for standardization in accordance with the recommendations of Kana [3]. For a combined single axis and narrow band test response, a multiplying factor of 0.5 has been used. For conversion of damping values, approximate factors have been obtained at various frequencies from a study of the existing data, preferably from the same test program.

---

*This work was performed under the auspices of the U.S. Nuclear Regulatory Commission.

Fragility data have been collected and stored in a computerized data bank at BNL for many electrical and control equipment pieces. The data collected for Switchgears and Motor Control Centers (MCCs) have been considered adequate to generically represent a majority of the respective equipment families. As such, a detailed fragility analysis of these two types of equipment has been performed. The fragility levels with the associated malfunctions have been included in the analysis. The front-to-back fundamental natural frequency of these equipment families varies from 5 Hz to 15 Hz primarily depending on the model, manufacturer, mounting configurations and modifications of the test specimen. The Phase I data indicate that the lower-bound fragility TRS levels for MCCs, Low Voltage Switchgears and Medium Voltage Switchgears have the respective ZPA values of 1.1 g, 1.5 g and 1.8 g.

In the process of collecting and evaluating test data, a number of important observations have been made regarding the amount and the quality of available fragility data, failure modes, device behavior, cautions to be exercised in defining a vibration input as the fragility level, etc. These observations are summarized as follows:

- In an equipment assembly (e.g., switchgear, motor control center) some devices are more vulnerable to seismic environment than others. Thus the overall fragility level of the equipment is limited by malfunction of such devices. These devices and their malfunctions are enumerated as follows:

    a) Contactors - chattering
    b) Motor Starter - chattering, dropping out load,
    changing state, erratic behavior
    c) Time Delay Relays - time setting
    d) Other Relays - chattering, non-operability
    e) Switches - chattering

  The presence of these devices and their effect on the fragility level should be carefully judged.

- Among the sensitive devices, certain types may withstand a substantially higher vibration level than others. Therefore, in evaluating the seismic margin or the risk of a specific plant, consideration should be given to the type of device used.

BEST COPY AVAILABLE

- In various test programs, certain electrical devices malfunctioned when subjected to the induced vibration and needed replacement. The fragility data discussed in this paper are applicable to those equipment pieces which do not contain such devices.

- Equipment design has evolved with time. Due to emphasis on stringent seismic qualification criteria since the mid-seventies, later products have been observed to withstand higher vibration inputs. Therefore, plants utilizing later products should not be unduly penalized by limiting the capacity level to that determined based on earlier products.

- Self-tapping screws have been observed to strip at a much lower vibration level than what the equipment frame can otherwise withstand. Proper consideration should be given if such screws are present.

- Sometimes in a fragility test the capacity level of a specimen in the horizontal direction is governed by the excitation level in the side-to-side direction. However, in application such equipment might be stiffened by the presence of a larger number of units or by some other means. Therefore, in such cases, the front-to-back vibration level, although higher, might be the governing fragility level in the horizontal direction in the actual installation.

- In multiaxis vibration tests, simultaneous test inputs in different directions should be considered while defining one input as the fragility level in that particular direction. For example, in a typical test program it has been observed that for the same input in one direction, the test specimen passed one test run but failed a subsequent run, due to the fact that the input in the second axis had been doubled. This is especially true for complex equipment for which a strong coupling effect is expected.

- Many electrical devices are frequency-sensitive. In a test program, the malfunction of a device was eliminated by reducing the low frequency content of the vibration input. In another test run, the vibration amplitude was very high at a high-frequency band with a high ZPA level, yet a low-frequency-sensitive device withstood this level without any sign of malfunction. These facts indicate that frequency content of the vibration input must be incorporated in the definition of a fragility level.

- A large amount of fragility data exists in the industry, residing especially with the manufacturers who conducted tests in the process of developing and improving their equipment. This information, if it can be made completely available, will greatly enhance the fragility data base and dramatically reduce the need and cost of any future fragility testing.

## 3. PHASE II ACTIVITIES

In current Phase II efforts of the Component Fragility Program, BNL is concentrating on collecting and analyzing the test data for the following equipment categories:

- Switchgear (additional data)
- Electrical distribution equipment
  - a) panelboards
  - b) other panels
- DC distribution switchboards
- Instrumentation and control panels and racks
  - a) nuclear instrumentation system
  - b) process control equipment
- Local Instruments
  - a) transmitters
  - b) switches
  - c) indicators
- Motor Control Centers (additional data)
- Relays
- Power Supplies

The above components have been selected primarily by considering their relatively low seismic capacity levels and importance in performing safety functions as indicated in a prioritization study performed by Lawrence Livermore National Laboratory. Other equipment categories identified in the prioritization study will also be included as part of the Phase II effort during FY 1987 and 1988.

Since PRA and the Margin Studies in their current forms cannot accept more than one fragility indicator, e.g., a g-value, in Phase II each fragility TRS data set is being reduced to a single g-value. To this end, three different approaches are being considered at this time: first, the ZPA of the TRS; second, an equivalent ZPA of a standard response spectrum comparable to the TRS; third, the spectral g-value at the natural frequency of the equipment. These g-values are then statistically used to determine a single-valued fragility descriptor for the equipment. The fragility descriptor used in this program is the HCLPF (High Confidence of a Low Probability of Failure) value at the equipment mounting location[4].

A study of the damping characteristics of selected equipment assemblies is being performed in Phase II by use of low level resonance search test data collected as part of the fragility information. For MCCs, the average damping values are observed from a limited data base to vary between 1.7% and 3.4% in the front-back direction at a sine sweep level of 0.2 g.

## 4. CONCLUSIONS

The fragility study is continuing. Phase I efforts demonstrated that fragility levels can be determined by use of existing test data. The information collected for the fragility study is increasingly being used for licensing decision-making purposes.

## 5. REFERENCES

1. Proceedings of the Thirteenth Water Reactor Safety Information Meeting, NUREG/CP-0072, Vol. 3, February 1986.

2. Seismic Fragility of Nuclear Power Plant Components (Phase I), NUREG/CR-4659, Vol. 1, June 1986.

3. A Research Program for Seismic Qualification of Nuclear Plant Electrical and Mechanical Equipment, NUREG/CR-3892, August 1984.

4. An Approach to the Quantification of Seismic Margins in Nuclear Power Plants, NUREG/CR-4334, August 1985.

## ACKNOWLEDGEMENT

This work is being performed under the auspices of the Division of Engineering Safety, Office of Nuclear Regulatory Research, U.S. Nuclear Regulatory Commission. The authors wish to express their special thanks to Dr. John A. O'Brien, NRC Project Manager, for his continued support and guidance throughout the course of this program. The authors also sincerely acknowledge the cooperation of the organizations and the individuals who participated in the BNL program providing valuable fragility data.

## NOTICE

The findings and opinions expressed in this paper are those of the authors and do not necessarily reflect the views of either the U.S. Nuclear Regulatory Commission or the organization of the authors.

BLANK PAGE

# SEISMIC MARGINS REVIEW OF NUCLEAR POWER PLANTS: PROGRAM OVERVIEW AND STATUS*

R. C. Murray, P. G. Prassinos, G. E. Cummings
Lawrence Livermore National Laboratory
P.O. Box 808
Livermore, California 94550

## ABSTRACT

In 1984, the Nuclear Regulatory Commission (NRC) initiated the Seismic Margins Program (SMP) because of regulatory needs and a changing perception of the seismic hazard. The NRC formed the "Expert Panel on the Quantification of Seismic Margins" and charged them to work closely with an in-house NRC staff "Working group on Seismic Margins" to provide technical guidance on the assessment of seismic margins. The overall goal of the SMP is the development of a methodology and guidelines that can be readily used by the NRC and industry for assessing the inherent quantitative seismic capacity of nuclear power plants [1].

The development of a soundly based and effective method for the assessment of how much margin actually exists in important components, systems and the plant will serve to minimize the need for changing regulatory requirements and licensing actions as the estimates of seismic hazards change. In addition, a seismic margins assessment can provide a basis for confidence in the capacity of nuclear power plants and can be applied when questions arise about their seismic capacity.

The purpose of this paper is to provide an overview and current status of the Seismic Margin Program.

## SEISMIC MARGINS APPROACH

The Expert Panel and its staff studied the available information on the quantification of seismic capacity of nuclear power plants and other industrial facilities. The results of several seismic probabilistic risk assessments of nuclear power plants were reviewed along with the behavior of industrial facilities during earthquakes. The PRAs included the utility sponsored analyses of Zion, Indian Point 2 & 3, Millstone 3, Limerick, Seabrook, and Oconee, and the NRC sponsored Seismic Safety Margins Research Program (SSMRP) study of Zion.

---

*This work was supported by the United States Nuclear Regulatory Commission under a Memorandum of Understanding with the United States Department of Energy.

These studies were used to develop a margins review approach that involves both the screening of components based on their importance to seismic core melt and their seismic capacity to simplify the margins assessment process. This approach is directed at reviewing a specific plant at a selected earthquake acceleration level greater than the SSE. The seismic margins review approach has been documented in the report "An Approach to the Quantification of Seismic Margin in Nuclear Power Plants" [2].

During the Panels' study of past seismic experience, they adopted the general definition of "seismic margin" given below:

> A general definition of seismic margin is expressed in terms of the earthquake motion level that compromises plant safety, specifically leading to melting of the reactor core. In this context, margin needs to be defined for the whole plant. The margin concept also can be extended to any particular function or component.

The Panel also adopted the measure of margin to be a high confidence, low probability of failure (HCLPF). The HCLPF is a conservative representation of capacity and in simple terms corresponds to the earthquake level at which it is extremely unlikely that failure will occur. Generally, the median capacity is at least a factor of two greater than the HCLPF value and, thus, there is no proverbial "cliff" or sudden failure which is expected to occur immediately above the HCLPF value. Although judgment is needed to establish a HCLPF value from a mathematical perspective of a failure probability distribution on capacity (fragility), the HCLPF value can be viewed as approximately equal to a 95 percent confidence of not exceeding about a five percent probability of failure.

## SYSTEMS SCREENING

The review of the available seismic PRAs indicated some key trends and insights useful in developing seismic margin review criteria. These trends and insights could only be obtained for pressurized water reactors (PWRs), for which there were seven available PRAs. For boiling water reactors (BWRs) additional reviews of seismic PRAs are required. These reviews are currently underway and include those PRAs of Kuosheng, LaSalle and GESAR.

Our review indicated that systems screening must be performed at the functional level due to the diversity of plant designs and system configurations. This led us to consider the general plant safety functions normally performed in PWRs:

1. Reactor Subcriticality
2. Normal Cooldown
3. Early Emergency Core Cooling (injection)
4. Late Emergency Core Cooling (recirculation)
5. Containment Heat Removal
6. Early Containment Overpressure Protection (injection)
7. Late Containment Overpressure Protection (recirculation)

When we examined the PRA results we noted that the dominant core melt plant damage states for seismic events are generally early core melt with early containment failure. In addition, these plant damage states generally involve core melt induced by failure of the first three functions listed above followed by loss of containment integrity early in the accident progression. This insight leads us to divide the plant safety function into two groups:

Group A - Functions 1-3
Group B - Functions 4-7

The systems screening approach is based on this insight. The dominant core melt plant damage states are caused by failure of the Group A functions and that these plant damage states are also characterized by functional failure of the Group B functions. Therefore, we consider core melt to occur whenever there is a failure of the systems that provide the initial quenching of the nuclear reaction and cooling of the reactor core followed by failure of the systems that provide the Group B functions so as to preclude the mitigation of consequences by performing containment protection and cooling.

The normal cooldown function is not considered in our screening criteria due to a loss of offsite power that is assumed to occur in all seismic PRAs as a result of "low capacity" switchyard components.

The relationship between the Group A and Group B functions indicated that they are highly coupled so that the combined failure of Group A and success of Group B (or the combined success of Group A and failure of Group B) is virtually precluded. This is because their weakest links are coupled. This insight indicates that only those systems and components needed to perform the Group A function must be considered.

We also discovered that seismic core melt can occur due to the failure of plant and site specific unique features. This implies that it will always be necessary to perform some kind of plant walkthrough to look for any unique features requiring a margin review. It must be emphasized that only major, unique features are of concern. Examples of these are the presence of a dam upstream of the plant or a free standing stack that could damage surrounding building.

The insights gained from our systems review of the PRAs and the development of a systems screening criteria to simplify the margin review process has resulted in the following conclusions:

1. It is possible only to come to conclusions regarding the relative importance of plant systems and safety function for PWRs for which six plants were studied (one by two different methods). No functions/systemic conclusions can be made about boiling water reactors (BWRs) at this date because the results of only one study are available at this time.

2. For PWRs, it is possible to categorize plant safety functions as belonging to one of two groups, one of which is important to the assessment of seismic margins and one of which is not.

3. The important group involves only two plant functions that must be considered for estimating seismic margin. These two functions are shutting down the nuclear chain reaction and providing cooling to the reactor core in the time period immediately following the seismic event.

4. It is possible to reasonably estimate the seismic margin of the plant by performing a margins study only involving the analysis of the plant systems and structures which are required in order to perform those two safety functions.

5. Not withstanding the previous conclusions, there are a number of limitations and restrictions on the analysis.

Using the systems screening criteria and combining it with fragility insights, we can establish functional/systemic guidelines for margin reviews, as illustrated in Table 1. This table shows that it is possible to perform a reasonable seismic margin review by concentrating on those functions (and associated systems) which are required in the early part of the seismic event and eliminating from the review those functions which are not required until later. Further, depending on the level of earthquake for which it is desirable to define a margin, certain initiating events would not have to be considered. This greatly reduced the level of effort and scope of the analysis.

Event trees need only be constructed up to the point of determining whether or not there was an early core melt. Fault trees would only have to be constructed for those front-line systems (and their support systems) that appear on these abbreviated event trees. By combining a fragility screening criteria with these systems models, it would only be necessary to include those components which have been determined to be required in the screening analysis. Our insight led us to believe that the resulting Boolean expressions from these models would represent the dominant contributor to seismic core melt frequency and risk.

## FRAGILITY SCREENING

The Panel reviewed and assessed the available fragility information based primarily on the detailed analysis of nuclear power plants performed for PRAs. This PRA information was supplemented by recent systematic investigations of historic earthquakes which were performed by the Seismic Qualification Utility Group (SQUG). The information includes past earthquake performance data for eight classes of equipment obtained by SQUG and reviewed by the Senior Seismic Review and Advisory Panel (SSRAP). Work is ongoing to document the historic earthquake performance and qualification data for additional components such as piping, valve operators, penetrations, diesel generators, battery racks, and electrical equipment. This work is being conducted by SQUG, the Electric Power Research Institute (EPRI) and the ASCE Dynamic Analysis Committee. Additionally, the collective knowledge of the Panel members with actual earthquake experience at nuclear and non-nuclear industrial facilities, performance test data, and other analyses were also included in the assessment.

These available sources of fragility information were used to arrive at conclusions about which components should be assessed from a seismic capacity standpoint. In making statements about the need for capacity assessments for each component, three ranges, stated in peak ground acceleration (pga), were used: (1) less than 0.3g, (2) 0.3g to 0.5g, and (3) greater than 0.5g. Each type of nuclear power plant component was assessed to have a HCLPF value within one of these ranges. This resulted in an extensive table of components indicating at what earthquake (pga) level each component will require a margin review or be removed from the review process. A sample of this table is given in Table 2.

This categorization of components is based on the available information and the fragility screening resulting from the use of this table should only be performed with consideration of the caveats, limitation and assumptions presented in Chapter 5 of Reference 2.

The fragility conclusions of the Panel can be summarized in simplified form by breaking the components evaluated into the categories established in the fragility table.

When reviewing for an earthquake up to 0.3g, the following components within or affecting important functional groups should be subjected to a review:

- steel containments *
- reactor internals *
- block walls
- heat exchanger supports
- tanks
- batteries and racks (walkdown inspection may suffice)
- soil liquefaction (for susceptible sites)
- dams, levees, and dikes

When reviewing for an earthquake between 0.3g and 0.5g, in addition to the above components the following components should be subjected to a review:

- recirculation pump supports (BWR)
- major containment penetrations
- control rod drive mechanisms
- unusual features of buildings

---

* Not enough data was available for the Panel to reach any conclusions.

BEST COPY AVAILABLE

- piping between buildings
- motor-operated valves on small lines
- active electrical equipment
- diesel generator peripherals
- pumps (certain types)
- fans and cooler unit supports
- ducting between buildings
- cable trays and cables
- control room ceilings

When reviewing for margin for an earthquake above 0.5g, all components should be subjected to a detailed review.

During the process of assessing the HCLPF values for the various nuclear power plant components, an extensive fragilities information base was developed from the available seismic PRAs. This fragilities information base is given in Ref. 3 and is available on diskettes for use on a personal computer.

## APPROACH FOR PERFORMING SEISMIC MARGINS REVIEWS

The Panel combined the insights gained on plant functions and systems, and component fragilities, and developed an outline of an approach for performing seismic margin reviews. The review approach consists of eight steps, the first of which is the selection of an earthquake review level for which it is desirable to demonstrate margin. The eight steps developed in Ref. 4 are outlined later in this paper and were used as the basis for developing guidelines for performing seismic margin reviews.

It is important to point out the assumptions and limitations of the approach.

1. The systems screening part of the approach presently applies only to PWRs.

2. The review approach is focused on earthquakes that could occur in the eastern part of the U.S., specifically east of the Rocky Mountains.

3. The assessment of component HCLPF values is limited to earthquakes of less than a Richter magnitude of about 6.5, which are characterized by 3 to 5 strong motion cycles with a total duration of 10 to 15 seconds.

4. Design and construction errors are not covered.

5. Possible vulnerabilities in hydraulic systems associated with sensors and pneumatic systems are not fully covered.

6. Electrical and control systems are incompletely covered because unrecoverable relay chatter and breaker trip cannot be adequately treated from a systems standpoint at this time.

7. Evaluation of the effect of wear and aging on equipment function is not fully covered.

8. Possible adverse human responses caused by earthquake-induced stress are not covered.

It is recognized that many of these topics are extremely important and deserve additional research.

## TRIAL GUIDELINES FOR SEISMIC MARGIN REVIEWS

With the insights gained from the study of available information and with an outline to an approach for the quantification of seismic margins, the Panel chartered its staff to develop guidelines for performing seismic margin reviews. Trial guidelines were prepared under the guidance and with the concurrence of the Panel and are presented in Ref. 4.

The objective of the seismic margin review guidelines [illegible] to provide guidance for determining whether a plant can resist with high confidence a specified earthquake level. To accomplish this objective, analyses are performed on components, systems, and the plant to determine what the HCLPF value is so that it can be compared to the specified earthquake level. Plant failure is defined as the onset of core melt.

A flow chart of the margin review process is shown in Figure 1. This process involves the screening of components based on their importance to plant safety and their seismic capacity. Inspection of Fig. 1 indicates that Steps 2, 5, and 7 are primarily concerned with plant safety functions and systems, and are performed by a team of systems analysts. Steps 3, 6, and 8 are primarily concerned with capacity assessment and are performed by a team of fragility analysts. Step 4 is performed by both teams of analysts. The entire process requires close cooperation between the two teams of analysts.

The initial step in the review process is the selection of the margin review earthquake level, stated in pga, for which it is desired to demonstrate margin.

In Step 2, plant information gathering, review and analysis is performed to determine those plant systems and components (structures and equipment) that are important contributors to plant safety and thus allow focusing of the effort of the components requiring a margin review. From the Panel's previous studies, it was found that, for PWRs, there are two plant safety functions that were identified as being major contributors to plant seismic safety: reactor subcriticality and early emergency core-coolant injection. For PWRs, those components that make up the systems that perform and support these two functions are then identified as the initial candidates of the margins review. All other systems and components are eliminated from further consideration. Also performed during Step 2 is an identification of the relevant seismic initiating events and the development of event trees that describe the systematic behavior of the plant following these initiating events.

Concurrently, in Step 3, knowledge of the inherent capacity of components is used to sort them into two groups, those with a generic HCLPF value larger than the review earthquake level and those that have smaller HCLPF values.

A first plant walkdown is performed in Step 4. This walkdown is performed to inspect the plant and confirm that the plants appearance is such that the rules developed for doing a margins assessment are applicable and that components can be screened out based on the generic evaluation. Assuming this is the case, the appropriate components are eliminated from further consideration. During this walkdown any system interactions, system dependencies and plant unique features will be identified along with confirmation of the accuracy of the system descriptions and configurations.

During Step 5, the information and understanding of the operation of the plant are used to review and revise, if necessary, the event trees developed in Step 3. In addition, for PWRs, systemic fault trees are developed for those systems that perform the two safety functions (subcriticality, early core cooling) and their support systems using those components remaining in the analysis. For BWRs, systemic fault trees have to be developed for all safety systems and their support systems at present although work is currently underway to develop systems screening criteria for BWR's.

A final plant walkdown is performed in Step 6. This walkdown is used to obtain additional specific information for determining the HCLPF values of the components that remain in the analysis. In addition, the systems models are verified for accuracy and any additional information needed to complete them is obtained.

During Step 7, the systems models developed in Steps 3 and 5, and finalized in Step 6 are analyzed to determine the Boolean expressions for the seismic induced core melt accident sequences. This step involves the analysis of the event trees to determine the accident sequences that lead to seismic core melt and the analysis of the fault trees to determine the Boolean expression for each system failure.

The final step in the margin review process, Step 8, is to calculate the HCLPF values for the important low capacity components, important systems, accident sequences and the plant. The HCLPF values are finalized for those components that appear in the Boolean expression derived from the above analyses. These HCLPF calculations may require detailed structural/mechanical analyses based on information gained in the previous steps. The HCLPF values for the components are then used to quantify the Boolean expressions for the system failures, accident sequences and the plant. This quantification provides information that can be used to make decisions about the seismic capacity of the plant, e.g., whether the plant HCLPF is above the review earthquake level or if below it, its actual value.

The guideline report also gives an estimate of the level of effort, staffing and an approximate schedule for completion of the various steps of a seismic margin review. It is estimated that a review would require about 27 engineering-months of effort and could be completed within about nine months from its initiation. Additional time is needed for a peer review of this effort.

## TRIAL PLANT SEISMIC MARGINS REVIEW

The performance of a trial plant review is needed to verify and test the review methodology and guidelines. In the best case, the trial plant would be a relatively new (design about 1972 or later) PWR in the eastern U.S. without a completed seismic PRA (so that the answer is not known before the trial).

The NRC negotiated with and selected the Maine Yankee plant for trial review.

Once the trial plant was selected, the two analysis teams (Systems Team and Fragility Team) were chosen. These teams were selected based on their technical approach, team make-up and cost. In addition, a Peer Review Group was selected and charters were developed for both this group and the Expert Panel. In addition, the seismic margin trial review project was organized accounting for the plant owner and their representative (Yankee Atomic Electric Company), the NRC Working Group on Seismic Design Margins and the appropriate NRC program managers.

The Peer Review Group was chartered to review the technical accuracy of the review including participation in the plant walkthrough and review of the result of the analysis. The Expert Panel was chartered to review the application of the margins methodology and guidelines to evaluate the overall usefulness of the margins review approach and identify any limitations whether previously recognized or not.

The trial plant review of Maine Yankee is about halfway complete. During the kick-off meeting with the utility in May, 1986, we assembled the analysis teams, briefed the NRC and utility on the review methodology and guideline and discussed the review earthquake level. The NRC Working Group was briefed on the trial plant review in June 1986.

The review earthquake level was chosen to be 0.3g with a NUREG/CR-0098 50th percentile spectral shape. The Maine Yankee SSE is 0.1g and the NRC would like to use this trial review to support license action and determine how well the plant seismic upgrades compare with a 0.18g earthquake level. In going through the process of selecting a review level earthquake, we discovered that more guidance is necessary on its selection and hope to address this in the future.

The first plant walkthrough was completed in July 1986. This effort was preceded by several meetings to identify and collect plant data, and to organize the logistics of the walkthrough. There was excellent interaction with the utility and plant personnel to organize the walkthrough and minimize unnecessary plant briefing.

The objectives of the first plant walkthrough are to collect data on the plant, verify that the systems drawings and information are correct and representative of the actual plant configuration, collect data to finalize the event trees and develop fault trees, and to verify that the generic data presented in the fragility screening table can be applied to the elimination of high capacity components from further review and analysis.

During the walkthrough, four groups of about five people each were escorted by knowledgeable plant personnel during the first two days of the walkthrough. These groups consisted of the Peer Review personnel, the NRC and staff, and the Analysis Team members. Each analysis group contained at least one Fragility and one System Team member. During the last three days of the walkthrough, two groups of Analysis Team members continued to review and collect data on the plant. The first walkthrough was completed with a productive interaction between all parties concerned and the walkthrough groups were well organized and worked efficiently. Preliminary results of the first walkthrough are given in Table 3. This table gives a discussion of the preliminary findings for each type of component reviewed.

We are currently working on Step 5 of the margins review. The systems models previously developed are being revised and fault trees of the appropriate front-line and support systems are being developed. Data on the seismic capacity of components collected during the first walkthrough is being analyzed and components not requiring further review are being identified. Important issues from the margins review to date are listed below:

1. Lack of qualification data on some components

2. Lack of data on reactor internals (new information is being reviewed)

3. Earthquake performance of threaded firewater piping (a systems interaction issue)

4. Seismic ruggedness of aged batteries (experience data being reviewed)

5. Applicability and use of the fragility screening table

We have found that interaction among the Analysis Teams and with the utility and Peer Review Group is a very important aspect of the review. The sharing of data and analyses results is essential to the successful completion of this project. Therefore, we have weekly conference calls between the analysis team and a monthly meeting to discuss current results and plan the upcoming effort. We also have bimonthly meetings with the Peer Review Group to keep them informed of our progress and exchange relevant information. In addition, we have some interaction with the Expert Panel to discuss our review procedure and ask guidance on important issues and the use of the fragility screening table.

The remainder of the SMP involves the completion of the PWR trial review, the determination of a systems screening criteria for BWRs, revising the seismic margin approach and guideline based on the trial review and the BWR screening criteria, and performing a trial review of a BWR.

## CONCLUSIONS

The Seismic Margins Program was initiated by the NRC to develop and try methods to study the inherent capacity of nuclear power plants to withstand earthquake accelerations greater than the SSE. The NRC formed an Expert Panel who developed a seismic margins review approach and guideline for the performance of seismic margin reviews.

The seismic margin approach is based on seismic PRAs of nuclear power plants and the behavior of other industrial facilities during earthquakes. This approach combines systems and fragility screening methods to review a specific plant for a selected earthquake level. The objective is to estimate the HCLPF capacity of components, systems, and the plant.

The seismic margin approach is currently being applied to a trial review of the Maine Yankee plant. This review is about half way complete at this time. The results of this review will be used to assess and possibly revise the seismic margin methodology and guideline.

The remainder of the Seismic Margins Program includes the possible revision of the seismic margin review methodology and the guidelines so that they are more prescriptive and can be readily applied to any light water reactor by the NRC and industry. In addition, a trial plant review of a BWR is planned.

## REFERENCES

1. G. E. Cummings, J. J. Johnson, and R. J. Budnitz, "NRC Seismic Design Margins Program Plan," UCID-20247 (October 1984).

2. R. J. Budnitz, P. J. Amico, C. A. Cornell, W. J. Hall, R. P. Kennedy, J. W. Reed, and M. Shinozuka, "An Approach to the Quantification of Seismic Margins in Nuclear Power Plants," NUREG/CR-4334, UCID-20444 (August 1985).

3. R. D. Campbell, M. K. Ravindra, A. Bhati, and R. C. Murray, "Compilation of Fragility Information from Available Probabilistic Risk Assessments," UCID-20571 (September 1985).

4. P. G. Prassinos, M. K. Ravindra, and J. B. Savy, "Recommendations to the Nuclear Regulatory Commission on Trial Guidelines for Seismic Margin Reviews of Nuclear Power Plants," NUREG/CR-4482, UCID-20579 (March 1986).

## TABLE 1

### Functions Requiring Detailed Evaluations in Seismic Margins Reviews

| Function | Screening Requirements | Remarks |
|---|---|---|
| Initiators: | | |
| Offsite Power | F | F = Assume Failure |
| RCS Integrity (LOCA) | X | |
| Containment Integrity | | |
| Functional Group A: | | |
| Reactor Subcriticality | X | X = Margin evaluation for all potential failure modes is required. |
| Normal Shutdown | F | |
| Emerg. Core Cooling (Early) | X | |
| Functional Group B: | | |
| Emerg. Core Cooling (Late) | A | A = Assume failure if core melt occurs resulting from failure of Functional Group A, assume successful if functional Group A is successful in preventing core melt. Conditional on plant walkdown not finding any extremely gross plant-specific differences. |
| Containment Heat Removal | A | |
| Cont. Overpres. Prot. (Early) | A | |
| Cont. Overpres. Prot. (Late) | A | |

## TABLE 2

## Selected Summary of Capacity Assessment of Nuclear Power Plant Components

| Component | Peak Ground Acceleration | | |
|---|---|---|---|
| | <.3g | .3-.5g | >.5g |
| 5. Structure Failures | | | |
| a. Shear walls, diaphragms and footings | C | (5) | X |
| b. Special non-ductile details | C | (6) | X |
| c. Impact between buildings | C | (7) | X |
| 6. Block Walls | X | X | X |
| 7. Piping | (8) | (8) | (9) X |

(5) Evaluation is required only for structures that do not comply with the requirements of either the ACI 318-71 or ACI 349-76 concrete building codes or have not been designed for a SSE of 0.1g or greater.
(6) Review of construction drawings, design criteria, and simplified analyses should be conducted to determine if a margin evaluation is required.
(7) Potential for relay chatter caused by impact should be evaluated.
(8) Walkdown of example piping-system runs should be conducted. Also, piping between buildings should be inspected and margins evaluated if problems are found.
(9) Margin evaluation should include detailed walkdown of all critical piping systems.
C High-confidence low-probability of failure (HCLPF) capacity exists for this acceleration range.
X Margin evaluation for all potential failure modes is required to determine the HCLPF capacity. In addition, margin evaluation (or exceptions) is required as discussed in (5) through (9) above.

## TABLE 3

## PRELIMINARY FINDING FROM THE FIRST PLANT WALKTHROUGH OF MAINE YANKEE

| COMPONENT | OBSERVATIONS/DISCUSSIONS |
|---|---|
| Structures | No obvious deficiencies found (to be confirmed by review of drawings |
| Impact Between Buildings | No problems; sufficient gaps exist between buildings |
| Block Walls | Data collected; some walls have been upgraded. |
| Tanks | Tanks conform to the design drawings. Data collected for HCLPF calculations. |
| Ceiling | Safety-wired (checked). |
| Dams | Not enough water to flood plant. Drainage in opposite direction to plan. |
| Cable Trays | Aluminum cable trays, rod hung trapeze supports; typical industrial cable trays. Pull tests have been done on rod inserts. |
| Pumps | Well anchored. Consistent with guidelines. |
| Active Electrical Equipment | More than sufficient anchorage; critical equipment had anchors further strengthened. |
| Batteries and Racks | Found to be anchored. Deficient spacers. Question about capacity of lead-antimony batteries. |
| Diesel Generators | Found to be well anchored. Ancillary component also well anchored. |
| Piping | No gross anomalies found. |
| Valves | Consistent with guidelines. Valves with long operators require evaluation. |
| HVAC Equipment | Some supported on vibration isolator. These require evaluation. |
| HVAC Systems | Ducting was rod hung. Consistent with guidelines. |
| Internals | Not reviewed during walkdown. |

BEST COPY AVAILABLE

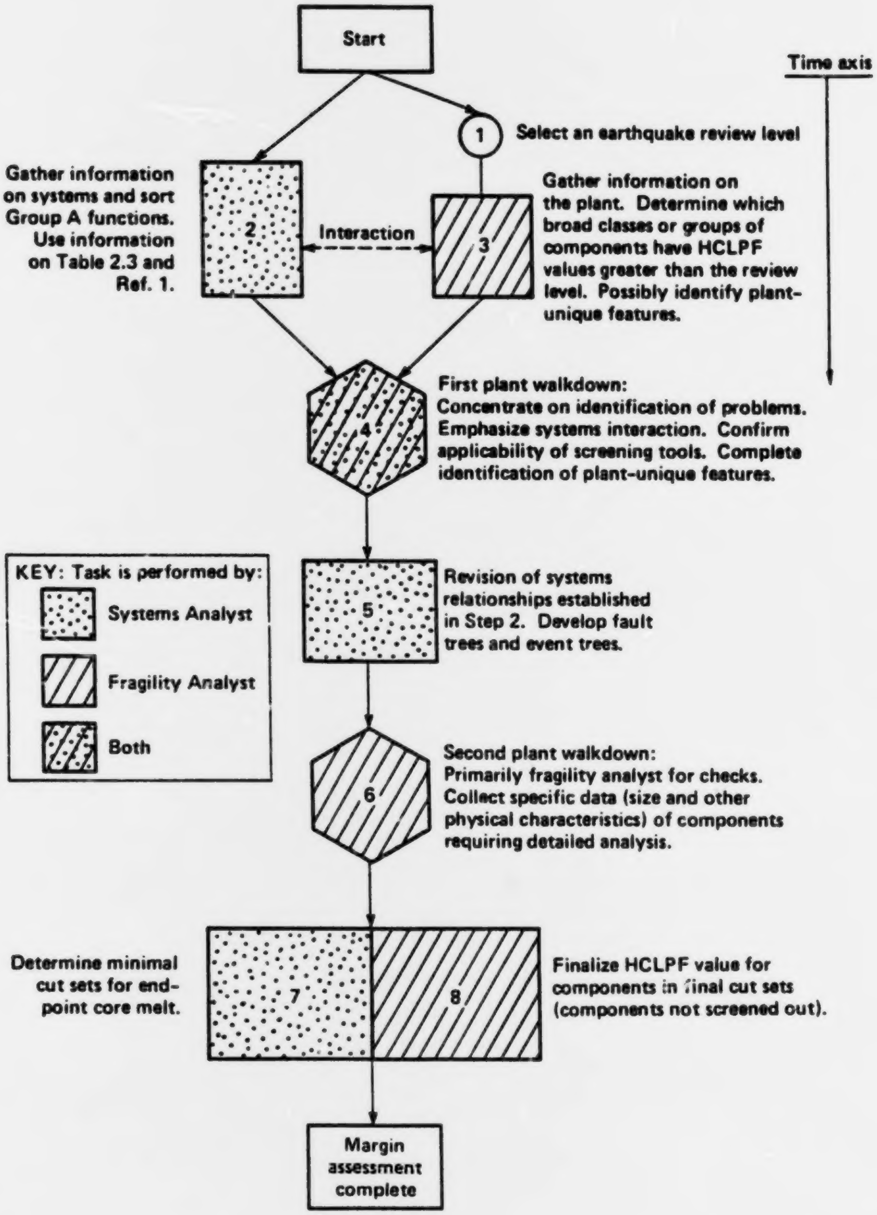
Start
Time axis
1
Select an earthquake review level
Gather information on systems and sort Group A functions. Use information on Table 2.3 and Ref. 1.
2
Interaction
3
Gather information on the plant. Determine which broad classes or groups of components have HCLPF values greater than the review level. Possibly identify plant-unique features.
4
First plant walkdown: Concentrate on identification of problems. Emphasize systems interaction. Confirm applicability of screening tools. Complete identification of plant-unique features.
KEY: Task is performed by:
Systems Analyst
Fragility Analyst
Both
5
Revision of systems relationships established in Step 2. Develop fault trees and event trees.
6
Second plant walkdown: Primarily fragility analyst for checks. Collect specific data (size and other physical characteristics) of components requiring detailed analysis.
Determine minimal cut sets for end-point core melt.
7
8
Finalize HCLPF value for components in final cut sets (components not screened out).
Margin assessment complete

Figure 1. Graphic Representation of the Screening Operations.

BLANK PAGE

# VALIDATION OF SEISMIC SOIL-STRUCTURE INTERACTION ANALYSIS METHODS

## EPRI/NRC Cooperation in Lotung, Taiwan, Experiments

**C. A. Kot, M. G. Srinivasan, and B. J. Hsieh**
**Argonne National Laboratory**
**Argonne, Illinois 60439**

**Y. K. Tang and R. P. Kassawara**
**Electric Power Research Institute**
**Palo Alto, California 94303**

## ABSTRACT

The cooperative program between NRC/ANL and EPRI for the validation of soil-structure interaction analysis methods with actual seismic response data is described. A large-scale model of a containment building has been built by EPRI/Taipower in a highly seismic region of Taiwan. Vibration tests were performed, first on the basemat before the superstructure was built and then on the completed structure. Since its completion, the structure has experienced many earthquakes. The site and structural response to these earthquakes have been recorded with field (surface and downhole) and structure instrumentation. The validation program involves blind predictions of site and structural response during vibration tests and a selected seismic event, and subsequent comparison of the predictions and measurements. The predictive calculations are in progress. The results of the correlation are expected to lead to an evaluation of the methods as to their conservatisms and sensitivities.

## INTRODUCTION

While much effort has been devoted to the development of seismic soil-structure interaction (SSI) analysis methods, relatively little has been done to verify these methods with seismic experimental data, i.e., structural and site response data recorded during natural earthquakes. Among the few notable exceptions is the work by Seed and Lysmer [1,2], which included comparisons of analytical predictions with measurements recorded in the Humboldt Bay Nuclear Power Station during a strong-motion earthquake. In general, the assumptions and approximations in the various SSI analysis methods used in the design, licensing, and risk assessment of nuclear power plants and the uncertainties they introduce into the results have not been systematically investigated vis-a-vis recorded data obtained specifically for this purpose. To remedy this situation, both the U.S. Nuclear Regulatory Commission (NRC) and the Electric Power Research Institute (EPRI) have undertaken programs for the validation of SSI analysis methods using experimental data that include motions recorded during natural earthquakes. A cornerstone of these efforts is the EPRI/NRC cooperation in the seismic experiment with scale-model containment structures built in Lotung, Taiwan, within the SMART-1 array.

The objective of the experiment is to verify or assess analytical predictions of important SSI aspects with extensive seismic ground motion and structural response data collected over a period of years at a site where strong motion events are known to occur frequently. Modeling techniques for site response, foundation input motions, and response of the structures and subsystems are among the major issues that will be subjected to verification. In addition to natural earthquakes, the model structures were subjected to dynamic testing with steady-state excitation to obtain baseline dynamic characteristics of the systems just after construction and before the occurrence of any strong-motion earthquake.

The validation process consists of blind predictions of site and structural response to the dynamic test excitation and to a selected strong motion seismic event, and subsequent comparison of predictions with corresponding measurement records. Different methodologies, varying from the relatively simple to the state-of-the-art, are used by different analysts to make the predictions. The predictions and comparisons will be made in distinct phases. In each phase, the same input data is provided to all the analysts and independent models are devised and blind predictions are made. After the predictions are completed, the analysts are provided with measurement data with which they perform comparisons. If the event modeled is the dynamic test, the comparison may lead to an improved model in the subsequent phase in which seismic response is predicted.

## DESCRIPTION OF LOTUNG SITE AND MODEL STRUCTURE

EPRI, in cooperation with the Taiwan Power Company (Taipower), has built two scale-model (1/4- and 1/12-scale) concrete containment structures in Lotung, Taiwan. The site is located in a highly seismic region and is within an NSF/U.C.-Berkeley array of strong-motion seismographs, the SMART-1 array [3]. The SMART-1 array consists of a central element and three concentric circles, each with 12 surface seismographs, with radii of 200 m, 1 km, and 2 km, respectively. The 1/4-scale EPRI model is located between the outer and middle circles of the array (Figure 1). From October 1980 (soon after the installation of the array began) through May 1984, 29 earthquakes with local magnitude ranging from 3.8 to 7.3 were recorded by the SMART-1 array [4]. Of the first nine, three were located directly below the array at focal depths of 59 to 76 km; the other six had shallow depths and epicentral distances from 7 to 193 km [3]. Thus, experience has shown that the site selected for the experiment is ideal for the collection of seismic data.

The soil at the site mainly consists of saturated sandy silt and silty sand with a shear wave speed in the range of 500 ~ 1000 fps. During the design stage, the results of a seismic refraction survey of the SMART-1 area [4] became available. More detailed data from additional site exploration and laboratory soil testing have since been obtained and will become available to the analysts for analytical modeling. Figure 2 shows a cross section of the 1/4-scale containment structure and its major dimensions. A scaled steam generator and piping loop are installed inside the building. The structure is not a replica model of a typical nuclear power plant containment building. The massive roof slab was necessary to ensure that the fundamental frequencies of the model fall within the frequency range of seismic excitation typical of the region. This program is not intended to scale up the measured response to a prototype containment structure. Soil-structure interaction is expected to occur during earthquakes and the measured responses will be directly used for verifying predictive methodologies.

## PERFORMANCE OF FORCED VIBRATION TESTS

The purpose of the low-level vibration tests--sponsored by NRC--was to define the dynamic characteristics of the soil-structure system in an as-built condition before the system was subjected to strong-motion events. The results of the tests are to be first predicted by the analysts and subsequently to be used for refining the predictive models. The testing was done in two stages. In the first stage, the tests were performed with only the basemat completed. The configuration of the basemat during the tests is shown in Figure 3. Since the water table was very close to the ground surface, water was pumped from the excavation during these tests. In the second stage, the tests were performed on the completed structure. The excavation was backfilled and the sheet piles shown in Figure 3 were removed before the start of the second-stage testing.

Steady-state excitation with a single eccentric-mass shaker was provided in each test. The two counter-rotating masses of the shaker resulted in a uniaxial force, the direction of which remained constant while the amplitude varied sinusoidally in time. The eccentricity of the rotating masses varied from test run to test run. In each run, the eccentricity was held constant as the shaker was operated at a number of discrete frequencies. The shaker was operated in each frequency long enough to obtain steady-state response at that frequency. For the basemat tests, the direction of forcing in any test run was one of the following: horizontal N-S (radial excitation), horizontal E-W (tangential excitation), or vertical. Figure 4 shows the shaker location and the placement of 15 accelerometers. Table 1 summarizes the details of excitation of the basemat. For the test on the completed structure, with the shaker located on the roof slab, the direction of forcing was either radial or tangential. Figure 5 shows the shaker location and the placement of the 20 accelerometers. Table 2 summarizes the details of excitation of the completed structure. The forcing of the basemat was designed to excite all translational and rotational degrees of freedom while that of the completed structure was designed to excite all fundamental modes except the purely vertical translational mode. The measurement locations were selected so that all rigid body motions of the basemat and the lowest modes of the completed structure could be determined from the measured data. The accelerometer (Endevco 5241A) signals were conditioned by anti-alias (low-pass) filter/differential amplifiers. The signal resolution was adequate to capture response of at least one percent g, the acceleration due to gravity. The response data were stored, for each excitation frequency, in the form of amplitude and phase (with respect to forcing), or alternatively as real and imaginary parts of the complex response.

Subsequent to the performance of tests, all the response data were normalized to a constant force of excitation. The data were evaluated by ANL for its quality and most of the data were found to have sufficiently high signal-to-noise ratio. The response data from the basemat tests were used to determine the following experimental soil impedance functions: vertical, $K_v$; torsional, $K_t$; sliding, $K_h$; rocking, $K_r$; and coupled sliding-rocking, $K_{hr}$. Approximate values of the resonant frequencies of the fundamental modes of the basemat were estimated by inspection of the data. The response data from the completed structure were used with the modal identification software of a HP 5451C system to determine a modal model of the system. The modal model consists of estimates of the lower natural frequencies, modal damping, mode shape vectors, and modal mass.

Since the validation plan also includes blind predictions of the vibration test response, the results obtained from the above noted analyses, performed at ANL, will be published only after the completion of the predictive calculations that are being performed by various analysts at present.

It should be noted that EPRI added six accelerometers to the piping system inside the model containment structure during the vibration tests. Also, independent low-level impact tests were performed on the piping system to define its dynamic characteristics.

## COLLECTION OF EARTHQUAKE DATA

Soon after the completion of construction (by the end of October 1985), all seismic instrumentation was installed by the Institute of Earth Sciences, Academia Sinica, who are responsible for maintaining, collecting, reducing and analyzing the seismic response data for Taipower and EPRI. Ground motion measurements on the surface and downhole in the field, and response measurements of the structure are made with triaxial strong-motion accelerometers. In addition, interfacial pressure transducers measure the contact pressure between the containment structure and the surrounding soil.

The surface instrumentation installed in the field consists of an array of three arms, as shown in Figure 6. Each arm contains five stations and in each station the accelerometer is set on a concrete pad and is enclosed by a fiberglass housing. The downhole instrumentation consists of two vertical arrays, aligned along arm 1 of Figure 6, and located as shown in Figure 7. Each vertical array has four downhole accelerometers at different depths, as indicated in Figure 7.

The structural instrumentation of the 1/4-scale containment model consists of 10 accelerometers installed inside the containment structure. Of these, four are installed at the base, four at the top below the roof slab, and one each at the base and at the top of the model steam generator. The schematic of the structural instrumentation is shown as Figure 8.

The interfacial instrumentation of the 1/4-scale containment structure consists of 13 pressure gages, as shown in Figure 9. Eight of these are buried underneath the basemat with two gages for each principal direction. Of the remaining, three are mounted below ground level along a vertical axis on the outside of the wall in the north side, and two are similarly mounted in the west side.

Since the model was completed in October 1985, the EPRI Lotung experiment has recorded more than a dozen seismic events. The recorded earthquakes ranged from magnitudes 5.3 to 6.5 (Richter scale) with epicenter distances varying from less than 2 km to over 80 km. Among them, the three most significant ones occurred on January 16, May 20, and July 30 of this year, with free-field peak ground accelerations recorded at 0.25 g, 0.2 g, and 0.18 g, respectively. Data reduction has indicated that a good earthquake data base has been obtained.

While the primary use of the records of the strong-motion event is in the validation exercise, the recorded structural response will also be used for the identification of modal parameters. The modal characteristics thus obtained will be compared with those derived from the vibration test response data to determine the change in the system during the earthquake.

## SSI METHODOLOGY VALIDATION PROGRAM

The methods selected for validation range from relatively simple lumped-parameter models to recently developed techniques involving detailed analytical/numerical treatment of the different aspects of the problem. The current program focuses on validating common practice in SSI analysis using existing methods. There will be no code/method development. Only the 1/4-scale model is covered in this program. While EPRI has selected different industrial practitioners to perform the tasks, NRC/ANL has sponsored a similar program in the universities, where many of the SSI analysis techniques originated. The methods selected include both the direct and the substructure techniques, while the site modeling may use finite-boundary or continuum approaches. The following methodologies or their variations have so far been selected for validation:

- Lumped-parameter models.
- FLUSH, a two-dimensional finite-element method that uses transmitting boundaries to model the site [5].
- CLASSI, a substructure approach to analyze linear three-dimensional SSI problems that involves determination of an impedance matrix, the foundation input motion, the modal analysis of the superstructure on a fixed-base, and the combination of the preceding to calculate the structural response [6].
- SASSI, a three-dimensional, substructure method that uses a flexible-volume technique that involves a single finite-element analysis to obtain solutions for the impedance and scattering problems [7].

Some of the analysts may use modified versions of FLUSH, CLASSI, or SASSI.

The plans for the validation program involve independent effort by each analyst to devise models, perform blind predictive calculations, and compare predictions with measurement leading to evaluation of the methodology. At least two models are to be constructed by each analyst in successive phases. In the earlier phase, the model(s) devised will be based only on information typically available in the nuclear plant design phase, i.e., soil boring and geophysical data. With such a model, the analyst will predict the response to dynamic excitation of the vibration tests, if the methodology will permit such calculations. In the latter phase, the model of the earlier phase may be modified, reflecting any additional knowledge gained from the vibration tests. The analysts will then use both the original and the modified models to predict both the site response and the structural response to a selected strong-motion seismic event, with only a measured free-field motion being given as input. Finally, the analyst will compare the predictions with measurements and document the results as well as descriptions of the approaches used and their justification.

A workshop is planned in which all analysts are expected to present and discuss their results. The evaluation of the methodologies, including the conservatisms (or their absence) and sensitivity of the results to different SSI parameters, will be based on the results. Although NRC/ANL and EPRI workscopes generally conform to the framework described above, there are some differences between the workscopes. The NRC/ANL plan is shown in Figure 10 and the EPRI plan in Figure 11.

## CONCLUDING REMARKS

This paper describes the cooperative program between EPRI and NRC/ANL on the validation of soil-structure interaction (SSI) analysis methods using the data from a seismic experiment. Since blind analytical predictions are being performed by different analysts with different methods, no measurement data are reported here. The results of this program are expected to form the basis for evaluating the methods as to their conservatism and the sensitivity of the results to various assumptions and procedures. The findings will be used in assessing plant seismic design conservatism/margins and for improving plant licensing procedures.

## REFERENCES

1. Seed, H. B., and J. Lysmer, "Soil-Structure Interaction Analyses by Finite Elements - State of the Art," Nuclear Engineering and Design, 46, (1978), pp. 349-365.

2. Seed, H. B., and J. Lysmer, "The Significance of Site Response in Soil-Structure Interaction Analyses for Nuclear Facilities," 2nd ASCE Conference on Civil Engineering and Nuclear Power, Vol. II: Geotechnical Topics, September 15-17, 1980, Knoxville, Tennessee, ASCE, pp. 14-1-1 - 14-1-61.

3. Bolt, B. A., Y. B. Tsai, K. Yeh, and M. K. Hsu, "Earthquake Strong Motions Recorded by a Large Near-Source Array of Digital Seismographs," Earthquake Engineering and Structural Dynamics, 10, (1982) pp. 561-573.

4. Wen, K. L., and Y. T. Yeh, "Seismic Velocity Structure Beneath the SMART-1 Array," Bulletin of the Institute of Earth Sciences, Academia Sinica, 4, (1984), pp. 51-72.

5. Lysmer, J., T. Udaka, C. F. Tsai, and H. B. Seed, FLUSH - A Computer Program for Approximate 3-D Analysis of Soil-Structure Interaction Problems, Report No. EERC 75-30, Earthquake Engineering Research Center, University of California, Berkeley, November 1975.

6. Wong, H. L., and J. E. Luco, Soil-Structure Interaction: A Linear Continuum Mechanics Approach (CLASSI), Department of Civil Engineering, University of Southern California, Los Angeles, California, CE79-03, 1980.

7. Lysmer, J., M. Tabatabaie-Raissi, F. Tajirian, S. Vahdani, and F. Ostadan, SASSI - A System for Analysis of Soil-Structure Interaction, Report No. UCB/GT/81-02, Geotechnical Engineering, Department of Civil Engineering, University of California, Berkeley, April 1981.

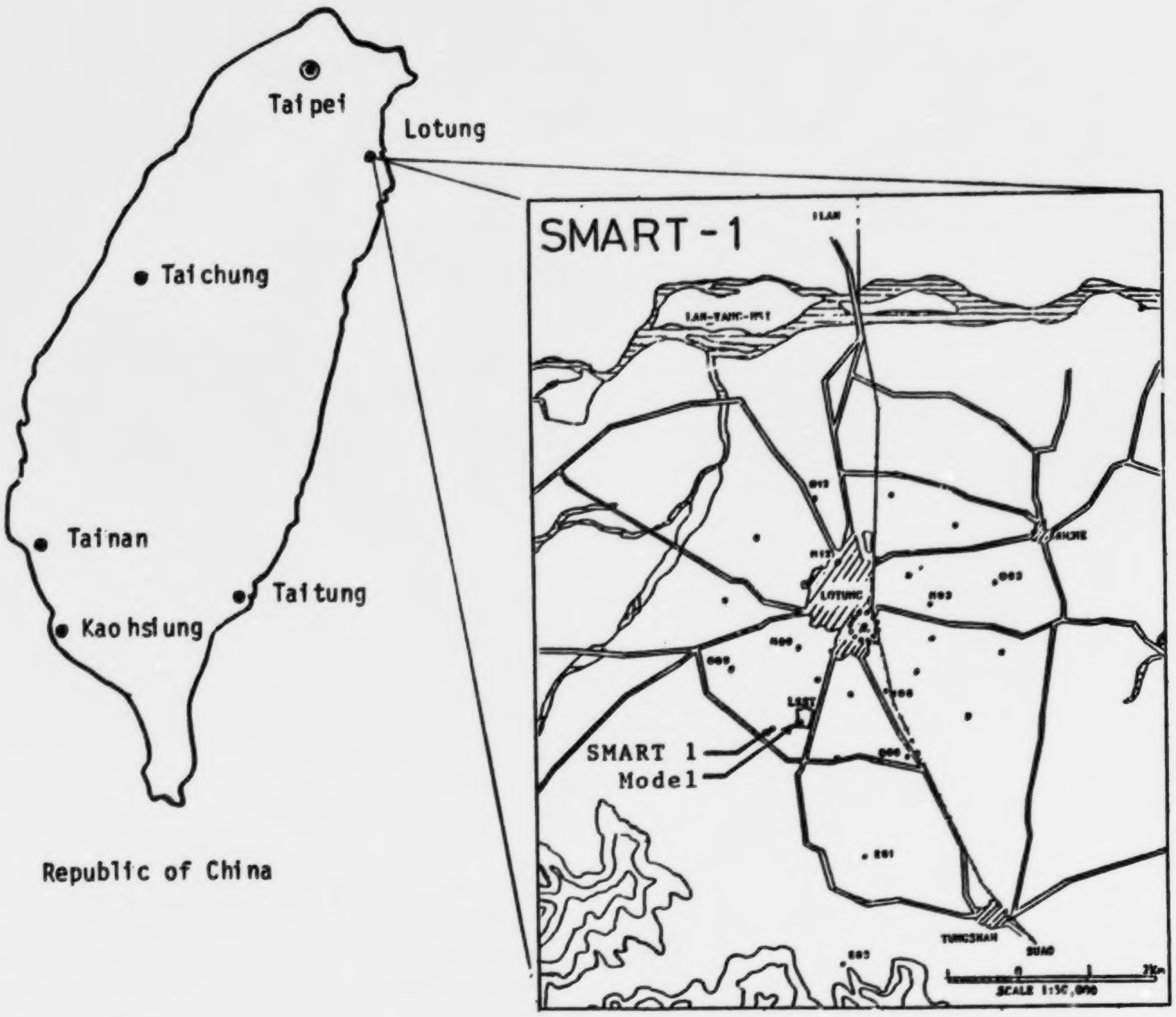
Taipei
Lotung
Taichung
Tainan
Taitung
Kaohsiung
Republic of China
SMART-1
ILAN
LOTUNG
SMART 1
Model
TUNGSHAN
SUAO
SCALE 1:50,000

Figure 1. Test Site Location

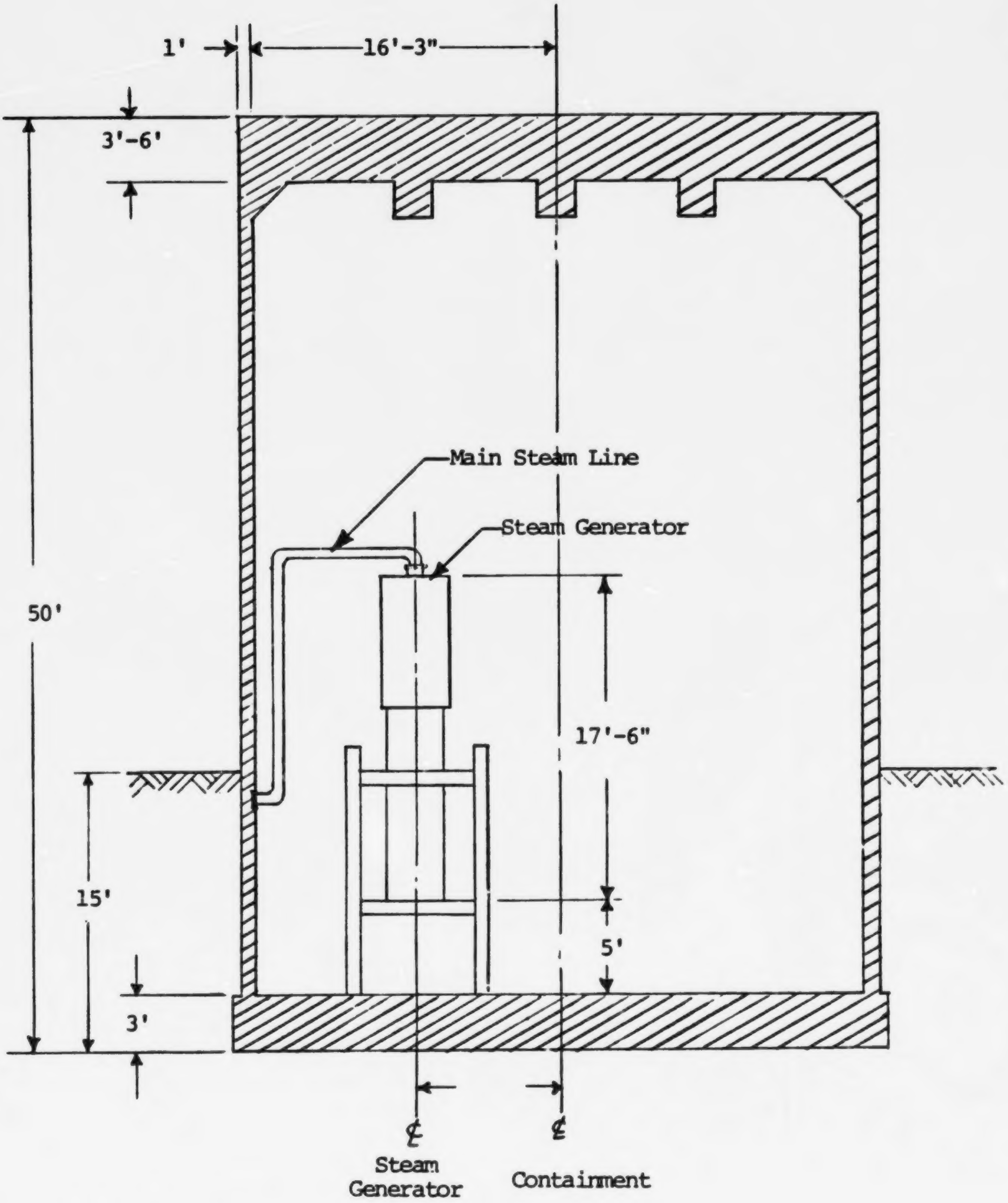
1'
16'-3"
3'-6'
50'
Main Steam Line
Steam Generator
17'-6"
15'
5'
3'
℄
Steam Generator
℄
Containment

Figure 2. Cross Section of 1/4-scale Containment Model

BEST COPY AVAILABLE

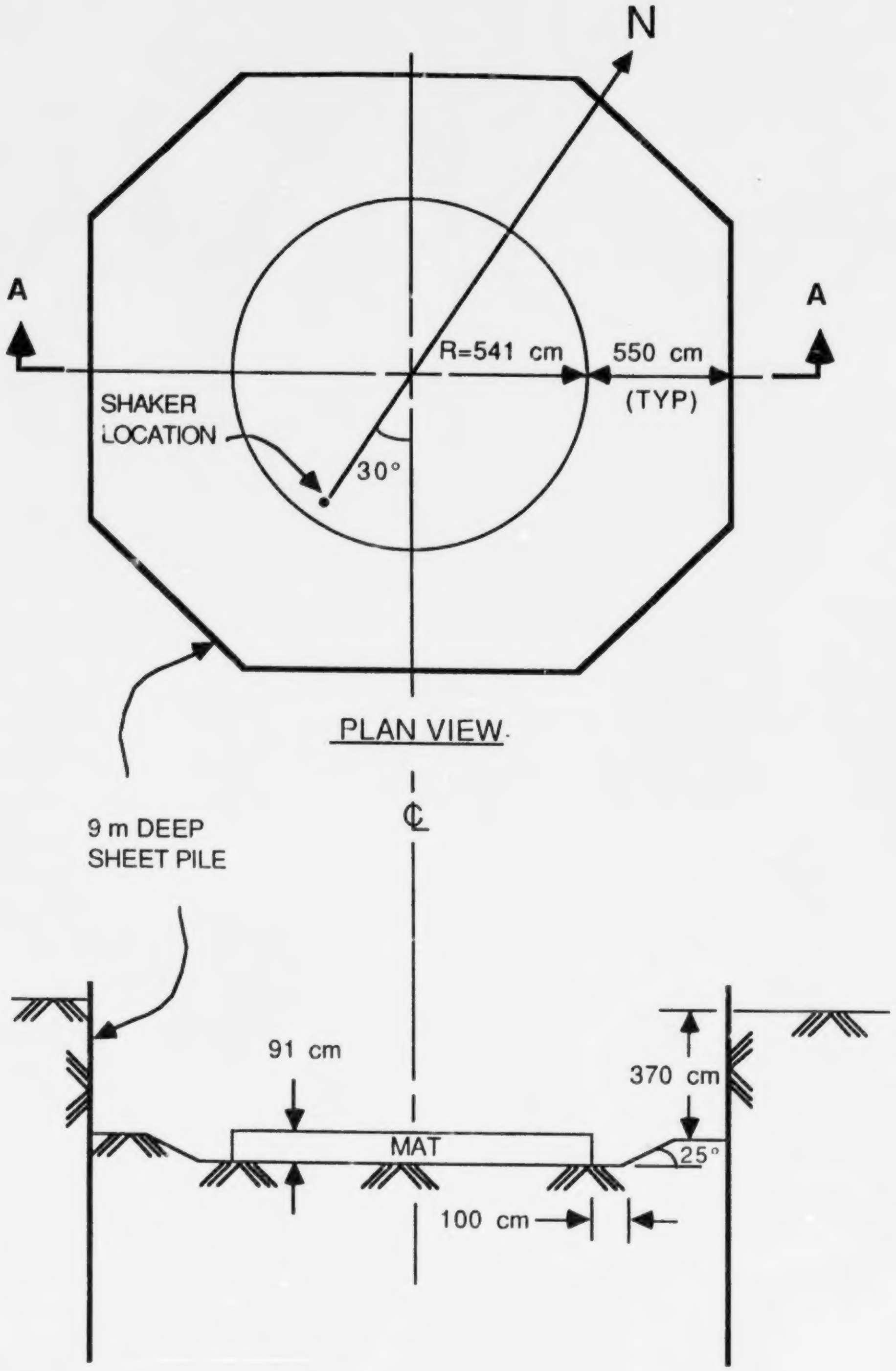
N
A
A
R=541 cm
550 cm
(TYP)
SHAKER
LOCATION
30°
9 m DEEP
SHEET PILE
℄
91 cm
370 cm
MAT
25°
100 cm

PLAN VIEW

SECTION A-A

Figure 3. Configuration during Vibration Tests on Basemat

BEST COPY AVAILABLE

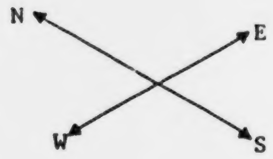

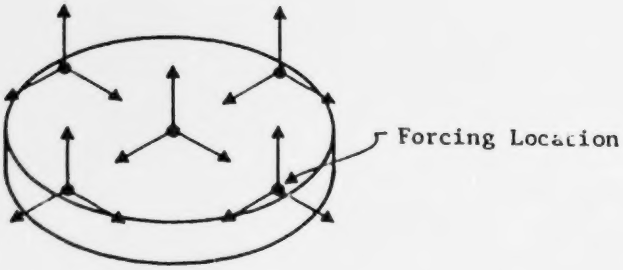
Forcing Location

Figure 4. Vibration Test Instrumentation of Basemat

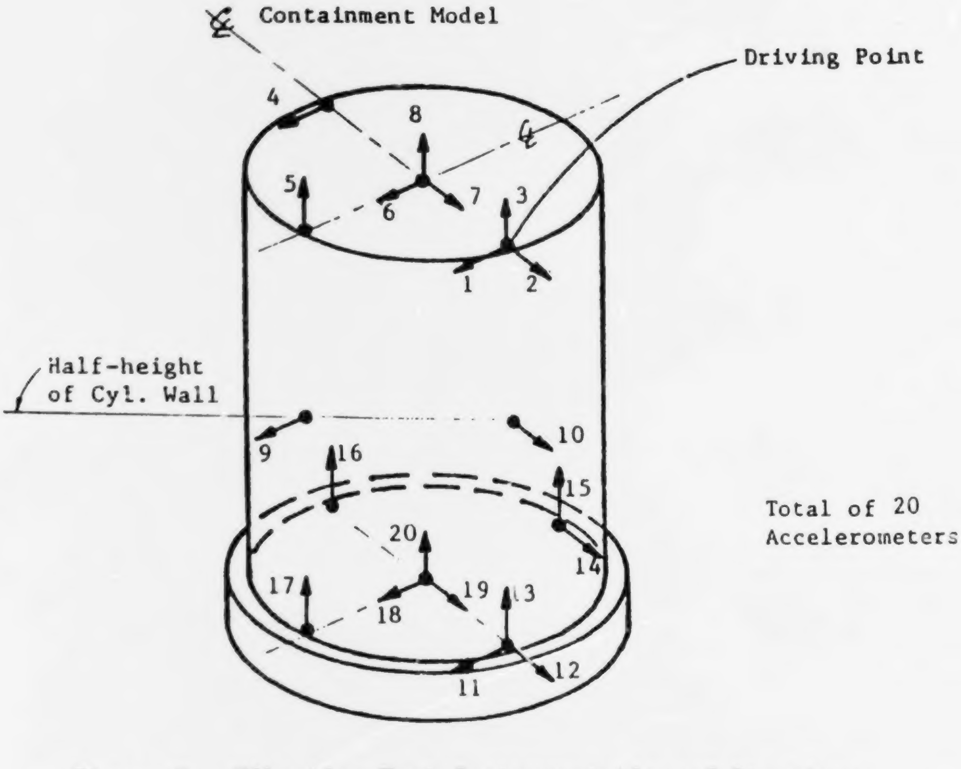
Containment Model
Driving Point
Half-height of Cyl. Wall
Total of 20 Accelerometers
1
2
3
4
5
6
7
8
9
10
11
12
13
14
15
16
17
18
19
20

Figure 5. Vibration Test Instrumentation of Structure

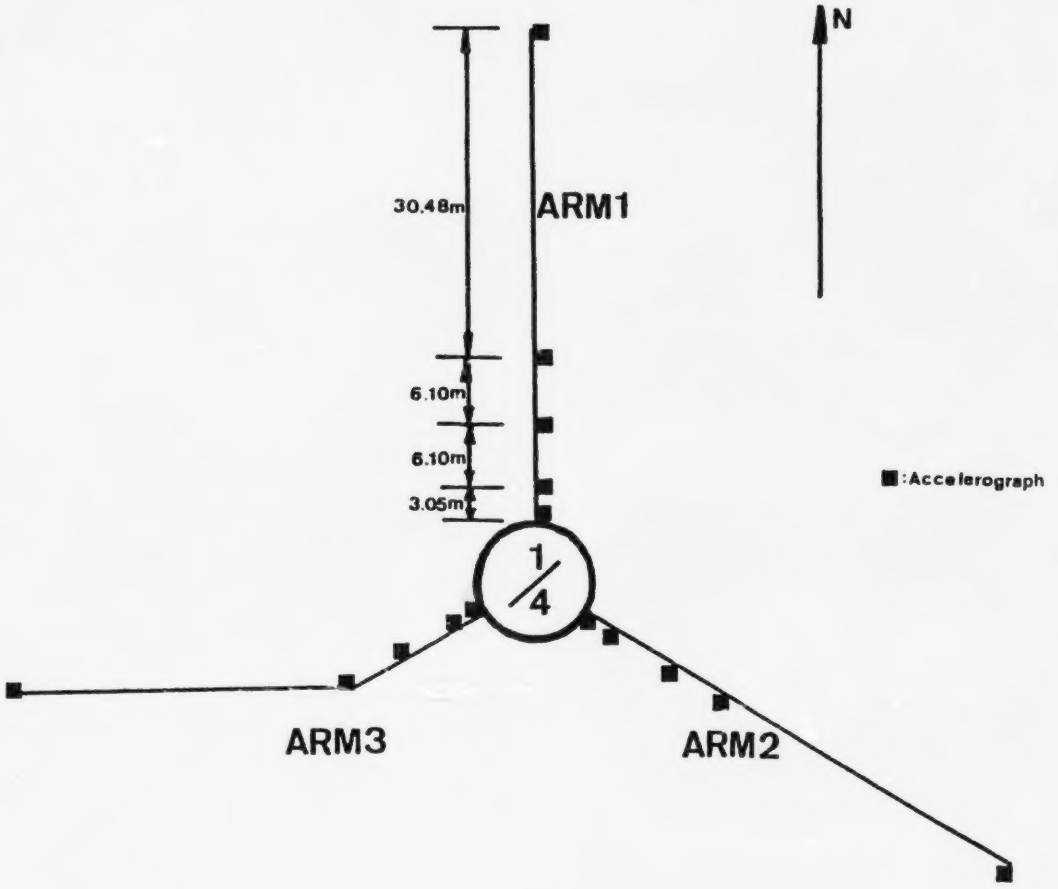
N
30.48m
ARM1
6.10m
6.10m
3.05m
■:Accelerograph
1/4
ARM3
ARM2

Figure 6. The Surface Instrumentation Array

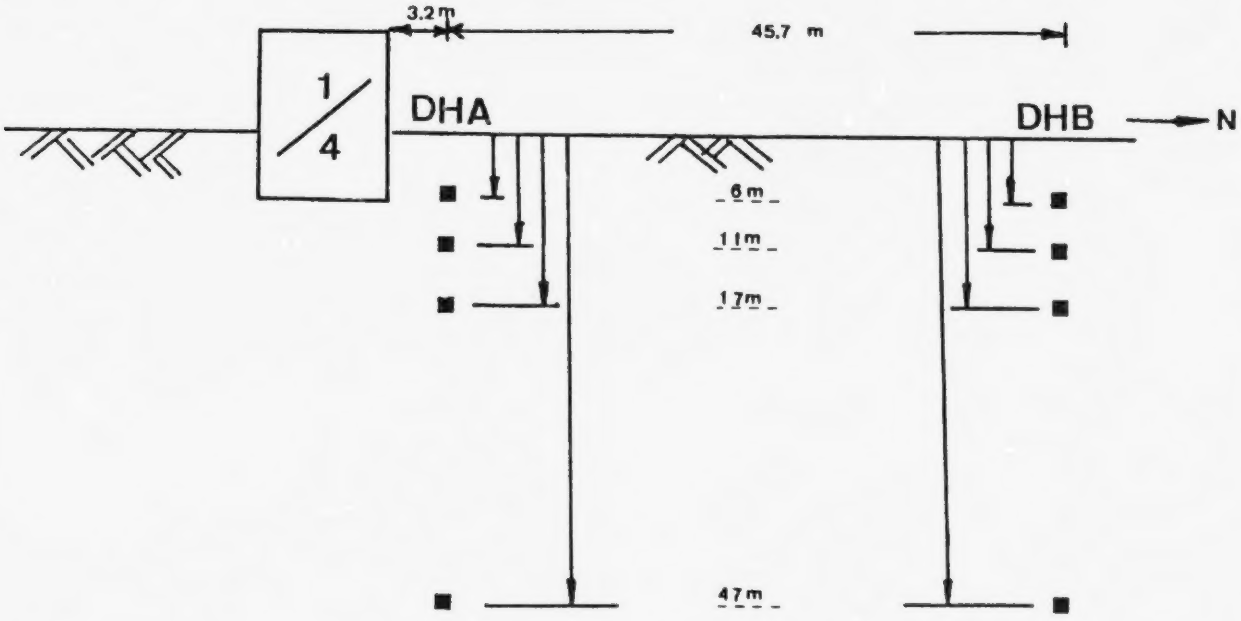
3.2m
45.7 m
1/4
DHA
DHB
N
6m
11m
17m
47m

Figure 7. The Downhole Instrumentation

289

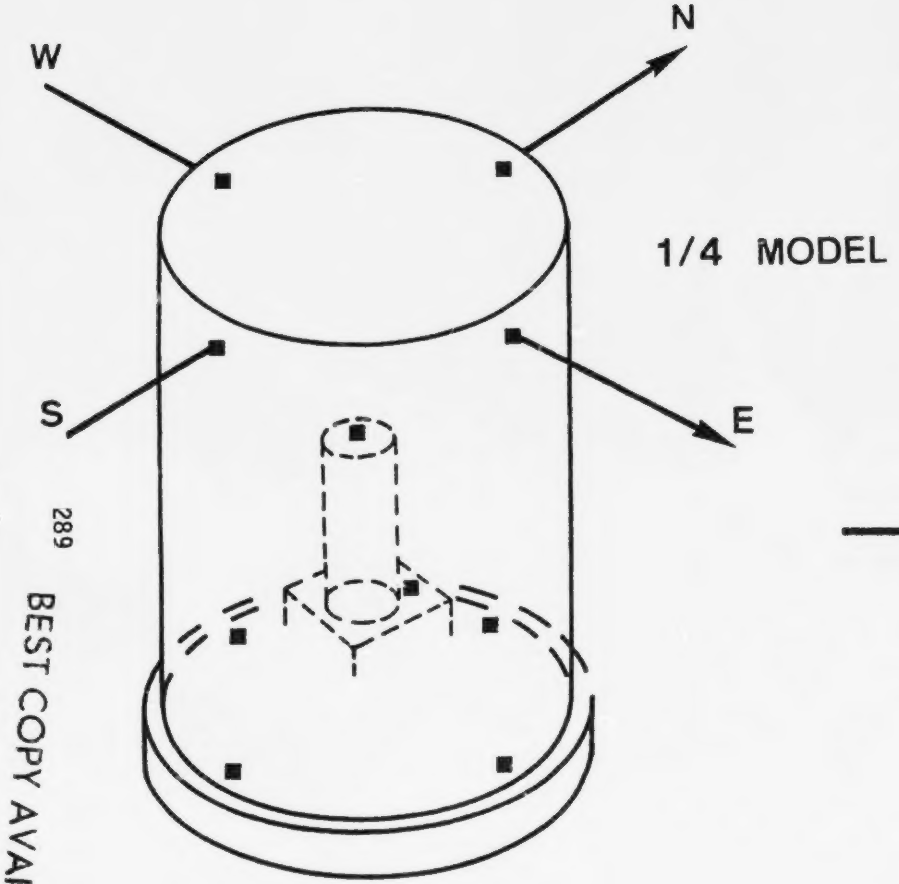

■ denote acclerometers

Figure 8. The Structural Instrumentation

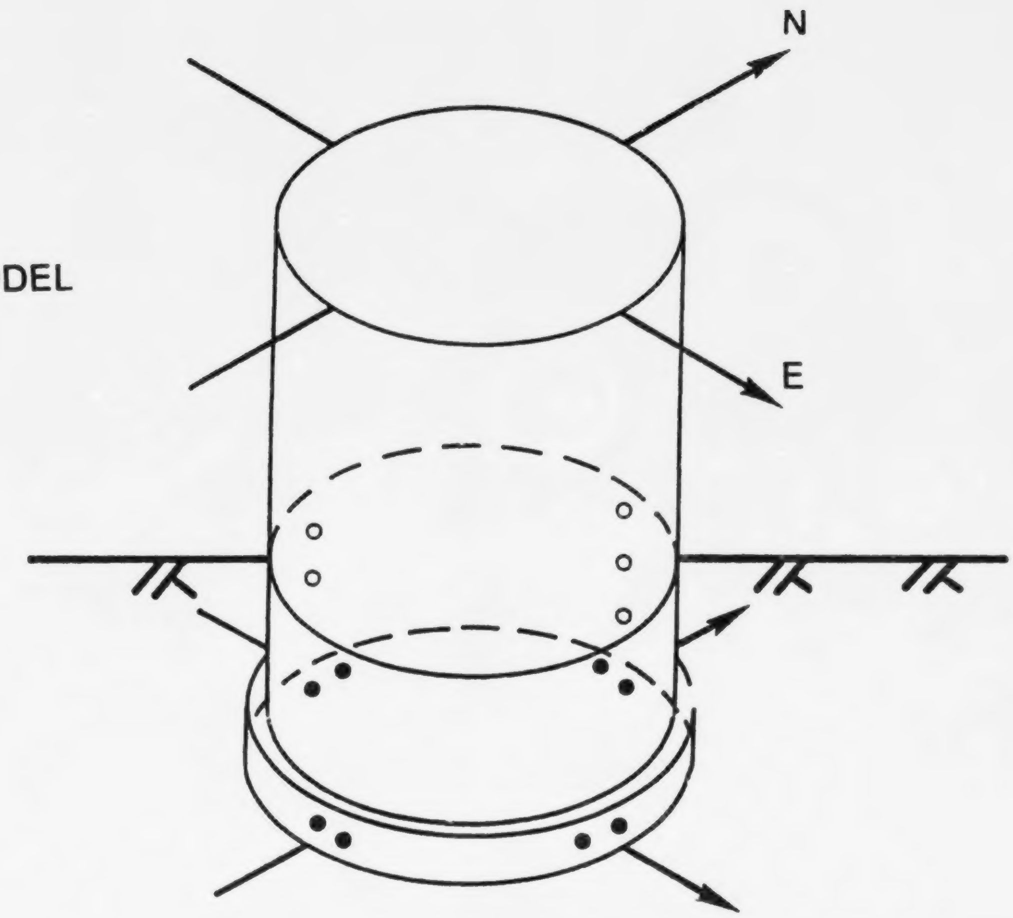

● denote pressure gages under basement

○ denote pressure gages on the side surface

Figure 9. The Interfacial Instrumentation

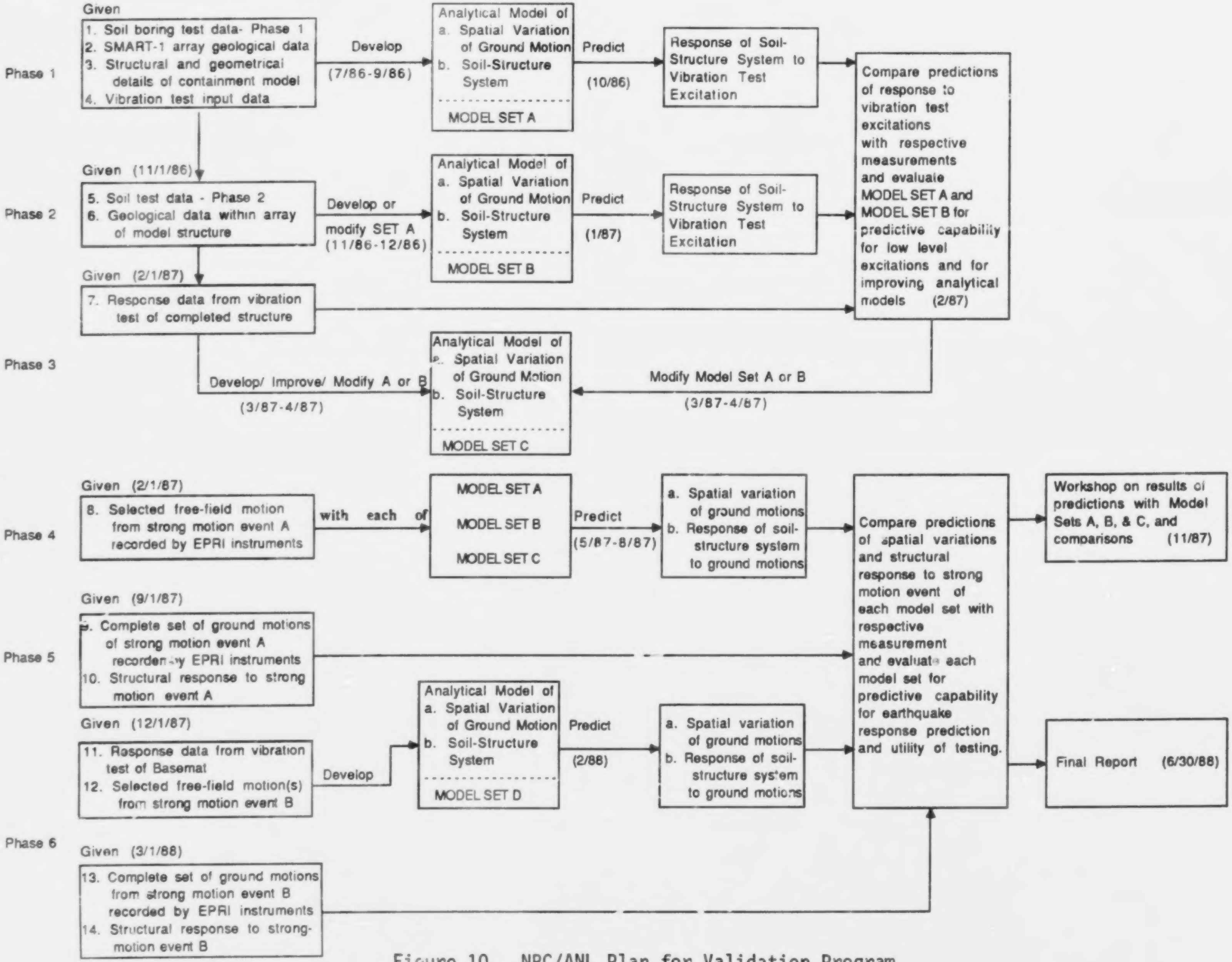
Phase 1
Given
1. Soil boring test data- Phase 1
2. SMART-1 array geological data
3. Structural and geometrical details of containment model
4. Vibration test input data
Develop
(7/86-9/86)
Analytical Model of
a. Spatial Variation of Ground Motion
b. Soil-Structure System
MODEL SET A
Predict
(10/86)
Response of Soil-Structure System to Vibration Test Excitation
Compare predictions of response to vibration test excitations with respective measurements and evaluate MODEL SET A and MODEL SET B for predictive capability for low level excitations and for improving analytical models (2/87)
Phase 2
Given (11/1/86)
5. Soil test data - Phase 2
6. Geological data within array of model structure
Develop or modify SET A
(11/86-12/86)
Analytical Model of
a. Spatial Variation of Ground Motion
b. Soil-Structure System
MODEL SET B
Predict
(1/87)
Response of Soil-Structure System to Vibration Test Excitation
Given (2/1/87)
7. Response data from vibration test of completed structure
Phase 3
Develop/ Improve/ Modify A or B
(3/87-4/87)
Analytical Model of
a. Spatial Variation of Ground Motion
b. Soil-Structure System
MODEL SET C
Modify Model Set A or B
(3/87-4/87)
Phase 4
Given (2/1/87)
8. Selected free-field motion from strong motion event A recorded by EPRI instruments
with each of
MODEL SET A
MODEL SET B
MODEL SET C
Predict
(5/87-8/87)
a. Spatial variation of ground motions
b. Response of soil-structure system to ground motions
Compare predictions of spatial variations and structural response to strong motion event of each model set with respective measurement and evaluate each model set for predictive capability for earthquake response prediction and utility of testing.
Workshop on results of predictions with Model Sets A, B, & C, and comparisons (11/87)
Phase 5
Given (9/1/87)
9. Complete set of ground motions of strong motion event A recorded by EPRI instruments
10. Structural response to strong motion event A
Given (12/1/87)
11. Response data from vibration test of Basemat
12. Selected free-field motion(s) from strong motion event B
Develop
Analytical Model of
a. Spatial Variation of Ground Motion
b. Soil-Structure System
MODEL SET D
Predict
(2/88)
a. Spatial variation of ground motions
b. Response of soil-structure system to ground motions
Final Report (6/30/88)
Phase 6
Given (3/1/88)
13. Complete set of ground motions from strong motion event B recorded by EPRI instruments
14. Structural response to strong-motion event B

Figure 10. NRC/ANL Plan for Validation Program

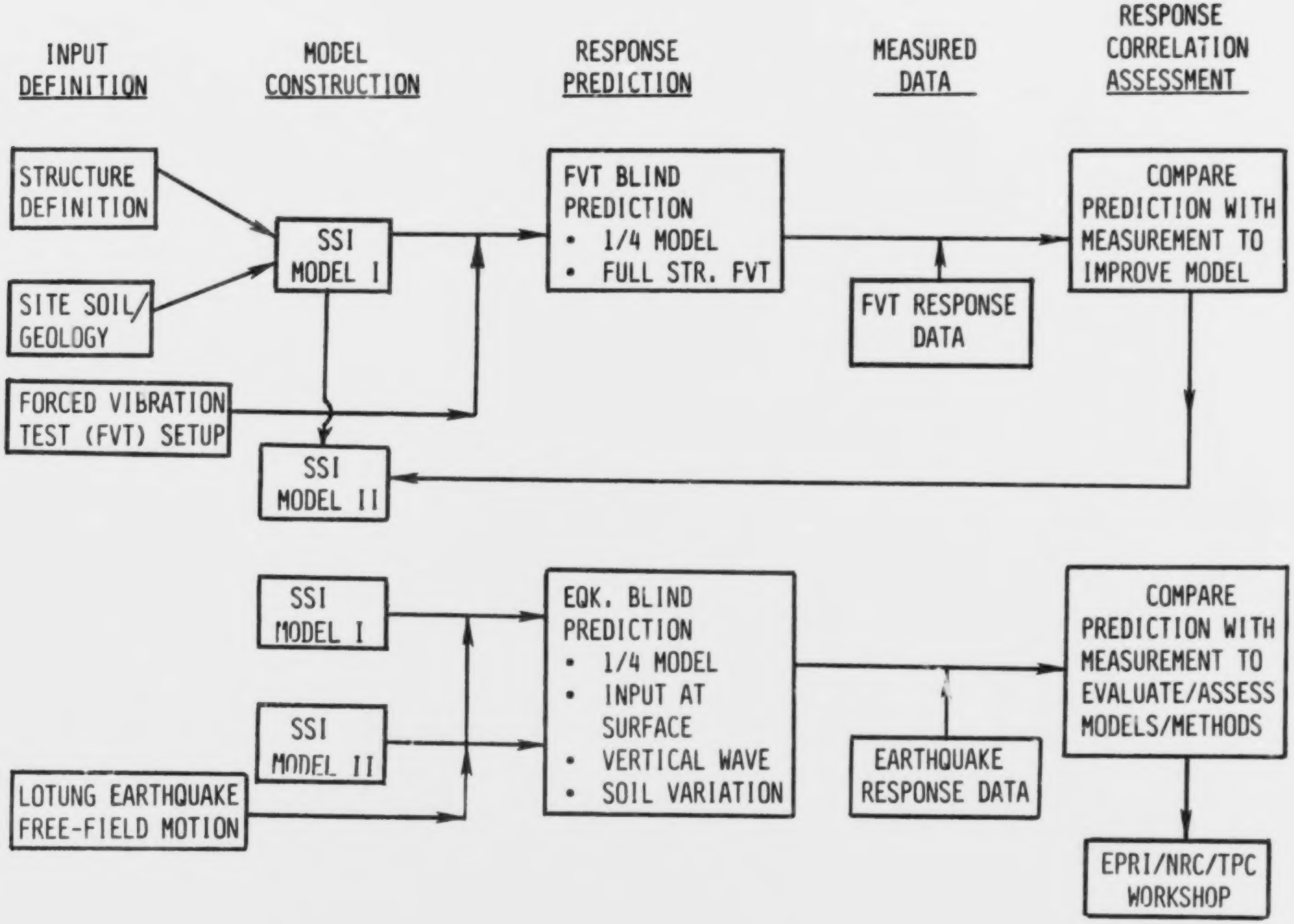
INPUT DEFINITION
MODEL CONSTRUCTION
RESPONSE PREDICTION
MEASURED DATA
RESPONSE CORRELATION ASSESSMENT
STRUCTURE DEFINITION
SITE SOIL/ GEOLOGY
FORCED VIBRATION TEST (FVT) SETUP
SSI MODEL I
SSI MODEL II
FVT BLIND PREDICTION
• 1/4 MODEL
• FULL STR. FVT
FVT RESPONSE DATA
COMPARE PREDICTION WITH MEASUREMENT TO IMPROVE MODEL
SSI MODEL I
SSI MODEL II
LOTUNG EARTHQUAKE FREE-FIELD MOTION
EQK. BLIND PREDICTION
• 1/4 MODEL
• INPUT AT SURFACE
• VERTICAL WAVE
• SOIL VARIATION
EARTHQUAKE RESPONSE DATA
COMPARE PREDICTION WITH MEASUREMENT TO EVALUATE/ASSESS MODELS/METHODS
EPRI/NRC/TPC WORKSHOP

Figure 11. SSI Analysis for Lotung Seismic Experiment (EPRI Program)

291

| Test No. | Run No. | Shaker | Eccentricity, in Kg-m | Direction of Forcing | Starting Frequency, in Hz | Ending Frequency, in Hz | No. of Freq.[4] | Force Amplitude, in N At Starting Frequency | Force Amplitude, in N At Ending Frequency |
|---|---|---|---|---|---|---|---|---|---|
| 1 | 2 | MK-12 | 0.545 | R[1] | 20.10 | 30.04 | 20 | 8693 | 19420 |
| 2 | 1 | MK-12 | 0.545 | T[2] | 20.20 | 30.13 | 26 | 8779 | 19530 |
| 3 | 1 | MK-12 | 0.545 | V[3] | 20.00 | 40.34 | 48 | 8606 | 35010 |
| 4 | 1 | MK-13 | 2.00 | R | 9.00 | 20.11 | 55 | 6395 | 31930 |
| 5 | 1 | MK-13 | 11.40 | R | 5.00 | 10.07 | 48 | 11250 | 45600 |
| 6 | 1 | MK-13 | 28.50 | R | 1.00 | 6.063 | 88 | 1125 | 41360 |
| 7 | 1 | MK-13 | 28.40 | T | 1.00 | 6.090 | 62 | 1121 | 41590 |
| 8 | 1 | MK-13 | 11.36 | T | 5.00 | 10.07 | 48 | 1121 | 45440 |
| 9 | 1 | MK-13 | 2.00 | T | 9.00 | 21.05 | 58 | 6395 | 34985 |
| 10 | 1 | MK-13 | 2.00 | V | 9.00 | 21.09 | 43 | 6395 | 35110 |
| 11 | 1 | MK-13 | 11.66 | V | 2.50 | 5.697 | 22 | 2877 | 14940 |
| 11 | 2 | MK-13 | 11.66 | V | 5.00 | 9.423 | 33 | 11510 | 40870 |

1. V = Vertical
2. R = Radial (North-South)
3. T = Tangential (East-West)
4. The frequencies are not equally spaced.

Table 1. Basemat Excitation

| Test No. | Run No. | Shaker | Eccentricity, in Kg-m | Direction of Forcing | Starting Frequency, in Hz | Ending Frequency, in Hz | No. of Freq.[3] | Force Amplitude, in N At Starting Frequency | At Ending Frequency |
|---|---|---|---|---|---|---|---|---|---|
| 1 | 1 | MK-12 | 0.55 | R[1] | 15.00 | 30.52 | 76 | 4885 | 19880 |
| 2 | 1 | MK-12 | 0.55 | T[2] | 15.00 | 30.10 | 71 | 4885 | 19670 |
| 3 | 1 | MK-13 | 2.00 | R | 9.00 | 18.06 | 71 | 6395 | 25760 |
| 4 | 1 | MK-13 | 11.50 | R | 5.00 | 10.07 | 57 | 1135 | 46070 |
| 5 | 1 | MK-13 | 28.50 | R | 1.00 | 6.007 | 97 | 1125 | 40600 |
| 6 | 1 | MK-13 | 28.50 | T | 1.00 | 6.020 | 79 | 1125 | 40770 |
| 7 | 1 | MK-13 | 11.50 | T | 5.00 | 10.11 | 47 | 1135 | 46400 |
| 8 | 1 | MK-13 | 2.00 | T | 9.00 | 18.06 | 71 | 6395 | 25760 |

1. R = Radial (North-South)
2. T = Tangential (East-West)
3. The frequencies are not equally spaced.

Table 2. Excitation of Completed Structure

293

BLANK PAGE

# HDR PHASE II VIBRATIONAL EXPERIMENTS

**L. Malcher, HDR Project**
**Kernforschungszentrum Karlsruhe, FRG**

**C. A. Kot, Argonne National Laboratory**
**Argonne, Illinois, U.S.A.**

## ABSTRACT

As part of the second phase of vibrational/earthquake investigations at the HDR (Heissdampfreaktor) Test Facility in Kahl/Main, FRG, high-level shaker tests (SHAG) were performed during June and July 1986. The purpose of these experiments was to investigate full-scale structural response, soil/structure interaction, and piping and equipment response under strong excitation conditions. While global safety considerations imposed load limitations, the HDR soil/structure system was nevertheless tested to its capacity limits. The performance of pipe support systems in as many as seven different multiple support pipe hanger configurations, ranging from flexible to stiff systems, was evaluated in the tests. Data obtained in the tests will be used to validate analysis methods.

## 1. Introduction

The HDR (Heissdampfreaktor) Test Facility (see Fig. 1) in Kahl/Main, FRG, has since 1975 been used to perform vibrational, thermal hydraulic, blowdown and other experiments related to the design and safety of nuclear power plants. During the first phase of the HDR Program of testing (PHDR), the HDR building and equipment were subjected to many low- and medium-level mechanical excitations (shaker, buried explosives, snapback). In the second phase of vibrational/earthquake investigations the HDR system is being tested at high levels of excitation. The centerpiece of these investigations is the high-level shaker tests (SHAG), which were performed at the HDR in June and July 1986. Their purpose was to investigate full-scale structural response, soil/structure interaction, and piping and equipment response under strong excitation conditions, i.e., under excitation levels that will induce significant strains in the structure and soil and produce nonlinear effects in the soil/structure system and piping. As with all HDR experiments, the primary intent is to use the SHAG tests to verify and validate calculational procedures and analysis methods. At the same time the experimental data provide direct information on the response and performance of structural systems, piping, and equipment under high dynamic loading; such information may have direct applicability to understanding the behavior of nuclear power plant systems.

The SHAG experiments were performed as part of the HDR Safety Project (PHDR) conducted by the Kernsforschungszentrum Karlsruhe (KfK), and were supported by the Government of the Federal Republic of Germany (FRG) and the U.S. Nuclear Regulatory Commission, Office of Research (NRC/RES). The NRC involvement is part of a program on the validation of seismic calculational methods conducted by Argonne National Laboratory (ANL) for NRC/RES. Additional participants in the SHAG experiments included the Electric Power Research Institute (EPRI), the Idaho National Engineering Laboratory (INEL), and German as well as U.S. industry.

## 2. Shaker Design and Operation

The shaker used in the SHAG experiments is a very large eccentric-mass coastdown shaker designed by ANCO Engineers, Inc., of Culver City, CA (Ref. 1). Most of the design and functional calculations of the shaker's dynamic behavior were performed by the Fraunhofer Institut für Betriebsfestigkeit (LBF), Darmstadt, FRG (Ref. 2). Safety calculations for the shaker, its mounting and the HDR soil/structure system were performed by the Engineering Firms of Zerna-Schnellenbach in Bochum, FRG (Ref. 3) and Hochtief AG in Frankfurt, FRG (Ref. 4).

The masses of each of the two shaker arms (which form the eccentricity) are made up of an assembly of steel plates mounted on the arm base-plate, and can be varied up to a total of 40 tons each. The shaker is capable of developing in excess of 1000 tons of force. It is mounted in a very stiff frame on the operating floor of the HDR building (see Fig. 2) to provide strong excitation to the entire HDR soil/structure/equipment system. The shaker was designed to develop maximum accelerations of the HDR building on the order of 5 $m/s^2$ and maximum displacement of about ± 7 cm. The total eccentricity of the shaker was designed to vary between 4,000 and 145,000 kgm. During operation the shaker is brought to the desired starting speed (1.6 - 8.0 Hz) with the two arms in a balanced condition. One of its arms is permanently fixed to the drive shaft, while the other arm is hinged to the shaft by a slightly eccentric support. In the balanced condition the movable arm is fixed by an explosive bolt. After the desired starting speed is reached the shaker arms are uncoupled from the drive system. Firing the explosive bolt releases the movable arm, which swings around and couples with the fixed arm, forming a large eccentric mass that provides a variable (in both magnitude and direction) force during coastdown. As the shaker coasts down through the fundamental frequencies of the HDR soil/structure system, strong resonances occur. During the entire shaker run there is strong coupling and feedback between HDR response and shaker forcing, resulting in a nonlinear coupled system. Details of shaker design and operation were discussed in the previous Water Reactor Safety Research (WRSR) Information Meeting (Ref. 5); a photograph of the shaker is shown in Fig. 3.

Preliminary tests were conducted in February 1986 to check out the functionality of the shaker. Five tests were planned, three with the shaker arms balanced (no loads on the HDR building) and two with the shaker arms unbalanced (providing excitation to the building). The tests with unbalanced shaker arms were completely successful, proving the design concept and operation of the shaker. In the experiments with the balanced arms, however, it was not possible to reach the desired shaker frequencies because the air resistance was much higher than expected, and the torque that could be generated by the drive system was limited. Thus, the maximum frequency reached with no plates on the shaker arms was 5.25 Hz rather than the desired 8.0 Hz. This problem was subsequently overcome by providing an enclosure for the shaker (see Fig. 4), which substantially lowered the aerodynamic drag. It was also found that the eccentricity of the bare arms of the shaker was substantially higher at 5,700 kgm than the estimated value of 4,000 kgm. Since this would have generated forces much higher than intended during the 8.0 Hz tests, the mass of the arms was reduced by cutting out part of the base plates. This reduced the eccentricity of the bare arms of the shaker to about 4,700 kgm. Just before the start of the SHAG experiments, the functionality of the shaker was tested again and all systems performed as expected.

## 3. SHAG Experiments

As stated earlier, the purpose of the SHAG tests was to investigate full-scale structure/soil, equipment, and piping response under strong vibrational excitation and to validate predictive analyses. While the interests of PHDR and NRC/RES includes all aspects of the SHAG testing, most other participants focused primarily on the behavior of piping systems. In particular, the response of the VKL (Versuchskreislauf) piping system with different multiple support (hanger) configurations was of interest to all participants.

The VKL piping (see Fig. 5) consists of a number of pipe runs ranging in nominal size from 100 to 250 mm. The piping is attached to the HDU vessel and associated manifolds and forms part of the experimental piping system at the HDR. The top of the pipe runs at about 28 m above ground level, just under the HDR operating floor (where the shaker is located). The original German hanger system provided primarily vertical dead weight support, and consisted of 11 spring and constant-force hangers and one threaded rod. The orignal intent was to compare in the SHAG tests the performance of this very flexible conventional support system with a typical U.S. stiff support system containing snubbers and struts. Also, as part of the NRC/RES Equipment Qualification Research Program, INEL intended to evaluate the performance of a typical U.S. gate valve during SHAG testing. Accordingly, an 8 in. valve was incorporated into the VKL piping system (see Fig. 6). INEL then designed a typical U.S. hanger system, adding six snubbers (see Fig. 7) and six rigid struts to the VKL hanger system and replacing one of the German spring hangers with a much higher rated hanger of the same type to accommodate the added weight of the valve as shown in Fig. 5.

EPRI and its industry associates intended to evaluate two additional hanger configurations. The first of these, designed by Bechtel Corporation, consists of energy absorber supports that damp out the motion of the piping through the plastic deformation of an assembly of steel plates incorporated into the support. The other configuration uses seismic stops, designed by R. L. Cloud and Associates, that replace the snubbers. This system allows free motion until a certain displacement is reached, at which the pipe impacts the stops, limiting further movement in the given direction. As part of German industry contribution to the SHAG experiments, Kraftwerk Union (KWU), Offenbach, FRG, designed a hanger system for the VKL piping, which uses, in addition to the dead weight supports, only five rigid struts placed so as to prevent large dynamic motions of the piping. All the alternative hanger designs of the VKL were motivated by the desire to replace snubbers, which have proved troublesome in nuclear power plants. Therefore, the objective of these experiments was to compare and evaluate the behavior of the VKL piping system with the different support systems under identical loading conditions.

## 3.1 Test Plans

In early March 1986 a meeting was held at the HDR Test Facility in Kahl/Main, FRG, to plan the SHAG test matrix and sequence. A test period of 6 weeks was foreseen, starting on 2 June 1986 and continuing through 11 July 1986. The tests were to include all five hanger configurations described above. All but two tests were designed to generate nominally the same peak force of $10^4$ kN, starting with different shaker frequencies. Higher shaker frequencies (8.0, 5.6 Hz) were intended primarily for piping excitation, while the lower frequencies (1.6, 2.1, 3.1 Hz) were intended primarily to challenge the soil/structure system.

Results of safety calculations (Ref. 3) and the functionality tests indicated that some of the test runs would severely challenge the HDR building. In particular, the 1.6 Hz runs were expected to strongly excite the rocking mode (nominally at 1.4 Hz) and the 3.1 Hz tests would strongly excite the out-of-phase bending mode at 2.5 Hz. In both cases it was thought that the foundation slab of the HDR would be severely challenged. Also, loads in the embedded portion of the outer shield building walls were expected to be high. Thus, in the resulting test matrix (Fig. 8) the test runs that would challenge the HDR structure were placed at the end of the test sequence. Four groups of five tests each were to compare the response of the VKL piping system with the different hanger configurations. Two of these test sequences (at 5.6 and 8.0 Hz) were to be run in hot conditions (210°C), permitting the evaluation of piping response under both hot and cold conditions. Also, under hot conditions it is possible to pressurize the VKL to 70 bars and thus better evaluate the performance of the gate valve under combined vibrational excitation and hydrodynamic loading.

More than 330 channels of instrumentation were planned by the HDR Central Measurement Facility (ZMA), with acceleration and strain being the primary measurements of structure and equipment response. All essential parts of the facility were instrumented, e.g., acceleratio[illegible] of the HDR building (structure) and ground accelerations in two orthogonal radial directions and at two depths were measured. Also, all piping systems of interest were instrumented, as were major components and vessels. Strain measurements in the HDR walls, foundation slab, piping and vessels were provided. Some of these measurements were intended as safety checks, as were some of the measurements of acceleration and velocity at the VAK (Versuchsatomkraftwerk) installation. The VAK (see Fig. 1) is a recently decommissioned experimental power reactor that shares the same site with the HDR and is located about 100 m from the HDR (see Ref. 6).

BEST COPY AVAILABLE

The HDR instrumentation was supplemented by more than 100 channels concentrated on the VKL piping system and the 8 in. U.S. gate valve. This instrumentation was provided by INEL under the sponsorship of primarily NRC/RES with additional support from EPRI. Again, accelerometers predominated, with some displacement, force and strain measurements. Specifically, acceleration of the HDR walls at the points of VKL piping support attachment were measured (see Fig. 9). These measurements are intended to serve as input to post-test piping analysis calculations. Also the detailed response of the piping was measured, as were all operating parameters of the valve.

### 3.2 Test Performance

The main series of SHAG tests began as planned on 2 June 1986 with Test No. 34, which was run with the minimum available eccentricity of 4700 kgm at 6 Hz starting frequency. While the peak forces, accelerations, and displacements were close to values predicted by LBF (Ref. 2), the duration of the shaker coastdown was much longer (~ 100 s) than predicted (40 s). The reason for this is the use of the enclosure around the shaker. Its effect is to reduce aerodynamic drag both during shaker spinup and coastdown. Because of the long test duration, more energy is radiated to the surrounding soil causing stronger than expected vibrational effects at some distance from the HDR, e.g., at the VAK installation. While the measured accelerations at the VAK were at least an order of magnitude lower than deemed acceptable, the experiment led to protests from the VAK management.

With the agreement of all major participants, two more pipe support configurations for the VKL were added to the test matrix. One test each was planned for viscous damper supports of GERB, Berlin, Germany, and for modified viscous dampers designed by ANCO Engineers. Two of the GERB supports were used, while six of the ANCO supports replaced all snubbers in the U.S. NRC system. In order to avoid possible permanent damage to the VKL piping, the original HDR dead weight support system was modified by retaining the two rigid struts of the U.S. support system which are located adjacent to the spherical Tee (see Fig. 5).

Additional safety calculations by Hochtief AG (Ref. 4), as well as a "best estimate" soil/structure interaction calculation and detailed stress analyses performed by Weidlinger Associates, Palo Alto, CA (Ref. 7), indicated that the 1.6, 2.1 and 3.1 Hz tests, when run at full load ($10^4$ kN), would provide a more severe challenge to the HDR structure than anticipated. Reexamination of the structural drawings also indicated lower capacity in the embedded region of the walls of the shield building. This led to a reordering of the test sequence, with the high-frequency tests for the piping being advanced in the schedule. Thus, while the first week of testing proceeded essentially as planned, in the second week of testing, 8.0 Hz experiments with three pipe hanger configurations were performed with the piping in cold conditions.

A test delay occurred at the end of the first week when Test 37 (at 2.1 Hz and less than half of full load) resulted in considerable shifting in a section of the outer shield wall (around the equipment hatch), which was made

BEST COPY AVAILABLE

of concrete blocks. The concrete blocks had to be secured by a steel structure. Other delays came about because of interference from the VAK management and protests of antinuclear intervenors. All these problems necessitated reevaluation, inspection, and reapproval for further testing by the Technical Evaluation Agency (TÜV) and the Licensing Agency of the Bavarian State Ministry. Hence, no tests were performed during the third week.

At the same time the concern for the global integrity of the HDR structure necessitated a detailed evaluation of crucial test data (accelerations, displacements, and strains) after each test. These measurements were compared with predictions and estimates of structural capacity to guide the progress of experiments. All these factors caused the test period to extend to nearly 8 weeks. The tests actually performed and their sequence are listed in Fig. 10. As indicated, only the 8.0, 5.6 and 6.0 Hz tests were performed at or near full load ($10^4$ kN); all other tests were performed at reduced loads. Only the 4.5 Hz runs were performed with hot conditions in the piping system. All tests at 3.1 Hz and 2.1 Hz (at full load) were dropped to avoid challenging the walls of the outer shield building, which experience their most severe strains in the out-of-phase bending mode. The 1.6 Hz tests, which involve the rocking mode, were limited to a maximum of about two-thirds of full load. A comparison of the planned and actual force-frequency region for the SHAG tests is shown in Fig. 11. All testing was completed on 22 July 1986. Detailed measurements of the response of the VKL piping and the performance of the 8 in. gate valve were carried out during nearly all experiments, except for the 1.6 Hz tests, which were conducted last (see Fig. 10).

Ambient response measurement tests (RAU) were carried out before, during, and after the performance of the SHAG experiments. The RAU tests provide a measure of the changes in dynamic characteristics that occur in the HDR soil/structure system due to high-level excitation produced by the SHAG testing. The combined SHAG and RAU results will allow the investigation of nonlinear effects.

## 4. Discussion

Pretest and blind post-test calculational predictions are performed by a number of organizations for many aspects of the SHAG tests. To allow for orderly completion of the post-test calculations, all experimental data are being held secure and will not be released until these calculations are completed. It is currently anticipated that at least the building response and soil/structure interaction data will be released in December 1986. The calculational efforts completed or in progress include predictions of the soil/structure interaction, building response (including stress analyses), and piping response. The piping response calculations are being done in the blind post-test mode and use measured building response as input.

The SHAG tests were planned to provide the maximum possible loading for the HDR soil/structure system and the piping without inducing global structure/soil failure, which would endanger the integrity of the containment. As indicated above, safety considerations for the HDR building necessitated some curtailment of the test plans (Fig. 11). In particular, the test runs that strongly excite the main structural modes (out-of-phase bending nominally at 2.5 Hz and rocking nominally at 1.4 Hz) had to be reduced in load or abandoned. The major reason for this is the weakness of the outer concrete HDR shield building, whose cylindrical walls have very little reinforcement in the embedded region and which could thus fail in tension during bending.

In spite of the limitations imposed on the testing, the overall goals of the SHAG tests were accomplished. Peak accelerations and displacements in the HDR building were quite substantial and nonlinear behavior of the soil/structure system was clearly observed. Much local damage occurred, such as concrete cracking and interior masonry wall collapse. Substantial amounts of energy were transferred to the surrounding soil, particularly during experiments challenging the rocking mode (1.6 Hz runs). This is evidenced by the high accelerations measured in the soil, cracking of soil (circumferential) away from the building, separation at the soil/structure interface, and soil subsidence. Impact occurred between the HDR building and the equipment tower as well as the connecting bridge to the office building. Strains in the HDR shield building walls approached or exceeded their estimated limit values. Accelerations and motions of the VKL piping measured in the SHAG tests are comparable with values expected during strong-motion earthquakes.

## References

1. "Suggestions for Dynamic Test at HDR," Technical Note, ANCO Engineers, Culver City, CA, June 1982.

2. H. Idelberger and H. Steinhilber, "Rechnerische Simulation des Shakerverhaltens bei exzentrischer Lagerung eines Shakerarms," LBF, Darmstadt, FRG, Berich Nr. 568., PHDR Nr. 4269/85, 1 August 1985.

3. "Sicherheitsrechnung Zur Lastabtragung der Shakerkräfte bei hohen Anregungen," Zerna, Schnellenbach und Partner, Bochum, FRG, PHDR Nr. 4285/85, July 1985.

4. H. Werkle, W. Weber, and G. Waas, "Sicherheitsberechnungen Zur Standsicherheit von Baulichen Anlagenteilen des HDR bei Shakerversuchen T40," Hochtief AG, Frankfurt, FRG, PHDR N4. 4298/86, July 1986.

5. L. Malcher, H. Steinhilber, and C. A. Kot, "Heissdampfreaktor Phase II Vibration Tests," Proceedings of the U.S. NRC - 13th Water Reactor Safety Research Information Meeting, NUREG/CP-0072, Vol. 3, pp. 159-178, NBS-Gaithersburg, MD, October 22-25, 1985.

6. H. Idelberger and L. Malcher, "Auslegungsbericht - Shakerversuche im Reaktorgebäude HDR-Versuchsgruppe SHAG," Vs.-Nr: T40, PHDR-Arbeitsbericht Nr. 4.280/85, October 1985, Revised March 1986.

7. R. Mak, T. Piland, and D. Vaughan, "Analysis of the HDR Containment Structure Subjected to High Level Shaker Loading," Weidlinger Associates, Palo Alto, CA, Report R866DV, October 1986.

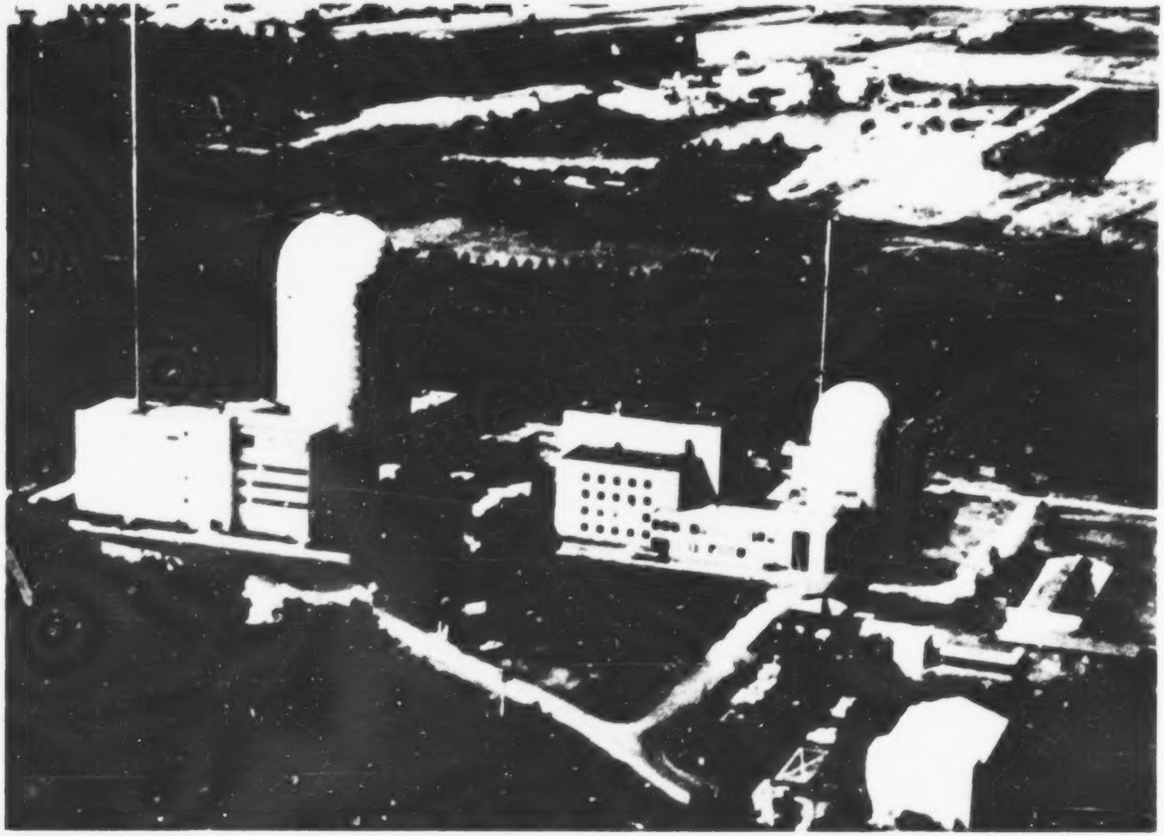

Fig. 1. Aerial View of HDR (left) and VAK (right) Facilities

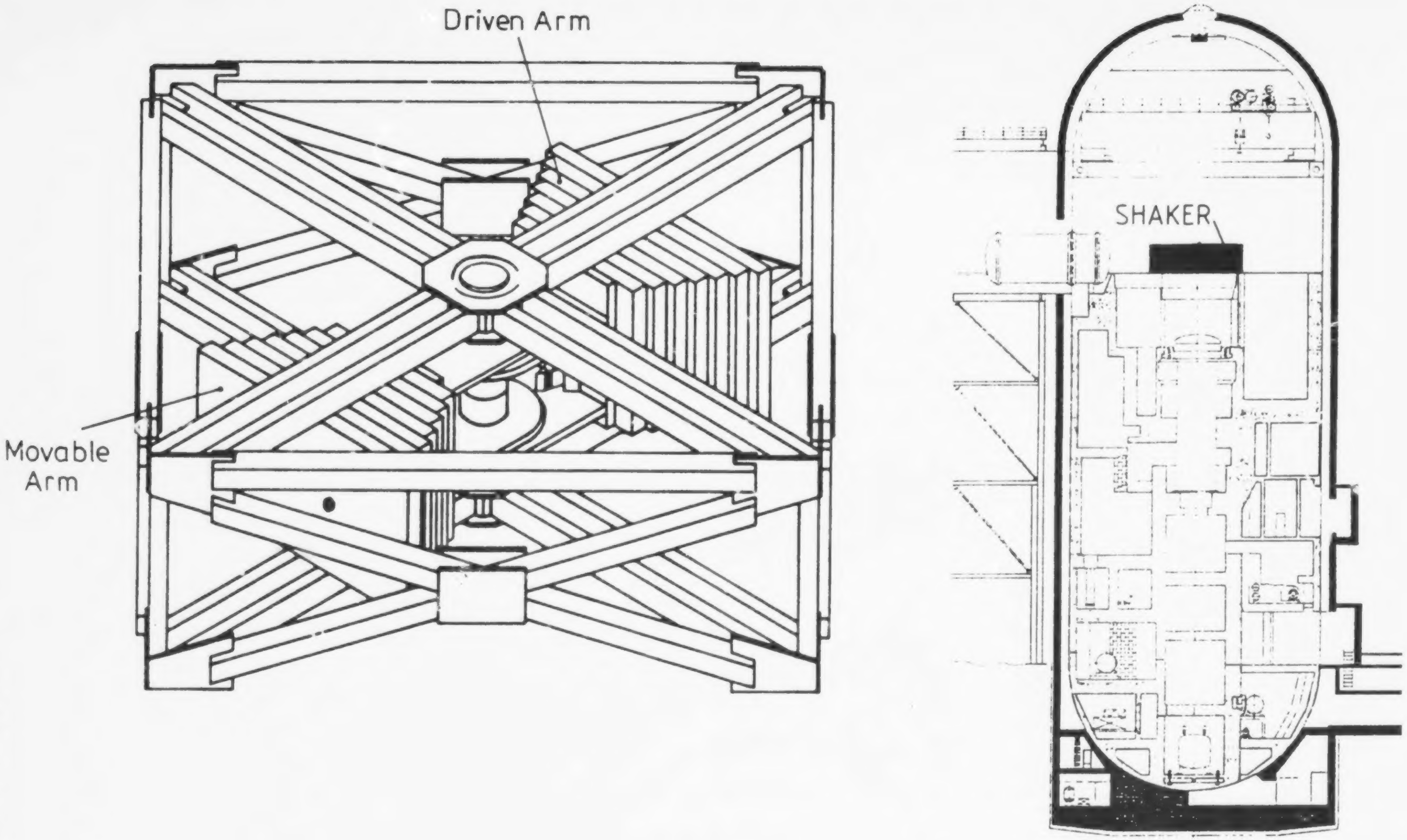
Driven Arm
Movable Arm
SHAKER

Fig. 2. ANCO MK16 Shaker (Final Design)

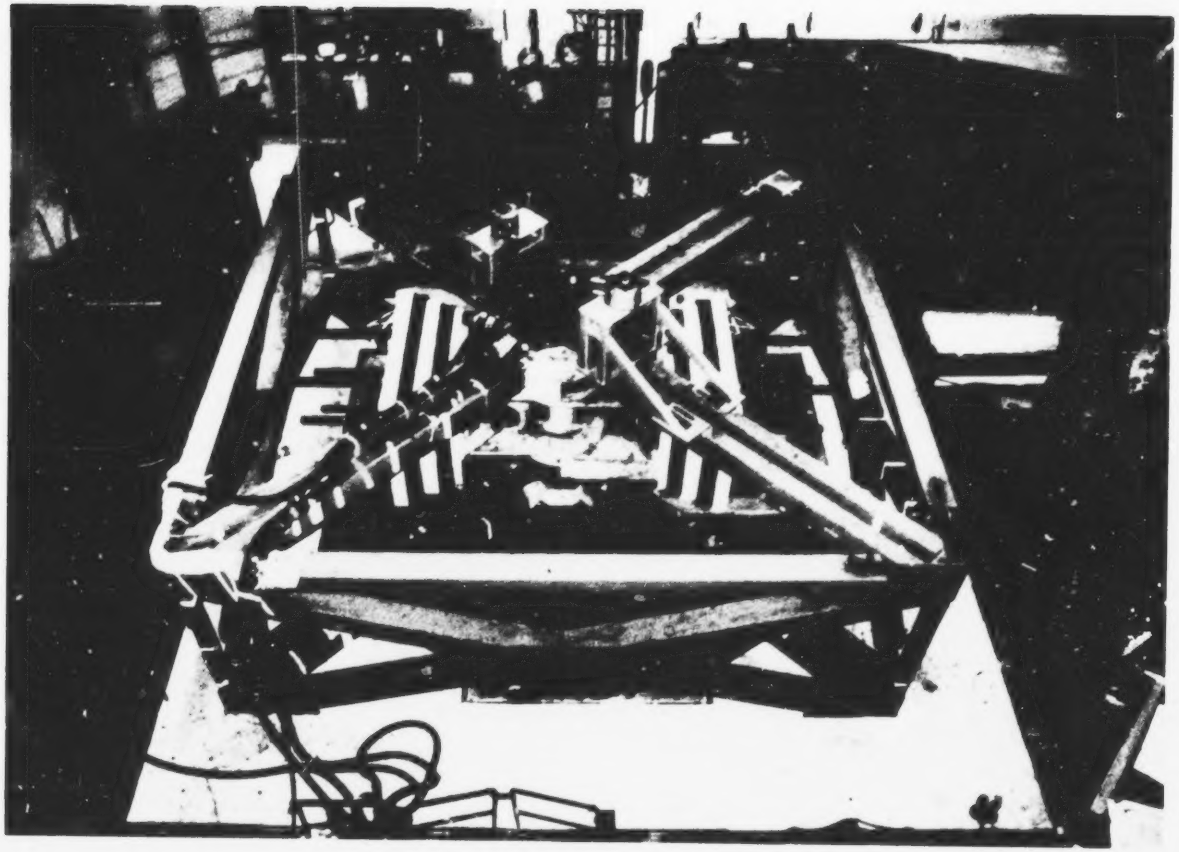

Fig. 3. Eccentric Mass Shaker in Balanced Condition

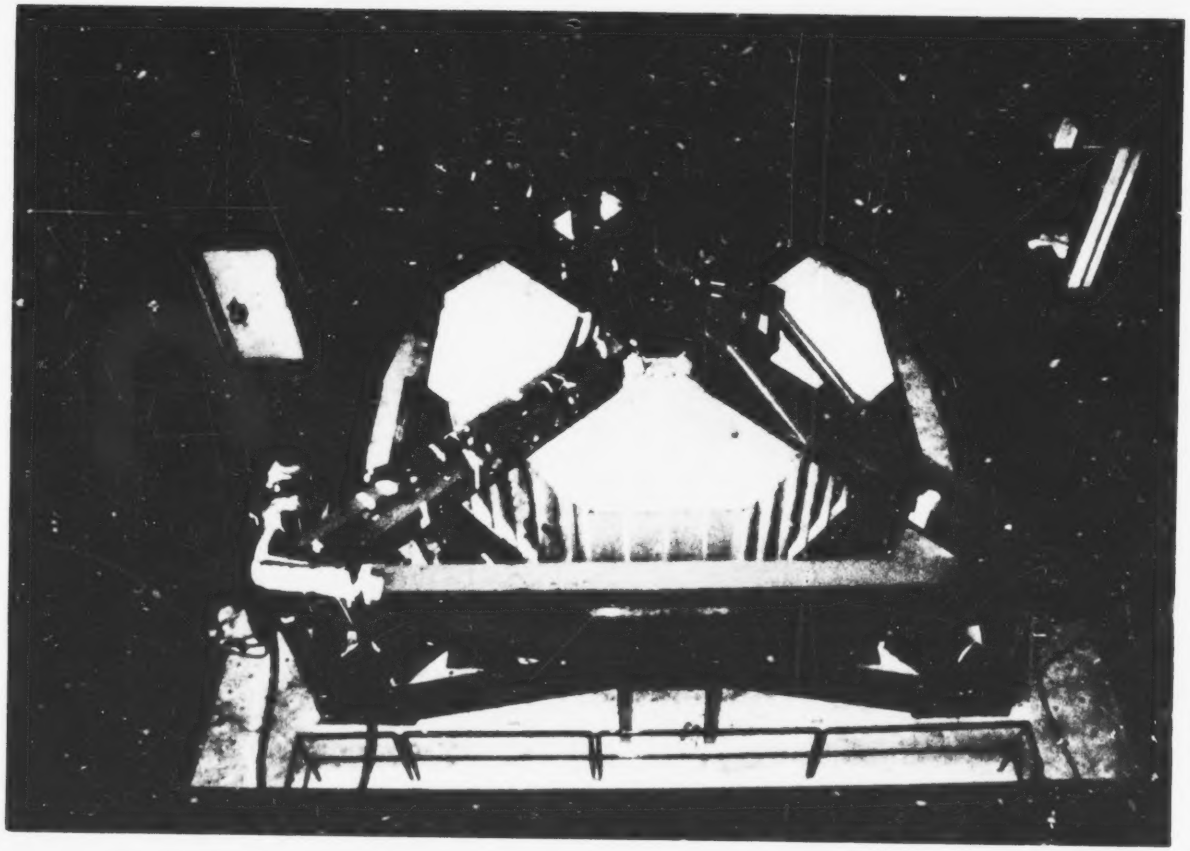

Fig. 4. Shaker Enclosure for Air Drag Reduction

305

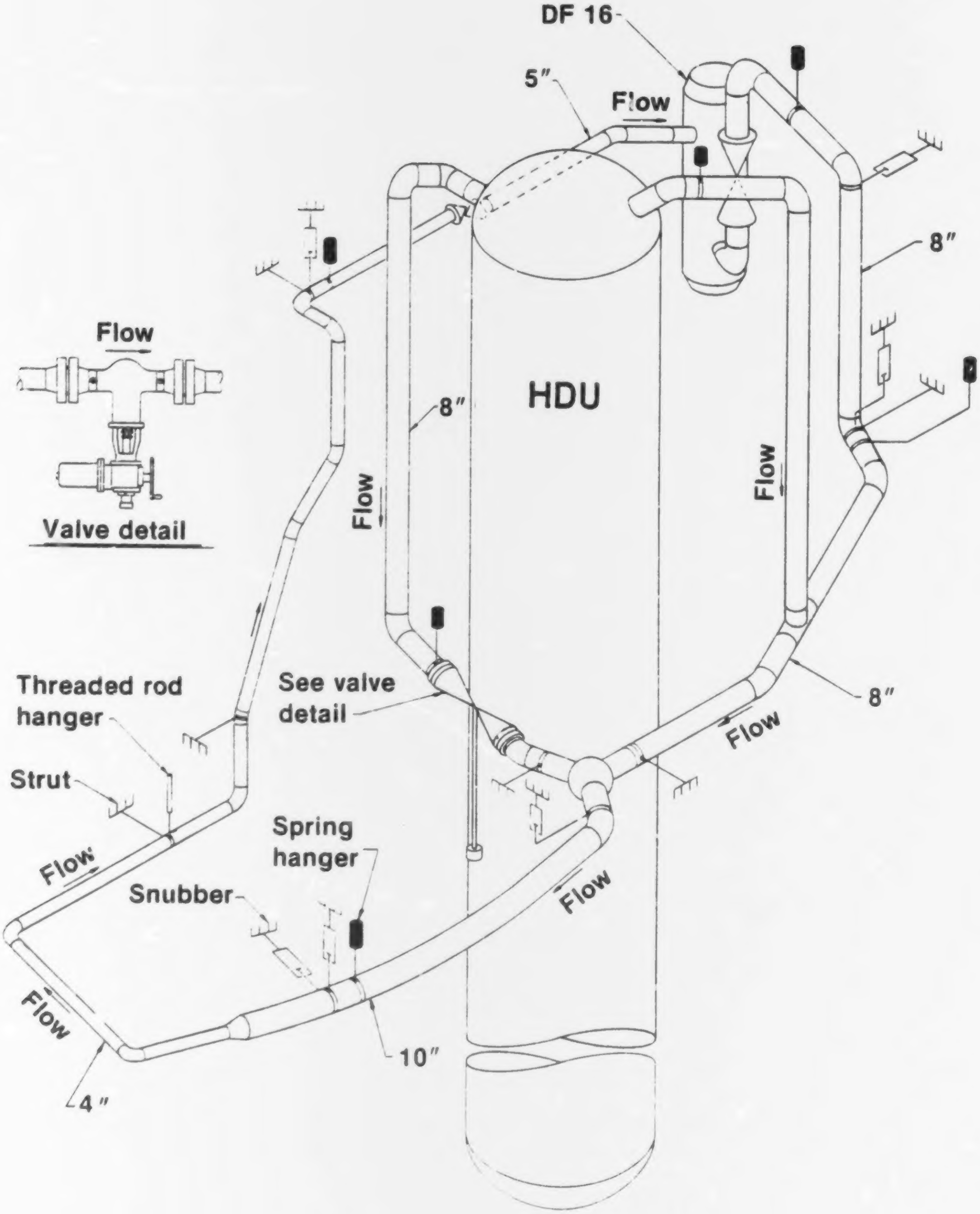
DF 16
5″
Flow
8″
Flow
Valve detail
8″
HDU
Flow
Flow
Threaded rod hanger
See valve detail
8″
Flow
Strut
Spring hanger
Flow
Snubber
Flow
Flow
10″
4″

Fig. 5. VKL Piping with U.S. Rigid Support System
(Courtesy of INEL, Idaho Falls, ID)

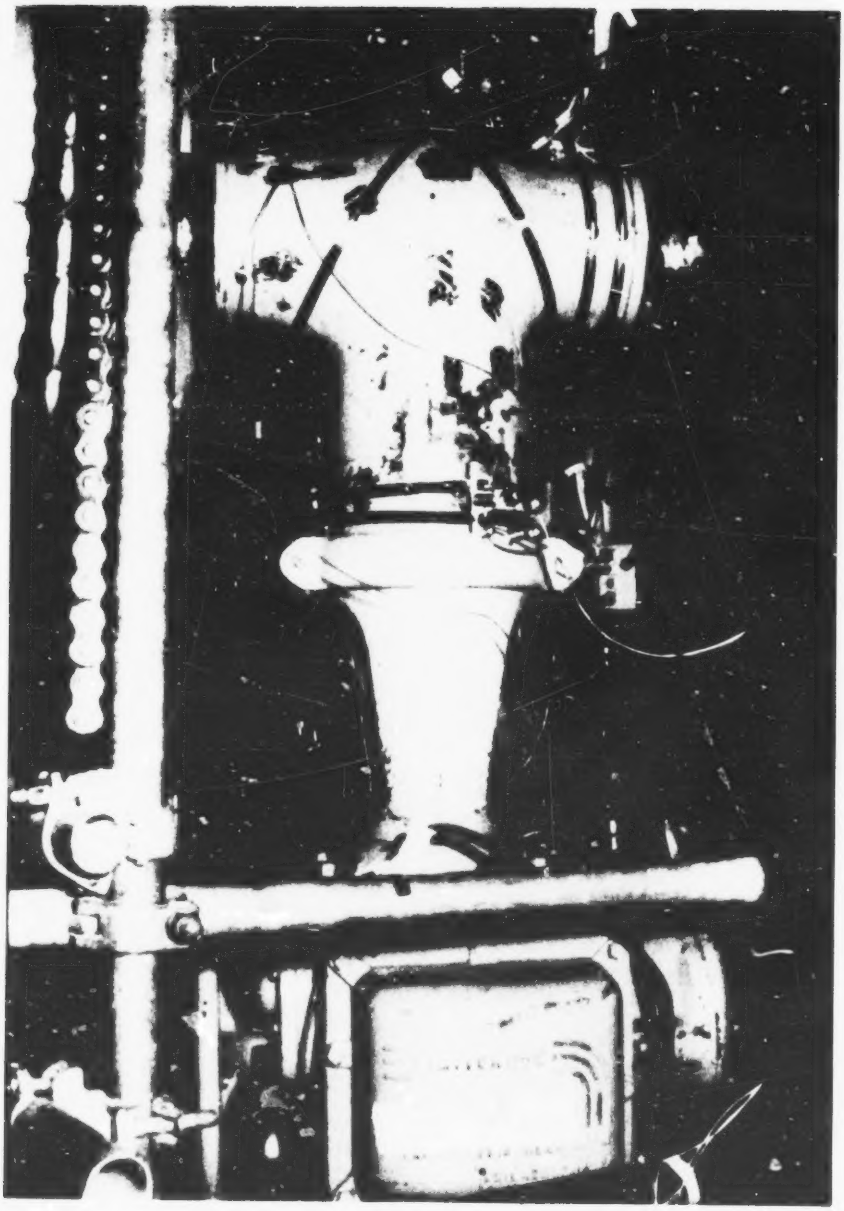

Fig. 6. U.S. 8" Gate Valve

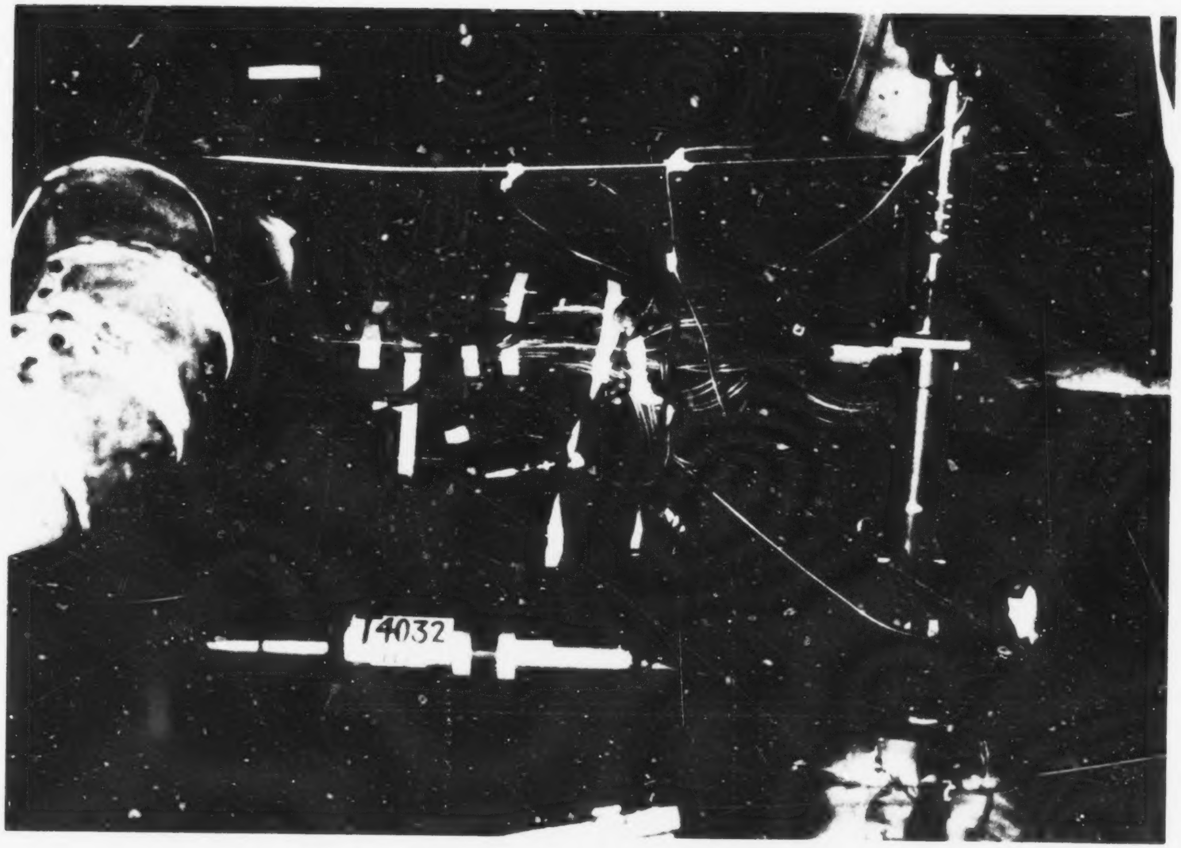

Fig. 7. Typical U.S. Snubber Installation

HDR T 40.
SHAG TEST MATRIX: PLANNED RUNS
2 June - 11 July 1986

| RUN NO. | TEMP. °C | VKL SUPPORT SYSTEM | ECCENTRICITY in kgm | STATRING FREQ. in Hz | MAX. FORCE in kN | TEST WEEK |
|---|---|---|---|---|---|---|
| 34 | 20 | USNRC | 4000 | 6 | 5600 | 1 |
| 35 | 20 | USNRC | 4000 | 8 | 10100 | |
| 36 | 20 | USNRC | 8200 | 5.6 | 10100 | |
| 37 | 20 | USNRC | 27800 | 2.1 | 4800 | |
| 32 | 20 | USNRC | 16800 | 4 | 10600 | 2 |
| 42 | 20 | EPRI/EA | 16800 | 4 | 10600 | |
| 52 | 20 | EPRI/SS | 16800 | 4 | 10600 | |
| 12 | 20 | HDR | 16800 | 4 | 10600 | |
| 22 | 20 | KWU | 16800 | 4 | 10600 | |
| 21 | 210 | KWU | 8200 | 5.6 | 10100 | 3 |
| 11 | 210 | HDR | 8200 | 5.6 | 10100 | |
| 51 | 210 | EPRI/EA | 8200 | 5.6 | 10100 | |
| 41 | 210 | EPRI/SS | 8200 | 5.6 | 10100 | |
| 31 | 210 | USNRC | 8200 | 5.6 | 10100 | |
| 30 | 210 | USNRC | 4000 | 8 | 10100 | 4 |
| 40 | 210 | EPRI/EA | 4000 | 8 | 10100 | |
| 50 | 210 | EPRI/SS | 4000 | 8 | 10100 | |
| 10 | 210 | HDR | 4000 | 8 | 10100 | |
| 20 | 210 | KWU | 4000 | 8 | 10100 | |
| 23 | 20 | KWU | 60000 | 2.1 | 10400 | 5 |
| 13 | 20 | HDR | 60000 | 2.1 | 10400 | |
| 33 | 20 | USNRC | 60000 | 2.1 | 10400 | |
| 43 | 20 | EPRI/NA | 60000 | 2.1 | 10400 | |
| 53 | 20 | EPRI/SS | 60000 | 2.1 | 10400 | |
| 58 | 20 | EPRI/SS | 27800 | 3.1 | 10500 | 6 |
| 48 | 20 | EPRI/EA | 27800 | 3.1 | 10500 | |
| 19 | 20 | HDR | 101800 | 1.6 | 10200 | |

Fig. 8. SHAG Test Matrix - Planned

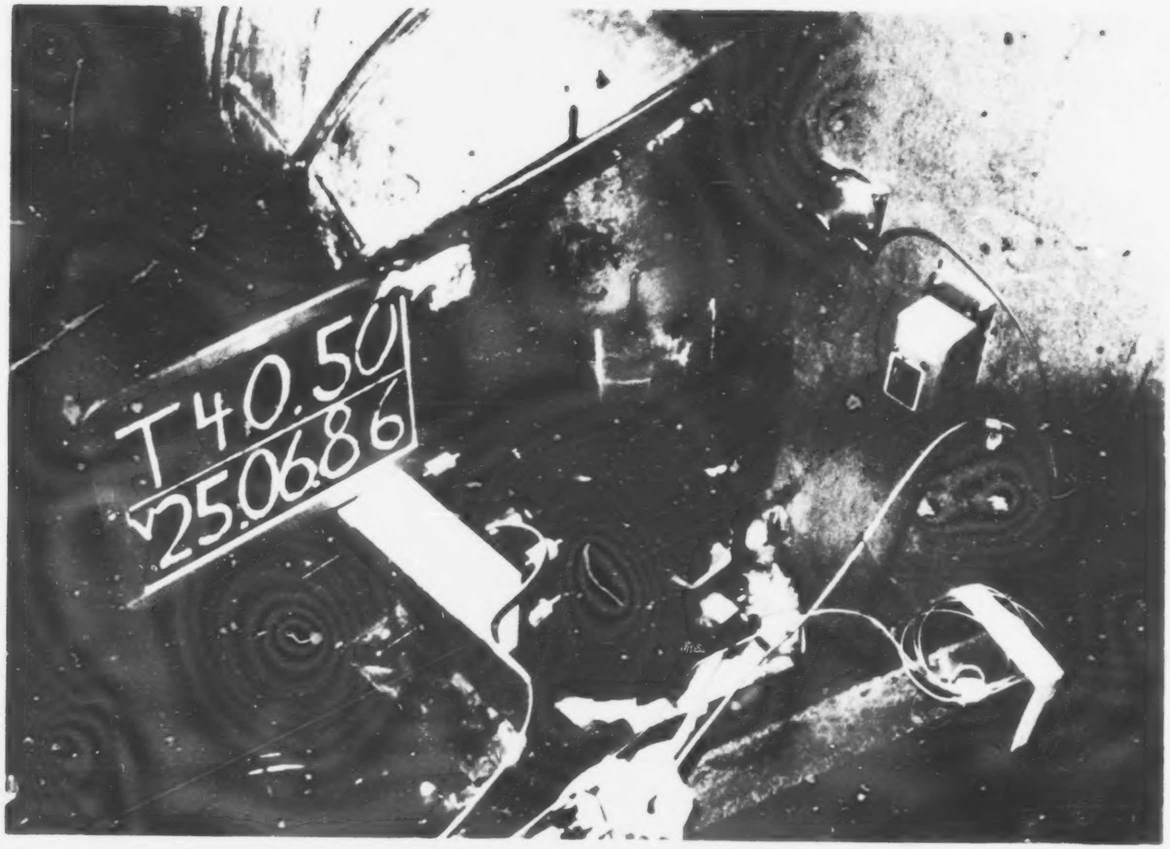
T40.50
25.06.86

Fig. 9. Wall Accelerometer Measuring Input to VKL Piping Support

# HDR T 40.
# SHAG TEST MATRIX: RUNS PERFORMED
## 2 June - 22 July 1986

| RUN NO. | TEMP. °C | VKL SUPPORT SYSTEM | ECCENTRICITY in kgm | STATRING FREQ. in Hz | MAX. FORCE in kN | TEST WEEK |
|---|---|---|---|---|---|---|
| 34 | 20 | USNRC | 4700 | 6 | 6600 | 1 |
| 35 | 20 | USNRC | 4700 | 8 | 11800 | |
| 36 | 20 | USNRC | 8200 | 5.6 | 10100 | |
| 37 | 20 | USNRC | 27800 | 2.1 | 4800 | |
| 40 | 20 | EPRI/EA | 4700 | 8 | 11800 | 2 |
| 20 | 20 | KWU | 4700 | 8 | 11800 | |
| 60 | 20 | GERB | 4700 | 8 | 11800 | |
| | | | | | | 3 |
| 50 | 20 | EPRI/SS | 4700 | 8 | 11800 | 4 |
| 70 | 20 | ANCO | 4700 | 8 | 11800 | |
| 10 | 20 | HDR | 4700 | 8 | 11800 | |
| 30 | 20 | USNRC | 4700 | 8 | 11800 | |
| 31 | 20 | USNRC | 6450 | 6 | 9100 | 5 |
| 41 | 20 | EPRI/EA | 6450 | 6 | 9100 | |
| 21 | 20 | KWU | 6450 | 6 | 9100 | |
| 11 | 20 | HDR | 6450 | 6 | 9100 | |
| 51 | 20 | EPRI/SS | 6450 | 6 | 9100 | |
| 52 | 210 | EPRI/SS | 8200 | 4.5 | 6500 | 6 |
| 32 | 210 | USNRC | 8200 | 4.5 | 6500 | |
| 42 | 210 | EPRI/EA | 8200 | 4.5 | 6500 | |
| 12 | 210 | HDR | 8200 | 4.5 | 6500 | |
| 22 | 210 | KWU | 8200 | 4.5 | 6500 | |
| 12.1 | 210 | HDR | 8200 | 4.5 | 6500 | 7 |
| 14 | 20 | HDR | 33000 | 1.6 | 3300 | |
| 16 | 20 | HDR | 54000 | 1.6 | 5400 | 8 |
| 13 | 20 | HDR | 67000 | 1.6 | 6700 | |

Fig. 10. SHAG Test Matrix - Performed

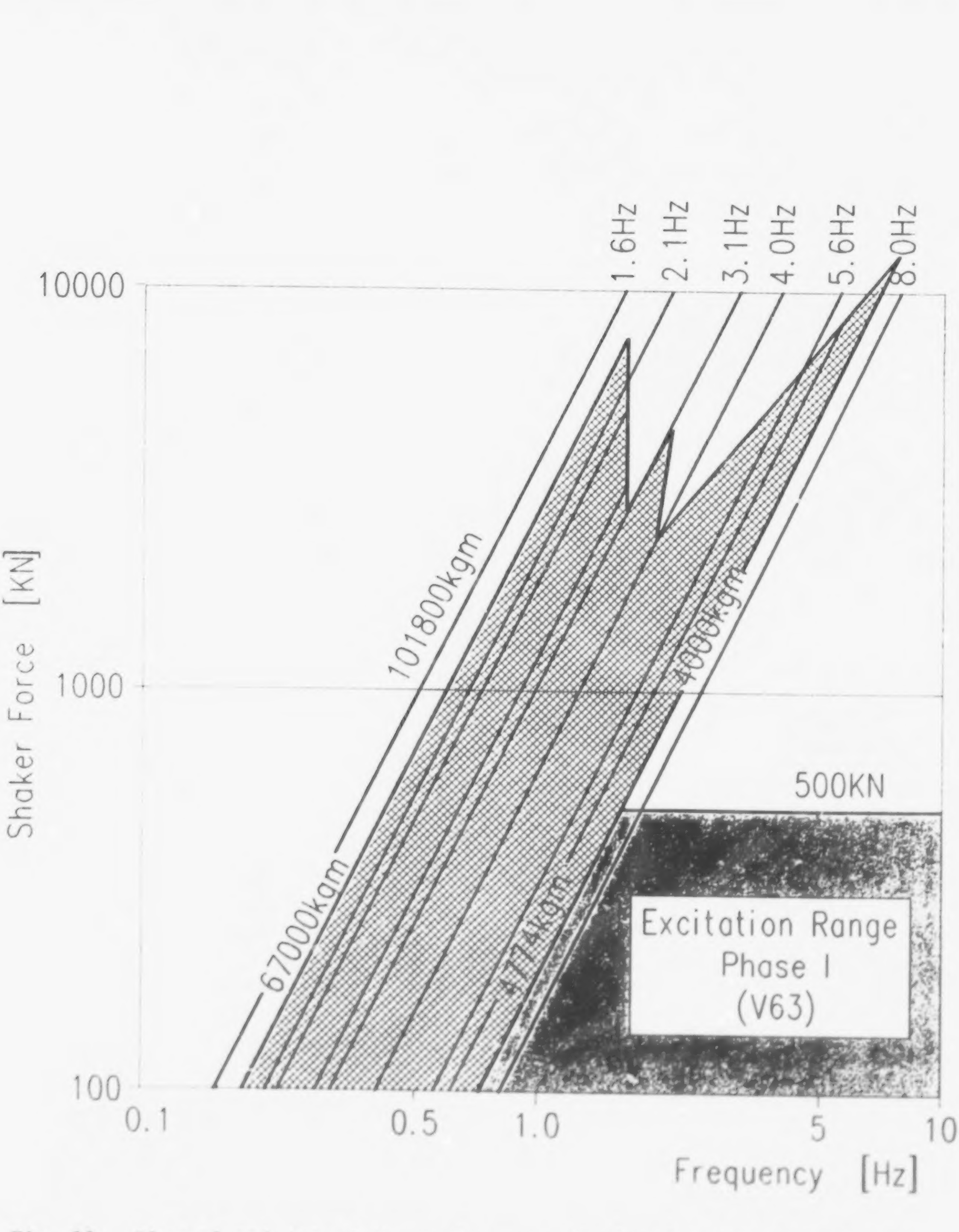

Fig. 11. Planned and Actual Force-Frequency Region for Shag Experiments

Shaded Region - planned
Crosshatched - actual

# THE SEISMIC CATEGORY I STRUCTURES PROGRAM

by

J. G. Bennett, C. R. Farrar, and W. E. Dunwoody
Los Alamos National Laboratory

## ABSTRACT

The Seismic Category I Structures Program entered a new phase at the end of FY 1984  During the prior fiscal years, tests on microconcrete scale model shear deformation dominated structures were completed. The results indicated that these structures responded to seismic excitations with frequencies that were reduced by factors of two or more over those calculated based on an uncracked cross section strength-of-materials approach. This reduction implies that stiffness associated with seismic working loads (loads resulting from an operating basis earthquake up to and including a safe shutdown earthquake) are down by a factor of four or more. These reductions were also consistent with those measured during quasistatic tests to an equivalent level of loading. Furthermore, though the structures themselves were shown to have sufficient reserve margin, the equipment and piping are designed to response spectra that are based on uncracked cross sectional member properties, and these spectra may not be appropriate for actual building responses.

The new phase of the program was aimed at verification of these conclusions using real concrete structures. These test structures were designed based on guidance from the program's Technical Review Group (TRG), a group of nationally recognized nuclear civil structure experts.

During FY 86, a large TRG type structure (4-inch walls of real concrete, No. 3 rebar, and with about 15 tons of added mass) was tested seismically at the construction Engineering Research Laboratory (CERL) in Champaign, IL.

When measured property values were used to predict the first mode frequency as opposed to using assumed design values, results again indicated stiffness reductions on the order of 4, consistent with previous results using microconcrete. Details of the results and floor response spectra obtained from measured results versus floor response spectra obtained from computed results are presented. A plan for further verifying and quantifying stiffness reduction for these structures as a function of shear wall aspect ratio, percentage steel reinforcing and load level is discussed.

## INTRODUCTION

The Seismic Category I Structures Program was begun at Los Alamos under the sponsorship of the United States Nuclear Regulatory Commission (USNRC) during the later part of FY 1980. The typical Category I Structure considered is a reinforced concrete structure (exclusive of the containment) that has an aspect ratio such that shear deformation rather than bending deformation governs the response. The primary lateral load carrying element of these structures, the shear wall, is a lightly reinforced wall that is designed to resist missile penetration. Seismic response is normally calculated based on elastic response using an uncracked strength-of-materials approach for calculation of the stiffness contribution to the seismic model. This practice has been followed in the past and specifically, Section 3.1.3.1 of the ASCE's Standard for the Seismic Analysis of Safety-Related Nuclear Structures states that reinforced concrete elements of a Category I structure may be modeled as uncracked sections for the purpose of computing stiffness because the anticipated stress state in the structural elements forming this type of building prior to a seismic event will be in the elastic (uncracked) range.

By the end of FY 84, a number or experimental studies on isolated shear walls, idealized scale model diesel generator buildings, and scale model auxillary buildings under both quasi-static and seismic loading conditions had been completed and reported (1,2,3). These models were considered scale models based on prototype wall thickness of 30 and 42 inches, but were not intended to serve as scale models of any particular larger structure. Models with 1 inch walls (1/30 and 1/42 scales) and 3 inch walls (1/10 and 1/14) made from microconcrete and simulated rebar were tested. These models were not intended to predict failure loads, crack patterns, etc. for any particular prototype structure. Rather, these structural elements were designed to exhibit under cyclic loading, the nonlinear, softening, hysteretic, stiffness-degradation characteristics that have been observed in other shear wall tests (4,5).

Shortly after the initiation of this program, a Technical Review Group (TRG) consisting of nationally recognized seismic and concrete experts on nuclear civil structures was established to both review the progress and make recommendations regarding the technical directions of the program. The recommendations of this group have been evaluated in light of the needs of the USNRC and, where possible, have been carefully integrated in the program.

This group has reviewed and commented about the program results on items such as aging (cure time), effect of increasing seismic magnitude damping levels, and floor response spectra changes etc. However, the two most commented about results were, (1) the scalability of the tests was illustrated both in the elastic and inelastic range, (2), the so-called "working load" secant stiffness of the models was lower than the computed uncracked cross-sectional values by a factor of about 4.

During their review, the TRG pointed out the following:

1. Design of prototype nuclear plant structures is normally based on an uncracked cross-section strength-of-materials approach which may or may not use a "stiffness reduction factor' for the concrete, but if one is used it is never as large as 4.

2. Although the structures themselves appear to have adequate reserve margin (even if the stiffness is only 25% of the theoretical), any piping and attached equipment will have been designed using inappropriate floor response spectra.

3. Given that a nuclear plant structure designed to have a natural response of about 12 Hz really has a natural frequency of 6 Hz (corresponding to a reduction in stiffness of 4), and allowing further that the natural frequency will decrease because of degrading stiffness, the natural response of the structure will shift well down into the frequency range for which an earthquake's energy content is the largest. This will result in increased amplification in the floor response spectra at lower frequencies, and this fact potentially has significant impact on the equipment and piping design response spectra and their margins of safety.

Note that all three points are related to the difference between measured and calculated stiffnesses of these structures.

To address these stiffness-related issues, it was agreed that credibility experiments should be carried out on a geometry that would appropriately address two important questions. Does our previous experimental data taken on microconcrete models represent behavior that would be observed in prototype structures? What is the appropriate value of the stiffness that should be used in design and for component response spectra computations in these structures?

To address the microconcrete issue, a structure was proposed having the following characteristics:

1. maximum predicted bending and shear mode natural frequency $\leq$ 30 Hz,
2. minimum wall thickness = 4 in. ,
3. height-to-depth ratio of shear wall $\leq 1$,
4. use actual No. 3 rebar for reinforcing,
5. use standard batch plant concrete,
6. use 0.1 to 1% steel (0.3% each face, each direction ideally),
7. use water blasted construction joints to assure good aggregate interlock.

These structures will be referred to as the TRG structures after the technical review group that established the above criteria.

## DESIGN OF THE TRG STRUCTURE AND MODELS

The initial design of the TRG structure was approached from a strength-of-materials point of view. An estimate of the required added mass indicated that on the order of three times the distributed structural mass would be necessary to meet the 30 Hz requirement. It was judged that the effect of the large added mass should be taken into account in arriving at the force-displacement relationship. To support the large added mass, the geometry of Fig. 1 was proposed and designed based on the following analysis. Using the free-body diagram of Fig. 2, and making the usual assumptions regarding bending, transformed sections and effective shear area, an expression for the strain energy for the structure can be written down. Assuming an elastic system, Castigliano's second theorem can be applied to the expression to show that the shear force (V) versus transverse displacement ($\delta$) relationship is

$$\delta = V\left(\frac{hL^2}{2E_cI_t} + \frac{L^3}{3E_cI_t} + \frac{L}{A_eG}\right), \tag{1}$$

where

$A_e$ = transformed section effective shear area,
$E_c$ = Young's modulus for concrete,
$G$ = shear modulus for concrete, and
$I_t$ = transformed section for moment of inertia*, and

the geometric parameters, L, h are defined in Fig. 2. In using the method of transformed sections for these thick wall lightly reinforced structures, we follow standard practice for an uncracked section and include the total concrete area in the calculation not just "compressive" concrete. From Equation 1, we define the stiffness quantities:

$$K_{CB} = K_{\text{Cantilever Bending}} = \frac{3E_cI_t}{L^3}$$

$$K_S = K_{\text{Shear}} = \frac{A_eG}{L}$$

$$K_{BM} = K_{\text{Bending Moment}} = \frac{2E_cI_t}{hL^2}$$

The expression for the total stiffness ($K_T$) then becomes:

$$\delta = V\left(\frac{1}{K_T}\right) = V\left(\frac{1}{K_{BM}} + \frac{1}{K_{CB}} + \frac{1}{K_S}\right)$$

---

* For the method of transformed sections as applied to beams of two materials, see Ref. 6, pp. 202-208.

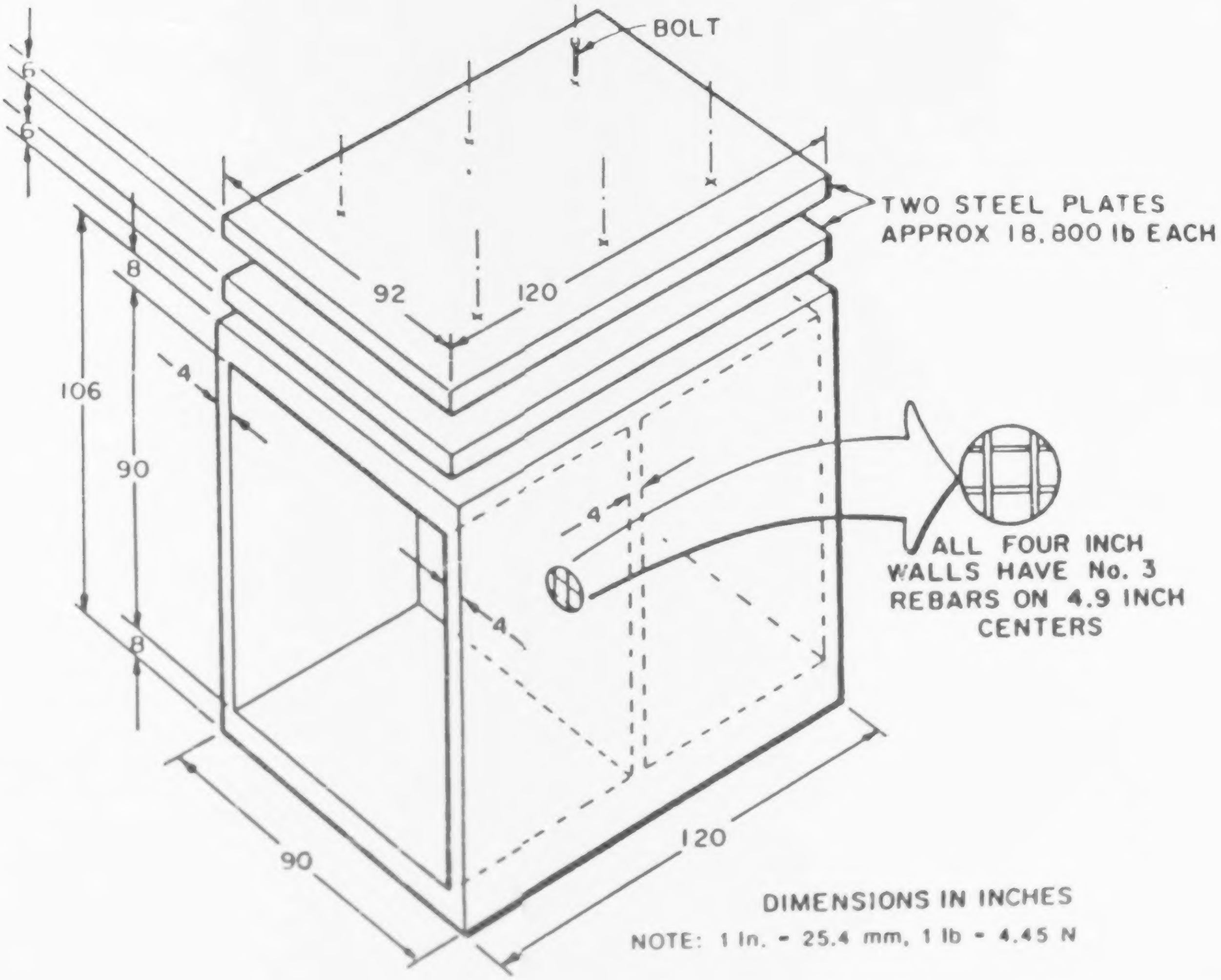
BOLT
6
6
TWO STEEL PLATES
APPROX 18,800 lb EACH
8
92
120
106
4
90
4
ALL FOUR INCH
WALLS HAVE No. 3
REBARS ON 4.9 INCH
CENTERS
4
8
90
120
DIMENSIONS IN INCHES
NOTE: 1 In. = 25.4 mm, 1 lb = 4.45 N

Fig. 1. Geometry of the TRG-3 model. There is a single rebar plane in the center of each 4 inch wall.

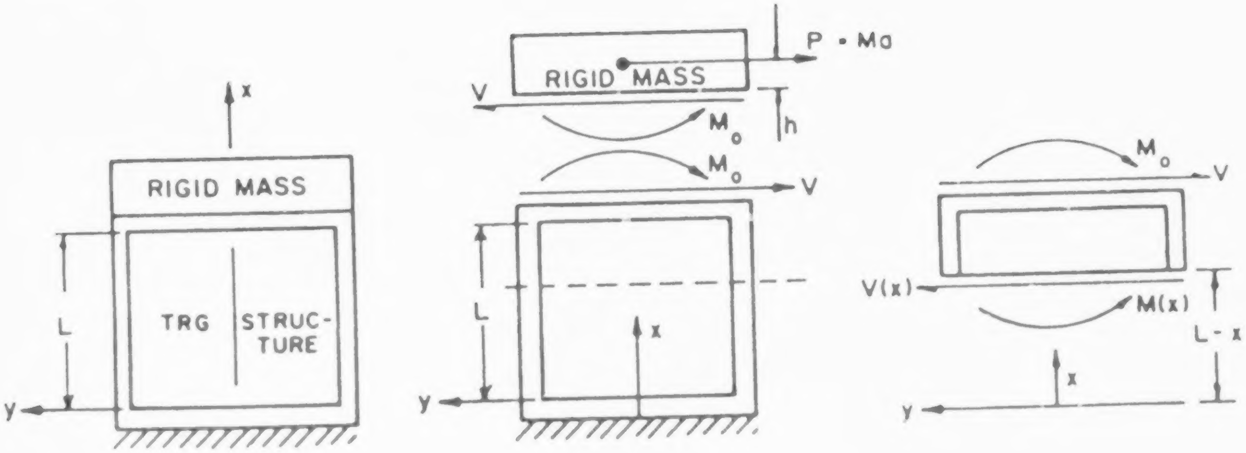
x
RIGID MASS
L
TRG
STRUCTURE
y
P = Ma
RIGID MASS
V
$M_o$
h
$M_o$
V
L
x
y
$M_o$
V
V(x)
M(x)
L - x
x
y

Fig. 2. Free body diagrams used to derive added mass effect on stiffness.

A simple expression for the first mode structural frequency (f) for the bending and shear response then becomes,

$$\omega = 2\pi f = \sqrt{\frac{K_T}{M_A + M_S + M_D}}$$

where,

$M_A$ = the added mass,
$M_S$ = the mass of the top slab of concrete,
$M_D$ = the distributed mass.

The expression for the added weight required for a targeted frequency can then be approximated as:

$$W_A = 386\left(\frac{K_T}{4\pi^2 f^2} - r\, M_{concrete}\right)$$

where,

$W_A$ = added weight in lbs,
$K_T$ = total stiffness in lb/in.,
$f$ = targeted natural frequency in Hz, and
$M_{concrete} = M_S + M_D$

The "r" is a multiplicative factor that relates the total structural mass to the effective distributed mass in the vibration mode of interest. Such a factor can be found from a "Rayleigh's Method" analysis of a cantilever beam. In our initial design we used a value for r of 0.3.

Using these equations, the structure of the geometry in Fig. 1 was designed to the recommendations of the TRG. The primary structural element of the TRG structure is a shear wall with an aspect ratio of 1.0. The calculated properties of the structure are given in Table 1. The method of transformed sections for beams of two or more materials was used to compute the geometric properties with a modular ratio of steel to concrete of 10 assumed for this computation and these results are shown in the first column. Because the as-fabricated steel spacing and concrete material properties differed slightly from the design values, column 2 of Table I shows the calculated values of the as-built structure for the geometric properties. Table II shows the various material properties and the basis for their determination that were used in the calculations of Table I.

The structure was constructed from "batch plant" structural grade concrete with a specified minimum compressive strength ($f'_c$) of 3000 psi. Two batch plant truck deliveries containing 3 yards of concrete each were used to facilitate construction. The base and bottom one-foot-heights of the wall sections were placed using the first truck and the remaining portions of the walls and the top slab were completed using the second

AVAILABLE

## TABLE I
## COMPUTED CHARACTERISTICS OF THE TRG-3 STRUCTURE

| Property | Design Value* | As-Built Value** |
|---|---|---|
| Uncracked section moment of inertia($I_t$) | = $2.06 \times 10^6$ in.$^4$ | $2.15 \times 10^6$ in.$^4$ |
| Area effective shear (transformed) | = 379 in.$^2$ | 392 in.$^2$ |
| Area (total) | = 1288 in.$^2$ | 1288 in.$^2$ |
| Total uncracked cantilever bending stiffness ($3E_cI_t/L^3$) | = $2.5 \times 10^7$ lb/in. | $1.8 \times 10^7$ lb/in. |
| Shear stiffness ($A_eG/L$) | = $5.3 \times 10^6$ lb/in. | $3.6 \times 10^6$ lb/in. |
| Mass contribution ($2E_cI_t/hL^2$) | = $2.5 \times 10^8$ lb/in. | $1.8 \times 10^8$ lb/in. |
| Total stiffness | = $4.3 \times 10^6$ lb/in. | $3.0 \times 10^6$ lb/in. |
| Max. dead weight normal stress | = 42 psi | ---- |
| Max. shear stress in flange at 5 g due to assumed 5% torsion (approx.) | = 35 psi | ---- |
| Total concrete | 6 cubic yards | ---- |
| Total added weight | 37600 lb | ---- |
| Total weight | 61600 lb | ---- |

---

* calculated using $E_c = 3.0 \times 10^6$ lb/in.$^2$ as the design value.

** calculated using $E_c = 2.0 \times 10^6$ lb/in.$^2$ from the strain gage measured value.

## TABLE II
## MATERIAL PROPERTIES FOR TRG-3

Concrete:

$E_c$ = assumed for design purposes = $3 \times 10^6$ psi
$E_c$ = (measured at $\sigma - \epsilon$ origin) = $2.0 \times 10^6$ psi
$f'_c$ = (compressive strength) = 3807 psi
$f_t$ = (split tensile test strength) = 351 psi
$E_c$ = $57000\sqrt{f'_c} = 3.5 \times 10^6$ psi

Steel - Standard No. 3 Rebar*

0.6% Both Directions
E = $30 \times 10^6$ psi
Yield Strength = 40 ksi min.
Ultimate Strength = 70 ksi min.
Elongation at failure = 11% min.
Diameter = 3/8 in.

---

* These are handbook values and have not as yet been measured.

truck. The entire concrete placement was completed within a four hour period using concrete vibrators and standard construction methods. At the same time standard 6 in.-diameter x 12 in.-high samples of the concrete were obtained from each truck, in accordance with ASTM C31-83 and C172-82 (Ref. 7, 8) specifications. Standard slump specimens were also obtained from each batch according to ASTM C143-78 (Ref. 9) to ensure proper water to cement ratios.

From Table II, the value of the Young's modulus for concrete is seen to vary from $2 \times 10^6$ psi for a strain gage measured value to $3.5 \times 10^6$ psi for a value based on $57,000\sqrt{f'_c}$. The reason for this difference is not clear and further samples taken from the structures itself (core samples) will be tested in FY 87 to verify the strain gage determined value. The results computed in the remainder of this paper will be stated using all 3 values of $E_c$.

## TESTING HISTORY OF TRG-3 IN BRIEF

The low load level testing history for the structure will be summarized. The structure was placed on foam pads for modal testing as a "free-free" structure to characterize the very low level vibrational frequencies and thus the structural "as-built" stiffnesses. First, a series of hammer tap tests was used to excite the structure. Second, a 300 lb. portable shaker was used to excite the structure with a random signal having frequency content of 0-500 Hz. For both of these modal analysis tests, accelerometer data was taken at 31 points shown schematically in Fig. 3 on the structure in three orthogonal directions. These tests gave some natural frequency and mode shape information, but the foam pads did not allow a true "free-free" condition to be simulated and coherence for the test signals below 200 Hz was poor. Next, the base of the structure was bolted to a load frame specifically constructed for low load level static testing and states testing was done keeping the load below a value that would produce a calculated maximum principal stress of 40 psi. The 37,600 lbs. of added weights arrived after these tests and were fitted to the structure and the transfer functions of the top slab acceleration to the base slab acceleration records were measured. The structure was then shipped to the Construction Engineering Research Laboratory (CERL) at Champaign, IL.

The structure was suspended from the CERL crane using nylon straps and "free-free" modal testing was again carried out using a portable shaker and random force excitation. In these tests coherence at lower frequencies was good and the modal analysis gave satisfactory results. The structure was next bolted to the CERL shaker table and a seismic test plan was carried out using a modified (properly time-scaled for a 1/5 scale structure and baseline corrected) El-Centro earthquake signal as the input time history.

## LOW LOAD LEVEL TESTING RESULTS

In these tests, the initial as-built stiffness of the structure was obtained to compare with theory.

The static load displacement curve was obtained by monotonically loading the structure to 10,000 lb. The results are shown in Fig. 4. A least squares fit of the data was performed (solid line) and the

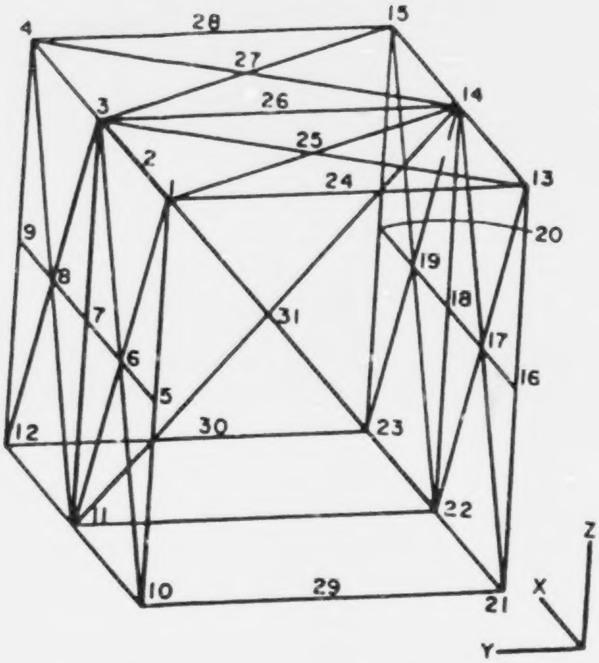

1
2
3
4
5
6
7
8
9
10
11
12
13
14
15
16
17
18
19
20
21
22
23
24
25
26
27
28
29
30
31
X
Y
Z

Fig. 3. Location of the accelerometers for the modal test data.

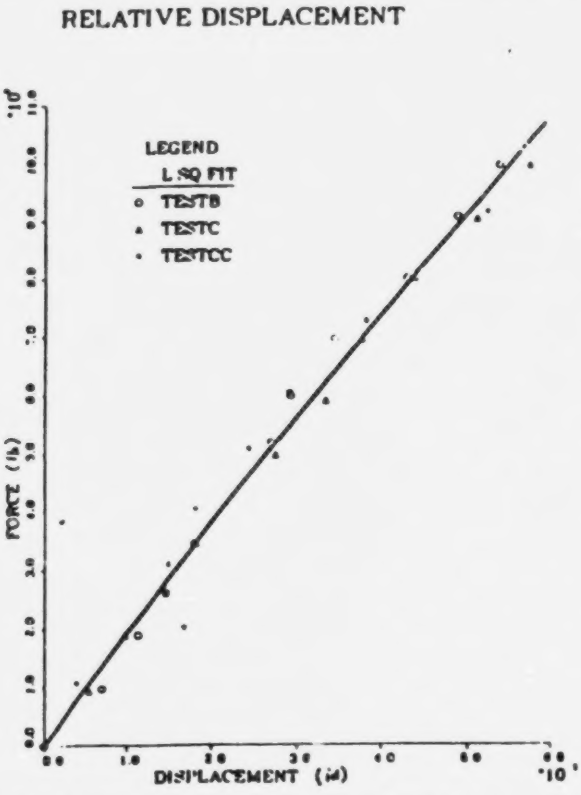

Fig. 4. Static load-displacement result 10,000 lb corresponds to about 40 psi maximum tensive stress in the concrete.

stiffness was evaluated as the slope of this curve at the origin. This value is 1.95 x $10^6$ lb/in., which is about 70% of the theoretical value based on an uncracked cross-section and using the strength-of-materials approach. This value is probably low as the connection effects at the base are unaccounted for.

The low load level modal test results gave similar information. The first two modes are the torsion mode and the free-free shear/bending mode. Table III shows the comparison of the measured frequencies.

TABLE III
MODAL TEST RESULTS

| | Frequency (Hz) Theoretical | Frequency (Hz) Measured |
|---|---|---|
| Mode 1 (Torsion) | | |
| $E_c$ - 2 x $10^6$ psi | 21 | 29 |
| $E_c$ - 3 x $10^6$ psi | 26 | 29 |
| $E_c$ - 3.5 x $10^6$ psi | 28 | 29 |
| Mode 2 (Shear/Bending) | | |
| $E_c$ - 2 x $10^6$ psi | 87 | 75 |
| $E_c$ - 3 x 106 psi | 106 | 75 |
| $E_c$ - 3.5 x $10^6$ psi | 115 | 75 |

Using the strain gage measured value of Young's modulus for the concrete and the static low load level test data and these modal tests results, it was concluded that the TRG-3 structure at the time of seismic testing had a stiffness value in the shear/bending mode of about 70-80% of the theoretical uncracked cross-sectional value.

## INITIAL HAVERSINE AND SEISMIC TEST RESULTS - WORKING LOAD STIFFNESSES

The working load stiffness is defined here as the equivalent linear stiffness that the structure has, as deduced from its response to applying any significant dynamic loading to the structure. In the seismic tests, the lowest load level that can be maintained with good shaker control for this structure is about 0.5 g which corresponds to about 0.1 g on a real Category I structure. This value is used here as the "working load" and corresponds to a typical operating basis earthquake (OBE) loading on a real structure.

A 0.5 g haversine base input pulse was designed to characterize the structure initially and to characterize damage between seismic tests on the CERL table. This type of test is assumed to cause less further damage to the structure than the 1/2 g broad band random type of characterization signal used between seismic tests on our previous models. Figure 5 shows the horizontal acceleration time history at the base of the structure and the corresponding horizontal top slab response in the plane of the shear wall. This record is from the first pulse applied to the structure by the CERL table. Figure 6 shows the real and

BEST COPY AVAILABLE

imaginary parts of the transfer function of this top slab acceleration to the base slab. Both records indicate a clear 10 Hz natural frequency for the shear-bending mode for this structure.

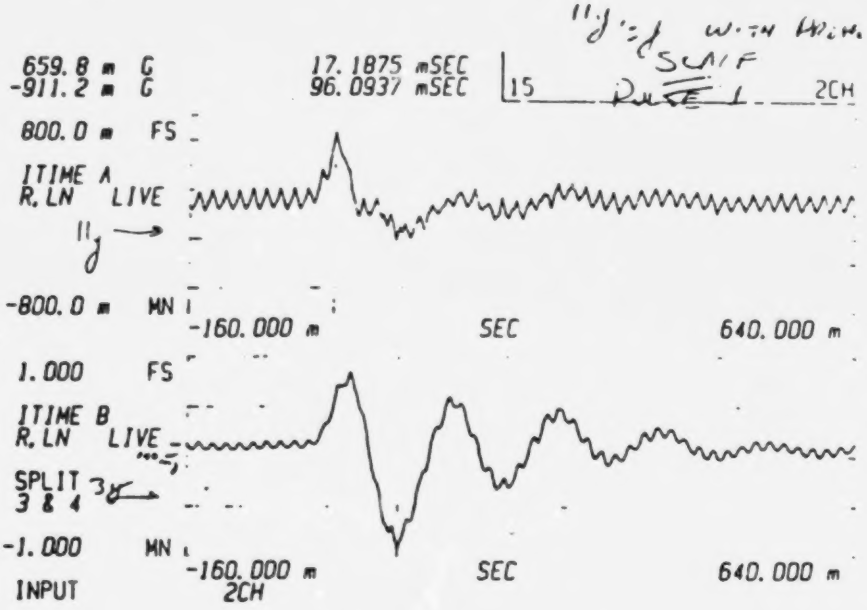

Fig. 5. Time history of the first base input haversine pulse (top trace) and the top response accelerometer. This record was taken "on-line" at CERL.

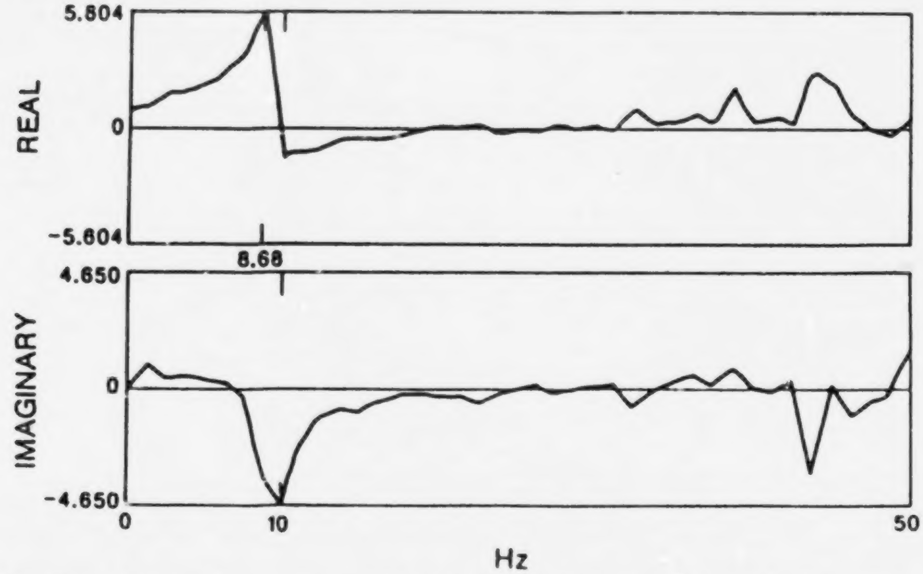

Fig. 6. Real and imaginary parts of the transfer function of the top accelerometer record to the base record for the haversine pulse of Fig. 5.

BEST COPY AVAILABLE

Figure 7 shows the time history of the base input 0.5 g nominal max peak seismic signal and Fig. 8 shows the response time history. As can be seen from Fig. 7, the base input magnitude was actually about 0.73 g max peak. Figure 9 shows the acceleration transfer function of the top to base for these two signals. The structure predominantly responds to the earthquake in the 10 Hz shear-bending mode.

The working load stiffness implied by this result is estimated by using the relationship that

$$\frac{f_{measured}}{f_{theoretical}} = \sqrt{\frac{k_{actual}}{K_{theoretical}}}$$

Henceforth, we will use $K_{actual}$ and $K_{measured}$ interchangeably, but natural frequency was the actual measured quantity.

The implications of these results with regard to measured versus theoretical stiffnesses will now be discussed. Three methods of approach to the design of the TRG-3 structure will be illustrated in order to quantify the magnitude of the various assumptions that are or have been used in the design of Category I structures.

The first method will be called the "design method". The assumptions for this method are as follows:

(1) Assume an uncracked concrete cross-section;
(2) Use the method of transformed sections to transform steel area to concrete and compute the transformed bending area moment of inertia for the cross-section,
(3) Use the strength-of-materials approach to compute the stiffness (i.e. Eq. 1),
(4) Assume the top and bottom concrete slabs are rigid compared to the cantilever cross-section and compute the effective MASS = $M_{ADDED} + M_{SLAB} + M_{DISTRIBUTED}$,
(5) Assume that the base is fixed.

As previously stated, in order to further quantify the magnitude of various effects, we will give results using the three different values of concrete modulus discussed previously. The ACI method, the design assumption, and the strain gage value. These values are:

(1) ACI Method $E_c = 57000\sqrt{f_c'} = 57000\sqrt{3807}$
$E_c = 3.5 \times 10^6$ lb/in.$^2$ ,
(2) Design assumption $E_c = 3 \times 10^6$ lb/in.$^2$ ,
(3) Strain gage value $E_c = 2 \times 10^6$ lb/in.$^2$ .

Table IV shows the results of calculating the stiffness and natural frequency of this structure based on these assumptions. Clearly the stiffness of this structure under working/loads is lower than theory would predict. Furthermore, it appears that the stiffness decreased in going from a low load level to a working load level.

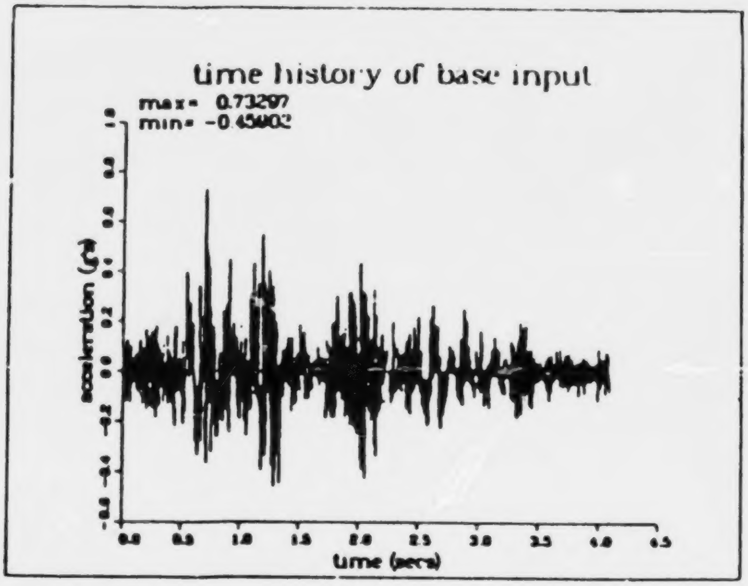

Fig. 7. Time history of the base input for the first seismic test of TRG-3 at CERL.

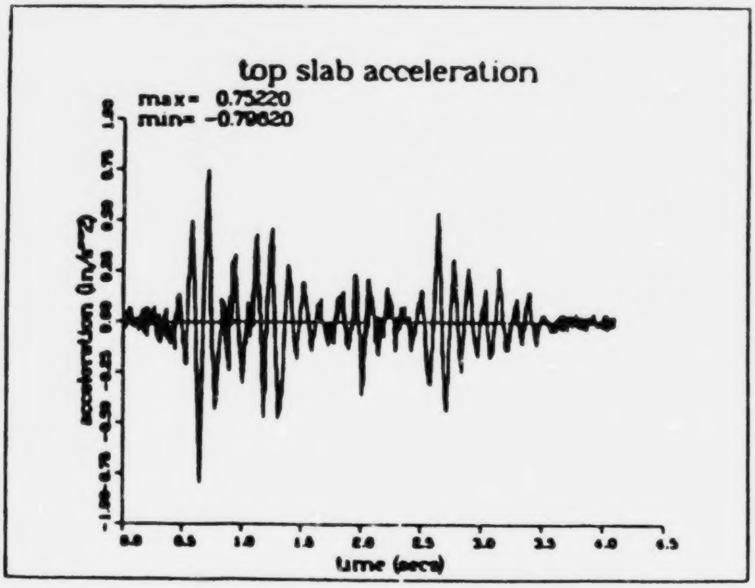

Fig. 8. Response acceleration of the top slab for the first seismic test of TRG-3 at CERL.

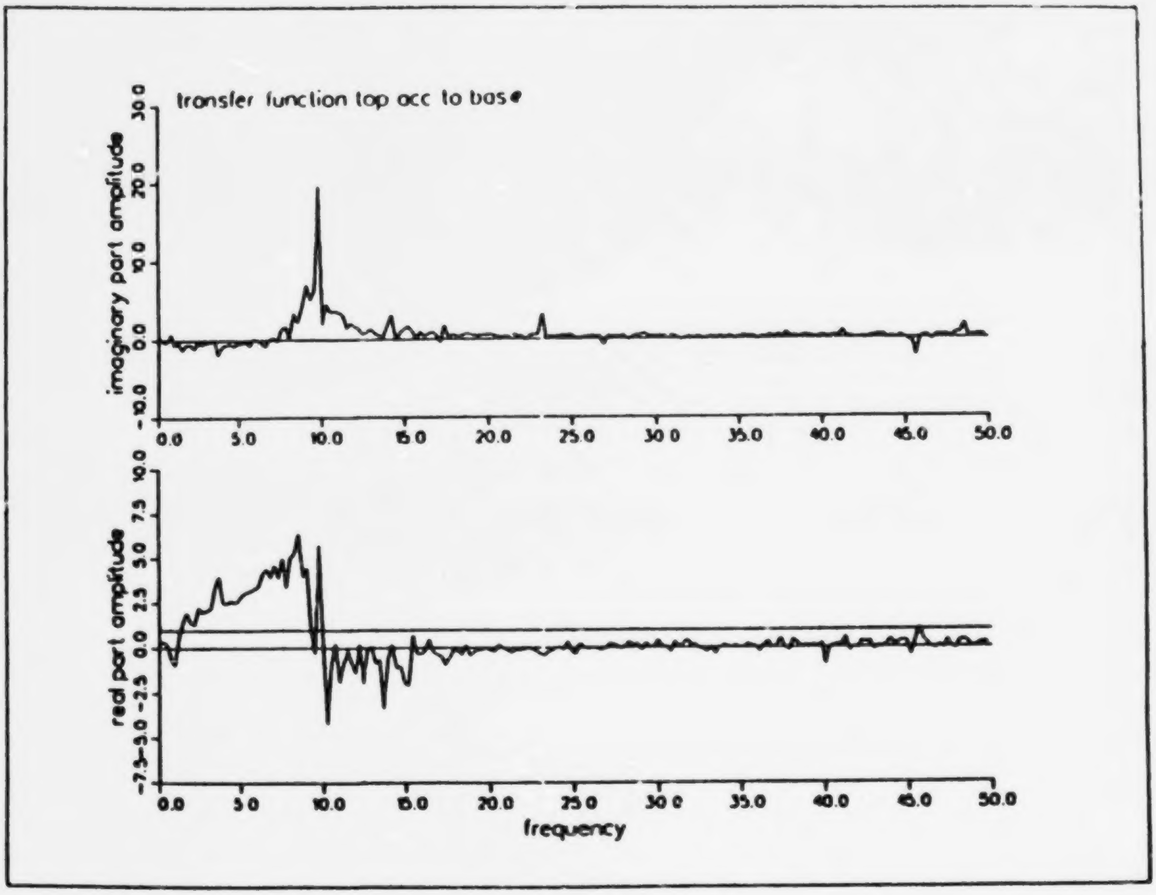

Fig. 9. Acceleration transfer function for the top slab to the base for the test of Figs. 12 and 13. The 10 Hz natural mode is clearly shown.

## TABLE IV
## SUMMARY OF RESULTS FOR WORKING LOAD STIFFNESSES BASED ON THE DESIGN METHOD

| | | | First Mode Frequency under E.Q. conditions | |
|---|---|---|---|---|
| $E_c$ lb/in.$^2$ | Computed Stiffness (lb/in.) | $K^*_{STRUCTURAL}$ / $K_{THEORY}$ | Predicted (Hz) | $f^{**}_{MEASURED}$ / $f_{PREDICTED}$ |
| $3.5 \times 10^6$ | $5.0 \times 10^6$ | 0.15 | 31.8 | 0.31 |
| $3.0 \times 10^6$ | $4.3 \times 10^6$ | 0.18 | 29.5 | 0.34 |
| $2.0 \times 10^6$ | $3.0 \times 10^6$ | 0.25 | 24.6 | 0.40 |

---

* $K_{STRUCTURAL}$ = 759,000 lb/in.

** $f_{MEASURED}$ = 10 Hz.

How much load is necessary, and the physical mechanism for stiffness changes has not been completely determined. All evidence points strongly to the fact that the structure does not respond to significant dynamic loads (i.e. working loads) as if it had uncracked shear walls.

The results presented in Table IV are representative of methods that were used by the architectural/engineering firms for existing nuclear plant structures of this type.

To further illustrate the magnitude of various effects an alternative analysis can be carried out. The engineering mechanics specialist might approach this problem from an energy methods point of view and use Hamilton's principle and shape functions to obtain the best single degree-of-freedom representation possible for the TRG-3 structure and its base connections. We will not go through all details in this paper, but the interested reader can obtain the theory from Ref. 10. The details are available from the author. The results for the TRG-3 structure are presented in Table V.

Finally Table VI illustrates modern analysis methods (the finite element method) that might be used on current and future nuclear plant structural designs. Both the fixed based assumptions and an attempt at modeling the connection effects are illustrated here for the three values of the concrete modulus. The ABAQUS finite element code was used with shell elements representing the structure and the smeared rebar option combined with the concrete material model to represent the material. The calculations are totally elastic. The structure was represented using the quarter model mesh shown in Fig. 10 with the appropriate symmetry boundary conditions for the vibration modes of interest. Table VI gives the results for the shear-bending mode.

The calculational basis for Tables IV - VI were chosen to represent three types of design methods of nuclear plant structures. The first basis, the design method, represents the method that was probably used for existing plants. The second basis, the engineering mechanics/structural dynamics basis, represents the best design method that could

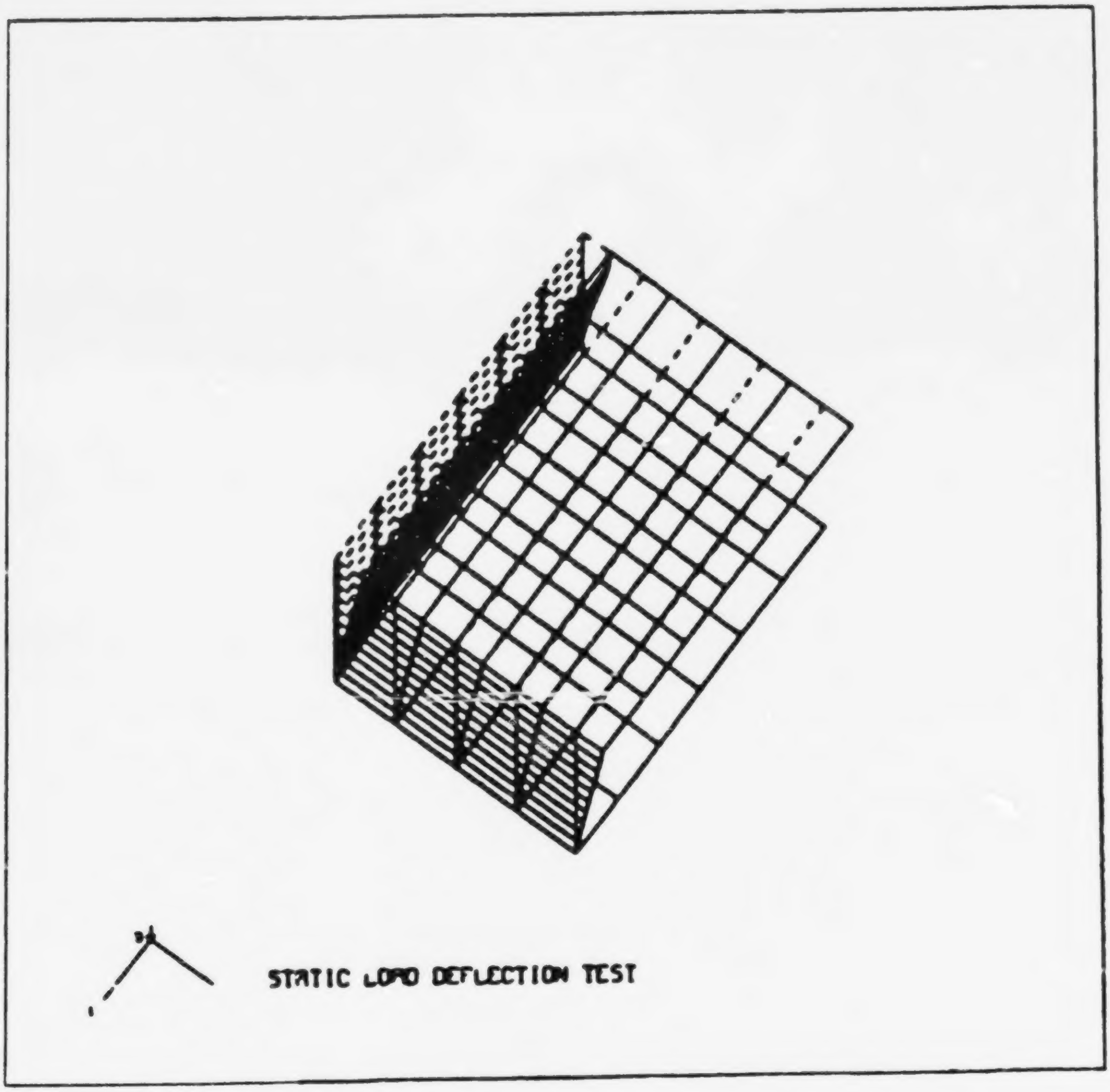
STATIC LOAD DEFLECTION TEST

Fig. 10. One-quarter model finite element mesh used for finite element calculations.

## TABLE V
## ENGINEERING MECHANICS/STRUCTURAL DYNAMIC "BEST EFFORT" SUMMARY

| | | | First Mode Frequency under E.Q. conditions | |
|---|---|---|---|---|
| Computed $E_c$ (lb/in.$^2$) | Stiffness (lb/in.) | $\frac{K^*_{STRUCTURAL}}{K_{THEORY}}$ | Predicted (Hz) | $\frac{f^{**}_{MEASURED}}{f_{PREDICTED}}$ |
| $3.5 \times 10^6$ | $2.76 \times 10^6$ | 0.23 | 18.9 | 0.53 |
| $3.0 \times 10^6$ | $2.59 \times 10^6$ | 0.25 | 18.8 | 0.53 |
| $2.0 \times 10^6$ | $2.11 \times 10^6$ | 0.31 | 18.0 | 0.56 |

---

* $K_{STRUCTURAL}$ = 647,000 lb/in.

** $f_{MEASURED}$ = 10 Hz.

## TABLE VI
## SUMMARY OF RESULTS FROM A FINITE ELEMENT MODEL CALCULATIONS

| | | | First Mode Natural Frequency under E.Q. conditions | |
|---|---|---|---|---|
| $E_c$ (lb/in.$^2$) | Calculated Stiffness (lb/in.) | $\frac{K^*_{STRUCTURAL}}{K_{THEORY}}$ | Predicted (Hz) | $\frac{f^{**}_{MEASURED}}{f_{PREDICTED}}$ |
| Fixed-Based Model: | | | | |
| $3.5 \times 10^6$ | $4.04 \times 10^6$ | 0.16 | 29.0 | 0.34 |
| $3.0 \times 10^6$ | $3.47 \times 10^6$ | 0.19 | 26.8 | 0.37 |
| $2.0 \times 10^6$ | $2.33 \times 10^6$ | 0.28 | 21.9 | 0.46 |
| Bolts Modeled with Axial Springs: | | | | |
| $3.5 \times 10^6$ | $2.71 \times 10^6$ | 0.24 | 22.7 | 0.44 |
| $3.0 \times 10^6$ | $2.38 \times 10^6$ | 0.27 | 21.2 | 0.47 |
| $2.0 \times 10^6$ | $1.68 \times 10^6$ | 0.38 | 17.9 | 0.56 |

---

* $K_{STRUCTURAL}$ = 647,000 lb/in.

** $f_{MEASURED}$ = 10 Hz.

methodology for "plant structures of the future". Study of these tables indicate that all calculational bases produce results that are consistent with one another and are probably within the variations that would be handled by NRC Regulatory Guides that cover peak broadening. The difference between Method 1 and 2, for example, might represent accounting for soil-structure interaction or not. The point is that the calculational method will not account for the stiffness reduction at working loads that has been consistently measured in this program. Figure 11 illustrates this consistency using the "design method" basis of calculation and strain gage determined concrete material properties.

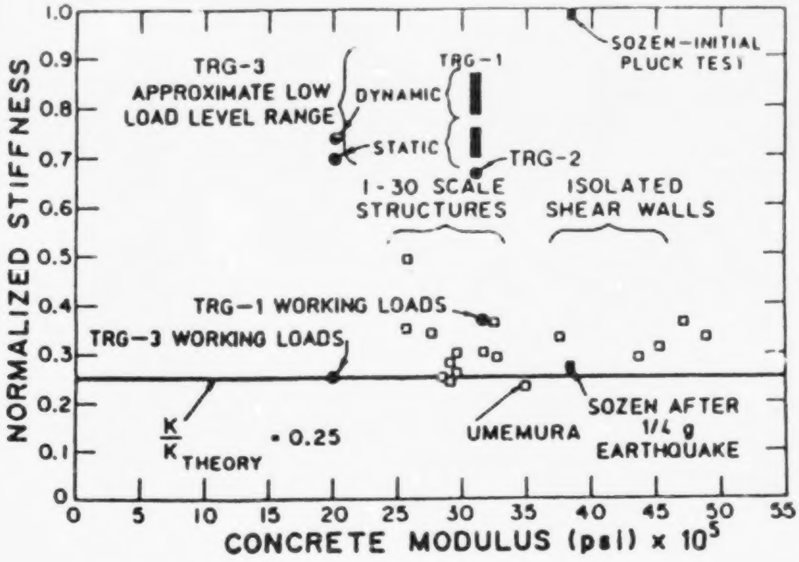

Fig. 11. Normalized stiffness for various tests at Los Alamos and elsewhere.

IMPLICATIONS WITH REGARD TO EQUIPMENT AND PIPING

To illustrate the implications of the "reduced working load stiffness," Figures 12 and 13 have been prepared using the first two calculational bases as discussed, and the response data taken from the top slab accelerometer for TRG-3. These figures compare the design floor response spectra for this particular aspect ratio shear wall structure.

The meaning of this result for existing and future Category I structures is under serious study by NRC, Los Alamos and industry. The ACI 349 code committee has been made aware the result as well as the ASCE Nuclear structures committee and its working groups.

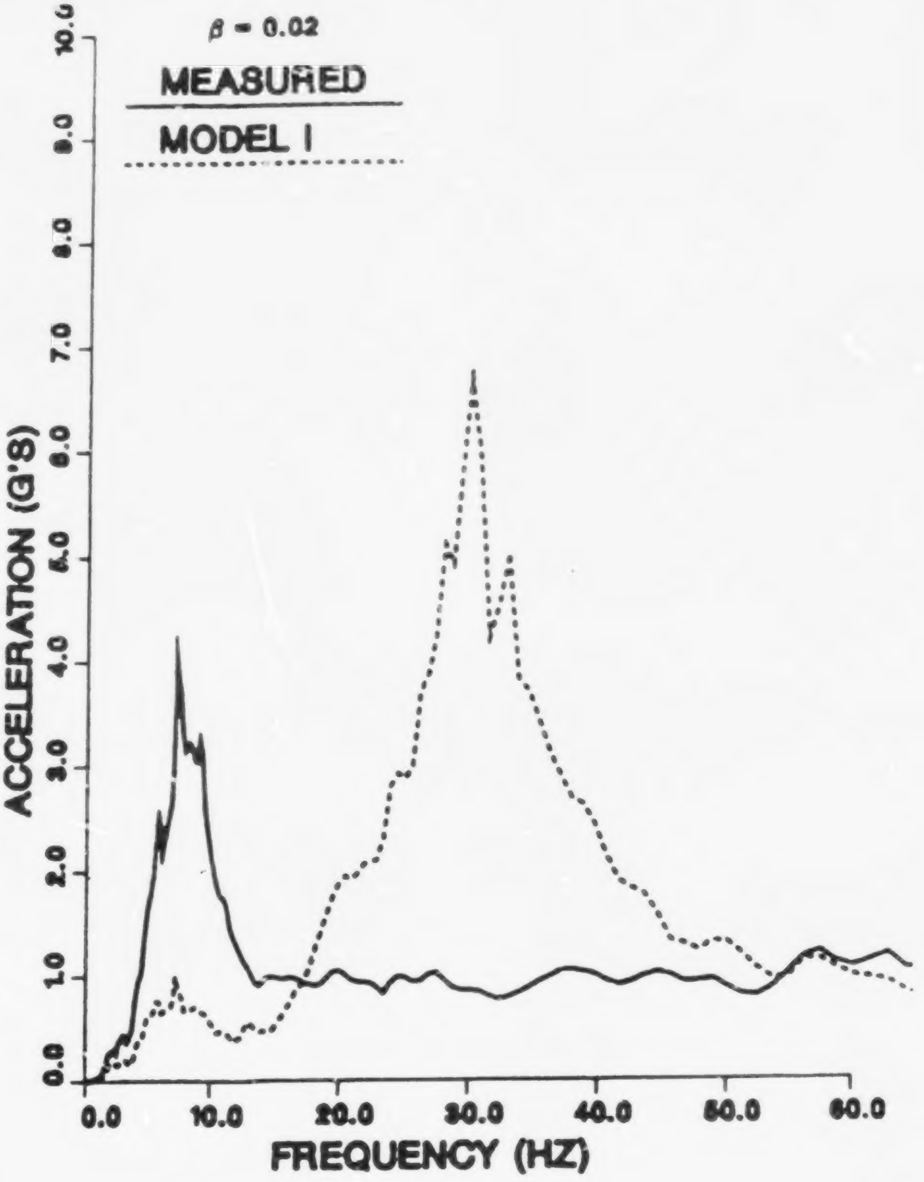

Fig. 12. The floor response spectra as calculated from the acceleration record using the "Design Basis" model compared with the floor response spectra calculated from the top slab accelerometer record.

BEST COPY AVAILABLE

Clearly further testing is necessary on real structures to verify this result. The TRG has recommended varying both aspect ratio and percentage reinforcing in these models in carrying out such verification. They have also recommended returning to a quasistatic cyclic loading. A set of experiments was laid out using statistical experimental design methods that will begin during FY 87. The end product of this effort should be a model that will predict the stiffness as a function of aspect ratio, percentage reinforcing and load level. The program will continue to work closely with NRC, the TRG, and code committees to make the best use of these research results.

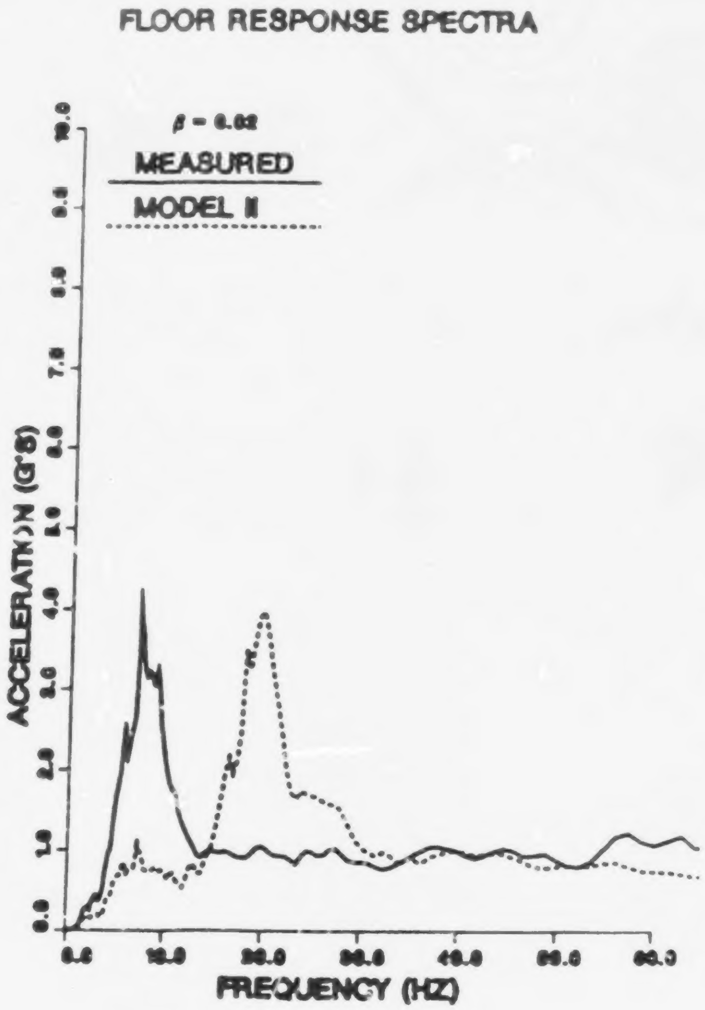

Fig. 13. The floor response spectra calculated from the "Engineering Mechanics" model of the structure compared with that calculated from the top slab accelerometer record.

## REFERENCES

1. Endebrock, E. G., Dove, R. C., Anderson, C. A., "Seismic Category I Structures Program," Proceedings of the 12th Water Reactor Safety Information Meeting, National Bureau of Standards, October 22, 1984, Bethesda, Maryland.

2. Dove, R. C., Endebrock, E. G., Dunwoody, W. E., Bennett, J. G., "Seismic Tests on Models of Reinforced Concrete Category I Buildings," 8th International Conference on Structural Mechanics in Reactor Technology, Brussels, Belgium, August 19-23, 1985.

3. Endebrock, E. G., Dove, R. C., Dunwoody, W. E., "Analysis and Tests on Small Scale Shear Walls - FY 82 Final Report," Los Alamos National Laboratory report NUREG/CR-4274, September 1985.

4. Oesterle, R. G. et al., "Earthquake Resistant Structural Walls - Tests of Isolated Walls - Phase II," NSF Report No. PB80-132418, Portland Cement Association, Skokie, IL, October, 1979.

5. Oesterle, R. G., et. al., "Earthquake Resistant Structural Walls - Tests of Isolated Walls," *NSF Report No. PB 271467/AS*, Portland Cement Association, Skokie, IL, November, 1976.

6. Popov, E. P., *Introduction to Mechanics of Solids*, Prentice-Hall (1968), Englewood Cliffs, NJ.

7. ASTM C31-83, "Standard Method of Making and Curing Concrete Specimens in the Field."

8. ASTM C172-82 "Standard Method of Sampling Freshly Mixed Concrete."

9. ASTM C143-78 "Standard Test Method for Slump of Portland Cement Concrete."

10. Clough, R. W., Penzien, T., *Dynamics of Structures*, McGraw-Hill (1975), New York, NY.

# RISK EVALUATIONS OF AGING PHENOMENA:
# THE LINEAR AGING RELIABILITY MODEL AND ITS EXTENSIONS*

W. E. Vesely
Science Applications International Corporation
Suite 245, 2929 Kenny Road, Columbus, Ohio 43221
(614) 451-0515

## ABSTRACT

A model for component failure rates due to aging mechanisms has been developed from basic phenomenological considerations. In the treatment, the occurrences of deterioration are modeled as following a Poisson process. The severity of damage is allowed to have any distribution, however the damage is assumed to accumulate independently. Finally, the failure rate is modeled as being proportional to the accumulated damage. Using this treatment, the linear aging failure rate model is obtained. The applicability of the linear aging model to various mechanisms is discussed. The model can be extended to cover nonlinear and dependent aging phenomena. The implementability of the linear aging model is demonstrated by applying it to the aging data collected in NRC's Nuclear Plant Aging Research (NPAR) Program. The applications show that aging as observed in collected data have significant effects on the component failure probability and component reliability when aging is not effectively detected and controlled by testing and maintenance.

## 1.0 INTRODUCTION

Aging occurs when physical and operating properties of structures and components degrade. Various mechanisms and stressors cause the physical and operating characteristics to degrade and hence cause aging. These mechanisms and stressors include neutron and gamma fluxes which cause irradiation damage, pressures and temperatures which cause fatigue and material toughness changes, and stress corrosion which causes cracking and fractures.

When the properties of structures and components degrade then their reliabilities can degrade. The reliability is determined by such quantities as the frequency of an initiating event (such as a pipe break), the component failure rate, and the structural unavailability. When the reliabilities of structures and components change then the safety and risk of the plant can be adversely affected.

The relationship whereby mechanisms cause property changes which cause reliability changes which in turn affects plant safety is the tie, or overall

---

* Work supported by the U.S. Nuclear Regulatory Commission, Office of Nuclear Regulatory Research, under DOE Contract No. DE-AC07-76ID01570.

relationship, between aging and plant safety. To understand and control the effects of aging on plant safety, it is important to identify and model the individual relationships involved in the overall relationship between aging and safety.

The identification and modeling of the individual relationships involves determining and measuring the property changes caused by various mechanisms occurring in plant environments and under plant operating conditions. It involves determining the relationships between property changes and reliability by relating failure rates and reliability parameters to property characteristics. It finally involves relating component and structure reliability to plant safety and risk by constructing and evaluating plant safety analyses and plant risk analyses.

In this work we will focus on the relationships involving aging mechanisms, property changes, and component failure rates. Specifically, we will develop models which express the component failure rate and component reliability in terms of parameters which characterize the rate and severity of occurring aging mechanisms. We thus relate the component failure rate to aging mechanism characteristics, bypassing the property and physical change relationships.

We proceed in this manner, relating the failure rate directly to aging mechanism parameters since available component failure data will allow us to directly estimate the aging mechanism parameters and hence the aging failure rates for the components. With estimates of the component aging failure rates, we can then determine the impacts of aging on public health risk, core melt probability, and other risk measures using risk models such as probabilistic risk analyses (PRA's).

The models which we will develop will allow physical property considerations and condition monitoring considerations to be incorporated in the future. This can be done by relating the aging mechanism characteristics to material and physical property changes. Using the models which relate failure rates to the aging mechanism characteristics, the component failure rates can then be expressed in terms of the material and physical property characteristics. This will allow condition monitoring measurements to be related to reliability implications, which is necessary for effective application of condition monitoring.

It is important that the component aging reliability models that are developed be compatible with the data and knowledge that exist. If the component model has more parameters than are meaningfully determinable from present information then the model will be overspecified. Examples of models which can be overspecified when sparse data are only available include the more or less standard statistical approaches which utilize the Weibull distribution, gamma distribution, etc. to statistically fit sequences of failure times. In these approaches, the time to failure distribution of an aging component is described by a statistical distribution with unknown parameters. The parameters are then empirically determined by fitting the data according to some criterion. The potential problem with these more or less standard approaches is that significant amounts of detailed failure time data are needed to estimate with any precision values for the parameters. Furthermore, the parameters are rather abstract and it is difficult to interpret their engineering implications.

Our objective in this work is to develop component aging reliability models which are compatible with sparse data and which have an engineering justification and an engineering interpretation. Because failure data exhibiting aging behavior is rather gross and summarized in its present form (see for example, 1, 2, 3, 4), the models need to be as parsimonious as possible, having as few parameters as possible but still having a valid foundation.

## 2.0 DERIVATION OF THE LINEAR AGING MODEL

Consider a specific aging mechanism which causes the component to deteriorate with age or use. The amount of deterioration can range from negligible to significant, depending upon the specific stresses the component experiences while on standby or while operating.

To be general, we will model the deterioration as being random in both the times at which the deteriorations occur and the severity of damage incurred by the component each time a deterioration occurs. If there is little variability associated with the deterioration then the component will undergo a very regular, continual deterioration, aging process. If there is high variability to the deterioration then the component will undergo a highly irregular aging process. We will develop our model to cover both extremes as well as intermediate cases.

To achieve the above flexibility in a parsimonious manner, we will model the occurrence of the deteriorations as following a Poisson process with a constant occurrence rate r. This implies that the probability of occurrence of a deterioration in some small age interval is proportional to the size of the interval and is independent of the past number of deteriorations which have occurred. The probability $P_n(t)$ of n deteriorations occurring in age t is then given by the Poisson distribution:

$$P_n(t) = \frac{(rt)^n e^{-rt}}{n!} \qquad n=0,1,\ldots \qquad (1)$$

The age t can be time, cycles, or some other relevant measure of age.

The Poisson covers the range from highly irregular deterioration ($m=rt<<1$) to highly regular deterioration ($m>>1$) and cases between. Since the damage from a particular deterioration occurrence has not been restricted and can be of any size, the spectrum of possible cumulative damage from the deteriorations which is covered by the model is quite general.

The restrictions the Poisson has in terms of age modeling are that the probability of a deterioration is proportional to the age interval (if the interval is small) and the occurrence of a deterioration is independent of past deteriorations which have occurred. The probability of a deterioration being proportional to the age interval implies that the age scaling is linear, to use the terminology of cumulative damage process modeling (5, 6).

Now that we have characterized the occurrences of deteriorations by a Poisson distribution we need to characterize the severity of deterioration incurred at each occurrence. The severity of deterioration can be the amount of damage incurred by an individual applied stress or the size of physical or material property change which occurs in a time interval in an aging environment. We shall allow the size of the deteriorations to have any distribution $f(x)$. The only constraint is that the distribution has a finite mean value say $\bar{x}$. We assume, however, that the severity of deteriorations in different occurrences, i.e. the severity increments, are independent and have the same general distribution $f(x)$.

As a last step in our development of the linear aging model, we need to relate the deterioration of the component at a given age to its failure rate. We will model the failure rate as being directly proportional to the deterioration which has occurred. This is the most straightforward characterization. To express the proportionality relationship between the failure rate and the deterioration, let the failure rate be denoted by $\lambda(t)$ for the component failing at age t due to a specific aging mechanism. The basic definition of the failure rate is given by:

$\lambda(t) =$ the probability per unit time that the component fails at age t due to a specific aging mechanism. (2)

This is a standard definition of a time dependent failure rate with the age measure replacing time. Note that in the above definition, the probability of failure is not conditioned on the fact that no failure occurred before t. The failure rate $\lambda(t)$ is thus not a first failure rate. The failure occurring at age t can be the first, second, or any subsequent failure. In general, based on the sparse data available it is often not known whether a failure is the first or not.

By the proportionality characterization, the failure rate is directly proportional to the specific amount of deterioration D the component has experienced from the aging mechanism to age t:

$$\lambda(t) = kD, \tag{3}$$

where k is the probability conversion constant.

Using the Poisson distribution for the number of deteriorations, the general distribution $f(x)$ for the size of each deterioration, and the deterio-

BEST COPY AVAILABLE

ration relationship given by Equation (3), the expected value for $\lambda(t)$ can be expressed in terms of the equation,

$$\lambda(t) = \sum_{n=0}^{\infty} P_n(t) \int_{0}^{\infty} f_n(D) kD dD \qquad (4)$$

$P_n(t)$ is the probability that n deteriorations occur and $f_n(D)$ is the probability distribution for the total deterioration D given n deteriorations have occurred. For a given deterioration D the failure rate $\lambda(t)$ is equal to kD which is the additional factor in the above equation. The failure rate for a specific deterioration kD is thus averaged over all possible values of n and D to obtain the expected failure rate $\lambda(t)$.

Equation (4) can be straightforwardly evaluated (see reference 7) to obtain

$$\lambda(t) = k\bar{x}rt \qquad (5)$$

where $\bar{x}$ is the average value of the distribution f(x) and is the average severity, or damage, associated with each deterioration occurrence. The parameter r is again the rate of occurrence of the deterioration and k is the proportionality constant.

We thus arrive at the linear aging model in which the aging failure rate $\lambda(t)$ is linearly proportional to the age t with the proportionality constant equal to $k\bar{x}r$,

$$\lambda(t) = at \qquad (6)$$

with

$$a = k\bar{x}r \qquad (7)$$

The parameter "a" can be termed the aging rate since it is the rate at which the failure rate increases due to the aging mechanism.

Based on its phenomenological development, the linear aging model is applicable for modeling aging mechanisms which cause an accumulated degradation in the component so as to continually increase its failure rate. The assumption of independent severity increments implies that the damage or material property changes accumulates as independent increments which are not significantly influenced by the past accumulated damage or change. The model is thus applicable to such aging processes as linear wear, linear material build-up, and linear elastic related phenomena.

Even where the damage build-up is not linear or independent, such as due to vibration, the linear aging model can provide first order linear approximations. Because of the sparseness and uncertainty in available data, the inaccuracies due to using the linear model will often be overshadowed by the data uncertainties. The subsequent sections discuss how the linear model can be extended to cover non-Poisson, nonlinear, and dependent aging phenomena when data allows these effects to be differentiated.

A linear failure rate may appear to be a rather strong time increasing failure rate when compared to Weibull failure rates which are sometimes obtained where the power of t is less than one. However it should be remembered that the linear aging failure rate applies to specific aging mechanisms while the Weibull and other such failure rates generally apply to the total failure rate. When a linear failure rate is combined with other failure rates, such as a random failure rate representing random failure mechanisms, the combined total failure rate will often have an effective power of t less than one.

Using phenomenologically based approaches similar to the above, additional formulas can be derived for the component failure rate which apply when the deterioration occurrences are nonlinear in time and when the damage incurred is dependent upon the past accumulated damage. These extensions to the linear aging model are summarized later in the paper and are described in detail in reference 7. The extended models can be used when sufficient data exist to discriminate among the models or when knowledge of the specific aging mechanism behaviors justify use of the extended models. Reference 7 shows that the linear aging model is also obtainable as a first order approximation of these more complex, extended models. (It is interesting to note that the linear aging model is furthermore obtainable from the Arrhenius equation for thermal, molecular deterioration of materials by assuming a constant operating temperature and assuming the failure rate is proportional to the accumulated reaction rate (for the Arrhenius equation, see for example (8))).

A strong feature of the linear aging model is its implementability. The macroscopic aging rate a can be determined from failure data using various data analyses techniques. Since the linear aging failure rate involves only one parameter, the aging rate a, the failure data do not need to be as detailed as needed for Weibull and other standard time dependent approaches. This need for less data is supplemented by engineering knowledge of the aging mechanisms involved and assessment of whether the behavior of these mechanisms is consistent with that modeled in the linear aging model.

When material properties or more detailed component condition monitoring is of interest, then the linear aging rate a can be decomposed into its more basic constituent factors k, r and $\bar{x}$. These factors can be related to the load conditions, environment, and material strength characteristics. In this manner, the load conditions, environment, and material properties can be directly tied to the component failure rate and resulting reliability. In the applications which have been performed, the linear aging model has proven to be a flexible model which is useable with gross data as well as detailed data. When time history data existed so as to be able to test the adequacy of the linear model versus its extension to more complicated models, the linear model was generally found to be consistent with the data. Reference 7 presents in more detail evaluations that were performed.

## 3.0 EXTENSION TO STATIONARY PROCESSES

If instead of using the Poisson model for $P_n(t)$, we only assume the deterioration occurrences are regular with an expected value proportional to the age then the only constraint on $P_n(t)$ is that

$$\sum_{n=0}^{\infty} P_n(t)n = rt \qquad (8)$$

where $P_n(t)$ is the general occurrence distribution and r is the expected occurrence rate of the deteriorations. It is shown in reference 7 that this is the only relationship needed to obtain the linear aging model and Equations (6) and (7). Processes characterized by Equation (8) are termed stationary processes in stochastic modeling (9). Thus the linear aging model is applicable not only to Poisson deterioration processes but to any deterioration occurrence process which is stationary and characterized by Equation (8).

## 4.0 EXTENSION TO NONLINEAR AGE SCALINGS

It is shown in reference 7 that if instead of an occurrence rate which is linear with time, we assume the deteriorations occur with some general time dependent rate Q(t) then we will obtain

$$\lambda(t) = k\bar{x}Q(t). \qquad (9)$$

Equation (9) is the generalization of the linear failure rate model to nonlinear aging phenomena. Instead of being proportional to the age t, the failure rate is generalized to be proportional to the deterioration scaling Q(t). For example, $Q(t) = at^b$, where a and b are constants, gives the Weibull process aging model or the power scaling model as sometimes termed in cumulative damage modeling (5, 6). When sufficient data are available then one can test whether a nonlinear scaling is needed for specific mechanisms and determine the estimate of Q(t) which best fits the phenomena.

## 5.0 APPLICATIONS WHEN SEVERAL AGING MECHANISMS ACT ON THE COMPONENT

Both the linear and nonlinear aging models derived in the previous sections can be straightforwardly applied to situations where different aging mechanisms act on the component. Because of the additive property of the Poisson the overall aging failure rate of the component is the sum of the individual aging mechanism failure rates. The individual aging mechanism failure rates can be either linear or nonlinear.

Consequently if K different aging mechanisms act on the component, each with failure rate $\lambda_k(t_k)$, then the total aging failure rate $\lambda_A$ is the sum of the individual mechanism failure rates,

$$\lambda_A = \lambda_1(t_1) + \lambda_2(t_2) + \ldots + \lambda_K(t_K) \qquad (10)$$

In the most general case indicated above, each aging mechanism can have its

BEST COPY AVAILABLE

own associated age which represents the time (or cycles) of exposure of the component to the particular aging mechanism.

## 6.0 INCORPORATION OF CONSTANT FAILURE RATE CONTRIBUTIONS

A constant failure rate contribution representing non-aging, random failure causes can be added to the aging failure rate to obtain the total component failure rate. If $\lambda_T$ is the total component failure rate then

$$\lambda_T = \lambda_0 + \lambda_A \tag{11}$$

where $\lambda_0$ is the constant failure rate contribution and $\lambda_A$ is the aging failure rate contribution given by Equation (10).

A constant failure rate contribution can also be added to a particular aging mechanism failure rate. The constant failure rate contribution can represent the residual failure rate when there is no deterioration experienced in the particular age interval. For example the residual failure rate may represent damage already existing in an installed component. For a residual constant failure rate contribution c, the linear aging rate generalizes to

$$\lambda(t) = c + at \tag{12}$$

where again

$$a = k\bar{x}r \tag{13}$$

## 7.0 EXTENSION OF THE LINEAR AGING MODEL TO COVER DEPENDENT AGING MECHANISMS

As stated, the linear aging model assumes the severity of deterioration which occurs at any time to be independent of the past accumulated deterioration or damage. To generalize this treatment we can extend the model in a straightforward manner to allow the severity to be linearly dependent on the size of the past deterioration. To still allow the deteriorations to be random, we shall model the mean of each severity occurrence as being linearly dependent upon the past accumulated deterioration. Since we allow the variation (variance) of each severity to be of any size, this dependency model is still rather general covering loose to very strong dependencies.

In terms of equations, the linear dependency model can be expressed as

$$\bar{x} = \alpha + \beta D \tag{14}$$

where $\bar{x}$ is the mean, or average size, of a deterioration occurrence given a past accumulated deterioration D, and $\alpha$ and $\beta$ are constants. The constant $\beta$ represents the strength of the dependency. If $\beta$ is zero then the deteriorations are independent of one another and we obtain the independence assumption in the linear aging model.

It is shown in reference 7 that using the above model, we obtain

$$\lambda(t) = k\frac{\alpha}{\beta}(e^{rt\beta}-1) \tag{15}$$

For small $\beta$, expanding the exponential to first order we have

$$\lambda(t) = k\frac{\alpha}{\beta}(1+rt\beta-1) = k\alpha rt \tag{16}$$

which is again the linear aging model with $\alpha = \bar{x}$. Thus the above model generalizes the linear aging model to cover nonlinear aging dependencies.

## 8.0 DEMONSTRATION OF THE COMPONENT RELIABILITY EFFECTS OF AGING

To determine the component reliability effects of aging using the linear aging model, we need to estimate the parameters in the model. For failure data used as the source of aging information, this means estimating the aging rate "a" for specific aging mechanisms acting on specific components. To demonstrate the application of the linear aging model, we will utilize aging rates that are consistent with the generic aging data described in references 1, 2, 3, and 4 and collected through the Nuclear Plant Aging Research (NPAR) Program (10) being conducted by the Office of Research for NRC. The data described in these references basically consist of the fractions of component failures that are due to categories of aging mechanisms. The data are averaged over different plants and different component ages, and the data have uncertainties associated with their classification and counting.

The aging data which we use is thus rather gross and has nonnegligible uncertainties. However even with the grossness and uncertainties, we will show how the data can be utilized in the linear aging model to investigate the effects of aging on component reliability. The example calculations will thus demonstrate that the linear aging model does not necessarily require detailed or precise data for exploratory evaluations.

To estimate the aging rate for a specific aging mechanism, or a category of aging mechanisms, we use a moments method type of estimation approach. The moments method approach is a common statistical estimation technique particularly useful for grosser data (see for example reference 11). The moments method approach as applied to the aging data is described in (7). For more detailed or precise applications, the aging root cause data collected in NPAR's Root Cause Data Program being conducted by the Idaho National Engineering Laboratory (12) can be used. This more precise data was used for the more detailed system unavailability evaluations that are described in reference 7.

Applying the moments method approach to the generic data collected in NPAR, Figure 1 shows the failure probability (or unreliability) F(t) versus age for a single component with an aging rate a of $2\times10^{-4}$ per year$^2$ (or $2\times10^{-12}$ per hour$^2$). The aging rate in Figure 1 is characteristic of foreign

BEST COPY AVAILABLE

## Figure 1. FAILURE PROBABILITY VERSUS AGE

Single Component Failing a=2E-04

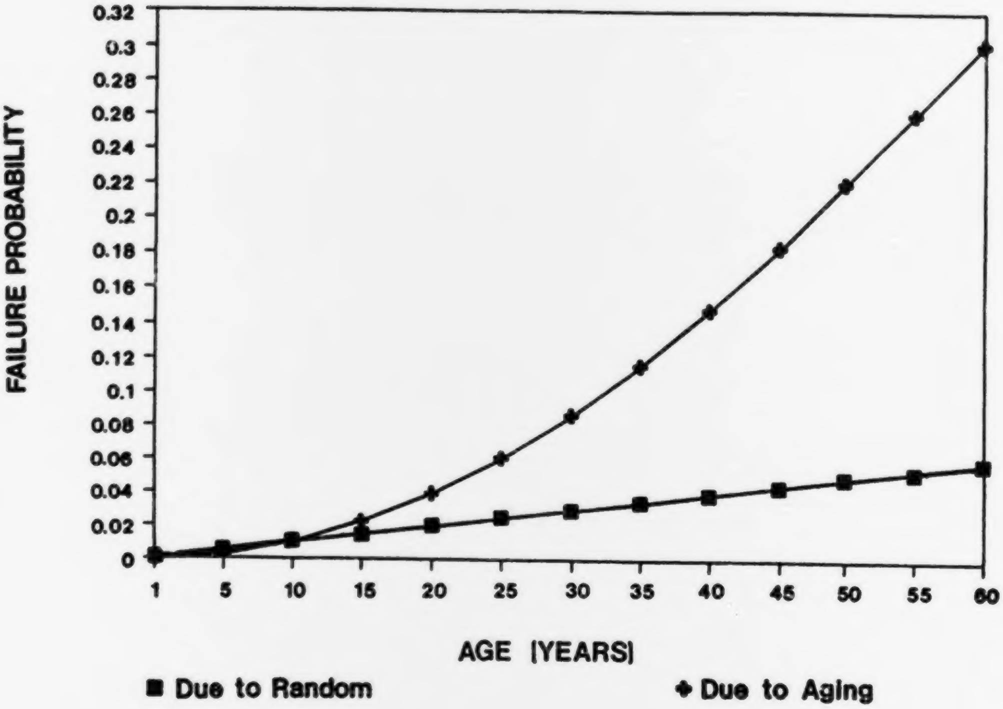

## Figure 2. FAILURE PROBABILITY VERSUS AGE

Single Component Failing a=2E-04

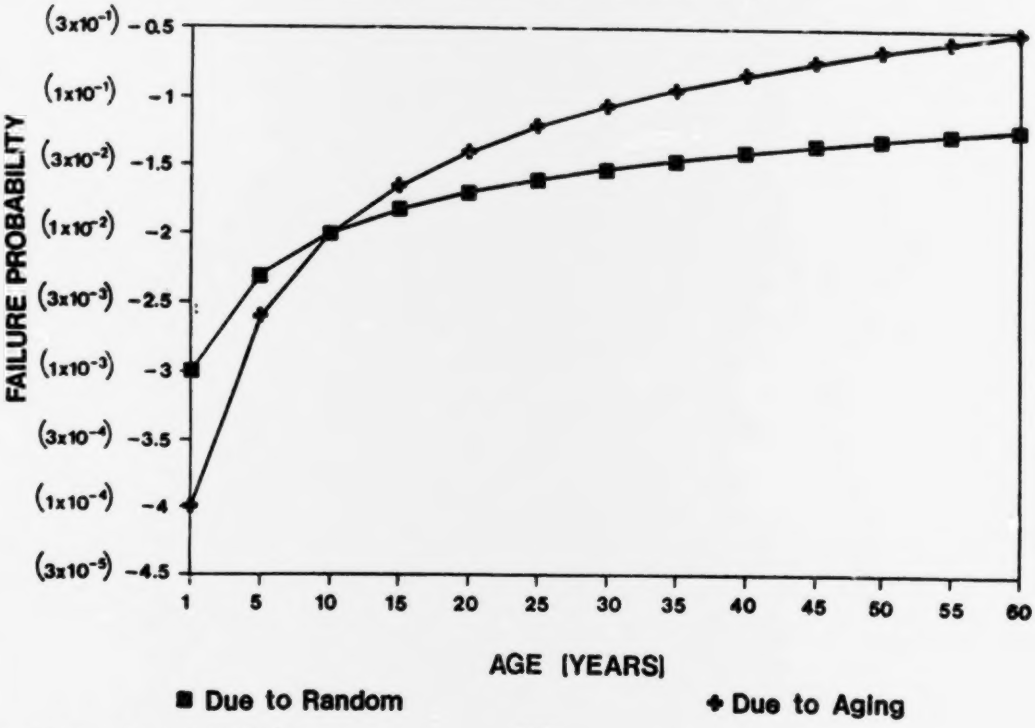

material buildup in a valve (1, 4). No surveillance tests and maintenances are assumed to be performed to detect or correct the buildup problem. The failure probability curve due to random failures is the failure probability from the constant failure rate for the component; it is basically the curve that would be obtained if all failures were treated as random as done in PRAs. As observed, the aging effects become increasingly significant after 25 years. Figure 2 shows the same results as Figure 1 but on a log scale (to the base 10); the unavailabilities are in parentheses beside their corresponding log values.

When multiple components age, then there is a multiplicative effect on the failure probability. Figures 3 and 4 show the failure probability for two components both failing and three components failing, respectively from aging and from random mechanisms. The figures plot the log of the failure probability. The individual components each have the failure probability shown in Figure 1. As observed, aging has a compounding effect on the probability of multiple components failing, in this case multiple valves failing due to material buildup.

To more explicitly show the impacts of aging, Figures 5, 6 and 7 show the ratio of the aging failure probability to the random failure probability. The figures are plots of the ratios of the curves of the previous figures and more vividly show the significant impacts of aging for the data used when no testing or maintenance is performed to detect or correct the aging mechanism.

In addition to the above calculations, various other calculations of the component failure probability (or unreliability) were performed and are described in (7). These calculations used the aging fractions in references (1, 2, 3, 4, and 12), which generally varied from 0.2 to 0.8 (i.e. 20% to 80% of the failures were aging related) depending upon the aging mechanism and component involved. In general, the aging observed, based on this nuclear experience caused the component failure probability to significantly increase above the random failure value, or PRA calculated value, at some age before 40 years. Aging caused the failure probability of a single component whose age was more than 20 years to increase anywhere from a factor of 3 to more than a factor of 30 over the random or PRA failure probability value. The specific size of increase and the time trend depended upon the specific component and mechanism.

These aging effects on single component failure probabilities were multiplied when the probabilities of two components failing or three components failing were calculated. The increases for two components failing ranged anywhere from a factor of 10 to more than a factor of 1000 over the random or PRA value. These multiplicative effects are an exhibit of the common cause effect of aging which simultaneously increases component failure rates and which can be due to the same or different aging mechanisms. The aging components can also be similar or different, which shows the broad pervasive effects of aging.

Figure 3. FAILURE PROBABILITY VERSUS AGE

Two Components Failing a=2E-04

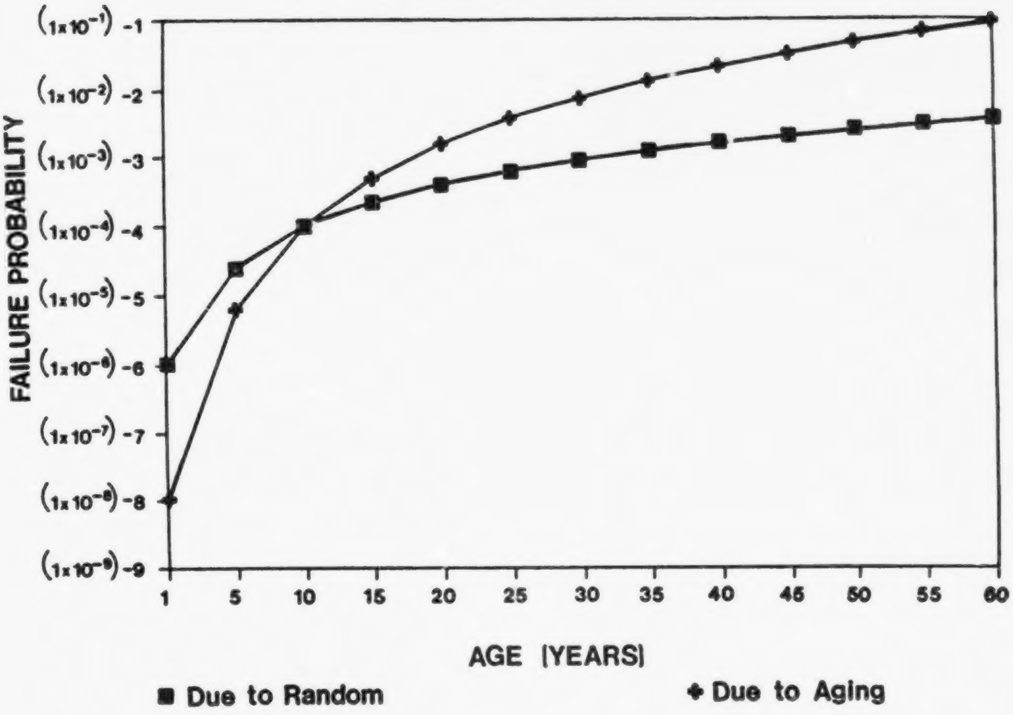

Figure 4. FAILURE PROBABILITY VERSUS AGE

Three Components Failing a=2E-04

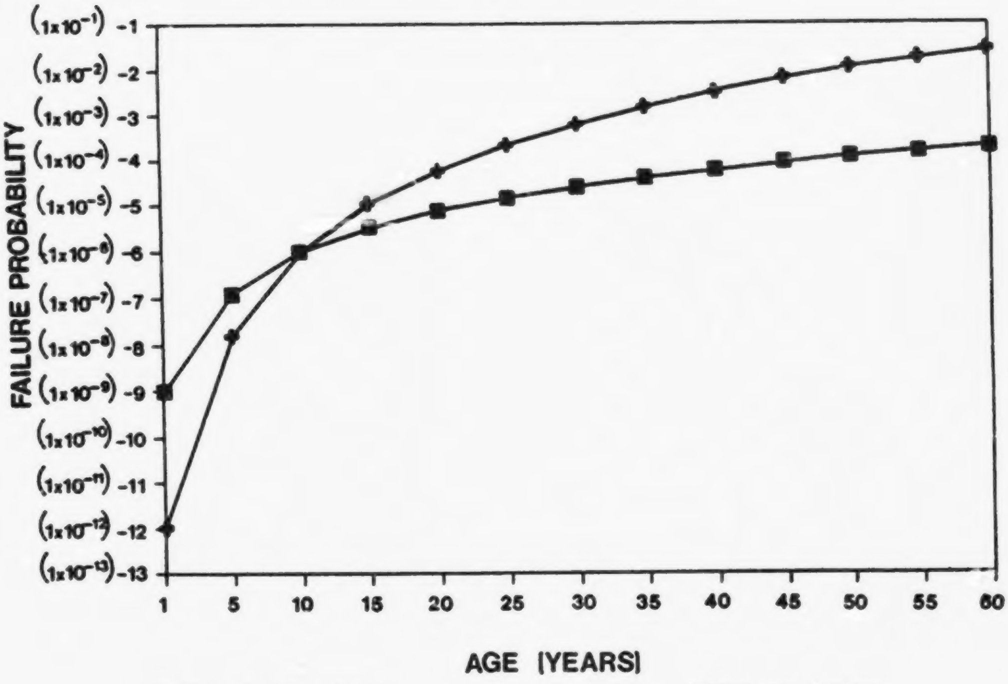

Figure5. RATIO OF AGING TO RANDOM FAILURE

Single Component Failing a=2E-04

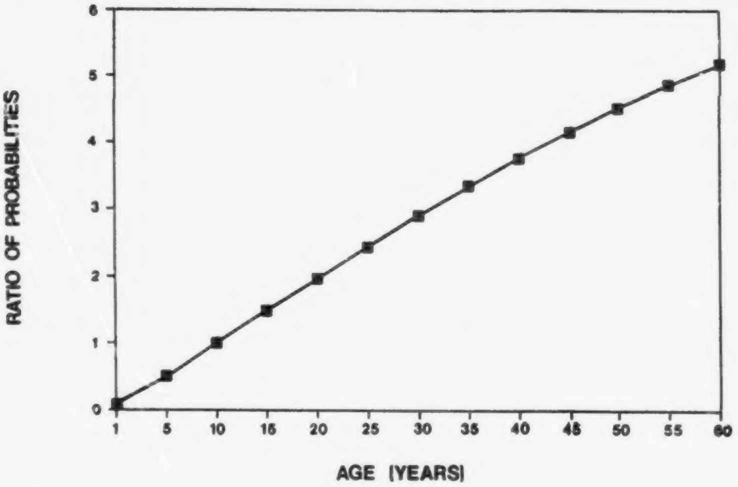

Figure 6. RATIO OF AGING TO RANDOM FAILURE

Two Components Failing a=2E-04

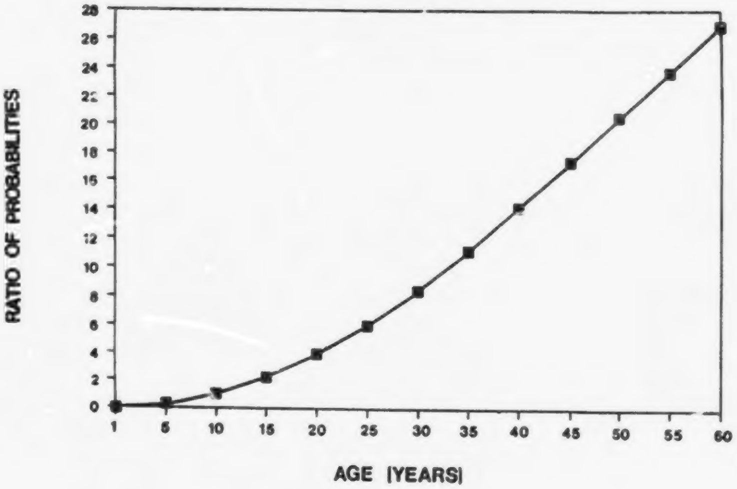

Figure 7. RATIO OF AGING TO RANDOM FAILURE

Three Components Failing a=2E-04

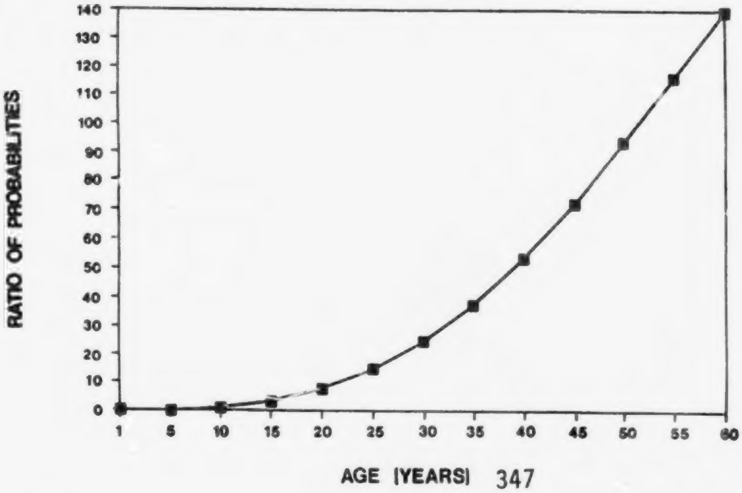

BEST COPY AVAILABLE

The above impacts of aging represent maximum impacts, obtained under the assumption that no testing or maintenance is performed to detect or control the aging mechanisms. In actual practice, testing and maintenance are performed and hence the aging impacts will generally be smaller than those which were obtained. However in specific cases the aging impacts can be as large as those obtained even if testing and maintenance is performed, if that testing and maintenance is ineffective in detecting and controlling aging mechanisms. For example, air tests or low pressure tests of piping are generally ineffective in detecting stress corrosion degradation. Valve controller tests are also ineffective in detecting fatigue or corrosion in valve bodies. Thus we must be careful in assessing the effectiveness of a test or maintenance on a specific aging mechanism then that test or maintenance is performed.

Even though the results we obtained are limited in assuming no testing or maintenance is performed on the aging mechanisms, they are very useful for several reasons. The results indicate that the models developed are practical for evaluating and studying the reliability impacts of aging even if gross data are only used. They further indicate what data needs to be obtained if more precise results are desired. Finally the results indicate that the data collected at nuclear plants imply that aging has significant effects on component reliability, if aging is not effectively detected and controlled.

Reference 7 describes more comprehensive applications of the linear aging model in which the linear model was used to not only evaluate component failure probability effects of different aging mechanisms, but also system unavailability effects of aging. For the system unavailability evaluations, different aging mechanisms affecting the components in the system were handled and the effects of testing and maintenance in controlling aging were studied.

## 9.0 SUMMARY AND CONCLUSIONS

The linear aging model is an attractive model for evaluating the reliability implications of aging because of its phenomenological basis and its implementability. Engineering information on the aging mechanisms and their behavior can be utilized to complement available data in utilizing the linear aging model in its macroscopic form. Less detailed data is thus required and even gross data can be used for exploratory evaluations.

For more detailed evaluations involving load conditions, environmental effects, and material properties the linear failure rate can be decomposed into its microscopic constituent factors. This decomposition offers the opportunity for directly tying condition monitoring to failure rate and reliability implications. The linear aging model can also be extended to cover nonlinear and dependent aging mechanisms when data are available to differentiate these effects.

The implementability of the linear aging model is demonstrated by applying it to the gross aging data collected in the NRC's NPAR program. The demonstrations show the significant effects aging mechanisms can have on component failure probabilities if the aging is not detected and corrected by testing and maintenance. Future work needs to be done to construct data bases to more thoroughly apply the linear aging model using more precise aging mechanism data. More detailed modeling of testing and maintenance effects on aging needs to be carried out to evaluate the effectiveness of present testing and maintenance. Uncertainty analyses needs to be incorporated to quantify uncertainties associated with the aging risk evaluations. Programs need to be developed for applying the models to identify the regulatory issues and research needs which are associated with aging. The models can then be utilized to evaluate strategies for controlling aging effects and for reducing uncertainties. The models should furthermore be extended to more explicitly incorporate component and environmental characteristics for condition monitoring applications. Thus, only a first step has only been taken in evaluating the risk and reliability implications of aging.

## REFERENCES

1. G.A. Murphy et. al., "Survey of Operating Experience from LERS to Identify Aging Trends," NUREG/CR-3543, January 1984

2. M. Subudhi et. al., "Operating Experience and Aging - Seismic Assessment of Electric Motors," Preliminary Report, NUREG/CR-4156, December 1984

3. D.M. Eissenberg et. al., "Aging and Surface Wear of Electric Motor-Operated Valves Used in Engineering Safety-Feature Systems," Preliminary ORNL Report, March 22, 1985

4. J.A. Rose et. al., "Survey of Aged Power Plant Facilities." [illegible]REG/KR-3819, June 1985

5. J.L. Bogdanoff and F. Kozen, *Probabilistic Models of Cumulative Damage*, Wiley and Sons, New York 1985

6. E. Cinlair, "Markov and Semi-Markov Models of Deterioration" in *Reliability Theory and Models*, ed. by M.S. Abdel-Hamerd, E. Cinlair and J. Quinn, Academic Press, New York 1984

7. W.E. Vesely, "Risk Evaluations of Aging Phenomena: The Linear Aging Reliability Model and Its Extensions," NUREG/CR-4769 (EG&G-2476) to be published

8. IEEE Standard 323 - 1974, "IEEE Standard for Qualifying Class IE Equipment for Nuclear Power Generating Stations"

9. S.M. Ross, *Applied Probability Models with Optimization Applications*, Holden Day, San Francisco, 1970

10. Division of Engineering Technology, "Nuclear Plant Aging Research (NPAR) Program Plan," NUREG-1144, July 1985.

11. C.R. Rao, *Linear Statistical Inference and Its Applications*. Wiley and Sons, New York, 1965

12. D.G. Satterwhite et. al., "Identification and Importance Quantification of Aging Root Causes of Component Failure for Service Water Systems and Class IE Electrical Power Distribution Systems," NUREG/CR-4744, (EGG-2472), to be published.

# AN INTERIM ASSESSMENT OF REACTOR PROTECTION SYSTEM AGING[a]

Patrick T. Jacobs
Idaho National Engineering Laboratory
Idaho Falls, Idaho 83415

## ABSTRACT

An interim assessment of reactor protection system aging is presented. The research approach is a Phase I study for the Nuclear Plant Aging Research Program of the United States Nuclear Regulatory Commission. Results addressing each of the program's technical objectives are presented. Plans for continuation of the work into Phase II are discussed.

## OBJECTIVES

The technical objectives of the United States (U.S.) Nuclear Regulatory Commission (NRC) Nuclear Plant Aging Research (NPAR) Program are to:

- Identify and characterize degradation that may impair plant safety
- Identify methods of inspection, surveillance, and monitoring (ISM) to detect degradation before loss of safety function
- Identify methods to control or mitigate the consequences of degradation.

## INTRODUCTION

The NPAR Program is a phased research program that follows the strategy described in NUREG-1144.[1] Figure 1 is an overview of the program strategy. The results of an interim aging assessment on the reactor protection system (RPS) are presented in this paper. The format followed will be that of the program, i.e., equipment/system selection, boundary definition, evaluation of operating experience, and the interim assessment summarizing Phase I progress.

## EQUIPMENT/SYSTEM SELECTION

Systems and components studied under the NPAR Program have been selected using a combination of expert knowledge, recorded failure experience, and studies assessing the frequency of failure events, their consequences on plant safety, and the development and application of risk assessment methodologies. The program started research on components identified by industry experts in a workshop to address aging impact on plant safety.[2] Several component studies were underway before the identification and research on specific safety systems.

---

[a] Work supported by the U. S. Nuclear Regulatory Commission, Office of Nuclear Regulatory Research, under DOE Contract No. DE-AC07-76ID01570.

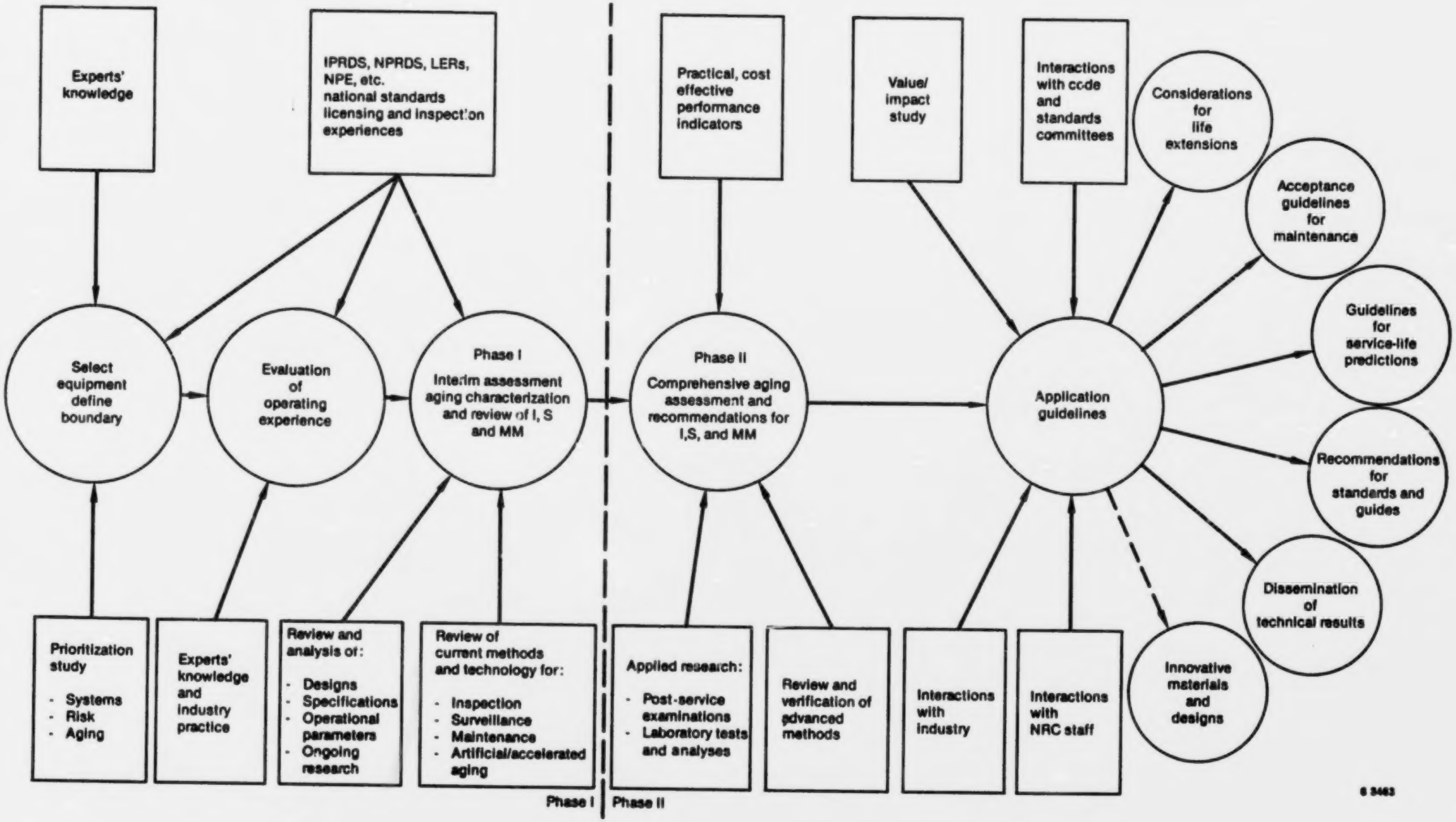
Experts' knowledge
IPRDS, NPRDS, LERs, NPE, etc. national standards licensing and inspection experiences
Practical, cost effective performance indicators
Value/ impact study
Interactions with code and standards committees
Considerations for life extensions
Acceptance guidelines for maintenance
Guidelines for service-life predictions
Select equipment define boundary
Evaluation of operating experience
Phase I Interim assessment aging characterization and review of I, S and MM
Phase II Comprehensive aging assessment and recommendations for I,S, and MM
Application guidelines
Recommendations for standards and guides
Dissemination of technical results
Innovative materials and designs
Prioritization study - Systems - Risk - Aging
Experts' knowledge and industry practice
Review and analysis of: - Designs - Specifications - Operational parameters - Ongoing research
Review of current methods and technology for: - Inspection - Surveillance - Maintenance - Artificial/accelerated aging
Applied research: - Post-service examinations - Laboratory tests and analyses
Review and verification of advanced methods
Interactions with industry
Interactions with NRC staff
Phase I
Phase II
6 3463

Figure 1. NPAR program strategy.

352

The first study performed by the Idaho National Engineering Laboratory (INEL) under NPAR[3] concluded that certain component failures were dependent on the system in which they operated and were caused by processes that degraded other system components as well. The identification of safety systems to be studied for aging degradation followed.[4] Existing research in the areas of risk assessment and systems interactions formed an important part of the basis for system selection.

The selection process involved a top-down look at plant safety, the design functions, and the systems that are needed to achieve the safety functions. It was decided to concentrate initially on those systems that protect the fuel and reactor coolant system pressure boundaries. Future efforts will include those systems that protect the containment boundary. Several systems were selected to begin the research: the RPS, emergency core cooling system (ECCS), Class 1E electrical power distribution system (EPDS), service water system, component cooling water system, and auxiliary feedwater system. The selection represents a cross section of electrical instrumentation and control systems and fluid-mechanical systems that are required to implement the various safety functions. Because of its central importance in the safety hierarchy, the RPS was selected for the pilot system study.

## REACTOR PROTECTION SYSTEM BOUNDARY

Significant variation exists among the Nuclear Steam Supply System (NSSS) designs in the systems used to achieve various safety functions, the components used in the various systems, and in the basic nomenclature used for the systems. The convention of IEEE Standard 603-1980 and the NRC's Standard Review Plan (NUREG-0800) were used in the study. Figure 2 shows the various functions, systems, components, and their interconnection within the safety system. The RPS boundary includes the reactor trip system (RTS) and the engineered safety features actuation system (ESFAS).

Figure 3 shows the components within the RPS that were included in the study. Specifically, the scope involved what IEEE Standard 603-1980 refers to as the "sense and command features of the safety system". The typical categories of components include: the process sensors, transducers, and transmitters that usually reside within the containment building (including the instrument piping that couples the process to various sensors); the cables, connectors, splices, terminal blocks, and electrical penetrations that are inside and outside of the containment; the signal processing electronics (amplifiers, square root extractors, comparators, bistables, etc.) and power supplies that usually reside in the control room; and the switches, relays, and breakers that are outside containment and usually in the control room.

## EVALUATION OF OPERATING EXPERIENCE

The evaluation of operating experience came from several sources: the plant-external data bases referenced in NUREG-1144 [licensee event reports (LERs), Nuclear Plant Reliability Data System (NPRDS), In-Plant

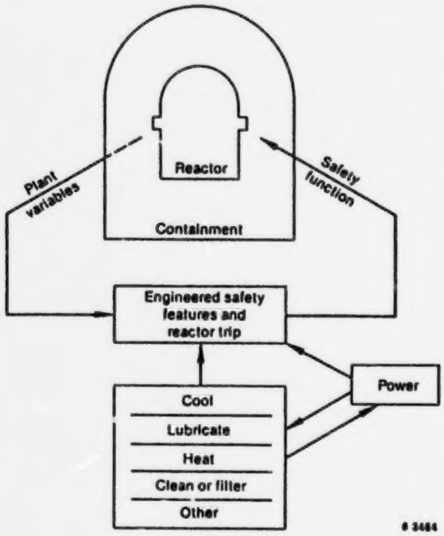
Reactor
Containment
Plant variables
Safety function
Engineered safety features and reactor trip
Power
Cool
Lubricate
Heat
Clean or filter
Other
6 3484

Figure 2. Typical safety system block diagram.

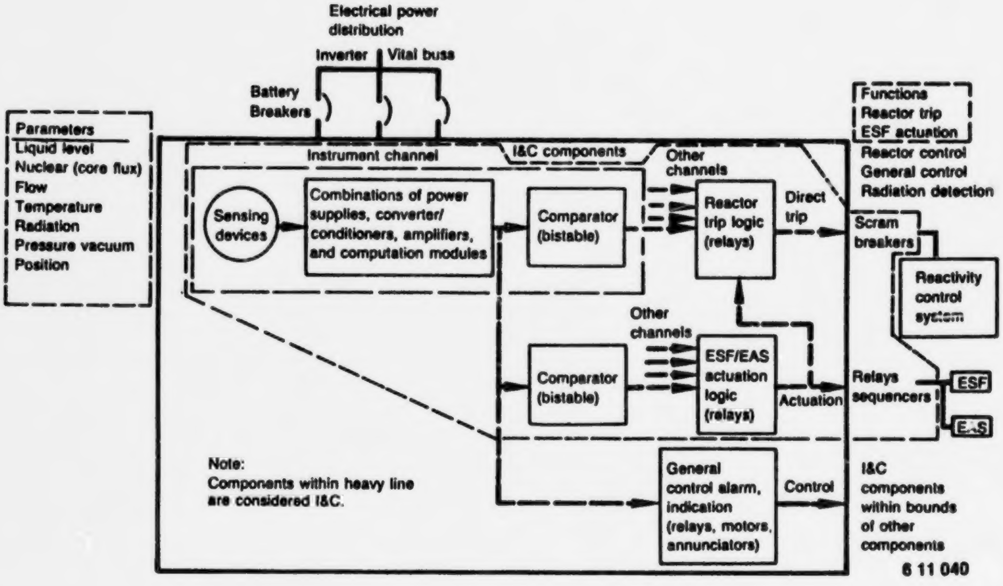
Electrical power distribution
Inverter
Vital buss
Battery
Breakers
Parameters
Liquid level
Nuclear (core flux)
Flow
Temperature
Radiation
Pressure vacuum
Position
Instrument channel
I&C components
Other channels
Sensing devices
Combinations of power supplies, converter/ conditioners, amplifiers, and computation modules
Comparator (bistable)
Reactor trip logic (relays)
Direct trip
Functions
Reactor trip
ESF actuation
Reactor control
General control
Radiation detection
Scram breakers
Reactivity control system
Other channels
Comparator (bistable)
ESF/EAS actuation logic (relays)
Actuation
Relays sequencers
ESF
EAS
Note:
Components within heavy line are considered I&C.
General control alarm, indication (relays, motors, annunciators)
Control
I&C components within bounds of other components
6 11 040

Figure 3. Simplified diagram showing boundary for RPS aging study.

Reliability Data System (IPRDS), and Nuclear Power Experience (NPE)] and from a cooperative research agreement with the Duke Power Company. Because of previous experience with the plant-external data, the approach was to use these sources as pointers for areas of investigation for the in-plant studies.

## Plant-External Data Source Results

Because the IPRDS is primarily a component-oriented data base for pumps (and their drivers), valves (and their operators), diesel generators, batteries, chargers, and inverters, it was not used in the RPS pilot study. However, the methodology used in creating the IPRDS was beneficial in conducting the in-plant portion of the study.[5] The sources used were the LERs and data bases based on the LERs, the NPE Automated Retrieval System and the volumes that contain the detailed event descriptions, and the NPRDS failure reports that were provided by the NRC.

A data base of selected LERs created for risk and reliability studies on instrumentation and control systems[6] was used for the RPS study[7]. The analysis was conducted using 1402 events reported on the RTS for the period 1976 to 1981. The categories of components reported most frequently are listed in descending order: sensors/transmitters, signal processing electronics, relays/breakers, power supplies, cables/connectors/terminals, and switches. The most frequent causes of reported events were (in descending order): drift, piece part failure, unknown, personnel maintenance, and electrical malfunction. Sixty-three percent of the events were detected through testing and thirty-four percent through normal operations. Fifty-six percent of the events were determined to be age-related (time in service), while twenty-five percent were found to be demand-related (frequency of use).

The NPE data base on the RPS contained 2487 events from over 25 years of experience through 1985 [1510 for RTS, 977 for engineered safety features actuating systems (ESFAS)]. The relative ranking of component categories varied slightly from the LER survey. Signal processing electronics, relays and breakers, and sensors ranked highest in the number of reported events. This is not totally unexpected because NPE draws heavily from documents available in the public domain. The variation could be due to the larger system boundary used with NPE (i.e., RPS includes ESFAS), the NPE survey included more years of data, or because NPE uses more references in their evaluations than just the LERs.

There was much more variation in the cause of failures, which could be attributed to the above differences as well as the methodology used in creating the NPE data base. Individual researchers analyze the events and request more information when, for example, the LER abstract provides insufficient data to complete the analysis. For this reason, a large percentage of the events attributed to unknown causes in the LER data base are resolved through further investigation. The analysis might also result in reclassification of other data fields for individual events. In analyzing the cause of the reported event, the following categories were found to be most dominant: operator/maintenance error, I&C component failure, design/construction error, mechanical wear, electronic drift, short/ground/arcing, and support system failure.

The NPRDS was used in a recent INEL NPAR task study[8] as a data source to aid in the quantification of risk attributable to aging degradation. For the nine LWR systems analyzed, approximately one-third of the events were categorized as aging and approximately one-half as "other". Failure records (3128) were provided by the NRC on the RPS for Westinghouse (which included ESFAS) and General Electric plants. The components exhibiting the most failures were: signal processing electronics, sensors and transmitters, switches, relays, and power supplies. This compares favorably with the results from the LER and NPE surveys. Failure events were assigned to one of five failure categories and their impact on the system determined with the results shown in Tables 1 and 2. The large percentage of events in the "other" category was attributed to lack of adequate failure analysis to resolve the cause.

TABLE 1. RPS FAILURE CATEGORY FRACTIONS FROM NPRDS

| Failure Category | Fraction |
|---|---|
| Design and installation | 0.145 |
| Aging and service wear | 0.233 |
| Test and maintenance | 0.062 |
| Human related | 0.008 |
| Other | 0.552 |

TABLE 2. RPS SYSTEM EFFECT FRACTIONS FROM NPRDS

| System Effect | Fraction |
|---|---|
| Loss of system function | 0.002 |
| Degraded system operation | 0.167 |
| Loss of redundancy | 0.170 |
| Loss of subsystem/channel | 0.393 |
| System function unaffected | 0.268 |

## Plant-Specific Sources

Having extracted what was felt to be the maximum amount of information from external data bases, coupled with the knowledge that the data bases contained only a subset of the recorded operating experience, several plant data sources were evaluated. The approach was to understand the data flow from a particular event to the report describing the event until it could be traced to either a LER, a NPRDS failure report, or some other document. The hypothesis is one could then estimate the fraction of events occurring that get reported in external data bases. Through this process, one could get a more complete picture of the history of the component or system.

## Incident Investigation Reports

Nonroutine events in the plant (including those that occurred during the pre-commercial operations phase) are evaluated. This evaluation may result in an incident investigation report (IIR) that captures the important details related to the event through interviews, analysis of logs, recorder strip charts, plant computer printouts, etc. The event may or may not require NRC notification. Hence, the LERs for the station are a subset of the IIRs.

The IIRs have been condensed to one-line summaries for ease in computer data base entry and analysis for trends, etc. There are 12 fields of data for each event: incident number, description, type, repetitive incident, date, time, unit, condition, cause, system, responsible group, and corrective action taken. The type field is coded to indicate the LER number (if the report is required). For each IIR event involving the RPS for the unit, the detailed report and the LER (if required) were obtained. Reports are prepared at the station by the Safety Review Group (SRG). The group does not report to station management and has the responsibility and the authority to conduct detailed investigations of the event. For events requiring an LER submittal, the SRG puts the information in the NRC-required format to assist the licensing staff in preparing the LER. Some of the information acquired from the investigation does not enter the reporting system, yet satisfies the reporting requirements. It is a practice of the utility to provide information to the NRC on operational events via the LER system even though the report may not be required. This was confirmed by comparing LERs with IIRs generated from RPS events. It is unknown how many licensees follow this practice.

Some of the events cause plant transients, which involve more detailed reporting. Transient assessment program (TAP) reports are a more recent form of internal reporting that is common to stations with the same NSSS. An investigation is performed after certain plant transients, e.g., a reactor trip. Several plant monitors record plant parameters preceding and following the transient. Interviews are conducted, the data analyzed, then a report is prepared and distributed internally and within the NSSS Owners Group. The data is also useful in tracking fatigue usage of various components. A comparison of design base information with actual plant experience allowed reduction of design conservatisms and prompted changes in plant operations to conserve fatigue usage.[9] Events that require TAP reporting are coded in the IIR system.

Because of the detail provided in the coded fields, the IIR data base of one-liners was adequate to construct a chronological history of nonroutine recorded events involving the RPS. Some observations based on sorts of the IIR data base are:

- Better resolution of information in the coded fields than LERs and NPRDS failure reports
- Pre-commercial operation events captured
- Report event frequency relatively constant up to 1984
- Approximately 5% of the events involve the RPS
- Coded reporting for LER and TAP tracking
- Infant mortality observable in component failure searches
- Learning curve observable in frequency of reactor trips
- Individual reports available for IIR, LER, NPRDS and TAP.

Plant Maintenance Records

A maintenance work request (MWR) can result from either an event noted by operations or an anomaly discovered in either surveillance or performance testing. Maintenance performance (preventive and corrective) is captured in the Nuclear Maintenance data base, which has been computer based since 1981. For equipment history before 1981, the information was recorded by component on separate cards that are now archived on microfilm. The initial review was conducted on data base information because of the labor-intensive effort required with the data on microfilm.

The Nuclear Maintenance data base contains approximately 50 fields of information. The fields contain MWR data coded for data base use. Typical fields include: MWR number, unit, priority, description, planning information, manhours spent and dates worked, failure codes, material, procedure numbers, etc. Records of surveillance and performance testing are also contained in the data base.

The Equipment data base is similar to the NPRDS component information, which contains pedigree and engineering information provided by Design Engineering, making it possible to track the performance of equipment by vendor, model, etc. Another data base available is the Nuclear Station Modification data base, which contains plant modifications and design changes. Efforts are underway to integrate the various plant data bases.

The NPRDS failure reports contain a subset of the information in these data bases because of reporting requirements, format, etc. It is also possible to track the NPRDS report within the Maintenance data system. Currently, there are more than 10,000 components included in the "NPRDS reportable scope" for the station. Even at that, not all components are reportable to the NPRDS data base. As one would expect, the level of detail provided in the plant data sources on equipment history exceeds that of the NPRDS.

## Other Data Sources

Another plant source of information that was useful in understanding the events involved in plant operations was the Environmental Qualification Reference Index (EQRI). The EQRI contains all the information regarding environmental qualification of plant equipment. The qualified life of various components dictates replacement even though there may be no problem observed. The EQRI documents the materials and parts that life limit certain hardware, required maintenance to guarantee continued qualification, references involving the testing reports that were used to qualify plant hardware, etc.

A number of other plants sources were used in the study: design information, operation and maintenance (O&M) manuals and procedures, and interviews with the staff involved in design, qualification, operation, maintenance and surveillance, performance testing, technical support, licensing, safety review, etc. The interviews were particularly important for an understanding that could never be achieved with data base analysis.

Comparison of Results. Because of the differences noted in the external data collection systems, the following comparisons are made using the NPE data to provide information for the RTS of the entire population, only pressurized water reactors (PWRs), and only Babcock & Wilcox (B&W) PWRs. The plant data for a specific B&W unit was used in the comparison. Tables 3 and 4 summarize the results for the RTS.

A sequential-event history was put together for the RPS at the reference plant. It included events from the LERs, NPE, NPRDS, IIRs, and the Nuclear Maintenance data base. Approximately 60% of the events were retained for comparison. Those discarded included corrective maintenance actions for RPS equipment with no safety consequence, e.g., replacing chart paper and ink pens on recorders. The majority of events retained involved maintenance and surveillance actions that may correct potential failures in the incipient stages. The IIRs accounted for approximately one-third of the remaining events, while the NPRDS failure reports accounted for approximately one-fourth of the events.

TABLE 3. FAILURE RANKING OF RTS COMPONENTS

| Component Categories | Total | PWR | B&W | Reference Plant |
|---|---|---|---|---|
| Sensing lines/instrument piping | 4 | 6 | 5 | 6 |
| Sensor/transducer/transmitter | 3 | 2 | 4 | 1 |
| Cables/connectors/terminals | 6 | 5 | 6 | 7 |
| Signal processing electronics | 1 | 1 | 1 | 2 |
| Power supplies | 5 | 4 | 3 | 4 |
| Relays/breakers | 2 | 3 | 2 | 3 |
| Switches/valves | 7 | 7 | 7 | 5 |

TABLE 4. EVENT CAUSE CATEGORY RANKING SUMMARY

| Cause Categories | Total | PWR | B&W | Reference Plant |
|---|---|---|---|---|
| Operator/maintenance error | 1 | 2 | 2 | 4 |
| Component failure | 2 | 1 | 7 | 1 |
| Design/construction error | 3 | 3 | 6 | 7 |
| Mechanical wear/malfunction | 4 | 4 | 3 | -- |
| Drift | 5 | 5 | 5 | 3 |
| Short/ground/arcing | 6 | 6 | 3 | 7 |
| Support system failure | 8 | 8 | 1 | 7 |
| Foul/block/foreign material | 9 | 7 | 7 | -- |
| Environment (therm/vib/moi) | 9 | 9 | 9 | 5 |
| Overload/overpressure | 11 | 11 | 10 | -- |
| Normal wearout | 12 | 12 | 12 | 5 |
| Corrosion | 13 | 13 | -- | -- |
| Other/miscellaneous | 7 | 10 | 10 | 2 |

## INTERIM ASSESSMENT OF AGING DEGRADATION

An interim assessment based on the operating experience review, coupled with a review and analysis of designs, specifications, operational parameters, and ongoing research plus a review of current methods and technology for inspection, surveillance, maintenance, and artificial/accelerated aging completes the Phase I portion of the research on RPS. These sources were examined with the goal of establishing how each addressed the technical objectives of the NPAR Program. The paper summarizes the highlights of Phase I by each objective.

### Identification/Characterization of Potential Safety Function Degradation

The RPS has been designed incorporating the fundamental concepts of reliability: redundancy, independence, and diversity. In order to assess the impact on risk or safety that has occurred or is occurring due to aging degradation, one must couple the frequency of the events with their consequences. Ranking component failure frequencies is a start to understanding the problem, but the failure consequences must also be understood.

The analysis of NPRDS failure reports indicated that approximately one-fourth of the RPS failures were due to aging causes, yet only 0.2% resulted in the loss of system function. The majority of failures were of lesser consequence because of the inherent reliability of the design. However, failures within the RPS continue to challenge plant safety through plant transients, forced shutdowns, and trips. Japanese experience also shows that failures within the RPS of sensors and signal processing electronics are a leading cause of plant trips.[10]

Because a failure analysis is often not performed, the failure mode but not the mechanism is reported. The large fraction of events that have unknown cause reported make a complete analysis impossible. Even with the plant records, a certain fraction of the events are due to unknown causes.

Several research efforts have shown that the nuclear operating experience with I&C equipment reveals a large percentage of failures in signal processing electronics and power supplies due to component failure (unreliability) and drift (instability)[11]. In the section on control and mitigation, a recent design solution to this problem is discussed.

The IIR data review for the reference plant showed that the majority categories of reported events are hardware failures requiring either replacement of components and subcomponents or calibration, software problems (procedures, technical specifications, etc.), and human errors in design, analysis, maintenance, and operations. The RPS is a four-channel system with only three required for plant operation; hence, most single failures are of minimal consequence. No single RPS hardware failure has caused a plant trip or engineered safety feature (ESF) actuation. The RPS-initiated transients were primarily human-dependent through maintenance or procedural errors. The experience at the reference plant reveals some historical problems with pressure transmitters and to a lesser extent nuclear instruments. More recently, the trend shows electrolytic capacitors in instrument power supplies to be failing more frequently.

## Cables, Connectors, Splices, Terminations, and Electrical Penetration Assemblies

Although the failure of cables is a relatively infrequent reported event (10 in the NPRDS failure reports obtained for the RPS study), the consequences can be very severe. The polymeric materials used in the insulation (also with equipment seals) are known to be vulnerable to thermal and radiation degradation. Some laboratory experiments have been performed to understand and model these processes and any possible synergisms that may exist. Efforts are underway in the United States, Japan, and Europe to characterize the thermal and radiation environment of containment so that material degradation and its impact on equipment function may be better understood.[12-15] There is still the safety concern that this degradation could provide a common cause challenge to the redundancy in safety system designs.

There are some cable in containment programs in existence. Duke Power Company installed sacrificial cable in the containment during construction at the Oconee station and samples segments at 5-year intervals.[16] There are samples of power, instrument, and control cable in trays with active cables. Some of the power cables are electrically loaded to simulate internal thermal sources. Tests performed on the 5- and 10-year samples showed no significant degradation.

The Electric Power Research Institute (EPRI) program[17] with the University of Connecticut, Northeast Utilities, and Detroit Edison is installing samples of cables and other equipment in the containments of eight U.S. reactors. The program is an extension of earlier research by the University of Connecticut sponsored by Northeast Utilities.

Although some of the programs are just beginning and some have been in existence for many years, the momentum seems to be changing to support the development of models to characterize the most severe environments experienced during normal operations. The information will be of value in understanding the qualified life of components and provide a realistic baseline for the estimation of abnormal conditions.

## Identify Method of Inspection, Surveillance, and Monitoring for Degradation Detection Before Failure

The review of the LER data revealed that 63% of the failures were discovered through testing and another 34% through normal operations. The IIR data for the reference plant shows similar results. Although it may be more desirable to know when a failure will occur through IS&M to minimize the consequences, most single failures are being detected by procedures already in place.

Technical specifications require three types of surveillance for the RPS. A channel check is performed each shift on channels displaying the same information. Any variation noted by the operations crew can initiate a MWR to investigate the anomaly. Because the containment at the reference plant is accessible during reactor operations, some checks can be performed without shutting the plant down. Depending on the limiting conditions for operation (LCO) in the technical specifications, the anomaly may or may not necessitate an immediate outage to correct the problem.

Channel functional tests are required monthly to verify that each channel is capable of performing its design function. Anomalies discovered during functional testing cause the test to be stopped and a MWR prepared to correct the problem before the test can be repeated. The record of this maintenance action ultimately gets entered into the Nuclear Maintenance data base. Unfortunately, the tests are primarily qualitative providing a "yes-no" answer to the question of operability. Quantitative information for trending is typically not required, hence not recorded. There has been concern that the frequent functional testing of highly reliable systems like the RPS increases system wear, unavailability, and challenges to the safety system. Several NSSS Owners Groups have successfully petitioned and have been granted an extension of the testing interval from monthly to quarterly. There has been insufficient experience with these changes to assess the impact.

Response-time testing is usually included in the technical specifications for the RPS. The test measures channel response to a trip signal to verify scram breakers open within a specified time from trip initiation. The technical specifications typically do not require response-time testing of the process sensors. It has been observed that the thermal cement used in some resistance temperature detector (RTD)

BEST COPY AVAILABLE

thermowells to improve heat transfer from the process fluid to the sensor is vulnerable to thermal degradation. Above certain temperatures, the material changes states decreasing the thermal conductivity and reducing the sensor response time. This degradation has been observed over relatively short time periods (between refueling outages). Although not observed during the in-plant study, the topic deserves further attention during Phase II studies.

The final required surveillance is the channel calibration that is usually required at a minimum of every 18 months (or to correspond with the fuel cycle), unless a problem occurs. Data from the calibrations that are end to end are of the "as found-as left" variety. No action is required unless the component exceeds its procedurally prescribed value or condition. In this case, the "as found" value or condition is recorded. If calibration is required, the operator also records the "as left" value or condition. It is more likely that repeated MWRs for a particular component will be the trend information used to initiate further action.

Duke Power Company is participating in a technology transfer program sponsored by the Department of Energy to evaluate Three Mile Island (TMI)-2-developed technology for use in commercial maintenance programs. A pilot program is underway at the Oconee Nuclear Station. The technology has been successfully used at TMI, Shippingport, and SONGS-1 to detect anomalies in circuits inside containment through measurements taken from outside the containment. Time domain reflectometry has been found to be particularly useful in detecting interface anomalies like loose connections, increased resistance due to corrosion, etc.

Franklin Research Institute is conducting research in an EPRI-sponsored program to assess a cable-indention methodology to estimate the state of the insulation.[18] It has been observed that the cable insulation mechanical degradation is observable before significant degradation in electrical properties is measured. Further, in the absence of flexural stresses to the insulation from cable movement, electrical property degradation appears to be unobservable.

Finally, as part of a control strategy [reliability-centered maintenance (RCM)] that has been successfully applied by the commercial aviation industry and the U.S. Navy, the functional indicators of degradation to weak links in the system are monitored to assess the system or component state. More will be said about RCM in the following section on control and mitigation.

## Identify Methods to Control or Mitigate the Effects of Degradation

It is a common belief that a good maintenance program is the best strategy for the control and mitigation of age-related degradation. Several efforts are underway, including NPAR, to determine the attributes of a "good" maintenance program. There are many philosophies on maintenance in the nuclear industry, both in the U.S. and abroad. The Japanese practices have received recent attention.[19] The U.S. Navy has performed studies that show for some classes of equipment, overhaul may either reduce the service life or have no impact at all.[20]

## Design Modification

One possible solution that shows merit is the redesign or modification of existing equipment. Several studies, including this one, on I&C equipment have found a significant number of failures occurring in signal processing electronics and power supplies due to component failure (unreliability) and electronic drift (instability). A recent effort by Science Applications International Corporation under EPRI-sponsorship demonstrated that by utilizing existing reliability prediction methods and high reliability components, the accuracy and reliability of a device could be improved by an order of magnitude and drift was virtually eliminated.[21] In a field dominated by a rapid change in technology reducing the time until obsolescence, design changes in the fundamental components used in the RPS have obvious benefits. A comparison of the nuclear environmental qualification with that conducted by the military also seems worthwhile.

Other examples of design practices that impact the degradation of electrical components are: providing thermal margins in electrical circuits and components (motors, cables, electrolytic capacitors, etc.) by sizing them for larger currents or voltages than those at which they are expected to operate. Duke Power Company's Design Engineering has followed this practice for many years. Power circuits are designed with No. 10 AWG conductors as minimum; control circuits use No. 12 AWG as a minimum. Providing cooling in cabinets and equipment spaces will prolong the lives of many electrical components because thermal degradation is the most significant challenge to extended life. The large number of part failures in signal processing electronics and power supplies are likely the result of thermal degradation.

## Installation

Common sense and good engineering in the installation of hardware also provides safety margins, frequently in unquantifiable ways. A practice in the Duke nuclear plants is the use of armor-sheathed cable. Initially more expensive, a long-term payback was envisioned due to reduced flexural stresses, added protection from external stressors, etc. It is unknown how many utilities have adopted this practice. The routing of cables in containment should be selected to receive minimal bending, thermal and radiation stress.

A recent Office for Analysis and Evaluation of Operational Data (AEOD) report on moisture intrusion[22] related the failure of qualified equipment operating in its normal environment. The proper orientation of junction boxes, equipment location with respect to conduit routing, maintenance of seals on boxes, transmitters, etc., after entry were just a few of the examples cited. Qualified equipment must be installed properly to have a chance at surviving its normal operating environment until the end of its qualified life.

### Operations, Surveillance, and Maintenance

Practices in operation including surveillance and maintenance may have an undetermined impact on equipment life. The movement of cables during surveillance or unrelated activities should be minimized or eliminated. High potential testing to determine the insulation resistance may be a destructive test if not controlled. Transmitter seals are replaced by procedure every time the device is opened at the reference plant, even though they are qualified for 4 years. Seals are the weak link in the transmitter, which has been otherwise qualified for 40 years.

A study[23] that identified some potential benefits to the nuclear industry from aviation industry experience led to a demonstration program on RCM.[24] An analysis of system history and design coupled with the identification of dominant failure modes led to a more effective preventive maintenance program. The estimated annual economic benefit for a single system at two operating plants was a 40% reduction in manhours expended and 30% reduction in materials costs.

## PHASE II PLANS

The major facets of Phase II in the NPAR Program involve more comprehensive assessments of the components and systems being studied. Particular goals are the determination of practical performance indicators for trending, applied research through post-service examinations, or lab tests and analyses. The review and verification of advanced methods is another important task.

The interfaces between RPS, the high pressure ECCS, and the Class 1E EPDS will provide the starting point for in-plant Phase I studies on the high pressure ECCS and the 1E-EPDS. Any interaction among the systems discovered during these studies may result in a Phase II study.

## REFERENCES

1. Nuclear Plant Aging Research (NPAR) Program Plan, NUREG-1144, U. S. Nuclear Regulatory Commission, 1985.

2. Proceedings of the Workshop on Nuclear Power Plant Aging, NUREG/CP-0036, U. S. Nuclear Regulatory Commission, 1982.

3. J. A. Rose et al., Survey of Aged Power Plant Facilities, NUREG/CR-3819, Idaho National Engineering Laboratory, 1985.

4. J. A. Close et al., Aging/Systems Interaction Study, Component Residual Lifetime Evaluation and Feasibility of Relicensing--Progress for FY 1985, EGG-REQ-7074, Idaho National Engineering Laboratory, 1985.

5. J. P. Drago et al., The In-Plant Reliability Data Base for Nuclear Power Plant Components: Data Collection and Methodology Report, NUREG/CR-2641, Oak Ridge National Laboratory, 1982.

6. C. F. Miller et al., *Data Summaries of Licensee Event Reports of Selected Instrumentation and Control Components at US Commercial Nuclear Power Plants*, NUREG/CR-1740, Idaho National Engineering Laboratory, 1981.

7. L. C. Meyer, *Nuclear Plant Aging Research on Reactor Protection Systems*, NUREG/CR-4740, EGG-2467, Idaho National Engineering Laboratory (To Be Published).

8. B. M. Meale and D. G. Satterwhite, *Aging Survey and Importance Quantification of Operational Data for Systems and Components*, NUREG/CR-4747, EGG-2473, Idaho National Engineering Laboratory (To Be Published).

9. C. W. Tally, "Ensuring the design life of a nuclear steam supply system," *Power Engineering*, April 1985, pp.48-50.

10. A. Sekiguchi, "Improvement Availability and Safety of Nuclear Power Plants in Japan," *Proceedings of ANS/ENS Topical Meeting on Operability of Nuclear Power Systems in Normal and Adverse Environments, September 29 - October 3, 1986, Albuquerque, NM* (To Be Published).

11. *Field-Hardened Instruments and Electrical Components for Nuclear Plant Applications-Project Planning*, EPRI-NP-3649, Science Applications, Inc., 1984.

12. K. T. Gillen and R. L. Clough, "General Approaches to Accelerated Aging Simulations," *Proceedings of ANS/ENS Topical Meeting on Operability of Nuclear Power Systems in Normal and Adverse Environments, September 29 - October 3, 1986, Albuquerque, NM.* (To Be Published).

13. G. Champion et al., "Exposure Doses Inside French PWR Containments Under Normal Operating Conditions," *Proceedings of ANS/ENS Topical Meeting on Operability of Nuclear Power Systems in Normal and Adverse Environments, September 29 - October 3, 1986, Albuquerque, NM.* (To Be Published).

14. T. Seguchi, "Analysis of Dose Rate Dependence on Radiation Thermal Combined Aging of Polymer Materials," *Proceedings of ANS/ENS Topical Meeting on Operability of Nuclear Power Systems in Normal and Adverse Environments, September 29 - October 3, 1986, Albuquerque, NM.* (To Be Published).

15. H. Schonbacher, "Life Experience with Aging of Organic Electrical Insulating Materials in Nuclear Radiation Environments," *Proceedings of ANS/ENS Topical Meeting on Operability of Nuclear Power Systems in Normal and Adverse Environments, September 29 - October 3, 1986, Albuquerque, NM.* (To Be Published).

16. T. J. Al-Hussaini and J. E. Stoner, "Ongoing Qualification of Cable in a Pressurized Water Reactor Environment," Procedings of the IEEE Nuclear Science Symposium, November 1, 1984, Orlando, Fl.

17. M. Shaw and G. Sliter, "In-plant Natural versus Artificial Aging Study," Proceedings of ANS/ENS Topical Meeting on Operability of Nuclear Power Systems in Normal and Adverse Environments, September 29 - October 3, 1986, Albuquerque, NM. (To Be Published).

18. G. J. Toman and G. Sliter, "Development of a Nondestructive Mechanical Condition Test for Electrical Cable Insulation," Proceedings of ANS/ENS Topical Meeting on Operability of Nuclear Power Systems in Normal and Adverse Environments, September 29 - October 3, 1986, Albuquerque, NM. (To Be Published).

19. A. J. Boegel et al., Analysis of Japanese-U.S. Maintenance Practices, NUREG/CR-3683, Battelle Pacific Northwest Laboratories, 1985.

20. J.W. Prichard, "Equipment Age-Reliability Analysis," Naval Engineers Journal, September 1984, pp. 65-70.

21. Improved Reliability for Analog Instrument and Control Systems, EPRI-NP-4483, Science Applications International Corporation, 1986.

22. M. El-Zeftawy, Operating Experience Related to Moisture Intrusion in Electrical Equipment at Commercial Power Reactors, AEOD/C402, U. S. Nuclear Regulatory Commission, 1984.

23. Commercial Aviation Experience of Value to the Nuclear Industry, EPRI-NP-3364, Los Alamos Technical Associates, Inc., 1984.

24. Application of Reliability-Centered Maintenance to Component Cooling-Water System at Turkey Point Units 3 and 4, EPRI-NP-4271, Los Alamos Technical Associates, Inc., 1985.

## NOTICE

This report was prepared as an account of work sponsored by an agency of the United States Government. Neither the United States Government nor any agency thereof, or any of their employees, makes any warranty, expressed or implied, or assumes any legal liability or responsibility for any third party's use, or the results of such use, or any information, apparatus, product, or process disclosed in this report, or represents that its use by such third party would not infringe privately owned rights. The views expressed in this report are not necessarily those of the U. S. Nuclear Regulatory Commission.

# Overview of Recent Operating Experience Regarding Plant Aging

M. A. Caruso and G. M. Holahan

U.S. Nuclear Regulatory Commission

## Abstract

In order to better understand all the factors which contribute to high reactor scram frequencies in new operating nuclear power plants, the authors have made a comparison of the frequency in early life between plants which went into operation in the 1960's and early 1970's and those which have gone into operation in the past four years. Scram frequency per unit operating time for the two plant groups is calculated and compared to see the extent to which design differences (e.g., capacity, thermal margin) affect scram frequency. In addition to this analysis a discussion of several recent operating reactor events involving age-related component failures is provided.

## Introduction

This paper provides a review of operating experience at domestic commercial nuclear power plants focusing on some operational safety problems with age-related causal factors. The paper is intended to provide some insight into the current aging trends of U.S. plants. The first section of the paper addresses the frequency of reactor scram events during the first three years of plant operation. This represents one way of establishing the "burn-in" (i.e., early failure phase) characteristics of plants. The second section includes a discussion of several recent events which involved age-related degradation of plant systems important to safety.

## 1.0 Reactor Scram Frequency Early in Plant Life

Studies of reactor scram frequency performed by the U.S. Nuclear Regulatory Commission have all shown that scram frequencies in newly-licensed plants generally tend to be several times greater than those of plants which have been in commercial operation for several years.[1, 2, 3] Figure 1 shows the relationship between scram frequency and plant age in terms of plant scram frequencies averaged over the first eight months of 1986. Here we clearly observe the burn-in (left hand) side of the familiar "bath tub" curve which is characteristic of the performance/age behavior of complex machines. Note that the figure does not appear to show the characteristically high failure rates at end-of-life (right hand side of the failure/age curve).

BEST COPY AVAILABLE

370

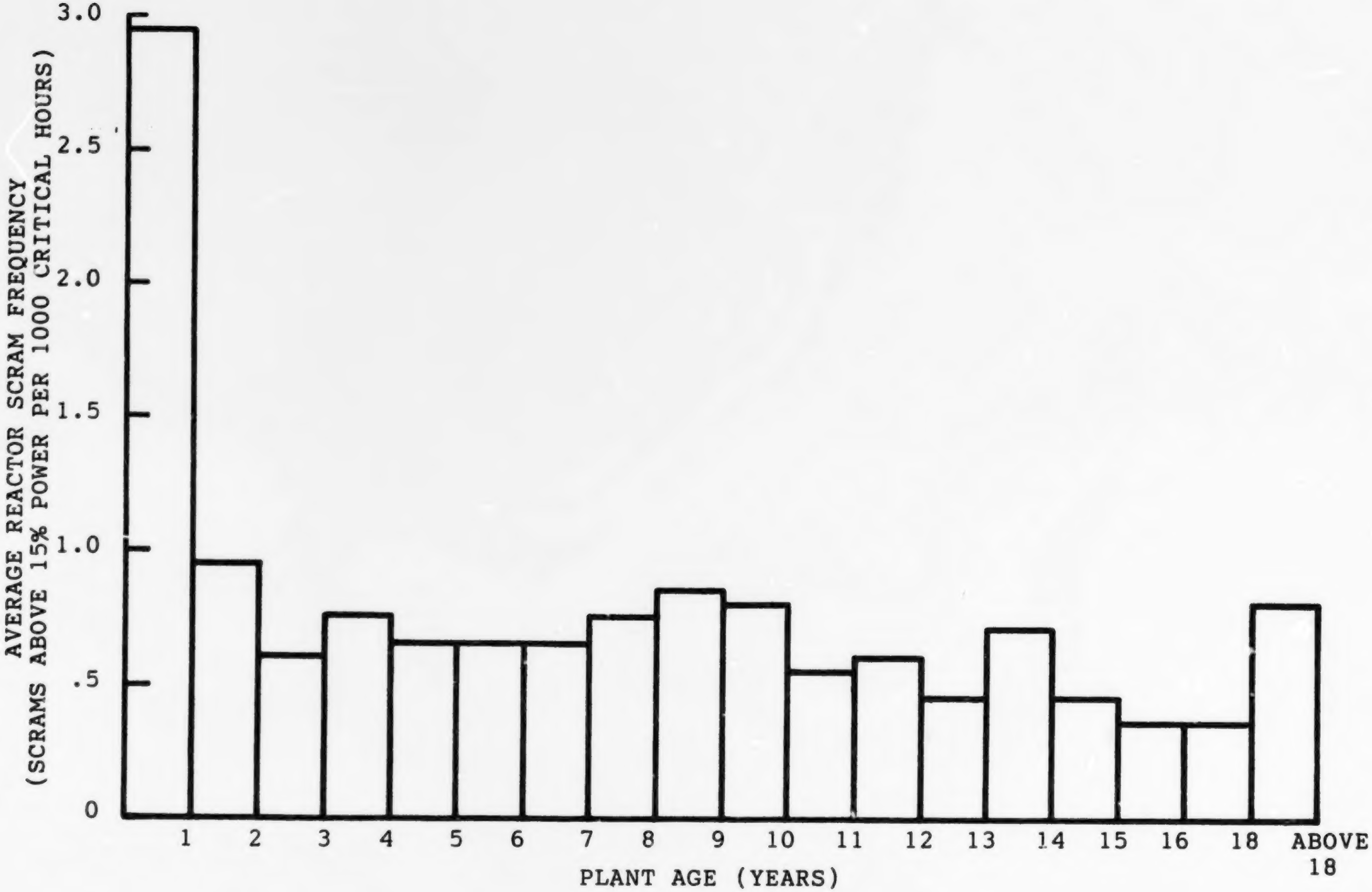

REACTOR SCRAM FREQUENCIES IN 1986 VERSUS PLANT AGE
FIGURE 1

370

As part of a larger staff study of performance at newly-licensed plants we have taken a closer look at new plant scram frequencies through a systematic analysis of scram rates in the early life of twenty-three modern plants licensed between June 1982 and June 1986, and twelve older and smaller facilities licensed between 1960 and 1972. The NRC staff is concerned with high scram frequencies in newly-licensed plants, particularly during the power ascension test period. This is when new systems are not completely tested, the plant staff is still gaining experience in the operation of the facility, yet the reactor may be operating with a significant heat load.

## 1.1 Data Compilation

In this study, scram counts for the modern facilities were determined from review of event reports made by licensees per the requirements of 10 CFR 50.72 (prompt notifications by licensees) and 10 CFR 50.73 (LERs). Scram events during plant startup, which have less safety significance (i.e., below 20% power) are not included. Scram counts for the twelve early vintage plants were obtained from a study of scram experience at these plants published in 1978.[4] In that study, the scram data, including pre-trip power level, was determined from reviews of plant logs and discussions with plant operations personnel. This was because consistent formal reporting requirements for reactor scram events did not exist at the time.

For purposes of direct comparisons between the modern and early vintage plants the scram counts were normalized with the same measure of reactor operating time. The measure used was thousands of effective full power hours of operation (1000 EFPH). It was determined as a function of time by dividing the gross number of megawatt-hours of electricity generated per unit time by the gross plant capacity in megawatt electric, i.e,

$$\text{Thousands of EFPH} = \frac{\text{Gross Electricity Generated (MWHrs)}}{\text{Plant Capacity (MWe) X 1000}}$$

This choice of normalization was dictated by the availability of historical data on operating time for the early vintage plants; and is not the preferred choice when one is simply trying to account for differences in down time among plants. This is because it includes the power the plant is operated at as well as the time; and is especially difficult to interpret when the period of interest includes power ascension testing, i.e., when the power level is varying significantly with time. Thus, while it serves our purpose of making direct comparisons between the performance of early vintage and modern plants, and perhaps provides additional insight regarding productivity during power ascension testing, it tends to exaggerate the rate of decrease of the normalized "scram frequency" versus time relationship in the period of power ascension testing.

Data for annual electricity production from the early vintage plants was obtained from a 1976 report by the then Energy Research and Development Administration (ERDA).[5] Electricity production figures for the modern plants and gross electrical capacities for all of the plants were obtained from monthly plant operating reports via the NRC "Grey Book", NUREG-0020[6] for the years 1982 through 1986. Since NUREG-0020 reports data on a monthly basis, operating time as well as scram frequency for the modern plants have been averaged on a quarterly basis as well as an annual basis.

## 1.2 Analysis

The scram count, productivity, and scram frequency (i.e., scrams/1000 EFPH) for the twenty-three modern plants are shown as functions of time after start-up in Tables 1, 2, and 3; and Figures 2, 3, and 4 respectively. The corresponding data for the twelve early vintage plants are shown in Tables 4, 5, and 6. The average trends over time for the two plant groups are observed to be quite similar. In both cases the first year of operation is generally characterized by a relatively large number of scrams; low but increasing productivity as the plant progresses through power ascension testing; and consequently a high yet decreasing scram frequency. In contrast the second and third years show relative stability in the general case. The horizontal dashed line shown in Figure 4 is the average scram frequency for plants in operation for more than three years during the first eight months of 1986. It has been included to provide a frame of reference.

These results suggest that plants which continue to have high scram rates and low productivity in the second year of operation have not been successfully debugged or have other specific problems whose root causes are not related to start-up activities.

## 1.3 Comparison Between Modern and Early Vintage Plants

Comparison of the quarterly scram counts in Tables 1 and 4 indicates that on the average the number of scrams experienced in the early years by the larger modern plants is higher than that for the early vintage plants. Tables 6 and 7 allow a comparison of normalized scram frequency for the two plant groups to be made. Here the differences do not follow as clear a trend. These tables show the frequency of scrams per 1000 EFPH averaged on a yearly basis. The choice of yearly time periods for averaging was essentially dictated by the periods in which electricity generation statistics were reported for the early vintage plants. The "year of start-up" column reflects the period from startup to the end of the calendar year and is therefore a partial year of different size for each plant. The remaining columns reflect full calendar years which follow. Thus, while the method of time averaging for the two plant groups is identical, it does not yield perfectly comparable performance versus time relationships and may be contributing to the difficulty in comparison. Tables 6 and 7 include both the average and median values for each of the years of interest. The median values may represent a more meaningful comparison, especially in the "year of startup" where the plant-to-plant variations are very large. Figure 5 shows a comparison of the median scram frequencies for the two plant groups. When all the data is considered (plant-specific, average and median values) it indicates that: (1) the performance differences between the modern plants and early vintage plants, on a group average (or median) basis are not significant relative to the significant design differences between the two plant groups, and (2) differences among and between individual plants of both groups are

## Table 1
## MODERN PLANTS

### NUMBER OF SCRAMS IN CALENDER QUARTERS FOLLOWING START-UP

| PLANT | START-UP DATE | CAPACITY (MWE) | FIRST QTR | SECOND QTR | THIRD QTR | FOURTH QTR | FIRST QTR | SECOND QTR | THIRD QTR | FOURTH QTR | FIRST QTR | SECOND QTR | THIRD QTR | FOURTH QTR |
|---|---|---|---|---|---|---|---|---|---|---|---|---|---|---|
| LASALLE 1 | 09/04/82 | 1078 | 1.00 | 5.00 | 2.00 | 5.00 | 5.00 | 2.00 | 5.00 | 3.00 | 1.00 | 0.00 | 5.00 | 3.00 |
| SAN ONOFRE 2 | 09/20/82 | 1127 | 0.00 | 3.00 | 4.00 | 4.00 | 1.00 | 3.00 | 2.00 | 0.00 | 2.00 | 0.00 | 0.00 | 2.00 |
| SUSQUEHANNA 1 | 11/16/82 | 1068 | 3.00 | [illegible] | 2.00 | 3.00 | 3.00 | 2.00 | 1.00 | 4.00 | 0.00 | 1.00 | 0.00 | 0.00 |
| SUMMER 1 | 11/16/82 | 900 | 5.00 | 3.00 | 1.00 | 6.00 | 4.00 | 3.00 | 1.00 | 1.00 | 1.00 | 1.00 | 3.00 | 3.00 |
| MCGUIRE 2 | 05/23/83 | 1225 | 1.00 | 1.00 | 4.00 | 2.00 | 4.00 | 3.00 | 6.00 | 0.00 | 3.00 | 2.00 | 3.00 | 1.00 |
| ST. LUCIE 2 | 06/13/83 | 882 | 2.00 | 4.00 | 1.00 | 3.00 | 0.00 | 1.00 | 5.00 | 0.00 | 2.00 | 3.00 | 0.00 | 1.00 |
| SAN ONOFRE 3 | 09/25/83 | 1127 | 1.00 | 9.00 | 1.00 | 2.00 | 0.00 | 1.00 | 1.00 | 3.00 | 0.00 | 0.00 | 1.00 | 1.00 |
| LASALLE 2 | 04/20/84 | 1078 | 2.00 | 4.00 | 2.00 | 0.00 | 0.00 | 0.00 | 1.00 | 1.00 | 1.00 | -3.00 | -3.00 | -3.00 |
| WNP 2 | 05/27/84 | 1155 | 4.00 | 2.00 | 7.00 | 6.00 | 1.00 | 2.00 | 1.00 | 0.00 | 1.00 | -3.00 | -3.00 | -3.00 |
| SUSQUEHANNA 2 | 07/03/84 | 1068 | 5.00 | 0.00 | 1.00 | 1.00 | 1.00 | 2.00 | 1.00 | 0.00 | -3.00 | -3.00 | -3.00 | -3.00 |
| GRAND GULF 1 | 10/20/84 | 1157 | 1.00 | 3.00 | 6.00 | 3.00 | 1.00 | 1.00 | 1.00 | -3.00 | -3.00 | -3.00 | -3.00 | -3.00 |
| CALLAWAY 1 | 10/24/84 | 1180 | 4.00 | 5.00 | 3.00 | 5.00 | 6.00 | 0.00 | 2.00 | -3.00 | -3.00 | -3.00 | -3.00 | -3.00 |
| DIABLO CANYON 1 | 11/11/84 | 1125 | 1.00 | 4.00 | 2.00 | 1.00 | 1.00 | 1.00 | 0.00 | -3.00 | -3.00 | -3.00 | -3.00 | -3.00 |
| CATAWBA 1 | 01/22/85 | 1145 | 2.00 | 3.00 | 1.00 | 2.00 | 1.00 | 3.00 | -3.00 | -3.00 | -3.00 | -3.00 | -3.00 | -3.00 |
| BYRON 1 | 03/01/85 | 1175 | 1.00 | 7.00 | 3.00 | 2.00 | 3.00 | 0.00 | -3.00 | -3.00 | -3.00 | -3.00 | -3.00 | -3.00 |
| WATERFORD 3 | 03/18/85 | 1104 | 2.00 | 5.00 | 5.00 | 4.00 | 1.00 | 2.00 | -3.00 | -3.00 | -3.00 | -3.00 | -3.00 | -3.00 |
| LIMERICK 1 | 04/13/85 | 1092 | 0.00 | 1.00 | 1.00 | 1.00 | 0.00 | -3.00 | -3.00 | -3.00 | -3.00 | -3.00 | -3.00 | -3.00 |
| PALO VERDE 1 | 06/10/85 | 1303 | 0.00 | 3.00 | 4.00 | 2.00 | 1.00 | -3.00 | -3.00 | -3.00 | -3.00 | -3.00 | -3.00 | -3.00 |
| WOLF CREEK 1 | 06/12/85 | 1170 | 1.00 | 6.00 | 2.00 | 1.00 | 2.00 | -3.00 | -3.00 | -3.00 | -3.00 | -3.00 | -3.00 | -3.00 |
| DIABLO CANYON 2 | 10/20/85 | 1124 | 10.00 | 5.00 | 2.00 | -3.00 | -3.00 | -3.00 | -3.00 | -3.00 | -3.00 | -3.00 | -3.00 | -3.00 |
| RIVER BEND 1 | 12/01/85 | 936 | 1.00 | 3.00 | 6.00 | -3.00 | -3.00 | -3.00 | -3.00 | -3.00 | -3.00 | -3.00 | -3.00 | -3.00 |
| MILLSTONE 3 | 01/23/86 | 1197 | 1.00 | 1.00 | -3.00 | -3.00 | -3.00 | -3.00 | -3.00 | -3.00 | -3.00 | -3.00 | -3.00 | -3.00 |
| PALO VERDE 2 | 05/20/86 | 1221 | 2.00 | -3.00 | -3.00 | -3.00 | -3.00 | -3.00 | -3.00 | -3.00 | -3.00 | -3.00 | -3.00 | -3.00 |
| AVERAGE | | 1023 | 2.17 | 3.64 | 2.86 | 2.79 | 1.84 | 1.62 | 2.08 | 1.20 | 1.22 | 1.00 | 1.71 | 1.57 |

-3 Period Not Yet Reached in Plant Life

Table 2

## MODERN PLANTS
## THOUSANDS OF EFFECTIVE FULL POWER HOURS IN CALENDER QUARTERS FOLLOWING START-UP

| PLANT | START-UP DATE | CAPACITY (MWE) | FIRST QTR | SECOND QTR | THIRD QTR | FOURTH QTR | FIRST QTR | SECOND QTR | THIRD QTR | FOURTH QTR | FIRST QTR | SECOND QTR | THIRD QTR | FOURTH QTR |
|---|---|---|---|---|---|---|---|---|---|---|---|---|---|---|
| LASALLE 1 | 09/04/82 | 1078 | 0.05 | 0.43 | 0.52 | 0.39 | 0.63 | 0.37 | 0.70 | 1.91 | 1.79 | 0.68 | 1.49 | 1.40 |
| SAN ONOFRE 2 | 09/20/82 | 1127 | 0.00 | 0.17 | 0.15 | 0.53 | 1.62 | 1.30 | 1.18 | 1.91 | 1.46 | 0.40 | 0.00 | 1.47 |
| SUSQUEHANNA 1 | 11/16/82 | 1068 | 0.32 | 1.08 | 0.52 | 1.73 | 1.38 | 0.24 | 2.09 | 1.84 | 1.75 | 0.77 | 0.35 | 2.17 |
| SUMMER 1 | 11/16/82 | 900 | 0.24 | 0.86 | 0.70 | 1.97 | 1.53 | 1.90 | 1.36 | 1.50 | 0.16 | 1.85 | 2.54 | 2.08 |
| MCGUIRE 2 | 05/23/83 | 1225 | -1.00 | -1.00 | -1.00 | 0.68 | 1.98 | 1.27 | 1.66 | 0.57 | 1.05 | 1.43 | 1.74 | 1.62 |
| ST. LUCIE 2 | 06/13/83 | 382 | 0.02 | 0.99 | 2.10 | 1.95 | 2.11 | 1.86 | 0.78 | 2.01 | 1.98 | 1.20 | 2.14 | 2.14 |
| SAN ONOFRE 3 | 09/25/83 | 1127 | 0.01 | 0.96 | 0.53 | 1.21 | 1.43 | 1.23 | 0.86 | 1.75 | 0.95 | 0.00 | 0.92 | 2.18 |
| LASALLE 2 | 04/20/84 | 1078 | 0.35 | 0.97 | 1.32 | 1.35 | 0.00 | 1.38 | 0.63 | 1.85 | 0.98 | -3.00 | -3.00 | -3.00 |
| WNP 2 | 05/27/84 | 1155 | 0.03 | 0.43 | 0.88 | 1.53 | 0.40 | 1.34 | 1.40 | 1.10 | 0.10 | -3.00 | -3.00 | -3.00 |
| SUSQUEHANNA 2 | 07/03/84 | 1068 | 0.59 | 0.34 | 1.38 | 1.84 | 1.94 | 1.96 | 1.96 | 1.50 | -3.00 | -3.00 | -3.00 | -3.00 |
| GRAND GULF 1 | 10/20/84 | 1157 | 0.03 | 0.31 | 1.23 | 1.82 | 0.59 | 1.23 | 1.49 | -3.00 | -3.00 | -3.00 | -3.00 | -3.00 |
| CALLAWAY 1 | 10/24/84 | 1180 | 0.53 | 1.70 | 1.67 | 1.96 | 1.85 | 1.34 | 1.14 | -3.00 | -3.00 | -3.00 | -3.00 | -3.00 |
| DIABLO CANYON 1 | 11/11/84 | 1125 | 0.23 | 0.71 | 1.17 | 2.08 | 1.65 | 1.96 | 2.12 | -3.00 | -3.00 | -3.00 | -3.00 | -3.00 |
| CATAWBA 1 | 01/22/85 | 1145 | -1.00 | 0.05 | 2.06 | 1.11 | 1.93 | 1.51 | -3.00 | -3.00 | -3.00 | -3.00 | -3.00 | -3.00 |
| BYRON 1 | 03/01/85 | 1175 | 0.01 | 0.86 | 0.85 | 0.71 | 1.53 | 1.81 | -3.00 | -3.00 | -3.00 | -3.00 | -3.00 | -3.00 |
| WATERFORD 3 | 03/18/85 | 1104 | 0.01 | 0.44 | 0.35 | 1.62 | 1.56 | 2.17 | -3.00 | -3.00 | -3.00 | -3.00 | -3.00 | -3.00 |
| LIMERICK 1 | 04/13/85 | 1092 | 0.00 | 0.16 | 0.98 | 1.74 | 1.02 | -3.00 | -3.00 | -3.00 | -3.00 | -3.00 | -3.00 | -3.00 |
| PALO VERDE 1 | 06/10/85 | 1303 | 0.05 | 0.37 | 0.61 | 0.86 | 0.82 | -3.00 | -3.00 | -3.00 | -3.00 | -3.00 | -3.00 | -3.00 |
| WOLF CREEK 1 | 06/12/85 | 1170 | 0.07 | 1.36 | 2.03 | 2.11 | 1.46 | -3.00 | -3.00 | -3.00 | -3.00 | -3.00 | -3.00 | -3.00 |
| DIABLO CANYON 2 | 10/20/85 | 1124 | 0.56 | 0.62 | 1.85 | -3.00 | -3.00 | -3.00 | -3.00 | -3.00 | -3.00 | -3.00 | -3.00 | -3.00 |
| RIVER BEND 1 | 12/01/85 | 936 | 0.00 | 0.17 | 1.06 | -3.00 | -3.00 | -3.00 | -3.00 | -3.00 | -3.00 | -3.00 | -3.00 | -3.00 |
| MILLSTONE 3 | 01/23/86 | 1197 | 0.28 | 1.49 | -3.00 | -3.00 | -3.00 | -3.00 | -3.00 | -3.00 | -3.00 | -3.00 | -3.00 | -3.00 |
| PALO VERDE 2 | 05/20/86 | 1221 | 0.20 | -3.00 | -3.00 | -3.00 | -3.00 | -3.00 | -3.00 | -3.00 | -3.00 | -3.00 | -3.00 | -3.00 |
| AVERAGE | | 1023 | 0.18 | 0.69 | 1.00 | 1.43 | 1.34 | 1.43 | 1.34 | 1.59 | 1.14 | 0.90 | 1.31 | 1.87 |

-1 Data Incomplete
-2 Plant Shutdown
-3 Period Not Yet Reached in Plant Life

Table 3

## MODERN PLANTS
## SCRAMS PER 1000 EFFECTIVE FULL POWER HOURS IN CALENDER QUARTERS FOLLOWING START-UP

| PLANT | START-UP DATE | CAPACITY (MWE) | FIRST QTR | SECOND QTR | THIRD QTR | FOURTH QTR | FIRST QTR | SECOND QTR | THIRD QTR | FOURTH QTR | FIRST QTR | SECOND QTR | THIRD QTR | FOURTH QTR |
|---|---|---|---|---|---|---|---|---|---|---|---|---|---|---|
| LASALLE 1 | 09/04/82 | 1078 | 20.73 | 11.52 | 3.86 | 12.93 | 7.90 | 5.40 | 7.10 | 1.57 | 0.56 | 0.00 | 3.36 | 2.15 |
| SAN ONOFRE 2 | 09/20/82 | 1127 | 0.00 | 17.43 | 27.32 | 7.58 | 0.62 | 2.32 | 1.69 | 0.00 | 1.37 | 0.00 | -2.00 | 1.36 |
| SUSQUEHANNA 1 | 11/16/82 | 1068 | 9.31 | 2.79 | 3.82 | 1.73 | 2.17 | 8.48 | 0.48 | 2.17 | 0.00 | 1.30 | 0.00 | 0.00 |
| SUMMER 1 | 11/16/82 | 900 | 20.74 | 3.51 | 1.43 | 3.04 | 2.61 | 1.58 | 0.74 | 0.67 | 6.16 | 0.54 | 1.18 | 1.44 |
| MCGUIRE 2 | 05/23/83 | 1225 | -1.00 | -1.00 | -1.00 | 2.96 | 2.02 | 2.36 | 3.62 | 0.00 | 2.85 | 1.40 | 1.73 | 0.62 |
| ST. LUCIE 2 | 06/13/83 | 882 | 103.76 | 4.02 | 0.48 | 1.54 | 0.00 | 0.54 | 6.39 | 0.00 | 1.01 | 2.51 | 0.00 | 0.47 |
| SAN ONOFRE 3 | 09/25/83 | 1127 | 93.92 | 9.33 | 1.88 | 1.65 | 0.00 | 0.82 | 1.17 | 1.72 | 0.00 | -2.00 | 1.09 | 0.46 |
| LASALLE 2 | 04/20/84 | 1078 | 5.72 | 4.14 | 1.52 | 0.00 | -2.00 | 0.00 | 1.59 | 0.54 | 1.02 | -3.00 | -3.00 | -3.00 |
| WNP 2 | 05/27/84 | 1155 | 132.00 | 4.70 | 7.94 | 3.92 | 2.49 | 1.49 | 0.71 | 0.00 | 10.13 | -3.00 | -3.00 | -3.00 |
| SUSQUEHANNA 2 | 07/03/84 | 1068 | 8.49 | 0.00 | 0.73 | 0.54 | 0.52 | 1.02 | 0.51 | 0.00 | -3.00 | -3.00 | -3.00 | -3.00 |
| GRAND GULF 1 | 10/20/84 | 1157 | 29.67 | 9.70 | 4.87 | 1.65 | 1.69 | 0.81 | 0.67 | -3.00 | -3.00 | -3.00 | -3.00 | -3.00 |
| CALLAWAY 1 | 10/24/84 | 1180 | 7.50 | 2.95 | 1.80 | 2.55 | 3.24 | 0.00 | 1.76 | -3.00 | -3.00 | -3.00 | -3.00 | -3.00 |
| DIABLO CANYON 1 | 11/11/84 | 1125 | 4.28 | 5.67 | 1.71 | 0.48 | 0.61 | 0.51 | 0.00 | -3.00 | -3.00 | -3.00 | -3.00 | -3.00 |
| CATAWBA 1 | 01/22/85 | 1145 | -1.00 | 61.34 | 0.49 | 1.81 | 0.52 | 1.98 | -3.00 | -3.00 | -3.00 | -3.00 | -3.00 | -3.00 |
| BYRON 1 | 03/01/85 | 1175 | 69.12 | 8.11 | 3.52 | 2.81 | 1.96 | 0.00 | -3.00 | -3.00 | -3.00 | -3.00 | -3.00 | -3.00 |
| WATERFORD 3 | 03/18/85 | 1104 | 315.43 | 11.48 | 14.19 | 2.47 | 0.64 | 0.92 | -3.00 | -3.00 | -3.00 | -3.00 | -3.00 | -3.00 |
| LIMERICK 1 | 04/13/85 | 1092 | 0.00 | 6.10 | 1.02 | 0.58 | 0.00 | -3.00 | -3.00 | -3.00 | -3.00 | -3.00 | -3.00 | -3.00 |
| PALO VERDE 1 | 06/10/85 | 1303 | 0.00 | 8.21 | 6.51 | 2.33 | 1.23 | -3.00 | -3.00 | -3.00 | -3.00 | -3.00 | -3.00 | -3.00 |
| WOLF CREEK 1 | 06/12/85 | 1170 | 14.62 | 4.42 | 0.99 | 0.47 | 1.37 | -3.00 | -3.00 | -3.00 | -3.00 | -3.00 | -3.00 | -3.00 |
| DIABLO CANYON 2 | 10/20/85 | 1124 | 17.76 | 8.04 | 1.08 | -3.00 | -3.00 | -3.00 | -3.00 | -3.00 | -3.00 | -3.00 | -3.00 | -3.00 |
| RIVER BEND 1 | 12/01/85 | 936 | -1.00 | 17.55 | 5.66 | -3.00 | -3.00 | -3.00 | -3.00 | -3.00 | -3.00 | -3.00 | -3.00 | -3.00 |
| MILLSTONE 3 | 01/23/86 | 1197 | 3.58 | 0.67 | -3.00 | -3.00 | -3.00 | -3.00 | -3.00 | -3.00 | -3.00 | -3.00 | -3.00 | -3.00 |
| PALO VERDE 2 | 05/20/86 | 1221 | 9.93 | -3.00 | -3.00 | -3.00 | -3.00 | -3.00 | -3.00 | -3.00 | -3.00 | -3.00 | -3.00 | -3.00 |
| AVERAGE | | 1023 | 43.33 | 9.60 | 4.54 | 2.69 | 1.64 | 1.76 | 2.03 | 0.67 | 2.57 | 0.96 | 1.23 | 0.93 |
| STD. DEVIATION | | | 74.83 | 12.76 | 6.31 | 3.00 | 1.84 | 2.23 | 2.28 | 0.84 | 3.42 | 0.97 | 1.25 | 0.74 |
| MEDIAN | | | 9.93 | 5.67 | 1.80 | 1.81 | 1.23 | 0.92 | 1.17 | 0.00 | 1.01 | 0.54 | 1.09 | 0.62 |

-1 Data Incomplete
-2 Plant Shutdown
-3 Period Not Yet Reached in Plant Life

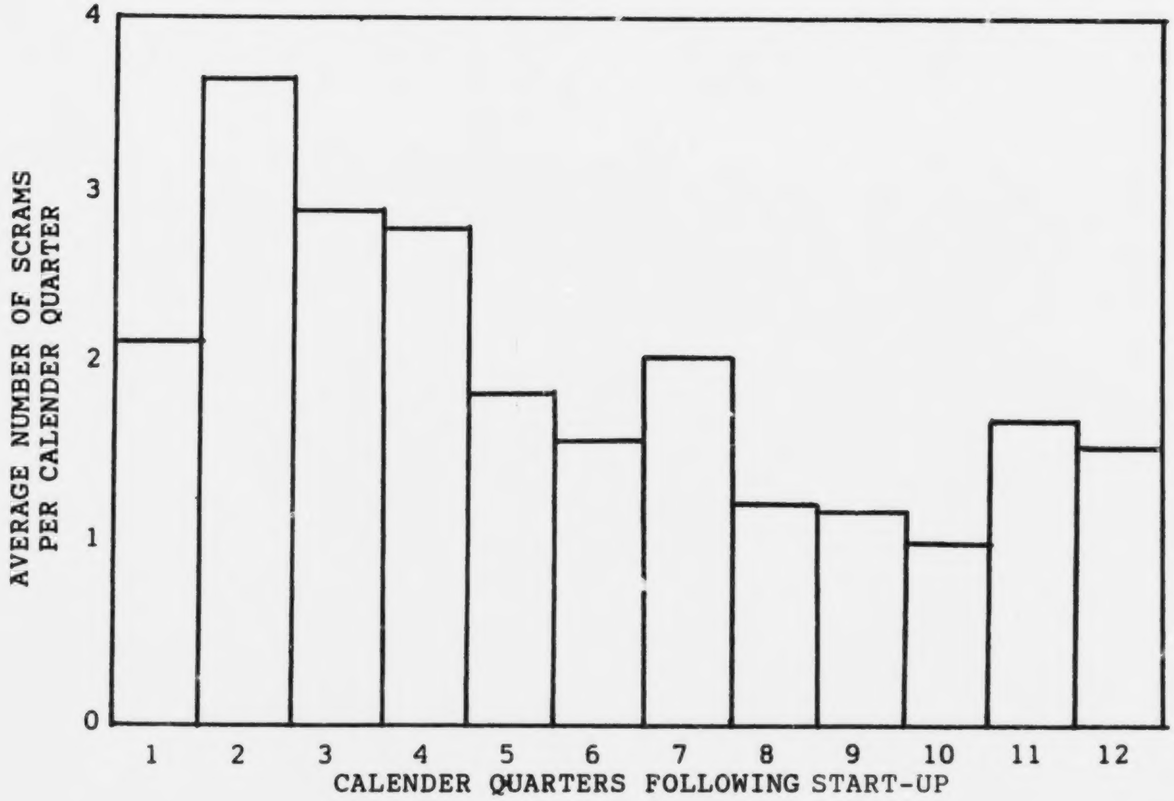

MODERN PLANT SCRAM COUNT VERSUS TIME
FIGURE 2

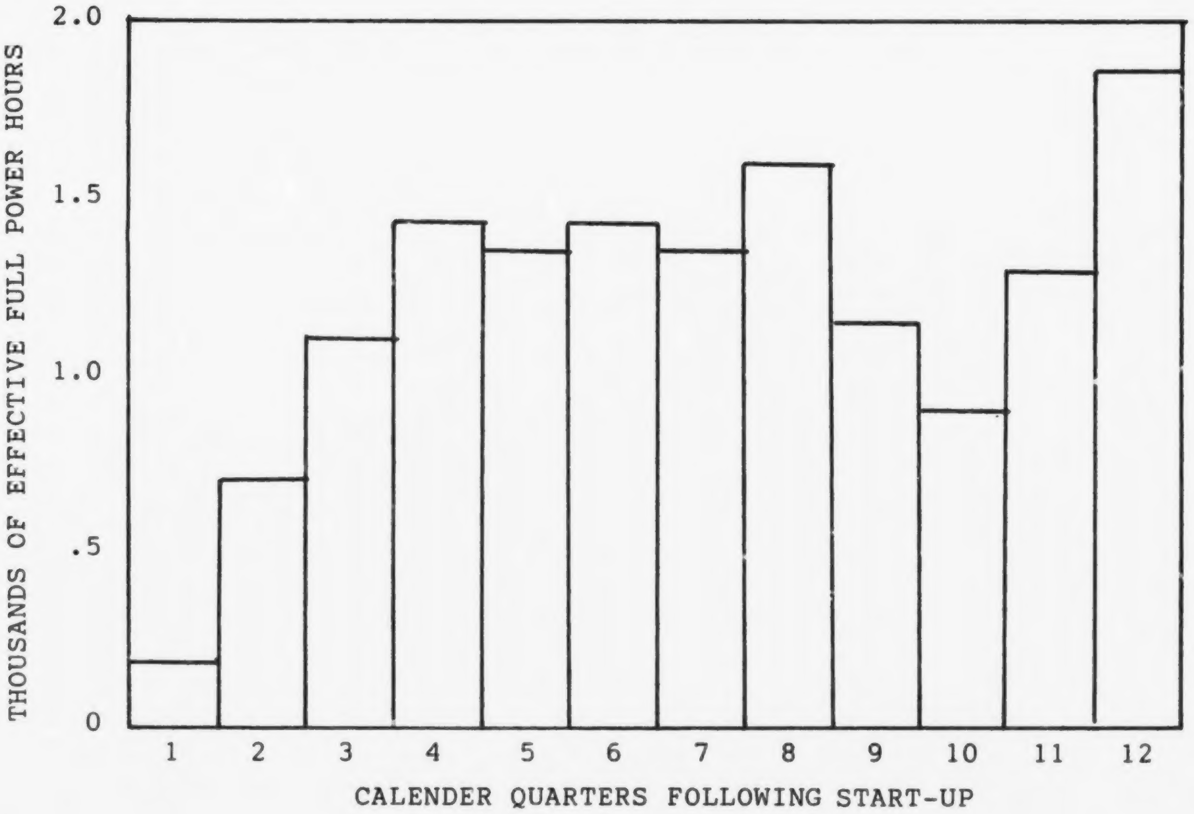

MODERN PLANTS
OPERATING TIME VERSUS CALENDER TIME
FIGURE 3

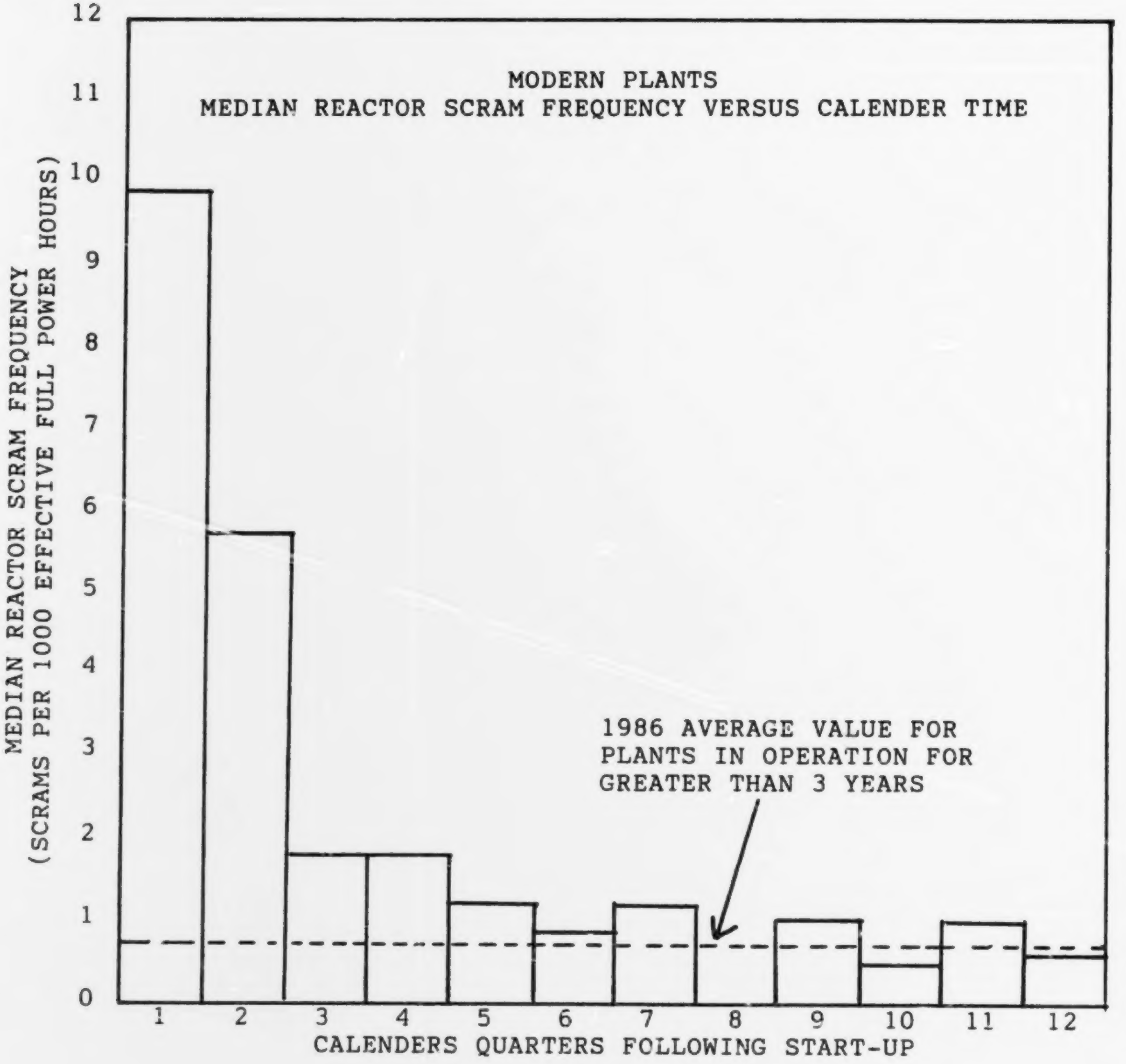
MODERN PLANTS
MEDIAN REACTOR SCRAM FREQUENCY VERSUS CALENDER TIME
MEDIAN REACTOR SCRAM FREQUENCY
(SCRAMS PER 1000 EFFECTIVE FULL POWER HOURS)
0
1
2
3
4
5
6
7
8
9
10
11
12
1986 AVERAGE VALUE FOR
PLANTS IN OPERATION FOR
GREATER THAN 3 YEARS
1
2
3
4
5
6
7
8
9
10
11
12
CALENDERS QUARTERS FOLLOWING START-UP

378 FIGURE 4

## Table 4

### EARLY VINTAGE PLANTS

### NUMBER OF SCRAMS IN CALENDER QUARTERS FOLLOWING START-UP

| PLANT | START-UP DATE | CAPACITY (MWE) | FIRST QTR | SECOND QTR | THIRD QTR | FOURTH QTR | FIRST QTR | SECOND QTR | THIRD QTR | FOURTH QTR | FIRST QTR | SECOND QTR | THIRD QTR | FOURTH QTR |
|---|---|---|---|---|---|---|---|---|---|---|---|---|---|---|
| YANKEE ROWE | 11/10/60 | 180 | 1.00 | 2.00 | 2.00 | 2.00 | 1.00 | 0.00 | 0.00 | 0.00 | 0.00 | 0.00 | 2.00 | 1.00 |
| BIG ROCK POINT | 12/08/62 | 70 | 5.00 | 1.00 | 0.00 | 0.00 | 4.00 | 2.00 | 0.00 | 0.00 | 0.00 | 0.00 | 0.00 | 1.00 |
| HUMBOLDT BAY | 04/18/63 | 65 | 0.00 | 2.00 | 0.00 | 0.00 | 2.00 | 0.00 | 2.00 | 0.00 | 1.00 | 1.00 | 0.00 | 0.00 |
| SAN ONOFRE 1 | 07/16/67 | 456 | 0.00 | 7.00 | 1.00 | 0.00 | 1.00 | 0.00 | 1.00 | 0.00 | 1.00 | 0.00 | 1.00 | 3.00 |
| HADDAM NECK | 08/07/67 | 596 | 0.00 | 4.00 | 1.00 | 3.00 | 3.00 | 4.00 | 2.00 | 1.00 | 3.00 | 4.00 | 0.00 | 1.00 |
| OYSTER CREEK | 09/23/69 | 650 | 0.00 | 19.00 | 3.00 | 3.00 | 3.00 | 3.00 | 0.00 | 0.00 | 0.00 | 1.00 | 0.00 | 3.00 |
| GINNA | 12/02/69 | 490 | 5.00 | 5.00 | 1.00 | 2.00 | 3.00 | 1.00 | 1.00 | 6.00 | 1.00 | 2.00 | 1.00 | 3.00 |
| ROBINSON 2 | 09/26/70 | 700 | 1.00 | 2.00 | 11.00 | 0.00 | 0.00 | 1.00 | 2.00 | 2.00 | 5.00 | 3.00 | 2.00 | 7.00 |
| POINT BEACH 1 | 11/06/70 | 519 | 2.00 | 7.00 | 0.00 | 0.00 | 1.00 | 1.00 | 1.00 | 0.00 | 0.00 | 0.00 | 2.00 | 0.00 |
| PALISADES | 12/31/71 | 675 | 2.00 | 3.00 | 0.00 | 1.00 | 2.00 | 2.00 | 1.00 | -1.00 | -1.00 | -1.00 | -1.00 | -1.00 |
| POINT BEACH 2 | 08/02/72 | 519 | 0.00 | 1.00 | 6.00 | 3.00 | 0.00 | 0.00 | 0.00 | 0.00 | -1.00 | -1.00 | -1.00 | -1.00 |
| AVERAGE | | 478 | 1.45 | 4.82 | 2.27 | 1.27 | 1.82 | 1.27 | 0.91 | 0.90 | 1.22 | 1.22 | 0.89 | 2.11 |

## Table 5

### EARLY VINTAGE PLANTS

### THOUSANDS OF EFFECTIVE FULL POWER HOURS IN YEARS FOLLOWING START-UP

| PLANT | START-UP DATE | CAPACITY (MWE) | YEAR OF START-UP | FIRST YEAR | SECOND YEAR | THIRD YEAR | FOURTH YEAR | FIFTH YEAR |
|---|---|---|---|---|---|---|---|---|
| YANKEE ROWE | 11/10/60 | 180 | 0.22 | 5.10 | 4.10 | 5.50 | 7.00 | 5.72 |
| BIG ROCK POINT | 12/08/62 | 70 | -1.00 | 1.85 | 2.91 | 2.72 | 7.57 | 6.41 |
| HUMBOLDT BAY | 04/18/63 | 65 | 2.70 | 5.84 | 4.18 | 2.60 | 5.20 | 7.20 |
| SAN ONOFRE 1 | 07/16/67 | 456 | 0.85 | 3.00 | 6.00 | 7.04 | 7.60 | 6.51 |
| HADDAM NECK | 08/07/67 | 596 | 0.94 | 5.30 | 6.44 | 6.24 | 7.38 | 7.55 |
| OYSTER CREEK | 09/23/69 | 650 | 0.54 | 5.52 | 6.10 | 6.92 | 5.72 | 5.86 |
| GINNA | 12/02/69 | 490 | 0.08 | 4.71 | 5.86 | 5.24 | 4.53 | 6.53 |
| DRESDEN 2 | 04/13/70 | 812 | -1.00 | -1.00 | 4.15 | 6.48 | 4.42 | 3.85 |
| ROBINSON 2 | 09/26/70 | 700 | 0.02 | 3.67 | 7.26 | 5.70 | 7.23 | 6.29 |
| POINT BEACH 1 | 11/06/70 | 519 | 0.41 | 6.60 | 5.93 | 5.60 | 6.38 | 5.93 |
| PALISADES | 12/31/71 | 675 | -1.00 | 2.81 | 3.72 | 0.14 | 3.91 | -1.00 |
| POINT BEACH 2 | 08/02/72 | 519 | [illegible] | 6.12 | 6.45 | 7.60 | -1.00 | -1.00 |
| AVERAGE | | 478 | 0.69 | 4.59 | 5.26 | 5.15 | 6.09 | 6.19 |

-1 Data Incomplete

379

### Table 6
## EARLY VINTAGE PLANTS

### SCRAMS PER 1000 EFPH IN YEARS FOLLOWING START-UP

| PLANT | START-UP DATE | CAPACITY (MWE) | YEAR OF START-UP | FIRST YEAR | SECOND YEAR | THIRD YEAR | FOURTH YEAR | FIFTH YEAR |
|---|---|---|---|---|---|---|---|---|
| YANKEE ROWE | 11/10/60 | 180 | 4.60 | 1.37 | 0.00 | 0.54 | 0.86 | 0.00 |
| BIG ROCK POINT | 12/08/62 | 70 | -1.00 | 3.23 | 2.40 | 0.37 | 0.19 | 0.00 |
| HUMBOLDT BAY | 04/18/63 | 65 | 1.47 | 0.51 | 0.24 | 0.39 | 0.57 | 0.70 |
| SAN ONOFRE 1 | 07/16/67 | 456 | 8.30 | 0.34 | 0.33 | 0.00 | 0.92 | 0.92 |
| HADDAM NECK | 08/07/67 | 596 | 4.25 | 2.08 | 1.55 | 0.64 | 0.68 | 0.40 |
| OYSTER CREEK | 09/23/69 | 650 | 35.20 | 2.20 | 0.16 | 1.16 | 1.04 | 0.17 |
| GINNA | 12/02/69 | 490 | 64.50 | 2.30 | 1.54 | 1.14 | 0.41 | 0.88 |
| DRESDEN 2 | 04/13/70 | 812 | -1.00 | -1.00 | 2.20 | 0.77 | 0.68 | 0.78 |
| ROBINSON 2 | 09/26/70 | 700 | 165.00 | 3.30 | 1.65 | 2.45 | 1.25 | 2.07 |
| POINT BEACH 1 | 11/06/70 | 519 | 4.90 | 1.05 | 0.51 | 0.36 | 0.78 | 0.34 |
| PALISADES | 12/31/71 | 675 | -1.00 | 2.13 | 1.34 | 0.00 | 0.26 | -1.00 |
| POINT BEACH 2 | 08/02/72 | 519 | 2.30 | 0.82 | 0.31 | 0.13 | -1.00 | -1.00 |
| AVERAGE |  | 478 | 32.28 | 1.76 | 1.02 | 0.66 | 0.69 | 0.63 |
| STD. DEVIATION |  |  | 54.07 | 1.02 | 0.85 | 0.68 | 0.32 | 0.61 |
| MEDIAN |  |  | 4.90 | 2.06 | 0.84 | 0.47 | 0.68 | 0.55 |

### Table 7
## MODERN PLANTS

### SCRAMS PER 1000 EFFECTIVE FULL POWER HOURS IN YEARS FOLLOWING START-UP

| PLANT | START-UP DATE | CAPACITY (MWE) | YEAR OF START-UP | FIRST YEAR | SECOND YEAR | THIRD YEAR |
|---|---|---|---|---|---|---|
| LASALLE 1 | 09/04/82 | 1078 | 12.44 | 7.34 | 1.77 | 1.93 |
| SAN ONOFRE 2 | 09/20/82 | 1127 | 17.29 | 3.35 | 0.81 | 1.44 |
| SUSQUEHANNA 1 | 11/16/82 | 1068 | 9.31 | 2.33 | 1.18 | 0.78 |
| SUMMER 1 | 11/16/82 | 900 | 20.74 | 2.77 | 1.22 | 1.17 |
| MCGUIRE 2 | 05/23/83 | 1225 | -1.00 | 2.69 | 1.67 | 0.61 |
| ST. LUCIE 2 | 06/13/83 | 882 | 2.25 | 1.34 | 0.68 | 0.35 |
| SAN ONOFRE 3 | 09/25/83 | 1127 | 10.25 | 0.91 | 1.13 | 0.64 |
| LASALLE 2 | 04/20/84 | 1078 | 3.04 | 0.30 | 0.71 | -3.00 |
| WNP 2 | 05/27/84 | 1155 | 9.72 | 2.14 | 0.83 | -3.00 |
| SUSQUEHANNA 2 | 07/03/84 | 1068 | 5.40 | 0.70 | 0.29 | -3.00 |
| GRAND GULF 1 | 10/20/84 | 1157 | 29.67 | 3.29 | 0.74 | -3.00 |
| CALLAWAY 1 | 10/24/84 | 1180 | 7.50 | 2.65 | 0.81 | -3.00 |
| DIABLO CANYON 1 | 11/11/84 | 1125 | 4.28 | 1.43 | 0.25 | -3.00 |
| CATAWBA 1 | 01/22/85 | 1145 | 2.49 | 1.16 | -3.00 | -3.00 |
| BYRON 1 | 03/01/85 | 1175 | 5.33 | 0.90 | -3.00 | -3.00 |
| WATERFORD 3 | 03/18/85 | 1104 | 6.63 | 0.80 | -3.00 | -3.00 |
| LIMERICK 1 | 04/13/85 | 1092 | 1.74 | 0.36 | -3.00 | -3.00 |
| PALO VERDE 1 | 06/10/85 | 1303 | 6.82 | 1.79 | -3.00 | -3.00 |
| WOLF CREEK 1 | 08/12/85 | 1170 | 2.61 | 0.84 | -3.00 | -3.00 |
| DIABLO CANYON 2 | 10/20/85 | 1124 | 17.76 | 2.83 | -3.00 | -3.00 |
| RIVER BEND 1 | 12/01/85 | 936 | -1.00 | 7.31 | -3.00 | -3.00 |
| MILLSTONE 3 | 01/23/86 | 1197 | 1.13 | -3.00 | -3.00 | -3.00 |
| PALO VERDE 2 | 05/20/86 | 1221 | 9.93 | -3.00 | -3.00 | -3.00 |
| AVERAGE |  | 1023 | 8.87 | 2.25 | 0.93 | 0.99 |
| STD. DEVIATION |  |  | 7.30 | 1.94 | 0.46 | 0.55 |
| MEDIAN |  |  | 6.82 | 1.79 | 0.81 | 0.78 |

-1 Data Incomplete
-2 Plant Shutdown
-3 Period Not Yet Reached in Plant Life

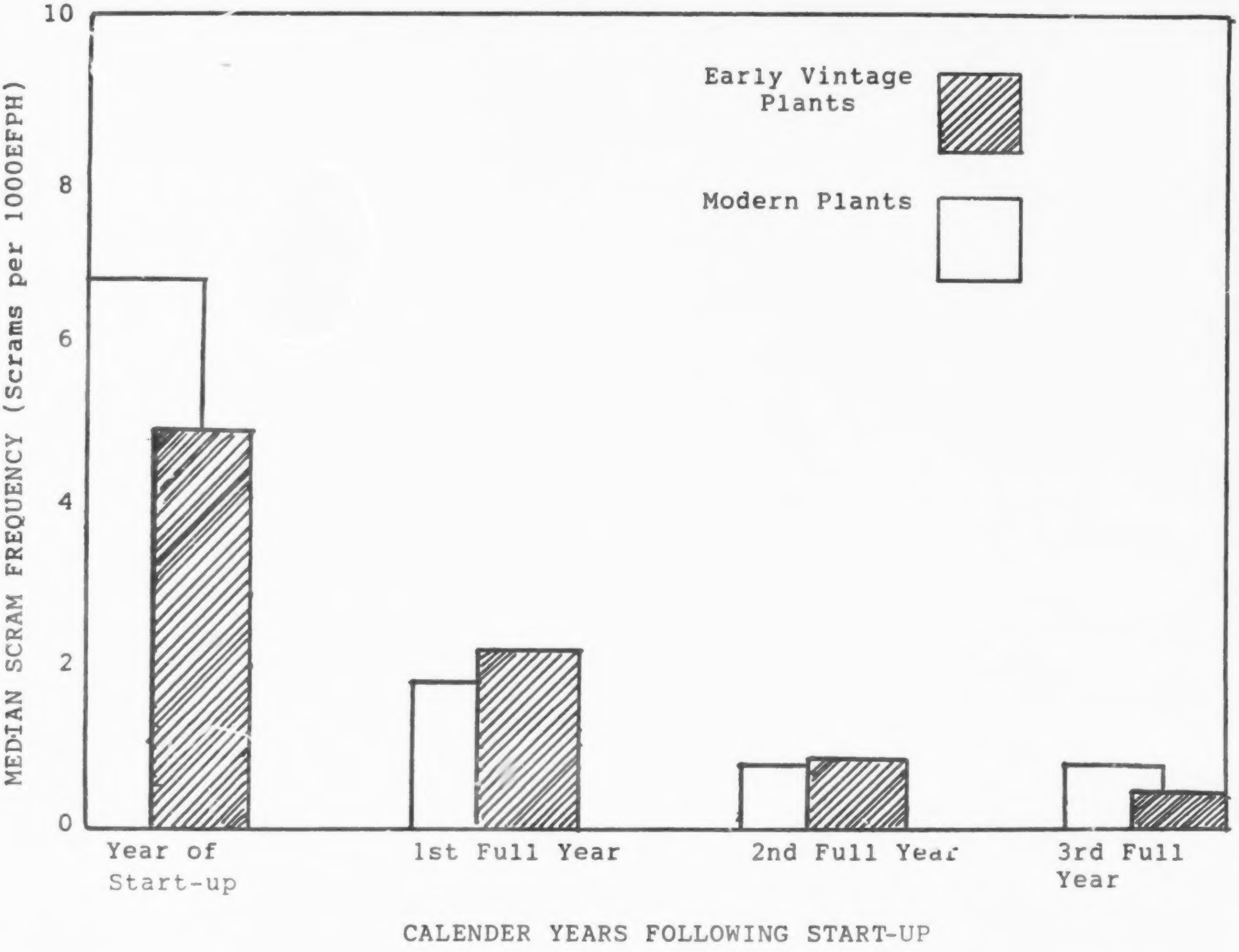

COMPARISON OF SCRAM FREQUENCIES FOR MODERN AND EARLY VINTAGE PLANTS
FIGURE 5

quite significant. These results tend to support the conclusion that design power level and other design changes which have taken place over the years are not significant factors regarding performance during initial startup and entry to commercial operation.

## 1.4 Comparison Between Plants at Multi-Unit Sites

Table 8 provides comparisons of performance statistics between first and follow-on units at multi-unit sites. The general trend appears to be significant reductions in scram frequency and increases in productivity, as one might expect. In the case of Diablo Canyon it is worth noting that while Unit 2 performance was typical for a second unit, the Unit 1 performance was unusually good.

## 2.0 Recent Significant Events Involving Age-Related Failures

While current plant performance indicators (e.g., reactor trip frequency) are not presently showing a significant impact from age-related failures, failures of plant components due to normal and accelerated aging are causing and contributing to significant operational events. This section of the paper provides a discussion of several recent significant events at domestic nuclear power plants which involved age-related degradation of systems and components. The events include: degradation of station batteries at Rancho Seco and Duane Arnold; degradation of solenoid valves used in BWR scram systems; loss of electrical power due to cable failures at San Onofre 1, and a damaging waterhammer at San Onofre 1 caused by multiple check valve failures. These events were identified through the NRC's current program for systematic review and assessment of operating experience and reporting of significant events.

## 2.1 Degradation of Station Batteries[7, 8]

Nuclear power station batteries are used to provide DC power for motive and control functions in safety-related equipment. They can also operate in conjunction with inverter to supply some AC instrumentation and control power. The batteries are crucial for successful mitigation of the station blackout accident in that they can successfully provide instrumentation and control to support equipment needed to maintain core cooling for several hours while AC power is being restored.

During licensee inspections conducted at the Rancho Seco Nuclear Power Plant in the spring of 1986, substantial degradation of all station batteries was revealed. The batteries exhibited flaking of the cell plates and flaking of the plate's hook area where the plates connect to the cell posts. Although the licensee performed visual inspections that included examination of the electrolyte level and accumulation of sediment in the bottom of the cell, the severe flaking went unnoticed. The deteriorated cells were of the Plante' design and over 15 years old. The batteries were expected to last about 20 years and an inspection by the battery vendor one year earlier did not reveal abnormal degradation. As a result of the flaking, the battery vendor advised the licensee that the batteries at Rancho Seco should be replaced and the licensee is now in the process of replacing the batteries.

## Table 8

## Comparison of First Year Average* Scram Frequency Between Units at Multi-Unit Sites

| Site | Unit | First Year Average Scram Frequency (Scrams/1000 EFPH) |
|---|---|---|
| Lasalle | 1 | 9.4 |
| | 2 | 5.7 |
| Susquehanna | 1 | 4.2 |
| | 2 | 1.7 |
| San Onofre | 2 | 13.0 |
| | 3 | 4.8 |
| Diablo Canyon | 1 | 3.3 |
| | 2 | 5.6 |
| Point Beach | 1 | 4.9 |
| | 2 | 2.3 |

*Average of first four quarters following start-up

On September 22, 1986, Iowa Electric Light and Power Company reported the results of station battery inspections at the Duane Arnold plant. Following a visual inspection of the battery in which white sediment was detected in the electrolyte, the licensee had the inside of the battery inspected by the vendor representative and found extensive erosion near the top of the plates between the plates and supports. Specifically, the vendor representative identified three plates separated in one cell and approximately 50% erosion of plate-to-bus bar connection in 11 other cells. The cells were 15 years old, having been installed in 1971. The licensee currently plans to replace 14 of the battery cells. The battery vendor believes that the root cause of the problem was accelerated aging due to variation in temperature in the room housing the batteries.

The principal technical concern with corrosion of the plates and plate connections is that it can weaken them which could render the battery inoperable during a seismic event. Tests of naturally-aged nuclear station safety-related batteries sponsored by the NRC have indicated that mechanical failure of internal connections, possibly due to erosion, is a significant failure mechanism.[9] The NRC staff is also concerned that this failure mechanism is not being identified using current surveillance test procedures.

## 2.2 Degradation of Scram Pilot Valve Solenoids

On December 24, 1985, at Millstone Unit 1, three control rods failed to insert during the performance of single rod scram time testing. In all cases, the control rod was immediately inserted and electrically disabled. The reactor was operating at 25% power during the event.

Investigation into the failures revealed that in the first case the cause for failure of one sticking solenoid operated valve (SOV) was attributed to deterioration of the BUNA-N disc material within the valve. The licensee's investigation of the other two control rod drop failures failed to reveal the causes for failure other than a misalignment problem of one SOV's internals, which prevented proper movement. However, in each case, the SOVs were disassembled, overhauled, retested satisfactorily, and returned to service.

Similar events involving control rod failures during surveillance testing have occurred in the past at other BWRs (e.g., Monticello, Pilgrim-1, and Big Rock Point). These failures were also caused by deterioration of BUNA-N components in the SOV. Inspections at Monticello following an event in 1978 revealed that the BUNA-N valve disc had become brittle over time and had broken into small pieces which blocked a port in the valve through which air was vented. These events prompted General Electric to issue several Service Information Letters (SIL) which discussed the deterioration of BUNA-N components via natural aging and advised their customers that components should be replaced after seven years of use by rebuilding the valves.

## 2.3 Electrical Cable Failure Resulting in Loss of Offsite Power[10]

On November 21, 1985, San Onofre Unit 1 experienced a loss of offsite power followed by a damaging waterhammer in the main feedwater system with the plant operating at 60% power. Offsite power was lost when a transformer was tripped by its differential relays because of a fault in the cable to the Class 1E 4160 volt bus and the main generator tripped following a manual reactor trip. Further inspection of the failed cable showed evidence of insulation degradation and arcing between two phases to the sheath of the cable. The most likely cause of the cable failure was determined to be temperature-induced accelerated aging and degradation of the cable insulation. The source of this heat was a bare high-temperature (400°F) feedwater line and flange in the immediate vicinity of the cable. The thermal insulation had been removed from the pipe during previous repair of a gasket leak and not replaced.

Southern California Edison Company established a special Cable Evaluation Task Force which has investigated and tested both 4160 and lower voltage cables and has identified several other degraded cables that also would have failed over time. The faulted cable and other cables have been replaced at San Onofre Unit 1. In addition, the staff has requested that the licensee develop a program for monitoring electrical cables.

### 2.4 Check Valve Failure Resulting in Waterhammer Damage

The damaging waterhammer which followed the loss of offsite power at San Onofre Unit 1 was due to the failure of five check valves to properly block backflow in the main feedwater system. Post-event disassembly and examination of the valves that contributed to waterhammer condition confirmed that check valve failures were the underlying causes for the occurrence of waterhammer. These inspections revealed significant wear on the internals of all valves, looseness of the disc-to-hinge nut with disc mispositioned in three valves, and separation of the disc from the hinge in two valves. The root cause of the check valve damage has been determined to be accelerated wear of the valve internals over several years due to a combination of factors including: improper sizing of the valves and a deficiency in the nut stud design; operation of the feedwater system at a reduced flowrate during the prior 4.5 year period, and turbulence in the check valve region from upstream disturbances. The licensee's detailed failure analysis[11] indicates that the latter two factors lead to large and rapid variation in the lift force on the disc which resulted in frequent impact of the disc against the upper stop.

## 3.0 Findings and Conclusions

The following findings are based on the analysis of the data presented in this paper:

1. Scram frequency is high during initial plant start-up, and in general drops significantly as commercial operation is begun.

2. Changes in plant design, including increases in design power level over the years have not been a significant contributor to high scram frequencies in modern plants during the first few years of operation.

3. Scram frequency in follow-on units during start-up generally tends to be lower than that of the lead unit by a significant amount.

Based on this information, we can draw the following conclusions. First, nuclear power plant overall performance as indicated by scram frequencies does appear to show the typical "burn-in" phase of most complex equipment. Second, none of the currently licensed plants appear to show the rapid increase in failures characteristic of equipment nearing the end-of-life. We conclude that "new" or "young" plants are those less than two years old. The age associated with an "old" plant cannot yet be established (i.e., it appears to be greater than 20 years). Third, individual plant components do show age-related failures and require repair or replacement to prevent overall plant performance from degrading unacceptably. These failures have been occurring at a sufficiently slow rate that corrective action has been effective. Fourth, the age-related failures which have occurred are in areas of known aging sensitivity (i.e., batteries and rubber seals and diaphragms).

In monitoring operating experience in the future, we will be better able to identify aging problems. The NRC's proposed Performance Indicator Program (which will initially monitor: scrams and safety system actuations, safety system failures, forced outage rates, enforcement actions, significant events, and mean-time between equipment-related forced outages) will provide more complete and uniform information for trending performance. Among other valuable uses, the Performance Indicator program will enhance our ability to identify age-related trends.

# List of References

1. 1983 Reactor Trip Statistics, D. G. Eisenhut, U.S. NRC, Washington, D.C., August 9, 1984.

2. Trends and Patterns Report of Unplanned Reactor Trips at U.S. Light Water Reactors in 1984, Office of Analysis and Evaluation of Operational Data, U.S. NRC, Washington, D.C., August 1985.

3. Trends and Patterns Report of Unplanned Reactor Trips at U.S. Light Water Reactors in 1985, Office of Analysis and Evaluation of Operational Data, U.S. NRC, Washington, D.C., August 1986.

4. G. E. Edison and M. T. Gerstner, Application of Reactor Scram Experience in Reliability Analysis of Shutdown Systems; Nuclear Safety, Volume 19, No. 6, November-December 1978.

5. ERDA-76/125, U.S. Central Station Nuclear Power Reactors - Operating History - 1975, Energy Research and Development Administration, Division of Nuclear Research and Applications, 1976.

6. NUREG-0020, Volumes 6-10, Licensed Operating Reactors, U.S. NRC, Washington, D.C.

7. U.S. NRC Office of Inspection and Enforcement, Information Notice No. 86-37: Degradation of Station Batteries, May 16, 1986.

8. Summary of the Operating Reactors Events Meeting on September 29, 1986, - Meeting 86-34, Gary M. Holahan, Internal Memorandum, U.S. NRC, Washington, D.C., October 6, 1986.

9. NUREG/CR-3923, Test Series 1: Seismic-Fragility Tests of Naturally-Aged Class 1E Gould NCX-2250 Battery Cells, September 1984.

10. U.S. NRC Office of Inspection and Enforcement, Information Notice No. 86-49: Age/Environment-Induced Cable Failures, June 16, 1986.

11. Letter and Enclosures from M. D. Medford (SCE) to A. E. Chaffee (USNRC) Forwarding Investigation Report of November 21, 1985, Waterhammer Event, April 4, 1986. Docket No. 50-206.

BLANK PAGE

# APPLICATION OF DIAGNOSTICS TO DETERMINE MOTOR OPERATED VALVE OPERATIONAL READINESS

D. M. Eissenberg

## ABSTRACT

ORNL has been carrying out an aging assessment of motor-operated valves (MOVs) with the primary objective of recommending diagnostic methods for detecting and trending aging.

As a result of experimental investigations at ORNL, it was discovered that the motor current during a valve stroke was a very useful diagnostic parameter for detecting and trending many MOV drive train load variations. The motor current signatures were analyzed at four levels: mean value for a stroke, gross trends during a stroke, transients, and noise frequency spectra. Examples illustrating the use of this technique are presented.

The use of motor current signature analysis was also shown to apply to other electric motor driven equipment.

Future work includes developing a data base of MOV diagnostics, including criteria for determining the extent of degradation and application of the technique to other LWR motor driven safety equipment.

## INTRODUCTION AND OBJECTIVES

As part of the Nuclear Regulatory Commission Nuclear Plant Aging Research (NPAR) program, Oak Ridge National Laboratory (ORNL) is carrying out a comprehensive aging assessment of the motor-operated valves (MOV's) used in safety systems of nuclear power plants.

A primary objective of the NPAR program is to identify and recommend diagnostic methods for detecting, differentiating, and trending time-dependent degradations and service wear (aging) of important components on nuclear plant safety systems such that timely maintenance can be performed prior to loss of safety function. The approach used to achieve the objective is to carry out comprehensive aging assessments of each component of interest.

The aging assessments contain these elements:

- review and analysis of the application of the component to specific nuclear plant safety systems, including identification of important design features and materials of construction, and the expected impact of the stressors to which they will be exposed under both normal and accident conditions.

- review and analysis of operating experience with that component in both nuclear power plants and other applications, in order to identify and characterize the significant failure modes and causes.
- identification and selection of diagnostic parameters to monitor during the operating life of the component which can be used to differentiate and trend defects and other degradations in the component prior to failure to perform its safety function.
- identification of suitable instrumentation and techniques with which the diagnostic parameters can be measured at appropriate times.
- demonstration, by means of laboratory and field tests, that the selected parameters can be monitored and trended, using suitable instrumentation, in an effective and reliable manner.

Early in the NPAR program life, motor-operated valves were identified as a component to be studied. Motor-operated valves are used in almost all nuclear plant safety systems. Failures of MOVs have resulted in a significant amount of plant maintenance and loss in operational readiness. A review of LERs and other failure data bases, IE Bulletins and Notices, and AEOD reports documented the types, frequency, and impacts of the failures. As a result of this and similar experiences with other types of valves, NRC has designated "In-situ Testing of Valves" as a high priority generic issue.

ORNL was assigned the task of performing a comprehensive aging assessment of motor-operated valves using the NPAR strategy, i.e, with the goal of identifying and demonstrating improved diagnostic techniques for use with motor-operated valves used in nuclear plant safety systems. Part of the task, including the first three elements listed above, has been completed and a Phase 1 report (1) issued. This paper describes activities in support of the final two elements listed above.

## BACKGROUND

Periodic surveillance tests are performed on motor-operated valves which are part of nuclear plant safety systems to demonstrate their operability. The tests are described in each licensed nuclear plant's Technical Specifications, and, by reference, in Subsection IWV (In-service Testing of Valves) which is part of Section XI of the ASME Boiler and Pressure Vessel Code. Additional leak test requirements (dealing with containment isolation valves) are described in the Code of Federal Regulations Title 10 Part 50. It should be noted that these tests apply to other types of valves in addition to motor-operated valves.

The surveillance tests are of three types:

- determination of movement of the obturator when actuated
- stroke time measurement
- leakage rate

The tests and the criteria associated with each are intended to demonstrate operability, i.e., they demonstrate that the valves meet the specified criteria under the test conditions and at the time of the test. They only indirectly demonstrate the operational readiness of the valves and the ability of the valves to actuate as required at future times under all anticipated operating conditions (including accident conditions) since there are no provisions for monitoring and trending degradation.

As part of Phase 1 of the comprehensive aging assessment, ORNL reviewed the current surveillance practices described above, and identified a list of diagnostic parameters that could be used to monitor and trend degradation on MOVs. In addition, ORNL reviewed recently developed surveillance techniques, including those developed by MOVATS Inc. (2) and by EPRI (3), to determine their applicability to measuring the effect of aging operational readiness. The results of the evaluation of the MOVATs technique has been published (4).

In order to carry out Phase 2 of the aging assessment, two MOVs (including a nuclear qualified valve obtained from a cancelled nuclear power plant) were obtained and installed in test stands. The valves were connected to switchgear so that they could be actuated, and instrumentation was obtained and installed which would demonstrate the feasibility and practicality of monitoring and trending the various diagnostic parameters identified in the Phase 1 report.

A typical motor-operated valve is shown in Figure 1, along with a cutaway drawing showing the internals of the operator. This operator was manufactured by Limitorque Corporation. Valve operators manufactured by that company account for an estimated 90% of all MOVs used in nuclear power plants in the United States.

As seen in Figure 1, the motor transmits power to the valve through a complex drive train. Included as a part of the operator in addition to the drive train elements are two switches which are used to control the voltage supplied

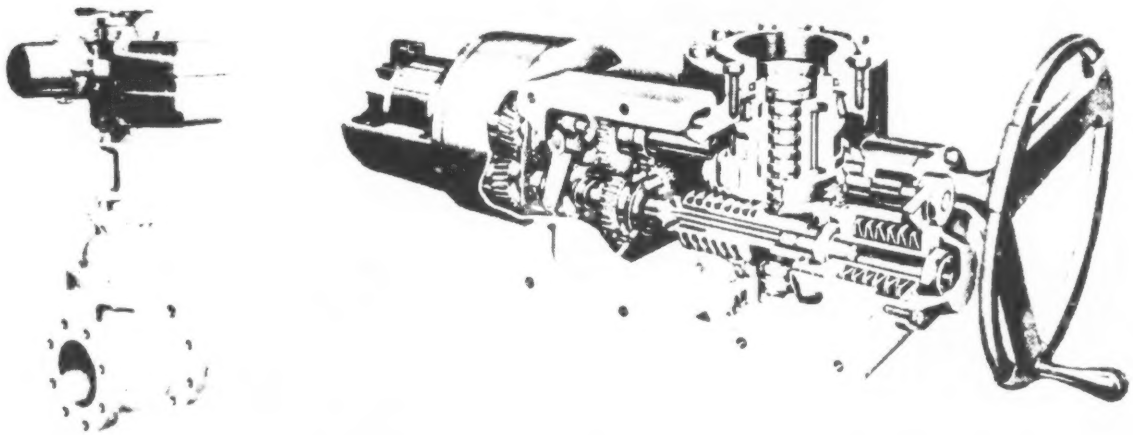

Figure 1. Limitorque motor operator installed on a gate valve.

BEST COPY AVAILABLE

to the valve motor. One switch indirectly senses the valve stem position and the second the torque or load being transmitted to the valve stem. The torque is measured by the amount of compression of a spring pack resulting from the axial translation of a worm.

Preliminary tests were carried out using the two valves in the test stand to determine the type and potential value of diagnostic information that could result from using instrumentation to measure the following MOV parameters:

- MOV vibration (three locations)
- motor temperature (two locations)
- motor current
- valve stem strain
- valve stem velocity and acceleration
- torque and limit switch (including torque switch angle)

Based on the results of the preliminary tests, it was concluded that although all of the parameters appeared to provide useful diagnostic information about the valve, the motor current signature appeared particularly attractive as the primary or initial diagnostic for detecting and trending degradation occurring in the MOV drive train. The other parameters then could be used to supplement motor current in cases where they would be useful in differentiating among possible degradations, or in detecting additional degradations not picked up by monitoring the motor current.

## MOTOR CURRENT AS A DIAGNOSTIC

The current flowing in the leads to the motor of the MOV was found to be a sensitive and selective indicator of the mechanical loads driven by the motor. From the standpoint of diagnostics, the motor is acting as a transducer, converting the drive train mechanical loads and their variations with time into variations in voltage across the windings. The resulting net current flow in the motor power leads then reflects the characteristics of the motor load. Changes over time reflect MOV degradations which appear as load changes.

## MEASUREMENT OF MOTOR CURRENT

The measurement of motor current has advantages compared to other parameters which could be used to monitor MOVs to provide similar information about MOV drive train loads (such as torque switch angle or spring pack deflection). The principal advantage is that it is capable of being measured remotely and non-obtrusively. It can as a result be measured during plant operation, since no leads need to be lifted to attach the sensor. Figure 2 shows the arrangement used to monitor motor current at the motor control center (MCC) of the MOV test stand. A clamp-on current sensor is attached to one lead of the power cable running between the MCC and the valve motor. The location of the attachment can be selected for convenience, since it does not affect the current reading. Clamp-on current sensors are inexpensive and can be simply installed. Reading and recording the motor current can be carried out rapidly, either manually or automatically.

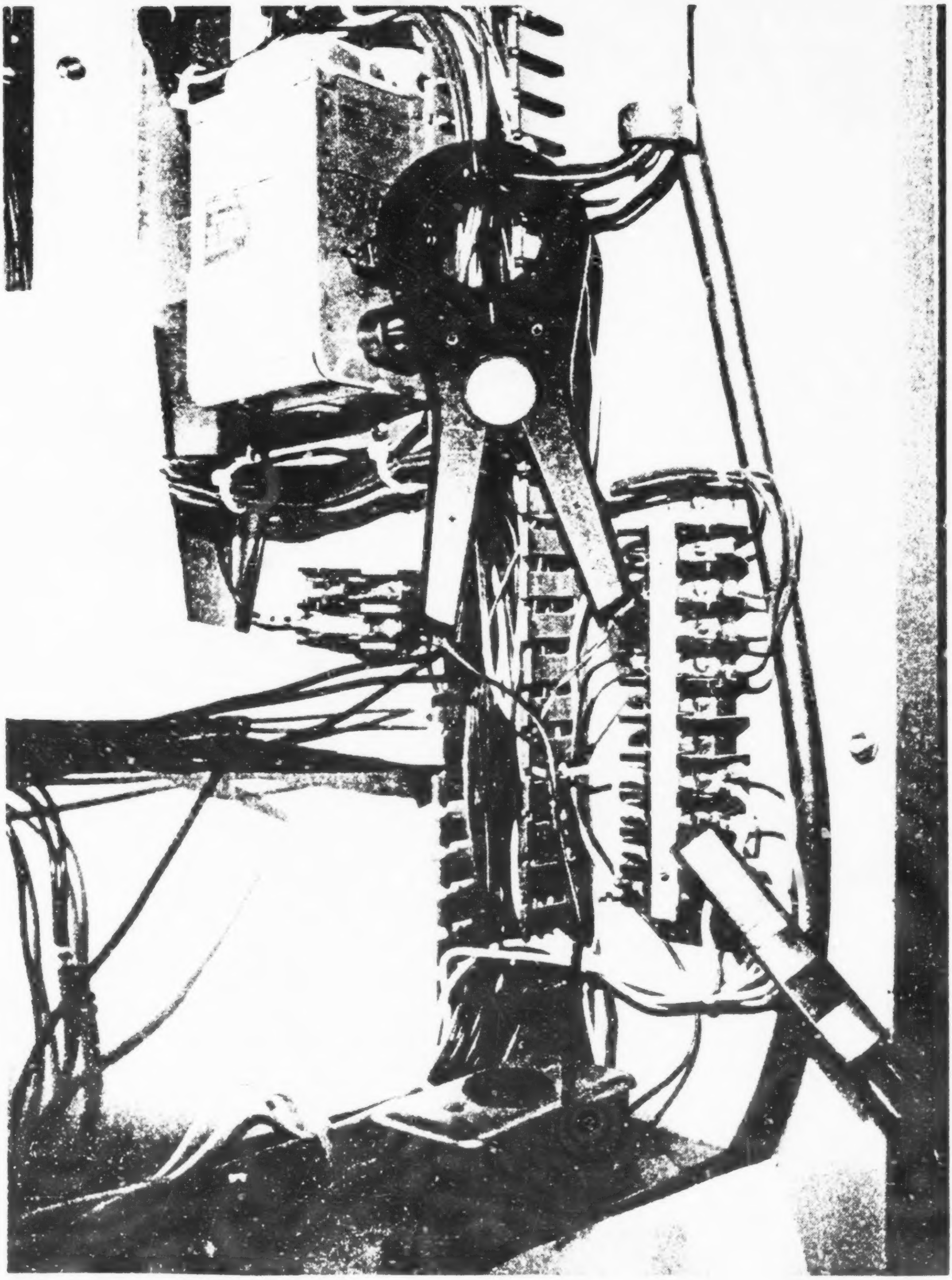

Figure 2. Measurement of motor current at the motor control center.

## INFORMATION CONTENT OF A MOTOR CURRENT SIGNATURE

A motor current signature has been found to contain four levels of information:

- mean value over a valve stroke
- gross variations during a stroke
- transients
- frequency spectrum of periodic variations

Each level of information has been found to be useful for detecting and trending different features of the MOV mechanical load. By analyzing all four levels of information during a valve actuation, it is expected that many types of degradation associated with MOV aging will be detected and trended in an incipient stage so that corrective measures can be taken prior to loss of safety function.

In the following discussion, examples will be presented of motor current signatures obtained from MOVs which clearly show different features of the mechanical train which the motor drives. In several instances, a defect (not necessarily serious) was identified and diagnosed using motor current signatures.

In addition, the application of motor current signature analysis to other motor driven mechanical equipment is demonstrated. It is anticipated that this technique will find application in the diagnostic monitoring of degradation in other motor driven components used in nuclear power plant safety systems, as well as in many nonnuclear applications.

A patent application has been submitted by the U. S. Department of Energy covering features of this technique.

## APPLICATIONS OF MOTOR CURRENT SIGNATURE ANALYSIS

### Stem Taper

The first example of the application of motor current signature analysis involves the gross variation observed during a valve stroke. In Figure 3 are two plots of motor current versus time, obtained for a type SMA-2 motor operator connected to an 8 inch globe valve. It is observed that, in these expanded scale plots, there is a gradual decrease in motor current with time in the open-to-close direction, while there is a slightly larger but symmetrical increase occurring in the close-to-open stroke. Although the magnitude of the decrease and increase is less than 2% of the current flow, it was found to be reproducible.

The diagnosis based on the gross variation was that there was a characteristic of the valve stem responsible, either near the stem nut or the packing. When the valve was disassembled, and the stem inspected, it was found (Figure 4) that the diameter of the valve stem changed monotonically in the region where the stem passes through the packing. Although the change was small, it was

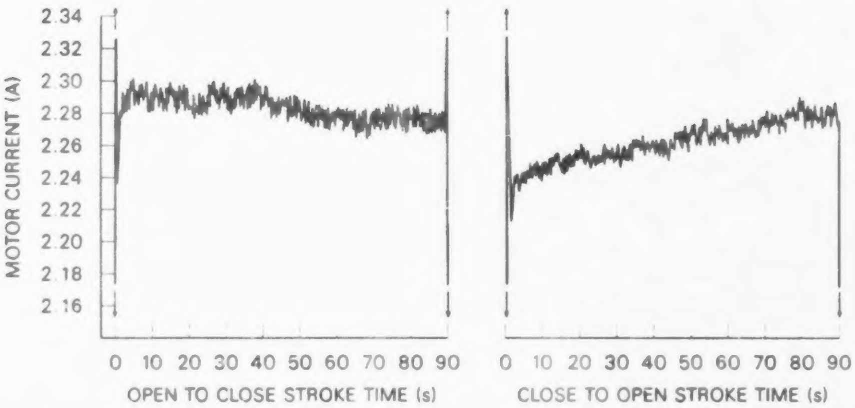

Figure 3. Motor current gross variation signatures from a limitorque operator connected to a six-inch gate valve.

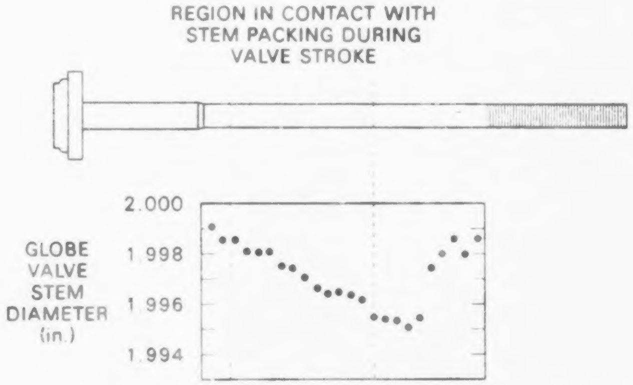

Figure 4. As-found stem dimensions of the six-inch globe valve.

sufficient to alter the friction coefficient between stem and packing. Subsequent tests have shown that the motor current variation is more or less pronounced as the packing is tightened or loosened.

WORM AND WORM GEAR LUBRICATION

Motor current signature analysis assisted in detecting and differentiating a problem in an MOV used for training purposes by a utility. The valve was being tested to develop a data base of motor current signatures of presumed normal valves. Figure 5 shows plots of open-to-close motor current signatures obtained from an SMB operator on a 3 inch gate valve. The as-found valve had loose packing, and the signature obtained (left) was that which would be expected in the open-to-close direction. The peak at the start of the stroke was due to the inrush current, while the peak at the end resulted from the seating of the gate. The magnitude of the peak current at seating was determined by the actuation of the torque switch, which occurred at a preset value of compression of the spring pack.

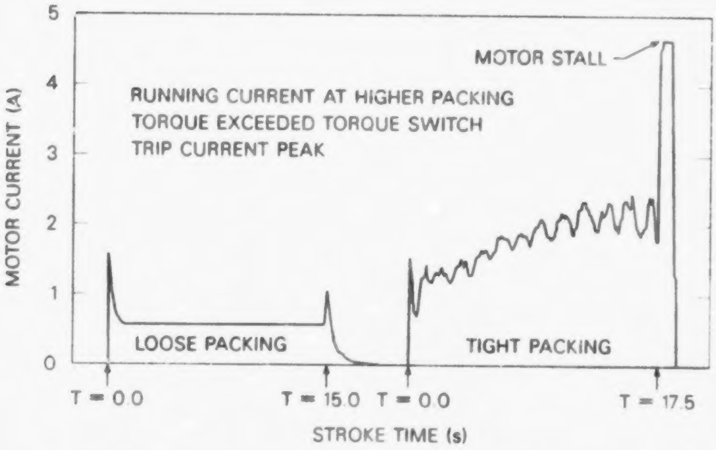

Figure 5. Motor current gross variation signatures for the as-found three-inch gate valve.

When the packing was tightened, the expected change in signature was a slight increase in the current during the middle portion of the stroke. The peak motor current at end of stroke should not have changed since it should have reflected the same spring pack deflection as before. What was found (right) was a gross increase in the motor current during the middle portion, and (in the case shown in Figure 5) a stalled motor at the end of stroke. This general effect was also observed in the close-to-open direction and was repeated in both directions at different packing tightness.

It was noted that with tight packing, the torque switch did not trip during the early part of the stroke, even though the motor current exceeded the amount at torque switch trip when the packing was loose. This observation led to the diagnosis that the increase in motor load must have been occurring in the drive train between the motor and the spring pack in a way that prevented the spring pack from compressing. This limited the problem to the drive train between the motor and the spring pack.

The operator was disassembled and inspected. It was found that there was essentially no lubricant in the region of the worm and worm gear. The operator drive train had been sprayed rather than packed with lubricant, since it was regularly disassembled and assembled as part of a classroom training program. When the operator was properly lubricated, the tests were rerun, with the results as shown, for both loose and tight packing, in Figure 6.

## SETTING TORQUE AND BYPASS SWITCHES

Motor current signatures can be used to capture transient events during a valve stroke. This is useful not only as a diagnostic for detecting and trending degradation but also can be used in the critical process of correctly setting the torque and bypass switches. This latter application is illustrated in Figure 7, which is a plot of the motor current during the first 2.5 seconds of a close-to-open stroke.

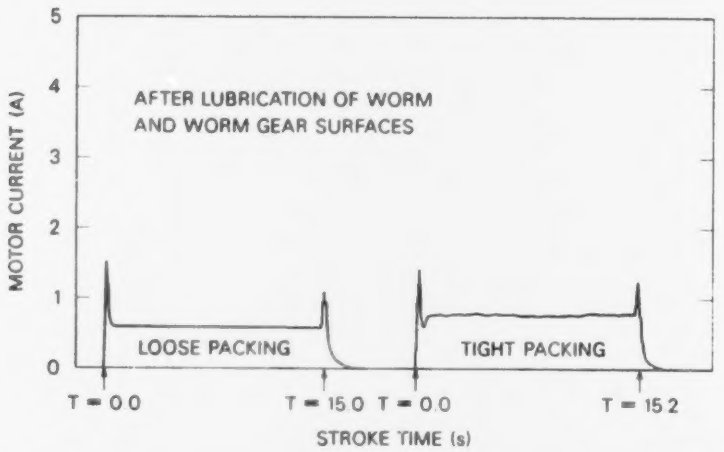

Figure 6. Motor current gross variation signatures for the three-inch gate valve following lubrication.

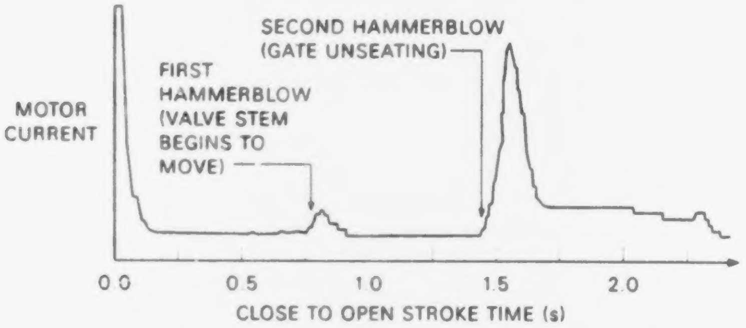

THIS METHOD IS SUPERIOR TO CURRENT PRACTICE WHICH INVOLVES DIRECT AND INTRUSIVE MEASUREMENTS

Figure 7. Motor current transient signature during open stroke.

The first transient event seen in the motor current plot is the first hammerblow, resulting from the contacting of the lugs on the worm gear with the lugs on the drive sleeve following rotation of the worm gear through approximately a one half turn. It signifies the start of motion of the valve stem. The second transient or hammerblow occurs after the valve stem rises sufficiently to use up the available clearance and start lifting the valve gate. Its magnitude, which is proportional to the load felt by the motor in overcoming the static friction between the gate and the valve seat and the inertia of the gate, is an important criteria in setting of the torque switch. Its location with regard to the start of the stroke determines the setting of the bypass switch.

Determining the switch settings using motor current transient signature analysis is superior to methods based on monitoring the compression of the spring pack, or alternately, listening to the noise associated with the hammerblows. Both of these methods require direct access to the valve. The method based on monitoring spring pack deflection requires, in addition, the direct installation and removal of complex test equipment as well as partial disassembly of the spring pack closure. The application of motor current signature analysis for this procedure may contribute to speeding up the process of verifying the torque switch/limit switch settings of safety related MOVs as required by IE Bulletin 85-03.

## MOTOR CURRENT SPECTRUM ANALYSIS

The motor current signature, when amplified and conditioned (see Figure 3), is seen to contain a "noise" component. When this "noise" was analyzed using a Fast Fourier Transform (FFT) spectral analyzer, it was observed that contained within the noise were discrete frequencies which could be associated with specific periodic phenomena.

Figure 8 is a plot of an MOV motor current signature after FFT analysis. The plot of relative amplitude versus frequency over the range 0-35 Hz shows peaks associated with the rotational speed of the worm (15.3 Hz) and its first harmonic (30.6 Hz), and the rotational speed of the motor shaft (29.3 Hz). Also appearing are peaks associated with the motor slip frequency [the difference between the synchronous speed of the motor (30 Hz), and the actual speed of the motor (29.3 Hz)]. The peaks occur at four times the slip frequency (2.8 Hz) and its first harmonic (5.6 Hz).

The relatively small magnitude of the first harmonic compared to the fundamental in each case is an indication that there is little or no degradation in either the worm gear or the motor bearings or shaft.

The motor slip frequency, because it is the difference between two larger numbers, is an accurate measure of the motor speed. The change in motor speed due to a change in load is determined by the motor design parameters, whereas

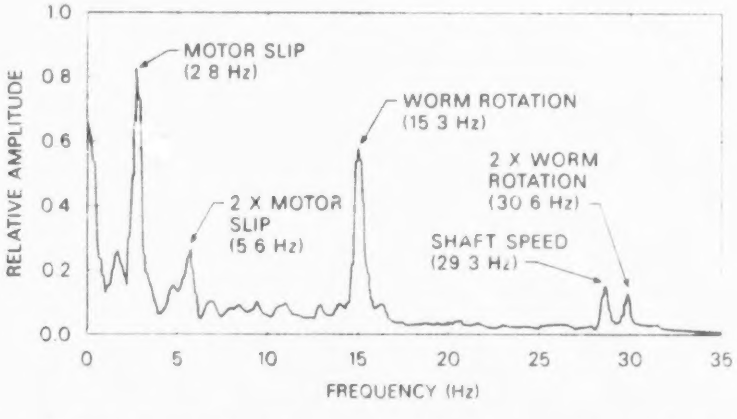

Figure 8. Motor current spectral signature (0-35 Hz) during MOV actuation.

the change in motor current due to a change in load is to some extent independent of the motor design. As a result, the relative change in motor speed with motor current may be used as a diagnostic of the performance of the motor itself.

The low frequency spectra of the MOV motor current provides additional details of the drive train loads. In Figure 9, the FFT spectrum in the range 0-1 Hz is shown. The peaks occur at the stem nut rotation frequency (0.268 Hz) and its first and second harmonic. It is observed that the second harmonic has about the same amplitude as the first. Subsequent tests show that the harmonics beyond the second also have similar amplitude, suggesting that the stem nut or stem may show degradation.

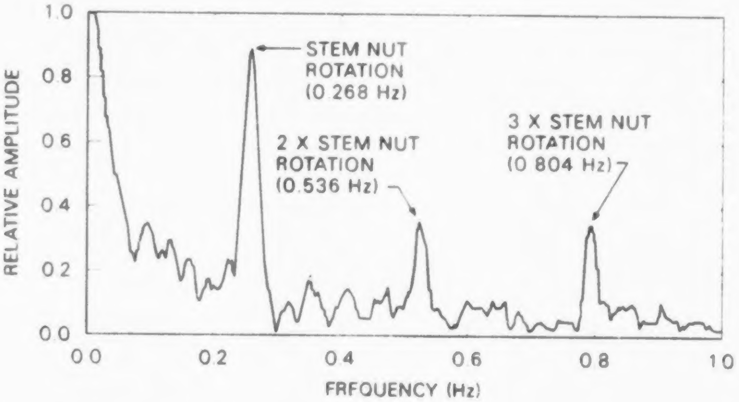

Figure 9. Motor current spectral signature (0-1 Hz) during MOV actuation.

OTHER MOTOR CURRENT SIGNATURES

Based on the experience with MOVs, it appears reasonable that motor current signature analysis should be useful for the diagnosis of other motor driven mechanical equipment. Several tests have been carried out to determine its feasibility.

Figure 10 is a motor current spectrum obtained from a 1/3 HP electric fan. The peaks shown are those due to the motor slip frequency and its first and second harmonic, and the motor shaft rotational speed. It is observed that in this case the harmonics decreased in amplitude, as expected for a simple system with little or no degradation.

The motor current spectrum for a portable laboratory vacuum pump is shown in Figure 11. The reciprocating pump was driven by a belt from an electric motor. The characteristic peaks occur at the calculated belt rotation speed and the pump rotational speed. A small peak occurs at the motor shaft speed. It is observed that the first harmonic of both belt and pump frequencies is greater than its respective fundamental frequencies. It is also

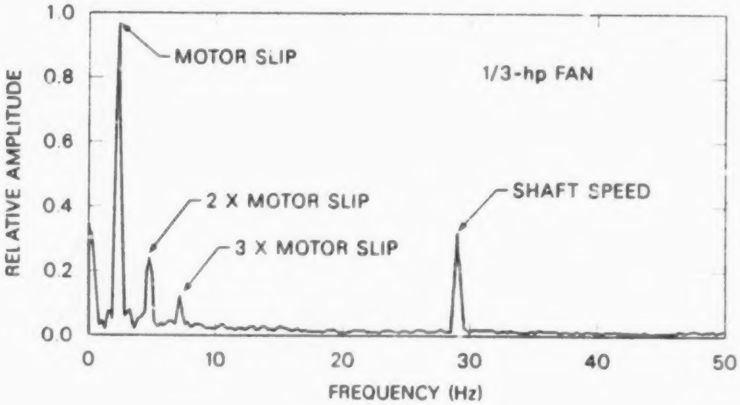

Figure 10. Motor current spectral signature for an electric fan.

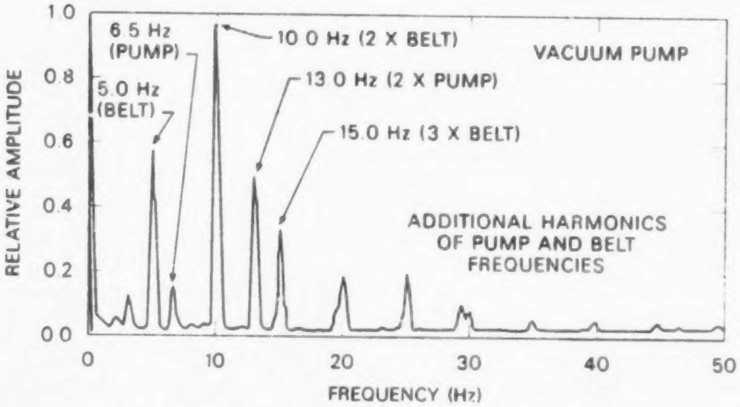

Figure 11. Motor current spectral signature for a motor-driven vacuum pump.

noted that the belt fundamental has many harmonics. In this case, it is likely that the cause of the strong pump first harmonic is simply that the pump is a reciprocating pump, with two direction (and load) changes per cycle. The harmonic content of the belt frequency may have been due to looseness or degradation of the belt.

## COMPARISON WITH VIBRATION SPECTRA

Since the cause of the spectra obtained from motor current FFT analysis (load variations) could also result in equipment vibration, a comparison was carried out between the spectra obtained from the motor current and that obtained from a portable accelerometer located on the pump housing. Signals from the motor current sensor and the accelerometer were fed to two separate FFT analyzers to produce the spectra shown in Figure 12. Although the relative magnitudes of the various peaks differ, substantially all of the peaks are seen in both spectra.

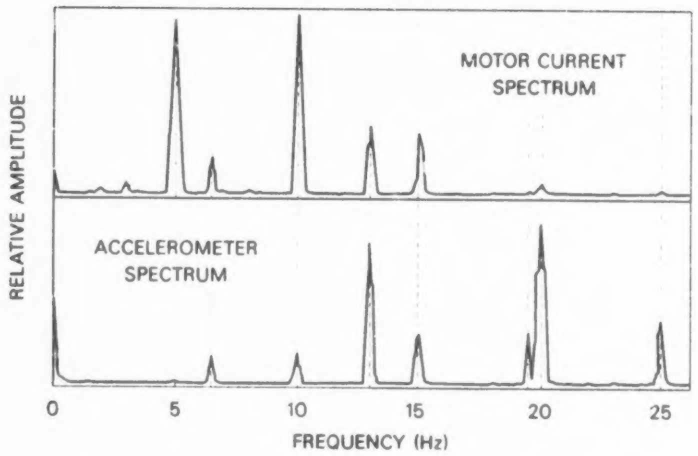

Figure 12. Comparison of spectral signatures based on motor current and on vibration.

Differences between motor current and accelerometer spectra should be expected based on differences in the nature of the signal being analyzed. These differences include the following:

- The motor current only detects load generated spectra, while the accelerometer can detect spectra generated frm outside sources, such as adjacent equipment
- The motor current acts as a single transducer, detecting all spectra generated from the power train, whereas the accelerometer spectra may be limited to one plane of vibration, and may be highly localized
- In the case of motor current, the transducer is directly linked to the load (i.e., the drive train), while the accelerometer is generally attached to a casing or other component, with the vibration signal passing through different materials from its source to the accelerometer.

In addition to these differences in the spectra, it is noted that the motor current sensor can be mounted remotely and non-intrusively, whereas the accelerometer must be directly linked to the device to be monitored.

## CURRENT AND FUTURE ACTIVITIES

The work reported here has confirmed that for MOVs and other motor driven mechanical equipment, the motor current signature provides four levels of information about the mechanical loads and its time dependent variations. However, it is recognized that in order to utilize this information for determining operational readiness, the relationship between the signatures (and their changes with time) and the degradations which may lead to loss of operational readiness must be determined.

To accomplish this a data base will be developed of diagnostics versus degradations. These will be developed from tests conducted at ORNL and also from field tests at nuclear power plants and other similar facilities.

The tests to be conducted at ORNL will involve implanting defects in the valve and operator in order to determine the effect that they will have on the motor current signatures. These tests are currently in progress.

The tests at nuclear plants will consist of obtaining motor current signatures of a large number of MOVs of different sizes and types during actuation both under shutdown conditions and where possible during operation. Where signatures are obtained that appear tc have unusual features, these will be reviewed with the utility and the valve examined at a future shutdown. The field tests are scheduled to begin in the next month.

REFERENCES

1. W. L. Greenstreet et al., "Aging and Service Wear of Electric Motor-Operated Valves Used in Engineered Safety-Feature Systems of Nuclear Power Plants", NUREG/CR-4234, Vol. 1, (June 1985).

2. U.S. Patent 4,542,649, "Motor-Operated Valve Analysis and Testing System."

3. R. A. S. Lee, "Improvements in Motor-Operated Valves", EPRI NP-4254 (November 1985).

4. J. L. Crowley and D. M. Eissenberg, "Evaluation of the Motor-Operated Valve Analysis and Test System (MOVATS) to Detect Degradation, Incorrect and Adjustments, and Other Abnormalities in Motor-Operated Valves "NUREG/CU-4380, (January 1986)

# The Interactive Effects of Relay and Circuit Breaker Aging in a Safety-Related System

G. J. Toman, V. P. Bacanskas
T. A. Shook, C. C. Ladlow

Franklin Research Center

W. Gunther

Brookhaven National Laboratory

## INTRODUCTION

This paper provides an overview of the results of a program to evaluate the aging of circuit breakers and relays and the effects of that aging on the function of a safety system used in nuclear power plants. The program was performed under the Nuclear Plant Aging Research (NPAR) Program of the U.S. Nuclear Regulatory Commission under subcontract to Brookhaven National Laboratory.

The full report of the program will be issued as a NUREG report in early 1987.

## PURPOSE OF THE PROGRAM

There were two primary aspects to the program. In the first, the aging and failure modes of relays and circuit breakers were determined by evaluating the construction, design, and materials and the failure data related to nuclear power plant service. In the second, the interactions between a safety system and its relays and circuit breakers were evaluated to determine the effects of relay and circuit breaker aging on the function of the safety system. The aging of relays and circuit breakers was assessed through evaluation of failure data bases, discussions with utility personnel, and evaluation of equipment operating and maintenance manuals. The interaction study was based on an analysis of the safety injection system of a pressurized water reactor. The effects of stresses from the system were analyzed for their tendency to cause deterioration of the relays and circuit breakers in the system. Then the effect of the deterioration of relays and circuit breakers on the functional capability of the safety system was evaluated.

## DESCRIPTION OF EQUIPMENT AND APPLICATIONS

### Relays

Three basic types of relays were studied: protective, auxiliary (or control), and time-delay. Each of these types is significantly different from the other in design and application. Protective relays are used to protect electrical equipment from the effects of overloads, faults, and abnormal voltage conditions. In most applications, the protective relay is connected to the control circuit of a circuit breaker and provides a control signal to the circuit breaker that causes it to open when an undesirable condition is detected.

Figure 1 provides a schematic diagram of a protective relay with an induction disc mechanism commonly used for overcurrent protection on busses and load circuits. In effect, it is a slip motor with magnetic damping to give it appropriate operating characteristics when responding to overcurrent conditions.

The auxiliary and control relays are similar to each other and use a solenoid or an armature to close or open a set of contacts upon energization of the relay coil. Figure 2 shows schematic diagrams of these relays. The auxiliary relay is used with protective relays, which have small contacts that cannot withstand the currents required to energize the trip coils of a number of circuit breakers. Therefore, the protective relay energizes an auxiliary relay having has many large contacts that are used to trip the circuit breakers. Control relays are used in the logic and control circuits of nuclear plant systems to detect changes in control signals and, in turn, initiate control and protective action for the reactor.

Time delay relays also are used in control and logic systems. They have either electronic or pneumatic time delay mechanisms that delay the opening or closing of the relay contacts upon energization or deenergization. They are used to prevent or cause safety system operation for a specific period of time.

### Circuit Breakers

Two types of circuit breakers were studied: low and medium voltage drawout types for metal clad switchgear, and low voltage molded-case types. Drawout circuit breakers, large circuit breakers that can interrupt high fault currents (tens of thousands to hundreds of thousands of amps), are used in safety-related power systems at 480 to 6900 V. Drawout circuit breakers are designed to unplug from the bus and load so that they are easily removed from their cabinets for testing and maintenance. They have sophisticated arc extinguishing systems, and complex mechanical linkages and control systems for rapid opening and closing of the main contacts.

Molded case circuit breakers used in nuclear plants are similar to those used in household electrical circuits. They have a molded phenolic or plastic case and are generally self contained (i.e., the overcurrent detection system is located within the circuit breaker). They are generally manually closed and have both a magnetic instantaneous trip device and a thermal trip device that heats up from excessive current and operates the trip latch. Like the drawout circuit breaker, the molded case has an arc extinguishing system but it is less sophisticated than that of the drawout circuit breaker.

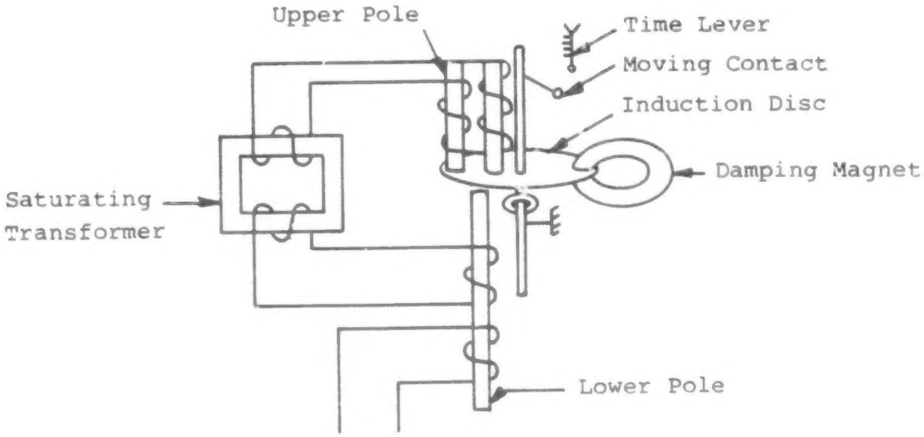
Upper Pole
Time Lever
Moving Contact
Induction Disc
Damping Magnet
Saturating Transformer
Lower Pole

Figure 1. Schematic Diagram for an Induction Disc Relay
(from Westinghouse Applied Protection Relaying [1])

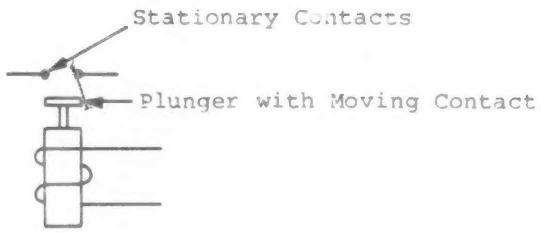
Stationary Contacts
Plunger with Moving Contact

a. Solenoid Operated Relay

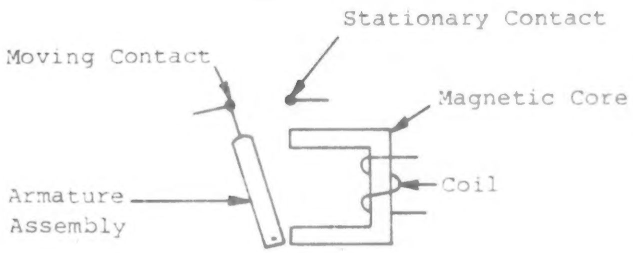
Stationary Contact
Moving Contact
Magnetic Core
Coil
Armature
Assembly

b. Armature Type Relay

Figure 2. Schematic Diagrams of Solenoid and Armature Type Relays (from Westinghouse Applied Protective Relaying [1])

## SYSTEM INTERACTION RELATING TO THE AGING OF CIRCUIT BREAKERS AND RELAYS

The interactions of the relays and circuit breakers within a safety system were studied through evaluation of the safety-injection (SI) system of a particular pressurized water reactor. Ways in which the operation of a safety system affects relays and circuit breakers and the effects of aged relays and circuit breakers on system function were evaluated. Figure 3 is a simplified diagram of one of the redundant trains of the SI system. The system forces high pressure water into the reactor at relatively low rates in the event of a small-break, loss-of-coolant accident. For the system to operate, the valves that connect the refueling water tank to the pump and the pump to the cold legs of the reactor system must open automatically and the pump motor must be energized.

Figure 4 is a diagram of the SI start path and valve opening circuits. Upon sensing a condition requiring SI, the reactor protection instrumentation causes the safeguards-actuation bistable circuits to deenergize the SI actuation relay, which energizes the SI master and slave initiation relays. The SI initiation relays cause the closing of the SI pump-motor circuit breaker and the energization of the contactors in the motor control centers that energize the motors of the valve actuators, causing the system valves to open.

## INTERACTIONS OF RELAYS AND CIRCUIT BREAKERS IN THE SYSTEM

### System Test and Operation Interactions

Figure 5 shows the interconnection of the relays and circuit breakers (CBs) in the SI system, with the reactor protection signal shown at top left. The diagram shows that each relay interconnects with at least one CB, either for receipt of control power or for affecting the position of main power CBs or both. Likewise, all of the CBs connect to relays and some are connected in series with others. The metal-clad switchgear CBs receive dc control power by way of molded-case CBs.

During normal plant operation, the SI system is inactive, except when it is exercised during surveillance tests (to verify its operability) and during infrequent, inadvertent operations caused by human error or misoperation of the initiating system. The periodic surveillance tests occur once per refueling cycle and once per month, depending on the type of tests. During the once-per-month test, the SI system is reconfigured so that the flow path from the outlet of the pump is returned to its refueling water storage tank and actual pump operation can be evaluated. A simulated reactor protection signal is used to initiate the operation of the SI system, allowing verification of the functioning of the system control relays. Valves in the system are exercised individually when they cannot be exercised with the system. During testing of the SI system with the reactor at power, flow cannot be routed to the reactor since injection of cold water will cause a thermal shock to reactor components and would also upset the stability of the reactor. During the once-per-refueling cycle tests, which occur during a refueling outage, full pump flow is verified by routing the SI system to the reactor.

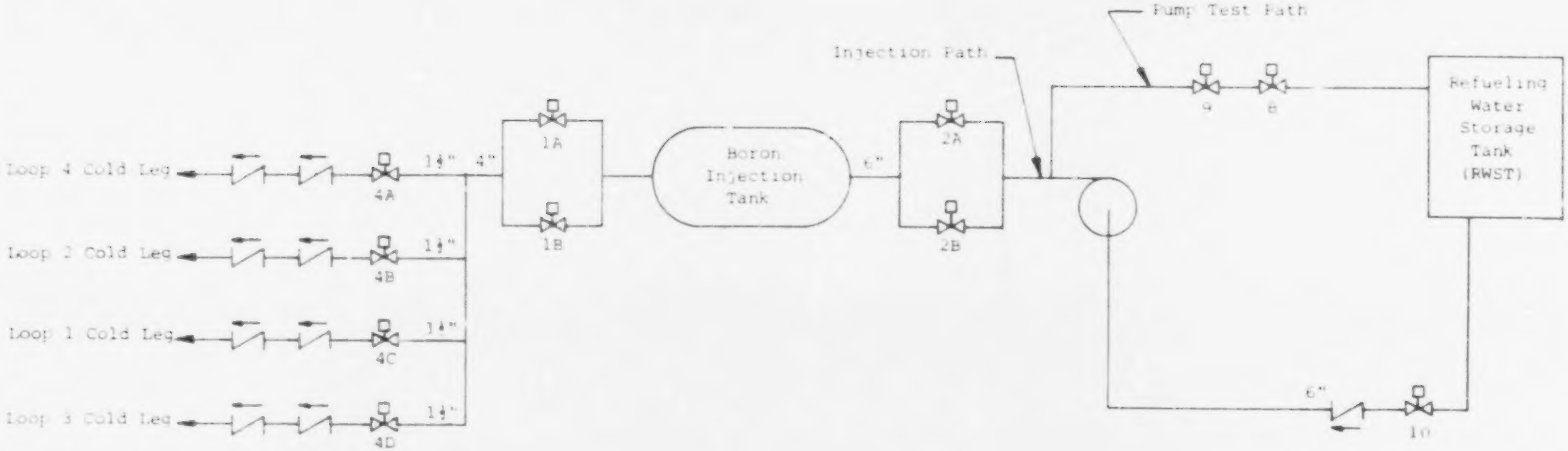
Pump Test Path
Injection Path
Loop 4 Cold Leg
Loop 2 Cold Leg
Loop 1 Cold Leg
Loop 3 Cold Leg
4A
4B
4C
4D
1½"
1½"
1½"
1½"
4"
1A
1B
Boron Injection Tank
6"
2A
2B
9
8
Refueling Water Storage Tank (RWST)
6"
10

Figure 3. Simplified Diagram of Safety-Injection System

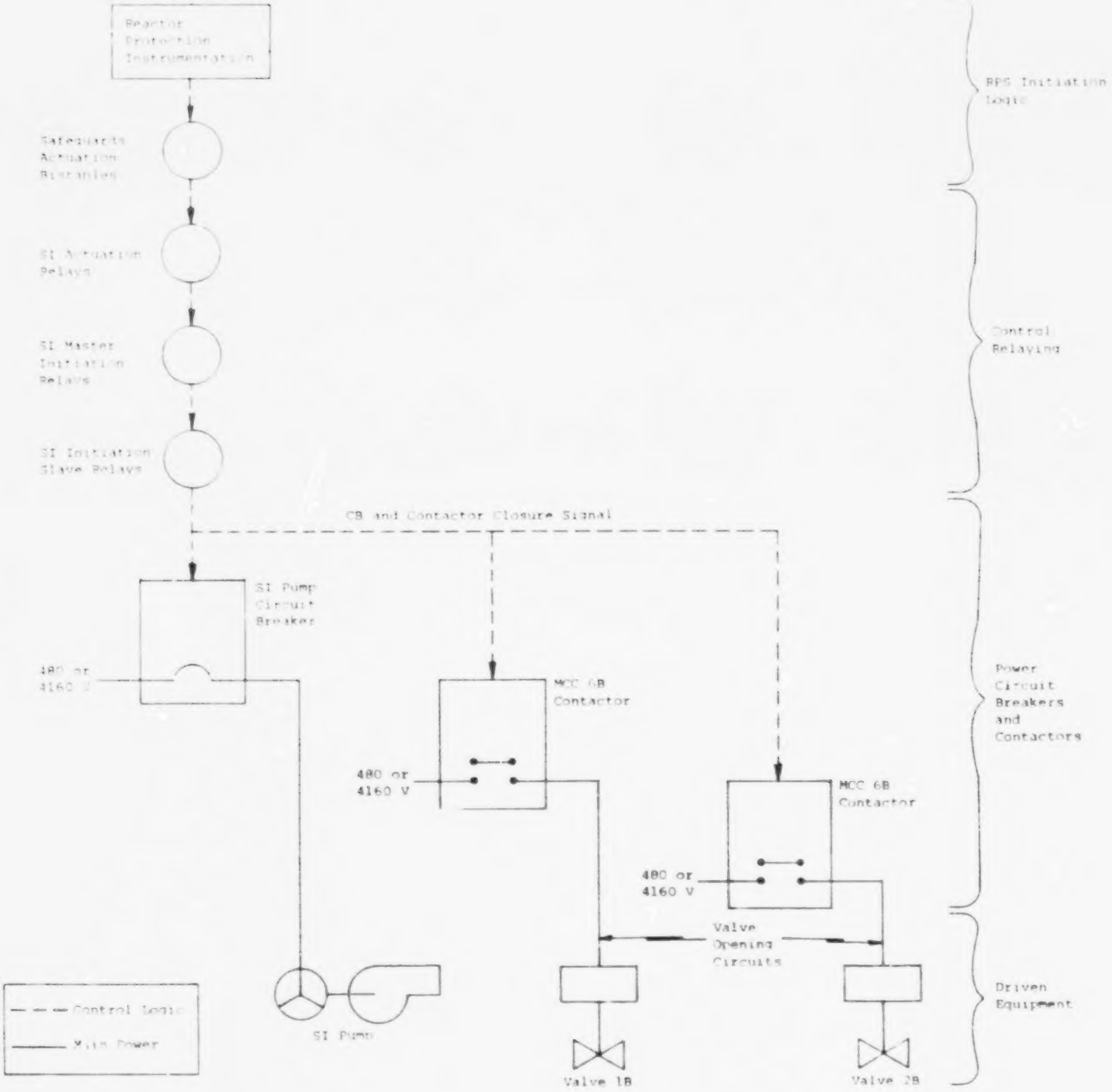
Reactor
Protection
Instrumentation
Safeguards
Actuation
Bistables
SI Actuation
Relays
SI Master
Initiation
Relays
SI Initiation
Slave Relays
CB and Contactor Closure Signal
SI Pump
Circuit
Breaker
480 or
4160 V
MCC 6B
Contactor
480 or
4160 V
MCC 6B
Contactor
480 or
4160 V
Valve
Opening
Circuits
SI Pump
Valve 1B
Valve 2B
Control Logic
Main Power
RPS Initiation
Logic
Control
Relaying
Power
Circuit
Breakers
and
Contactors
Driven
Equipment

Figure 4. Safety-Injection Pump Start Path

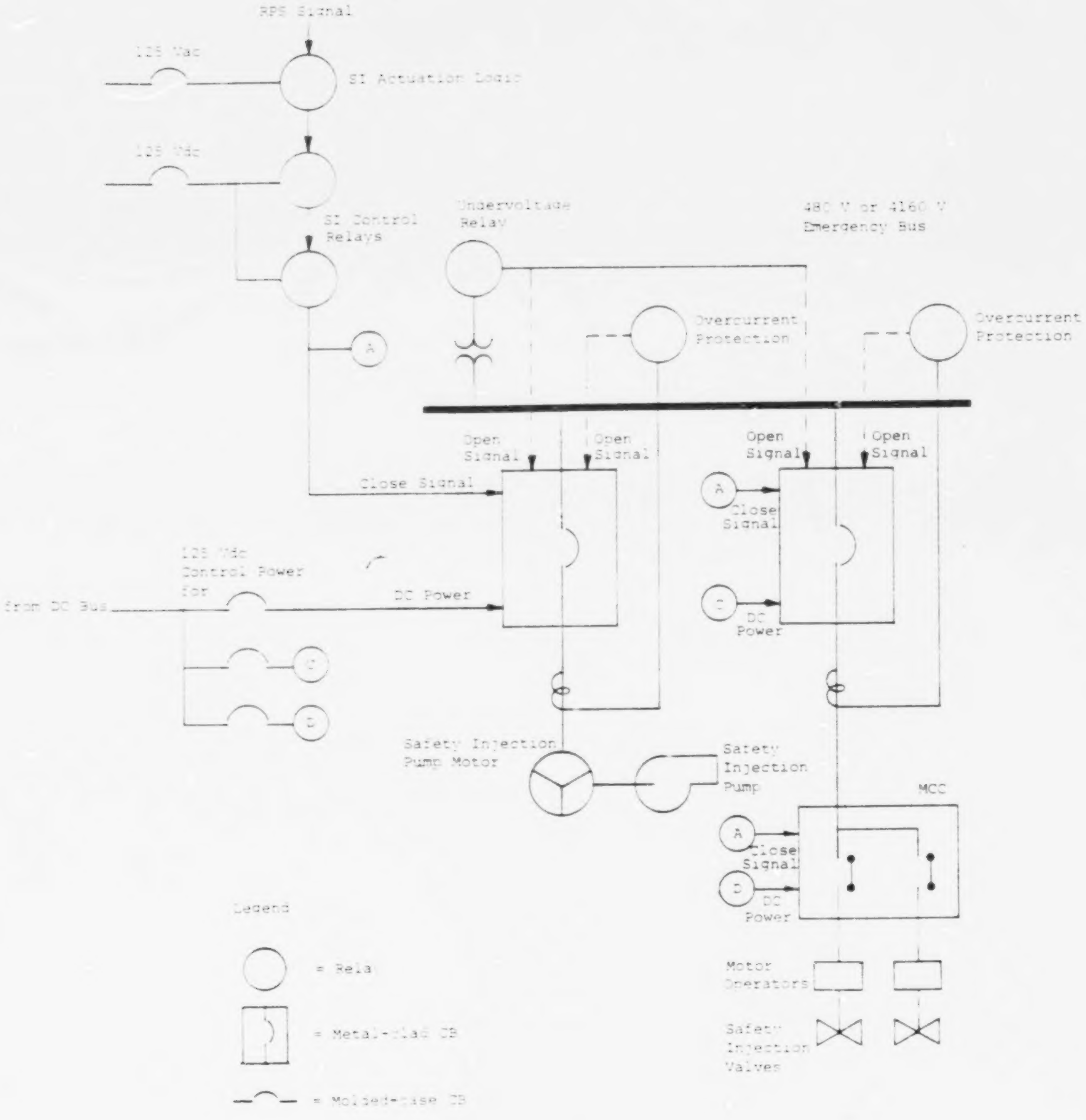
RPS Signal
125 Vac
SI Actuation Logic
125 Vdc
SI Control Relays
Undervoltage Relay
480 V or 4160 V Emergency Bus
Overcurrent Protection
Overcurrent Protection
A
Open Signal
Open Signal
Open Signal
Open Signal
Close Signal
A
Close Signal
125 Vdc Control Power for
from DC Bus
DC Power
C
DC Power
C
D
Safety Injection Pump Motor
Safety Injection Pump
MCC
A
Close Signal
D
DC Power
Legend
= Relay
= Metal-clad CB
= Molded-case CB
Motor Operators
Safety Injection Valves

Figure 5. Interconnection of Protective and Control Relays with Primary Power Sources via Circuit Breakers

The testing of the system is beneficial because it redistributes lubricants and the contacts of the switches and relays tend to wipe over each other and help remove minor amounts of dirt and corrosion. Such monthly testing should not cause heavy wear of the system relays and CBs. However, it is during such tests that the coils, switch contacts, and mechanical components of the circuit breakers and control relays are challenged and do experience slight amounts of degradation. This degradation adds to the slow gradual deterioration that is continuously occurring to the organic materials and surfaces of metallic components.

## Component Failure Challenges to Other Components

Electrical faults within the system cause the largest increment of rapid CB wear. When a fault occurs in a circuit protected by a molded-case CB, it will cause the thermal trip device to open the CB. The heat generated by the high fault current damages the thermal trip device by affecting the annealing of the bi-metal strip that causes the CB to trip, thereby lowering the trip point of the CB. As few as two faults can cause the molded-case CB to trip below its rated load so that random trippings of the CB may occur at normal current levels. Most manufacturers recommend replacement of molded-case CBs when they have tripped twice under fault current conditions.

Faults in circuits protected by metal-clad switchgear CBs generally do not damage the protective relays or CB control system other than to add one more wear cycle. The only real challenge to the contacts and arc extinction systems occurs when the CBs open under fault conditions. The 480-Vac CBs with a 1200 A normal rating may be rated for 60,000 A or more fault current. It can be seen that such currents can be expected to produce damage even from a one-time occurrence. Manufacturers recommend inspection of the contacts and arc chutes after high current faults, especially those that cause the instantaneous portion of protective relays to operate (which indicates that a high current fault has occurred).

## System Voltage Condition Interactions

A sustained increase in the voltage of the control power sources (i.e., 125 Vdc and 120 Vac) can lead to more rapid deterioration of relay coils when the coils are continously energized. Self heating in the coils can increase the rate of thermal deterioration rapidly.

During internal research at FRC, testing of dc solenoid valve coils that are similar to relay coils showed that the temperature at the key elastomeric components increased from 73°C (164°F) to 83°C (182°F) when the voltage was changed from 120 to 142 Vdc (as would occur when the station battery is placed on floating charge). Such a temperature change can double the rate of thermal degradation for many materials used in relay coils.

In the SI system of the power plant evaluated in this study, the 120-Vac system was regulated to preclude overvoltage on the SI actuation relays. The SI initiation relays were energize-to-operate types; therefore, they were not subject to additional continous thermal aging caused by self-heating.

## Human Interactions with the System

During maintenance, testing, and operation, there is always a potential for damage to components due to mishandling or inadvertent abuse by personnel.

In general, the molded-case CBs and the control relays are usually not subject to mishandling and inadvertent abuse. The metal-clad CBs and the protective relays do require preventive maintenance or calibration. For the metal-clad CBs, most errors will be detected when the CB is functionally tested prior to return to service.

In the case of protective relays, human error during calibration is of concern for it is only during calibration that the relay is out of its protective case. Improper calibration of the relays or introduction of dirt and contaminants into the close tolerance mechanism can prevent operation or cause inadvertent operation. In most cases, the operation of the protective relay cannot be verified once it is returned to service. Most tests are performed by placing simulated voltages and currents on the relay terminals rather than by causing real changes to system operating voltages and currents.

## EFFECTS OF CIRCUIT BREAKER AND RELAY AGING ON SYSTEM OPERATION

As a safety-related system, the most important function of the SI system is to provide cooling water to the reactor during an accident. It must not start up inadvertently for it will cause an unwanted temperature transient and negative reactivity insertion in the reactor. To study the consequences of CB and relay aging effects on the SI system, the five chains of events listed in Table 1 were evaluated. These are the key events in which relays and circuit breakers in the SI system are required to perform a safety function. Events 1, 2, and 5, which are a loss-of-coolant accident (LOCA), a LOCA with loss of off-site power, and a seismic event, are analyzed as part of the licensing basis for nuclear plants. The other two events were included in the program since they allow the functions of all of the relays and CBs to be analyzed regarding the effect on system operation. In this paper, only Events 1 and 4, a LOCA by itself and a LOCA coupled with a seismic event, are described to show the nature of the evaluation.

In the following description, the failure causes found to be of highest interest during the failure data evaluations for relays and CBs were used to evaluate system operation. Brief statements about the causes are included in this paper for clarity. More details are contained in the report from the project that will be published as a NUREG report in 1987.

Figure 5 shows the main electrical power control and protective components in the SI system. The 480-V emergency power bus is shown only with SI system loads. In reality, there are three power source circuit breakers and a number of other safety loads connected to the bus.

A LOCA by itself will not affect the protective relays (i.e., the under-voltage and overcurrent relays connected to the bus and SI loads); the voltage and currents experienced at the onset of a LOCA are the same as during a test of the SI system. The SI control relays and the metal-clad switchgear CB for the SI pump are challenged. If the normally energized 120-Vac SI actuation relay has experienced an age-related coil bobbin failure[1] which causes

---

[1] At least two types of continuously energized control relays were reported in U.S. Nuclear Regulatory Commission IE Information Notices to experience coil bobbin melting after coil insulation failure caused overheating. The melted material flowed into the contact carrying components and caused the contacts to be held in the position associated with the relay coil being energized. These failures were also reported in the failure data bases that were analyzed.

Table 1. Assumed Chains of Events That Could Challenge the Safety Injection System

| Device Challenged or Affected by Event | Event | | | | |
|---|---|---|---|---|---|
| | LOCA Alone | LOCA with Offsite Power Loss | LOCA and Adjacent Electrical Failure | Seismic With LOCA | Seismic Event Alone |
| Protective Relays and Auxiliary Relays | No | Yes, 1 | Yes, 2 | Yes, 3 | 3 |
| Control Relays | Yes | Yes | Yes | Yes, 3 | 3 |
| Metal-Clad Circuit Breakers | Yes | Yes | Yes | Yes, 3 | 3 |
| Molded-Case Circuit Breakers | Possibly | Possibly | Possibly | 3 | 3 |

1. Undervoltage and return of voltage relays affected.
2. Overcurrent and differential relays challenged.
3. Physical challenge from seismic vibration.

binding of its solenoid core, the SI system start sequence will not occur. In this case, the relay acts as if it had never been deenergized and its contacts will not energize the SI master initiation relay. (Note: A second SI chain exists in each plant and provides redundancy; failure of one relay will not prevent operation of the second chain.)

If the SI actuation relay works properly, the normally deenergized SI master initiation and slave initiation relays can be expected to operate properly, provided the molded-case CBs for the dc power do not trip when the relays are energized. (Tripping would be expected only if the molded case CBs had been degraded by interrupting too many electrical faults on the associated circuit.[2])

Proper initiation of the SI initiation relays will cause close signals to be sent to the SI pump motor metal-clad CB and to the SI valve control contactors in the motor centers (MCC). With respect to the SI pump motor CB, three subsystems may have experienced age-related failures. The closing solenoid may have failed, the charging motor or the charging mechanism may have failed (a CB trouble alarm should indicate such a failure), or the close latch and closing mechanism may have failed. If any of these fail, the SI train will not perform its function since the pump motor will not be energized. The CB will also fail to close if dc control power has been lost, as in the case of molded-case CB deterioration described above.

Finally, the valve control circuits must work properly. The main metal-clad CB for the MCC does not have to change position (it is normally closed). Therefore, electrical power will be available. The molded-case CBs in series with each valve contactor could trip when the contactor is energized if it has interrupted too many electrical faults. It would be expected that only a limited number of molded-case CBs will have interrupted two or more faults. Therefore, at most, one valve would be affected. In the case of the SI chain that was evaluated (see Figure 3), failure of any one valve to open will not prevent SI system operation.

### Seismic Event with a LOCA

The most likely problems to be added to the LOCA chain of events by a simultaneous seismic event are associated with unwanted operation of metal-clad CBs or relays (control and protective). The energized SI actuation relay (shown in Figure 5) will not change position since the holding force is greater than the forces generated by the expected seismic vibrations. The deenergized SI master and slave relays may change state since the springs that hold the relays in the deenergized state do not exert the same level of force as the coil when it is energized. (Note: Seismic qualification of the relay should verify that unwanted operation will not occur.) If unwanted operation

---

[2] The thermal trip device for a molded case CB is operated by a bimetallic strip that is heated by the current passing through the CB. Under fault conditions, the bimetallic strip is annealled. Subsequently, it will trip at a lower current; after a while, it may trip at normal load currents.

BEST COPY AVAILABLE

of the SI initiation relays did occur, operation of the SI system would be prematurely initiated. In the case of a simultaneous LOCA, no problem would be encountered.

Malfunctioning of most types of protective relays would not be expected. Such relays do not have an aging mechanism that would affect their operation during a seismic event. Only certain types of electromechanical differential relays for the diesel generator would tend to have their contacts drift closed and operate during seismic events. This condition occurs because the diesel is not energized and there are no currents through the relay to keep the contacts in the proper position. When these types of differential relays are energized, they do not malfunction during seismic events.

The metal-clad CB trip and close latch could malfunction due to causes that could be coupled with aging wear. The main CB for the MCC could open due to unwanted trip latch operation. The SI pump CB could close inadvertently due to close latch operation caused by seismic vibration. Early closure of the SI pump motor CB should not be detrimental since system operation will be required under this scenario. Unwanted opening of the CB should not disable the CB in the open position.

Additional malfunctions of molded-case CBs would not be expected under this event.

## OVERALL CONCLUSIONS FROM THE SYSTEM INTERACTION EVALUATION

The evaluation of the age-related interaction between relays and circuit breakers and the SI system indicated that aging will affect the performance of the SI system if no preventive actions are taken. This study evaluated only two categories of the equipment used in the SI system: relays and CBs. Many paths to system failure are possible if key molded-case or metal-clad CBs fail or if control or protective relays fail. Failures of other key components, such as the SI system motor, could also prevent system operation.

Most of the failures that can be expected are detectable during surveillance testing, calibration, or periodic preventive maintenance. These actions detect aging after failure or significant deterioration of the CBs or relays has occurred. These actions do not provide predictions of when CB and relay components will fail. Surveillance, calibration, and maintenance, as presently performed, help prevent failures from going undetected for long periods so that multiple safety systems and redundant safety trains are not simultaneously out of service.

Once recognized, the types of failures described above can be precluded as a source of common mode failure (i.e., those types of failure that will affect significant number of units of a particular type of device in redundant systems when the function of the devices are necessary) through failure evaluations and appropriate corrective action. For example, the relay coil failures due to long-time thermal effects from energization were detected and IE Information Notices were issued to all operating plants [2, 3, 4], allowing replacement of the failure-prone coils.

The key problem that may allow aging-related failures is that 18 months may elapse between functional tests of the initiation relays and the power CBs. The length of time between tests requires a knowledge of the rate of deterioration expected during the interval before the next test. With this knowledge, the interval between maintenance inspections can be set so that gradual deterioration does not cause loss of function.

At present, the aging of the mechanical and control portions of metal-clad switchgear CBs is only evaluated by visual inspection and observation of operation performed during preventive and corrective maintenance. More sophisticated, automated evaluation techniques are not used for the mechanical and control portions of the metal-clad CBs. Most of the monitoring and evaluative testing of these CBs is associated with the verification of the adequacy of the electrical insulation of the power path. Analysis of the LER, NPRDS, and IPRDS data has shown that very few failures of the power path insulation have occurred. This does not mean that the monitoring of the electrical insulation should be stopped. Failure of the insulation of a CB is catastropic, causing a fault on the emergency power bus. The concern is that more sophisticated test methods do not exist for the more failure-prone portions of the CBs (i.e., the mechanism and control circuits).

With regard to assuring the continued operability of the SI system, the following areas should receive the most attention:

- o Verification that coil deterioration is under control on the SI actuation relays.
- o Verification that setpoint drift of protective relays is not excessive over an 18-month period.
- o Periodic performance of detailed inspections of the mechanical and control portions of the SI system metal-clad switchgear CBs.
- o Replacement of any molded-case CB used in control power circuits that has interrupted fault current more than once.

Development of diagnostic and predictive condition monitoring tests for metal-clad switchgear CBs is desirable for the mechanical and control subsystem as a longer term effort.

## REFERENCES

1. Applied Protective Relaying, Westinghouse Electric Corporation, 1976

2. IE Information Notice No. 82-02, "Westinghouse NBFD Relay Failures in Reactor Protection Systems at Certain Nuclear Plants," U.S. Nuclear Regulatory Commission, Office of Inspection and Enforcement, Washington, DC, January 27, 1982

3. IE Information Notice No. 82-13, "Failures of General Electric Type HFA Relays," U.S. Nuclear Regulatory Commission, Office of Inspection and Enforcement, Washington, DC, May 10, 1982

4. "Service Life of Relays in Safety-Related Systems," IE Information Notice No. 84-20, U.S. Nuclear Regulatory Commission, March 2, 1984

# NUCLEAR SERVICE EMERGENCY DIESEL GENERATOR AGING RESEARCH

K. R. Hoopingarner
J. W. Vause III
D. A. Dingee

Battelle, Pacific Northwest Laboratory

## ABSTRACT

This paper reports the progress of diesel-generator aging research currently underway at PNL.

Nuclear service diesel generators have been selected to be studied as a part of the Nuclear Plant Aging Research (NPAR) Program by the Nuclear Regulatory Commission's Office of Nuclear Regulatory Research, Division of Engineering Safety. Equipment aging can potentially reduce the capability of a nuclear plant to operate safely. This program is intended to identify, evaluate and recommend ways to mitigate aging.

The preliminary results of this research program, using a statistical technique based upon expert analysis, shows that diesel-generator aging can be detected, and quantified. The results are positive in that the components that fail, how they fail and what measures for correction have been used have all been analyzed and reported. The chief results of this first study phase are presented in this paper.

The analysis shows that the aging of diesel generators is related most often to a few major components and engine systems and that these can be repaired or replaced to maintain the emergency power function. Further the study indicated that the percentage of aging related failures increases with plant age and that certain practices and maintenance/surveillance methods have the potential to mitigate safety concerns.

## INTRODUCTION AND METHODOLOGY

Diesel-generators occupy a unique position in the NRC research program. Even though they are on the list of components to be evaluated, diesel-generators are complex systems: actually, small power plants within the larger nuclear facility. As a complex of systems, the diesel generator comprises the engine, auxiliary systems, and interfacing equipment. This includes the fuel, lubrication, air start, cooling, and electrical systems as well as special components such as the governor, and turbocharger. An additional complication is that more than ten vendors and several diesel power systems contractors supply diesel generators to the nuclear industry, each with several models, modifications, and applications in service.

Because of the complexity of this task, the identification of aging degradation was separated into two major phases: 1) an evaluation of current expert and operational experience; and 2) detailed component aging assessments.

Under Phase I of the research, an evaluation was performed of a representative sample of several existing data bases to formulate one large database of failures evaluated for aging degradation. The purpose of the evaluation was to determine which components failed; why the components failed; if the failure was due to an aging mechanism; and what were the preliminary corrective actions that should be suggested. The methods to resolve these issues included the participation of expert diesel consultants, who reviewed the available data with knowledgeable objectivity and considerable past diesel experience.

Each failure was categorized by a predetermined and coded list of components and subcomponents. Then, the failure was evaluated for the primary and secondary causes of failure, primary and secondary recommended corrective actions for the listed failure, and whether aging may have contributed to the failure. The failure causes and recommended corrective actions were also coded to represent a predetermined selection of evaluation categories for each component and subcomponent. Accompanying each aging evaluation was a comments section of up to 250 words that amplified details of the evaluation.

The data was entered on an IBM-PC using the dBase III relational database management system. Using the dBase III programming language, programs were developed to formulate component/analysis and component/recommended-corrective-action matrices to total the number of failures for each component in each failure category and each associated recommended corrective action category. Because the comments field was word searchable, many relevant topical areas could be segregated and reviewed.

Due to the diversity of information in the database, interesting and valuable computer sorts could be selected. The resulting output provided an indication of aging processes and a basis for the aging analysis. As a result, 50 matrices plus selected word searchable topical sorts were produced that eventually were categorized into four major groups of nuclear service diesel-generator aging indicators.

## RESEARCH RESULTS

An example of a small portion of a failure matrix is shown in Figure 1, which shows a typical aging-wear computer printout. This partial matrix is for the instrument and control subsystem which is one of 10 major subsystems associated with the diesel-generator system. Of all subsystems and components examined in the study's first phase, this subsystem has the most failures, with 296 of the 1984 failures in the data base. The matrix also shows the 14 preassigned alpha code letters at the top and their brief identification. These were common to all failure matrices. It may be interesting to note that it would take about 500 illustrations of the complexity of Figure 1 to show all the matrices produced in this study.

Summary of Diesel Engine Failure Data ,All Failures ,Aging and Wear Only

| | POOR DESIGN/APPLICAT. | POOR QC-QA MANUFACT. | OVERSTRESS | VIBRAT. - BAD CONDITIONS | ENVIRONMENT - DUST | INSTALLATION ERROR | BAD ADJUST/ALIGN | GALVANIC & STRAY CURRENTS | HUMAN ERROR - OPS. | HUMAN ERROR - MAINT. | CASUALTY | GRID UPSET | UNKNOWN/OTHER | POOR SYSTEM DESIGN | |
|---|---|---|---|---|---|---|---|---|---|---|---|---|---|---|---|
| INSTRUMENTS AND CONTROLS | a | b | c | d | e | f | g | h | i | j | k | l | m | n | TOTAL |
| - GOVERNOR | 3 | 31 | 0 | 22 | 13 | 0 | 10 | 0 | 2 | 14 | 0 | 0 | 14 | 0 | 109 |
| - OVERSPEED GOVERNOR | 0 | 2 | 0 | 6 | 3 | 0 | 2 | 0 | 3 | 3 | 0 | 0 | 2 | 0 | 20 |
| - CONTROL VALVES | 0 | 0 | 0 | 3 | 1 | 0 | 0 | 0 | 0 | 0 | 0 | 0 | 1 | 0 | 5 |
| - ALARMS AND SHUTDOWNS | 0 | 1 | 0 | 18 | 2 | 0 | 0 | 0 | 0 | 0 | 0 | 0 | 2 | 0 | 23 |
| - LINKAGES | 0 | 0 | 0 | 5 | 5 | 0 | 0 | 0 | 1 | 2 | 0 | 0 | 2 | 0 | 15 |
| STARTUP SYSTEM | 1 | 0 | 0 | 1 | 2 | 0 | 1 | 0 | 0 | 0 | 0 | 0 | 5 | 0 | 10 |
| - CONTROL AIR SYSTEM | 1 | 0 | 0 | 17 | 3 | 0 | 0 | 0 | 0 | 4 | 0 | 0 | 1 | 0 | 26 |
| - WIRING & TERMINATIONS | 0 | 3 | 0 | 13 | 0 | 0 | 0 | 0 | 0 | 0 | 1 | 0 | 2 | 0 | 10 |
| - RELAYS | 1 | 2 | 0 | 6 | 3 | 1 | 1 | 0 | 0 | 0 | 0 | 0 | 12 | 0 | 26 |
| - SENSORS | 1 | 6 | 0 | 7 | 3 | 0 | 3 | 1 | 0 | 1 | 0 | 0 | 7 | 0 | 29 |
| - OTHER | 0 | 1 | 0 | 4 | 1 | 0 | 0 | 0 | 0 | 0 | 0 | 0 | 8 | 0 | 14 |

296

Figure 1. Illustrating a Portion of a Typical Failure Matrix

The results gained from analysis of the matrices indicate that the aging of diesel-generators: is observable, follows recognizable patterns, experiences changes in the type of degradation mechanism with time, is confined to a relatively few, major components and subsystems, and increases as a percentage of all failures with time. To illustrate two of these points, Figure 2 shows a graph of how the percentage of aging related failures increases with time. The first point is, that based upon the definition of aging in this study, aging was more than just observable and amounted to 50 percent of all failures. The second point is that the trend is upward with increasing time. The methodology used in this study was such as to make the trend more certain than the absolute amounts of the failure percentage. For example, a more restrictive aging failure definition would reduce the amounts of aging found. Because, the same personnel and criteria were used for coding all entries from one data source the trend seems to be quite certain.

The years from 14 to 20 are a problem and are labeled poor data. So few older plants contribute data that these only amount to 2-3 data points per year. It is not logical to assume that the older plants have less aging related failures.

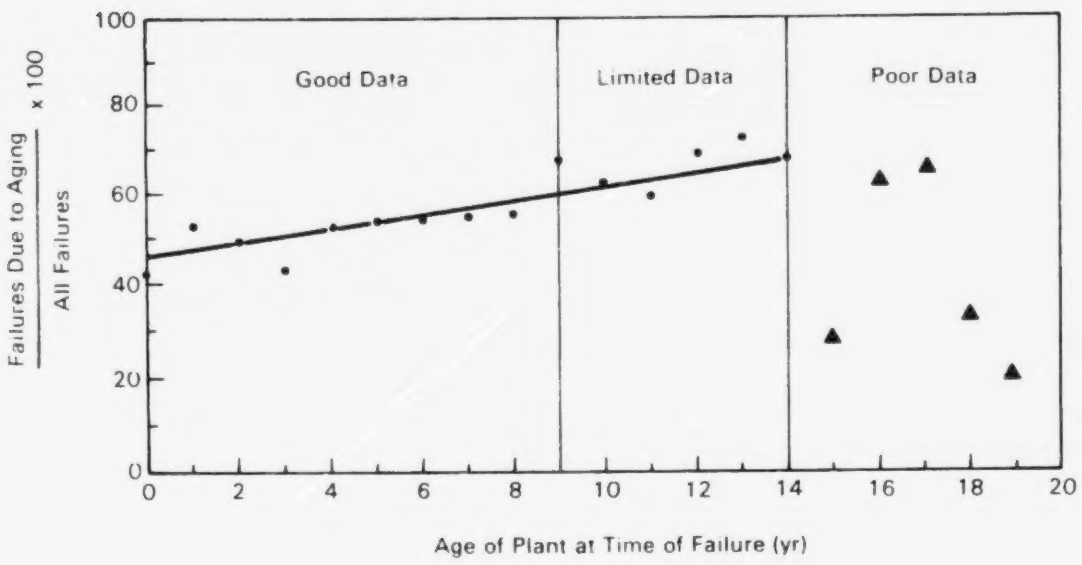

Figure 2. Graph of Aging Failure Rate versus Time in Years

The predominate aging stressors were in order of significance vibration, inferior component quality and an adverse environment. Normal engine vibration caused persistent problems with fastener loosening and fitting failures. Engine mounted piping also suffered vibration damage, as did other engine mounted components. Vibration sensitivity was also noted in poorly manufactured components and in those affected by poor installation and maintenance practices.

Problems of inferior quality were related to various design application and manufacturing causes. Often a component failed due to how it was applied on an engine, e.g., too near a heat source, or due to specific engine design variables and compromises.

Many times adverse environmental factors such as dust, high humidity, engine oil, and similar engine environmental conditions seemed to be the cause of engine failures. These affected the control, air start, and fuel systems in particular.

Human error was the cause of many direct and indirect engine failures. For example, omitted maintenance, incorrect adjustments and sometimes a lack of training or specific knowledge was the engine stressor that lead to failure. For this study, indirect human error was listed as an engine stressor. It is indirect in that it did not cause an immediate failure, but ultimately with time it did lead to a failure.

## DIESEL-GENERATOR AGING MITIGATION

The research work completed emphasized the identification and quantification of the aging process. The next phase will emphasize corrective and preventative measures. However, ten corrective actions were coded into the computer inputs, as applicable, the diesel experts reviewing the data base sources. These corrective actions were listed as a primary and a secondary corrective action for each entry, where possible. The corrective action taken was often listed in the original data source. These listed actions were reviewed by the diesel experts to ensure that they were correct, if not, they were modified.

Examination of the computer output matrices for aging mitigation revealed that the majority (78%) of the aging failures could be corrected by either maintenance and/or simple replacement. The most common recommended overall corrective actions were identified as follows:

| Recommend Corrective Action | Percent Applied |
|---|---|
| Replacement with same component | 52 |
| Maintenance | 26 |
| Replacement with upgraded component | 13 |
| Repair required | 5 |
| Preventative maintenance | 2 |
| Redesign | 1 |

Major subsystems of the diesel generator were also evaluated for corrective actions and separate matrices were produced for each of these subsystems. Generally the results were related to the overall recommended corrective actions tabulated above. This implies that a significant fraction of aging related failures may be prevented or corrected by replacing or repairing only a few components.

Primary corrective actions are intended to return the component and system to service and thus restore the diesel generator emergency power function. Secondary corrective actions tend to reinforce primary actions and also focus more on preventing the reoccurrence of the failure, for example, for a vibration loosening problem the primary action is to retorque the fitting or fastener; the secondary action is usually enhanced preventive maintenance.

## SAFETY AND RELIABILITY IMPROVEMENT

Quantification of the safety function of the diesel generators was not an objective of the first study phase. However, the affect of aging related to safety considerations was the primary objective of the program. Thus, the database developed has significant safety information capabilities which have only been partly explored and developed. The next phase of the study will further relate aging to safety and safety and reliability improvement.

The study did produce insights with significant safety aspects. One insight was that failures are primarily concentrated into a relatively few systems. Efforts for improvement that are concentrated on those systems and components that fail most often will give the greatest safety improvement. Likewise concentrating efforts on the greatest aging related failure causes and mitigating measures will give the greatest benefits. The results of this first phase study tell the regulators and the utilities where to focus their attention.

The study has shown that the primary corrective action of replacement and maintenance restore the safety function in about three quarters of the events studied. This type of simple direct action alone will not prevent the same failure occurring again in the same general time period unless the aging stressor is reduced or eliminated. This study describes what is failing most often and why it does so. Utilities may use this information to improve the safety function and reliability of their diesel generators.

In addition to the general safety actions discussed the following preliminary recommendations are offered for reliability improvement. These are actions within the control of the licensees.

- Conduct an active trend analysis program
- Develop a dedicated maintenance program
- Develop an aggressive design review/change program
- Maintain and improve vendor/contractor communications with the owner

## CONCLUSIONS

The original research and evaluations by diesel experts performed in the initial part of the NPAR program did detect aging effects. It also helped in understanding the influence of aging on the safety function of the diesel generators. The methodology used and the database developed provided realistic insights into diesel-generator aging and the general safety impacts. Although much work remains to be done, the good news is that no aging trends or safety problems were found of such a nature or magnitude to threaten either current nuclear plant safety or plant life extension. This does not imply that cost effective improvements cannot be made in the regulatory, operations and maintenance aspects of the diesel generator emergency power function.

NRC FORM 335
(2-84)
NRCM 1102,
3201, 3202

U.S. NUCLEAR REGULATORY COMMISSION

# BIBLIOGRAPHIC DATA SHEET

SEE INSTRUCTIONS ON THE REVERSE

1 REPORT NUMBER (Assigned by TIDC add Vol No, if any)
NUREG/CP-0032
Vol. 3

2 TITLE AND SUBTITLE
Proceedings of the Fourteenth Water Reactor Safety Information Meeting

3 LEAVE BLANK

4 DATE REPORT COMPLETED

| MONTH | YEAR |
|---|---|
| January | 1987 |

5 AUTHOR(S)
Compiled by Allen J. Weiss, BNL

6 DATE REPORT ISSUED

| MONTH | YEAR |
|---|---|
| February | 1987 |

7 PERFORMING ORGANIZATION NAME AND MAILING ADDRESS (Include Zip Code)
Office of Nuclear Regulatory Research
U. S. Nuclear Regulatory Commission
Washington, D. C. 20555

8 PROJECT/TASK/WORK UNIT NUMBER

9 FIN OR GRANT NUMBER
A-3283

10 SPONSORING ORGANIZATION NAME AND MAILING ADDRESS (Include Zip Code)
Same as Item 7 above

11a TYPE OF REPORT
Proceedings of conference on safety research

b PERIOD COVERED (Inclusive dates)
October 27-31, 1986

12 SUPPLEMENTARY NOTES
Proceedings prepared by Brookhaven National Laboratory

13 ABSTRACT (200 words or less)

This six-volume report contains 156 papers out of the 175 that were presented at the Fourteenth Water Reactor Safety Information Meeting held at the National Bureau of Standards, Gaithersburg, Maryland, during the week of October 27-31, 1986. The papers are printed in the order of their presentation in each session and describe progress and results of programs in nuclear safety research conducted in this country and abroad. Foreign participation in the meeting included thirty-four different papers presented by researchers from Canada, Czechoslovakia, Finland, Germany, Italy, Japan, Mexico, Spain, Sweden, Switzerland and the United Kingdom. The titles of the papers and the names of the authors have been updated and may differ from those that appeared in the final program of the meeting.

14 DOCUMENT ANALYSIS - a KEYWORDS/DESCRIPTORS
reactor safety research
nuclear safety research

b IDENTIFIERS/OPEN ENDED TERMS

15 AVAILABILITY STATEMENT
Unlimited

16 SECURITY CLASSIFICATION
(This page)
Unclassified
(This report)
Unclassified

17 NUMBER OF PAGES

18 PRICE

425

BEST COPY AVAILABLE